31st Benelux Meeting

on

Systems and Control

March 27 – 29, 2012

Heijen, The Netherlands

Book of Abstracts

The 31^{st} Benelux Meeting on Systems and Control is sponsored by

and supported by

Hans Stigter and Ton van den Boom (eds.)
Book of Abstracts 31st Benelux Meeting on Systems and Control

Wageningen University – Biometris
P.O. Box 9101
6700 HB Wageningen
The Netherlands

A catalog record is available from Wageningen University Library.

ISBN: 978-94-6173-317-7

Part 1

Programmatic Table of Contents

Tuesday, March 27, 2012

P0 **Jasmijn**
Welcome and opening
Chair: Hans Stigter **11.25–11.30**

Plenary: P1 **Jasmijn**
Dynamic Value Functions
Alessandro Astolfi
Chair: Ton van den Boom **11.30–12.30**

Plenary: P2 **Jasmijn**
Model Reduction by Moment Matching
Alessandro Astolfi
Chair: Ton van den Boom **13.45–14.45**

TuP01 **Jasmijn**
Systems Theory A
Chair: Jan van Schuppen **15.10–16:50**

TuP01-1 **15.10–15.35**

N.W. Bauer Eindhoven University of Technology
M.C.F. Donkers Eindhoven University of Technology
N. van de Wouw Eindhoven University of Technology
Maurice Heemels

TuP01-2 **15.35–16.00**

R. M. Hermans Eindhoven University of Technology
M. Lazar Eindhoven University of Technology
A. Jokic Eindhoven University of Technology
R. H. Gielen

TuP01-3 **16.00–16.25**

Ilya Tkachev Delft University of Technology
Alessandro Abate Delft University of Technology

TuP01-4 **16.25–16.50**

T.M.P. Gommans Eindhoven University of Technology

TuP02 **Gerbera**
System Identification A
Chair: Peter Heuberger **15.10–16:50**

TuP02-1 **15.10–15.35**

Marco Forgione Delft University of Technology
Xavier Bombois Delft University of Technology
Paul M.J. Van den Hof Eindhoven University of Technology
Ali Mesbah

TuP02-2 **15.35–16.00**

A. G. Dankers Delft University of Technology
P. M. J. Van den Hof Eindhoven University of Technology
P. S. C. Heuberger Delft University of Technology
X. J. A. Bombois

TuP02-3 **16.00–16.25**

Adeline Decuyper Université Catholique de Louvain
Vincent D. Blondel Université Catholique de Louvain
Luis E.C. Rocha Université Catholique de Louvain

TuP02-4 **16.25–16.50**

P.G.M. Hoeijmakers Eindhoven University of Technology
V.N. Kornilov Eindhoven University of Technology
I. Lopez Arteaga Eindhoven University of Technology
H. Nijmeijer, L.P.H. de Goey

TuP03 **Hyacinth**
Optimal Control A
Chair: Jacob van der Woude **15.10–16:50**

TuP03-1 **15.10–15.35**

M. Hajiahmadi Delft University of Technology
B. De Schutter Delft University of Technology
H. Hellendoorn Delft University of Technology

TuP03-2 **15.35–16.00**

Vital van Reeven Eindhoven University of Technology
Theo Hofman Eindhoven University of Technology
Rudolf Huisman DAF Trucks NV
Frank Willems, Maarten Steinbuch

TuP03-3 **16.00–16.25**

Y. Zeinaly TU Delft
B. De Schutter TU Delft
J. Hellendoorn TU Delft

TuE01-4 **18.35–19.00**
Higher Order Approximations for Verification of Stochastic Hybrid Systems 46
S. Esmaeil Zadeh Soudjani Delft University of Technology
A. Abate Delft University of Technology

TuE02 **Gerbera**
System Identification B
Chair: Karel Keesman **17.20–19.00**

TuE02-1 **17.20–17.45**
Design of multilevel signals for identifying the Best Linear Approximation of Nonlinear Systems 47
Hin Kwan Wong University of Warwick
Johan Schoukens Vrije Universiteit Brussel
Keith R. Godfrey University of Warwick

TuE02-2 **17.45–18.10**
Identification of nonlinear systems via a powerful block-oriented nonlinear model 48
Laurent Vanbeylen Vrije Universiteit Brussel

TuE02-3 **18.10–18.35**
Detecting the time variation in an assumed linear, time invariant measurement 49
John Lataire Vrije Universiteit Brussel
Ebrahim Louarroudi Vrije Universiteit Brussel
Rik Pintelon Vrije Universiteit Brussel

TuE02-4 **18.35–19.00**
Nonlinear block-oriented identification for insulin-glucose models 50
Anna Marconato Vrije Universiteit Brussel
Maarten Schoukens Vrije Universiteit Brussel
Koen Tiels Vrije Universiteit Brussel
Amjad Abu-Rmileh, Johan Schoukens

TuE03 **Hyacinth**
Optimal Control B
Chair: Jacob van der Woude **17.20–19.00**

TuE03-1 **17.20–17.45**
Distributed Dynamic Price Mechanism in The New Gas Chain 51
Desti Alkano University of Groningen
Jacquelien M.A. Scherpen University of Groningen

TuE03-2 **17.45–18.10**
A plug and control strategy for simulated moving bed processes 52
P. Suvarov Université de Mons
A.V. Wouwer Université de Mons
A. Kienle Max-Planck-Institut

TuE03-3 **18.10–18.35**
Time-energy optimal control of a driveline by multi-objective dynamic programming 53
Maarten Witters Flanders' Mechatronic Technology Centre
Gregory Pinte Flanders' Mechatronic Technology Centre
Wim Symens Flanders' Mechatronic Technology Centre

TuE03-4 **18.35–19.00**
Online MPC on Industrial Programmable Logic Controllers 54
Bart Huyck KAHO Sint-Lieven
Filip Logist KU Leuven
Jos De Brabanter KAHO Sint-Lieven
Jan Van Impe, Bart De Moor

TuE04 **Iris**
Optimization B
Chair: Ton Backx **17.20–19.00**

TuE04-1 **17.20–17.45**
Large-scale optimization for component analysis of fMRI resting brain data 55
R. Liégeois University of Lige
A. SodduCyclotron Research Centre, University of Lige
R. Sepulchre University of Lige

TuE04-2 **17.45–18.10**
LS-SVM approach for solving linear descriptor systems 56
Siamak Mehrkanoon KU Leuven
Johan A. K. Suykens KU Leuven

TuE04-3 **18.10–18.35**
A geometric subgradient descent algorithm for the economic load dispatch problem 57
P.B. Borckmans Université catholique de Louvain
S. Easter Selvan Université catholique de Louvain
N. Boumal Université catholique de Louvain
P.-A. Absil

TuE04-4 **18.35–19.00**
Expected MSE minimization in linear regression over ellipsoidal uncertainty sets 58
Can Bikcora Eindhoven University of Technology

TuE05 **Klaproos**
Non-Linear Control B
Chair: Rodolphe Sepulchre **17.20–19.00**

TuE05-1 **17.20–17.45**
Controllability and stabilizability of piecewise affine dynamical systems 59
L.Q. Thuan University of Groningen
M.K. Camlibel University of Groningen

TuE05-2 **17.45–18.10**
Solving algebraic riccati equation real time for integrated vehicle dynamics control 60
A. Kunnappillil Madhusudhanan Delft University of Technology
M. Corno Politecnico di Milano
E. Holweg Delft University of Technology
B. Bonsen

TuE05-3 **18.10–18.35**
Quantized average consensus with delay 61
M.Jafarian University of Groningen
C.De Persis University of Groningen

TuE05-4 **18.35–19.00**
A little kick to synchronization models 62
R. Sepulchre University of Liege

TuE06 **Klaproos**
Robotics B
Chair: Daniel Dirksz **17.20–19.00**

TuE06-1 **17.20–17.45**
The flying hand: Control of an aerial manipulator interacting with a remote environment 63
Matteo Fumagalli Twente University
S. Stramigioli Twente University
R. Carloni Twente University

TuE06-2 **17.45–18.10**
Force Feedback of a Manipulator System in the port-Hamiltonian Framework 64
M. Munoz-Arias University of Groningen
J.M.A. Scherpen University of Groningen
D.A. Dirksz Eindhoven University of Technology

TuE06-3 **18.10–18.35**
An Update on the RoboEarth Architecture 65
R.J.M. Janssen Eindhoven University of Technology
M.J.G. van de Molengraft Eindhoven University of Technology
M. Steinbuch Eindhoven University of Technology

TuE06-4 **18.35–19.00**
Coordinating robots in water polo matches using modified snowdrift games 66
Chen Wang University of Groningen
Bin Wu Peking University
Ming Cao University of Groningen
Guangming Xie

Wednesday, March 28, 2012

WeA01 **Jasmijn**
Systems Theory C
Chair: Jan Willem Polderman **08.30–10.10**

WeA01-1 **08.30–08.55**
Simulation on the edge 67
P. van der Hulst Technische Universiteit Eindhoven
A. Veltman Technische Universiteit Eindhoven
P.P.J. van den Bosch Technische Universiteit Eindhoven

WeA01-2 **08.55–09.20**
An overview of input-to-state stability analysis methods for delay difference inclusions 68
R.H. Gielen Eindhoven University of Technology
M. Lazar Eindhoven University of Technology
A.R. Teel University of California, Santa Barbara

WeA01-3 **09.20–09.45**
Multimesh $\mathcal{H}_\in$ model reduction and extensions . 69
Samuel Melchior Université catholique de Louvain
Vincent Legat Université catholique de Louvain
Paul van Dooren Université catholique de Louvain

WeA01-4 **09.45–10.10**
Stability analysis for linear systems with state reset 70
Svetlana Polenkova University of Twente
Jan Willem Polderman University of Twente
Rom Langerak University of Twente

WeA02 **Gerbera**
System Identification C
Chair: Johan Schoukens **08.30–10.10**

WeA02-1 **08.30–08.55**
Nonparametric Identification of Linear Periodically Time-Varying Systems Using Arbitrary Inputs 71
Ebrahim Louarroudi Vrije Universiteit Brussel
John Lataire Vrije Universiteit Brussel
Rik Pintelon Vrije Universiteit Brussel

WeA02-2 **08.55–09.20**
Identifcation of 2D interconected systems using multilevel semi separable gradient method. 72
P. Torres Delft University of Technology
J.W van Wingerden Delft University of Technology
M. Verhaegen Delft University of Technology

WeA02-3 **09.20–09.45**
Two dimensional spline interpolation for slowly time-varying systems 73
Péter Zoltn Csurcsia Vrije Universiteit Brussel,Budapest University of Technology and Economics
Johan Schoukens Vrije Universiteit Brussel
Istvn Kollr Budapest University of Technology and Economics

WeA02-4 **09.45–10.10**
State space identification for linear parameter-varying systems 74
J. Goos Vrije Universiteit Brussel

WeA03 **Hyacinth**
Optimal Control C
Chair: Anton Stoorvogel **08.30–10.10**

WeA03-1 **08.30–08.55**
Solution for State Constrained Optimal Control Problems 75
T. van Keulen DAF Trucks N.V. Eindhoven
B. de Jager Eindhoven University of Technology

WeA03-2 **08.55–09.20**
Iterative Learning Control with Multiple Pass Points 76
Tong Duy Son Katholieke Universiteit Leuven
Hyo-Sung Ahn Gwangju Institute of Science and Technology (GIST)

WeA03-3 **09.20–09.45**
Iterative feedback tuning to learn steering control of an autonomous tractor 77
E. Hostens Flanders' Mechatronics Technology Centre
G. Pinte Flanders' Mechatronics Technology Centre
W. Symens Flanders' Mechatronics Technology Centre

WeA03-4 **09.45–10.10**
Multi-agent control for coordination of freight transport hubs 78
J. Xin Delft University of Technology
R. R. Negenborn Delft University of Technology
G. Lodewijks Delft University of Technology

WeA04 **Iris**
Optimization C
Chair: Ton van den Boom **08.30–10.10**

WeA04-1 **08.30–08.55**
Mobile phone communications help identify stable regions in France 79
Pierre Deville Université catholique de Louvain
Vincent Blondel Université catholique de Louvain
Paul Van Dooren Université catholique de Louvain
Zbigniew Smoreda

WeA04-2 **08.55–09.20**
Model predictive railway traffic management . . . 80
B. Kersbergen Delft University of Technology
T.J.J. van den Boom Delft University of Technology
B. De Schutter Delft University of Technology

WeA04-3 **09.20–09.45**
Traffic Counts Estimation Based on Urban Properties 81
Y. Hu Delft University of Technology
J. Hellendoorn Delft University of Technology

WeA04-4 **09.45–10.10**
Optimal trajectory planning for trains under operational constraints 82
Yihui Wang Delft University of Technology
Bart De Schutter Delft University of Technology
Ton van den Boom Delft University of Technology

WeA05 **Klaproos**
Mechanical Engineering A
Chair: Paul van den Hof **08.30–10.10**

WeA05-1 **08.30–08.55**
Stability analysis of networked control systems with periodic protocols and uniform quantizers . 83
S.J.L.M. van Loon Eindhoven University of Technology
M.C.F. Donkers Eindhoven University of Technology
N. van de Wouw Eindhoven University of Technology
W.P.M.H. Heemels

WeA05-2 **08.55–09.20**
Steer-by-wire: a study into the bandwidth requirements 84
T.P.J. van der Sande Eindhoven Universtiy of Technology
I.J.M. Besselink Eindhoven Universtiy of Technology
H.Nijmeijer Eindhoven Universtiy of Technology

WeA05-3 **09.20–09.45**
Experimental control of a mobile robot by an electronic brain 85
T.G.M. Vromen Eindhoven University of Technology
E. Steur Eindhoven University of Technology
H. Nijmeijer Eindhoven University of Technology

WeA05-4 **09.45–10.10**
Energy-optimal time allocation for a series of point-to-point motions 86
Pieter Janssens KU Leuven
Goele Pipeleers KU Leuven
Jan Swevers KU Leuven
Moritz Diehl

WeA06 **Lelie**
Medical Applications
Chair: Hans Stigter **08.30–10.10**

WeA06-1 **08.30–08.55**
Dielectric Spectroscopy for Non-Invasive Glucose Measurements 87
Oscar Olarte Vrije Universiteit Brussel
Wendy Van Moer Vrije Universiteit Brussel
Kurt Barbé Vrije Universiteit Brussel
Yves Van Ingelgem, Annick Hubin

WeA06-2 **08.55–09.20**
Anisotropy preserving interpolation of diffusion tensors 88
Anne Collard University of Lige
Silvre Bonnabel Mines Paris Tech
Rodolphe Sepulchre University of Lige
Christophe Phillips

WeA06-3 **09.20–09.45**
Design of a teleoperated palpation device 89
A. Buttafuoco Université Libre de Bruxelles (U.L.B.)
M. Kinnaert Université Libre de Bruxelles (U.L.B.)

WeA06-4 **09.45–10.10**
Piezoelectric Tactile Tissue Differentiation Sensor System: Concepts and Measurement Challenges . 90
David Oliva Uribe Vrije Universiteit Brussel
Johan Schoukens Vrije Universiteit Brussel
Jrg Wallaschek Leibniz University of Hannover

WeP01 **Jasmijn**
Systems Theory D
Chair: Jan van Schuppen **10.35–12.15**

WeP01-1 **10.35–11.00**
Memory Elements: A Paradigm Shift in Lagrangian Modeling of Electrical Circuits 91
Dimitri Jeltsema Delft University of Technology

WeP01-2 **11.00–11.25**
Metrics for oscillator models: an input-to-phase approach 92
Pierre Sacré University of Lige
Rodolphe Sepulchre University of Lige

WeP01-3 **11.25–11.50**
From rational representations to minimal output nulling and driving variable representations of a Behavior 93
Sasanka V. Gottimukkala University of Groningen
Prof. Harry L. Trentelman University of Groningen

WeP01-4 **11.50–12.15**
Sarymsakov matrices and coordination tasks for multi-agent systems 94
Weiguo Xia University of Groningen
Ming Cao University of Groningen

WeP02 **Gerbera**
System Identification D
Chair: Rik Pintelon **10.35–12.15**

WeP02-1 **10.35–11.00**
Parameter reduction of SISO Wiener-Schetzen models 95
Koen Tiels Vrije Universiteit Brussel
Peter S.C. Heuberger Delft University of Technology
Johan Schoukens Vrije Universiteit Brussel

WeP02-2 **11.00–11.25**
Identifying linear systems from binary output data 96
Bruno Depraetere K U Leuven
Julian Stoev Flanders Mechatronics Technology Centre
Gregory Pinte Flanders Mechatronics Technology Centre
Jan Swevers

WeP02-3 **11.25–11.50**
Prediction Error Methods and Polynomial Root-finding 97
Kim Batselier KU Leuven
Philippe Dreesen KU Leuven
Bart De Moor KU Leuven

WeP02-4 **11.50–12.15**
Robust or fast local polynomial method: How to choose? 98
Griet Monteyne Vrije Universiteit Brussel
Diana Ugryumova Vrije Universiteit Brussel
Gert van der Steen Vrije Universiteit Brussel
Rik Pintelon

WeP03 **Hyacinth**
Optimal Control D
Chair: Michel Kinnaert **10.35–12.15**

WeP03-1 **10.35–11.00**
Multi-level control for intelligent intermodal transport networks 99
L. Li Delft University of Technology
R. Negenborn Delft University of Technology
B. De Schutter Delft University of Technology

WeP03-2 **11.00–11.25**
Optimal control of electricity generation from μ-CHPs in a network 100
G. K. H. Larsen Univerisity of Groningen
N. D. van Foreest University of Groningen
J. M. A. Scherpen University of Groningen

WeP03-3 **11.25–11.50**
Moving horizon estimation for airborne wind energy systems 101
Kurt Geebelen KU Leuven
Jan Swevers KU Leuven
Moritz Diehl KU Leuven

WeP03-4 **11.50–12.15**
Asymptotic Characteristics of Toeplitz Matrix in SISO Model Predictive Control 102
Quang N. Tran Eindhoven University of Technology
Leyla Ozkan Eindhoven University of Technology
Jobert H.A. Ludlage Delft University
A.C.P.M. Backx

WeP04 **Iris**
Optimization D
Chair: Ton van den Boom **10.35–12.15**

WeP04-1 **10.35–11.00**
Low-rank optimization on the set of low-rank non-symmetric matrices 103
Bamdev Mishra University of Liege
Rodolphe Sepulchre University of Liege

WeP04-2 **11.00–11.25**
Numerical modelling and calibration of an ultrasonic separator 104
H.J. Cappon HZ University of Applied Sciences
K.J. Keesman Wageningen University

WeP04-3 **11.25–11.50**
Community detection via kernel spectral clustering 105
R. Langone kU LEUVEN
C. Alzate kU LEUVEN
J. A. K. Suykens kU LEUVEN

WeP04-4 **11.50–12.15**
Riemannian MADS for range-based ICA estimation 106
S. Easter Selvan Université Catholique de Louvain
P. B. Borckmans Université Catholique de Louvain
P.-A. Absil Université Catholique de Louvain

WeP05 **Klaproos**
Mechanical Engineering B
Chair: Jan Willem van Wingerden **10.35–12.15**

WeP05-1 **10.35–11.00**
Controllability and energy performance of the drying process 107
J C Atuonwu Wageningen University
G van Straten Wageningen University
H C van Deventer TNO
A J B van Boxtel

WeP05-2 **11.00–11.25**
Benchmarking for CVT in CS-PTO Applications 108
Irmak Aladagli Eindhoven University of Technology
Theo Hofman Eindhoven University of Technology
Maarten Steinbuch Eindhoven University of Technology
Bas Vroemen

WeP05-3 **11.25–11.50**
Control for Low Emission, High Efficiency Diesel Engines 109
C.H.A. Criens Eindhoven University of Technology
F.P.T. Willems Eindhoven University of Technology
M. Steinbuch Eindhoven University of Technology

WeP05-4 **11.50–12.15**
A New Robust Delay-Variable Repetitive Controller With Application to Media Transport in a Printer 110
E. Bajonero Canonico Eindhoven University of Technology
E. van der Laan Océ-Technologies BV
S. Koekebakker Océ-Technologies BV
Maarten Steinbuch

WeP06 **Lelie**
Robotics C
Chair: Jan Swevers **10.35–12.15**

WeP06-1 **10.35–11.00**
Port-Hamiltonian approach to deployment on a line 111
E. Vos University of Groningen
J.M.A. Scherpen University of Groningen
A.J. van der Schaft University of Groningen

WeP06-2 **11.00–11.25**
Probabilistic Multiple Hypothesis Reasoning in Robotics 112
Sjoerd van den Dries Technische Universiteit Eindhoven
Jos Elfring Technische Universiteit Eindhoven
dr.ir. M.J.G. van de Molengraft Technische Universiteit Eindhoven
prof.dr.ir. M. Steinbuch

WeP06-3 **11.25–11.50**
Global asymptotic tracking of one-DOF mechanical systems without velocity measurements 113
Yuxin Su Katholieke Universiteit Leuven
Jan Swevers Katholieke Universiteit Leuven
Joris De Schutter Katholieke Universiteit Leuven

WeP06-4 **11.50–12.15**
ROP: Developing a Robotic Open Platform . . . 114
Janno Lunenburg Eindhoven University of Technology
René van de Molengraft Eindhoven University of Technology
Maarten Steinbuch Eindhoven University of Technology

WeP07 **Mimosa**
Systems Biology
Chair: Eric Bullinger **10.35–12.15**

WeP07-1 **10.35–11.00**
A Novel Phase Portrait to Understand Neuronal Excitability 115
Guillaume Drion University of Lige
Rodolphe Sepulchre University of Lige
Alessio Franci Univ Paris Sud 11
Vincent Seutin

WeP07-2 **11.00–11.25**
Decision making in noisy bistable switches: a local analysis for non local predictions 116
Laura Trotta University of Lige
Eric Bullinger University of Lige
Rodolphe Sepulchre University of Lige

WeP07-3 **11.25–11.50**
The Modeling Cycle in Genetic Network Reconstruction: the XlnR Regulon of Aspergillus niger 117
J. Omony Wageningen University
A.R. Mach-Aigner TU Vienna
L.H. de Graaff Wageningen University
G. van Straten, A.J.B. van Boxtel

WeE01 **Jasmijn**
Systems Theory E
Chair: Rodolphe Sepulchre **13.45–15.00**

WeE01-1 **13.45–14.10**
Invariance and contractiveness via comparison systems 118
Nikolaos Athanasopoulos Eindhoven University of Technology
George Bitsoris University of Patras

WeE01-2 **14.10–14.35**
An observer for a piecewise-affine hybrid system on a polytope 119
Luc C.G.J.M. Habets Eindhoven University of Technology
Jan H. van Schuppen CWI

WeE01-3 **14.35–15.00**
An evaluation list for model complexity assessment 120
George A.K. van Voorn Wageningen University & Research

WeE02 **Gerbera**
System Identification E
Chair: Rik Pintelon **13.45–15.00**

WeE02-1 **13.45–14.10**
How to obtain a broad band FRF with constant uncertainty? 121
Egon Geerardyn Vrije Universiteit Brussel
Yves Rolain Vrije Universiteit Brussel
Johan Schoukens Vrije Universiteit Brussel

WeE02-2 **14.10–14.35**
Full scall dynamics of biological sulfide oxidation at halo alkaline 122
johannes B.M. Klok University of Wageningen
Karel J. Keesman University of Wageningen

WeE02-3 **14.35–15.00**
Optimal input design for model discrimination . 123
Karel J. Keesman Wageningen University
Eric Walter CNRS, SUPELEC

WeE03 **Hyacinth**
Optimal Control E
Chair: Michel Kinnaert **13.45–15.00**

WeE03-1 **13.45–14.10**
Lyapunov based design of robust linear-feedback for time-optimal periodic quadcopter motion . . . 124
J. K. Gillis KU Leuven
K. Geebelen KU Leuven
J. Sternberg KU Leuven
J. Sternberg, S. Gros, M. Diehl

WeE03-2 **14.10–14.35**
Time-optimal robot path tracking with cartesian acceleration constraint 125
Frederik Debrouwere KU Leuven
Wannes Van Loock KU Leuven
Moritz Diehl KU Leuven
Joris De Schutter, Jan Swevers

WeE04 **Iris**
Optimization E
Chair: Ton van den Boom **13.45–15.00**

WeE04-1 **13.45–14.10**
Comparison of mechanical-hybrid vehicle concepts 126
K. van Berkel Technische Universiteit Eindhoven
S. Rullens Technische Universiteit Eindhoven
T. Hofman Technische Universiteit Eindhoven
B. Vroemen, M. Steinbuch

WeE04-2 **14.10–14.35**
Towards Integrated Energy and Thermal Management for Parallel Hybrid Electric Vehicle 127
H.T. Pham Eindhoven University of Technology
J.T.B.A. Kessels Eindhoven University of Technology
P.P.J. van den Bosch Eindhoven University of Technology

WeE04-3 **14.35–15.00**
Cooperative planning of a class of heterogeneous multi-vehicle systems 128
J.F. Determe Université Libre de Bruxelles
E. Garone Université Libre de Bruxelles
R. Naldi University of Bologna

WeE05 **Klaproos**
Mechanical Engineering C
Chair: Jan Willem van Wingerden 13.45–15.00

WeE05-1 **13.45–14.10**
Optimal design of reduced-order LPV controllers 129
G. Hilhorst KU Leuven
G. Pipeleers KU Leuven
J. Swevers KU Leuven

WeE05-2 **14.10–14.35**
Transfer-Function-Data-based computation of closed-loop poles for lightly damped MIMO systems 130
R. Hoogendijk Eindhoven University of Technology
M.J.G. van de Molengraft Eindhoven University of Technology
M. Steinbuch Eindhoven University of Technology

WeE05-3 **14.35–15.00**
Model-based control design for inferential and over-actuated control of lightweight motion systems 131
Frank Boeren Eindhoven University of Technology
Robbert van Herpen Eindhoven University of Technology
Tom Oomen Eindhoven University of Technology
Okko Bosgra, Marc van de Wal

WeE06 **Lelie**
Robotics D
Chair: Jan Swevers **13.45–15.00**

WeE06-1 **13.45–14.10**
Teleoperated endoscopic injection 132
Jérme Janssens Université Libre de Bruxelles
Michel Kinnaert Université Libre de Bruxelles

WeE06-2 **14.10–14.35**
World Modeling in Robotics 133
Jos Elfring Eindhoven University of Technology
Sjoerd van den Dries Eindhoven University of Technology
René van de Molengraft Eindhoven University of Technology
Maarten Steinbuch

WeE07 **Mimosa**
Systems Biology
Chair: Eric Bullinger **13.45–15.00**

WeE07-1 **13.45–14.10**
Dynamic metabolic flux analysis using dynamic optimization techniques 134
Dominique Vercammen Katholieke Universiteit Leuven
Eva Van Derlinden Katholieke Universiteit Leuven
Jan Van Impe Katholieke Universiteit Leuven

WeE07-2 **14.10–14.35**

Robustness analysis of apoptosis signalling 135
Monica Schliemann Université de Lige
Eric Bullinger Université de Lige

WeE07-3 **14.35–15.00**

Estimating the prediction uncertainty of biological models 136
S. van Mourik Wageningen University
JD Stigter Wageningen University
J. Molenaar Wageningen University

DISC Event: P3 **Jasmijn**
DISC Certificate Awards
Chair: Paul van den Hof **15:20–15:30**

Mini Course: P4 **Jasmijn**
Port Based Thinking: Introduction
Stefano Stramigioli
Chair: Ton van den Boom **15.30–16.30**

Part 1: Port Based Thinking: What is it and why is this useful? . . . . . .
Stefano Stramigioli

Mini Course: P5 **Jasmijn**
Port Based Modeling for Robotics
Stefano Stramigioli
Chair: Ton van den Boom **16.45–17.45**

Part 2: Port Based Modeling for Robotics . . . .
Stefano Stramigioli

Mini Course: P6 **Jasmijn**
Port Based Control for Robotics
Stefano Stramigioli
Chair: Ton van den Boom **18.00–19.00**

Part 3: Port Based Control for Robotics . . . . .
Stefano Stramigioli

Thursday, March 29, 2012

Plenary: P7 **Jasmijn**
Event-Based Control
Jan Lunze
Chair: Hans Stigter **8.30–9.30**

Event-Based Control: Theory and Application . . 219
Jan Lunze

Plenary: P8 **Jasmijn**
Synchronization of Autonomous Agents
Jan Lunze
Chair: Hans Stigter **09.45– 10.45**

Synchronization of Autonomous Agents with Individual Dynamics 220
Jan Lunze

ThM01 **Jasmijn**
Games and Agent-Based Models A
Chair: Jacob Engwerda **11.15–12.30**

ThM01-1 **11.15–11.40**

Game-theoretical approach to multi-agent synchronization 137
S. Haesaert Delft University
R. Babuska Delft University
F.L. Lewis University of Texas at Arlington

ThM01-2 **11.40–12.05**

Neuromorphic reinforcement learning 138
Julie Dethier University of Liege
Damien Ernst University of Liege
Rodolphe Sepulchre University of Liege

ThM01-3 **12.05–12.30**

Randomized averaging algorithm: decoupling accuracy and convergence rate 139
Paolo Frasca Politecnico di Torino
Julien M. Hendrickx Université catholique de Louvain

ThM02 **Gerbera**
Electro-Mechanical Engineering A
Chair: Bram de Jager **11.15–12.30**

ThM02-1 **11.15–11.40**

Port Hamiltonian modeling of Power Networks . 140
F. Shaik University of Groningen
A.J. van der Schaft University of Groningen
J.M.A. Scherpen University of Groningen
D. Zonetti, R. Ortega

ThM02-2 **11.40–12.05**

Sensors for control of nuclear fusion plasmas . . 141
G. HommenEindhoven University of Technology/Dutch Institute for Fusion Energy Research

ThM03 **Hyacinth**
Modeling for Control A
Chair: Bayu Jayawardhana **11.15–12.30**

ThM04 **Iris**
Biochemical Engineering A
Chair: Hans Stigter **11.15–12.30**

ThM05 **Klaproos**
Non-Linear Control C
Chair: Kanat Camlibel **11.15–12.30**

ThM06 **Lelie**
Distributed Parameter Systems A
Chair: Jacquelien Scherpen **11.15–12.30**

ThP01 **Jasmijn**
Games and Agent-Based Models B
Chair: Julien Hendrikx **13.45–15.50**

ThP01-3 **14.35–15.00**
Performance of a synchronized community detection algorithm 157
Arnaud Browet UCLouvain
Paul Van Dooren UCLouvain
Pierre-Antoine Absil UCLouvain

ThP01-4 **15.00–15.25**
Stability and synchronization analysis of multi-agent systems with switching topologies 158
Nima Monshizadeh University of Groningen
Harry L. Trentelman University of Groningen
M. K. Camlibel University of Groningen

ThP01-5 **15.25–15.50**
Consensus on nonlinear spaces and graph coloring 159
Alain Sarlette Ghent University

ThP02 **Gerbera**
Electro-Mechanical Engineering B
Chair: Thijs van Keulen **13.45–15.50**

ThP02-1 **13.45–14.10**
Real-time control of electrical power systems . . . 160
A. Virag Eindhoven University of Technology
A. Jokic Eindhoven University of Technology
P.P.J. van den Bosch Eindhoven University of Technology

ThP02-2 **14.10–14.35**
Boiling-based thermal conditioning in battery electric vehicles 161
R.W. van Gils Eindhoven University of Technology
M.F.M. Speetjens Eindhoven University of Technology
H. Nijmeijer Eindhoven University of Technology

ThP02-3 **14.35–15.00**
Idealized voltage control of variable reluctance actuators 162
A. Katalenic Eindhoven University of Technology
C.M.M. van Lierop Eindhoven University of Technology

ThP02-4 **15.00–15.25**
An axisymmetric rotational inertia shaker for the active structural acoustic control of rotating machinery 163
Guoying Zhao KULeuven
Dr. Gregory Pinte Flanders' Mechatronics Technology Centre
Dr. Wim Symens Flanders' Mechatronics Technology Centre
Paul Sas

ThP02-5 **15.25–15.50**
Cooperative Adaptive Cruise Control: Tradeoffs Between Control and Network Specifications . . . 164
S. Oncu Eindhoven University of Technology
N.v.d. Wouw Eindhoven University of Technology
H. Nijmeijer Eindhoven University of Technology

ThP03 **Hyacinth**
Modeling for Control B
Chair: Bayu Jayawardhana **13.45–15.50**

ThP03-1 **13.45–14.10**
Joint order and dependency reduction for LPV state-space models 165
Muhammad Mohsin Siraj Eindhoven University of Technology
Dr. ir. Roland Toth Delft University of Technology

ThP03-2 **14.10–14.35**
Modal decoupling of a lightweight motion stage using algebraic constraints on the decoupling matrices 166
E. Silvas Technische Universiteit Eindhoven
R. Hoogendijk Technische Universiteit Eindhoven
W. Aangenent ASML Holding NV
M.M.J. van de Wal, M. Steinbuch

ThP03-3 **14.35–15.00**
Dynamic Simulation and Control of a Recirculating Aquaculture System 167
P. Almeida University of Mons
A. Donoso Bravo University of Mons
A. Vande Wouwer University of Mons

ThP03-4 **15.00–15.25**
Pre-crash passenger safety in cars: a model based control approach 168
Mark Mutsaers Eindhoven University of Technology
Siep Weiland Eindhoven University of Technology
Lex van Rooij TNO Science and Industry
Olaf op den Camp

ThP03-5 **15.25–15.50**
Modeling of a waste heat recovery system for control purposes 169
E. Feru Technische Universiteit Eindhoven
F.P.T. Willems Technische Universiteit Eindhoven
M. Steinbuch Technische Universiteit Eindhoven

ThP04 **Iris**
Biochemical Engineering B
Chair: Karel Keesman **13.45–15.50**

ThP04-1 **13.45–14.10**
Some Preliminary Results on Modeling and Control of MBR Process 170
Guilherme Araujo Pimentel Université de Mons
Alain VANDE WOUWER Université de Mons
Alain RAPAPORT INRA/SupAgro
Daniel COUTINHO

ThP04-2 **14.10–14.35**
Comparative study of a few state estimation techniques for monitoring microalgae cultures 171
Micaela Benavides Université de Mons
Alain Vande Wouwer Université de Mons
Jan Van Impe Katholieke Universiteit Leuven

ThP04-3 **14.35–15.00**
Identification and modeling of distillation columns from transient response data 172
D. Ugryumova Vrije Universiteit Brussel
G. Vandersteen Vrije Universiteit Brussel
B. Huyck Katholieke Universiteit Leuven
F. Logist

Part 2

Contributed Lectures

Observer-Based Decentralized Control via Networked Communication[1]

N.W. Bauer, M.C.F. Donkers, N. van de Wouw, W.P.M.H Heemels
Dept. of Mechanical Engr., Eindhoven University of Technology, P.O. Box 513, 5600 MB Eindhoven, The Netherlands
{N.W.Bauer, M.C.F.Donkers, N.v.d.Wouw, W.P.M.H.Heemels}@tue.nl

1 Introduction

Recently, there has been an enormous interest in control of large-scale systems that are physically distributed over a wide area. Examples of such distributed systems are electrical power distribution networks, water distribution networks, industrial factories and energy collection networks (such as wind farms).

2 Problem Statement

This work considers stability analysis and controller design for this class of systems. The control structure we consider has a number of features that complicate the design enormously. First of all, the controller is decentralized in the sense that it consists of a number of local controllers that do not share information (see Fig. 1). Although a centralized controller can be considered, the achievable bandwidth associated with using a centralized structure would be limited by long delays from distant sensors and actuators.

Secondly, when considering control of a large-scale system, it would be unreasonable to assume that all states are measured. Therefore an observer-based design is suitable to estimate the states that cannot be directly measured. Moreover, with an observer-based controller it is possible to reduce the number of sensors, which alleviates the demands on the network design. However, it has been proven that, in general, it is hard to obtain decentralized observers that will converge to the 'true' state estimate [2]. Despite this fact, stability of the closed-loop system can still be achieved, but design is of course challenging.

Finally, the controller needs to have certain robustness properties when using communication networks. Indeed, the advantages of using a wired/wireless network are inexpensive and easily modifiable communication links. However, the drawback is that the control structure is susceptible to undesirable (possibly destabilizing) side-effects: varying delays, packet dropouts, varying transmission intervals, quantization and a shared communication medium. In this work, we design our controller such that the closed loop remains stable given bounds on the varying transmission intervals and given the communication medium is shared. Since the communication medium is shared, a protocol (we assume is periodic) is needed to orchestrate in what order sensor and actuator data is sent over the shared network.

3 Decentralized Networked Control System

The continuous-time linear plant we consider is decomposed into N discrete-time subsystems $\mathcal{P}_1, ..., \mathcal{P}_N$. The corresponding subsystem controllers $\mathcal{C}_1, ..., \mathcal{C}_N$ are switched discrete-time systems consisting of a switched-observer structure to deal with the presence of a shared communication medium. The general setup is depicted in Fig. 1 (see [1] for details).

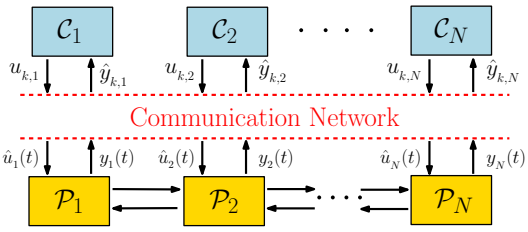

Fig. 1. Decentralized networked control system (NCS).

4 Decentralized Controller Synthesis

We provide LMI-based conditions for analysis and synthesis of the aforementioned controller. The main features of the synthesis are the following:

- Although transmission time variability introduces an non-linear uncertainty in the closed-loop, a *convex over-approximation* of the uncertain switched system can be achieved using well-developed techniques.
- To deal with the decentralized structural constraints, the overapproximated closed-loop system is formulated as a *multi-gain* switched static feedback system (with additive uncertainty) for which sufficient LMI-based synthesis conditions can be formulated by extending recent output-feedback synthesis results.

The LMI-based synthesis conditions, if satisfied, provide stabilizing gains for *both* the decentralized problem setting and the NCS problem setting in isolation, as well as the unification of these two problem settings.

[1] This work is supported by the Innovational Research Incentives Scheme under the VICI grant "Wireless control systems: A new frontier in automation" (No. 11382) awarded by NWO (The Netherlands Organization for Scientific Research) and STW (Dutch Science Foundation), and the European 7th Framework Network of Excellence "Highly-complex and networked control systems" (HYCON2).

References

[1] N.W. Bauer, M.C.F. Donkers, W.P.M.H. Heemels, and N. van de Wouw. Observer-based decentralized control via networked communication. *Submitted.*

[2] Dragoslav D. Siljak. *Decentralized control of complex systems / Dragoslav D. Siljak.* Academic Press, Boston, 1991.

Non-centralized Stabilization via Parameterized Storage Functions

Ralph Hermans, Mircea Lazar, Andrej Jokić, Rob Gielen
Department of Electrical Engineering
Eindhoven University of Technology
P.O. Box 513, 5600 MB Eindhoven, The Netherlands
Emails: {r.m.hermans, m.lazar, a.jokic, r.h.gielen}@tue.nl

1 Introduction

Electrical power networks, water supply infrastructures, autonomous vehicles on automated highways and coupled chemical processes are but a few examples of systems that consist of a large number of interacting dynamical subsystems. Many of these networked dynamical systems (NDS) feature significant nonlinearities, strict input and state constraints and, most importantly, coupling dynamics.

A key challenge in NDS research is to establish asymptotic stability in a scalable fashion, which is crucial in the design of stabilizing control laws for such systems. Conventionally, stability is determined by verifying the existence of a quadratic Lyapunov function (LF), given a linearized description of the network dynamics. Yet, the large size of NDS renders this method infeasible, as the required full system model is usually difficult to obtain and the LF synthesis problem, formulated as a semi-definite program (SDP), comes with prohibitively large computational burdens.

2 Problem Statement

The issues associated with the application of classical Lyapunov methods to large-scale NDS motivate the need for decentralizing the conditions for asymptotic stability. Non-centralized stability analysis typically relies on dissipativity theory to generate a LF from a set of local storage and supply functions. Perhaps the simplest dissipativity-based stabilization method for linear systems employs fixed-parameter, quadratic storage functions and constant supply rates to obtain a separable set of SDP problems that are solved off-line, in a decentralized fashion. Although such approaches are attractive because of their low complexity, they are often conservative, which significantly limits their applicability.

Advanced scalable Lyapunov methods aim to increase flexibility with respect to decentralized synthesis via *state-parameterized supply functions* that can be generated in a distributed fashion. As an example, we mention the scheme proposed in [1] that employs a set of parameterized supply rates and fixed, positive-definite storage functions, i.e., *structured LFs*, whose sum yields a Lyapunov candidate for the overall network. However, the existing tractable methods for a-priori generating a set of quadratic structured LFs and supply rates for linear NDS (see, e.g., [2]) come with communication requirements that are incompatible with many large-scale applications. In [3], a partial solution to this issue was provided, which employs "max-type dissipativity conditions". Such conditions do not require distributed optimization and allow for max-construction of a LF for the full network, which provides more flexibility than the sum-construction employed by the structured LF scheme. Even so, both the decentralized and distributed schemes described above suffer from the impediment that is characteristic to *a-priori fixed* storage function synthesis.

3 Contribution

In this talk, we illustrate the conservatism of off-line LF synthesis with an example network that does not admit LF construction from a set of fixed-parameter storage functions, but that is stable nonetheless. Then, the objective is to find a solution to this issue, by endowing the storage functions with a finite set of state-dependent parameters. Stability conditions similar to the ones provided in [3] are used to allow for max-construction of a Lyapunov function for the full closed-loop network, while neither of the parameterized storage functions is required to be a local LF. The merit of this approach is that the storage functions can be constructed *on-line*, via a set of coupled convergence conditions. In this way, the impediment of off-line structured LF synthesis from fixed storage functions is removed. The proposed stability conditions are efficiently exploited in devising a decentralized control scheme that relies on non-iterative communication among directly coupled systems only, and that can stabilize NDS for which conventional non-centralized methods, based on off-line generated fixed quadratic storage functions, fail.

References

[1] A. Jokić and M. Lazar, "On decentralized stabilisation of discrete-time nonlinear systems," in *American Control Conference*, St. Louis, USA, 2009, pp. 5777–5782.

[2] C. Langbort, R. S. Chandra, and R. D'Andrea, "Distributed control design for systems interconnected over an arbitrary graph," *IEEE Transactions on Automatic Control*, vol. 49, no. 9, pp. 1502–1519, 2004.

[3] R. M. Hermans, M. Lazar, and A. Jokić, "Almost decentralized Lyapunov-based nonlinear model predictive control," in *American Control Conference*, Baltimore, MD, USA, 2010, pp. 3932–3938.

Formal verification of discrete-time Markov processes with an application to Risk Theory

Ilya Tkachev and Alessandro Abate
Delft Center for Systems and Control
Technische Universiteit Delft
Mekelweg 2, 2628 CD, Delft
The Netherlands
Email: {i.tkachev,a.abate}@tudelft.nl

1 Introduction

The primary goal of formal verification is, given a model and a specification over this model, to verify if the model satisfies such a specification. This approach was developed in the Computer Science field where specifications are expressed as formulas over certain modal logics: CTL, LTL, etc. [3]. Research in this field was mostly focused to the case of discrete state spaces. On the other hand, specifications (properties) widely used in Systems and Control area, such as reachability, stability and convergence, are usually stated for models evolving on more general (e.g. continuous or hybrid) state spaces. Moreover, in areas of application such as Systems Biology and Financial Mathematics probabilistic phenomena play an important role and should thus be embedded in models.

The focus of our work is on developing methods of formal verification for probabilistic models over general state spaces. There are two classes of properties to be verified: binary (which hold with probability 0 or 1) or quantitative (within $(0,1)$) [3]. The obtained results for the first class are more theoretical in nature, while those attained for the second class are more computational. Special attention is placed on the accuracy of the computation of a probability that a certain property holds. As an example, we provide a method to compute the ruin probability, which is one of the most important problems in Risk Theory [2].

2 Current State of Research

Due to our focus on the precise computation of probabilities, we currently work with discrete-time problems. The framework is given by discrete time Markov processes (dtMP) which are large enough to include discrete-time Stochastic Hybrid Systems. There are two main approaches to this problem:

1. a direct one, where the specification (or a property) is verified against the original dtMP and

2. one based on abstractions, where the specification is verified against a dtMP which is an abstraction of the original process (e.g. with a discrete state space). The distance between the two processes is used then to export the results from the abstraction to the original dtMP.

For the latter case, we have shown that the problem of finding the distance between the original dtMP and its abstraction on the infinite time horizon is usually as hard as the direct approach to verification [4], so that it is not always optimal to use abstractions.

As for the direct approach, the computation of probabilities of finite time horizon specifications has been studied in [1], so with a focus on an infinite time-horizon we have developed a "decomposition technique." This technique allows one to find the value of the probability of certain infinite-horizon properties (e.g.reachability) with any given precision in a finite number of steps. It is as well useful for the study of binary properties. As an application, we selected the study of ruin probabilities in Risk Theory and successfully tailored the decomposition technique to this problem.

3 Future Work

We are focusing on the extension of the class of properties that can be verified using the obtained results. We are also interested in the generalization of the modeling framework, which can be obtained both by relaxing the assumptions raised on dtMPs and by extending the developed methods to the continuous time case.

References

[1] A. Abate, J.-P. Katoen, J. Lygeros, and M. Prandini. Approximate model checking of stochastic hybrid systems. *European Journal of Control*, 16:624–641, December 2010.

[2] Søren Asmussen. *Ruin probabilities*, volume 2 of *Advanced Series on Statistical Science & Applied Probability*. World Scientific Publishing Co. Inc., River Edge, NJ, 2000.

[3] C. Baier and J.P. Katoen. *Principles of model checking*. The MIT Press, 2008.

[4] I. Tkachev and A. Abate. On infinite-horizon probabilistic properties and stochastic bisimulation functions. In *Proceedings of the 50th IEEE Conference on Decision and Control and European Control Conference*, pages 526–531, Orlando, FL, December 2011.

Compensation-Based Control for Lossy Communication Networks

T.M.P. Gommans W.P.M.H. Heemels N.W. Bauer N. van de Wouw

Eindhoven University of Technology

Department of Mechanical Engineering,

P.O. Box 513, 5600 MB Eindhoven, The Netherlands

{t.m.p.gommans, m.heemels, n.w.bauer, n.v.d.wouw}@tue.nl.

1 Introduction

Networked Control Systems (NCSs) offer various benefits such as ease of maintenance and low cost. However, the presence of a network in the control loop causes network-induced imperfections, such as packet dropouts, which degrade performance an can even lead to instability.
To mitigate the effect of dropouts on stability and also performance of the NCS, we propose a novel dropout compensation strategy.

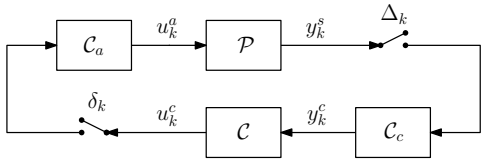

Figure 1: Schematic overview of the NCS.

2 NCS model with compensation-based strategy

In this work, we consider a NCS consisting of a discrete-time linear time-invariant plant and a discrete-time static output feedback controller communicating over a network which is subject to dropouts. We introduce compensators $\mathcal{C}_c$ and $\mathcal{C}_a$ to mitigate the effect of packet dropouts, as shown in Figure 1.

The main idea behind the functioning of each of the compensators is the following:

- If a packet arrives, the compensator forwards the packet and, additionally, acts as a model-based closed-loop observer;
- If a packet drops, the compensator acts as an open loop predictor and, additionally, forwards its best prediction based on its estimate of the plant state.

Hence, the proposed compensators have the following structure

$$\mathcal{C}_c: \begin{cases} x_{k+1}^c &= Ax_k^c + Bu_k^c + \Delta_k L_{j_{k-1}}^c \left(y_k^s - Cx_k^c\right) \\ y_k^c &= \begin{cases} Cx_k \left(= y_k^s\right) & \text{if} \quad \Delta_k = 1 \quad \text{(receive)} \\ Cx_k^c & \text{if} \quad \Delta_k = 0 \quad \text{(drop)}, \end{cases} \end{cases}$$

$$\mathcal{C}_a: \begin{cases} x_{k+1}^a &= Ax_k^a + Bu_k^a + \delta_k L_{i_{k-1}}^a \left(u_k^c - KCx_k^a\right) \\ u_k^a &= \begin{cases} Ky_k^c \left(= u_k^c\right) & \text{if} \quad \delta_k = 1 \quad \text{(receive)} \\ KCx_k^a & \text{if} \quad \delta_k = 0 \quad \text{(drop)}, \end{cases} \end{cases}$$

where $i_k, j_k \in \mathbb{N}$ are successive dropout counters, which count the number of successive dropouts and reset to zero if a packet is received. To obtain a closed-loop representation of the NCS with the compensation-based strategy, we define the augmented state $\xi_k^{cb} := [\ x_k^T \quad (x_k - x_k^a)^T \quad (x_k - x_k^c)^T\ ]^T$. The closed-loop dynamics can then be given by a discrete-time switched system

$$\xi_{k+1}^{cb} = A_{\delta_k, \Delta_k, i_{k-1}, j_{k-1}}^{cb} \xi_k^{cb}. \tag{1}$$

3 Dropout Models

In modeling the dropout behavior, we consider two approaches: worst-case bound models, which only require an upper bound on the maximum number of successive dropouts, and stochastic models, which use stochastic information on the occurrence of dropouts, given in the form of Bernoulli or Gilbert-Elliott models.

4 Stability Analysis and Compensator Synthesis

Based on parameter dependent Lyapunov functions we derive the following results: for the worst-case bound models we obtain sufficient conditions for global asymptotical stability of (1) and the upper bound on the dropouts, whereas for the stochastic models we obtain necessary and sufficient conditions for (exponential) mean square stability of the Markov jump linear system given by (1) and the transition probabilities. For both dropout models we provide LMI-based conditions for the synthesis of the compensator gains $L_{i_{k-1}}^a$ and $L_{j_{k-1}}^c$.

5 Compare with basic strategies

We compare the compensation-based strategy with two basic compensation strategies: the zero strategy, which sets the networked version of a signal to zero if a transmission fails, and the hold strategy, which holds the value of the last successfully transmitted signal. Simulation results show significantly increased robustness with respect to packet dropouts, and therefore indicate the importance of the proposed class of dropout compensators.

This work is supported by the Innovational Research Incentives Scheme under the VICI grant "Wireless control systems: A new frontier in automation" (No. 11382) awarded by NWO (The Netherlands Organization for Scientific Research) and STW (Dutch Science Foundation).

[1] T.M.P. Gommans, "Compensation-Based Control for Lossy Communication Networks," *MSc Thesis*, 2011.

Batch-to-batch control of supersaturation in cooling crystallization with a measurement-based model update

Marco Forgione, Ali Mesbah, Xavier Bombois
Delft Center for Systems and Control
Delft University of Technology
Mekelweg 2, 2642BD, Delft
The Netherlands
Email: m.forgione@tudelft.nl

Paul M.J. Van den Hof
Department of Electrical Engineering
Eindhoven University of Technology
P.O. Box 513, 5600 MB Eindhoven
The Netherlands

1 Introduction

Batch cooling crystallization is often applied as a separation and purification step, e.g. in the pharmaceutical industry. Supersaturation is the driving force of crystallization, and a tight control of this variable is expected to improve the quality of the final product. In this paper we present a Batch-to-Batch (B2B) strategy for supersaturation control in batch cooling crystallization. Based on the desired supersaturation profile and the measurement from previous batches, the B2B algorithm computes after each batch an improved profile for the temperature in the crystallizer. The B2B algorithm is put on top of a PI temperature controller in order to reject the disturbances in the temperature dynamics. Two B2B algorithms are introduced in this paper, namely an Iterative Learning Control (ILC) and an Iterative Identification Control (IIC) algorithm. The performance of the control scheme based on both algorithms is assessed in a simulation study.

2 The control scheme

The B2B+PI control scheme is shown in Figure 1. The two leftmost blocks represent the controller: the PI temperature controller and the B2B controller, which drives the reference of the latter in a master-slave configuration.

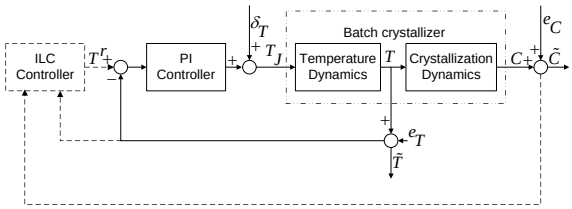

Figure 1: the control scheme

Assume we have a model $F_{ST^r}(\mathbf{T}^r;\theta_0)$ from the temperature reference $\mathbf{T}^r$ to the supersaturation $\mathbf{S}$, where θ_0 is the nominal parameter. The ILC algorithm performs these steps [1]:

1. The profile $\mathbf{T}^r_k$ is set as the input to the PI controller and the batch is executed. Measurements of solute concentration $\tilde{\mathbf{C}}_k$ and temperature $\tilde{\mathbf{T}}_k$ are collected. The corresponding supersaturation $\tilde{\mathbf{S}}_k$ is computed.
2. A corrected model $S^c_{k+1}(\mathbf{T}^r) = F_{ST^r}(\mathbf{T}^r;\theta_0) + \alpha_{k+1}$ is found. The correction vector α_{k+1} is computed using the approach in [2].
3. The corrected model is used to design the temperature profile for the next iteration to track a set-point $\bar{\mathbf{S}}_k$.

The IIC algorithm is based on 3 similar steps. However, the model correction at step 2 of IIC is a recursive identification of the parameter vector: $S^c_{k+1}(\mathbf{T}^r) = F_{ST^r}(\mathbf{T}^r,\theta_{k+1})$ with

$$\theta_{k+1} = \arg\min_{\theta\in R^4} \left(||\tilde{\mathbf{S}}_k - F_{ST^r}(\tilde{\mathbf{T}}_k,\theta)||^2_{\Sigma_e^{-1}} + ||\theta-\theta_k||^2_{\Sigma_{\theta_k}^{-1}} \right).$$

The design of the weighting matrices Σ_e and Σ_{θ_k} is performed in a bayesian framework.

3 Results

The B2B+PI configuration is shown to give better results compared to the pure B2B control driving the jacket temperature directly. IIC achieves the fastest convergence when the assumed model structure contains the true system. Furthermore, it is able to effectively follow a set-point that changes from batch to batch. As a drawback, the method fails to converge to the desired set-point in case of structural mismatches. ILC is shown to be able to converge to the desired set-point even in the presence of model mismatches: this is the main advantage of the algorithm. However, the speed of convergence observed is somewhat lower. Furthermore, tuning of the algorithm is delicate.

References

[1] M. Forgione, A. Mesbah, X. Bombois, and P.M.J. Van den Hof. Iterative learning control of supersaturation in batch cooling crystallization. Submitted to *American Control Conference*, June 2012.

[2] M. Volckaert, M. Diehl, and M. Swevers. A two step optimization based iterative learning control algorithm. In *Dynamic Systems and Control Conference*, pages 579–581, Cambridge, Massachusetts, USA, September 2010.

Dynamic Network Identification with Known Interconnection Architecture

Arne Dankers
Delft Center for Systems and Control
Delft Univeristy of Technology
Email: a.g.dankers@tudelft.nl

Paul M.J. Van den Hof
Department of Electrical Engineering
Eindhoven University of Technology
Email: p.m.j.vandenhof@tue.nl

Peter S.C. Heuberger and Xavier Bombois
Delft Center for Systems and Control
Delft Univeristy of Technology
Email: {p.s.c.heuberger, x.j.a.bombois}@tudelft.nl

1 Introduction

In the control field there is a trend towards distributed and networked control. When it is desired to use model based control for complex interconnected systems, good models are necessary. The goal of the work presented here is to generate good models from data recorded from the network.

A dynamic network is defined as an interconnection of modules, where each of the modules are interconnected according to an interconnection architecture. The identification of the dynamics of the modules and the interconnection architecture will be referred to as network identification.

Here it will be assumed that the interconnection architecture of the network is known, and the goal is to identify the dynamics of each of the modules in the network. This is a natural generalization of the classical closed-loop identification problem, to the situation of interconnected systems.

The measured variables, w_j, can be described as:

$$w_j = \sum_{\substack{i=1 \\ i\neq j}}^{L} G_{ji} w_i + v_j + r_j \tag{1}$$

where, G_{ij} represents the module dynamics, v_i represents a noise source,r_i represents an external input, and L is the number of measured variables. The noise source and external input may or may not be present. The noise sources are considered to be independent colored noise. An example of a network is shown in Fig. 1.

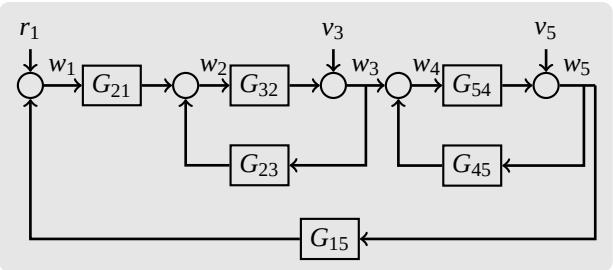

Figure 1: Network which satisfies the conditions stated.

2 Methods

Two methods will be presented. Both methods are based on the prediction error framework. The one-step-ahead predictor for w_j is:

$$\hat{w}_j(\theta) = H_j(\theta)^{-1} \sum_{\substack{i=1 \\ i\neq j}}^{L} G_{ji}(\theta) w_i + (1 - H_j^{-1}(\theta)) w_j. \tag{2}$$

The unknown coefficients, θ, are found by minimizing the sum of squared errors:

$$V_j(\theta) = \frac{1}{N} \sum_{k=0}^{N-1} (w_j(k) - \hat{w}_j(k))^2 \tag{3}$$

Method 1: Direct Identification. If all noise sources are present, i.e. $\Phi_v(\omega) > 0$, then the classical direct identification method can be applied to consistently estimate all transfers. This necessarily includes the modelling of dynamic noise models for all measured variables. For this result to hold a condition needs to be satisfied on the absence of algebraic loops in the network, which can be verified using graph-theoretic tools. This is a slight generalization of the results presented in [1].

If only a subset of noise sources is present, i.e. $\Phi_v(\omega) \geq 0$, then a direct identification method (including noise modelling) can be applied to a part (subset) of the network, that can be specified, and consistent estimates can be achieved for this subset.

Method 2: Two Stage Identification. If one or more external excitation signals r are present, then (parts of) the network can be identified consistently without noise modelling, while using output error predictors. Dependent on the location of the *r*s, a particular subset of the network can be identified. This subset can be specified by using graph-theoretical tools. The presented method to achieve this, is a natural generalization of the two-stage (or IV) method of closed-loop identification.

References

[1] D. Materassi, and M. Salapaka, "Relations between structure and estimators in Networks of Dynamical Systems," *Proc. of IEEE CDC*, Orlando, 2011.

Numerical Model of Epidemic Spreading in a Temporal Network

Adeline Decuyper
Adeline.Decuyper@uclouvain.be [1]

Vincent D. Blondel
Vincent.Blondel@uclouvain.be [2]

Luis E.C. Rocha
Luis.Rocha@uclouvain.be [3]

1 Introduction

We build a model of a temporal contact network. The goal is to build a numerically simulated network that allows the analysis of spreading processes, and reproduces some of the characteristics observed in empirical data of epidemics. In order to do this, we first build a model of a temporal network, and then run simulations of spreading processes on it. We then analyze the results when we vary certain parameters.

2 Network Model

To build the network, we only set one parameter, i.e. the distribution of the time between two activations of one node. We set it first to be a power-law distribution with exponential cutoff (PLCO) [1], and compare the results with the case of a geometric (GEO) distribution. We thus have a simple network model that assumes no information about degree distribution or attachment preference. A stochastic process determines the activation times of each node, i.e. when they can make a link with another active node. The PLCO case is a distribution that has been observed in many real world networks, such as sexual contacts networks, mobile phone, and many more, hence our choice for the inter-event time distribution between two activations of a same node.

3 Spreading Process

The study of spreading processes on our model is still work in progress. We run simulations of spreading processes following different models (SI, SIR,...) on a 1000-nodes network, built as explained. In order to see the impact that the PLCO distribution has on the spreading process, we also run all our simulations on a network built as before using a geometric (GEO) distribution instead of the PLCO, to represent the discrete equivalent of a Poissonian process.
To start the process, we infect one node at random at t=0. Then, for each contact between a susceptible node and an infected node, the susceptible is infected with probability β.

4 Results

Results of the simulations show that the main effect that the PLCO distribution has on spreading processes is that it slows down the diffusion of epidemics, especially for high transmission probabilities. The difference between PLCO and GEO can also be observed in the distribution of the number of infected nodes only a short time after the start of the process. The PLCO case presents a fat tail, whereas a higher proportion of the processes have already started in the GEO case.

5 Conclusions and Perspectives

We have built a simple stochastic network model, where the structure characteristics appear as a result of the stochastic process of activations of the nodes. We observe that the activation times of the edges is also broadly distributed purely as a result of the stochastic process. The main effect of the PLCO distribution is the slowing down of spreading processes in agreement with other studies in the literature ([2], [3]). This project is a work in progress, so we are now studying more deeply different epidemic models on this temporal network, finite size properties and extensions of the model by adding more characteristics to the network.

References

[1] A. Clauset, C.R. Shalizi, M. E. J. Newman,
Power Law Distributions in Empirical Data,
arXiv:0706.1062v2 [physics.data-an] 2 Feb 2009

[2] M. Karsai, M. Kivelä, R. K. Pan, K. Kaski, J. Kertész, A.-L. Barabási and J. Saramäki,
Small But Slow World: How Network Topology and Burstiness Slow Down Spreading,
arXiv:1006.2125v2 [physics.soc-ph] 11 Jun 2010

[3] A. Vazquez, B. Rácz, A. Lukács and A.-L. Barabási,
Impact of non-Poisson activity patterns on spreading processes,
arXiv:physics/0609184v2 [physics.data-an] 12 Apr 2007

[1]Department of Mathematical Engineering, UCLouvain, Belgium. A.D. is a Research Fellow with the Fonds National de la Recherche Scientifique.

[2]Department of Mathematical Engineering, UCLouvain, Belgium.

[3]Department of Mathematical Engineering, UCLouvain, Belgium. LECR is beneficiary of a FSR incoming post-doctoral fellowship of the Academie universitaire Louvain, co-funded by the Marie Curie Actions of the European Union.

Transfer function identification of burners for domestic boilers

Maarten Hoeijmakers*, Viktor Kornilov, Ines Lopez Arteaga, Philip de Goey, and Henk Nijmeijer
Department of Mechanical Engineering
Eindhoven University of Technology
P.O. Box 513
5600 MB Eindhoven, The Netherlands
Email: *p.g.m.hoeijmakers@tue.nl

1 Introduction

Many practical combustion devices are suspect to a strong resonance phenomena called a thermoacoustic instability. These instabilities usually manifest themselves by the generation of acoustic tone(s) within a combustion system and consist of a feedback loop between acoustic waves and the unsteady flame heat release rate.

Due to the very nature of the phenomenon both the acoustics of the combustor and the thermo-acoustics of the burner are important. In many cases the total system behavior (e.g. stability) can be represented by a network of transfer matrices for one-dimensional wave propagation. One of the key ingredients in the model is the so called flame transfer function which represents the response of the flame or burner heat release to acoustic modulation. In this work, the focus is on the measurement and model fitting of the flame transfer function.

2 Flame frequency response measurement

In order to measure the burner transfer function, the burner is mounted on an experimental setup to which a mean flow and acoustic perturbations are supplied. The acoustic fluctuations u' $[m/s]$ just below the burner deck are measured by a hot wire probe, and the resulting heat release rate fluctuations Q' $[W]$ are sensed by a photo-multiplier with OH filter. In this setting, the flame transfer function $\mathscr{F}$ can be defined as

$$\mathscr{F} = \frac{Q'}{u'}\frac{\overline{u}}{\overline{Q}}, \tag{1}$$

where $\frac{\overline{u}}{\overline{Q}}$ is the ratio of mean velocity to mean heat release and acts as a normalization factor. A typical frequency response function resulting from a stepped sine measurement is shown in figure 1. Note that the almost linear phase decrease with frequency which is typical of a time delay.

3 Model fit

In order to incorporate the flame in the thermoacoustic model, the transfer function is fitted on the frequency response by a simple rational model.

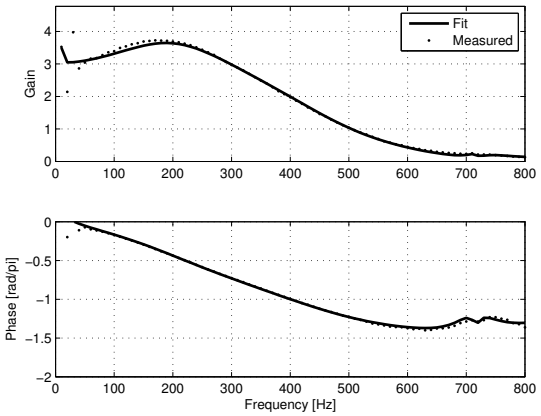

Figure 1: Measured flame response and fit, $n = 10$, $d = 11$

$$H(s,P) = \frac{\sum_{k=0}^{n} a_k s^k}{\sum_{k=0}^{d} b_k s^k}, \tag{2}$$

were a_k ad b_k are the coefficients, and n and d are the orders of the numerator and denominator polynomial respectively. Note that P is the parameter vector $P = [a_1, ...a_n, b_1, ...b_d]$. In contrast to many simple mechanical systems, the a-priori choice of model orders is a quite difficult task for this system due to the non-standard gain form and the time delay behavior of the phase. However, a model order of $n = 10$ and $d = 11$ gives good results for a wide range of flames and operating conditions. The fit for the measurement is also shown in figure 1.

4 Conclusions

It is shown that given a properly measured flame frequency response a simple rational fit is sufficient to provide a good model. Although such task seems trivial from the system/control community viewpoint, the transfer function fit is often neglected in combustion literature and the frequency response itself is used instead, leading to fundamentally wrong results in the subsequent stability analysis of the complete thermo-acoustic system. The author gratefully acknowledges STW for the financial support of this work.

Model Predictive Control for Traffic Networks: A Mixed-Logical Dynamic Approach Based on the Link Transmission Model

M. Hajiahmadi, B. De Schutter, and H. Hellendoorn
Delft Center for Systems and Control
Delft University of Technology, Mekelweg 2, 2628 CD Delft, The Netherlands
Email: {m.hajiahmadi,b.deschutter,j.hellendoorn@tudelft.nl}

1 Introduction

With the increasing number of vehicles, the highways are becoming more and more congested. This along with increasingly stringent traffic requirements necessitates use of efficient large-scale traffic management and control algorithms. One particular solution to this problem is based on Model Predictive Control (MPC), where a finite-horizon constrained optimal control problem is solved in a receding horizon fashion using the Link Transmission Model (LTM) proposed by [1]. This model provides fast yet accurate predictions. However, the underlying optimization problem is nonlinear nonconvex. One way to mitigate this is to use the methods developed in [2] to recast the problem as a mixed integer linear programming (MILP). In the sequel, we will describe our approach in detail.

2 Approach

The LTM uses links to model homogeneous sections of a road and nodes to model origins, destinations, on-ramps, off-ramps, intersections, etc. The LTM is capable of determining time-dependent link volumes and route travel times in traffic networks. To this aim, the LTM uses the cumulative number of vehicles as a representation for the traffic evolution. The cumulative number of vehicles that passed the upstream and downstream boundaries of the links are tracked and their values are updated using flow functions of links and nodes. These flow functions are characterized by capacities of the links, link travel times, demand profiles, available storage space at origins, etc. First, sending and receiving flows of all links are determined and subsequently, transition flows of the nodes are obtained using the flow functions of their incoming and outgoing links. For each type of the nodes a different formulation for the transition flow is defined. For instance, for a merge node in the LTM framework a *median* function of the sending/receiving flows of the connected links is used. The reader is referred to [1] for more details about the LTM equations.

However, since the LTM model is nonlinear in nature, the optimization problem that has to be solved to obtain the optimal control signals is nonlinear nonconvex. Hence, in every control time step, there is no guarantee to have a unique global solution. Furthermore, the nonlinear optimization takes considerable time to find a (local) optimal and for some initial points there is no feasible point. In order to get rid of the nonlinear nonconvex original optimization problem, one can use the approach proposed in [2] to end up with a mixed-integer linear optimization problem. The main idea is to define some binary variables to describe the hybrid nature of the system. Then by using the binary variables and adding some inequality constraints, we will come up with a system of linear equalities and inequalities consisting of real and integer variables.

3 Case Study

For testing the proposed approach, a benchmark traffic network example has been selected from [3]. The network consists of a mainstream freeway with a metered on-ramp and it is modeled using a modified version of the LTM that includes the metering signals. The flows of the vehicles from the mainstream origin and the on-ramp are controlled in order to have a minimum total time spent on the road for the vehicles. The control signals are obtained first by using an MPC controller based on the original nonlinear LTM model and next by using the MLD-MPC approach. The performance of the two approaches is compared in terms of computational efficiency and total cost.

4 Acknowledgements

This research is supported by the BSIK project "Next Generation Infrastructures (NGI)", and the European 7th Framework Network of Excellence "Highly-complex and networked control systems (HYCON2)".

References

[1] I. Yperman, *The Link Transmission Model for Dynamic Network Loading*. Ph.D. dissertation, Katholieke Universiteit Leuven, Leuven, Belguim, 2007.

[2] A. Bemporad, and M. Morari. Control of systems integrating logic, dynamics, and constraints. *Automatica*, 35(3): 407-427, 1999.

[3] A. Hegyi, B. De Schutter, and H. Hellendoorn. Model predictive control for optimal coordination of ramp metering and variable speed limits. *Transportation Research Part C*, 13(3): 185-209, 2005.

Towards Integrated Energy Management for Hybrid Commercial Vehicles

Vital van Reeven, Theo Hofman, Frank Willems, Maarten Steinbuch
Department of Mechanical Engineering, Eindhoven University of Technology
P.O.Box 513, 5600 MB Eindhoven, The Netherlands
v.v.reeven@tue.nl

Rudolf Huisman
DAF Trucks NV
P.O.Box 90065, 5600 PT Eindhoven, The Netherlands

Why Integrated Energy Management?

In order to be competitive in commercial road transportation, methods are needed to increase transport efficiency, while complying to increasingly stringent emission legislation. Hybrid Electric Vehicles (HEVs) can improve transport efficiency by reducing fuel consumption. To make optimal use of the HEV's components, all essential energy aspects of the vehicle have to be taken into account, both in the traction, thermal and emission domain: Integrated Energy Management. A real-time (supervisory) controller will be developed that optimally allocates the power resources of the HEV. This controller will however not influence the route, velocity or hardware of the vehicle.

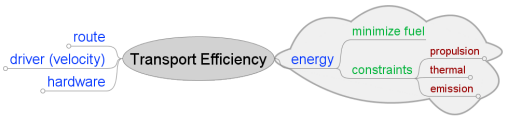

Vehicle System Layout

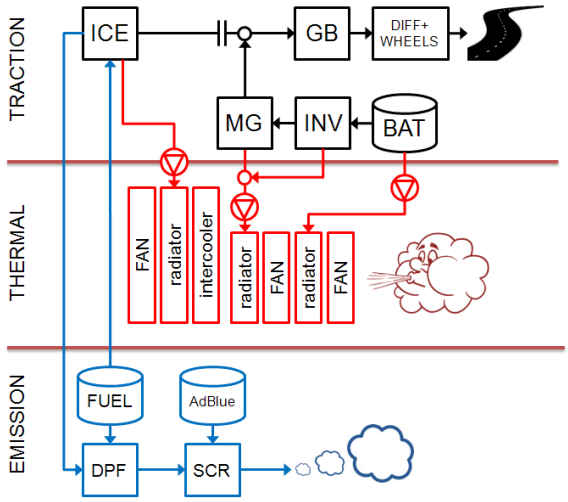

The system layout of the HEV is schematically shown above. Not only the traction subsystems (e.g. Internal Combustion Engine (ICE), Motor Generator (MG), Battery (BAT), Gear Box (GB), clutches), but also thermal subsystems (e.g. fans, radiators, pumps and valves) and emission subsystems (e.g. Diesel Particulate Filter (DPF), Selective Catalytic Reductor (SCR)) are to be considered for the integrated energy optimization.

Intermediate result

For a subset of the energy components an optimal control based algorithm is developed that controls, not only the power distribution between ICE (P_{ICE}) and MG (P_{MG}), but also explicitly gear selection i_{GB} and clutch activation i_{CL}. The solution of the resulting Mixed Integer Program (MIP) is converted to a piecewise affine control function to allow for real-time control on the vehicle [1]. On a validated vehicle simulation the new controller shows the hybrid functionality at reduced fuel and shift count compared to the same controller without gear and clutch integration.

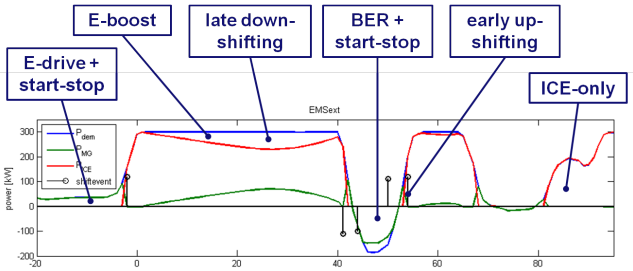

Next steps

To arrive at Integrated Energy Management, the emission and thermal aspects of the HEV will be incorporated in the control framework and validated on a prototype vehicle.

References

[1] V.v.Reeven e.a., Extending Energy Management in Hybrid Electric Vehicles with Explicit Control of Gear Shifting and Start-Stop, ACC2012 [submitted]

A Model Predictive Control Approach for Line Balancing Problem

Yashar Zeinaly, Bart De Schutter, Hans Hellendroon
Delft Center for Systems and Control
2628 CD Delft
The Netherlands
Email: {y.zeinaly, b.deschutter, j.hellendoorn@tudelft.nl}

1 Introduction

Modern baggage handling systems at large airports transport luggage in an automated way using so-called destination coded vehicles (DCVs), which are tubs moving on a network of conveyor belts or unmanned carts that transport the bags at high speeds on a network of railway-like tracks. A DCV-based baggage handling system consists of several parts: loading stations (where the bags enter the system after having the check-in and security), unloading stations (where the bags leave the system to be loaded onto the planes), a network of single-direction tracks with several (local) loops (for loading, unloading, and temporary storage of DCVs), and the early baggage storing, where the bags that enter the system too early can be stored. From a high-level point of view, the control problems in automated baggage handling system can be divided into three categories: (i) route choice control for DCVs, (ii) line balancing, and (iii) empty cart management.

2 Problem Statement

Tarău et al. [1] have developed methods for predictive route choice control of DCVs by assuming there is always a sufficient number of free DCVs at the loading stations such that the bags are immediately transported upon arrival. In practice, the total number of DCVs is limited, necessitating dynamical assignment of free DCVs to the loading stations. Line balancing is the problem of assigning a limited number of free DCVs in the central or local depots to the loading stations. It is required that the overall time delay in the loading stations is minimized and that the energy consumption and wear and tear due to extensive utilization of the resources are as low as possible. This translates into a balanced trade-off between minimizing the baggage queue lengths and the number of DCVs moving around in the network.

3 Approach: MPC

One particular solution to the line balancing problem is based on Model Predictive Control (MPC), where a finite-horizon constrained optimal control problem is solved in a receding horizon fashion using a dynamic model of the system [2]. For the sake of simplicity we consider a simple configuration of the baggage handling system. We derive a continuous-time event driven model for such a configuration to use as the prediction model. It will be shown that the proposed control scheme can achieve an acceptable balance between the overall baggage waiting time and the energy consumption. Furthermore, it provides some degree of robustness against uncertainties on the future baggage demand. As the system under consideration is piece-wise affine, the optimal control problem can be recast as (with some simplifying assumptions) a mixed integer linear programming optimization, for which efficient solvers exist.

4 Next Steps

Using the methods based on work of Michiels and Niculescu for control of time delay systems [3], we seek to design an internal controller that deals with the time delays in the system. An MPC controller is then designed for the closed-loop system in order to satisfy the performance requirements of Sect. 2. This will essentially be multi-level approach with the internal controller at the bottom level and the MPC controller at the top level.
The possibility of recasting the problem as a finite horizon optimal control of linear systems should be investigated. If possible, this will allow making use of the classical optimal control results (e.g., the Hamilton-Jacobi-Bellman equations and Pontryagin's maximum principle) [4].

5 Acknowledgment

This research is supported by the BSIK project "Next Generation Infrastructures (NGI)".

References

[1] A. Tarău, B. De Schutter, and H. Hellendoorn, "Predictive route choice control of destination coded vehicles with mixed integer linear programming optimization," *IEEE Trans. on Systems, Man, and Cybernetics, Part C: Application and Reviews*, vol. 40, no. 3, pp. 341-351, 2010.

[2] C. Garcia, D. Prett and M. Morari,"Model predictive control: theory and practive-a survey," *Automatica*, vol. 25, no. 3, pp. 335-348, 1989.

[3] W. Michiels and S.-I. Niculescu, *Stability and Stabilization of Time-delay Systems. An Eigenvalue Based Approach*, SIAM Publications, Philadelphia, 2007

[4] D. Naidu, *Optimal Control Systems*, CRC Press, Boca Raton, Florida, 2003

Energy Optimal Point-to-point Motion of A Badminton Robot Using Model Predictive Control

Xin Wang[1], Julian Stoev[2], Gregory Pinte[2], Jan Swevers[1]
[1] Department of Mechanical Engineering, Division PMA, KU Leuven
[2] Flanders Mechatronics Technology Centre

1 Abstract

This presentation discusses energy optimal point-to-point motion using Model Predictive Control (MPC). MPC [1] is a model-based control approach that predicts the future behaviour of the system and the control signals over a prediction horizon are calculated by solving an optimization problem while taking into account system constraints. The considered system is the linear motor based first axis of FMTC's badminton robot. This robot has to perform energy optimal point-to-point motion and arrive at a given set point within a required time. Energy optimality is achieved by setting the object function of the MPC optimization problem equal to the system's energy losses. The key issue is to utilize the strategy of the prediction horizon to ensure that the motion time is exactly equal to the required motion time.

2 Problem Description

The badminton robot of FMTC shown in Figure 1 is a 3 degree of freedom robot equipped with a badminton rocket. The robot controller receives estimation of the interception position and time in real-time from a central computer. This presentation discusses the application of MPC to the first axis of the badminton robot, in order to arrive at the in real-time generated interception position and time in an energy optimal way. It is assumed that linear motor is a perfect velocity controlled system so that the system can be regarded as an integrator. The input and the output are the velocity and the position of the robot respectively. According to the limitations of the system, the considered limits on position, velocity and acceleration are: $\pm 5[m], \pm 3[m/s]$ and $\pm 30[m/s^2]$ respectively.

[1]**Acknowledgement** This work has been carried out within the framework of projects IWT-SBO 80032 (LeCoPro) of the Institute for the Promotion of Innovation through Science and Technology in Flanders (IWT-Vlaanderen). This work also benefits from K.U.Leuven-BOF PFV/10/002 Center-of-Excellence Optimization in Engineering (OPTEC), the Belgian Programme on Interuniversity Attraction Poles, initiated by the Belgian Federal Science Policy Office (DYSCO), and K.U.Leuvens Concerted Research Action GOA/10/11.

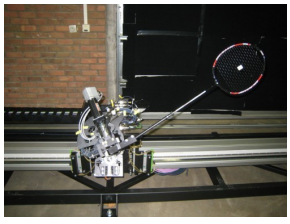

Figure 1: Badminton robot

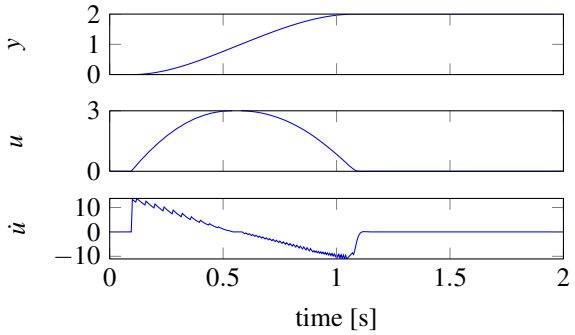

Figure 2: position (y), velocity (u) and acceleration ($\dot{u}$)

3 Energy Optimal MPC Approach

The developed energy optimal MPC approach is based on Time Optimal MPC [2]. Assuming that friction forces are negligible, the motion energy losses are copper losses in the motor and hence proportional to square of the motor current, which is taken as the object function of the MPC. An important constraint to consider in this optimal control problem is the given time of arrival at the interception position or the motion time T. If the system arrives at the interception point early, more energy is consumed, hence the solution won't be energy optimal. If the system arrives late, there's a chance the robot can't hit the shuttle.

4 Simulation results and conclusion

Figure 2 shows the simulation result for a motion of $2[m]$ and $T = 1[s]$, requested at time $0.1[s]$. The non-smooth acceleration is caused by the blocking [2]. The blocking is required to achieve prediction horizons that are sufficiently long to allow large displacements with a limited number of control variables.

References

[1] Francesco Borrelli and Manfred Morari. Offset free model predictive control. volume 1, pages 12451250, 2007.

[2] Lieboud Van den Broeck, Moritz Diehl, Jan Swevers, A model predictive control approach for time optimal point-to-point motion control Mechatronics, Vol. 21, No. 7, 2011, pp. 1203-1212

Unfolding of nodes with the same behavior in large networks

Maguy Trefois Jean-Charles Delvenne

Department of Applied Mathematics
Université catholique de Louvain (UCL)
Bâtiment Euler-4, Avenue G. Lemaître B-1348 Louvain-La-Neuve
Belgium
Email: maguy.trefois@uclouvain.be

1 Introduction

A graph, also called network, is a mathematical structure which allows to model complex systems with interacting agents like the Internet or the human societies. Such structures can be partitioned into subgraphs, called communities, with few links between them. This problem of graph partitioning is called community detection and is fundamental for the understanding of the underlying system. Several methods have been developed to detect communities in large graphs. We present an adaptation of these methods in order to detect groups of nodes with the same behavior, that is we partition the graph so that all the nodes of a group communicate in the same way with the nodes of the other groups.

2 Community detection

Several objective functions have been defined in order to partition the graph into communities. We briefly present two of them : the cut and the modularity.

2.1 The cut

The cut function is defined in order to divide the graph into two communities C_1 and C_2. This function counts the number of edges between the two groups of nodes, that is :

$$R = \sum_{i \in C_1, j \in C_2} A_{ij},$$

where A_{ij} denotes the $(i,j)-$entry of the adjacency matrix of the graph to partition.

A relevant partition is a partition minimizing R (see [1] for efficient algorithms).

2.2 The modularity

The modularity function compares the fraction of edges between two nodes in a same community with the expected fraction of edges between these two nodes if the edges were placed randomly in the graph (respecting the degrees of the nodes), that is :

$$Q = \frac{1}{2m} \sum_{ij} \left(A_{ij} - \frac{k_i k_j}{2m} \right) \delta(c_i, c_j),$$

where m is the number of edges in the graph, k_i is the degree of node i, δ is the Kronecker symbol and c_i is the community index to which node i belongs.

A relevant partition is a partition maximizing Q (see [1] and [2] for efficient algorithms).

3 Detecting groups of nodes with the same behavior

We will say that some nodes have the same behavior (or are of the same type) if they communicate in the same way with the nodes of the other groups. Illustrate this with the following examples.

- A movie-actor network : in this graph, a node is either a movie or an actor. If an actor plays in a movie, then their corresponding nodes are connected. So, the movies are only connected to actors and vice versa. In this network, there are two kinds of nodes : the movies and the actors.
- A food web network : in this directed graph, a node represents an individual. If there is an edge from node i to node j, that means that individual i eats individual j. In this graph, all individuals of species A only eat individuals of species B, and so on. So, a group of nodes with the same behavior matches with the individuals belonging to a same species.

The objective functions described in previous section have been generalized to detect such groups of nodes. We will study the flow of information in the system whose communication topology is described by the graph in order to detect nodes with the same behavior.

References

[1] M.E.J. Newman. *Networks : An introduction*. Oxford University Press, Oxford UK, 2010.

[2] V.D. Blondel, J.-L. Guillaume, R. Lambiotte, and E. Lefevre. *Fast unfolding of communities in large networks.* Journal of Statistical Mechanics: Theory and Experiment, page P10008, 2008.

Energy flow scheduling for parallel running batch processes[1]

Mark Mutsaers, Leyla Özkan, Ton Backx

Department of Electrical Engineering, Eindhoven University of Technology
P.O. Box 513, 5600 MB Eindhoven, The Netherlands
Email: {M.E.C.Mutsaers,L.Ozkan,A.C.P.M.Backx}@tue.nl

Introduction

Nowadays, manufacturing systems are becoming complex due to the large number of processes they consist of. To be able to deal with this complexity, advanced control and scheduling techniques are used to ensure that the complete production process runs in a more efficient and reliable way then controlling and making decisions manually. At this moment, this is quite often done using model predictive controllers (MPC), which is still an important research topic in the field of systems and control. In this talk however, we focus on the definition and optimization of scheduling problems instead.

We focus on a specific type of manufacturing systems that consists of batch processes running in parallel. These batch processes can interact with each other, and therefore influence the production of different batches in these parallel processes. The interaction will be used as the decision variable in the scheduling problem as illustrated in Figure 1. These scheduling problems will be modeled using the so called max-plus approach, which can also be used for doing optimization afterwards.

We will show results for a case study for factories of the compny Xella, where the production of calcium silicate stones is done in parallel batches, and where the steam flow between the processes will be the scheduling variable.

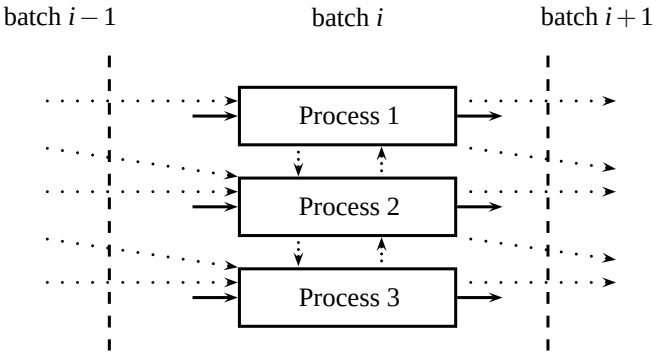

Figure 1: Scheduling for three parallel batch processes with interaction between them.

[1]This work was supported by AgentschapNL. The authors would also like to thank dr.ir. Ton J.J. van den Boom from Delft University of Technology for the discussions on max-plus systems.

Max-plus systems

In scheduling problems, one tries to take decisions that influence the finishing times of (intermediate) products of each sub-process. Modeling the finishing times using the general framework of (linear) dynamical systems is not as easy as usual, hence another strategy should be taken to model these discrete event systems. Instead of using the regular operations as addition an multiplication, another algebra will be used where the basic operations are taking the maximum value of two elements, and adding them together. This is named the max-plus algebra. Without giving too much detail in this abstract, we can use this algebra to represent discrete event systems as linear max-plus systems

$$\Sigma: \quad \begin{cases} x[k+1] = A \otimes x[k] \oplus B \otimes u[k], \\ y[k] \quad = C \otimes x[k], \end{cases}$$

where $\oplus$ and $\otimes$ denote $x \oplus y = \max(x,y)$ and $x \otimes y = x + y$. Here, $x[k]$ is denoting *time instances* when a process is ready with the production of a *batch k*. This is the mayor difference with normal (linear) dynamical systems. Earlier research has been shown that this kind of models can be used in optimization problems, hence can be applied to the problem we are dealing with.

To solve the scheduling problem of a factory where batches are produced in parallel, with interaction as decision variable, we have to make the following steps:

1. *Modeling of the batch process:* Each batch process that is running in parallel needs to be modeled, implying that the different stages for each batch of product are modeled using the max-plus algebra. Also the interaction moments with other parallel running processes need to be included in this model.
2. *Defining interaction constraints:* It is not possible to define interactions between arbitrary processes at any time or batch. This can, for example, be due to physical constraints in the factory. Therefore, we need to define these constraints, possibly also using the max-plus algebra, so that we can take them into account when solving the scheduling problem.
3. *Defining the objective and start optimization:* Now the model and the constraints are available, an objective function needs to be specified that needs to be minimized during optimization.

Reducing the Bullwhip Effect in Supply Chain Management by Applying a Model Predictive Control Ordering Policy

Dongfei Fu, Clara Mihaela Ionescu, Robin De Keyser
EeSA - Department of Electrical energy, Systems & Automation, Ghent University,
Technologiepark 913, 9052 Gent, Belgium
E-mail: Dongfei.Fu@UGent.be

1 Introduction

The tendency of demand variability to increase as one moves upward a supply chain, is commonly known as bullwhip effect [1]. In this research we model and control a four nodes supply chain network consisting of a factory F_a, a distributor D_i, a wholesaler W_h and a retailer R_e as shown in Figure 1. Our own model based predictive control, namely the Extended Prediction Self-Adaptive Control strategy (EPSAC) is applied to generate optimal ordering decision that can reduce the bullwhip effect. In order to evaluate the efficiency of the control performance, we use quantifying measures of the bullwhip effect to compare various strategies.

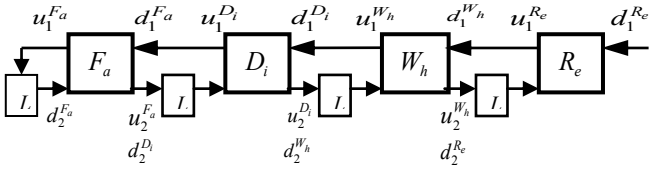

Figure 1. Block diagram of a four nodes supply chain

2 Process model

Consider a node $i \in \{F_a, D_i, W_h, R_e\}$ and the information and material exchange with its supplier and customer. A material balance around any network node involves the inventory level as well as the total incoming products from upstream node and total outgoing products to downstream node. The inventory position balance can be derived as:

$$y_1^i(t) = \frac{1}{1-z^{-1}}(d_2^i(t) - u_2^i(t)) \tag{1}$$

where z^{-1} is the discrete time shift operator and corresponds to unit sample period delay. If we make a linearization assumption that there is always enough stock at node i to meet customer demand, then (1) can be simplified to

$$y_1^i(t) = \frac{z^{-1}}{1-z^{-1}}(u_1^i(t) - d_1^i(t)) \tag{2}$$

which will be used as the prediction model in MPC control.

3 Control strategy

In order to calculate bullwhip, we need the ordering policy transfer function. Therefore, it's in principle necessary to formulate a closed loop expression for the MPC. We apply distributed EPSAC controllers to the system and each of them makes control decision for each node respectively. There is no information sharing in this control strategy and it is based on the SISO model (2) of supply chain. The closed loop transfer function of ordering policy can then be derived from the block diagram in Figure 2.

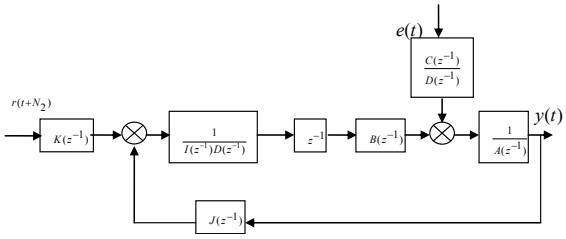

Figure 2. MPC closed form structure

4 Results

A measure of the bullwhip is defined as the ratio of the variance of the orders and the variance of the demand. The analytical expression for bullwhip metric can be in the following form. We assume an ARMA demand pattern (4), which is a weakly stationary stochastic process.

$$\text{Bullwhip} = \sum_{m=0}^{M} Z^{-1}\left\{T_{u/n}(z)\right\}^2 = \sum_{m=0}^{M} T_{u/n}[m]^2 \tag{3}$$

We then calculate the bullwhip for classical *order-up-to* and fractional ordering policy, using (3).

$$n(t) = \frac{\Theta(z^{-1})}{\Phi(z^{-1})}e(t) = \frac{1-0.6z^{-1}}{1-0.8z^{-1}}e(t) \tag{4}$$

The result given in Table 1 shows that MPC-EPSAC can produce a significantly lower demand variability compared to conventional *order-up-to* ordering policies.

Table 1. Bullwhip results

Ordering Policy	*Order-up-to*	Fractional	MPC
Bullwhip	10.7396	2.4429	1.3578

References

[1] Disney, S.M., Towill, D.R., "On the bullwhip and inventory variance produced by an ordering policy." *The International Journal of Management Science*, volume (31),157-167, 2003.
[2] De Keyser, R., "A Gent'le approach to predictive control." U*NESCO Encyclopedia of Life Support Systems*.Eolss Publishers Co.Ltd, Oxford, 2003.

Time optimal point-to-point motion trajectories: a convex optimization approach

Wannes Van Loock, Goele Pipeleers, Jan Swevers
KU Leuven, Department of Mechanical Engineering, Division PMA
Celestijnenlaan 300B, B-3001 Heverlee
Email: wannes.vanloock@mech.kuleuven.be

1 Introduction

Calculating time-optimal point-to-point motion trajectories for second order systems is known to be a non-convex optimization problem. However, by transforming the problem to a geometric path following problem, this presentation shows that a convex relaxation can be found, allowing for efficient calculation of time optimal point-to-point motion trajectories. As an illustration the effect of the dynamic friction term on the optimal time is investigated. It appears that in certain cases it is beneficial to include dynamic friction in the mechanical system.

2 Optimization problem

We consider the problem of moving a constrained one-dimensional second order mass-damper system, with mass m and viscous friction coefficient c, time-optimally from x_0 to x_T. Geometrically the time optimal double dwell trajectory is a monotonically increasing function from x_0 to x_T. Therefore, for one dimensional systems, the optimization problem can be transformed into a time optimal geometric path following problem. To this end, we write the position x as a function of a scalar path coordinate $s \in [0,1]$. Then $x(s)$ describes the spatial geometry of the path whereas the time dependency follows from the relation $s(t)$.

Using [1], we formulate following non-convex time optimal path-following problem

$$\begin{aligned} \underset{a(\cdot),b(\cdot)}{\text{minimize}} \quad & \int_0^1 \frac{1}{\sqrt{b(s)}} ds \\ \text{subject to} \quad & b(0) = 0, b(T) = 0 \\ & b'(s) = 2a(s) \\ & \underline{F} \leq x'(s)\left(ma(s) + c\sqrt{b(s)}\right) + mx''(s)b(s) \leq \overline{F} \end{aligned}$$

where $a(s) = \ddot{s}$, $b(s) = \dot{s}^2$ and $x'(s) = dx(s)/ds$. Note that the non-convexity enters in the upper bound of the last constraint due to the term $\sqrt{b(s)}$.

This presentation discusses how a convex relaxation of the above problem can be found by lifting it to a higher dimensional space. As the problem is rendered convex, relaxed solutions are found very efficiently. Moreover, in all our simulations, the solutions from the relaxed problem were indistinguishable from the true solution.

3 Faster with friction

We can now efficiently solve many problem instances by varying the parameters c and $\underline{F}$ (Figure 1). Note that for $\underline{F} < -\overline{F}$ it is advantageous with respect to the optimal time to introduce some viscous friction. For strongly asymmetric bounds gains can be as high as 30 %. Due to a faster deceleration with viscous friction, the maximal force can be applied longer and hence results in a shorter travel time. However, when introducing too much viscous friction, a slower acceleration counteracts this positive effect.

References

[1] D. Verscheure, B. Demeulenaere, J. Swevers, J. De Schutter, and M. Diehl. Time-optimal path tracking for robots: A convex optimization approach. *Automatic Control, IEEE Transactions on*, 54(10):2318 –2327, oct. 2009.

Acknowledgement

Goele Pipeleers is a Postdoctoral Fellow of the Research Foundation – Flanders (FWO – Vlaanderen). This work benefits from K.U.Leuven – BOF PFV/10/002 Center-of-Excellence Optimization in Engineering (OPTEC), the Belgian Programme on Interuniversity Attraction Poles, initiated by the Belgian Federal Science Policy Office (DYSCO), , G.0377.09, G.0320.08 of the Research Foundation – Flanders (FWO – Vlaanderen), and K.U.Leuven's Concerted Research Action GOA/10/11 and GOA/10/09.

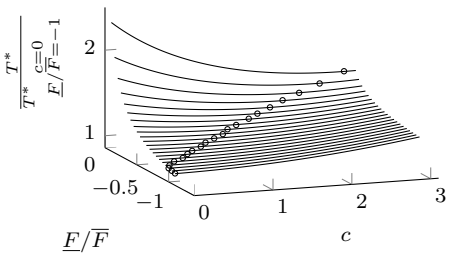

Figure 1: The optimal time T^* compared to T^* for $c = 0$ and $\underline{F}/\overline{F} = -1$ in function of the damping coefficient c and the ratio $\underline{F}/\overline{F}$. The circles indicate the optimal damping coefficient for a given $\underline{F}/\overline{F}$.

Stabilization of double integrator with output saturation

Wisnu Pradana
Department of Applied Mathematics
University of Twente
P.O. Box 217, 7500 AE Enschede
The Netherlands
Email: w.a.pradana@utwente.nl

Anton Stoorvogel
Department of Applied Mathematics
University of Twente
P.O. Box 217, 7500 AE Enschede
The Netherlands
Email: a.a.stoorvogel@utwente.nl

1 Introduction

Linear systems subject to input saturation have been extensively studied. See, for instance, the papers in the two special issues [1, 4]. However, the control of systems subject to saturating sensors have received little attention. The paper [2] studied the issue of observability of systems subject to output saturation while [3] studied the problem of stabilization of linear systems subject to output saturation. However, the latter paper has many limitations for practical implementation. It is in some sense an open loop design and, moreover, it is extremely sensitive to noise.

2 Problem formulation

In this talk we discuss some issues related to this problem. Our prime objective is to design stabilizing controllers for linear systems subject to sensor saturation. We are looking for closed-loop designs which can handle sensor and system noise. Clearly local stabilization is trivial since the saturation will not be active. The goal is to handle a large potential set of initial conditions. On the other hand if the sensor and system noise is too large one might expect that it becomes impossible to stabilize the system since the sensor noise will overwhelm the true measurement which is saturated and hence limited in size. Our objective is to improve upon the earlier design presented in [3] which can only handle uncertainty in the initial condition. We will see that measurement noise does require a quite different design than the one in [3] but also quite different from a classical observer/state feedback design methodology.

3 Results

Recently a design has been developed to find stabilizing controllers for neutrally stable systems with output saturation which showed how an observer and a state feedback can be integrated to obtain internal stability. It is clear that we cannot rely on the classical seperation principle in our design. In this presentation we look at the natural extension of the problem: a double integrator both with output saturation. It is not hard to verify that the earlier design cannot be used in this case and we will present a different design for this special system to illustrate how the design needs to be modified. Finally we briefly describe the intrinsic problems when we want to design stabilizing controllers for more complex unstable systems.

References

[1] D.S. BERNSTEIN AND A.N. MICHEL, guest eds., *Special Issue on saturating actuators*, Int. J. Robust & Nonlinear Control, 5 (1995), pp. 375–540.

[2] R. KOPLON, E.D. SONTAG, AND M.L.J. HAUTUS, "Observability of linear systems with saturated outputs", Lin. Alg. Appl., 205-206 (1994), pp. 909–936. Third Special Issue on Systems and Control.

[3] G. KREISSELMEIER, "Stabilization of linear systems in the presence of output measurement saturation", Syst. & Contr. Letters, 29 (1996), pp. 27–30.

[4] A. SABERI AND A.A. STOORVOGEL, guest eds., *Special issue on control problems with constraints*, Int. J. Robust & Nonlinear Control, 9 (1999), pp. 583–734.

Stability analysis for a system with hysteresis

Ruiyue Ouyang
Dept. Discrete Technology and Production Automation
University of Groningen
r.y.ou.yang@gmail.com

Bayu Jayawardhana
Dept. Discrete Technology and Production Automation
University of Groningen
bayujw@ieee.org

1 Introduction

Hysteresis is a common phenomena that presents in diverse systems, such as piezo-actuator, ferromagnetic material and mechanical systems. From the perspective of input-output behavior, the hysteresis phenomena can have counterclockwise (CCW) input-output (I/O) dynamics [1], clockwise (CW) I/O dynamics, or even, butterfly I/O maps.
In our previous results in [2], we show that for a certain class of Duhem hysteresis operator $\Phi : AC(\mathbb{R}_+) \times \mathbb{R} \to AC(\mathbb{R}_+)$, we can construct a storage function $H : \mathbb{R}^2 \to \mathbb{R}_+$ which satisfies

$$\frac{\mathrm{d}H((\Phi(u,\eta))(t),u(t))}{\mathrm{d}t} \leq \langle (\dot{\widetilde{\Phi(u,\eta)}})(t), u(t)\rangle \qquad (1)$$

for all $u \in AC(\mathbb{R}_+)$ and $\eta \in \mathbb{R}$, where η is the initial condition and AC is the space of absolutely continuous functions. This inequality immediately implies that such Duhem hysteresis operator has CCW input-output dynamics [1].
The aim of this work is to study the stability of feedback interconnections between a linear system and a CCW Duhem hysteresis operator. In our main results, we extend it by exploiting the dissipative characterization of CCW Duhem operator from our previous result [2] that also allows the analysis of positive feedback interconnection.

2 Main results

Depending on the input-output dynamics (CCW or CW) of the linear system, we present sufficient conditions that guarantee the stability of the closed-loop systems as shown in the following two theorems.

Theorem 2.1 Consider a negative feedback interconnection between a single-input single-output linear system and a Duhem operator Φ satisfying the hypotheses in Theorem 3.3 in [2] as follows

$$\left.\begin{array}{rl} \dot{x} &= Ax + Bu_1, \\ y &= Cx + Du_1, \\ z &= \Phi(y, z_0), \\ u_1 &= -z, \end{array}\right\} \qquad (2)$$

where $A \in \mathbb{R}^{n\times n}$, $B \in \mathbb{R}^{n\times 1}$, $C \in \mathbb{R}^{1\times n}$ and $D \in \mathbb{R}$. Assume that there exist $P = P^T > 0$, L and $\varepsilon > 0$ such that the following linear matrix inequalities (LMI)

$$P\begin{bmatrix} 1 \\ 0^{n\times 1} \end{bmatrix} = \begin{bmatrix} D \\ C^T \end{bmatrix}, \qquad (3)$$

$$\frac{1}{2}\left(P\begin{bmatrix} 0 & 0^{n\times n} \\ B & A \end{bmatrix} + \begin{bmatrix} 0 & B^T \\ 0^{n\times n} & A^T \end{bmatrix} P\right) + \varepsilon L^T L \leq 0, \qquad (4)$$

hold. Then for every initial conditions, the state trajectories of the closed-loop system (2) is bounded and all state trajectories converges to the largest invariant set in $\{(x,z) | L\left[\begin{smallmatrix} -z \\ x \end{smallmatrix}\right] = 0\}$.

Theorem 2.2 Consider a positive feedback interconnection between a single-input single-output linear system and a Duhem operator Φ satisfying the hypotheses in Theorem 3.3 in [2] as follows

$$\left.\begin{array}{rl} \dot{x} &= Ax + Bu_1, \\ y &= Cx, \\ z &= \Phi(y, z_0), \\ u_1 &= z, \end{array}\right\} \qquad (5)$$

where $A \in \mathbb{R}^{n\times n}$, $B \in \mathbb{R}^{n\times 1}$ and $C \in \mathbb{R}^{1\times n}$. Let $\varepsilon := (CB)^{-1}$ where we assume $CB > 0$ and there exist $\delta > 0$ and $Q = Q^T > 0$ such that

$$\frac{1}{2}(A^T Q + QA) + \varepsilon A^T C^T C A \leq 0, \qquad (6)$$

$$QB + A^T C^T = 0, \qquad (7)$$

$$Q - \delta C^T C > 0, \qquad (8)$$

hold and the anhysteresis function f_{an} satisfies $(f_{an}(\xi) - \delta\xi)\xi \leq 0$, for all $\xi \in \mathbb{R}$ (i.e. f_{an} belongs to the sector $[0, \delta]$). Then for every initial conditions, the state trajectory of the closed-loop system (5) is bounded and converges to the largest invariant set in $\{(x,z) | CAx + CBz = 0\}$.

Based on these stability results, a control strategy can be designed for a linear plant with hysteretic actuator by solving the LMIs given in (3)-(4) or (6)-(8).

References

[1] D. Angeli, "Systems with Counterclockwise Input-Output Dynamics," *IEEE Transactions on automatic control*, vol. 51, no. 7, pp. 1130-1143, 2006.

[2] B. Jayawardhana, Ruiyue Ouyang, V. Andrieu, "Dissipativity of general Duhem hysteresis models," Proc. IEEE Conf. Dec. Contr., Orlando, 2011.

Comparison of Model Predictive Control and Linear Quadratic Regulator when applied to a single reach.

M. Breckpot, O.M. Agudelo and B. De Moor
KU Leuven, Department of Electrical Engineering (ESAT), SCD-SISTA,
Kasteelpark Arenberg 10, 3001 Leuven, Belgium
{maarten.breckpot,mauricio.agudelo, bart.demoor}@esat.kuleuven.be

1 Introduction

Several studies can be found in literature where control strategies are used to control reaches or irrigation canals, such as PI controllers, heuristic controllers, predictive controllers and optimal controllers [1]. The dynamics of such a reach can be described by the Saint-Venant equations: two nonlinear partial differential equations. Because of computational reasons these controllers do not work directly with these equations but use approximating models, e.g. models based on the linearized Saint-Venant equations. The Linear Quadratic Regulator (LQR) is an example of a control strategy working with such a linear model. [2, 3, 4] show that this technique can be used for set-point control. However as we will show, this controller cannot be used at the same time for flood control.

2 Model predictive control

This problem does not exist with Model Predictive Control (MPC). MPC is a control strategy originating from the process industry and is used in various applications going from chemicals and food processing to automotive and aerospace applications. Just as for LQR, one can find many studies in literature where MPC is used for set-point control [5, 6, 7]. However these works do not focus on flood control. In previous work [8] we have been using a very simplified conceptual model which models the water levels of a river system only at a very limited number of points for set-point control in combination with flood control. In this work we use a linear version of the Saint-Venant equations with a very fine spatial discretization for designing and implementing the control strategies.

3 Results

We have compared the control performance of LQR and MPC for three different test cases: set-point control, disturbance rejection and flood control. For each of these cases MPC outperforms LQR. For the case of set-point control, MPC reaches new set-points after a change in the reference signal earlier than LQR. When a disturbance is present, the resulting steady state offset is much smaller when MPC is used, and for large disturbances MPC succeeds in preventing the river from flooding by temporaly creating extra buffer capacity. This is not the case for LQR.

In future work we will test MPC on river systems with multiple reaches, gates and junctions. Furthermore, an estimator will be added to the current control scheme in order to estimate the discharges and water levels of a river system from only a small number of measurements.

4 Acknowledgements

M. Breckpot is a Ph. D. fellowship of the Research Foundation - Flanders (FWO) at the KU Leuven, M. Agudelo is a post-doc at the KU Leuven, B. De Moor is a full professor at the KU Leuven, Belgium. Research Council KUL: GOA/11/05 Ambiorics, GOA/10/09 MaNet, CoE EF/05/006 Optimization in Engineering (OPTEC) en PFV/10/002 (OPTEC), IOF-SCORES4CHEM, several PhD/postdoc & fellow grants; Flemish Government: FWO: PhD/postdoc grants, projects: G0226.06 (cooperative systems and optimization), G0321.06 (Tensors), G.0302.07 (SVM/Kernel), G.0320.08 (convex MPC), G.0558.08 (Robust MHE), G.0557.08 (Glycemia2), G.0588.09 (Brain-machine) research communities (WOG: ICCoS, ANMMM, MLDM); G.0377.09 (Mechatronics MPC); IWT: PhD Grants, Eureka-Flite+, SBO LeCoPro, SBO Climaqs, SBO POM, O&O-Dsquare; Belgian Federal Science Policy Office: IUAP P6/04 (DYSCO, Dynamical systems, control and optimization, 2007-2011); IBBT; EU: ERNSI; FP7-HD-MPC (INFSO-ICT-223854), COST intelliCIS, FP7-EMBOCON (ICT-248940), FP7-SADCO (MC ITN-264735), ERC HIGHWIND (259 166); Contract Research: AMINAL; Other: Helmholtz: viCERP; ACCM.

References

[1] P. Malaterre, D. Rogers, and J. Schuurmans, "Classification of canal control algorithms," *Journal of Irrigation and Drainage Engineering*, vol. 124, pp. 3–10, January/February 1998.

[2] A. Clemmens and J. Schuurmans, "Simple optimal downstream feedback canal controllers: Theory," *Journal of Irrigation and Drainage Engineering*, vol. 130, pp. 26–34, February 2004.

[3] P. Malaterre, "Pilote: Linear quadratic optimal controller for irrigation canals," *Journal of Irrigation and Drainage Engineering*, vol. 124, pp. 187–194, July/August 1998.

[4] O. Balogun, M. Hubbard, and J. DeVries, "Automatic control of canal flow using linear quadratic regulator theory," *Journal of Hydraulic Engineering*, vol. 114, pp. 75–102, January 1988.

[5] P. van Overloop, *Model Predictive Control of Open Water Systems*. PhD thesis, Technische Universiteit Delft, 2006.

[6] M. Xu, P. van Overloop, and N. van de Giesen, "On the study of control effectiveness and computational efficiency of reduced saint-venant model in model predictive control of open channel flow," *Advances in Water Resources*, vol. 34, pp. 282–290, 2011.

[7] B. Wahlin and A. Clemmens, "Automatic downstream water-level feedback control of branching canal networks: theory," *Journal of Irrigation and Drainage Engineering*, vol. 132, no. 3, pp. 208–219, 2006.

[8] M. Breckpot, T. Barjas Blanco, and B. De Moor, "Flood control of rivers with nonlinear model predictive control and moving horizon estimation," in *49th IEEE Conference on Desicion and Control*, pp. 6107–6112, 2010.

A flexible, efficient software package for nonlinear ILC

Marnix Volckaert[1]
Department of Mechanical Engineering
KU Leuven, Belgium
marnix.volckaert@mech.kuleuven.be

Jan Swevers
Department of Mechanical Engineering
KU Leuven, Belgium
jan.swevers@mech.kuleuven.be

1 Introduction

Iterative learning control (ILC) is an open loop control strategy that aims to reject repeating disturbances and improve tracking control of repeated motions by using information about the tracking performance of the previous motion, also called trial or iteration. The large collection of ILC algorithms can be divided in LTI versus LTV and nonlinear approaches, model based versus data driven, first order versus higher order, indirect versus direct, unconstrained versus constrained, etc. While most of these approaches have been implemented as distinct variants of ILC, their underlying principles are often identical.
This abstract presents an open source software package that is a generic approach to model based optimal ILC, and therefore incorporates many of the existing algorithms. It allows the user to adapt the ILC algorithm in the most flexible way. It can be applied both to tracking control problems and to point to point motion control problems, to MIMO systems, and systems that experience a sudden change in dynamic behavior. By using a sparse implementation of an interior point method to solve the underlying optimization problems, the algorithm can efficiently handle very long data records.

2 Theoretical background

The presented ILC approach is model based, and therefore it is assumed that a discrete-time state-space model $\hat{P}$ is available, which can be either linear or nonlinear. However, in order to introduce learning, the nominal model is augmented by one or more model correction vectors α, such that the corrected model $\hat{P}_c$ can be written as:

$$\hat{P}_c : \begin{cases} \mathbf{x}(k+1) = f_c[\mathbf{x}(k), \mathbf{u}(k), \alpha(k)] \\ \hat{\mathbf{y}}_c(k) = h_c[\mathbf{x}(k), \mathbf{u}(k), \alpha(k)] \end{cases}$$

The user has the freedom to determine how the nominal model is corrected by α. The ILC algorithm now consists of two steps: in the first step, an optimal value of α is estimated to best describe the previous trial's measurement, which corresponds to the following optimization problem:

$$\min_{\alpha} J_\alpha = (\mathbf{y}_i - \hat{\mathbf{y}}_c)^T \mathbf{Q}_\alpha (\mathbf{y}_i - \hat{\mathbf{y}}_c)$$
$$\hat{\mathbf{y}}_c = \hat{P}_c(\mathbf{u}_i, \alpha)$$

During the second step, an optimal value of the input signal is calculated, using the corrected model with the estimated value of α, corresponding to the following optimization problem:

$$\min_{\mathbf{u}} J_\mathbf{u} = (\mathbf{y}_r - \hat{\mathbf{y}}_c)^T \mathbf{Q}_u (\mathbf{y}_r - \hat{\mathbf{y}}_c)$$
$$\hat{\mathbf{y}}_c = \hat{P}_c(\mathbf{u}, \alpha_i)$$

These optimization problems can easily be extended with additional objectives and constraints. Both problems are formulated automatically in the gILC software, and then sent to a third party solver, which is a sparse implementation of an interior point method. This results in a very efficient algorithm, even for long data records.

3 The gILC package

The gILC package consists of a number of Python class definitions, combined with the third party software packages CasADi [1] (for automatic differentiation and formulation of the optimization problems) and IPOPT [2] (for the minimization of said problems). It allows the user to create a gILC object, to provide a model for the system, and to easily set the properties of the algorithm. The software then provides an update function of the following form:

```
u_ip1 = gilc.update(u_i,y_i)
```

All algorithm settings can be adapted during operation, without extra computational effort.

4 Conclusions

More information about the gILC software package, including download and install instructions, can be found at `www.kuleuven.be/optec/software`.

References

[1] CasADi, implementing automatic differentiation by means of a hybrid symbolic/numeric approach, `sourceforge.net/apps/trac/casadi/`, 2012

[2] IPOPT, a software package for large-scale nonlinear optimization, `projects.coin-or.org/Ipopt`, 2012

[1]This work benefits from FWO-project G.0422.08, K.U.Leuven-BOF PFV/10/002 Center-of-Excellence Optimization in Engineering (OPTEC), IWT-SBO-project 80032 (LeCoPro) and the Belgian Programme on Interuniversity Attraction Poles, initiated by the Belgian Federal Science Policy Office (DYSCO).

Control System Design for Wireless Electromagnetic-Based Micromanipulation System

Islam S. M. Khalil*, Leon Abelmann† and Sarthak Misra*
*MIRA-Institute for Biomedical Technology and Technical Medicine
†MESA+ Institute for Nanotechnology
University of Twente
P.O. Box 217, 7500 AE Enschede
The Netherlands
Email: {i.s.m.khalil, l.abelmann, s.misra}@utwente.nl

Abstract

Control strategy to accomplish precise point-to-point positioning and trajectory tracking of magnetically-guided microparticles is analyzed in this work. External disturbances and model mismatch were modeled as inputs to the magnetic force governing equation. First, the problem is formulated by modeling the magnetic force experienced by the microparticles in the presence of viscous drag, buoyancy force, force due to gravity, external disturbances and model mismatch [1]; the resulting model is utilized to design an observer to estimate the mismatch over the nominal and actual values of these forces. Hereafter, the current-magnetic force map is derived by minimizing the two-norm square of the magnetic field-to-current map constrained with the magnetic force equation. The result of this minimization problem along with the designed observer were utilized in the realization of a control input for the attainment of robustness by compensating for the model mismatch of the electromagnetic system and rejecting the disturbance forces on the microparticles.

The proposed control strategy is based on designing two control loops, an inner-loop for the robustness attainment and an outer-loop to achieve stability of the overall electromagnetic system. In the inner-loop, the force-current map and its inverse were utilized for estimating the disturbance forces and the model mismatch, in addition to computing the required current to reject the disturbances and compensate for the model mismatch. On the other hand, the outer-loop enforces stability by achieving stable error dynamics without the necessity to identify the actual system parameters and exact model. This was shown to be valid in the electromagnetic system's low frequency range through analyzing the tradeoffs between robustness and stability using frequency response analysis [2].

In order to examine the validity of the control strategy and the performance of the overall electromagnetic-based micromanipulation system, experiments were conducted on an experimental setup consisting of four electromagnets as shown in Figure 1. The electromagnets are oriented around a reservoir at which microparticles with average diameter of 100 μm navigate in a fluidic body with unknown parameters and in the presence of external disturbance forces [3].

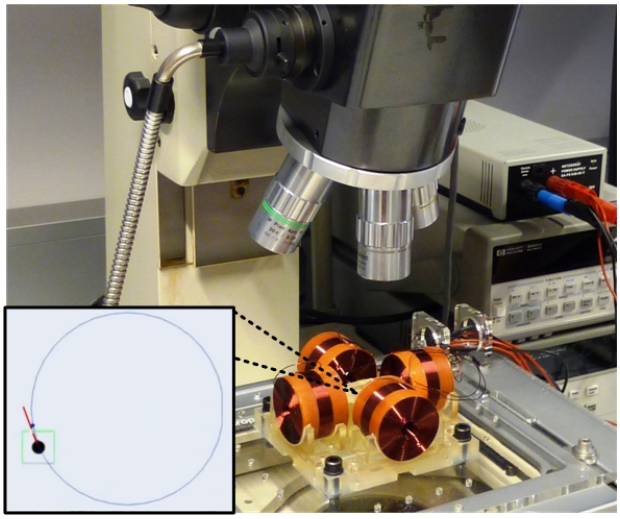

Figure 1: The electromagnetic system developed for the wireless control of microparticles under magnetic field. The inset shows a 100 μm spherical microparticle in a reservoir tracking a circular trajectory through the controlled magnetic fields.

References

[1] J. J. Abbott, Z. Nagy, F. Beyeler, and B. J. Nelson, "Robotics in the Small, Part I: Microbotics," *IEEE Robotics & Automation Magazine*, vol. 14, no. 2, pp. 92-103, 2007.

[2] Z. J. Yang, S. Hara, S. Kanae, K. Wada, and C. Y. Su, "An adaptive robust nonlinear motion controller combined with disturbance observer," *IEEE Transactions on Control System Technology*, vol. 18, no. 2, pp. 454-462, 2010.

[3] J. D. Keuning, J. de Vries, L. Abelmann, and S. Misra, "Image-based magnetic control of paramagnetic microparticles in water," In *Proceeding of the IEEE International Conference on Intelligent Robots and Systems (IROS)*, pp. 421-426, San Francisco, USA, September 2011.

Foot placement for balance in planar bipeds with point feet

Pieter van Zutven and Henk Nijmeijer
Eindhoven University of Technology, Dynamics and Control Group
P.O. Box 513, 5600 MB Eindhoven, The Netherlands
Email: p.w.m.v.zutven@tue.nl, h.nijmeijer@tue.nl

1 Introduction

When humanoid robots are going to be used in society, they should be capable to maintain their balance. Knowing where to step appears to be important to remain balanced. Here we present an algorithm to determine proper foot placement (FP) for balance of planar bipeds with point feet [1]. The algorithm is based on conservation of energy, taking into account energy losses at impact.

2 Biped model

We model a biped as a chain of N rigid bodies from stance to swing foot interconnected by revolute joints. The stance and swing leg swap immediately at the impact of the swing foot with the ground, so that the biped can be modeled as a system with impulsive effects:

$$\begin{cases} D(q)\ddot{q}+C(q,\dot{q})\dot{q}+G(q)=u, & q_- \notin S, \\ \dot{q}_+=\Delta(q_-)\dot{q}_-, & q_- \in S, \end{cases} \quad (1)$$

where $q \in \mathbb{T}^N$ is the state vector, $D \in \mathbb{R}^{N\times N}$ is the inertia matrix, $C\dot{q} \in \mathbb{R}^N$ is the Coriolis and centrifugal vector, $G \in \mathbb{R}^N$ is the gravity vector and $u \in \mathbb{R}^N$ is the input vector. The impact map is given by $\Delta \in \mathbb{R}^{N\times N}$ and S is the impact surface. Subscripts $_-$, $_+$ and $_b$ indicate states just before impact, just after impact and in a balanced configuration respectively.

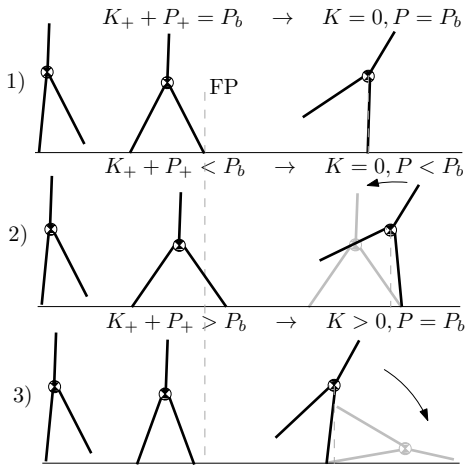

Figure 1: Schematic drawing of the relation between foot placement and balance. The kinetic and potential energy are K and P respectively ($_+$ indicates just after impact). The potential energy in a balanced configuration is P_b.

3 Foot placement and balance

A balanced configuration is a configuration in which the center of mass of the biped lies exactly above its stance foot. A biped is in balance as long as it can still place its swing foot at a location such that it evolves to a balanced configuration, see Figure 1:

1) The biped steps onto the FP point and it stops exactly at the balanced configuration.
2) The biped steps after the FP point, does not reach the balanced configuration and falls backward.
3) The biped steps before the FP point, does not stop at the balanced configuration and falls forward.

The desired FP for balance can now be found if we assume that the sum of the kinetic energy K and the potential energy P is conserved after impact:

$$K(q_+,\dot{q}_+)+P(q_+)=K(q_-,\Delta(q_-)\dot{q}_-)+P(q_-)=P_b. \quad (2)$$

Solving (2) for q_- yields the desired location that indicates where the foot would need to be placed to balance the biped if the impact were to occur in the next instant.

4 Simulation results

We model a three link biped according to (1). At each time step we solve (2) for q_- and use this as reference q_r for a feedback tracking controller. Results of simulations of situation 2) and 3) are shown in Figure 2. The simulations show that the biped is continuously in balance and that it can be controlled to stably walk or stop by proper foot placement.

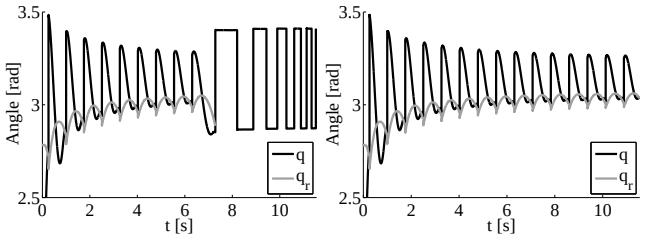

Figure 2: Simulation results: actual configuration (q) and desired one at the end of a step (q_r) for stepping after (left) and before (right) the FPE

References

[1] P. v. Zutven, D. Kostić, and H. Nijmeijer. Foot placement for planar bipeds with point feet. *ICRA*, 2012, in press.

Motion control of Philips Arm using joint torque sensors

Marinkov S., Janssen, R.J.M., Molengraft, M.J.G. van de and Steinbuch, M.
Dept. of Mechanical Engineering
Eindhoven University of Technology
P.O. Box 513, 5600 MB Eindhoven
The Netherlands
Email: s.marinkov@tue.nl

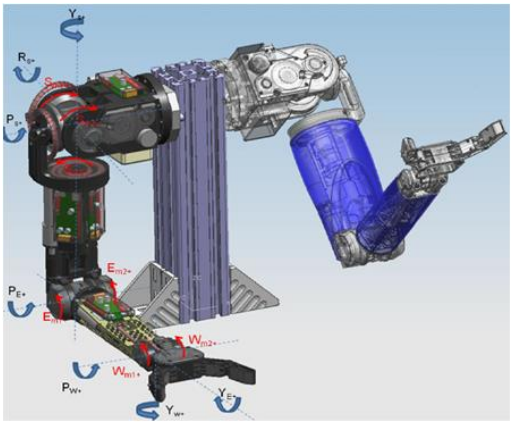

Figure 1: The left and the right Philips Arm

1 Introduction

In the past couple of decades a number of model-based control schemes has been proposed as a solution to the problem of motion control of a robotic arm *e.g.,* resolved acceleration control or the computed torque method. To be able to cope with model uncertainties and changing dynamics due to for instance varying payloads, these classical methods that utilize full manipulator dynamics have been further extended to their more complex, adaptive and robust counterparts. However, their shared characteristic of a heavy computational burden which they put upon the control computer, often makes them difficult to apply in real time.

Alternatively, a simpler approach has been treated in literature that, unlike the aforementioned cases, does not require a dynamical model of the robot links. Namely, using joint torque feedback [1], and providing that the additional torque measurement is available at the joint level, the robotic arm system can be reduced to the rotor dynamics only. Nevertheless, precise measurement of the torque, accurate friction model and directly driven joints are a common assumption.

2 Concept

Figure 2 illustrates the general idea of the joint torque feedback control system. The external disturbance τ_J (effect of

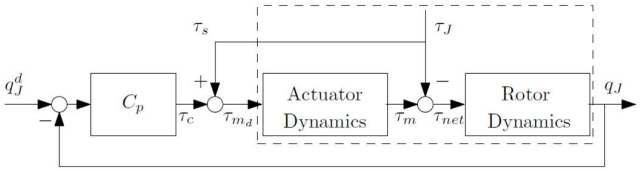

Figure 2: Positive torque feedback control system

the link dynamics), is measured via a torque sensor τ_s and the resulting torque signal is fed back for compensation. In the case of an ideal actuator, *i.e.,* when $\tau_m = \tau_{m_d}$, it can be seen that the load torque τ_J is trivially compensated with the measured sensor torque. As a consequence the load dynamics becomes exactly decoupled, resulting in $\tau_{net} = \tau_c$.

Within this scope, a new algorithm has been implemented for the motion control of an anthropomorphic robotic manipulator with a differential drivetrain structure – the Philips Arm, see Figure 1. The control solution is based on the available joint torque sensing capabilities of the arm, and in the adaptive context compensates for the friction and inertia related effects of the drivetrain dynamics. The stability of the system has been proven analytically. Furthermore, the topics of accurate calibration of the (nonlinear) optical torque sensors and real-time velocity estimation, have been treated as well.

3 Implementation

The real-time controller implementation was achieved by means of Orocos Real-Time Toolkit (RTT), a tool for the development of real-time robotics applications using modular, run-time configurable software components [2].

References

[1] M. Buehler, F. Aghili, and J. M. Hollerbach. Motion control systems with hinfinity positive joint torque feedback. *Control Systems Technology, IEEE Transactions on*, 9(5):685695, 2001.

[2] H. Bruyninckx. Open robot control software: the OROCOS project. *Robotics and Automation, 2001. IEEE International Conference on*, 2523-2528 vol.3, 2001.

Internal and external force-based impedance control for cooperative manipulation

Dennis Heck[1], Henk Nijmeijer[2]
Dynamics and Control
Eindhoven University of Technology
P.O. Box 513, 5600 MB Eindhoven
The Netherlands
Email: { [1]d.j.f.heck, [2]h.nijmeijer } @tue.nl

Introduction

The manipulation of an object by multiple robot arms is called cooperative manipulation. It can be useful in complex tasks that cannot be executed by a single arm. In this research, an asymptotically stable cascaded control algorithm is proposed for cooperative manipulation of a common object. This algorithm controls motion and internal forces of the object, as well as the contact forces between the object and environment.

Control strategy for cooperative manipulation

The considered system consists of multiple non-redundant rigid manipulators that tightly grasp a rigid object. A cascade control structure (depicted in Figure 1) is designed to control the motion and forces of the system [1].

The motion of the system is controlled by applying inverse dynamic controllers to each manipulator. Knowledge of dynamics of the manipulated object is not required, since the interaction forces and moments between the object and manipulators are measured.

The internal stresses in the object are controlled with enforced impedance relationships between the object and each manipulator:

$$D_i(\ddot{x}_{id} - \ddot{x}_{ir}) + B_i(\dot{x}_{id} - \dot{x}_{ir}) + S_i(x_{id} - x_{ir}) = h_{Iid} - h_{Ii}.$$

With a desired trajectory of the internal force h_{Id} the internal stresses of the object can be specified. The internal forces and moments are computed using the object kinematics.

Contact with the environment is controlled with an enforced impedance relationship between the object and the environment:

$$D_o(\ddot{x}_{oc} - \ddot{x}_{od}) + B_o(\dot{x}_{oc} - \dot{x}_{od}) + S_o(x_{oc} - x_{od}) = h_{e,c} - h_{e,d}.$$

A commanded contact force $h_{ext,c}$ can be applied to the environment. The contact dynamics can be shaped with the impedance parameters D_o, B_o and S_o.

Asymptotic stability of each controller is proven using Lyapunov stability theory and LaSalle's invariance principle. Up to now, asymptotic stability of the internal force-based impedance controller was only presumed in [2], but never proven. Guidelines are suggested to compute the control parameters of the internal impedance parameters. Consequently, the parameters of all controllers can be tuned intuitively. Successful implementation of the control algorithm is demonstrated in simulations.

Conclusion

With the cascade controller, motion, internal and external forces of the object can be controlled. Asymptotic stability is proven for the controlled system.

References

[1] D.J.F. Heck, D. Kostić, A. Denasi and H. Nijmeijer, "Internal and external force-based impedance control for cooperative manipulation," Robotics and Autonomous Systems, (submitted).

[2] R.G. Bonitz and T.C. Hsia, "Internal Force-based Impedance Control for Cooperating Manipulators," Tr. on Robotics and Automation, 1996.

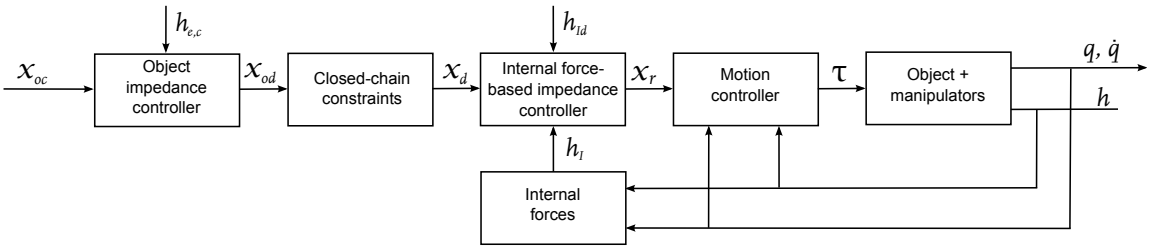

Figure 1: Feedback control structure.

On the reachability of discrete time linear systems with convex output constraints

M. D. Kaba and M. K. Camlibel

JBI for Mathematics and Computer Science, University of Groningen, Nijenborgh 9, 9747 AG Groningen, the Netherlands

Email: {m.d.kaba, m.k.camlibel}@rug.nl

1 Abstract

We characterize the reachability of a right-invertible discrete time linear system with convex output constraints using techniques of geometric control and convex analysis.

2 Introduction

We consider the discrete time linear system Σ, given by the equations

$$x_{k+1} = Ax_k + Bu_k, \tag{1a}$$
$$\mathscr{Y} \ni Cx_k + Du_k, \tag{1b}$$

where the input, state and output dimensions are m, n and s, respectively. Here $\mathscr{Y}$ denotes a closed convex set in $\mathbb{R}^s$, which contains the origin.

Let $\mathscr{W}$ be a subspace of the input space $\mathbb{R}^m$. We denote by $(\Sigma, \mathscr{W})$, the system obtained by restricting the inputs of Σ to $\mathscr{W}$. The weakly unobservable subspace of $(\Sigma, \mathscr{W})$ will be denoted by $\mathscr{V}^*(\Sigma, \mathscr{W})$. Similarly, $\mathscr{V}_g^*(\Sigma, \mathscr{W})$ denotes the stabilizable weakly unobservable subspace of $(\Sigma, \mathscr{W})$ (See [1] for the definitions).

The discrete time linear system (1) can be written as a difference inclusion

$$x_{k+1} \in F(x_k) \tag{2}$$

where $F : \mathbb{R}^n \rightrightarrows \mathbb{R}^n$ is a convex set-valued mapping given by

$$F(x) = Ax + BD^{-1}(\mathscr{Y} - Cx).$$

Then the dual of F is given by

$$F^\circ(q) = A^T q - C^T[((D^T)^{-1}B^T q) \cap \mathscr{Y}^\circ].$$

where $\mathscr{Y}^\circ$ denotes the polar of $\mathscr{Y}$, which is defined as $\mathscr{Y}^\circ := \{q | \langle q, x\rangle \leq 1 \text{ for all } x \in \mathscr{Y}\}$. Similarly, we have the negative polar cone $\mathscr{Y}^- := \{q | \langle q, x\rangle \leq 0 \text{ for all } x \in \mathscr{Y}\}$ and the barrier cone $\mathscr{Y}^b := \{q | \sup_{x\in\mathscr{Y}} \langle q, x\rangle < \infty\}$. Clearly F° is closely related to the dual system Σ^T.

Let $R(F) = \bigcup_{i\geq 1} F^i(0)$ and $X(F)$ be the set of initial conditions q_0 from which an infinite trajectory of (2) starts. We say that the system (1) is reachable if

$$X(F) \subseteq R(F). \tag{3}$$

Our aim is to provide necessary and sufficient conditions for (3) to be true, especially when (1) is right-invertible.

3 Main Result

We prove

Theorem 1 *Suppose that the system* (1) *is right-invertible. Then the following are equivalent*

1. *The system* (1) *is reachable.*
2. $R(F) = \mathbb{R}^n$.
3. $X(F^\circ) = \{0\}$.
4. *All of the followings hold*
   (a) *For all* $\lambda \in [0, +\infty)$,
   $$\begin{bmatrix} A^T - \lambda I \\ B^T \end{bmatrix}^{-1} \begin{bmatrix} C^T \\ D^T \end{bmatrix} \mathscr{Y}^- = \{0\}.$$
   (b) $\mathscr{V}^*(\Sigma^T, \mathscr{Y}^\perp) = \{0\}$.
   (c) *For all* $\lambda \in [0, 1]$,
   $$\begin{bmatrix} A^T - \lambda I \\ B^T \end{bmatrix}^{-1} \begin{bmatrix} C^T \\ D^T \end{bmatrix} \mathscr{Y}^\circ = \{0\}.$$
   (d) $\mathscr{V}_g^*(\Sigma^T, \mathscr{Y}^b \cap (-\mathscr{Y}^b)) = \{0\}$.

References

[1] Harry L. Trentelman, Anton A. Stoorvogel, and Malo Hautus. *Control theory for linear systems*. Communications and Control Engineering Series. Springer-Verlag London Ltd., London, 2001.

Reachability Analysis of Autonomous Max-Plus-Linear Systems

Dieky Adzkiya, Bart De Schutter, Alessandro Abate
Delft Center for Systems and Control
TU Delft – Delft University of Technology
Mekelweg 2
2628 CD Delft
The Netherlands
Email: {d.adzkiya,b.deschutter,a.abate}@tudelft.nl

1 Abstract

Max-Plus-Linear (MPL) systems are discrete-event models [1] with a continuous state space characterizing the timing of the underlying discrete events. The finite-horizon forward reachability analysis of autonomous MPL models has been discussed in [2], under a finiteness assumption on the cardinality of the set of initial conditions. This work investigates the infinite-horizon forward and backward reachability analysis of autonomous MPL models, where the set of initial conditions is uncountable and characterized by a Difference-Bound Matrix (DBM) [3].

2 Introduction

This section introduces the definition of an autonomous MPL model, an irreducible max-plus matrix and a DBM. Define $\mathbb{R}_\varepsilon$ and ε as $\mathbb{R}\cup\{\varepsilon\}$ and $-\infty$, respectively. Given an integer $k\in\mathbb{N}$, the max-algebraic power of $A\in\mathbb{R}_\varepsilon^{n\times n}$ is denoted by $A^{\otimes^k}$ and corresponds to $A\otimes\cdots\otimes A$, k times. The base case $A^{\otimes^0}$ represents a max-plus identity matrix. An autonomous MPL model [1] is defined as follows:

$$x(k+1) = A\otimes x(k),$$

where $A\in\mathbb{R}_\varepsilon^{n\times n}$, $x(0)\in\mathbb{R}^n$. The independent variable k denotes an increasing discrete-event counter, whereas the state variable defines the (continuous) timing of the discrete events.

A max-plus matrix $A\in\mathbb{R}_\varepsilon^{n\times n}$ is called irreducible if the non-diagonal elements of $A\oplus\cdots\oplus A^{\otimes^{n-1}}$ are finite (not equal to ε). Finally, a DBM $D\subseteq\mathbb{R}^n$ is a finite intersection of $x_i - x_j \simeq \alpha$, where $\simeq\in\{<,\leq\}$, $1\leq i,j\leq n$ and $\alpha\in\mathbb{R}\cup\{+\infty\}$.

3 Problem Formulation

We assume the set of initial conditions $\emptyset\subset D_0\subseteq\mathbb{R}^n$ is a DBM and A is an irreducible max-plus matrix. As stated before, we consider the infinite-horizon forward and backward reachability analysis of autonomous MPL models:

$$F_{+\infty} = \bigcup_{k=0}^{+\infty}\{A^{\otimes^k}\otimes x : x\in D_0\},$$
$$B_{+\infty} = \bigcup_{k=0}^{+\infty}\{x\in\mathbb{R}^n : A^{\otimes^k}\otimes x\in D_0\}.$$

4 The Results

For each D_0, since A is an irreducible max-plus matrix, there exist $m_0, n_0\in\mathbb{N}$ such that $\cup_{k=0}^{M}\{A^{\otimes^k}\otimes x : x\in D_0\}$ and $\cup_{k=0}^{N}\{x\in\mathbb{R}^n : A^{\otimes^k}\otimes x\in D_0\}$ are the same for $M\geq m_0$, $N\geq n_0$. This leads to conclude that we can compute $F_{+\infty}$ and $B_{+\infty}$ with a finite-time procedure, which however may not handle large dimensional autonomous MPL systems due to the complexity of the involved operations.

Since $D_0\subseteq F_{+\infty}$ and $D_0\subseteq B_{+\infty}$, we know that $F_{+\infty}$ and $B_{+\infty}$ are non-empty sets. It can be shown that both the image and the inverse image of a DBM are finite unions of DBMs. By induction, it can be concluded that $F_{+\infty}$ and $B_{+\infty}$ are finite unions of DBMs.

5 Conclusions and Future Work

This work has put forward the infinite-horizon reachability analysis of autonomous MPL systems. We have designed a procedure to solve this problem. The authors are currently investigating the extension to the controlled case.

References

[1] F. Baccelli, G. Cohen, G.J. Olsder, and J.P. Quadrat. *Synchronization and Linearity, An Algebra for Discrete Event Systems*. John Wiley and Sons, 1992.

[2] S. Gaubert, and R. Katz. Reachability and Invariance Problems in Max-plus Algebra. In *Positive Systems*, vol. 294 of *LNCIS*, pp. 15-22. Springer Berlin / Heidelberg, 2003.

[3] D. Dill. Timing assumptions and verification of finite-state concurrent systems. In *Automatic Verification Methods for Finite State Systems*, vol. 407 of *LNCS*, pp. 197-212. Springer Berlin / Heidelberg, 1990.

Optimal sampler with preview from a system theoretic viewpoint

Hanumant Singh Shekhawat
Department of Applied Mathematics
University of Twente
P.O. Box 217, 7500 AE Enschede
The Netherlands
Email: h.s.shekhawat@utwente.nl

Gjerrit Meinsma
Department of Applied Mathematics
University of Twente
P.O. Box 217, 7500 AE Enschede
The Netherlands
Email: g.meinsma@utwente.nl

1 Introduction

Most of the signals in real world are analog in nature (e.g. speech). For high quality transmission, these analog signals are often discretized before transmission. At the receiving end, the discretized signal is converted back to analog signal. The problem of reconstructing the original signal from the discretized signal is known as signal reconstruction problem. One approach to solve the signal reconstruction problem uses the sampled data system theory (see e.g. [1]) whose setup is shown in Figure 1. This theory uses a signal generator G driven by a standard signal w to model the analog signal y. Generally G is a causal linear continuous-time (LCTI) system driven by impulse or white noise. The analog signal y is converted into discrete $\bar{y}$ with the help of a sampler $\mathcal{S}$ by sampling at interval h. This discrete signal $\bar{y}$ is converted back to analog signal u with the help of a Hold $\mathcal{H}$. This reconstructed signal u must be as close as possible to the analog signal y (or v if a model of another process like noise during transmission is incorporated in $\mathcal{G}$). The quality of the reconstruction process in sampled-data system theory is generally measured by L^2 (or H^2) or L^∞ (or H^∞) norm of the error system $\mathcal{G}_\mathrm{e} := \mathcal{G}_\mathrm{v} - \mathcal{H}\mathcal{S}\mathcal{G}_\mathrm{y}$ where $\mathcal{G} = \begin{bmatrix}\mathcal{G}_\mathrm{v} & \mathcal{G}_\mathrm{y}\end{bmatrix}^T$ (see [1] and the references therein). The problem that we

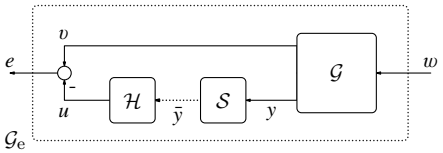

Figure 1: Sampled-data setup

consider is that of design of optimal sampler with given preview, for a given Hold $\mathcal{H}$ and $\mathcal{G}$. More precisely, we allow sampler to be l-causal meaning that it is non-causal upto lh time (so for $l = 0$ it is just causal and for $l = 1$ we allow preview of h time et cetera). Systems are considered stable if its 2-norm induced operator norm is finite. The problem we consider is:

Problem $\boldsymbol{\mathcal{P}_1}$: Given causal $\mathcal{G}_\mathrm{v}$ and $\mathcal{G}_\mathrm{y}$, causal and stable $\mathcal{H}$, and $l \geq 0$, find an l-causal and stable sampler $\mathcal{S}$ that renders $\mathcal{G}_\mathrm{e} := \mathcal{G}_\mathrm{v} - \mathcal{H}\mathcal{S}\mathcal{G}_\mathrm{y}$ stable and minimizes $\|\mathcal{G}_\mathrm{e}\|_{\mathrm{L}^2}$.

2 Design of a optimal sampler with given preview

We use the lifting Fourier transform (see e.g. [1]) to obtain the solution of the Problem $\boldsymbol{\mathcal{P}_1}$. We represent the lifted Fourier domain equivalent of $\mathcal{G}_\mathrm{v}$, $\mathcal{G}_\mathrm{y}$, $\mathcal{H}$ and $\mathcal{S}$ by $\breve{G}_\mathrm{v}$, $\breve{G}_\mathrm{y}$, $\grave{H}$ and $\acute{S}$ respectively. Also, we denote the space of all stable l-causal systems by $z^l\mathrm{H}^\infty$. The Problem $\boldsymbol{\mathcal{P}_1}$ in lifted frequency domain is given by:

Problem $\boldsymbol{\mathcal{P}_2}$: Given causal $\breve{G}_\mathrm{v}(z)$ and $\breve{G}_\mathrm{y}(z)$, $\grave{H} \in \mathrm{H}^\infty$ and $l \geq 0$, find $\acute{S} \in z^l\mathrm{H}^\infty$ that renders $\breve{G}_\mathrm{e} := \breve{G}_\mathrm{v} - \grave{H}\acute{S}\breve{G}_\mathrm{y} \in \mathrm{L}^\infty \cap \mathrm{L}^2$ and minimizes $\|\breve{G}_\mathrm{e}\|_{\mathrm{L}^2}$.

Now, we describe the solution of the Problem $\boldsymbol{\mathcal{P}_2}$.

Proposition 2.1. *Assume that $\mathcal{G}_\mathrm{y}$ is rational and $\breve{G}_\mathrm{y}(\mathrm{e}^{\mathrm{j}\theta})\breve{G}_\mathrm{y}(\mathrm{e}^{\mathrm{j}\theta})^* > 0$ for all $\theta \in [0, 2\pi]$. Also assume that there exist a factorization of $\grave{H} = \grave{H}_\mathrm{i}\bar{H}_\mathrm{o}$ such that $\grave{H}_\mathrm{i}$ is inner and $\bar{H}_\mathrm{o}$ is bistable and bicausal outer function. Now, a solution to Problem $\boldsymbol{\mathcal{P}_2}$ exists iff*

1. *There exists a coprime factorization over H^∞ of $\breve{G} := \begin{bmatrix}\breve{G}_\mathrm{v} & \breve{G}_\mathrm{y}\end{bmatrix}^T$ of the form $\breve{G} = \begin{bmatrix}I & \breve{M}_\mathrm{v} \\ 0 & \breve{M}_\mathrm{y}\end{bmatrix}^{-1}\begin{bmatrix}\breve{N}_\mathrm{v} \\ \breve{N}_\mathrm{y}\end{bmatrix}$ with $\breve{M}_\mathrm{y}, \breve{N}_\mathrm{y} \in \mathrm{H}^\infty$ left coprime and $\breve{N}_\mathrm{y}$ co-inner.*
2. *$(I - \grave{H}_\mathrm{i}\grave{H}_\mathrm{i}^\sim)\breve{G}_\mathrm{v} \in \mathrm{L}^2 \cap \mathrm{L}^\infty$ and there exists a $\acute{V} \in \mathrm{L}^\infty$ such that $\acute{M}_\mathrm{h} := \grave{H}_\mathrm{i}^\sim\breve{M}_\mathrm{v} - \acute{V}\breve{M}_\mathrm{y} \in z^l\mathrm{H}^\infty$.*

Then, $\acute{S}_\mathrm{opt} = \bar{H}_\mathrm{o}^{-1}(\acute{S}_{\alpha,\mathrm{opt}}\breve{M}_\mathrm{y} - \acute{M}_\mathrm{h})$ solves Problem $\boldsymbol{\mathcal{P}_2}$ where $\acute{S}_{\alpha,\mathrm{opt}} = \mathrm{proj}_{z^l\mathrm{H}^2}(\grave{H}_\mathrm{i}^\sim\breve{N}_\mathrm{v}\breve{N}_\mathrm{y}^\sim - \acute{V})$ and proj is the orthogonal projection on $z^l\mathrm{H}^2$ (the space of l-causal systems with finite L^2 norm). Moreover, the error norm satisfies

$$\|\breve{G}_\mathrm{v} - \grave{H}\acute{S}_\mathrm{opt}\breve{G}_\mathrm{y}\|_2^2 = \|\breve{G}_\mathrm{v} + \grave{H}_\mathrm{i}\acute{M}_\mathrm{h}\breve{G}_\mathrm{y}\|_2^2 - \|\acute{S}_{\alpha,\mathrm{opt}}\|_2^2$$

It can shown that if $\mathcal{T}_l(\grave{H}_\mathrm{i}^\sim\breve{M}_\mathrm{v}\breve{M}_\mathrm{y}^{-1}) \in z^l\mathrm{H}^\infty$ (where $\mathcal{T}_l(\sum_{k\in\mathbb{Z}} a_k z^{-k}) = \sum_{k<l} a_k z^{-k}$) then there exists a $\acute{V} \in \mathrm{L}^\infty$ such that $\acute{M}_\mathrm{h} := \grave{H}_\mathrm{i}^\sim\breve{M}_\mathrm{v} - \acute{V}\breve{M}_\mathrm{y} \in z^l\mathrm{H}^\infty$.

References

[1] G. Meinsma and L. Mirkin. Sampling from a system-theoretic viewpoint: Part I—concepts and tools. *IEEE Trans. Signal Processing*, 58(7):3578–3590, July 2010.

Higher Order Approximations for Verification of Stochastic Hybrid Systems

Sadegh Esmaeil Zadeh Soudjani and Alessandro Abate
Delft Center for Systems and Control
Technische Universiteit Delft
Mekelweg 2, 2628 CD, Delft
The Netherlands
Email: {S.EsmaeilZadehSoudjani,A.Abate}@tudelft.nl

1 Abstract

This work investigate approximate solutions of the probabilistic safety (invariance) problem for Stochastic Hybrid Systems. Algorithms for the efficient computation of the approximate solution with specific bounds on the error are presented. Depending on the selected procedure, which is based on a state space partitioning approach, the approximation error is proportional to a higher order function of the chosen partition size.

2 Introduction

Stochastic Hybrid Systems (SHS) provide an excellent framework to model the interaction of discrete, continuous, and probabilistic dynamics. Developing efficient numerical methods for formal analysis and verification of SHS models is a topic of research in recent years. These numerical approaches are based on state space partitioning: [1] proposes a gridding that is uniform in the abstraction step, and which suffers from heavy computational costs. The work in [2] provides adaptive gridding to improve the abstraction error and to reduce the numerical costs, whereas [3] generalizes the procedure to mixed deterministic-stochastic models.

3 Problem Statement

Stochastic Hybrid Systems can be modelled as a Markov process over a general state space. Consider a discrete time Markov process over the state space $\mathscr{S}$ with one-step conditional distribution function $t_s(.|s)$. We are interested in the probabilistic invariance problem, i.e. in computing the probability that an execution associated to the process with the initial condition $s_0 \in \mathscr{S}$ remains within a bounded set A over a finite time horizon $[0,N]$:

$$p_{s_0}(A) \doteq P\{s(k) \in A, \forall k \in [0,N] | s(0) = s_0\}. \quad (1)$$

Defining the following operator over the set of continuous functions

$$T(f)(s) = \mathbb{I}_A(s) \int_{\mathscr{S}} f(\bar{s}) t_s(\bar{s}|s), \quad (2)$$

we are able to characterize the solution of problem (1) by applying the operator T^N on the indicator function of the set A. The solution of this procedure is rarely analytic. Hence, we have to propose some numerical procedure to approximate it.

4 Numerical Approach

Suppose Π is a given linear operator on a set of functions that satisfies the inequality in (3). Under some regularity conditions on the argument function f:

$$\|\Pi(f) - f\|_\infty \leq \varepsilon. \quad (3)$$

Using this operator we stablish the following inequality:

$$\|T^N(\mathbb{I}_A) - (\Pi T)^N(\mathbb{I}_A)\|_\infty \leq \mathscr{K}\varepsilon, \quad (4)$$

where the constant $\mathscr{K}$ depends on the structure of the conditional density function $t_s(.|s)$.

We employ interpolation theorems for function approximation to construct the operator Π. The newly developed algorithms require finite number of function evaluations in each step. They provide specific bounds on the approximation error that are proportional to a higher order function of the grid size, depending on the operator Π.

We have implemented the results on a one dimensional case study taken from financial mathematics. We have also applied the algorithms to a chemical reaction network characterized by species with heterogeneous concentrations.

References

[1] A. Abate, J.-P Katoen, J. Lygeros, and M. Prandini, "Approximate Model Checking of Stochastic Hybrid Systems," European Journal of Control, nr. 6, pp. 624-641, 2010.

[2] S. Esmaeil Zadeh Soudjani and A. Abate, "Adaptive Gridding for Abstraction and Verification of Stochastic Hybrid Systems," Proceedings of the 8th International Conference on Quantitative Evaluation of SysTems, QEST11, Aachen (DE), Sept. 2011, pp. 59–69.

[3] S. Esmaeil Zadeh Soudjani and A. Abate, "Probabilistic Invariance of Mixed Deterministic-Stochastic Dynamical Systems," ACM Proceedings of the 15th International Workshop on Hybrid Systems: Computation and Control, Apr 2012, Beijing, PRC. To appear.

Design of multilevel signals for identifying the Best Linear Approximation of Nonlinear Systems

Hin Kwan Wong
School of Engineering, University of Warwick, Coventry, CV4 7AL, U.K.
Hin.Wong@warwick.ac.uk

Johan Schoukens
ELEC dept., Vrije Universiteit Brussel, 1050 Brussels, Belgium
Johan.Schoukens@vub.ac.be

Keith R. Godfrey
School of Engineering, University of Warwick, Coventry, CV4 7AL, U.K.
K.R.Godfrey@warwick.ac.uk

Abstract

There are many kinds of excitation signals with different advantages. In identification of a nonlinear system one may be interested in linearisation, involving the estimation of the Best Linear Approximation (BLA) [1-5] of the said system. The BLA is 'best' in terms of the minimisation of errors in least square sense. The BLA depends on the types of input signal used; more specifically, the amplitude distribution or the higher order moments of the signal. BLA obtained from Gaussian signals (Gaussian BLA) is well studied and has well known properties. For example, in a cascaded block structured system, the Gaussian BLA is directly proportional to the cascaded linear dynamics.

The use of any other signals would result in a BLA with a bias compared with the Gaussian BLA [6]. The amount of bias depends on the details of the system – the linearities, nonlinearities, and the higher order moments of the input signal. It is therefore possible to tune a random signal to mimic 'Gaussianity' to drive down the bias. Here the term Gaussianity simply refers to a qualitative measure of how close a signal matches a zero-mean random Gaussian signal in terms of their higher order moments. With signal power (i.e. second order moment) normalised, by adjusting signal levels and the probabilities of a signal being at these levels, it is possible to match exactly one higher order moment term for a ternary sequence, two for a quaternary sequence, three for a quinary sequence and so on. When these sequences are used as inputs to identify the BLA of a simple Wiener system with a polynomial nonlinearity, the BLA would contain precisely zero bias for nonlinearity up to and including the third degree for ternary sequences, fifth degree for quaternary sequences and seventh degree for quinary sequences.

Two simulation experiments were conducted; Firstly, with signal power normalised, symmetric ternary sequences with levels $\{+a, 0, -a\}$ were generated with different probabilities of symbols at level zero. These sequences were used to identify the BLA of a Wiener system with a pure cubic nonlinearity. Theory suggested that for this system, when the probability of being at level zero is set as 2/3 and the probability at either levels of high and low is set as 1/6, one would obtain a BLA with exactly zero bias. This was tested along with the case where the pure cubic nonlinearity is replaced by a saturation nonlinearity. Secondly, discrete sequences with 3, 4 and 5 levels were designed to mimic Gaussianity as close as possible. Along with their uniformly distributed counterparts, these sequences were used to identify the BLA of a Wiener system with a seventh degree polynomial nonlinearity. Their performance was compared with the Gaussian case.

References

[1] M. Enqvist and L. Ljung, "Linear approximations of nonlinear FIR systems for separable input processes," Department of Electrical Engineering, Linköping University, SE-581 83 Linköping, Sweden, Tech. Rep. LiTH-ISY-R-2718, Dec. 2005.

[2] R. Pintelon and J. Schoukens, *System identification: a frequency domain approach*. John Wiley and Sons, Jan. 2001.

[3] P. Mäkilä and J. Partington, "Least-squares LTI approximation of nonlinear systems and quasistationarity analysis," *Automatica*, vol. 40, pp. 1157–1169, Jul. 2004.

[4] P. M. Mäkilä, "On optimal LTI approximation of nonlinear systems," *IEEE Trans. on Automatic Control*, vol. 49, no. 7, pp. 1178– 1182, Jul. 2004.

[5] P. Mäkilä, "LTI approximation of nonlinear systems via signal distribution theory," *Automatica*, vol. 42, pp. 917–928, Jun. 2006.

[6] H. K. Wong, J. Schoukens, and K. R. Godfrey, "Analysis of best linear approximation of a WienerEHammerstein system for arbitrary amplitude distributions," *IEEE Trans. on I&M*, DOI:10.1109/TIM.2011.2169615.

Identification of nonlinear systems via a powerful block-oriented nonlinear model

Laurent Vanbeylen
Vrije Universiteit Brussel (Dept. ELEC)
Pleinlaan 2, B-1050 Brussel, Belgium

1 Motivation and goal

Nonlinear operation of devices is ubiquitous in practical application examples. When the nonlinearities are small, a linear system may be sufficient. In such a situation, a well-established framework of system identification theory and methods can be used. However, in nonlinear identification, there is still a lot of work to be done. This topic is concentrating on the identification of the most general block-oriented nonlinear model structure with the restriction that there is no more than one static nonlinearity (SNL), shown in Figure 1, a.k.a. Linear Fractional Representation (LFR) model in the literature. Its flexibility (power) comes from the multiple-input-multiple-output, linear time-invariant (MIMO-LTI) part of the model, which realizes an arbitrary interconnection between the model input u, model output y, input y_2 and output u_2 of the SNL. As suggested by Figure 1, the model encompasses, e.g., the Wiener-Hammerstein and nonlinear feedback block-oriented models. Besides, the model structure is also reasonably parsimonious, since it involves a relatively low number of parameters. The model may be a good starting point as a first nonlinear model candidate, and serve as an initial guess for other nonlinear identification methods, such as the polynomial nonlinear state-space model [1], relying now on a linear initialization (Best Linear Approximation), which may otherwise be located too far from the global solution of the nonlinear optimization procedure.

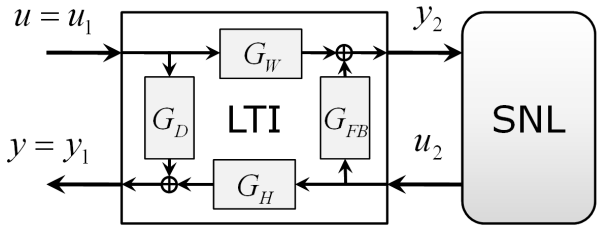

Figure 1: The considered nonlinear LFR model structure, consisting of a MIMO-LTI and a SNL part.

2 The underlying ideas of the method

The method, aiming at generating initial estimates for the LFR model, is based on Best Linear Approximations constructed at 2 different input amplitude levels. Making the approximation that the input of the SNL (signal y_2) is Gaussian, results in a BLA obtained by replacing the SNL by an amplitude-dependent gain. Written in state-space form, it turns out that a certain rank-one modification acts on the state-space matrices, when the input amplitude varies, leading to a variation of the gain related to the SNL. The method essentially equates the BLA's at both levels (state-space representations obtained via a frequency domain subspace method) to the theoretical expression, taking the (unavoidable) similarity transformations into account. As a result (after solving the matrix equations), both gains related to the BLA and the MIMO-LTI part are retrieved. Next, the SNL can be fitted in a nonparametric way from a scatter plot of the inner signals (reconstructed via u, y, and the MIMO-LTI). A weighted least-squares method then yields a parametric estimate. See [2] for more details. The simulation results for an arrow-shaped validation signal show that the initial estimate of the nonlinear LFR model outperforms both BLA models (see Figure 2).

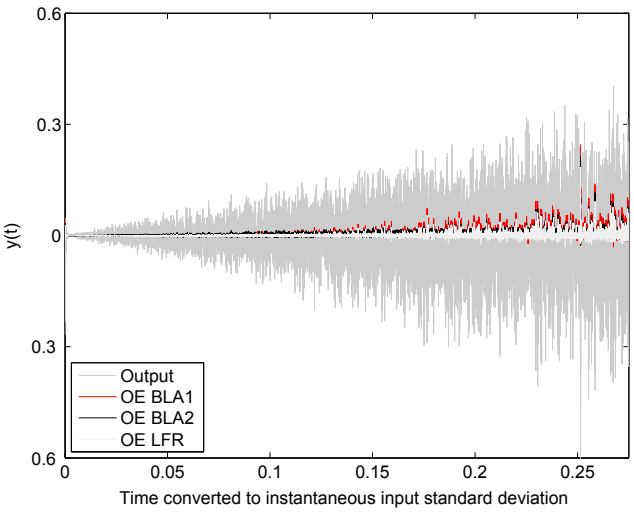

Figure 2: Validation output and model errors vs. time (converted to instanteneous standard deviation). OE-BLA1: simulation output error of the BLA at amplitude 1. White: simulation output error of the obtained LFR model.

References

[1] J. Paduart, L. Lauwers, J. Swevers, K. Smolders, J. Schoukens, and R. Pintelon, "Identification of nonlinear systems using polynomial nonlinear state space models," *Automatica*, vol. 46, no. 4, pp. 647–656, 2010.

[2] L. Vanbeylen, "Initial estimates for the LFR nonlinear model structure via the Best Linear Approximation," submitted to *IFAC Symposium on System Identification* (SYSID), 2012.

Detecting the Time Variation in an Assumed Linear, Time Invariant Measurement

John Lataire, Ebrahim Louarroudi and Rik Pintelon
Vrije Universiteit Brussel, Dept. ELEC, Pleinlaan 2, 1050 Elsene, Belgium,
Email: jlataire@vub.ac.be

1 Motivation

What are the consequences of processing measurements, made on a linear time-varying (LTV) system, by tools meant for linear time invariant (LTI) systems? This question is relevant in applications where the use of LTI models is preferred, and one wants to assert the validity of the LTI assumption. This is to be done by means of a minimal additional amount of processing power.

2 Problem formulation

Given an LTV system, its associated best LTI approximation is defined such that it minimises the output error in the least squares sense, for white noise or random phase multisine excitations. As shown in Fig. 1, the LTV system G_{V} is equivalent to the LTI system G_{BLTIA}, the output of which is disturbed by N_{TV}, an additional error term. BLTIA stands for Best Linear Time Invariant Approximation. G_{BLTIA} is determined such as to minimise N_{TV} in the least squares sense.

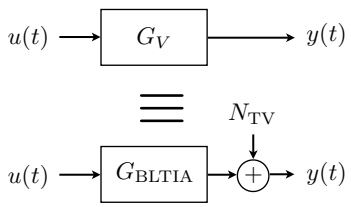

Figure 1: Approximating the LTV system G_{V} as a linear time invariant system and an error term N_{TV}.

If G_{V} is time-varying, the error term N_{TV} will be non-stationary. As a result, the spectrum of N_{TV} is correlated over the frequency. This property gives a means to detect time variations in measurements.

3 Methodology

For given measurements of the input and the output signals, the FRF (Frequency Response Function) of the system is estimated using the Local Polynomial Method (LPM) described in [2]. This method smooths the FRF estimate, and is shown to provide an unbiased estimate of the BLTIA of the system [1].

If the hypothesis of the system being time-varying is true, then, assuming a slow variation, an order of magnitude of the ratio of the variance of N_{TV} to its correlation at lag 1 can be computed, *viz.*

$$\frac{\mathbb{E}\left\{|N_{\mathrm{TV}}(k)|^2\right\}}{\mathbb{E}\left\{N_{\mathrm{TV}}(k)\overline{N_{\mathrm{TV}}(k+1)}\right\}} = \frac{\pi^2}{6} \tag{1}$$

At those frequencies where this ratio, estimated using the measured signals, is significantly higher than $\pi^2/6$, the time variation is below the noise floor. Otherwise, the time variation is visible in the data.

This is illustrated in Fig. 2, where the BLTIA of a system with slowly time-varying resonance frequency is estimated. The uncertainty on this estimate is shown to be mainly due to the time variation in the lower half of the frequency band ('o' in the figure) and due to noise in the upper half ('x').

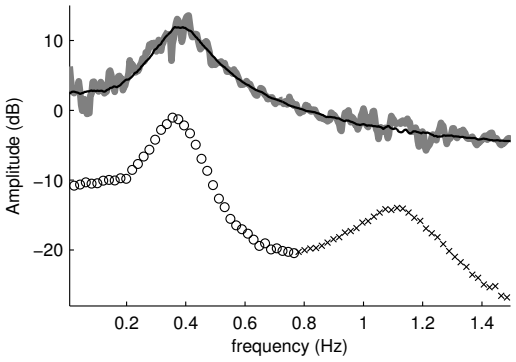

Figure 2: Black full line: BLTIA, Grey line: estimated BLTIA, Circles and crosses: variance on estimated BLTIA with dominating time variation and noise respectively.

Acknowledgement - This work was supported in part by the Fund for Scientific Research (FWO-Vlaanderen), by the Flemish Government (Methusalem Fund, METH1), and by the Belgian Federal Government (IUAP VI/4).

References

[1] J. Lataire, E. Louarroudi, and R. Pintelon. Nonparametric best linear time invariant approximation of a linear time-varying system. Under review for the IEEE transactions on Instrumentation and Measurement, special Issue on Measurements, 2012.

[2] R. Pintelon, J. Schoukens, G. Vandersteen, and K. Barbé. Estimation of nonparametric noise and FRF models for multivariable systems–Part I: Theory. *Mechanical Systems and Signal Processing*, 24(3):573 – 595, 2010.

Nonlinear block-oriented identification for insulin-glucose models

Anna Marconato[1], Maarten Schoukens[1], Koen Tiels[1], Amjad Abu-Rmileh[2], Johan Schoukens[1]
(1) Dept. ELEC, Vrije Universiteit Brussel, Pleinlaan 2, 1050 Brussels, Belgium
Email: anna.marconato@vub.ac.be
(2) GRECS group, University of Girona, Campus Montilivi, 17071 Girona, Spain

1 Introduction

The application of advanced identification techniques to model insulin-glucose systems represents a crucial step towards the development of the artificial pancreas for diabetes patients. Type 1 diabetes mellitus (T1DM) is a disease characterized by the fact that the pancreas is not able to produce a sufficient amount of insulin. Therefore, when treating patients with exogenous insulin delivery, the level of glucose in the blood needs to be carefully regulated to avoid severe problems such as hypoglycemia, retinopathy or cardiovascular diseases.

Several mathematical descriptions (mainly first principle models) have been considered to represent the diabetic patient, and automated closed-loop control systems based on these models are currently under study [1]. The main difficulties associated to the existing models are related to the fact that the tuning of parameters differs for each patient, and that the model parameters cannot be identified in practice.

The objective of this work is the identification of models to describe the glucoregulatory system, based on input-output data. In particular, nonlinear system identification methods for block structures are combined with the use of nonlinear functions from statistical learning, e.g. Neural Networks (NNs).

2 Model structure

In this work, a Wiener structure is considered to model the insulin-glucose system, on the basis of a set of input-output simulation data generated using the Hovorka model (see [1]).

Figure 1 shows the considered model structure. Since the data were collected for 12 different operating points of the system, the linear part in the Wiener model consists of 12 different linear blocks, i.e. for each operating point the Best Linear Approximation (BLA) is estimated [2]. Hence the nonlinear part should contain switching functions to describe the system behavior in the different regions. The nonlinear block consists of the sum of one-input one-output piecewise linear functions. As an alternative, a 12-input one-output one-hidden-layer NN with saturation basis functions is also considered [3].

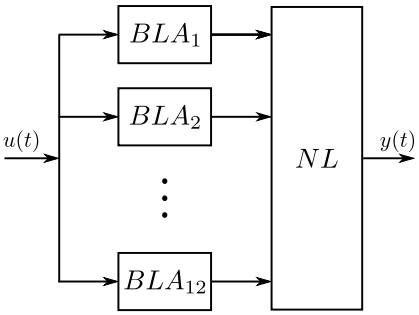

Figure 1: Wiener structure used to model the insulin-glucose system.

3 Simulations

Different excitation signals have been employed for the estimation and validation of the Wiener model: a Random Phase Multisine with five different amplitude levels, and a pulse excitation. For the nonlinear part of the model, several kinds of basis function were tested, including polynomial, sigmoidal and RBF nonlinearities, obtaining the best results using a simple piecewise linear function.

Preliminary investigations proved to be quite successful, resulting in models characterized by good levels of accuracy for all the 12 different operating points of the system (more than 95% of the output power is captured by the models). Future steps will aim at reducing the number of parameters in the model. Finally, a different description of the insulin-glucose system (the Meal model, see [1]) will also be taken into account, for which a single linear block in the Wiener structure might be sufficient to capture the dynamics of the system.

References

[1] A. Abu-Rmileh, W. Garcia-Gabin, “Smith Predictor Sliding Mode Closed-loop Glucose Controller in Type 1 Diabetes”, 18th IFAC World Congress, Milano, Italy, 2011.

[2] R. Pintelon, J. Schoukens, System Identification. A Frequency Domain Approach, IEEE Press, New Jersey, 2001.

[3] T. Hastie, R. Tibshirani, J. Friedman, The Elements of Statistical Learning: Data Mining, Inference, and Prediction, Springer-Verlag, 2009.

Distributed Dynamic Price Mechanism in The New Gas Chain

Desti Alkano and Jacquelien M.A. Scherpen
Faculty of Mathematics and Natural Sciences
University of Groningen
The Netherlands
Email: d.alkano@rug.nl, j.m.a.scherpen@rug.nl

1 Introduction

In the near future, the Dutch gas distribution is changing due to the decline of domestic gas production and the increase of renewable gas from a share of 0.1% to 8 - 12% and 15 - 20% in 2020 and 2030, respectively [1]. The renewable gas are mainly produced by farmers. Hence, they can be both producer and consumer (prosumer) in the gas grid. This leads the gas infrastructure change toward a multi-producer multi-consumer market. Along with the possibilities that the prosumers have gas storage, the future gas grid can no longer be passive. The grid needs monitoring and controlling over the balance among gas production, consumption, and storage within the network.

The research aims at providing a fair and optimal price mechanism for heterogeneous prosumers in the gas grid. The expected outcome is a balance among supply, demand, and storages in the network. The developments will be built upon the results of the Flexines project which is developed for the electricity grid [2].

2 Research Framework

Given a similar case applied to the electricity chain, we intend to translate the dynamical price mechanism into the new gas value chain. The main difference between the gas and electricity network is that the objective function in the electricity network is to balance between the supply and demand in the grid as the electricity cannot be efficiently stored at a large scale [2]. Additionally, the gas grid needs to maintain the gas pressure within a certain range corresponding to the desired service level to the prosumers in the gas grid. Moreover, there are a number of quality issues involved in the gas value chain. The gas from different fields has different gas quality in terms of energy content and its chemical composition. In this research, we focus on a local gas network. Thus, it is assumed that the gas within the grid has the same quality.

The state space representation used to describe the system of a local gas grid is given by

$$x(t+1) = Ax(t) + Bu(t) + Cv(t) + d(t), \qquad (1)$$

where $x(t)$, $u(t)$, $v(t)$, and $d(t)$ represent imbalance, change in supply $(p(t+1)-p(t))$, amount of gas stored in a storage device, and change in demand, respectively.

We aim to include small and large prosumers in the dynamic pricing. Hence, topology of the network and the input matrix shown in A and B matrix, respectively, play important role in representing the heterogeneous prosumers.

The objective function is then to minimize global cost of the gas network.

$$J_u(K) = \lim_{K\to\infty} \frac{1}{K} \sum_{k=1}^{K} E\left[|x(k)|^2 + |u(k)|^2 + |v(k)|^2\right] \qquad (2)$$

over the solution of the equation (1)

The procedure in obtaining the optimization problem fully distributed can be found in [2]. The distributed dynamic price mechanism is then achievable.

We also intend to discuss price schemes under optimal storage shown in [3]. It proposes a balance by satisfying the demand with renewable gas production and storing the excess gas supply at peak prices and the reverse order at lower prices.

3 Acknowledgements

This research is supported by the Edgar project. The partners of this project are the University of Groningen, KEMA, and Gasterra BV.

References

[1] J. Wempe, "Let's give full gas! The role of green gas in the Dutch energy management system," Senter November, 2007.

[2] G. Larsen, J.M.A. Scherpen, and N.D. vanForeest, "Local supply demand Balancing through Prices: Distributed MPC for controlling micro-CHPs in a network," Submitted.

[3] P. Harsha, and M. Dahlel, "Optimal sizing of energy storage for efficient integration of renewable energy," The 50th IEEE Conference on Decision and Control and European Control Conference. Orlando, 2011.

A plug and control strategy for simulated moving bed processes

Paul Suvarov, Alain Vande Wouwer
Service d'Automatique, Université de Mons,
B-7000 Mons, Belgium
Email : Paul.Suvarov@umons.ac.be;
Alain.VandeWouwer@umons.ac.be

Achim Kienle
Max-Planck-Institut für Dynamik komplexer
technischer Systeme,
D-39106 Magdeburg, Germany
Email : Kienle@mpi-magdeburg.mpg.de

1. Introduction

The simulated moving bed (SMB) is a continuous chromatographic separation process used for separation of chemical mixtures. It has been used in the industry for separations of cheap products like sugar and hydrocarbon, and high-added value products like enantiomers and proteins. Various processes have been developed to exploit the different degrees of freedom of the SMB, in this way improving the productivity and the cost of the separation. In the industry, most of these processes are operated in open-loop at suboptimal operating points, so as to have a security margin to face disturbances, at the expense of longer separation time and higher costs. Hence, besides the selection of optimal operating conditions, the regulation of the SMB process has attracted considerable attention.

In [1] a simple adaptive control scheme has been proposed for the SMB process, based on linear adsorption isotherms, a discrete-time model of the front wave position and an adaptation scheme for the wave velocity. This control scheme has the advantage of simplicity, as even a proportional controller can be sufficient in most cases, but also to require little prior knowledge about the adsorption properties (isotherm parameters), and to be self-optimizing as it allows the concentration fronts to be moved in optimal locations.

In the present study, the control concept is further analysed for the case of linear and nonlinear adsorption isotherms based on two case studies, i.e. the separation of Fructo-OligoSaccharides (FOS) and cyclopentanone – cycloheptanone [2]. Extensive simulation tests are conducted to investigate the control performance and robustness.

2. Control design and parameter estimation

In order to control the purities at the outputs, feedback regarding the position of the waves, forming the inner concentration profiles, is required. The position of the waves is determined from concentration measurements performed by UV detectors placed in the middle of each zone, and can be adjusted by manipulating the external flow-rates and the duration of the cycle. The manipulated variables are computed at the beginning of the cycle and are considered to be constant until the next one.

To face perturbations, the following feedback control law is considered:

$$w_i(k) = \theta_i \left(1 - K\left(y_{REF,i} - y_i(k)\right)\right),\ i = I,...,IV \qquad (1)$$

where θ_i are the optimal open-loop inputs of the process, K is the controller gain, $y_i(k)$ and $y_{REF,i}$ are the measured and reference position of the waves. The external flow-rates and the duration of the new cycle are computed from $w_i(k)$ by imposing the feed flow-rate.

To face parameter changes (or lack of prior knowledge), a parameter estimator is introduced.

$$\hat{\theta}_i(k+1) = \hat{\theta}_i(k) + (1 - K_\theta)\tilde{\theta}_i(k),\ 0 \le K_\theta \le 1 \qquad (2)$$

where K_θ is the estimator gain and $\tilde{\theta}_i(k)$ are the parameter errors computed from the measurements and the estimation of the position of the wave given by a foot-point model.

The control strategy is summarized in figure 1.

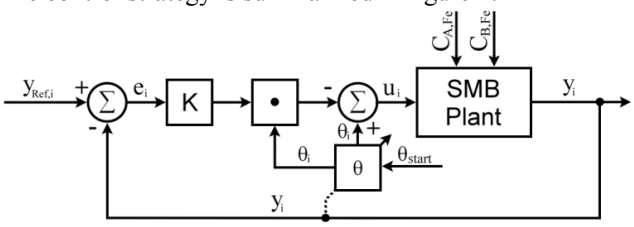

Fig. 1. Controller with parameter estimation

Acknowledgments

The authors gratefully acknowledge the support of the Belgian Network DYSCO (Dynamical Systems, Control, and Optimization), funded by the Interuniversity Attraction Poles Programme, initiated by the Belgian State, Science Policy Office. The scientific responsibility rests with its author(s).

References

[1] Fütterer M., "*An adaptive control concept for Simulated Moving Bed plants in case of complete separation*", Chemical Engineering and Technology 31 (10), p. 1438–1444, 2008.

[2] Grosfils, V., Levrie, C., Kinnaert, M. and Wouwer, A.V., "*A systematic approach to SMB processes model identification from batch experiments*", Chemical Engineering Science 62 (15), pp. 3894-3908, 2007.

Time-energy optimal control of a driveline by multi-objective dynamic programming

M. Witters[1], G.Pinte[1], W. Symens[1]
[1] Flanders' Mechatronic Technology Centre,
Celestijnenlaan 300D, B-3001 Leuven, Belgium.
e-mail: maarten.witters@fmtc.be

1 Introduction

This paper presents a multi-objective dynamic programming algorithm to determine the trade-off between time-optimal and energy efficient control of a driveline for a heavy duty vehicle. The driveline consists of an internal combustion engine, a torque converter and a gear box with three gear ratios, actuated with wet clutches. In the past decade, fuel economy has become more and more important for automotive industry. Rule-based supervisory control strategies are commonly used to schedule the gear shifts. These algorithms typically neglect the efficiency characteristics of the driveline components, yielding a suboptimal performance. Dynamic programming [1] is often proposed for the energy efficient control of automotive drivelines [2]. However, most publications are limited to simulation studies and ignore time-optimality.

The developed multi-objective control algorithm allows to determine the trade-off between time-optimal and energy-efficient control of the driveline. The algorithm uses physical models for the driveline components which describe their efficiency characteristics and are identified based on experimental data. The developed approach is experimentally validated on a wet clutch driveline test set-up, shown in figure 1. The obtained results show a significant reduction both in time and in fuel consumption can be achieved with respect to an industrial rule-based control algorithm currently used in heavy duty vehicles.

Figure 1: a wet clutch driveline test set-up

2 Multi-objective dynamic programming

To determine the trade-off between time-optimal and energy efficient control of a driveline, a multi- objective dynamic programming (*MO-DP*) algorithm is developed. In dynamic programming (*DP*), discretization decomposes the optimal control problem into smaller sub-problems for which the optimal driveline inputs, gear ratio and required engine torque, are easily computed. Next, a combinatorial search is performed to retrieve the optimal inputs for the entire manoeuvre. Opposed to the *DP* approach, *MO-DP* threats the output speed as an additional degree of freedom, which allows to compromise time-optimality and energy efficiency. The algorithm uses experimentally identified physical models for the driveline components which describe their efficiency characteristics. The engine efficiency is given by the specific fuel consumption map. A look-up table describes the speed-dependent characteristics of the torque converter. The transmission model includes the drag losses in the clutches and heat losses in the gears.

The developed *MO-DP* algorithm returns a set of pareto-optimal control signals with respect to time and fuel consumption. The right graph of figure 2 gives this pareto-front for an acceleration from *100* to *600 rpm*. The graphs at the left show respectively the scheduled gear and the fuel consumption for two points of the pareto-front (*DP1* and *DP2*) and the rule-based control strategy that targets a maximum tractive effort (*MTE*). These experiments demonstrate that accelerating in first gear is slightly faster, but consumes about *10 %* more fuel than when an up-shift is included. The rule-based control schedules the up-shift earlier which is suboptimal, as it falls beyond the pareto-front.

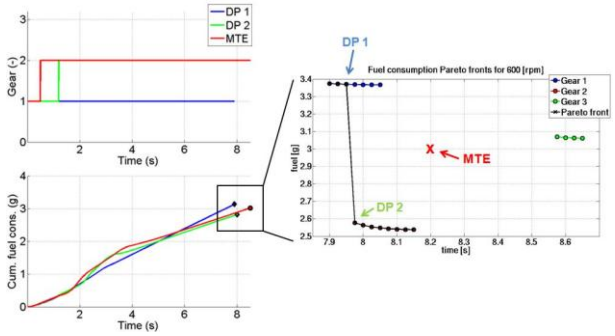

Figure 2: Left: Experimental results: output speed and cumulative fuel consumption; **Right:** Pareto-fronts

3 Conclusions

The multi-objective dynamic programming approach is a powerful control technique to analyse the achievable performance and efficiency of a driveline. Furthermore, the developed technique is flexible and can for instance be easily extended to hybrid drivelines. Future research focuses on deriving real-time implementable strategies from the obtained results.

References

[1] D. Bertsekas, *Dynamic Programming and Optimal Control*, Athena Scientific, 2007
[2] A. Sciaretta, L. Guzella, *Control of Hybrid Electric Vehicles*, IEEE Control Systems Magazine, 2007

Online MPC on Industrial Programmable Logic Controllers

Bart Huyck, Jos De Brabanter
KAHO Sint-Lieven - Departement Industrieel Ingenieur
Email: bart.huyck@kahosl.be jos.debrabanter@kahosl.be

Filip Logist, Jan Van Impe
KU Leuven - Department of Chemical Engineering (CIT)
Email: filip.logist@cit.kuleuven.be jan.vanimpe@cit.kuleuven.be

Bart De Moor
KU Leuven - Department of Electrical Engineering (ESAT - SCD)
Email: bart.demoor@esat.kuleuven.be

1 Introduction

Model Predictive Control has been studied intensively during the past 30 years and is nowadays applied in many industries. Current research, however, now focuses on embedded applications. Attempts to run MPC on industry standard controlling hardware like Programmable Logic Controllers (PLC) are limited to explicit MPC because of computation speed [1]. Explicit MPC is much faster for small (SISO) systems with only a few states and a limited prediction and control horizon. For a MIMO-system with a prediction and control horizon larger then 10, explicit MPC is not recommended. If the sample time is in the order of seconds, an online MPC strategy is possible. This research investigates and validates the use of an online QP solver to implement MPC on a industry standard PLC for a MISO-system. To this end, the Hildreth algorithm [2] and qpOASES [3] are exploited.

2 Set-up

As a small scale and flexible test set-up, a hairdryer is considered. This device is adapted to a multiple input-single output (MISO) system with one controlled variable (i.e., the air temperature) and two manipulated variables (i.e., the resistor power and the fan speed). The PLC is a Siemens S7-315T CPU programmed with S7-SCL, a language similar to the computer language Pascal.

3 The MPC controller

The MPC controller is formulated as an optimization problem with only constraints on the inputs. This choice has been made to facilitate the translation of the qpOASES code to S7-SCL. The model of the system is of fourth order. The control horizon is 7 steps and the prediction horizon is 22 steps of one second. All data that could be computed offline is precomputed and stored on the PLC.

4 Results

Both algorithms follow a predefined reference trajectory accurately. The Hildreth algorithm solves the online operation (estimation, reading of in- and outputs, composition of the matrices for the QP solver and generation of optimal inputs) in maximum 20 ms. The qpOASES algorithm is much more complex compared to the Hildreth algorithm and therefore takes 407 ms to calculate the solution. These results are obtained on the practical set-up. Although it takes more time for the latter algorithm, qpOASES can be aborted early, which is an advantage for online use. Currently, there is still some room to speed up the S7-SCL implementation of qpOASES. Future work will therefore focus on the speed up of employed matrix operations.

5 Conclusion

This work describes the successful implementation and validation of an online MPC on a PLC. Although the Hildreth algorithm is not recent, it serves very well in this small problem. If the system size increases, qpOASES will be used as this algorithm can be aborted early. Future work will focus on the speed up of the S7-SCL implementation of qpOASES.

References

[1] G. Valencia-Palomo, J. Rossiter, "Efficient suboptimal parametric solutions to predictive control for PLC applications," Control Engineering Practice, vol. 19, pp. 732743, 2011.

[2] C. Hildreth, "A quadratic programming procedure," Naval Research Logistics Quarterly, vol. 4, p. 7985, 1957

[3] H. J. Ferreau, H. G. Bock, and M. Diehl, "An online active set strategy to overcome the limitations of explicit MPC," International Journal of Robust and Nonlinear Control, vol. 18, no. 8, pp. 816830, 2008

Acknowledgements

Work supported in part by Projects OT/10/035, PFV/10/002 (Center-of-Excellence Optimization in Engineering), IOF-SCORES4CHEM (KP/09/005) of the Research Council of the KULeuven and IUAP VI/4. Interreg IVa-7-022-BE i-MOCCA. J. Van Impe holds the chair Safety Engineering sponsored by the Belgian chemistry and life sciences federation essenscia.

Large-scale optimization for component analysis of fMRI resting brain data

Raphaël Liégeois[1], Andrea Soddu[2] and Rodolphe Sepulchre[1]
[1] Department of Electrical Engineering and Computer Science, University of Liège, Belgium
[2] Coma Science Group, Cyclotron Research Centre, University of Liège, Belgium
Email : {R.Liegeois, Andrea.Soddu, R.Sepulchre}@ulg.ac.be

The use of component analysis on fMRI data is an important neuroimaging computational tool. In this paper we focus on the particular application of extracting the so-called default mode neuronal network from resting brain data ([**?**] and references therein). While independent component analysis (ICA) is currently the method of choice in this application, we investigate the advantages and limitations of using sparse PCA as an alternative to ICA. Indeed, the searched neuronal networks are mostly intrinsically very sparse and it has been suggested that ICA is a prior for sparsity rather than for statistical independence in neuroimaging [**?**].

1 Methods

We denote by $\mathbf{X}_{(m,T)}$ the fMRI signal, with m the number of voxels and T the number of time samples. Dimensionality reduction of the initial data can be expressed by :

$$\mathbf{Y}_{(n,T)} = \mathbf{W}_{(n,m)}\mathbf{X}_{(m,T)} \tag{1}$$

where $\mathbf{Y}_{(n,T)}$ is the new representation of the dataset in a n-dimensional space with $n \leq m$ since we want to reduce the dimensions of the data, and $\mathbf{W}_{(n,m)}$ is the matrix that expresses the base switch from the m to n-dimensional space.

In order to implement the ICA approach we used the fastICA algorithm which aims to achieve statistical independence between the components of $\mathbf{Y}_{(n,T)}$. On the other hand, sPCA aims to induce sparsity in the principal components contained in $\mathbf{W}_{(n,m)}$ (See [**?**] for more details) and we used the generalized power method [**?**] to implement sPCA. The optimization problem to extract one sparse principal component can be written :

$$\phi_{l_i}(\gamma) = \max_{w \in B^m} \sqrt{w^T \mathbf{C}_x w} - \gamma ||w||_i \tag{2}$$

where w is a column of $\mathbf{W}_{(n,m)}$, $\mathbf{C}_x$ is the sample covariance matrix of the data matrix, l_i indicates that the norm-i of w is used ($i = 0$ or 1), B^m is the unit ball and γ is the *sparsity-controlling* parameter.

When applied to simulated fMRI data our results suggest that sPCA gives better results than ICA when the sparsity of the networks composing the simulated data is higher than a certain threshold. However, this advantage is lost in real data because it appears that sPCA is less robust than ICA to some perturbations that exist in real fMRI data such as the motion of the patient during acquisition of the data. We then use real fMRI data from nine control patients and we design three different experiments. Those experiments aim to evaluate the ability of both techniques to extract neuronal information out of the fMRI signal.

2 Experimental results

In each experiment ICA gives better results than sPCA. We can retain two important drawbacks of sPCA compared to ICA. First, the neuronal networks extracted through sPCA appear to be more affected by perturbations such as motion of patients, making the extraction of neuronal components from one subject to another less robust than with ICA. Second, sPCA does not seem to be able to isolate neuronal information in a few components only, whereas ICA does.

3 Ongoing work

In addition to sparsity, neuronal networks are also highly structured. We currently investigate an optimization problem of the form :

$$\phi(\gamma) = \min_{w \in B^m} f(w) + \gamma \Omega(w) \tag{3}$$

as presented in [**?**] in which the regularization term $\Omega(w)$ induces sparsity *and* structure in w.

References

[1] R. Liégeois, Structured sparse PCA for fMRI Imaging, *Master's thesis*, University of Liège, June 2011.

[2] I. Daubechies, E. Roussos, S. Takerkarta, M. Benharrosh, C. Golden, K. DArdenne, W. Richter, J.D. Cohen, and J. Haxby. Independent component analysis for brain fMRI does not select for independence. *Proceedings of the National Academy of Sciences*, 106(26):10415-10422, 2009.

[3] M. Journée, Y. Nesterov, P. Richtarik, and R. Sepulchre. Generalized power method for sparse principal component analysis. *Journal of Machine Learning Research*, 11:517-553 2010.

[4] R. Jenatton, A. Gramfort, V. Michel, G. Obozinski, E. Eger, F. Bach, B. Thirion. Multi-scale Mining of fMRI data with Hierarchical Structured Sparsity. *Technical report, HAL-inria-00589785*, 2011

LS-SVM approach for solving linear descriptor systems

Siamak Mehrkanoon and Johan A. K. Suykens
KU Leuven, ESAT-SCD, Kasteelpark Arenberg 10, B-3001 Leuven (Heverlee), Belgium.
Email: {Siamak.Mehrkanoon,Johan.Suykens}@esat.kuleuven.be

1 Introduction

Differential algebraic equations (DAEs) arise frequently in numerous applications including mathematical modelling, circuit and control theory [1]. DAEs are known under a variety of names, depending on the area of application for instance they are also called descriptor, implicit or singular systems. The most general form of DAE is given by $F(\dot{x},x,t)=0$. where $\frac{\partial F}{\partial \dot{x}}$ may be singular. DAEs are characterized by their index. DAEs with an index greater than 1 are often referred to as higher-index DAEs and the index of an ODE is zero. Generally, the higher the index, the more difficult it is to solve the DAE numerically and an alternative treatment is the use of index reduction techniques. On the other hand, there are several reasons to solve differential algebraic equations directly, rather than convert it to a system of ODEs [2]. In this study, the solution of linear time varying initial value problems in differential algebraic equations is approximated by using Least Squares Support Vector Machines [5, 6].

2 Formulation of the method for IVPs in DAEs

Consider a linear time varying DAE

$$C(t)\dot{X}(t)=A(t)X(t)+B(t)u(t),\ t\in[t_{in},t_f],\ X(t_{in})=X_0, \tag{1}$$

where $C(t)=[c_{ij}(t)]$, $A(t)=[a_{ij}(t)]\in\mathbb{R}^{m\times m}$ and $B(t)\in\mathbb{R}^{m\times r}$. The state vector $X=[x_1,...,x_m]^T\in\mathbb{R}^m$, the input vector $u\in\mathbb{R}^r$ and $\dot{X}(t)=\frac{dX}{dt}$. $C(t)$ may be singular on $[t_{in},t_f]$ with variable rank and the DAE may have an index that is larger than one. When C is nonsingular, equation (1) can be converted to an equivalent explicit ODE system. Assume that a general approximate solution to i-th equation of (1) is of the form of $\hat{x}_i(t)=w_i^T\varphi(t)+d_i$, where $\varphi(\cdot):\mathbb{R}\rightarrow\mathbb{R}^h$ is the feature map and h is the dimension of the feature space. To obtain the optimal value of w_i and d_i, a collocation method is used [3] with a discretization of the interval $[t_{in},t_f]$ into a set of points $\{t_i\}_{i=1}^N$. The parameters w_i and d_i, for $i=1,...,m$, follow from [6]:

$$\begin{aligned}\underset{w_i,d_i,e_\ell^i}{\text{minimize}}\quad & \frac{1}{2}\sum_{\ell=1}^{m}w_\ell^Tw_\ell+\frac{\gamma}{2}\sum_{\ell=1}^{m}e_\ell^Te_\ell\\ \text{subject to}\quad & CW^T\Psi=A\left[W^T\Phi+D\right]+G+E,\\ & W^T\varphi(t_1)+D_{:,1}=X_0\end{aligned} \tag{2}$$

where $W=[w_1|\cdots|w_m]\in\mathbb{R}^{h\times m}$, $\Phi=[\varphi(t_2)|\cdots|\varphi(t_N)]\in\mathbb{R}^{h\times(N-1)}$, $\Psi=[\frac{d\varphi}{dt}|_{t=t_2}|\cdots|\frac{d\varphi}{dt}|_{t=t_N}]\in\mathbb{R}^{h\times(N-1)}$, $D=\begin{bmatrix}d_1\cdots d_1\\ \vdots\ \ \vdots\\ d_m\cdots d_m\end{bmatrix}$, $E=\begin{bmatrix}e_1(t_2)\cdots e_1(t_N)\\ \vdots\ \ \vdots\\ e_m(t_2)\cdots e_m(t_N)\end{bmatrix}$ and $G=\begin{bmatrix}g_1(t_2)\cdots g_1(t_N)\\ \vdots\ \ \vdots\\ g_m(t_2)\cdots g_m(t_N)\end{bmatrix}$. N is the number of collocation points (which is equal to the number of training points) and $g(t)=[g_1(t)|\cdots|g_m(t)]=B(t)u(t)$. The solution in the dual form becomes $\hat{x}_\ell(t)=\sum_{v=1}^{m}\sum_{i=2}^{N}\alpha_i^v(c_{v\ell}(t_i)[\nabla_1^0K](t_i,t)-a_{v\ell}(t_i)[\nabla_0^0K](t_i,t))+\beta_\ell[\nabla_0^0K](t_1,t)+b_\ell,\ \ell=1,...,m.$ where $[\nabla_0^0K](t,s)$ and $[\nabla_1^0K](t,s)$ are the kernel function and its derivative respectively. α_i^v and β_ℓ are Lagrange multipliers associated with (2). $D_{:,1}$ is the first column of matrix D.

Problem 1: Consider the singular system of index-3 [4]:

$$C(t)\dot{X}(t)=A(t)X(t)+B(t)u(t),\ t\in[0,20],\ X(0)=X_0$$

where $C=\begin{bmatrix}0&-t&0\\1&0&t\\0&1&0\end{bmatrix}$, $A=\begin{bmatrix}-1&0&0\\0&-1&0\\0&0&-1\end{bmatrix}$ and $B(t)=0$ with $x(0)=[0,e^{-1},e^{-1}]^T$. The problem is solved on domain $t\in[0,20]$ for $N=70$. Fig. 1 shows the residuals $e_i(t)=x_i(t)-\hat{x}_i(t)$ for $i=1,2$ and 3.

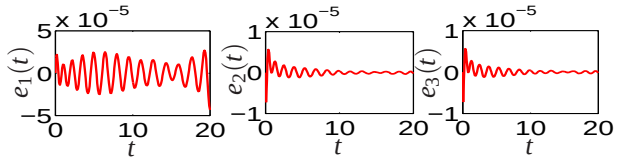

Figure 1: Obtained model errors for problem 1.

Acknowledgments. This work was supported by Research Council KUL: GOA/11/05 Ambiorics, GOA/10/09 MaNet, CoE EF/05/006 Optimization in Engineering(OPTEC), IOF-SCORES4CHEM, several PhD/postdoc & fellow grants;Flemish Government:FWO: PhD/postdoc grants, projects: G0226.06 (cooperative systems and optimization), G0321.06 (Tensors), G.0302.07 (SVM/Kernel), G.0320.08 (convex MPC), G.0558.08 (Robust MHE), G.0557.08 (Glycemia2), G.0588.09 (Brain-machine) research communities (WOG: ICCoS, ANMMM, MLDM); G.0377.09 (Mechatronics MPC) IWT: PhD Grants, Eureka-Flite+, SBO LeCoPro, SBO Climaqs, SBO POM, O&O-Dsquare; Belgian Federal Science Policy Office: IUAP P6/04 (DYSCO, Dynamical systems, control and optimization, 2007-2011); EU: ERNSI; FP7-HD-MPC (INFSO-ICT-223854), COST intelliCIS, FP7-EMBOCON (ICT-248940); Contract Research: AMINAL; Other:Helmholtz: viCERP, ACCM, Bauknecht, Hoerbiger. Johan Suykens is a professor at the K.U.Leuven, Belgium.

References

[1] K. Bernan. "Numerical simulation of trajectory prescribed path control problems," *IEEE Trans. Automat. Control*, AC-31, pp. 266-269, 1986.

[2] H.S. Wang, W.L. Jhu, C.F. Yung, P.F. Wang. "Numerical Solutions of Differential-Algebraic Equations and Its Applications in Solving TPPC Problems," *Journal of Marine Science and Technology*, 19(1), 76-88, 2011.

[3] D.R. Kincaid, E.W. Cheney. *Numerical Analysis*, Mathematics of Scientific Computing, third ed., Brooks/Cole, Pacific Grove, CA, 2002.

[4] K. Murugesan, V. Balakumar. "Study on singular systems of index three via runge-kutta method of order-10", *IJPAM*: 70(5), 723-733, 2011.

[5] J.A.K. Suykens,T. Van Gestel, J. De Brabanter,B. De Moor, J. Vandewalle., *Least Squares Support Vector Machines*, World Scientific, Singapore, 2002.

[6] S. Mehrkanoon, J.A.K. Suykens. "LS-SVM approximate solution to linear time varying descriptor systems", Internal Report 11-205, ESAT-SISTA, K.U.Leuven (Leuven, Belgium), 2011, submited.

A geometric subgradient descent algorithm for the economic load dispatch problem

P. B. Borckmans, S. Easter Selvan, N. Boumal and P.-A. Absil
Department of Mathematical Engineering, ICTEAM Institute
Université catholique de Louvain
B-1348 Louvain-La-Neuve
Belgium
Email: {pierre.borckmans,easter.suviseshamuthu,
nicolas.boumal,pa.absil}@uclouvain.be

1 Introduction

The economic load dispatch problem (ELDP) is a classical problem in the power systems community. It consists in the optimal (minimal cost) scheduling of the output of n power generating units to meet the required load demand subject to unit and system inequality and equality constraints:

$$\min_{\mathbf{p}\in\mathbb{R}^n} f_T(\mathbf{p}) = \sum_{i=1}^{n} a_i p_i^2 + b_i p_i + c_i + |d_i \sin\left[e_i\left(p_i^{\min} - p_i\right)\right]|,$$

$$\text{s.t.} \qquad p_i^{\min} \le p_i \le p_i^{\max}, \qquad \sum_{i=1}^{n} p_i = p_d + p_l,$$

$$p_l = \sum_{i=1}^{n}\sum_{j=1}^{n} p_i B_{ij} p_j + \sum_{i=1}^{n} b_i^0 p_i + b^{00}.$$

This optimization problem is challenging on three different levels: the geometry of its feasible set, the non-differentiability of its cost function and the multimodal aspect of its landscape. For this reason, ELDP has received much attention in the past few years and numerous derivative-free techniques have been proposed to tackle its multimodal and non-differentiable characteristics [1]. However, all these heuristic solutions face difficulties to respect the load equality constraint, and they are not endowed with convergence guarantees.
In this work, we propose a different approach exploiting the rich geometrical structure of the problem. We show that the equality constraint can be handled in the framework of Riemannian manifolds and we develop a projected subgradient descent algorithm to provide fast and robust convergence to local minima.

2 Projected subgradient descent for the ELDP

The equality constraint defines the surface of an ellipsoid in $\mathbb{R}^n$, which is a smooth embedded manifold. The canvas of optimization on manifolds allows to produce a sequence of iterates that belong to the feasible set at all times. Consequently, the original problem is turned into a simpler bound-constrained problem. In order to do so, we develop the necessary tools specifically for the ellipsoid manifold.

Next, we study the cost function and show that it is piecewise smooth. This suggests to use Clarke's generalized calculus to obtain the associated subgradient. Although this set can be hard to compute in general, we show that the cost function at hand can be expressed as the pointwise maximum of smooth functions; therefore the subgradient is easily available, following the canvas presented by Dirr *et al.* in [2]. We then describe how a deterministic descent direction can be obtained by solving a simple, low-dimensional quadratic program. Finally, we use the result of this subproblem to perform a classical descent iteration using line search with Armijo's rule, which ensures convergence to a Clarke stationary point.

3 Experimental validation

We tested our approach on 4 real data sets of dimensions 3, 5, 6 and 15. We also implemented some state-of-the-art heuristic competitors for comparison purpose, namely, cross-entropy, particle swarm optimization and differential evolution. The proposed method surpasses the competitors both in terms of convergence speed and precision. Furthermore, our approach presents the major advantages of scaling well with respect to the problem dimension and producing valid iterates at all times. On the other hand, the competitors provide better exploration of the search space. Therefore, a possible extension of our work will be to incorporate exploration techniques into the proposed approach.

References

[1] J. Vlachogiannis, and K. Lee, "Economic Load Dispatch - A Comparative Study on Heuristic Optimization Techniques With an Improved Coordinated Aggregation-Based PSO," *IEEE Transactions on Power Systems*, vol. 24, no. 2, pp. 991–1001, 2009.

[2] G. Dirr, U. Helmke, and C. Lageman, "Nonsmooth Riemannian Optimization with Applications to Sphere Packing and Grasping," *Lecture Notes in Control and Information Sciences*, vol. 366, pp. 29–45, Springer, 2007.

Expected MSE Minimization in Linear Regression over Ellipsoidal Uncertainty Sets

Can Bikcora
Department of Electrical Engineering, Eindhoven University of Technology
P.O. Box 513, 5600 MB Eindhoven, The Netherlands
Email: c.bikcora@tue.nl

1 Introduction

In this work, we investigate the parameter estimation problem in linear regression models where the parameters are known to belong to a given ellipsoidal uncertainty set. Optimization over this set is usually performed by minimizing the maximum mean-squared error (MSE) in order to guarantee performance specifications that hold for all elements in the ellipsoid [1]. However, an explicit solution is only available for a few specific cases. As an alternative, we analyze the minimization of the expected MSE which has an explicit solution and point out its properties.

2 Problem formulation

Let $\mathbf{y} = \mathbf{H}\mathbf{x} + \mathbf{v}$ be the linear regression model where $\mathbf{y} \in \mathbb{C}^p$ is the measured data, $\mathbf{x} \in \mathbb{C}^n$ is the deterministic parameter vector to be estimated, $\mathbf{H}$ is a known model matrix with full column rank and $\mathbf{v}$ is a zero-mean random vector with a positive definite covariance matrix $\mathbf{C}$. Considering a linear estimator of the form $\hat{\mathbf{x}} = \mathbf{G}\mathbf{y}$, the MSE which is defined as $\mathbb{E}\{\|\hat{\mathbf{x}} - \mathbf{x}\|^2\}$, becomes a function of the unknowns $\mathbf{G}$ and $\mathbf{x}$: $\varepsilon(\mathbf{G},\mathbf{x}) = \mathbf{x}^*(\mathbf{I} - \mathbf{G}\mathbf{H})^*(\mathbf{I} - \mathbf{G}\mathbf{H})\mathbf{x} + \mathrm{Tr}(\mathbf{G}\mathbf{C}\mathbf{G}^*)$ where $\mathbf{I}$ denotes the identity matrix and $(\cdot)^*$ returns the conjugate transpose of its argument. In the least-squares estimator (LS), $\varepsilon(\mathbf{G},\mathbf{x})$ is minimized by imposing the constraint $\mathbf{G}\mathbf{H} = \mathbf{I}$ so that the resultant estimator is unbiased and only minimizes the variance. As a different approach, we assume that $\mathbf{x}$ is known to lie in the ellipsoidal uncertainty set $\mathscr{U} = \{\mathbf{x} \in \mathbb{C}^n | \mathbf{x}^*\mathbf{T}\mathbf{x} \leq r^2\}$ with $\mathbf{T} \succ 0$ and $r > 0$ and utilize this knowledge to find a biased estimator that has a better expected MSE when compared to the LS. The provided improvement over the LS increases as $\mathbf{H}$ gets more ill-conditioned. The minimization problem can be formulated as

$$\min_{\mathbf{G}} \mathop{\mathbb{E}}_{\mathbf{x}\in\mathscr{U}} \{\varepsilon(\mathbf{G},\mathbf{x}) - \varepsilon(\mathbf{G}_{\mathrm{LS}})\} \tag{1}$$

where $\varepsilon(\mathbf{G}_{\mathrm{LS}})$ is the MSE of the LS.

3 The solution and its properties

The unique minimizer of (1) is given by

$$\mathbf{G}_{\mathrm{EXP}} := \mathbf{G} = (\mathbf{H}^*\mathbf{C}^{-1}\mathbf{H} + ((n+2)/r^2)\mathbf{T})^{-1}\mathbf{H}^*\mathbf{C}^{-1}. \tag{2}$$

As the solution reveals and in accordance with our expectations, $\mathbf{G}_{\mathrm{EXP}}$ converges to $\mathbf{G}_{\mathrm{LS}}$ as $\mathscr{U} \to \mathbb{C}^n$.

Apparent from the structure in (2), $\mathbf{G}$ is in the form of the Tikhonov (ridge) estimator. The parameter estimate $\hat{\mathbf{x}}_{\mathrm{EXP}} = \mathbf{G}_{\mathrm{EXP}}\mathbf{y}$ is also equal to the solution to the regularized least-squares problem $\min_{\hat{\mathbf{x}}_{\mathrm{EXP}}} \{(\mathbf{y} - \mathbf{H}\hat{\mathbf{x}}_{\mathrm{EXP}})^*\mathbf{C}^{-1}(\mathbf{y} - \mathbf{H}\hat{\mathbf{x}}_{\mathrm{EXP}}) + \hat{\mathbf{x}}_{\mathrm{EXP}}^*\mathbf{M}\hat{\mathbf{x}}_{\mathrm{EXP}}\}$ where $\mathbf{M} = ((n+2)/r^2)\mathbf{T}$.

Admissibility Result: An estimator $\hat{\mathbf{x}}$ is admissible on $\mathscr{U}$ if it is not dominated by any other linear estimator, meaning that there is no other estimator having a MSE that is never larger than the MSE of $\hat{\mathbf{x}}$ for all $\mathbf{x} \in \mathscr{U}$, and is strictly smaller for some $\mathbf{x} \in \mathscr{U}$ [2]. In [1], it is derived that the Tikhonov estimator is admissible on $\mathscr{U}$ if and only if $\mathrm{Tr}(\mathbf{T}\mathbf{M}^{-1}) \leq r^2$. Applying this result to our case yields: $\hat{\mathbf{x}}_{\mathrm{EXP}}$ is always admissible on $\mathscr{U}$ since $n < n+2$. Therefore, admissibility is a shared property of the current approach and the minimax estimator (MX) which is obtained via (1) after replacing the $\mathbb{E}$ with the *max* operator. Moreover, $\hat{\mathbf{x}}_{\mathrm{EXP}}$ has the *admissibility robustness* of $\alpha := 100\big(1 - \sqrt{n/(n+2)}\big)\%$, meaning that admissibility is retained for all $\{\mathbf{x} \in \mathbb{C}^n | \mathbf{x}^*\mathbf{T}\mathbf{x} \leq \gamma^2\}$ where $\gamma \in [(1 - 0.01\alpha)r, \infty)$. In Fig. 1, the analyzed method is compared against the LS and the MX with respect to the MSE for a given model and an ellipsoid ($\mathbf{T} = \mathrm{diag}(1,4), r^2 = 4$) in 2-D. Although it does not dominate the LS as the MX does, it outperforms the MX at a large region in the ellipsoid. Similar simulations are carried out under various model settings to distinguish different relative performances.

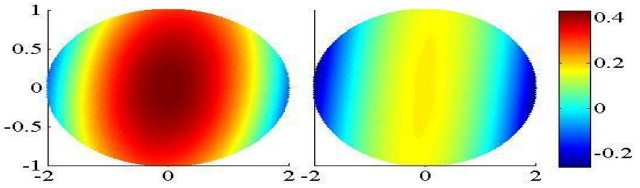

Figure 1: MSE differences within a given ellipsoid in 2-D. Left: $\varepsilon(\mathbf{G}_{\mathrm{LS}}) - \varepsilon(\mathbf{G}_{\mathrm{EXP}},\mathbf{x})$, Right: $\varepsilon(\mathbf{G}_{\mathrm{MX}},\mathbf{x}) - \varepsilon(\mathbf{G}_{\mathrm{EXP}},\mathbf{x})$.

References

[1] Y. C. Eldar, "Comparing between estimation approaches: Admissible and dominating linear estimators," *IEEE Trans. Signal Process.*, vol. 54, no. 5, May 2006.

[2] E. L. Lehmann and G. Casella, *Theory of Point Estimation*, 2nd ed. New York: Springer, 1999.

Controllability and stabilizability of piecewise affine dynamical systems

Le Quang Thuan
Department of Mathematics
University of Groningen
P.O. Box 800, 9700 AV Groningen,
The Netherlands.
Email: t.q.le@rug.nl

M. Kanat Camlibel
Department of Mathematics
University of Groningen
P.O. Box 800, 9700 AV Groningen,
The Netherlands.
Email: m.k.camlibel@rug.nl

1 Introduction

The controllability concept was born in the early sixties in Kalman's work [1] and it has played a central role throughout the history of modern control theory. In the context of linear systems, the well-known Kalman rank condition and Popov-Belevitch-Hautus test are among the classical results of modern control theory. For nonlinear systems, only local controllability results are available.

In this work, we consider the controllability and stabilizability problem for (continuous) piecewise affine dynamical systems. A piecewise affine dynamical system is an input/state/output system for which the product of the state and output spaces is partitioned into polyhedral regions and an affine dynamics is active on each of these regions. It is well-known that checking certain controllability properties of even very simple such systems is a undecidable problem [2], i.e. there is no algorithm to decide whether such a system is controllable.

Our main goal is to derive algebraic necessary and sufficient conditions for global controllability of piecewise affine dynamical systems. Based on achieved results, we also provide algebraic characterizations for stabilizability of such systems.

2 Piecewise affine dynamical systems. Main results

Let $\{\mathscr{Y}_1,\ldots,\mathscr{Y}_h\}$ be a polyhedral subdivision (see e.g. [3] for the details) of $\mathbb{R}^p$, and let $f:\mathbb{R}^p\to\mathbb{R}^n$ be a continuous piecewise affine function with $f(y)=F_iy+g_i$ whenever $y\in\mathscr{Y}_i$. Consider the dynamical systems of the form

$$\dot{x}(t)=Ax(t)+Bu(t)+f(y(t)) \tag{1a}$$

$$y(t)=Cx(t)+Du(t) \tag{1b}$$

where $x\in\mathbb{R}^n$ is the state, $u\in\mathbb{R}^m$ is the input, $y\in\mathbb{R}^p$ is the output, and all considered matrices have appropriate sizes. We call such a system *piecewise affine dynamical system*.

Definition 2.1. An absolutely continuous function $x:\mathbb{R}\to\mathbb{R}^n$ is called a solution of the system (1) for the initial state x_0 and locally integrable input u if $x(0)=x_0$ and the pair (x,u) satisfies the system (1) for almost all $t\in\mathbb{R}$.

Since the function f is continuous, the right-hand side of (1a) is globally Lipschitz. Thus, the system (1) must admit a unique solution for each initial state x_0 and locally integrable input u which is denoted by $x^u(t;x_0)$.

Definition 2.2. We say that the system (1) is *globally controllable* if for any two states x_0,x_1 there exist $T>0$ and a locally integrable input u such that $x^u(T;x_0)=x_1$; *stabilizable* if for any state x_0 there exists a locally integrable input u such that $\lim_{t\to\infty}x^u(t;x_0)=0$.

The main contribution of this work is that we derive algebraic characterizations for controllability as well as stabilizability of piecewise affine dynamical systems. These characterizations recover the former results in [4, 5] as special cases and make a premise for future work on controllability issue of similar system classes such as linear complementarity systems and affine differential variational inequalities, and also on feedback stabilization issue.

References

[1] R.E. Kalman, "On the general theory of control systems", In Proceeding of the first World Congress of the International Federation of Automatic Control, 481-493, 1960.

[2] V.D. Blondel and J.N. Tsitsiklis, "Complexity of stability and controllability of elementary hybrid systems", Automatica, 35(3):479-490, 1999.

[3] L.Q. Thuan and M.K. Camlibel, "Continuous piecewise affine dynamical systems do not exhibit Zeno behavior", IEEE Transaction on Automatic Control, 56(8):1932-1936, 2011.

[4] M.K. Camlibel, W.P.M.H. Heemels, and J.M. Schumacher, "Algebraic necessary and sufficient conditions for the controllability of conewise linear systems", IEEE Transaction on Automatic Control, 53(3):762-774, 2008.

[5] M.K. Camlibel, W.P.M.H. Heemels, and J.M. Schumacher, "A full characterization of stabilizability of bimodal piecewise linear systems with scalar inputs", Automatica, 44(5):1261-1267, 2008.

Solving Algebraic Riccati Equation Real Time for Integrated Vehicle Dynamics Control

Anil Kunnappillil Madhusudhanan
Delft Center for Systems and Control
Delft University of Technology
Mekelweg 2 (3mE building)
2628CD Delft
a.k.madhu@tudelft.nl

Matteo Corno
Dipartimento di Elettronica e Infomazione
Politecnico di Milano
Via Ponzio 34/5
20133 Milano
corno@elet.polimi.it

Bram Bonsen
Philips Innovation Services
High Tech Campus 7
5656AE Eindhoven
bram.bonsen@philips.com

Edward Holweg
Delft Center for Systems and Control
Delft University of Technology
Mekelweg 2 (3mE building)
2628CD Delft
edward.holweg@skf.com

1 ABSTRACT

Since the beginning of the 20^{th} century, the number of vehicles on streets has been increasing almost monotonically. Although traffic rules are imposed to avoid accidents, the number of accidents is not decreasing as desired. This demands better vehicle safety. One of the active safety systems for facilitating better vehicle safety is Vehicle Dynamics Control (VDC). VDC supports the driver in emergency situations by producing a yaw torque in the case of exceedance of a certain yaw rate. Such emergency situations could arise from unexpected disturbances. In such situations, an average driver might not be able respond quickly enough to avoid an accident, whereas a VDC generates required corrective yaw moments and thereby assists the driver.

Modern vehicles have many active and semi-active VDCs such as Electronic Stability Program (ESP), Active Front Steering (AFS), etc. As these systems are designed individually, when used in a vehicle, they might counteract each other. Therefore integration of such systems i.e., Integrated VDC (IVDC) is important for better vehicle safety.

To design a VDC, various control methods are available. Many of them are linear. However vehicle states could go outside the linearizing point depending on driving conditions. In such cases, linear controllers may not stabilize the vehicle. Another approach is based on Linear Parameter Varying (LPV) model based on longitudinal vehicle velocity. In terms of accuracy of the model, the LPV model might be better than a LTI model. However this excludes model variations with respect to parameters other than longitudinal vehicle velocity. Therefore a nonlinear as well as Integrated VDC (IVDC) approach is preferable to cover the operating region and nonlinearity, and to avoid possible intereferences with individual controllers.

State Dependent Riccati Equation (SDRE) based control is one of the promising nonlinear control methods [1] and SDRE based IVDC has demonstrated promising simulation [2] as well as practical [3] test results. In this method, an Algebraic Riccati Equation (ARE) is solved at each sample to generate the control signal. However solving ARE is computationally complex.

In this work, Extended Kalman Filter (EKF) iterative, Schur, Eigenvector, and Hamiltonian methods to solve ARE real time are implemented and studied for their timing, accuracy, and feasibility. The three methods, Schur, Eigenvector, and Hamiltonian are found to have an average calculation time of 3.9, 2.5, and 1.6 milliseconds on a dSPACE real time processor. In addition to the least processing time, the Hamiltonian based approach yields the lowest quadratic cost for SDRE based Integrated Vehicle Dynamics Control (IVDC).

References

[1] J. R. Cloutier, C. N. D'Souza and C. P. Mracek, "Nonlinear Reguation and Nonlinear H_∞ Control via the State-Dependent Riccati Equation Technigue: Part 1, Theory", *International Conference on Nonlinear Problems in Aviation and Aerospace*, 1996.

[2] T. Acarman, "Nonlinear optimal integrated vehicle control using individual braking torque and steering angle with on-line control allocation by using state-dependent Riccati equation technique", *Vehicle System Dynamics*, vol. 47, no. 2, 2009, pp 155-177.

[3] B. Bonsen, R. Mansvelders and E. Vermeer, "Integrated Vehicle Dynamics Control using State Dependent Riccati Equations", *10th International Symposium on Advanced Vehicle Control*, Loughborough, UK, 2010.

Quantized average consensus with delay

Matin Jafarian, Claudio De Persis
Faculty of Mathematics and Natural Sciences, ITM
University of Groningen
Nijenborgh 4, 9747AG Groningen
The Netherlands
Email: {m.jafarian,c.de.persis}@rug.nl

1 Introduction

Average consensus problem is a special case of cooperative control in which the agents of the network asymptotically converge to the average state (*i.e.*, position) of the network by transferring information via a communication topology. One of the issues of the large scale networks is the cost of communication and computational burden. Quantized information, in which the agents transmit the information sporadically, can be a solution for this problem. So far, there has been studies on the average consensus problem with quantization e.g. [1], however the effect of one of the most common problem in communication networks, delay, in combination with quantization is not well understood. In this work we introduce the continuous-time average consensus problem of a network of agents with quantized transferred data and constant heterogeneous communication delays.

2 On the limitations of uniform quantizers

We consider a network of N single integrators connected by a weight-balanced and weakly-connected graph topology. Each agent is communicating with its own neighboring agents via a quantized communication channel. The quantized position of agents (x) with quantization level Δ is the following:

$$q(x) = \left\lfloor \frac{x}{\Delta} + \frac{1}{2} \right\rfloor \tag{1}$$

We assume the communication of each two agents is affected by a constant delay, τ_{ij}, where i and j are neighbours. We do not consider the effect of self-delay ($\tau_{ii} = 0$). The overall system equation is the following in which D is a diagonal matrix whose diagonal entries are the degrees of each agent, also the non-zero values of the graph adjacency matrix are assumed to be equal to one:

$$\dot{x}(t) = -Dq(x(t)) + \begin{pmatrix} \sum_{i\in N_1} q(x_i(t-\tau_{i1})) \\ . \\ . \\ . \\ \sum_{i\in N_n} q(x_i(t-\tau_{in})) \end{pmatrix} \tag{2}$$

For simplicity we rewrite the above equation in the form $\dot{x}(t) = -Dq(x(t)) + A(q(x_t))$, where $x_t = x(t+\theta)|_{\theta\in[-\tau_{\max},0]}$ and $\tau_{\max} \geq t_{ij}$ for all i, j.

Let $\phi : [-\tau_{\max}, 0] \to \mathbb{R}^n$ be any absolutely continuous function with the following properties: $\phi_j(0) = (k+\frac{1}{2})\Delta$ for some $k \in \mathbb{Z}$, and $\phi_i(0) \neq (h+\frac{1}{2})\Delta$ for any $h \in \mathbb{Z}$ and all $i \neq j$; moreover, for any i, j and for any $h \in \mathbb{Z}$, $\phi_i(-\tau_{ji}) \neq (h+\frac{1}{2})\Delta$. Take now any absolutely continuous function $x : [-\tau_{\max}, \varepsilon] \to \mathbb{R}^n$, with $\varepsilon > 0$, which agrees with ϕ on the interval $[-\tau_{\max}, 0]$ and is such that $A(q(x_t))$ is equal to a constant c for all $t \in [0, \varepsilon]$. Observe that such a function x always exists by definition of ϕ and provided that ε is sufficiently small.
Consider now the auxiliary system $\dot{\xi}(t) = -Dq(\xi(t)) + c =: f(\xi(t))$ and let ξ one of its Krasowskii solution defined on $[0, \varepsilon]$ starting from $\phi(0)$. Because the rhs of (2) computed along $\xi(t)$ and the rhs of the auxiliary system agrees on $[0, \varepsilon]$, we define $\xi(t)$ as a solution to (2). Following [1], let $I(\xi(0))$ be a neighborhood of $\xi(0)$ such that, for any $\xi \in I(\xi(0))$, it holds that $\xi_j \neq (h+\frac{1}{2})\Delta$ for any integer $h \neq k$, and $\xi_i \neq (h+\frac{1}{2})\Delta$ for any i and any $h \in Z$. Let $I^+(\xi(0)) = \xi \in I(x(0)) : \xi_j > (k+\frac{1}{2})\Delta$ and $I^-(\xi(0)) = \xi \in I(\xi(0)) : x_j < (k+\frac{1}{2})\Delta$. Let f^+ be the value of the auxiliary system vector field in $I^+(\xi(0))$ and f^- be the corresponding value in $I^-(\xi(0))$. The j-th components of f^+ and f^- can be written as:

$$f_j{}^+ = c_j - d_j q(\xi_j(0)) = c_j - d_j(k+1)\Delta, \quad f_j{}^- = f_j{}^+ + d_j\Delta$$

where d_j is the degree of node j. As in [1], we conclude that $\xi(t)$ evolves along the discontinuity surface $\xi_j = (k+\frac{1}{2})\Delta$ for $t \in [0, \varepsilon]$. In practice this might cause chattering and request fast information transmission on a short period of time, an undesirable scenario in networked systems.

3 Conclusion and Future work

We showed that sliding mode (and chattering in practice) can happen in the presence of delays and quantization. To overcome this limitation, research on implementing hybrid (hysteretic) quantizers ([1]) is in progress.

References

[1] F. Ceragioli, C. De Persis, P. Frasca "Discontinuities and hystersis in quantized average consensus" Automatica, 2011.

A little kick to synchronization models

Rodolphe Sepulchre
Systems and Modeling Research Unit, ULg
10 Grande Traverse, B-4000 Liege, Belgium
Emails: r.sepulchre@ulg.ac.be

1 Introduction

Synchronization is a pervasive phenomenon in physics, biology, and engineering. The topic has attracted much attention also in the systems and control community in the recent years. In this talk we discuss and revisit two important models of synchronization in networks of oscillatory systems: the *diffusive coupling* model, in which synchronization results from a feedback interconnection akin to a negative output feedback of the synchronization error, and the *impulsive coupling* model, in which each oscillator impulsively kicks the connected oscillators at every zero-crossing of some phase variable.

2 Synchronization in Systems and Control

Synchronization is a system theoretic concept: it is a property that results from interconnecting open systems in the right fashion. The early connection between master-slave synchronization and observer design [1] popularized the concept in the systems and control community. It has stimuated many recent efforts to generalize stability concepts to incremental stability concepts, see e.g. the use of contraction analysis[2], incremental Lyapunov stability [3], and incremental passivity [4] in synchronization studies. All these contributions pertain to the *diffusive* coupling model.

3 Synchronization experiments

Experimental manifestations of synchronization have become popular in the recent years, see e.g. [5]. Highlight YouTube examples include flashing fireflies, metronomes, and revisiting the historical pendula experiment of Huygens. In those and most experiments reported in the literature, the kicks appear as the central ingredient. Diffusive coupling, when hypothetized, plays at best a secondary role. But the mathematical literature on kick-induced synchronization in networks is scarse.

4 Pulse-coupled versus diffusively-coupled models of oscillators

Based on recent and older –e.g. [6] – literature, the talk will provide a short introduction the mathematical modeling of spking networks through their reduction to phase models. I will stress the importance of the phase response curve, present recent synchronization results from [7] and [8], a basic conjecture, and hopefully inspiring connections with consensus and diffusive coupling models in the limit of weak coupling. At the time of many developments in hybrid systems theory, the talk will primarily be an invitation to pay more system-theoretic attention to a barely touched topic of importance in many areas of applications.

References

[1] H. Nijmeijer and I. Mareels, "An observer look at synchronization," *IEEE Trans. on Circuits and Systems I*, vol. 44, no. 10, pp. 882–890, 1997.

[2] J.-J. Slotine and W. Wang, "A study of synchronization and group cooperation using partial contraction theory," in *Cooperative control, V. Kumar, N. Leonard, A. Morse (eds.)*, vol. 309. Spinger-Verlag, London, 2004, pp. 207–228.

[3] D. Angeli, "A Lyapunov approach to incremental stability properties," *IEEE Trans. on Automatic Control*, vol. 47, pp. 410–422, 2002.

[4] G.-B. Stan and R. Sepulchre, "Analysis of interconnected oscillators by dissipativity theory," *IEEE Transactions on Automatic Control*, vol. 52, no. 2, pp. 256–270, 2007.

[5] S. Strogatz, *Sync: the emerging science of spontaneous order*. Hyperion, 2003.

[6] R. Mirollo and S. H. Strogatz, "Synchronization of pulse-coupled biological oscillators," *SIAM Journal on Applied Mathematics*, vol. 50, pp. 1645–1662, 1990.

[7] A. Mauroy, "On the dichotomic collective behaviors of large populations of pulse-coupled firing oscillators," Ph.D. dissertation, University of Liege, October 2011.

[8] P. Wieland, G. S. Schmidt, R. Sepulchre, and F. Allgöwer, "Phase synchronization through entrainment by a consensus input," in *Proc. 49th IEEE Conf. Decision and Control*, 2010, pp. 534–539.

The Flying Hand: Control of an Aerial Manipulator Interacting with a Remote Environment

Matteo Fumagalli, Stefano Stramigioli and Raffaella Carloni
Control Engineering - University of Twente, The Netherlands
Email: {m.fumagalli, s.stramigioli, r.carloni}@utwente.nl

1 Introduction

Physical interaction between Unmanned Aerial Vehicles (UAVs) and the surrounding environment is a research trend that is currently receiving great attention in the field of aerial robotics. The goal is to exploit in real applicative scenarios the potentialities of systems that are able not only to fly autonomously, but also to interact safely with remote objects to accomplish tasks such as data acquisition by contact, sample picking, objects repairing and assembling. To achieve this, several methodological and technological challenges have to be faced. In particular, most aerial configurations are underactuated mechanical systems, which means that not all their degrees of freedom (DoFs) can be actually controlled simultaneously. This feature affects the design of the control law, in particular because stability has to be preserved even in presence of disturbances deriving from physical interaction.

2 Control Design

The interaction between the aerial robot, the manipulator and the environment are investigated both during free-flight and in the case in which docking to a vertical surface is achieved. Building upon this analysis, an energy-based control strategy is proposed. The main idea is to "passify" [1] the position dynamics of the vehicle relying upon a cascade control strategy [2], in which the attitude is considered virtually as an available control input. The closed-loop passive system can be then controlled as a standard robotic manipulator, implementing hybrid force/position and impedance control strategies suitable to handle both contact and no-contact cases.

3 The Flying Hand System

From a technological viewpoint, the flying hand integrates a commercial quadrotor helicopter with a custom-made manipulation system (see Fig. 1). We constructed a fast and robust prototype that can perform cartesian movements to compensate for the aerial vehicle's dynamics, in both free flight and during contact, and can realize interactions. The manipulation system uses a three DoFs Delta structure together with an end-effector, realized by a Cardan gimbal that allows a compliant interaction. The Cardan gimbal is endowed with a small actuator for the roll motion, a compliant element to correct its orientation in the direction of interaction and two passive compliant rotational DoFs [3].

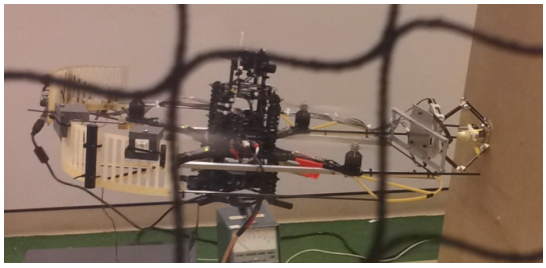

Figure 1: AscTec Pelican quadrotor during interaction with a wall by means of the manipulation system.

4 Experiments

The first experiment consists in tracking a desired point, which is fixed in the workspace with respect to the inertial frame. Two different cases are compared: (a) the manipulation system is kept rigid in a certain configuration as if it were a rigid tool; (b) the manipulation system is exploited in all its seven degrees of freedom. In the second experiment, the system is controlled so to realize an interaction with the wall by means of the manipulation system. During the second experiment, the quadrotor approaches a vertical surface. The reference position of the manipulator is fixed with respect to the vehicle. A reference position is set to the quadrotor, such that the system enters in contact with the wall. When the system touches the wall, the manipulator moves as a consequence of the intrinsic compliance of the low-level control. The impedance behavior of the quadrotor generates a virtual force on the vehicle that depends on its position and velocity error.

References

[1] A. van der Schaft. *L2-Gain and Passivity Techniques in Nonlinear Control*. Springer, 2000.

[2] A. Isidori, L. Marconi, and A. Serrani. *Robust Autonomous Guidance: An Internal Model Approach*. Advances in Industrial Control. Springer-Verlag London, 2003.

[3] A.Q.L. Keemink, M. Fumagalli, S. Stramigioli, and R. Carloni. Mechanical design of a manipulation system for unmanned aerial vehicles. In *Proceedings of the IEEE International Conference on Robotics and Automation*, 2012.

Force Feedback of a Manipulator System in the port-Hamiltonian Framework

Mauricio Muñoz-Arias[1] Jacquelien M.A. Scherpen[1] Daniel A. Dirksz[2]

[1]Faculty of Mathematics and Natural Sciences, University of Groningen, Nijenborgh 4, 9747 AG Groningen, the Netherlands

[2]Department of Mechanical Engineering, Eindhoven University of Technology, P.O. Box 513, 5600 MB Eindhoven, the Netherlands

Email: m.munoz.arias@rug.nl; j.m.a.scherpen@rug.nl; d.a.dirksz@tue.nl

Skilled manipulation is required when a robot is in contact with the environment. The interaction robot-environment is intentional in industrial applications such as grinding, polishing, cutting, excavating and non-industrial such as domotics [1] and [2]. Implementation of all these tasks requires motion and force control due to the non-contact to contact transitions. The motion and force control in robot manipulators is thoroughly discussed in [3] and [4] in the Euler-Lagrange framework. It is the aim of this paper to propose a dynamic extension in the form of a standard mechanical system and based in the port-Hamiltonian (PH) formulation [5].

Except for [6], in a specific multi-fingered robotic hand and [7], where friction and tyre forces are used for a wheel slip control, the PH framework has not been exploited for force modeling and control purposes.

In this paper, a dynamic extension and a coordinate transformation are introduced on the state space of a port-Hamiltonian standard mechanical system. The new dynamic state and the coordinate transformation are realized for force feedback purposes. The new dynamic state is the sum of the internal and external forces of the mechanical system. The internal forces are given by a set of storing kinetic and potential energy elements, and a set of energy dissipation elements. The external forces are exerted from the environment and are modeled as generalized vector forces. In order to realize the coordinate transformation, an integral action over the dynamic extension is proposed. The force feedback is included through the coordinate transformation and a new Hamiltonian function is introduced. Furthermore, the dynamic state and the coordinate transformation are realized in order to preserve the structure and also to have a passive output of the transformed port-Hamiltonian system. The present work is inspired by the previous results of [8] and [9].

References

[1] G. Zeng, A. Hemami "An Overview of Robot Force Control" Robotica, vol. 15, 1997, pp 473-482.

[2] T. Yoshikawa "Force Control of Robot Manipulators" Proceedings - IEEE Int. Conf. on Robotics & Automation, vol. 1, 2000, pp.220-226.

[3] C. Canudas de Wit, B. Siciliano and G. Bastin "Theory of Robot Control", Springer-Verlag London Limited, 1996.

[4] M. Spong, S. Hutchinson, and M. Vidyasagar "Robot Modeling and Control", John Wiley & Sons, 1998.

[5] B.M. Maschke, A.J. van der Schaft "Port-controlled Hamiltonian systems: modeling origins and system-theoretic properties" Bordeaux, France, in Proc. 2nd IFAC NOLCOS, 1992, pp. 282-288.

[6] F. Ficuciello, R. Carloni, L.C. Visser and S. Stramigioli "Port-Hamiltonian Modeling for Soft-Finger Manipulation" Taipei, Taiwan, IEEE/RSJ Int. Conf. On Intelligent Robots and Systems, 2010, pp. 4281-4286.

[7] J. Koopman, D. Jeltsema and M. Verhaegen "Wheel Slip Control Using Energy Shaping" Atlanta, GA., 49th IEEE Conference on Decision and Control, 2010, pp. 2916-2921.

[8] D.A. Dirksz and J.M.A. Scherpen "Port-Hamiltonian and power-based integral type control of a manipulator system", Milan, Italy, 18th IFAC Symposium on Nonlinear Control System, 2011, pp. 13450-13455.

[9] A. Donaire, A. and S. Junco "On the addition of integral control action to port-controlled Hamiltonian systems", Automatica, 45(8), 2009, pp 1910-1916.

An Update on the RoboEarth Architecture

Rob Janssen, René van de Molengraft and Maarten Steinbuch
Control Systems Technology
Eindhoven University of Technology
P.O. Box 513, 5600 MB Eindhoven
The Netherlands
Email: R.J.M.Janssen@tue.nl

1 Introduction

The core idea of the RoboEarth project [**?**] is to develop a global WWW-style database where service robots operating in domestic and healthcare environments can share and re-use any obtained knowledge of their everyday activities. This common knowledge consists for instance of the maps they create for navigation, learned object models for perception and manipulation, and hierarchically stored plan descriptions of their commanded tasks. The partners in the RoboEarth project consist of multiple research institutes throughout Europe, which all bring their own area of expertise. The RoboEarth project was launched in December 2009 in the European FP7 framework programme.

Part of the projects dissemination consists of yearly real-life demonstrations to the general audience. One of these demonstrators was presented in 2011, where the custom-build service robot AMIGO was introduced and instructed to 'serve a drink' to a patient in a hospital room. The main components that were required for this task, object models, semantic maps and modularized plan components were downloaded through RoboEarth.

Figure 1: The TU/e AMIGO 'serving a drink'.

2 The 2012 Demonstrator

The demonstrator planned for February 2012 will expand to an illustrative multi-robot scenario, where both the TU/e AMIGO and Willow Garage's PR2 will collaboratively improve upon their task specific knowledge during execution of the 'serve-a-drink' action plan. With respect to the second demonstrator, improvements will be made towards a first generic high level executive, merging of navigational maps on the database side, sharing of articulation models for opening doors and increased robustness for task execution.

3 RoboEarth Architecture

Fig. **??** depicts the current implementation of the RoboEarth architecture. On top the RoboEarth database is shown, with 4 containers for maps, task descriptions and physical/semantic object descriptions. Upon user instruction, a plan is composed based on the RoboEarth hierarchical plan components by the CRAM plan executive. Plan composition is based on the current status of the world (a combination of self-sensing and the environmental belief state stored in RoboEarth) and the reasoner module KnowRob [**?**]

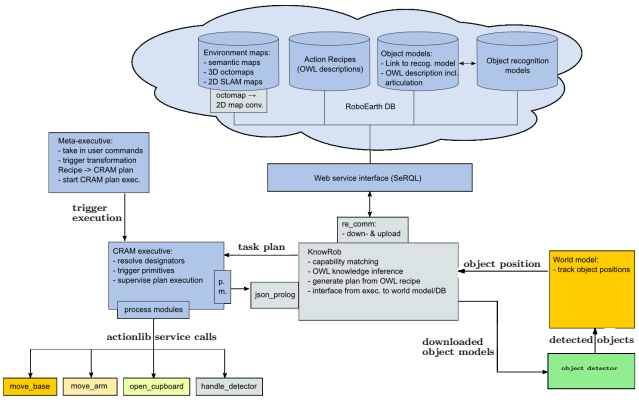

Figure 2: The RoboEarth component architecture

One of the goals in the project is to eventually execute most of these local components on the RoboEarth database itself, allowing also less sophisticated robots to assist in complex domestic tasks.

References

[1] M. Waibel et all, "RoboEarth: A World Wide Web For Robots", IEEE Robotics & Automation Magazine, 2011.

[2] M. Tenorth and M. Beetz, "Knowledge Processing for Cognitive Robots", Künstliche Intelligenz, 2010

Coordinating robots in water polo matches using modified snowdrift games

Chen Wang[1,2] Bin Wu[2] Ming Cao[1] Guangming Xie[2]

[1]Faculty of Mathematics and Natural Sciences, University of Groningen, Nijenborgh 4, 9747 AG Groningen, The Netherlands

[2]Intelligent Control Laboratory, College of Engineering, Peking University, 100871 Beijing, China

Email: wangchen@pku.edu.cn; bin.wu@evolbio.mpg.de; m.cao@rug.nl; xiegming@pku.edu.cn

1 Introduction

One key research topic in the study of coordinating multiple robots is to understand under what conditions the *synergy effect* emerges. While most of the previous work on cooperative robots confirms the existence of synergy effects, less is known about how to quantify them and more importantly, how they affect autonomous robots' tendencies to cooperate. In this paper, using game theoretic ideas, we propose a modified snowdrift game to study the emergence and evolution of cooperation among robots in multi-robot water polo matches. We first formulate a game setting in which groups of robots play matches repeatedly that are modeled by modified snowdrift games. Then by introducing a cooperation coefficient we investigate how evolutionary stability is affected by cooperation efficiency through replicator dynamics in infinite populations. We are able to identify evolutionarily stable strategies (ESS) under different fixed values of the cooperation coefficient. We further study the co-evolution of the cooperation efficiency with game dynamics using simulations of Fermi processes in finite populations. It is found that the cooperation efficiency improves when robots are capable to learn.

2 Modified snowdrift game

We consider a simplified scenario in robotic water polo matches, in which the team of players under study cares only scoring more goals without paying attention to the defense. The match is played in repeated rounds and in each round there are two field players from the team who may choose to or not to shoot. The strategies can be described in a game theoretic setting as follows: strategy C, to cooperate, is to shoot while strategy D, to defect, is to wait for the other teammate to shoot. The base game can then be described by a two-player, two-strategy symmetric game, whose payoff matrix M is

$$M = \begin{array}{c} \\ C \\ D \end{array} \begin{array}{c} \begin{array}{cc} C & D \end{array} \\ \begin{pmatrix} b-kc & b-c \\ b & 0 \end{pmatrix} \end{array}, \qquad (1)$$

where b is the benefit when at least one player shoots because of the potential to score, c is the cost of shooting alone, and $k > 0$ is a parameter, which is called the *cooperation coefficient*, introduced to quantify the synergy effect between the two players. Here we assume $b > c > 0$. When both of the two players opt for C, each of them shares the cost c discounted by the cooperation coefficient k. So smaller k implies higher cooperation efficiency and thus greater synergy effects. We use G to denote this base game and call it a modified snowdrift game since the standard snowdrift game is a special case of G when $k = \frac{1}{2}$.

3 Evolutionary game

We consider three reactive strategies in this paper: (a) the *ALLC strategy* is the strategy that a player always plays C; (b) the *tit-for-tat (TFT) strategy* is the one that the player plays C in the first round and does what his opponent did in the previous round; (c) the *suspicious Tit-for-tat (STFT) strategy* is the one that the player plays D in the first round and does what his opponent did in the previous round. For a given constant $m > 0$, every time when the base game G has been played m times, one has a stage game $\overline{G}$, which is a two-player, three-strategy symmetric game. We analyze the evolutionary stability of the formulated modified snowdrift games $\overline{G}$ with the cooperation coefficient k as the parameter with fixed different values. We can reinterpret the analysis result in the context of the robotic water polo matches. A robot player prefers to shoot together with its teammate when the cooperation efficiency is high. In contrast, when the cooperation efficiency is low, robots are more motivated to shoot alone.

4 Adaptive cooperation efficiency

Using the stage game $\overline{G}$, we study the co-evolution of the cooperation efficiency k with game dynamics using simulations of Fermi processes [1] in a group of 12 agents. We assume that k is bounded by $k_{min} \leq k \leq k_{max}$. The update rule of k is

$$k(g+1) = \begin{cases} k_{max} & \text{if } \tilde{k}(g) > k_{max} \\ k_{min} & \text{if } \tilde{k}(g) < k_{min} \\ \tilde{k}(g) & \text{otherwise} \end{cases} \qquad (2)$$

where $\tilde{k}(g) = k(g) + 1 - \eta \frac{n_{cc}(g)}{2m}$ and $\eta > 0$ is called the *learning coefficient*, which quantifies the robots' learning capability to improve their cooperation efficiency. The simulation results show the capability of the robots to improve their cooperation efficiency has great influence on the dynamics of the adaptive cooperation coefficient k and the dynamics of the strategies. Better learning capability leads to better cooperation efficiency and cooperation is preferred.

References

[1] L. E. Blume. The statistical mechanics of strategic interaction. *Games and Economic Behavior*, 5:387–424, 1993.

Simulation on the edge

Paul van der Hulst
Department of Electrical Engineering
Eindhoven University of Technology
Postbus 513
5600 MB Eindhoven
The Netherlands
Email: p.v.d.hulst@tue.nl

André Veltman
Department of Electrical Engineering
Eindhoven University of Technology
Postbus 513
5600 MB Eindhoven
The Netherlands
Email: a.veltman@piak.nl

P.P.J. van den Bosch
Department of Electrical Engineering
Eindhoven University of Technology
Postbus 513
5600 MB Eindhoven
The Netherlands
Email: p.p.j.v.d.bosch@tue.nl

1 Introduction

Many software packages are available for simulation of dynamical systems. They may differ in input method, or may target a specific application by having specific building blocks. For simulation, they will however all 'solve' a model by (assuming a known initial state) calculating the state some interval later, and then based on that extrapolated state, again an interval later, etc. .

Discrete-time systems are calculated only on the simulation samples. Continuous-time systems are more difficult to solve since the state of a continuous integrator also depends on its input *during* the interval, which is not calculated explicitly and thus must be interpolated using numerical integration methods such as 'Runge Kutta' or 'Adams-Bashford'. An implicit assumption of continuous-time solvers is that the states and signals in the model are continuous. When a continuous-time system is confronted with a discontinuous signal, simulation accuracy and causality problems will arise. This is a serious issue in systems with a high frequency of discontinuities compared to the frequency of the signal of interest (e.g. switching power converters). Currently available commercial simulation programs inadequately try to work around this problem by reducing the step size around the discontinuity. The proper solution is a modification of conventional numerical integration methods, which is not available on the market at this time.

2 External discontinuities

When a signal with discontinuities (e.g. a sawtooth) is fed to a continuous-time system, the integration step which contains the discontinuity is problematic. Although reducing the time step reduces the possible error, it is not a true solution.

A first modification to the solver is to insert a simulation sample at the discontinuity. This forces the discontinuity to be exactly at the end of the interval instead of 'somewhere in the interval'. For some integration methods (such as Euler) this solution is perfect. However, solvers which take an intermediate step at the end of the interval such as Runge-Kutta 4, will still make an integration error because the intermediate evaluation at the end of the interval will be calculated with the discontinuous signal having the value of the following interval. Thus a discontinuity will have an effect in the preceding interval, effectively making the system simulation behave acausal.

3 Internal discontinuities

A more difficult situation occurs when the system contains blocks with zero crossing detection (state events). These blocks can insert additional samples which allow for example a comparator to switch at precisely the right time. In this case also a simulation with Euler solver can run into problems because the zero crossing detection algorithm uses the finished sample at the end of the interval. Since this sample's value can be affected by the discontinuity through a feedback loop, the zero crossing time may be a function of itself. The discontinuity can even negate itself, leading to simulation deadlock.

A modification of the conventional solver algorithms will be proposed which truly solves the above problems, which are present in all of the current state of the art simulation programs.

An overview of input-to-state stability analysis methods for delay difference equations

Rob Gielen and Mircea Lazar
Eindhoven University of Technology
Eindhoven, The Netherlands
Email: {r.h.gielen,m.lazar}@tue.nl

Andrew Teel
University of California at Santa Barbara
Santa Barbara, United States of America
Email: teel@ece.ucsb.edu

1 Abstract

Systems affected by delay can be found in many applications within the control field, see the monograph [1] for an excellent overview. In the discrete-time setting, such systems are modeled by a delay difference equation (DDE). In this research DDEs that are subject to external disturbances are considered. For the input-to-state stability (ISS) analysis of DDEs two different approaches that are based on Lyapunov theory exist. Firstly, the Krasovskii approach which is an extension of classical Lyapunov theory to systems with delay, see, e.g., [2]. Secondly, the Razumikhin approach which is an application of the small-gain theorem to systems with delay, see also [2]. Both methods have particular advantages and disadvantages. For example, the Krasovskii approach is non-conservative but not computationally tractable for large delays. On the other hand, as the Razumikhin approach is an application of the small-gain theorem it simplifies the ISS analysis at the cost of some conservatism. Both methods have proven to be effective in a wide variety of control problems involving the ISS analysis and stabilization of DDEs.

Alternatively, based on the fact that a DDE can be expressed as an interconnected system, the ISS analysis can also be performed using dissipativity theory [3]. Thus, sufficient conditions, involving storage and supply functions, for ISS can be formulated. Moreover, similar conditions can also be used to establish $\mathscr{KL}$-stability or to guarantee ℓ_2 disturbance attenuation for DDEs. This technique is less conservative than Razumikhin theorems and shares the advantages of such theorems when compared to the Krasovskii approach, i.e., the method remains computationally tractable for large delays and provides a set with invariance properties that are particular to systems with delay. Moreover, for linear DDEs, when quadratic storage and supply functions are considered, the synthesis algorithm corresponding to the dissipativity based conditions recovers the corresponding synthesis algorithm for the Razumikhin approach as a particular case. Apart from that, the stability analysis can be performed by solving a linear matrix inequality (LMI) while the stability analysis via the Razumikhin approach requires solving a *bilinear* matrix inequality. Furthermore, stabilizing controller synthesis for linear DDEs can also be formulated as an LMI. As such dissipativity theory provides a third alternative for the ISS analysis and stabilization of DDEs.

In what follows, the three ISS analysis techniques are compared via an example. In Section 6.1 of [2] a controller was designed for a DC-motor controlled over a communication network. In particular, the maximal admissible delay (MAD) for which a certain rate of convergence could be guaranteed, was established. Results were obtained using both the Razumikhin and the Krasovskii approach. Obviously, the dissipativity based approach can also be used to solve this problem. In Table 1 the MAD and the complexity of the corresponding controller synthesis algorithm are shown for all three approaches. These results confirm that the stabilizing controller synthesis method based on the Krasovskii approach is the least conservative. Furthermore, the stabilizing controller synthesis method based on the Razumikhin approach has the lowest complexity. The method based on dissipativity theory on the other hand is less conservative than the Razumikhin approach and of lower complexity than the Krasovskii approach. As such it provides a trade-off between the advantages of the Razumikhin and the Krasovskii approach.

Table 1: The MAD and the dimension of the corresponding controller synthesis LMI for each method.

method:	MAD	dimension of the LMI
Razumikhin approach	4.24ms	26×26
Dissipativity approach	4.40ms	32×32
Krasovskii approach	4.80ms	36×36

References

[1] V. Kolmanovskii and A. Myshkis, *Introduction to the theory and applications of functional differential equations*. Dordrecht, The Netherlands: Kluwer Academic Publishers, 1999.

[2] R. H. Gielen, M. Lazar, and I. V. Kolmanovsky, "Lyapunov methods for time–invariant delay difference inclusions," *SIAM Journal on Control and Optimization*, vol. 50, no. 1, pp. 110–132, 2012.

[3] J. C. Willems, "Dissipative dynamical systems," *Archive for Rational Mechanics and Analysis*, vol. 45, pp. 321–393, 1972.

Multimesh $\mathscr{H}_2$ model reduction and extensions

Samuel Melchior
CESAME
Université catholique de Louvain
4 Avenue G. Lemaître
B-1348 Louvain-la-Neuve
Belgium
Email: samuel.melchior@uclouvain.be

Vincent Legat
CESAME
Université catholique de Louvain
4 Avenue G. Lemaître
B-1348 Louvain-la-Neuve
Belgium
Email: vincent.legat@uclouvain.be

Paul Van Dooren
CESAME
Université catholique de Louvain
4 Avenue G. Lemaître
B-1348 Louvain-la-Neuve
Belgium
Email: paul.vandooren@uclouvain.be

We describe a multimesh approach for model reduction of large scale dynamical systems [1], modelled via generalized state-space systems $\{M,A,B,C\}$ of the type

$$\begin{cases} M\dot{\mathbf{x}}(t) &= A\mathbf{x}(t)+B\mathbf{u}(t) \\ \mathbf{y}(t) &= C\mathbf{x}(t) \end{cases}$$

(with input $\mathbf{u}(t)\in\mathbb{R}^m$, state $\mathbf{x}(t)\in\mathbb{R}^N$ and output $\mathbf{y}(t)\in\mathbb{R}^p$), obtained from a finite element discretization constructed on a fine mesh. The basic step of the algorithm is a fixed point iteration used to solve the $\mathscr{H}_2$ model reduction problem [2]. This iteration requires the solution of a pair of Sylvester equations defined in terms of the state space equations and a current low order approximation $\left\{\hat{M},\hat{A},\hat{B},\hat{C}\right\}$ of the dynamical system.

We show how this fixed point can be efficiently obtained using a multilevel approach where the fixed point iteration is applied only a few steps on each grid level. We illustrate these ideas on the construction of low order models for a particular example of advection–diffusion equations.

We also describe extensions of the scheme to time-varying and nonlinear dynamical systems. The nonlinearity can be tackled using alternatively the DEIM interpolation technique [3] . The idea is to use $\mathscr{H}_2$ model reduction in order to iteratively compute the dominant signal space of the state $\mathbf{x}(t)$ instead of using POD. Some of the main advantages of this approach are:

- an output $\mathbf{y}(t)$ can be taken into account,
- no a priori simulated solutions are needed,
- theoretical bounds on $\mathscr{H}_2$ optimal model reduction can be used.

Ideally, the goal is to apply only one or two nonlinear iterations on the finest mesh.

Finally, we investigate the connections between Model Order Reduction and iterative schemes. On the one hand, Krylov solvers preconditioned with multigrid can be used as inexact solver for the Sylvester equations in the $\mathscr{H}_2$ iterations. On the other hand, we show that a reduced order model can be used as a preconditioner.

References

[1] A. Antoulas. Approximation of Large-Scale Dynamical Systems. SIAM Publications, Philadelphia (2005)

[2] P. Van Dooren, K.A. Gallivan, P.-A. Absil, $\mathscr{H}_2$-optimal model reduction with higher order poles. SIAM J. Matr. Anal. Appl., Vol.31(5), 2738–2753, 2010.

[3] S. Chaturantabut, D.C. Sorensen, Discrete Empirical Interpolation for nonlinear Model reduction. SIAM J. Sci. Comp., Vol.32(5), 2737–2764, 2009.

Stability analysis for linear systems with state reset

Svetlana Polenkova
Department of Applied Mathematics
University of Twente
P.O. Box 217
7500 AE Enschede, The Netherlands
Email: s.v.polenkova@utwente.nl

Jan Willem Polderman
Department of Applied Mathematics
University of Twente
P.O. Box 217
7500 AE Enschede, The Netherlands
Email: j.w.polderman@math.utwente.nl

Rom Langerak
Department of Computer Science
University of Twente
P.O. Box 217
7500 AE Enschede, The Netherlands
Email: langerak@cs.utwente.nl

Introduction

In our work we focus on reset control systems. The basic concept in reset control is to reset all states or subset of states of a linear controller to zero whenever its input meets a threshold.

Reset control actions are similar to a number of popular nonlinear control strategies such as relay control, sliding mode control and switching control. A common feature to all of them in the use of a switching surface to trigger a control signal. One of the main disadvantages of reset controllers is that the reset action may destabilize a stable feedback system. Reset control systems can also be considered as a special case of hybrid systems. Stability analysis for a seemingly simple situation, a single linear planar system with a state reset, is considered by the authors in [3].

Motivation and Problem Statement

The main motivation for using reset control comes from the urge to reduce overshoot in a step response since reset controllers can overcome limitations present in all linear controllers [2].

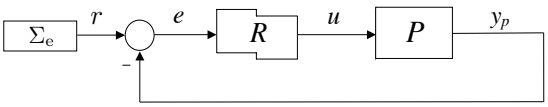

Figure 1: Block diagram of a reset control system

Indeed, by invoking reset of the controller states dramatic performance improvement may result. A major drawback, however, is the potential risk of loosing stability. In this paper, inspired by this effect, we study stability of systems with state reset in an abstract setting. Our results may be applied to reset control systems but are also of interest in their own right.

The reset systems that we study can conveniently be modeled as in Figure 2. Here A is a Hurwitz matrix, $\mathcal{V}$ is a linear sub space of the state space and Π is a projection operator.

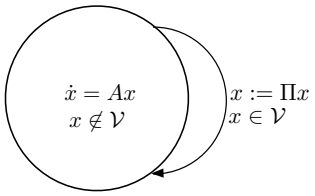

Figure 2: Linear system with state reset

The main result that we derive is a sufficient condition in term of a system of linear matrix inequalities. Furthermore, we introduce the concept of project gain. Through the projection gain we provide quantitative insight in the effect of switching on the overall stability of the reset system.

References

[1] Orhan Beker, C. V. Hollot, Y. Chait, and H. Han. Fundamental properties of reset control systems. *Automatica*, 40(6):905–915 (2005), 2004.

[2] C. V. Hollot, Orhan Beker, Yossi Chait, and Qian Chen. On establishing classic performance measures for reset control systems. In *Perspectives in robust control (Newcastle, 2000)*, volume 268 of *Lecture Notes in Control and Inform. Sci.*, pages 123–147. Springer, London, 2001.

[3] S.V. Polenkova, J.W. Polderman, and R. Langerak. Stability criteria for planar linear systems with state reset. In *Proceedings of the 19th International Symposium on Mathematical Theory of Networks and Systems (MTNS 2010)*, Budapest, 5-9 July, 2010.

Nonparametric Identification of Linear Periodically Time-Varying Systems Using Arbitrary Inputs

Ebrahim Louarroudi, John Lataire and Rik Pintelon
Vrije Universiteit Brussel, Dept. ELEC, Pleinlaan 2, 1050 Elsene, Belgium,
Email: elouarro@vub.ac.be

1 Introduction

Periodically time-varying (PTV) systems appear in a lot of engineering applications [1]. Examples can be found in control, sampled data systems, multi-rate filter banks, mechanical processes, and so on. For instance, mechanical systems that sustain a periodic motion (at constant angular speed) exhibit a PTV behavior due to the rotating parts in the system.

Recently, a nonparametric scheme was developed to obtain an estimate of the evolution of the time-varying dynamics of continuous-time PTV systems, [2]. The proposed method imposes restrictions on the type of input (i.e. a broad band periodic signal). In this work, this assumption is relaxed to arbitrary inputs.

2 Output-error framework

The problem that is tackled here is shown schematically in Fig. 1 where the time-varying dynamics of an LPTV system are described by the *instantaneous transfer function* (ITF), $G(j\omega,t)$. Loosely spoken, the ITF can be seen as being the time-varying response to a complex exponential, $u_0(t) = e^{j\omega t}$,

$$u_0(t) = e^{j\omega t} \rightarrow y_0(t) = |G(j\omega,t)|e^{j(\omega t + \angle G(j\omega,t))}. \qquad (1)$$

The similarity in (1) with the LTI-response is obvious, except that the amplitude change and the phase shift are now time-dependent.

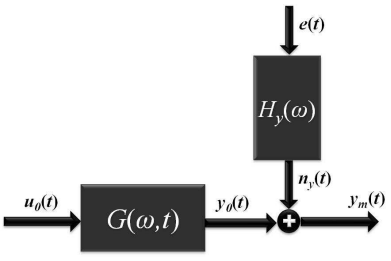

Figure 1: LPTV system, described by the ITF $G(j\omega,t)$ with known input $u_0(t)$ and disturbed output $y_m(t)$. The output noise $n_y(t) = H_y\{e(t)\}$ is written as filtered band-limited white noise $e(t)$.

Acknowledgement - This work was supported in part by the Fund for Scientific Research (FWO-Vlaanderen), by the Flemish Government (Methusalem Fund, METH1), and by the Belgian Federal Government (IUAP VI/4).

Since most physical systems exhibit a smooth dynamic behavior, their dynamics can locally be well-described by a polynomial, as is thoroughly elaborated in [2]. This powerfull algorithm is applied to the ITF, $G(j\omega,t)$ in (1).

3 a PTV Mass-Damper-Spring System

The simulated system is a *linear* PTV mass-damper-spring system with equation of motion

$$m\frac{d^2y_0(t)}{dt^2} + c(t)\frac{dy_0(t)}{dt} + k(t)y_0(t) = k_m u_0(t). \qquad (2)$$

Both the natural frequency and the damping ratio of the system are selected to be PTV. The input $u_0(t)$ is chosen to be normal distributed, $\mathcal{N}(0,1)$. The true output $y_0(t)$ was disturbed by stationary, band-limited colored noise with a time domain SNR of 20 dB. The results are summarized in Fig. 2 by looking at the estimated ITF for some time instants.

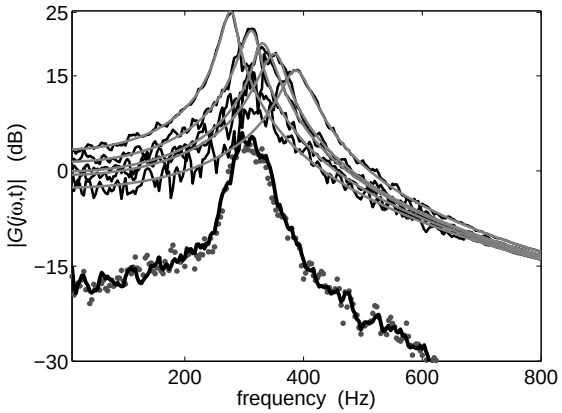

Figure 2: The true ITF at some time instants (grey), estimated ITF (black). The averaged uncertainty of the ITF over time (bold black), mean RMS over time (grey dots).

References

[1] S. Bittanti and P. Colaneri. *Periodic Systems: Filtering and Control*. Springer, 2008.

[2] Ebrahim Louarroudi, R. Pintelon, and J. Lataire. Nonparametric tracking of the time-varying dynamics of weakly nonlinear periodically time-varying systems using periodic inputs. *IEEE Trans. on Instrumentation and Measurement*, **(accepted for publication)**.

Identification of 2D interconected systems using Multilevel Semi-Separable Gradient method.

Patricio Torres, J.W. van Wingerden and Michel Verhaegen
Delft Center of Systems and Control, TU Delft, Mekelweg 2, 2628 CD Delft, The Netherlands
Email: {p.i.torrestapia, j.w.vanwingerden, m.verhaegen}@tudelft.nl

1 Introduction

In this work, a new identification method for large interconnected systems is presented. A 2D grid of systems which have full state-space parametrization is considered. The proposed method optimizes the Output-Error of the lifted system by using a structure exploiting Steepest-Descent method. It is shown that the computational burden can be efficiently managed by using Multilevel Sequentially Semi-Separable (M-SSS) matrix operations. A numerical example is provided.

2 Problem formulation

We consider a grid of MN sub-systems as depicted in Fig.1. Every sub-system is described by the following set of equations:

$$\begin{bmatrix} x_{k+1}^{(v,h)} \\ y_k^{(v,h)} \\ e_k^{(v,h)} \\ w_k^{(v,h)} \\ N_k^{(v,h)} \\ S_k^{(v,h)} \end{bmatrix} = \begin{bmatrix} A_{(v,h)} & B_{(v,h)} & B_e^{(v,h)} & B_w^{(v,h)} & B_N^{(v,h)} & B_S^{(v,h)} \\ C_{(v,h)} & D_{(v,h)} & F_e^{(v,h)} & F_w^{(v,h)} & F_N^{(v,h)} & F_S^{(v,h)} \\ C_e^{(v,h)} & D_e^{(v,h)} & W_e^{(v,h)} & 0 & 0 & 0 \\ C_w^{(v,h)} & D_w^{(v,h)} & 0 & W_w^{(v,h)} & 0 & 0 \\ C_N^{(v,h)} & D_N^{(v,h)} & 0 & 0 & W_N^{(v,h)} & 0 \\ C_S^{(v,h)} & D_S^{(v,h)} & 0 & 0 & 0 & W_S^{(v,h)} \end{bmatrix} \begin{bmatrix} x_k^{(v,h)} \\ u_k^{(v,h)} \\ e_k^{(v,h-1)} \\ w^{(v,h+1)} \\ N^{(v-1,h)} \\ S_k^{(v+1,h)} \end{bmatrix}, \quad (1)$$

where $x_k^{(v,h)} \in \Re^{n\times 1}$ is the state vector, $u_k^{(v,h)} \in \Re^{r\times 1}$ is the input vector, $y_k^{(v,h)} \in \Re^{\ell\times 1}$ is the output vector, $e_k^{(v,h)} \in \Re^{q\times 1}$, $w_k^{(v,h)} \in \Re^{q\times 1}$, $N_k^{(v,h)} \in \Re^{q\times 1}$ and $S_k^{(v,h)} \in \Re^{q\times 1}$ are the interconnection variables. Then, the lifted system of the grid can be obtained by performing consecutive substitutions in (1):

$$\begin{bmatrix} \overline{\overline{x}}_{k+1} \\ \overline{\overline{y}}_k \end{bmatrix} = \begin{bmatrix} \overline{\overline{A}} & \overline{\overline{B}} \\ \overline{\overline{C}} & \overline{\overline{D}} \end{bmatrix} \begin{bmatrix} \overline{\overline{x}}_k \\ \overline{\overline{u}}_k \end{bmatrix}, \quad (2)$$

where $\overline{\overline{x}}_k \in \Re^{(MN)n\times 1}$ is the interconnected state vector that contains all the local states stacked together. Similar definitions hold for $\overline{\overline{x}}_{k+1} \in \Re^{(MN)n\times 1}$, $\overline{\overline{u}}_k \in \Re^{(MN)r\times 1}$, and $\overline{\overline{y}}_k \in \Re^{(MN)\ell\times 1}$. On the other hand, $\overline{\overline{A}} \in \Re^{(MN)n\times(MN)n}$, $\overline{\overline{B}} \in \Re^{(MN)n\times(MN)r}$, $\overline{\overline{C}} \in \Re^{(MN)\ell\times(MN)n}$, and $\overline{\overline{D}} \in \Re^{(MN)\ell\times(MN)r}$ are M-SSS matrices [1]. Thus, the identification problem can be formulated as follows: Given the input-output data:

$$\{u_k^{(v,h)}, y_k^{(v,h)}\}_{k=\{1,\ldots,K\}}^{v=\{1,\ldots,M\},h=\{1,\ldots,N\}},$$

find the distributed system matrices $A_{(v,h)}$, $B_{(v,h)}$, $B_e^{(v,h)}$, $B_w^{(v,h)}$, $B_N^{(v,h)}$, $B_S^{(v,h)}$, $C_{(v,h)}$, $C_e^{(v,h)}$, $C_w^{(v,h)}$, $C_N^{(v,h)}$, $C_S^{(v,h)}$, $D_{(v,h)}$, $D_e^{(v,h)}$, $D_w^{(v,h)}$, $D_N^{(v,h)}$, $D_S^{(v,h)}$, $F_e^{(v,h)}$, $F_w^{(v,h)}$, $F_N^{(v,h)}$, $F_S^{(v,h)}$, $W_e^{(v,h)}$, $W_w^{(v,h)}$, $W_N^{(v,h)}$ and $W_S^{(v,h)}$, for all $v \in \{1,2,\cdots,M\}$ and $h \in \{1,2,\cdots,N\}$ up to a set of similarity transformations.

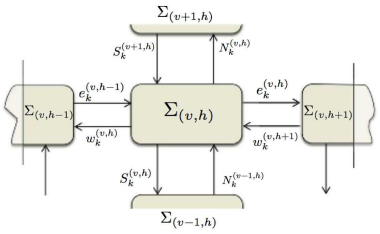

Figure 1: Subsystem (v,h).

3 Output error identification

In the Output-Error model approach, the following objective function has to be minimized:

$$J_K(\overline{\theta}) = \frac{1}{K}\sum_{k=1}^{K} ||\overline{\overline{y}}_k - \hat{\overline{\overline{y}}}_k(\overline{\theta})||_2^2 = \frac{1}{K}\sum_{k=1}^{K} \varepsilon_k(\overline{\theta})^T \varepsilon_k(\overline{\theta}), \quad (3)$$

where $\overline{\overline{\theta}}$ is the vector that contains all the parameters of the matrices described above. For the sake of simplicity and in order to minimize (3), the Steepest-Descent method is considered. In this case, the update law becomes:

$$\overline{\overline{\theta}}_{i+1} = \overline{\overline{\theta}}_i + \mu J_K' \quad (4)$$

where $\mu \in [0,1]$ is the step size and J_K' is the Jacobian that satisfies the following equation:

$$J_K' = -\frac{2}{K}\Big(\sum_{k=1}^{K}\left(\frac{\partial\overline{\overline{A}}(\overline{\overline{\theta}})}{\partial\overline{\overline{\theta}}}\hat{\overline{\overline{x}}}_k(\theta)\right)^T \overline{\overline{X}}_k(\overline{\overline{\theta}}) + \sum_{k=1}^{K}\left(\frac{\partial\overline{\overline{B}}(\overline{\overline{\theta}})}{\partial\overline{\overline{\theta}}}\overline{\overline{u}}_k\right)^T \overline{\overline{X}}_k(\overline{\overline{\theta}}) + \quad (5)$$

$$\sum_{k=1}^{K}\left(\frac{\partial\overline{\overline{C}}(\overline{\overline{\theta}})}{\partial\overline{\overline{\theta}}}\hat{\overline{\overline{x}}}_k(\overline{\overline{\theta}})\right)^T \varepsilon_k(\overline{\overline{\theta}}) + \sum_{k=1}^{K}\left(\frac{\partial\overline{\overline{D}}(\overline{\overline{\theta}})}{\partial\overline{\overline{\theta}}}\overline{\overline{u}}_k\right)^T \varepsilon_k(\overline{\overline{\theta}})\Big), \quad (6)$$

$$\overline{\overline{X}}_{k-1}(\overline{\overline{\theta}}) = \overline{\overline{A}}^T(\overline{\overline{\theta}})\overline{\overline{X}}_k(\overline{\overline{\theta}}) + \overline{\overline{C}}^T(\overline{\overline{\theta}})\varepsilon_k(\overline{\overline{\theta}}) \quad (7)$$

where $\hat{\overline{\overline{x}}}_k(\overline{\overline{\theta}})$ and $\varepsilon_k(\overline{\overline{\theta}})$ are obtained by simulating the model given in (2). Since we are considering a distributed identification problem, the system matrices all have M-SSS structure (denoted by $\overline{\overline{*}}$). Therefore, partial derivatives, matrix-vector product and matrix transpose operations can be performed in complexity $\mathcal{O}(MN)$, (see [1]).

References

[1] J.K Rice, "Efficient Algorithms for Distributed Control: A Structured Matrix Approach," Ph.D. Thesis, TU Delft, 2010.

[2] J.W. van Wingerden, P. Torres "Identification of spatially interconected systems using Sequentially Semi-Separable Gradient method.," submitted to IFAC SYSID 2012.

Two dimensional spline interpolation for slowly time-varying systems

Péter Zoltán Csurcsia[1,2], Johan Schoukens[1] and István Kollár[2]
[1] Vrije Universiteit Brussel, Pleinlaan 2, 1050 Elsene, Belgium
[2] Budapest University of Technology and Economics, Magyar tudósok krt. 2, 1117 Budapest, Hungary
Email: peter.zoltan.csurcsia@vub.ac.be

1 Introduction

The goal of this paper is to present a new method which estimates non-parametrically slowly time-varying systems (STV). If the parameter changing of the observed system is sufficiently slow, we can use a new algorithm based on modified, generalized B-spline basis functions. In case of STV systems the output is determined by a two dimensional impulse response function h_{LV} as $y[n] = \sum_{k=-\infty}^{\infty} h_{LV}[n,k]u[k]$. Assume that the length of $u[n]$ is N and the length of $y[n]$ is N, then $h[n,k](n = 0,...,N-1$ and $k = 0,...,N-1)$ consists of N^2 unknown values, to be determined on the basis of those measurements. Infinitely many solutions are equally possible. Among all the possible solutions, we select a smooth solution. This can be done using smoothing methods, e.g.: spline interpolation or approximation.

2 Spline technique

Assuming that only a few parameters are slowly changing and plotting the frequency response function (FRF) step by step next to each other we get a smooth surface that can be estimated with several methods (e.g.: polynomial-fitting) or with the new approach: the B-spline [1] based spline interpolation method generalized to two dimensions [2]. With the spatial technique we can measure the FRF matrix [4] as a collection of different time realizations of FRFs. Namely, we measure the FRF of the system at certain time instant, then we put the result into a matrix and repeat this procedure a few times. With that a double smoothing can be used to decrease the number of parameters to be stored i.e. decrease the degree of freedom and the computing time: once over the different excitation time (which refers to the system memory) and once over the actual excitation (referring to the system behavior).

3 An example

Consider a very simple simulation example: a time-varying system represented by a second order inverse Chebyshev low-pass filter with changing ripple ratio and resonance frequency (see Fig. 1. on the left). Using a (to the resonance frequency reactive, see Fig. 1. on the right) weighted cost function we can judge the goodness of estimation. The acceptance level in rms sense is 27.76 (in this example there are 301x256 points, with an average error in the whole domain is -40 dB on each measured point). Figure 2. shows the generalized estimate with double smoothing B-splines of degrees [1] 3/2 using each twelfth knot (the point that is used for fitting the surface) on frequency and time axis.

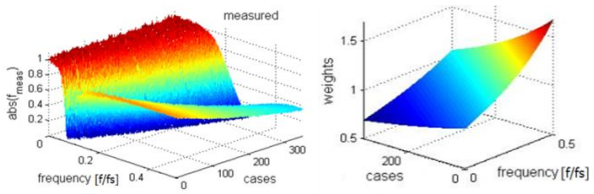

Figure 1: On the left side the system under test is shown. On the right side the weights are shown.

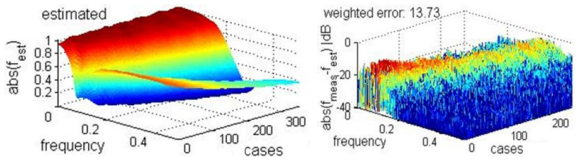

Figure 2: On the left side the B-spline estimation is shown. On the right side the rms value of the Euclidean distance between true and estimated systems in decibel scale is shown.

4 Summary

In this work we developed a new non-parametric estimation method for slowly time-varying systems with modified and generalized B-spline technique. This technique is very useful because it is more flexible and faster than the single polynomial fitting, the computing time is linear in the number of points (knots) and much faster than traditional methods. The only cost that we have to pay that either the knot sequences or the matrices of B-spline must be stored.

References

[1] H. Prautzsch, W. Boehm, M. Paluszny, "Bézier and B-spline techniques," Springer-Verlag, Berlin, 2001

[2] P. Dierckx,"An algorithm for surface-fitting with spline function," IMA J. for NA, vol. 1, pp. 267-283, 1981

[3] R. Pintelon, J. Schoukens: "System identification, a frequency domain approach," New Jersey, January 2001

[4] S. Vanlanduit, "High spatial resolution experimental modal analysis," Vrije Universiteit Brussel, May 2001

State Space Identification for Linear Parameter-Varying Systems

Jan Goos
ELEC
Vrije Universiteit Brussel
Pleinlaan 2 1050 Brussel
Belgium
Email: jan.goos@vub.ac.be

1 Introduction

Although the linear time-invariant (LTI) system identification framework has proven its merits for many years, in quite some applications the linearity and time-invariance hypotheses are only approximately true or not valid at all. The need to operate processes with higher accuracy and efficiency has therefore resulted in the realization that the non-linear (NL) and time-varying (TV) nature of many physical systems must be handled by the control design.

In the linear parameter varying (LPV) framework, the dynamic relation between the input and output signals is still assumed to be linear, but it is continuously adapted based on the actual value of the scheduling parameters. Besides the excitation one should also choose a periodic or non-periodic scheduling. A common assumption is the bounded rate of variation of the coefficients and parameters.

2 Gain scheduling

Because LTI-systems have become a well-known framework, they have given rise to an intuitive form of LTV modelling, called gain-scheduling [3]. Here, the basic concept is to linearize the NL system model at different operating points, resulting in a set of local LTI descriptions. Next, the LTI model or the according controller designs are interpolated to obtain a global solution of the entire operation regime. The obvious advantage of this approach is that only LTI system should be estimated. However, a full measurement must be carried out for each operating point, and we cannot capture dynamics w.r.t. the varying parameters. We will therefore opt for a direct, global identification method.

3 Model class

The goal of this research is the development of algorithms for the identification of time-varying dynamical systems. The calculations will be done directly in the frequency domain, in contrast to [2]. In a first step, a non-parametric estimate of the noise and system model is estimated, as described in [1]. In a second step, one of three specific model structures can be extracted:

1. A differential or difference equation with parameter-varying coefficients [5, 6]
2. A parallel structure of LTI systems, each followed by a parameter-varying gain [6]
3. A state space model with parameter-varying A,B,C,D matrices

Acknowledgement - This work was supported in part by the Fund for Scientific Research (FWO-Vlaanderen), by the Flemish Government (Methusalem Fund, METH1), and by the Belgian Federal Government (IUAP VI/4).

4 LTV state-space

Although some promising work has already been done on 1. and 2. in [5, 6], we know from [4] that a conversion from one model class to another is not as straightforward as in the LTI case. We will concentrate on the latter class, because state space can be used directly in control applications. The research is therefore immediately relevant to the industry, which results in a variety of applications and test setups. The drawback of using the state-space representation

$$\dot{x}(t) = A(p(t))x(t) + B(p(t))u(t) \quad (1)$$
$$y(t) = C(p(t))x(t) + D(p(t))u(t) \quad (2)$$

is that we do not have a direct relation between the input u and the output y, while these are the only measured values. It will therefore be necessary to estimate the states x, e.g. by adapting a sub-space algorithm to cope with the time variation.

References

[1] R. Pintelon & J. Schoukens: "System Identification: A Frequency Domain Approach" IEEE Press, 2001

[2] V. Verdult & M. Verhaegen "Subspace identification of multivariable linear parameter-varying systems" AUTOMATICA Volume: 38 Issue: 5 Pages: 805-814, 2002

[3] J. De Caigny: "Contributions to the Modeling and Control of Linear Parameter-Varying Systems" Doctoral Thesis, KUL 2009

[4] R. Toth: "Modeling and Identification of Linear Parameter-Varying Systems" Springer Germany, 2010.

[5] E. Louarroudi: "Identificatie van Lineaire Periodieke Tijdsvariërende Systemen" Master thesis, VUB 2011

[6] J. Lataire: "Frequency Domain Measurement and Identification of Linear, Time-Varying Systems" Doctoral Thesis, VUB 2011

Solution for State Constrained Optimal Control Problems

Thijs van Keulen
DAF Trucks N.V. Eindhoven
Email: Thijs.van.Keulen@daftrucks.com

Bram de Jager
Eindhoven University of Technology
Email: A.G.deJager@tue.nl

1 Problem description

This paper presents a numerical solution for scalar state constrained optimal control problems for which we can formulate the Hamiltonian which is assumed to be convex in the control variable:

$$H = g(x,u,r) + pf(x,u,r) + \lambda_1(x-\bar{x}) + \lambda_2(\underline{x}-x). \quad (1)$$

Here, g is the integrant of the cost function $J = \int_0^T g(x,u,r)dt$ to be optimized, x the scalar state variable, u the scalar control variable, and r the extraneous input, p the Lagrange multiplier, f the state dynamic equation, λ_1 and λ_2 the multiplier functions for the state constraints, $\bar{x}$ the upper state constraint, $\underline{x}$ the lower state constraint. Besides, the terminal constraints are given: $x(0) = x_0$, and $x(T) = x_T$. Using Pontryagin's Maximum Principle [3], the necessary conditions of optimality can be derived:

- the differential equation on the multiplier function:

$$\dot{p} = \frac{\partial H}{\partial x} = \frac{\partial g(x)}{\partial x} + p\frac{\partial f(x)}{\partial x} + \lambda_1 - \lambda_2, \quad (2)$$

- the complementary slackness condition:

$$\lambda_1(t) = 0 \quad \text{for} \quad t \in [q : x^*(q) < \bar{x}], \quad (3)$$

$$\lambda_2(t) = 0 \quad \text{for} \quad t \in [q : x^*(q) > \underline{x}], \quad (4)$$

- the discontinuity of the multiplier trajectory p given by the following jump condition (for details, see [1]):

$$p(\tau^+) = p(\tau^-) + \mu_1(\tau) - \mu_2(\tau), \quad (5)$$

with $\mu_1 \geq 0$ and $\mu_2 \geq 0$. Under the assumption that ξ_1 and ξ_2 have a piecewise continuous derivative, it is possible to set $\lambda_1(t) = \dot{\xi}_1(t)$, $\lambda_2(t) = \dot{\xi}_2(t)$, for every t for which ξ_1 and ξ_2 exist and $\mu_1(\tau) = \xi_1(\tau^-) - \xi_1(\tau^+)$, $\mu_2(\tau) = \xi_2(\tau^-) - \xi_2(\tau^+)$, for all $\tau \in [0,\ T]$ where ξ_1 and ξ_2 are not differentiable,

- the Hamiltonian H has a global minimum with respect to control u:

$$u^* = \arg\min_{u \in \mathscr{U}(r)} H(x^*, u, p^*, r), \quad (6)$$

where u^* the optimal control trajectory, $\mathscr{U}$ the set of admissible controls, x^* is the optimal state trajectory, and p^* the corresponding optimal adjoint multiplier trajectory.

2 Solution

Ignoring the state constraints ($\lambda_1 = \lambda_2 = 0$), from the necessary conditions of optimality an initial value problem can be constructed. Given a prescribed extraneous input r and an initial multiplier value of p, (6) can be solved at each time step. The initial value problem $(\dot{x}, \dot{p}) = f(x(0), p(0))$ subject to the terminal constraint $x(T) = x_T$ can be solved with a single shooting algorithm. If $f(t, x^0, p^0)$ denotes the solution of the initial value problem subject to the initial conditions $x(0) = x_0$ and $p(0)$, the problem reduces to finding $p(0) = p^*(0)$. A root finding algorithm can be used to obtain $p^*(0)$, e.g., bisection.

Our approach [2] will adopt the unconstrained solution and extends it for the state constrained case. The procedure is briefly outlined:

- the unconstrained optimal trajectory is calculated,
- if state constraints are exceeded, the problem is split in two subproblems at the time where the unconstrained solution exceeds the state constraint the most,
- the subproblem for times before the time where the maximum exceeding is reached, has an endpoint constraint at the boundary that is reached, while the subproblem for times after the time where the maximum is reached has an initial condition at the boundary,
- this procedure is repeated until none of the subtrajectories exceeds a bound (recursion).

A proof for optimality of the solution is given.

3 Example

The approach is applied to the power split control for hybrid vehicles for a predefined power and velocity trajectory and is compared with a Dynamic Programming solution. The computational time is, at least, one order of magnitude less than for the Dynamic Programming algorithm for a superior accuracy.

References

[1] R.F. Hartl, S.P. Sethi, and R.G. Vickson. A survey of the maximum principles for optimal control problems with state constraints. SIAM review, 37:181-218, 1995.

[2] T. van Keulen, J. Gillot, B. de Jager, M. Steinbuch. Solution for State Constrained Optimal Control Problems Applied to Power Split Control for Hybrid Vehicles. Subm. for journal publication.

[3] R. Vinter. Optimal Control. Springer, USA, 2000.

Iterative Learning Control with Multiple Pass Points

Tong Duy Son
Division PMA, Department of Mechanical Engineering, Katholieke Universiteit Leuven
Celestijnenlaan 300B, B-3001 Heverlee, Belgium
Email: duyson.hut@gmail.com

Hyo-Sung Ahn
Department of Mechatronics, Gwangju Institute of Science and Technology (GIST)
1 Oryong-dong, Buk-gu, Gwangju 500-712, Korea
Email: hyosung@gist.ac.kr

1 Introduction

This work presents iterative learning control [1] (ILC) algorithms for multiple points tracking problems, developed at DCAS Laboratory, GIST, under supervision of Professor Hyo-Sung Ahn.

Existing ILC approaches solve the multiple points tracking problem in two consecutive steps: the first step generates a reference trajectory that passes through all given points at given times. In the second step, ILC controller learns the control input in order to follow this reference trajectory. However, these approaches show drawbacks under certain circumstances. First, even though the given reference trajectory plays an important role in the performance of the ILC controller, there is no connection between trajectory planning and the control algorithm. Hence, it is not certain to guarantee that the specified trajectory is the optimal trajectory for the ILC implementations. Second, most planning algorithms face difficulties in generating optimal reference trajectories. In particular, the existence of a large number of data points can lead to a significant increase in the computational analysis. Third, when there is a change in the motion profile, the whole two step procedure has to be repeated. In order to overcome these drawbacks, ILC controllers that combine both steps are developed.

2 ILC algorithms

First, we present a new learning technique that investigates the relationship between two stages. The key point here is the flexible selection of reference trajectory. Specifically, we identify a class of reference trajectories and their relationships. Then, we develop an update law for the reference trajectory such that the convergence rate of the ILC controller is improved, that is, the reference trajectory is updated by the ILC scheme instead of being fixed in the iteration domain. After that, the control input is learned for the updated reference trajectory. The advantage of this approach is faster convergence, resulting in a reduced cost and complexity on practical implementations.

Second, we propose a concurrent approach that learns both the reference trajectory and the control signal iteratively. The strength of the proposed formulation is the methodology to obtain a control signal through learning laws that take into accounts the reference points and system dynamics. Here, we apply the norm optimal ILC algorithms for analysis purposes. However, our approach is different since the cost function considers errors only at the given reference points, which leads to a new learning algorithm where the dimension of the learning vector is equal to the number of reference points. Thus, the approach also reduces the memory requirements. Proofs of and conditions for stability and monotonic convergence are given.

In addition, we extend the second approach by studying learning algorithms in the case where we allow the reference points to vary inside an interval in the iteration domain. This problem happens naturally in many applications since the reference points might not be defined exactly because of non-repetitive measurement noise, sensor noises, disturbances... The approach is presented through three main steps. First, we formulate the new optimization based ILC problem including the non-repetitive uncertainties, which is bounded, at the reference points. Then, the problem is formulated as a two objectives optimization model. Second, by solving the min-max problem, we achieve an optimized adaptive ILC algorithm. Last, a convergence analysis is performed.

3 Acknowledgement

Tong Duy Son is currently a phd student at the KU Leuven, supported by the FP7 Marie Curie Initial Training Network ITN IMESCON (GA 264672).

References

[1] H.S. Ahn, Y.Q. Chen, and K.L. Moore, "Iterative learning control: Brief survey and categorization", *IEEE Transactions on Systems, Man and Cybernetics Part C: Applications and Reviews*, vol. 37, no. 6, pp. 1099–1121, 2007.

Iterative feedback tuning to learn steering control of an autonomous tractor

E. Hostens, G. Pinte, W. Symens
FMTC (Flanders' Mechatronics Technology Centre)
Celestijnenlaan 300D, 3001 Heverlee, Belgium
Email: erik.hostens@fmtc.be

1 Introduction

A vast majority of controllers in industry are simple feedback controllers with a limited number of control parameters, e.g. PIDs. In order to tune such a controller properly, some experiments in open loop, e.g. step tests, are typically carried out on the machine to estimate the system's behavior and calculate the optimal controller settings. Afterwards, the settings of the controller are seldomly adjusted, either because the operator lacks the appropriate knowledge, or because it is practically undesired to carry out more open loop experiments. It appears in many cases however that further adjusting is necessary to guarantee optimal control behavior. Iterative feedback tuning (IFT) [1] offers an answer to this issue.

2 Iterative Feedback Tuning

IFT is a method to automatically adjust the controller's setting in an iterative procedure while the control loop remains closed. In each iteration a particular excitation, calculated from observed input and output signals, is fed to the controlled system as a reference. From the observed behavior, one can estimate the partial derivatives of a quadratic cost function to the control parameters. One can then adjust these parameters based on a gradient-descent method, in order to iteratively minimize the error in the long run.

A number of adaptations of the original algorithm of Ref. [1] have been made, mainly in view of practical applicability. As it is undesired that the excitation disturbs the controlled system too much, transitions should be bumpless. Furthermore, a trade-off can be made between the magnitude of the excitation and the accuracy of the gradient estimate. Finally, IFT is combined with feed forward in parallel.

3 Experimental validation on an autonomous tractor

In this research, IFT is applied to control an autonomous tractor. Autonomous tractors become more and more important in agriculture as operator costs increase. An important challenge in the control of such tractors is to deal with varying soil conditions. Learning control provides a solution. To investigate and test advanced learning control methods for autonomous tractor steering in practice, a field robot has been built in the LeCoPro project (Fig. 1) [2].

Figure 1: The autonomous tractor in action.

The idea is to steer the tractor along a predefined trajectory, guided by a GPS system with an accuracy of a few centimeter. When the tractor is off track, e.g. after a headland turn, it is crucial that the controller puts the tractor back on track as quickly as possible to avoid production loss. The result of applying IFT in combination with feed forward on a trajectory of parallel lines is shown in Fig. 2 for a simulation of the system. Initially, the tractor is ill-tuned and oscillates. After a few turns, the tractor more quickly corrects for the track offset without oscillating.

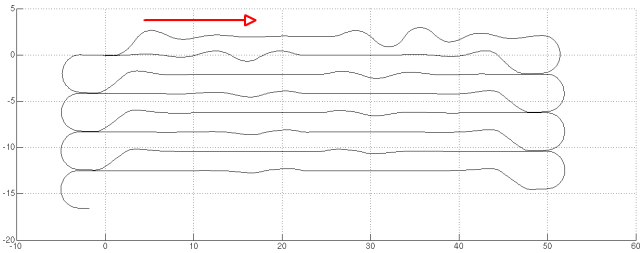

Figure 2: The tracking behavior of the autonomous tractor improves after a few iterations of IFT (axes units are in m).

References

[1] H. Hjalmarsson, M. Gevers, S. Gunnarsson and O. Lequin, *Iterative feedback tuning : theory and applications*, IEEE Control Systems Magazine, vol. 18, No 4, pp. 26-41, August 1998.

[2] http://www.lecopro.org

Multi-agent control for coordination of freight transport hubs

J. Xin, R. R. Negenborn, G. Lodewijks
Department of Marine and Transport Technology, Delft University of Technology
Mekelweg 2, 2628 CD Delft, The Netherlands
E-mail: {J.Xin,R.R.Negenborn,G.Lodewijks}@tudelft.nl

Framework

Over the last decades there has been a considerable growth in freight transportation. Most of consumer goods are shipped in standardized containers across different modalities of transportation. The requirements of high productivity and container throughput at low cost bring operational challenges to terminal operators as physical infrastructure is limited and the volume of container transshipment increases. Therefore, how to effectively manage the volume growth is investigated by considering a more integrated way of looking at transport of freight in an inter-modal way. Multi-agent techniques for control will be developed to solve complex, real-time problems of container terminals in an uncertain and changing environment. A hierarchical control structure is envisioned for the control of multiple container terminals as shown in Fig. 1, enabling a more flexible container transshipment. The research hereby focuses on coordination both within and among such transport hubs.

Problem Formulation & Approach

Single container terminal modeling and control

A container terminal provides the interface [1] between transportation using vessels, trains, and trucks as an intermodal transport hub. The growth of freight transported by containers motivates efficient management to minimize the turn-around time of vessels and reduce delays of containers. The efficiency is influenced by how modeling of a container terminal is close to the behavior of a real one. The existing models proposed are either too detailed or too abstract. How to model and control container terminals from a systematic point of view at the operational level still remains unclear.

We propose to describe the characteristics of the operation in a container terminal as a hybrid dynamical model using the Mixed-Logic Dynamics framework [2]. For such a model we will propose a model predictive control (MPC) strategy. The modeling of a container terminal using such a hybrid system representation can be addressed at the operational level in order to obtain a trade-off between details of modeling and feasibility of solving the MPC problem. The cost function in the MPC formulation focuses on the economic costs with respect to turn-around time of vessels, along with the costs of using resources available in the terminal.

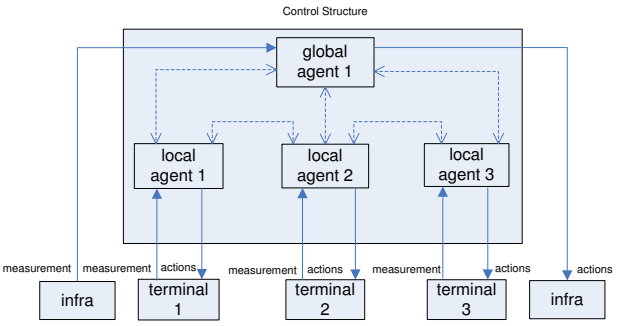

Fig. 1: Control structure for multiple container terminals.

Multiple container terminal modeling and control

Multiple container terminals can be regarded as a large-scale networked system. The centralized control of such a complex networked system brings a large computational burden and low reliability. Multi-agent technique is proposed for coordinating the flow of containers among multiple container terminals in a tractable way. At the port level, an overall agent could coordinate the actions of a lower level of container terminal agents and the vessels that transport containers. Each container terminal agent can on its turn coordinate the actions of agents associated with each machine inside the terminal. The challenge is then to determine what models each agents should use and what objectives should be achieved to obtain the best performance as a whole network of terminals. Techniques such as distributed MPC using augmented Lagrangians [3] will be investigated.

Acknowledgments Supported by the China Scholarship Council and the VENI project "Intelligent multi-agent control for flexible coordination of transport hubs" (project 11210) of the Dutch Technology Foundation STW, a subdivision of the Netherlands Organization for Scientific Research (NWO).

References

[1] F. A. Vis and R. de Koster, "Transshipment of containers at a container terminal: An overview," European Journal of Operational Research, vol. 147, no. 1, pp. 1-16, 2003.

[2] A. Bemporad and M. Morari, "Control of systems integrating logic, dynamics, and constraints," Automatica, vol. 35, no. 1, pp. 407-427, 1999.

[3] R.R. Negenborn, B. De Schutter, J. Hellendoorn. Multi-Agent Model Predictive Control for Transportation Networks: Serial versus Parallel Schemes. Engineering Applications of Artificial Intelligence, vol. 21, no. 3, pp. 353-366, 2008.

Mobile phone communications help identify stable regions in France

Pierre Deville [1]
pierre.deville@uclouvain.be

Vincent Blondel [1]
vincent.blondel@uclouvain.be

Paul Van Dooren[1]
paul.vandooren@uclouvain.be

Zbigniew Smoreda[2]
zbigniew.smoreda@orange.com

1 Introduction

We describe a network constructed from anonymized communications between 17 million mobile phone users in France over a period of 5 months. We use this network and the "Louvain method" to automatically identify cohesive communities in France. The identified communities are contiguous and coincide for a large part with the administrative regions in France. We further analyze the stability of the communities obtained by modifying the detection algorithm and the time frame used for the detection.

2 Identification of the regions

Based on the dataset described above we construct a network of geographically located nodes. The nodes are the antennas (roughly 20000 of them) and the strength of the connection between two antennas is measured by the total number of calls, or by the total communication time between them. The location of the antenna is their physical location. We then use the so-called "Louvain method" [3] to detect communities in this network. No community detection has ever been performed on similar networks for France (see [2] and [5] for studies in Belgium and in Great Britain) . The visualization of the communities obtained is represented on Figure 1. All communities are contiguous (a property that is not imposed by the algorithm) and the communities closely follow the administrative regions of France, with a few noticeable exceptions. The map that we produce here was published in the December 17, 2011 issue of the newspaper "Le Monde" and the map has since then been scrutinized and commented by many blog contributors. The differences between the communities found by our algorithm and the official administrative regions in France is discussed at length in several of these blogs.

3 Stability analysis

One could ask whether the community borders are stable or if they vary with the community detection algorithm or with the time frame used.

We present four different techniques that aim at quantifying the stability of communities. These techniques have a low computational complexity which is one of our major concern since we are dealing with very large networks. The results of our techniques provide detailed stability information about community decompositions. For network with geographically located nodes this helps to address natural questions such as: are community borders stable? do cities play a role in the community stability? Finally, we propose several visualizations of our network in order to capture complex social features in France but also the complexity of the community detection process on our network.

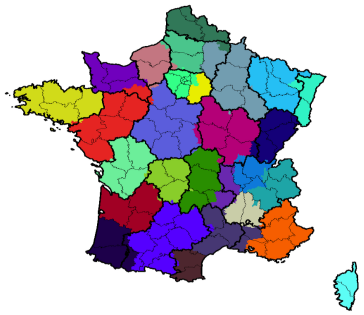

Figure 1: Automatic detection of mobile phone communities in France. The communities coincide for a large part with the administrative regions. Map reproduced in the newspaper "Le Monde" [1].

References

[1] Le mobile, reflet des frontières françaises, in "Le Monde", 17/12/2011.

[2] Blondel VD, G Krings, I Thomas, Regions and borders of mobile telephony in Belgium and around Brussels, Brussels Studies 42, ISSN 2031-0293, 2010.

[3] Blondel VD, Guillaume J-L, Lambiotte R and Lefebvre E, Fast unfolding of communities in large networks, J. Stat. Mech P10008, (2008)

[4] Blondel VD, P Deville, F Morlot, Z Smoreda, P Van Dooren, C Ziemlicki. Voice on the Border: Do Cellphones Redraw the Maps? ParisTechReview, November 15, 2011.

[5] Ratti C, S Sobolevsky, F Calabrese, C Andris, J Reades. Redrawing the Map of Great Britain from a Network of Human Interactions. PLoS ONE 5(12): e14248, (2010)

[1]Department of Mathematical Engineering, Université catholique de Louvain, Belgium.

[2]Sociology and Economics of Networks and Services Department, Orange Labs, Issy-les-Moulineaux, France

Model Predictive Railway Traffic Management

Bart Kersbergen, Ton van den Boom, Bart De Schutter
TU Delft, DCSC, Mekelweg 2, 2628 CD Delft, The Netherlands
{B.Kersbergen, A.J.J.vandenBoom, B.DeSchutter}@tudelft.nl

Introduction

Due to the increased traffic on the roads people are looking for an attractive alternative to reach their destination. Especially for longer trips railway transportation is such an attractive alternative. This results in more people traveling by train, which in turn results in the railway networks being operated closer to their maximum capacity. The effect of this is that trains have less buffer time to reduce their delays, resulting in more and longer delays, which may spread over large parts of the network. It is therefore important that these delays are dealt with as well as possible.

Currently dispatchers try to minimize the effects of delays in their dispatching area by rerouting trains or changing the order in which trains run over the infrastructure. They do this, based on the current situation in their dispatching area, by using a set of dispatching rules and their experience. In general they do not know the situation of the entire network and are not aware of the consequences of their actions outside of their dispatching area. Because of that the chosen dispatching actions may not be ideal for the entire network.

The main focus of our research is to develop a method that, based on the current state of the network, allows the dispatchers to determine which dispatching actions they should take to achieve an optimal solution for the entire network, where optimal relates to minimizing a cost function based on the total delay and the number of missed connections.

Model Description

The railway traffic will be modeled as a discrete-event system, where the events are the arrivals and the departures of the trains at specific points of the network. The running, dwell, and headway times are fixed values based on real-life data. The resulting discrete-event model is a macroscopic model and can be described using max-plus algebra, resulting in a max-plus-linear model. The default max-plus-linear model cannot model the dispatching actions; for that an extension to switching max-plus-linear systems [1] is needed, where each dispatching action is described by a different max-plus-linear model and a dispatching action is implemented by a switch to the corresponding max-plus-linear model.

Model predictive control is used to predict the future state of the network and return the network back to the desired state as quick as possible. The prediction is done by using the switching max-plus-linear model to simulate several periods of the railway traffic. The dispatching actions are determined by solving a mixed integer linear optimization problem, where the switching max-plus-linear model determines the constraints and the dispatching actions are the control variables of the optimization problem. Although the problem can be written as a mixed integer linear optimization problem, due to the large number of constraints and control variables it may take a long time to find an optimal solution, while the dispatcher needs a solution as soon as possible. So the main limitation for implementing this in practice is the required computation time.

Research Goals

The goal of our current research will be to reduce the required computation time. We intend to do this by determining an initial solution to the optimization problem based on properties of the network model. We will analyze the steady-state behavior of the model describing the railway traffic and its relation to the control variables.

Because our model is a switching max-plus-linear model, we can use the analysis tools available to max-plus algebra to analyze the steady-state behavior and its relation to the control variables. The steady-state behavior is determined by the max-plus eigenvalue and the max-plus eigenvectors of the system matrix for each dispatching action. When the network is running in steady-state the eigenvalue describes the minimum possible period of the timetable and the eigenvectors describe the moment the arrival and the departure events happen. By determining the eigenvalues and eigenvectors that match the current situation in the network as closely as possible, with a minimum accumulated delay, we can select the control variables related to these eigenvalues and eigenvectors and use them as the initial solution to the mixed integer linear optimization problem.

Acknowledgements

Research funded by the STW project Model-Predictive Railway Traffic Management (11025).

References

[1] T.J.J. van den Boom and B. De Schutter, “Modelling and control of discrete event systems using switching max-plus-linear systems”, *Control Engineering Practice*, vol. 14, no. 10, pp. 1199-1211, Oct. 2006

Traffic Counts Estimation Based on Urban Properties

Yu Hu
Delft Center for Systems and Control
Delft University of Technology
Mekelweg 2
2628 CD Delft
The Netherlands
Email: yu.hu@tudelft.nl

J. Hellendoorn
Delft Center for Systems and Control
Delft University of Technology
Mekelweg 2
2628 CD Delft
The Netherlands
Email: j.hellendoorn@tudelft.nl

1 Introduction

With the rapidly increasing use of mobile vehicles, the traffic networks are suffering two main problems: traffic jam and increasing scale, especially in urban areas. Most of the state-of-the-art researches point out that a large scale hierarchical control structure is one of the solutions to solve these two problems. But on the way to there, there are still several difficulties. One of the problems in the existing situations is the lack of traffic count data: researchers use the data of traffic counts to build up the models. The problem is: is the traffic count data reliable? In most of the urban areas traffic count data are lacking, and many of the data are corrupted by measurement errors. The state-of-the-art literature about the estimation of traffic counts are mainly focusing on decreasing the systematic errors to improve the accuracy of the estimation of traffic counts, as Szeto and Gazis [1] and A. Ehlert et al. [2] propose, but the problem of lacking traffic counts data is still existing. This paper introduces urban properties, such as number of cars, number of residences, age composition etc. of urban blocks, with which the traffic count data can be completed without detectors.

2 Urban Properties

Urban properties are essential attributes of traveling behavior of urban blocks. According to different research scales, an urban block could contain of one building, a small area with several buildings, a group of street blocks, or even the whole city in some cases. In each urban block, its function can be divided into several types: living, working, shopping etc. Those different types of blocks have their own traveling time table of floating inside and outside the urban blocks, which is influencing the related traffic networks directly. For example, the urban properties of living blocks have three main properties: $P_{node} : (\delta, \lambda)$ is used to indicate the geometric coordinate position of a node, C_{node} is the number of cars that can be produced or absorbed by the node, $A_{node} : \{a \rightarrow [0,1] | a \in [age\ ranges]\}$ is the age composition of a node.

Thus, the traffic count data based on the urban property data can be generated. Denote

$$f(node,t) : \{(node,\ C_{node},\ A_{node},\ t) \rightarrow N_c\}$$

as the in-flow or out-flow dynamic function of urban blocks, where N_c is the number of cars the block generated in a certain time point.

3 Case Study and Discussion

In order to expound that similar urban blocks have similar dynamic traffic performance in general, we take the area of Kruithuisweg in Delft, the Netherlands, as shown in Figure 1. The traffic count data of nodes G, H, I and the data on the link between J and K, K and M, and M and N are determined. According to the environment, node D is similar to node G, and node E is similar to node I. Similar nodes should have similar dynamic traffic behavior due to the same amount and similar behavior of inhabitants. Thus, we use the Node G and I to estimate the performance of node D and E respectively. The result of the case study shows that

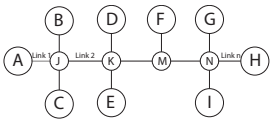

Figure 1: Graph of Kruithuisweg area

the error rate of the estimated model is lower than 20% after 6:00 a.m. until 10:00 p.m., which is accurate enough for the estimation of traffic counts. In the future, more detailed analytics of the influencing of the urban properties on the traffic networks will be researched. Urban properties based estimation to obtain O-D matrices will be used to improve the control of the traffic networks in the future.

References

[1] M.W. Szeto, D.C. Gazis, "Application of Kalman Filtering to the Surveillance and Control of Traffic Systems", Trasportation Science, 1972.

[2] A. Ehlert, M. G.H. Bell, S. Grossotitle, "The optimisation of traffic count locations in road networks", Transportation Research Part B: Methodological, 2006.

Optimal Trajectory Planning for Trains under Operational Constraints

Yihui Wang, Bart De Schutter, Ton van den Boom

Delft Center for Systems and Control, Delft University of Technology
Mekelweg 2, 2628 CD, Delft, The Netherlands
Email: {yihui.wang, b.deschutter, a.j.j.vandenboom}@tudelft.nl

1 Introduction

Advanced train control systems enable energy-efficient driving of trains, which becomes more and more important because of the rising energy prices and environmental concerns [1]. The automatic train operation (ATO) subsystem of the advanced train control system drives the train according to an optimal trajectory and recalculates it when operational conditions change [1]. Therefore, it is important to develop an efficient algorithm to find the optimal speed-distance reference trajectory.

2 Operational Constraints

Wang et al. [2] have proposed a mixed-integer linear programming (MILP) approach to calculate the optimal trajectory. The varying line resistance, variable speed restrictions, and varying maximum traction force are taken into account in the optimal trajectory planning problem in [2]. However, there exist other constraints that can result from the timetable or from real-time operational restrictions [3]. For example, in order not to get hindered by a preceding train, a train may be required not to pass a location earlier than a certain time. On the other hand, in order not to hinder a following train, a train may have to be at a certain location not later than a scheduled time.

Albrecht et al. [3] classified these operational constraints into two groups: target points and target windows. Target points correspond to fixed passing times, which could e.g. be arrival and departure times at stations. In dense networks, target points could also be passing times at certain places where overtaking and crossing of trains is planned. If the passing time is not that strict but is characterized by an earliest arrival time and a tolerated delay, then it forms a target window constraint. The scheduled arrival times at minor stations without connections with other trains can be regarded as target windows.

3 Solution Approaches

The methods for the optimal trajectory planning problem in the literature can be grouped into two main categories: analytical solutions and numerical optimization [4]. The optimal driving style of analytical solutions typically contains four optimal regimes: maximum acceleration, cruising at a constant speed, coasting, and maximum deceleration. Based on these four optimal regimes, Albrecht et al. [3] proposed an analytical algorithm for the optimal trajectory planning problem under operational constraints that yields the minimal number of regime changes. In general, a traction force that can take values in a interval (instead of in a limited set of fixed values) and frequent changes in the traction force are not easy to follow for the driver. Therefore, the approach in [3] is easier for the driver as it is characterized by a small number of regime changes.

However, numerical optimization is a better choice for an advanced train control system with an ATO subsystem. On the one hand, the entire freedom of traction force and frequent changes in traction force is not a problem for an ATO subsystem. On the other hand, the analytical methods often meet difficulties if more realistic conditions are considered that introduce complex nonlinear terms into the model equations and the constraints as stated in [4]. Numerical optimization approaches involves dynamic programming, genetic algorithms, collocation methods, MILP, and so on.

In this presentation, we explain how the MILP approach of [2] can be extended to include these operational constraints, i.e. target points and target windows. Furthermore, we also extend the approach of [2] to solve trajectory planning problems for multiple trains.

References

[1] R. Liu and I. M. Golovicher, "Energy-efficient operation of rail vehicles," *Transportation Research Part A: Policy and Practice*, vol. 37, no. 10, pp. 917–931, Oct. 2003.

[2] Y. Wang, B. De Schutter, B. Ning, N. Groot, and T. van den Boom, "Optimal trajectory planning for trains using mixed integer linear programming," in *14th International IEEE Conference on Intelligent Transportation Systems (ITSC 2011)*, Washington, DC, USA, Oct. 2011.

[3] T. Albrecht, C. Gassel, A. Binder, and J. van Luipen, "Dealing with operational constraints in energy efficient driving," in *IET Conference on Railway Traction Systems (RTS 2010)*, Birmingham, UK, Apr. 2010.

[4] R. Franke, M. Meyer, and P. Terwiesch, "Optimal control of the driving of trains," *Automatisierungstechnik*, vol. 50, no. 12, pp. 606–614, Dec. 2002.

Stability analysis of networked control systems with periodic protocols and uniform quantizers

S.J.L.M. van Loon[1] M.C.F. Donkers[1] N. van de Wouw[2] W.P.M.H. Heemels[1]

Eindhoven University of Technology

[1] Mechanical Engineering, Hybrid and Networked Systems Group, PO Box 513, 5600 MB Eindhoven, The Netherlands

[2] Mechanical Engineering, Dynamics and Control Group, PO Box 513, 5600 MB Eindhoven, The Netherlands

Email: {S.J.L.M.v.Loon, M.C.F.Donkers, N.v.d.Wouw, W.P.M.H.Heemels}@tue.nl

1 Introduction

Networked Control Systems (NCSs) offer many advantages, such as increased architectural flexibility and reduced wiring. However, NCSs are inherently subject to quantization effects, packet dropouts, time-varying transmission intervals and delays and communication constraints. In this research, we develop a unified framework for the stability and performance analysis of NCSs in joint presence of all these network-induced phenomena.

2 NCS Model

We focus on linear plants and controllers, and periodic protocols (with the well-known Round-Robin protocol as a special case), which leads to a modeling framework for NCSs based on discrete-time switched linear uncertain systems of the form

$$\bar{x}_{k+1} = \tilde{A}_{\sigma_k,h_k,\tau_k}\bar{x}_k + \tilde{B}_{\sigma_k,h_k,\tau_k}\bar{\epsilon}_k, \qquad (1)$$

in which $\bar{x}_k$, $k \in \mathbb{N}$ contains here the state of the plant, the state of the controller and some other (memory) variables. The value for σ_k is determined by the scheduling protocol and the parameters h_k and τ_k denote the uncertain (but bounded) time-varying transmission interval and delay, respectively. In (1), the quantization effects $\bar{\epsilon}_k$, induced by uniform quantizers, are modeled as norm-bounded additive disturbances on both plant and controller signals.

3 Stability Analysis

Based on a suitable overapproximation of the NCS model (1), see [1], we develop LMI-based conditions that guarantee exponential input-to-state stability (EISS). EISS is characterized by the existence of an EISS Lyapunov function V that satisfies the following inequality constraints

$$\alpha_1\|\bar{x}_k\|^2 \leqslant V(\bar{x}_k,k) \leqslant \alpha_2\|\bar{x}_k\|^2$$
$$V(\bar{x}_{k+1},k+1) - V(\bar{x}_k,k) \leqslant -\alpha_3\|\bar{x}_k\|^2 + \kappa\|\bar{\epsilon}_k\|^2, \qquad (2)$$

for some $\alpha_1,\alpha_2,\alpha_3,\kappa > 0$. The satisfaction of (2) implies EISS with a certain upper bound on the ISS gain γ_{ISS}. The conditions (2) can be used for NCSs equipped with uniform quantizers, to guarantee the following ultimate bound (UB) on the state of the system (1) as $k \to \infty$;

$$\limsup_{k\to\infty}\|\bar{x}_k\| \leqslant \gamma_{\text{ISS}}\sup_{s\in\mathbb{N}}\|\bar{\epsilon}_s\| \leqslant \gamma_{\text{ISS}}\sqrt{\sum_{i=1}^{n_z}\left(\frac{\zeta_i}{2}\right)^2}, \qquad (3)$$

in which $\zeta_i > 0$, $i \in \{1,\ldots,n_z\}$, with n_z the total number of quantized signals, denotes the step sizes of the uniform quantizers.

4 Illustrative Example

We illustrate the theory using a benchmark example of a batch reactor, which communicates its two plant outputs, each having their own uniform quantizer, over a network.

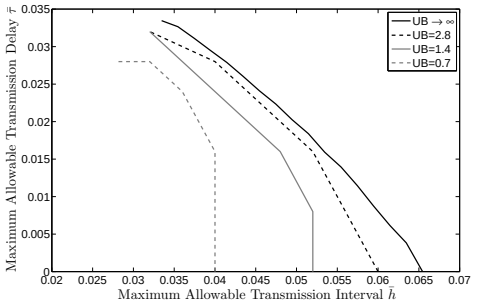

Figure 1: Numerical results for various upper bounds on the UB.

For this example with quantization step sizes $\zeta_i = 10^{-3}$, $i = \{1,2\}$, the numerical results for various upper bounds on the UB as function of the maximum allowable transmission interval and delay are depicted in Fig. 1.

5 Further Work

In [1], we demonstrate that the framework as presented here also allows to consider quadratic protocols, with the well-known Try-Once-Discard protocol as a special case, and other types of quantizers, such as logarithmic quantizers. We show that based on a suitable overapproximation of the NCS model (1), we can guarantee EISS and a certain ℓ_2-gain using newly developed conditions based on LMIs. Using these notions of EISS and ℓ_2-gain, we can assess closed-loop stability and performance of the NCS and make trade-offs between the various network properties, such as bounds on transmission intervals and delays, the quantization properties and control criteria, such as ultimate bounds (in case of uniform quantizers) and global exponential stability (in case of logarithmic quantizers).

References

[1] S.J.L.M. van Loon, M.C.F. Donkers, N.W. Bauer, N. van de Wouw, and W.P.M.H. Heemels, "Stability Analysis of Networked and Quantized Control Systems: A Switched Linear Systems Approach", (submitted), 2011.

This work is supported by the Innovational Research Incentives Scheme under the VICI grant "Wireless control systems: A new frontier in automation" (No. 11382) awarded by NWO (The Netherlands Organization for Scientific Research) and STW (Dutch Science Foundation), and the European 7th Framework Network of Excellence "Highly-complex and networked control systems" (HYCON2).

Steer-by-wire: A study into the bandwidth requirements

Tom van der Sande, Igo Besselink, Henk Nijmeijer
Section Dynamics and Control
Eindhoven University of Technology
P.O. Box 513, 5600MB Eindhoven
The Netherlands
Email: t.p.j.v.d.sande@tue.nl

1 Introduction

Numerous papers show the benefits of steer-by-wire (SbW), however, hardware limitations are rarely discussed. In Ackermann [1] a minimum required actuator bandwidth is determined using a linear vehicle model, however a maximum effective bandwidth is not mentioned. To define these requirements the maximum effective steering frequency will be explored here using a multibody model of a Jaguar XF that includes all suspension kinematics and non-linear tire behavior.

2 Results

The additional functionality of steer-by-wire will be most useful at large lateral acceleration and yaw-rate, usually experienced in limit handling situations. This means that vehicle characteristics are far from linear. Therefore, to determine up to which frequency an additional steering action is useful, the vehicle is steered up to a lateral acceleration of 7 m/s^2. The steering wheel angle is then varied sinusoidal with an amplitude δ_Δ. The steering angle thus reads

$$\delta_{sw} = \delta_{ss} + \delta_\Delta \sin(2\pi f t) \tag{1}$$

with $f = 0.1, 0.2 \ldots 49Hz$. The steady state angle is chosen

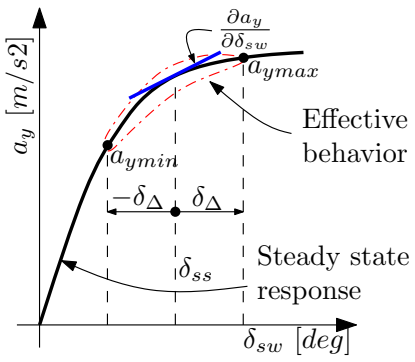

Figure 1: Lateral acceleration as a function of steering wheel angle.

to be $\delta_{ss} = 50°$ and the varying steering angle $\delta_\Delta = 20°$. As a result, the vehicle will experience a change in lateral acceleration as is indicated in figure 1. As a result of damping in the vehicle, a hysteresis loop will occur. To get insight into the frequency up to which a steering action is useful, the derivative of the lateral acceleration to the steering wheel angle $\left.\frac{da_y}{d\delta_{sw}}\right|_{\delta_{sw}=\delta_{ss}}$ is calculated.

The results of the simulations can be seen in figure 2. It is clear that for increasing frequency the lateral acceleration can not be influenced as much as with a low frequency steering action. It furthermore has to be noted that due to tire relaxation effects the derivative has a negative sign for $f = 1.4Hz$. The negative sign beyond $f = 24Hz$ can be explained by a combination of the limited stiffness in the steering system and tire relaxation effects.

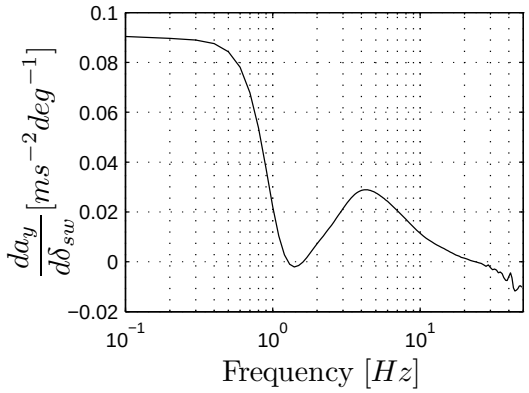

Figure 2: Influence of varying steering wheel angle on lateral acceleration.

3 Conclusion

It is shown that there exists an upper limit up to which steering actions are useful. Already for low frequencies a drop in effectiveness can be observed.

4 Acknowledgements

This work is a part of the HTAS VERIFIED II project which is a common project of TU/e, TNO, NXP, Verum and Tractive Suspension.

References

[1] J. Ackermann, “Actuator rate limitis in robust car steering control”, *Proc. IEEE Conf. on Decision and Control*, 1997; Volume 5, pp 4726-4730.

Experimental control of a mobile robot by an electronic brain

Thijs Vromen, Erik Steur, Henk Nijmeijer
Department of Mechanical Engineering, Eindhoven University of Technology
P.O. Box 513, 5600 MB Eindhoven, The Netherlands
Email: t.g.m.vromen@tue.nl

1 Introduction

Autonomous navigation of robots is an important research topic nowadays. These mobile robots are usually controlled by predefined laws, which makes it difficult to explore unknown environments and to deal with poor defined situations. On the other hand, biological examples like the human brain show networks of billions of neurons that coordinate all our actions. From these examples, the idea arose to make an "intelligent system" using a network of neurons. The goal of this research is to train a network of electronic neurons [1] to control a two-wheel mobile robot.

2 Neuronal controller with training procedure

A neuronal controller with a structure as shown in Figure 1 is used. The network has three sensor neurons whose input voltages are related to the measured distances by the (left, middle and right) sensors of the robot. The period time of

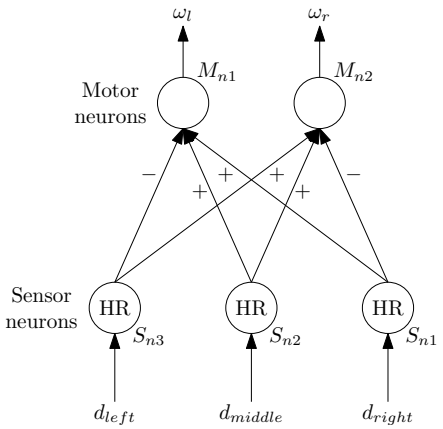

Figure 1: Network structure with HR neurons in the input layer.

the sensor neurons is determined by the input voltage and therefore influenced by the measured distance to an obstacle. The sensor neurons are coupled with the motor neurons and the spiking behavior of the sensor neurons determines the response of the motor neurons. Next, the number of spikes of the motor neurons determine the angular velocities of the driving wheels of the mobile robot.

The electronic neurons show mutual differences, which limits the performance of the controller. To improve the results, clusters of nonidentical neurons are trained to replace the sensor neurons. To act as a single (average) neuron, the neurons in the clusters should be synchronized. The training procedure is shown in Figure 2. Within the adaptation mech-

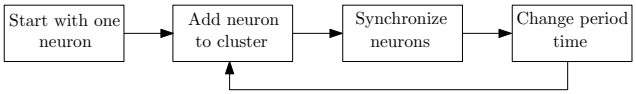

Figure 2: Flowchart of the steps in the training algorithm.

anism the coupling gains between the neurons are changed to match the period time of the cluster with the period time of a, beforehand chosen, reference neuron. After changing the period time, an extra neuron can be added to the cluster to improve the correspondence with the reference period.

3 Experimental results

Experiments have been performed with clusters of five neurons. The robot drives around and the distances to obstacles are the inputs for the trained clusters. In the plot on the left hand side in Figure 3 we see the difference in trajectory between an untrained (white) and trained (gray) network. Without training, the robot has a preferential driving direction, caused by the differences between the neurons. However, after training the clusters, the robot is able to drive in a straight line. The other experiment demonstrates that the robot is able to detect and avoid obstacles, using the neuronal controller.

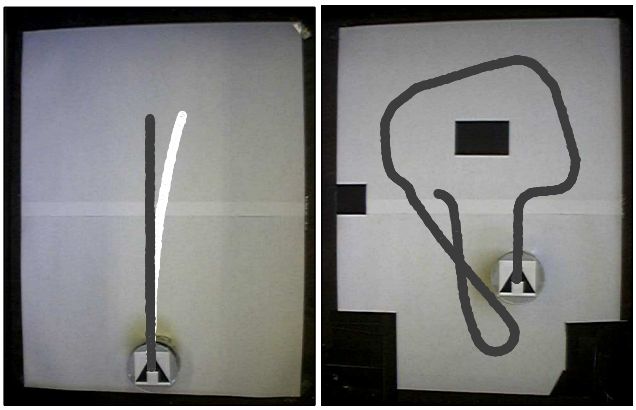

Figure 3: Experimental results of the robot driving around.

References

[1] P.J. Neefs, E. Steur and H. Nijmeijer, "Network Complexity and Synchronous Behavior - An Experimental Approach", International Journal of Neural Systems, 3:233-247, 2010

Energy-optimal time allocation for a series of point-to-point motions

Pieter Janssens[1], Goele Pipeleers[1], Moritz Diehl[2], Jan Swevers[1]
KU Leuven, Department of Mechanical Engineering, Div. PMA[1],
KU Leuven, Department of Electrical Engineering, Div. SCD[2],
Heverlee 3001, Belgium
Email: Pieter.Janssens@mech.kuleuven.be

1 Introduction

There is a growing interest in reducing the energy consumption of mechatronic systems such as pick-and-place machines. For linear time-invariant (LTI) systems, energy-optimal point-to-point (PTP) motion trajectories can easily be computed by solving a convex optimization problem. The dissipated energy is minimized subject to linear equality constraints, which ensure that the system reaches the desired endpoint at the specified time instants. Other system limitations such as maximum input current, maximum velocity, etc. can be incorporated in the optimization problem by formulating them as linear inequality constraints.

The same approach can also be used to compute the energy-optimal system input for a series of PTP motions with specified time instants for each of the dwells. In many practical situations, however, the exact dwell times of the intermediate PTP motions are irrelevant, and therefore free to minimize the energy required for the series of PTP motions. We present an algorithm for LTI systems to compute the energy-optimal time allocation for a series of PTP motions. The presented algorithm is able to account for linear constraints, such as maximum input and maximum velocity constraints.

2 Energy-optimal time allocation algorithm

Consider a series of Q PTP motions to be executed within N_{tot} samples. The first step of the energy-optimal time allocation algorithm is to compute the minimally dissipated energy $E_j(N), \text{for} j \in \{1,\dots,Q\}$ as a function of the execution time N. The second step is computing the minimal energy $E_{12}(N)$ for the first two PTP motions, and the number of samples $N_2(N)$ allocated to the second PTP motion as a function of the execution time N:

$$E_{12}(N) = \underset{N_2}{\text{minimize}} \quad E_1(N-N_2)+E_2(N_2).$$

These minimization problems are solved by simply finding the smallest element of the vector $E_1(N-N_2)+E_2(N_2)$.

Next, the third PTP motion is added to the first two in the same way resulting in the minimal energy $E_{123}(N)$ to perform the first three PTP motions, and the number of samples $N_3(N)$ allocated to the third PTP motion as a function of the execution time N:

$$E_{123}(N) = \underset{N_3}{\text{minimize}} \quad E_{12}(N-N_3)+E_3(N_3).$$

This procedure is repeated until the last PTP motion is added and we obtained (i) the minimal energy to perform the series of PTP motions within N_{tot} samples, and (ii) the number of samples $N_Q^* = N_Q(N_{\text{tot}})$ allocated to the last PTP motion. $N_{Q-1}^*,\dots,N_2^*$ are obtained by recursively going back through the solutions $N_{Q-1},\dots,N_2$ and $N_1^* = N_{\text{tot}} - \sum_{j=2}^{Q} N_j$.

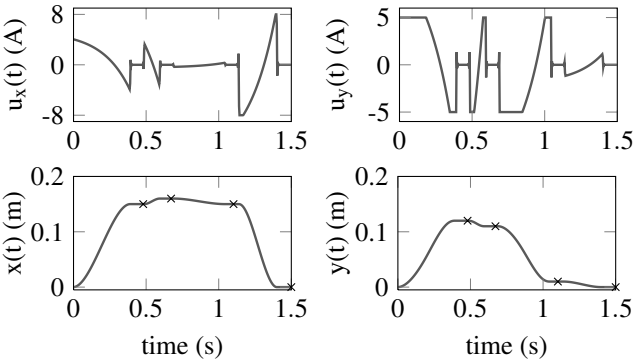

Figure 1: Energy-optimal input currents and trajectories.

3 Simulation results

The proposed algorithm is numerically validated using a model of an XY-positioning system consisting of 2 permanent magnet linear motors. The energy losses in the internal motor resistance, and the energy losses due to viscous friction are minimized subject to input constraints.

The XY-positioning system is commanded to execute a series of 4 PTP motions. The optimal end time of each PTP motion is indicated in Fig. 1 by a black cross. Fig. 1 shows the energy-optimal current signals and trajectories of the 2 linear motors as a function of time.

Acknowledgement

Goele Pipeleers is Postdoctoral Fellow of the Research Foundation - Flanders. This work has been carried out within the framework of projects IWT-SBO 80032 (LECO-PRO) of the Institute for the Promotion of Innovation through Science and Technology in Flanders (IWT-Vlaanderen) and G.0422.08 and G.0377.09 of the Research Foundation - Flanders (FWO - Flanders). This work also benefits from K.U.Leuven-BOF PFV/10/002 Center-of-Excellence Optimization in Engineering (OPTEC) and from the Belgian Programme on Interuniversity Attraction Poles, initiated by the Belgian Federal Science Policy Office.

Dielectric Spectroscopy for Non-Invasive Glucose Measurements

Oscar Olarte, Wendy Van Moer, Kurt Barbé, Yves Van Ingelgem, Annick Hubin
Vrije Universiteit Brussel
Pleinlaan 2, B-1050 Brussels Belgium
Email: oolarter@vub.ac.be

1 Introduction

A common non-invasive measurement technique is based on dielectric spectroscopy (DS). This technique allows measuring the properties of the system as a function of the frequency as well as distinguishing between the different processes that could be involved [1]. When developing a non-invasive glucose measurement system, one must deal with different noise sources that need to be identified and quantified in order to provide confidence bounds for the estimated glucose level. Hence advanced signal processing techniques are needed to quantify, detect and discriminate the presence of noise sources as well as the non-linear distortions inherent to the system. Combining non-linear identification techniques and odd random phase multisines (ORPM) [2], together with the DS will allow for an accurate non-invasive glucose measurement system.

In a first step towards the in-vivo identification of blood glucose levels, in-vitro experiments are performed using different solutions. It let us identify the influence of various constituents of human blood on the system response as well as the variance in the experimentation. In this report three principal blood components are tested given its prevalence in blood or its influence over the conductivity process. During the experiments the concentration of the investigated substances is maintained and its impedance is evaluated over a number of physiological glucose levels.

2 Experimental Setup

In order to identify the effect of glucose on the obtained impedance spectra three different solutions at five glucose concentrations were used. The three solutions were: demineralized water (Milipore MilliQ Element), human Albumin at 4gr/dL (Baxter) and a Sodium-Chloride solution at 350mg/dL (VWR). In each solution glucose was added at 0, 70, 120, 240 and 400 mg/dL (D-Glucose - Merck).

The hardware used was a Bank POS2 potentiostat, with signals generated and recorded by a NI 4461 PCI DAQ card. The excitation signals are ORPM. The frequency range employed for the impedance evaluation was from 1Hz to 30 kHz with a resolution of 1Hz. The electrochemical cell consists of a working (4 mm diameter) and counter electrode of Platinum and a reference electrode of Silver (Dropsens). These sensors exhibit a high electrochemical activity and good repeatability [3]. All the experiments were performed at 21 and 37 degrees Celsius.

3 Results

Experiments using incremental experimentation, room and body temperature and different repetitions show the influence of these factors over the glucose impedance measurement. According with the results a low variance in the experimentation is obtained at body temperature as well as in high glucose concentrations.

The BLA combined with ORPM generates information related to the linear behavior of the system under test, as well as the noise level and the non-linearities present in the system. Based on the results, the BLA describes appropriately the impedance behavior of each one of the analyzed systems.

4 Conclussions

The capabilities of an ORPM to perform glucose measurements are studied. The measurement technique is based on DS and uses an ORPM excitation signal analysis. Although the results are preliminary, they clearly elucidate the capabilities of random phase multisine analysis for glucose measurements. In the future more complex sampled matrices should be analyzed (plasma, complete blood, over the skin, fat, etc). Besides, this is also necessary to test the effect of environmental factors. However, the proposed approach shows a great capacity to detect the impedance levels in the most prevalent blood components.

Acknowledgment

This research was funded by a postdoctoral fellowship of the Research Foundation-Flanders (FWO), the Flemish Government (Methusalem Fund METH1), and the Belgian Government (IUAP VI/4, DYSCO).

References

[1] M. Orazem and B. Tribollet, 'Electrochemical Impedance Spectroscopy,' John Wiley & Sons, 2008

[2] J. Schoukens, R. Pintelon And T. Dobrowiecki 'Linear Modeling in the Presence of Nonlinear Distortions,' IEEE Trans. Instrum. Meas., Vol.16, 2002.

[3] O. Kadara, N. Jenkinson And C. Banks, 'Characterisation of Commercially Available ELectrochemical Sensing Platforms,' Sensors B: Chemical, vol. 138. 2009.

Anisotropy preserving interpolation of diffusion tensors

Anne Collard[1], Silvère Bonnabel[2], Christophe Phillips[3] and Rodolphe Sepulchre[1]
[1] Department of Electrical Engineering and Computer Science, University of Liège, B-4000 Liège, Belgium
[2] Robotics Center, Mathématiques et Systèmes, Mines Paris Tech, Paris, France
[3] Cyclotron Research Centre, University of Liège, B-4000 Liège, Belgium
Emails: {Anne.Collard, C.Phillips, R.Sepulchre}@ulg.ac.be, Silvere.Bonnabel@mines-paristech.fr

The growing importance of statistical studies of Diffusion Tensor Images (DTI) requires the development of a processing framework that accounts for the non-scalar and nonlinear nature of diffusion tensors. This motivation led a number of authors to consider a Riemannian framework for DTI processing because a Riemannian structure on the data space is sufficient to redefine most processing operations. As a prominent example, the Log-Euclidean metric proposed in [1] has emerged as a popular tool because it accounts for the tensor nature of DTI data at a computational cost that remains competitive with respect to standard tools. A limitation of the Log-Euclidean metric is its tendency to degrade the anisotropy of tensors through the standard operations of processing. Because anisotropy is the core information that motivates tensor imaging, the present paper proposes a novel metric that is anisotropy preserving while retaining the desirable properties of the Log-Euclidean metric. The properties of the proposed metric are illustrated on the basic operation of interpolating between diffusion tensors.

1 Methods

The proposed Riemannian geometry is rooted in the spectral decomposition of the tensors, which models any positive definite matrix as a diagonal positive scaling in a basis appropriately rotated from the canonical basis. This parametrization suggests a metric that weighs separately the rotation and the scaling using the geometries of both groups. This basic idea appears in early work on DTI [2] but we introduce additional features to make it practical and relevant for DTI processing. First, we use the invariant metrics of each group in order to recover the invariance properties of the Log-Euclidean metric by scaling and rotation. Second, the anisotropy of the tensor is used to balance the contributions of rotation and scaling: by making rotations of isotropic tensors cheaper, one obtains a geometric framework that inherently accounts for the uncertainty about the measured directions of diffusion. Third, we use quaternions for all computations involving rotations. The computational saving is significant and analog to the one obtained when working with the Log-Euclidean metric as opposed to the affine invariant metric.

2 Results

The benefits of the proposed framework are illustrated on the basic operation of interpolation. Figure 1 compares the interpolation of two anisotropic tensors within both the Log-Euclidean and the proposed frameworks. The Log-Euclidean interpolation causes a large decrease of the relative anisotropy (RA), resulting in degraded anisotropy information for the average tensor, while the proposed framework overcomes this limitation because the RA evolves monotonically between the two tensors. Thanks to the use of quaternions, the computational cost of generating these results is comparable in both frameworks.

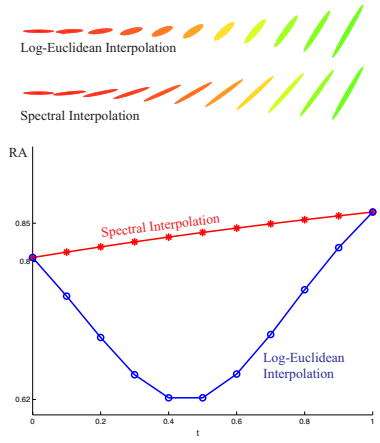

Figure 1: (Top) Interpolation between two tensors with the Log-Euclidean and the spectral framework. (Bottom): Evolution of the relative anisotropy through the interpolation with the Log-Euclidean and the spectral framework.

References

[1] V. Arsigny, P. Fillard, X. Pennec and N. Ayache. Log-Euclidean metrics for fast and simple calculus on diffusion tensors. *Magnetic Resonance in Medicine*, 56(2), 411-421, 2006.

[2] C. Chefd'hotel, D. Tschumperlé, R. Deriche and O. Faugeras. Regularizing flows for constrained matrix-valued images. *Journal of Mathematical Imaging and Vision*, 20(1), 147-162, 2004.

Design of a teleoperated palpation device for minimally invasive thoracic surgery

Angelo Buttafuoco and Michel Kinnaert
Université Libre de Bruxelles (U.L.B.)
50, Av. F.D. Roosevelt-CP 165/55, B-1050 Brussels, Belgium
angelo.buttafuoco@ulb.ac.be, michel.kinnaert@ulb.ac.be

1 Introduction

Minimally invasive surgery (MIS) consists in operating through small incisions in which a camera and adapted instruments are inserted. It allows to perform many interventions with reduced trauma for the patient. One of these is the ablation of peripheral pulmonary nodules [1].

Nevertheless, the means for detecting nodules during MIS are limited. In fact, because of the lack of direct contact, the surgeon cannot palpate the lung to find invisible lesions, as he would do in classical open surgery. As a result, only clearly visible nodules can be treated by MIS presently.

Our work aims at designing, building and controlling a teleoperated palpation instrument, in order to extend the possibilities of MIS in the thoracic field. Such an instrument is made of a master device, manipulated by an operator, and a slave device which is in contact with the patient and reproduces the task imposed by the master. Adequate control laws between these two parts allow to restore the operator's haptic sensation [2].

2 The palpation device

The palpation device has been designed in collaboration with thoracic surgeons and is represented on figure 1. A pantograph has been built to be used as the master of the palpation tool. The slave is made of a 2 degrees of freedom (dof) clamp, which can be actuated in compression and shear. The compression corresponds to vertical moves of the pantograph, and the shear to horizontal ones. Force sensors have been designed to measure the efforts along these directions, both at the master and the slave side, in order to implement advanced force-feedback control laws and for validation purposes.

Since the slave device has not been built yet, the dynamical behaviour of the complete teleoperation device has been modelled based on the CAD drawings and teleoperation control laws have been applied in simulation. Position-position, force-position and 3-channel control schemes have been tested and compared using classical performance criteria.

Figure 1: Teleoperated palpation device

3 Future work

On-going work aims at introducing a visco-elsatic model of the lung, including the presence of nodules, into the simulation of the teleoperation device [3], in parallel with the realisation of the slave. Once the latter is built, further modeling of the teleoperation device using frequency domain identification will be carried on, in order to take manufacturing errors into account. Based on that model, control laws that best suit the needs of palpation will be studied and experimentally tested [4].

Acknowledgments

The work of Angelo Buttafuoco is supported by a FRIA grant.The experimetal setup is financed by the FNRS. This paper presents research results of the Belgian Network DYSCO (Dynamic Systems, Control and Optimization), funded by the Interuniversitary Attraction Poles Programme, initiated by the Belgian State, Science Policy Office. The scientific responsibility rests with its authors.

References

[1] J. Lin, M.D. Iannettoni, The role of thoracosocopy in the management of lung cancer, In *Surgical Oncology*, vol. 12, pp. 195–200, 2003.

[2] P.F. Hokayem, Bilateral teleoperation : an historical survey, In *Automatica*, vol. 42, pp. 2035–2047, 2006.

[3] M. Nicotra, A. Buttafuoco, M. Kinnaert, Hybrid Model for haptic Lung Palpation, In *16th IFAC Symposium on System Identification* (under submission), Brussels, 2012.

[4] M.C. Cavusoglu, Bilateral Controller Design for Telemanipulation in Soft Environments, In *Proceedings of the 2001 IEEE International Conference on Robotics and Automation*, Korea, 2001.

Piezoelectric Tactile Tissue Differentiation Sensor System: Concepts and Measurement Challenges

David Oliva Uribe[*], Jörg Wallaschek[+] and Johan Schoukens[*]
[*]Department ELEC, Vrije Universiteit Brussel, Belgium
[+]Institute of Dynamics and Vibration Research, Leibniz University of Hannover, Germany
Email: dolivaur@vub.ac.be

Introduction

In this contribution the development of a piezoelectric tactile sensor system for the differentiation of soft tissues and phantoms is presented. The aim of this system is to provide a medical tool that can help neurosurgeons with the critical task of brain tumour resection, where in particular, the most important characteristic is to offer the surgeon the capability to find accurately tumour boundaries during surgery. The differentiation among distinct tissues and phantoms that have similar mechanical characteristics is a technique based on the detection and evaluation of different electrical parameters, where frequency response function measurements utilizing multisine excitation are performed to obtain the transfer function of the bimorph's voltages $U_{Sensor}/U_{Actuator}$. The system was tested on a series of gelatine gel phantoms at different concentrations. The bimorph sensor system is able to detect even minimal differences.

Materials and Methods

I. Mimicking Phantoms Materials

Biological tissues are materials with a complex internal structure which exhibits viscoelastic behaviour. At early phases of investigations, it is not recommendable to work with real biological tissues due to its highly demanded care and narrow window time to perform measurements. Instead, it is commonly used to work with phantoms fabricated with polymers or gelatine, which expose comparable viscoelastic behaviour than the real tissue (e.g. brain tissue). Phantoms, also have the advantage that they present a higher stability (i.e. their physical or chemical structure will not change rapidly), being possible to use them for a considerable time [1].

II. Measurement Concept.

The sensor system is based on the use of a piezoelectric bimorph. As shown in Fig. 1, one of the piezoelectric layers is used as a driving element to generate vibrations and the second layer is used as a sensor. When the contact ball tip touches the tissue, the mechanical impedance will change. To evaluate a tissue sample, frequency response function measurements using multisine excitation are performed and the changes from the no-load condition (i.e. no contact with tissue) in the resonance peaks as well as

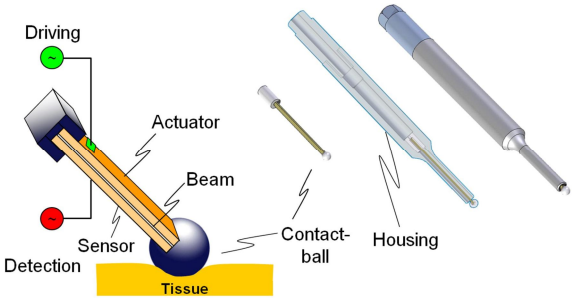

Fig. 1. Left: Piezoelectric bimorph tactile sensor in contact with tissue. Right: assemble of the sensor into a housing.

the transfer function of both piezo layers' signals, $U_{Sensor}/U_{Actuator}$, are used to determine the alteration in the consistency of the sample. The use of multisine excitation to obtain the FRF is justified due to the need of a fast measurement procedure. One of the resonance modes is used to estimate the transfer function, where the position of the poles functions as differentiation criteria.

Results

Experiments performed on a series of gelatine phantoms using different amplitude levels were carried out to analyse influence of the nonlinearities. The results of these experiments indicate that nonlinear distortions are present but still a linear model can be obtained to differentiate phantoms with high accuracy. Moreover, the sensor was tested at several contact forces to determine the influence of this variable in our results. Differentiation of phantoms was achieved successfully even at small forces (i.e. 1 cN). Higher contact forces lead to a better quality in the measurement, although this increases the risk of damage on the tissue.

References

[1] D.O. Uribe, H. Zhu and J. Wallaschek, "Automated measurement system for mechanical characterization of soft tissues and phantoms," *2010 Intl Conf on Electronic Devices, Systems and Applications*, pp 227-231, Kuala Lumpur, Malaysia,11-14 April 2010.

Memory Elements: A Paradigm Shift in Lagrangian Modeling of Electrical Circuits

Dimitri Jeltsema
Delft Institute of Applied Mathematics
Delft University of Technology
Mekelweg 4, 2628 CD Delft
The Netherlands
Email: d.jeltsema@tudelft.nl

1 Introduction

Memristors, meminductors, and memcapacitors [1] constitutive an increasingly important class of two-terminal circuit elements whose resistance, inductance, and capacitance retain memory of the past states through which the elements have evolved. All three elements are nonlinear and can be identified by their pinched hysteresis loop in the voltage versus current plane, current versus flux plane, and voltage versus charge plane, respectively; see Figure 1. While there are many discovered experimental realizations and applications of systems that exhibit memristive behavior, ranging from applications in non-volatile nano memory to intelligent machines with learning and adaptive capabilities, the number of systems showing memcapacitive and meminductive behavior is still somewhat limited. Nevertheless, several applications of these concepts are foreseen in the field of logic and arithmetic operations using memristive and memcapacitive devices, and field-programmable quantum computation using meminductive and memcapacitive devices [2].

2 Contribution

In this presentation, we consider circuits made from memristors, meminductors, and memcapacitors and their conventional counterparts in the Lagrangian framework [3]. It will be shown that meminductors and memcapacitors do not allow a Lagrangian formulation in the classical sense since these elements are nonconservative in nature and the associated energies are not state functions. To circumvent this problem, a different configuration space is considered that, instead of the usual loop charges, consist of time-integrated loop charges. The Lagrangian is defined by the difference between two novel state functions in a fashion similar to the usual magnetic co-energy minus electric energy setup, but having the dimensions of energy times time-squared which is equivalent to action times time. As a result, the corresponding Euler-Lagrange equations provide a set of integrated Kirchhoff voltage laws in terms of the element fluxes. Memristive and resistive losses can be included via the introduction of a second scalar function that has the dimension of action. A dual variational principle follows by considering variations of the integrated node fluxes and yields a set of integrated Kirchhoff current laws in terms of the charges. Although integrated charge, which in SI units is measured in Coulomb times seconds, is a somewhat unusual quantity in circuit theory, it may be considered as the electrical analogue of a mechanical quantity called absement. Absement (a contraction of absence and displacement) is measured in meters times seconds and its rate of change coincides with position. One meter-second corresponds to being absent one meter from a reference point for the duration of one second. Based on this analogy, simple mechanical devices are presented that can serve as didactic examples to explain memristive, meminductive, and memcapacitive behavior.

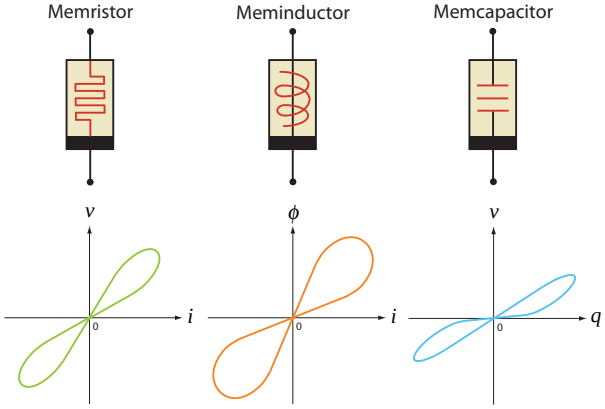

Figure 1: Memory circuit elements.

Selected References

[1] Di Ventra, M., Pershin, Y., and Chua., L. (2009). Circuit elements with memory: memristors, memcapacitors and meminductors. *Proc. of the IEEE*, 97(10), 1717–1724.

[2] Pershin, Y. and Di Ventra, M. (2011). Memory effects in complex materials and nanoscale systems. *Advances in Physics*, 60(2), 145–227.

[3] Jeltsema, D. and Scherpen, J. (2009). Multi-domain modeling of nonlinear networks and systems: energy- and power-based perspectives. *IEEE Control Systems Magazine*, 29(4), 28–59.

Metrics for oscillator models: an input-to-phase approach

Pierre Sacré and Rodolphe Sepulchre
Montefiore Institute, University of Liège, Belgium
{pierre.sacre,r.sepulchre}@ulg.ac.be

1 Introduction

Oscillatory behaviors are observed in every field of science. They arise from the interactions between multiple processes, which often makes their design principles not intuitive. To uncover the rules that map networks to functions we have to adapt tools from linear to nonlinear systems theory.

A central notion in systems theory is the notion of distance between dynamical systems. It arises naturally in system identification, model reduction, robustness analysis, to cite a few. The few existing measures to compare oscillator models focus on steady-state information (*e.g.* period, amplitude of oscillations, or periodic orbit).

In this paper, we motivate the use of infinitesimal phase response curve as an input-to-phase characteristics of an oscillator. We introduce new metrics for oscillator models based on their phase response curves and derive their sensitivities.

2 Infinitesimal phase response curves as an input-to-phase oscillator characteristics

In this paper, an oscillator is modeled as an open dynamical system defined by a set of differential equations

$$\dot{x} = f(x) + \varepsilon g(x)u(t), \quad x \in \mathbb{R}^n, \quad u \in \mathbb{R}.$$

We assume that the 'zero-input' system has a *hyperbolically stable* periodic orbit and that the open system is perturbed by a *weak* input ($0 < \varepsilon \ll 1$). This assumption implies that trajectories remain confined in the vicinity of the periodic orbit.

Using an asymptotic method of reduction [1], the system is reduced into a one-dimensional phase model

$$\dot{\theta} = \omega + \varepsilon q_u(\theta)u(t), \quad \theta \in \mathbb{S}^1, \quad u \in \mathbb{R},$$

in which $\omega \in \mathbb{R}_{>0}$ is the angular frequency of the oscillator. The *(input) infinitesimal phase response curve* is the map $q_u(\cdot) : \mathbb{S}^1 \to \mathbb{R}$ which measures the asymptotic phase-shift response to an infinitesimal δ-function. It serves as an impulse response characteristics in the direction of phase-shift.

The characterization of this phase model is used to study the entrainment and the synchronization of the system. The infinitesimal phase response curve $q_u(\cdot)$ plays thus a leading role in those properties. Moreover, there are many applications where the phase response curve can be measured experimentally.

3 Metrics between oscillator models

We define the distance between two oscillator models as a distance between their infinitesimal phase response curves. Depending on the nature of the oscillator and the question, we define a metric which fulfills none, one, or both following invariance properties.

Circular-shift invariance. The choice of a reference position (associated to a zero-phase) along the periodic orbit is often artificial. In those cases, we require that

$$d(q_1(\cdot), q_2(\cdot)) = d(q_1(\cdot), q_2(\cdot + \sigma))$$

with $\sigma \in \mathbb{S}^1$.

Magnitude-scale invariance. The actual magnitude of the input signal is not always known (*e.g.* in systems biology). This uncertainty about the input magnitude induces an uncertainty on the phase response magnitude. In those cases, we require that

$$d(q_1(\cdot), q_2(\cdot)) = d(q_1(\cdot), \lambda q_2(\cdot))$$

with $\lambda \in \mathbb{R}_{>0}$.

Moreover, we derive the metric sensitivity involving the sensitivity of the infinitesimal phase response curve which measures the effect of perturbing a parameter on an infinitesimal phase response curve.

4 Applications

We illustrate our approach by answering systems theory questions on simple oscillator models from different fields: cellular rhythm in systems biology [2], spike generation in neurodynamics [3], and low-noise clock synthesis in electronics [4].

References

[1] F C Hoppensteadt and E M Izhikevich. *Weakly Connected Neural Networks*. Springer, 1997.

[2] A Goldbeter. *Biochemical Oscillations and Cellular Rhythms: The Molecular Bases of Periodic and Chaotic Behaviour*. Cambridge University Press, 1996.

[3] E M Izhikevich. *Dynamical Systems in Neuroscience: the Geometry of Excitability and Bursting*. The MIT Press, 2007.

[4] I Vytyaz, D C Lee, P K Hanumolu, U-K Moon, and K Mayaram. Sensitivity Analysis for Oscillators. *IEEE Trans. Comput.-Aided Design Integr. Circuits Syst.*, 27(9):1521–1534, 2008.

From rational representations to minimal output nulling and driving variable representations of a Behavior

Sasanka V. Gottimukkala[1] Harry L. Trentelman[1]

1 Introduction

In this talk, we deal with a special category of representations of linear time invariant differential systems (LTIDS) in the behavioral framework. In the behavioral framework, a behavior, $\mathfrak{B}$, of a LTIDS admits many representations such as the kernel of a polynomial differential operator [2], the kernel of a rational differential operator [4], etc. In modeling of LTIDS, we often need variables other than the manifest ones, called latent variables. Representations involving these are called *latent variable representations*. These latent variable representations in general involve polynomial, and/or rational differential operators. There are also special class of latent variable representations called *state representations*, in which the latent variable satisfies a special property called the axiom of state. This axiom states that this variable has the property that it parametrizes the memory of the system, i.e., it splits the past and future of the behavior. A behavior admits different kinds of state representations such as classical *input/state/output (I/S/O) representations*, *driving variable representations*, *output nulling representations* [3], [1]. In this talk we shall limit our attention to driving variable and output nulling representations.

2 Problem Description

In this talk we show that given a behavior $\mathfrak{B}$ and a rational kernel representation with a proper real rational matrix, any realization of the above matrix yields an output nulling representation of this behavior. Similarly, we show that given a controllable behavior $\mathfrak{B}$ and a rational image representation with a proper real rational matrix, any realization of the above matrix yields a driving representation of this behavior.

Minimality of a representation is defined differently for each of the state space representations that a behavior admits [3]. An I/S/O representation is minimal if the state dimension is minimal over all I/S/O representations of $\mathfrak{B}$. A driving variable representation is minimal if the state and the driving variable dimensions are minimal over all driving variable representation of $\mathfrak{B}$. An output nulling representation is minimal if the state dimension and the dimension of output space are minimal over all output nulling representations of $\mathfrak{B}$. It is well known that every proper real rational matrix admits a realization such that the underlying constant real matrices form a controllable and an observable pair. In the classical I/S/O setting, a representation obtained from such realization is always minimal. However this is not the case with driving variable and output nulling representations. The controllability and observability conditions on the underlying constant real matrices are not sufficient to ensure minimality of the output nulling and driving variable representations.

This motivates us to pose the following questions:

1. Given are a behavior $\mathfrak{B}$, its rational kernel representation with a proper real rational matrix and a realization of the above matrix such that the underlying constant real matrices form a controllable and an observable pair. Find conditions under which the above realization yields a minimal output nulling representation of the behavior.
2. Given are a controllable behavior $\mathfrak{B}$, its rational image representation with a proper real rational matrix and a realization of the above matrix such that the underlying constant real matrices form a controllable and an observable pair. Find conditions under which the above realization yields a minimal driving variable of the behavior.

We show that for a given behavior, there always exists a proper real rational matrix such that a realization exists which yields a minimal output nulling (driving variable) representation of the behavior.

[1]Johann Bernoulli Institute for Mathematics and Computer Science, University of Groningen, P. O Box 800, 9700 AV Groningen, The Netherlands Phone:+31-50-3633999, Fax:+31-50-3633800 s.v.gottimukkala@rug.nl, and h.l.trentelman@math.rug.nl.

References

[1] M. Kuiper, *First-Order Representaions of Linear Systems*, Birkhäuser, 1994.

[2] J.W. Polderman and J.C. Willems, *Introduction to Mathematical Systems Theory: a Behavioral Approach*, Springer-Verlag, Berlin, 1997.

[3] J.C. Willems, "Input-output and state-space representations of finite-dimensional linear time-invariant systems," *Linear Algebra and its Applications*, Vol. 50, pp. 581-608, 1983.

[4] J.C. Willems and Y. Yamamoto, "Behaviors defined by rational functions," *Linear algebra and its applications*, Vol. 425, pp. 226-241, 2007.

Sarymsakov matrices and coordination tasks for multi-agent systems

Weiguo Xia and Ming Cao
Faculty of Mathematics and Natural Sciences, ITM, University of Groningen, The Netherlands
Email: {w.xia,m.cao}@rug.nl

1 Introduction

The convergence of products of stochastic matrices has proven to be critical in establishing the effectiveness of distributed coordination algorithms for multi-agent systems. After reviewing some classic and recent results on infinite backward products of stochastic matrices, we provide a new necessary and sufficient condition for the convergence in terms of matrices from the Sarymsakov class of stochastic matrices. We further generalize some conditions in the definition of the Sarymsakov class and prove that the resulted set of matrices is exactly the set of indecomposable, aperiodic, stochastic matrices. In the end, we investigate a specific coordination task with asynchronous update events. Then the set of scrambling stochastic matrices, a subclass of the Sarymsakov class, is utilized to establish the convergence of the system's state even when there is no common clock for the agents to synchronize their update actions.

2 Products of stochastic matrices

A square matrix $P=\{p_{ij}\}_{n\times n}$ is said to be *stochastic* if $p_{ij}\geq 0$ for all $i,\ j\in\{1,\dots,n\}$ and $\sum_{j=1}^{n}p_{ij}=1$ for all $i=1,\dots,n$. For a stochastic matrix P and all $\mathscr{A}\subseteq\{1,\dots,n\}$, let $F_P(\mathscr{A})$ be the set of *one-stage consequent indices* of $\mathscr{A}$ defined by

$$F_P(\mathscr{A})=\{j:\ p_{ij}>0 \text{ for some } i\in\mathscr{A}\}.$$

We say P is indecomposable and aperiodic and thus called an *SIA* matrix if $\lim_{m\to\infty}P^m=\mathbf{1}c^T$, where $\mathbf{1}$ is an n-dimensional all-one column vector, and $c=[c_1,\dots,c_n]^T$ is some column vector satisfying $c_i\geq 0$ and $\sum_{i=1}^{n}c_i=1$. We say P belongs to the *Sarymsakov class* $\mathscr{K}$ if for any two disjoint nonempty subsets $\mathscr{A},\ \tilde{\mathscr{A}}\subseteq\{1,\dots,n\}$, either $F_P(A)\cap F_P(\tilde{\mathscr{A}})\neq\varnothing$, or $F_P(\mathscr{A})\cap F_P(\tilde{\mathscr{A}})=\varnothing$ and $|F_P(\mathscr{A})\cup F_P(\tilde{\mathscr{A}})|>|\mathscr{A}\cup\tilde{\mathscr{A}}|$, where $|A|$ denotes the cardinality of $\mathscr{A}$. We say P is a *scrambling* matrix if for any pair of distinct row indices i and j, there always exists a column index k such that both p_{ik} and p_{jk} are positive. Consider a compact set $\mathscr{P}$ of $n\times n$ stochastic matrices. The following four conditions are proved to be equivalent.

C1. For each integer $k\geq 1$ and any $P(i)\in\mathscr{P},\ 1\leq i\leq k$, the stochastic matrix $P(k)\cdots P(1)$ is SIA.
C2. There is an integer $\nu\geq 1$ such that for each $k\geq\nu$ and any $P(i)\in\mathscr{P},\ 1\leq i\leq k$, the matrix $P(k)\cdots P(1)$ is scrambling.
C3. There is an integer $\mu\geq 1$ such that for each $k\geq\mu$ and any $P(i)\in\mathscr{P},\ 1\leq i\leq k$, the matrix $P(k)\cdots P(1)$ has a column with only positive entries.
C4. There is an integer $\alpha\geq 1$ such that for each $k\geq\alpha$ and any $P(i)\in\mathscr{P},\ 1\leq i\leq k$, the matrix $P(k)\cdots P(1)$ belongs to the Sarymsakov class $\mathscr{K}$.

Theorem 1. Let $\mathscr{P}$ be a compact set of stochastic matrices, and $P(i)\in\mathscr{P}$. Then $P(k)\cdots P(1)$ converges to a rank-one matrix $\mathbf{1}c^T$ as $k\to\infty$ if and only if any of the four conditions C1, C2, C3 or C4 holds.

3 The Sarymsakov class and SIA matrices

For a stochastic matrix P and all $\mathscr{A}\subseteq\{1,\dots,n\}$, let $F_P^k(\mathscr{A})$ be the set of *k-stage consequent indices* of any nonempty set $\mathscr{A}\subseteq\{1,\dots,n\}$, which is defined by $F_P^k(\mathscr{A})=F_P(F_P^{k-1}(\mathscr{A}))$ for $k\geq 2$ and $F_P^1(\mathscr{A})=F_P(\mathscr{A})$. We say a stochastic matrix P belongs to the class $\mathscr{W}$ if for any two disjoint nonempty subsets $\mathscr{A},\ \tilde{\mathscr{A}}\subseteq\{1,\dots,n\}$, there exists an integer k such that either $F_P^k(\mathscr{A})\cap F_P^k(\tilde{\mathscr{A}})\neq\varnothing$, or $F_P^k(\mathscr{A})\cap F_P^k(\tilde{\mathscr{A}})=\varnothing$ and $|F_P^k(\mathscr{A})\cup F_P^k(\tilde{\mathscr{A}})|>|\mathscr{A}\cup\tilde{\mathscr{A}}|$. It is easy to see that $\mathscr{K}\subseteq\mathscr{W}$ since we can always take $k=1$.

Theorem 2. A stochastic matrix P is in $\mathscr{W}$ if and only if P is SIA.

4 Asynchronous updates in multi-agent systems

Consider a system consisting of n agents, which is described by

$$x(t+1)=Px(t),\ t=0,1,\dots, \tag{1}$$

where P is an $n\times n$ stochastic matrix, and $x(t)=[x_1(t),\dots,x_n(t)]^T\in R^n$ is the state of the system. we consider a possible asynchronous implementation of system (1). Assume that the agents' clocks have the same skew but different offsets and thus one can program into each agent the notion of the length a period of time T. We consider the case when the agents update exactly once within each T and ignore the unlikely event that two agents update exactly at the same time.

Theorem 3. Assume each agent updates exactly once within T. If the stochastic matrix P in (1) is scrambling, then with asynchronous implementation the states of all the agents become the same asymptotically.

Parameter reduction of SISO Wiener-Schetzen models

Koen Tiels, Johan Schoukens
Dept. ELEC
Vrije Universiteit Brussel
Pleinlaan 2, 1050 Brussel
Belgium
Email: (Koen.Tiels, Johan.Schoukens)@vub.ac.be

Peter Heuberger
Delft Center for Systems and Control
Delft University of Technology
Mekelweg 2
2628 CD Delft
The Netherlands
Email: P.S.C.Heuberger@tudelft.nl

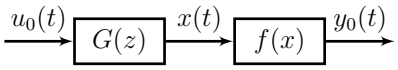

Figure 1: A discrete time SISO Wiener system (G is a linear dynamic system and f is a nonlinear static system)

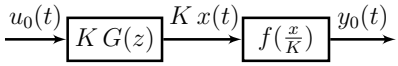

Figure 2: An equivalent representation of the Wiener system shown in Fig. 1

1 Introduction

The class of Wiener-Schetzen models can describe a large variety of nonlinear systems. The dynamical part of these models is formulated in terms of orthonormal basis functions (OBFs), while the nonlinearity is modeled through a multivariate polynomial. The parameters of the model are the coefficients of this polynomial. Generally, this polynomial contains a relatively large number of significant terms, resulting in a large number of parameters. This abstract is based on [1].

2 Problem formulation

The identification of a discrete time single input single output (SISO) Wiener system, shown in Fig. 1 is considered. The excitation signal $u_0(t)$ is considered to belong to the class of extended Gaussian excitations.

In [2], it is shown how a set of poles gives rise to a set of OBFs and that if the poles are close to the true poles of the underlying linear dynamical system, this system can be well approximated with only a limited number of these OBFs. In the general case with possibly multiple real and complex valued poles, the Takenaka-Malmquist OBFs are obtained.

In [3], we estimate the pole locations using the best linear approximation (BLA) of the system. For the Wiener system shown in Figure 1 and with $u_0(t)$ belonging to the class of extended Gaussian excitations, the BLA of the system is equal to:

$$G_{BLA}(z) = cG(z) \quad , \tag{1}$$

in which c is a constant. Since the BLA has the same poles as the linear dynamic subsystem G, the poles of the estimated G_{BLA} are excellent candidates to be used in the construction of the OBFs. Although the quality of the pole estimates is very good, the number of parameters can still be large. Therefore, a parameter reduction step is considered.

3 Basic idea

An equivalent representation of the Wiener system shown in Figure 1, resulting in the same input-output behavior, is shown in Fig. 2, in which K is an arbitrary non-zero constant. Since the BLA can represent the system dynamics very well (see equation 1), we propose to replace one of the OBFs by the BLA. In that way, most of the dynamics are represented by only one basis function. The other basis functions can then be seen as correction terms. Many of the parameters resulting from these basis functions can be considered small compared to those resulting from the BLA.

4 Results

Simulation results show a major reduction of the number of parameters, with only a minor increase in the rms error on the simulated output.

References

[1] K. Tiels, P.S.C. Heuberger, and J. Schoukens, "Reducing the number of parameters in a Wiener-Schetzen model," submitted for presentation at the 16^{th} IFAC Symp. Syst. Identification, Brussels, Belgium, 2012.

[2] P.S.C. Heuberger, P.M.J. Van den Hof, and B. Wahlberg [Eds.], "Modelling and Identification with Rational Orthogonal Basis Functions," Springer, 2005.

[3] K. Tiels, and J. Schoukens, "Identifying a Wiener system using a variant of the Wiener G-Functionals," 50^{th} IEEE Conference on Decision and Control and European Contol Conference, Orlando, FL, USA, December 2011.

Identifying linear systems from binary output data

Bruno Depraetere[1], Julian Stoev[2], Gregory Pinte[2], Jan Swevers[1]
[1] Department of Mechanical Engineering, Division PMA, Katholieke Universiteit Leuven
[2] Flanders' Mechatronics Technology Centre
Email: bruno.depraetere@mech.kuleuven.be

1 Motivation

This work considers the identification of linear systems based on binary output measurements. This can be useful for applications where sensors measuring the output are too costly or impractical to install. If it is possible to determine whether the output is above or below a given threshold, this information can then be used instead. An example is a moving object whose position is not measured, but where an optical sensor can detect when it passes a specific point.

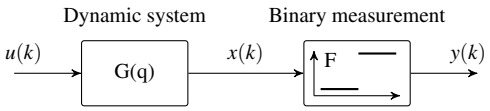

Figure 1: Schematic representation of considered systems.

Fig. 1 gives a schematic representation of the considered systems, with the binary measurement represented by a non-linear function F. It relates the output of the linear system $x(k)$ to the binary value $y(k)$ through

$$y(k) = F(x(k)) = \begin{cases} 0 & \text{if} \quad x(k) < x_{th}, \\ 1 & \text{if} \quad x(k) \geq x_{th}, \end{cases}$$

where x_{th} is the threshold at which the binary output changes in value between 0 and 1. The goal is now to identify a good model $\hat{G}(q)$ without measuring $x(k)$, using only $u(k)$ and $y(k)$, as well as the known behavior of F.

2 Methodology

In contrast to existing techniques with strict requirements on the excitation signals, the available data is assumed to be obtained from short and independent experiments, during which only a single transition of the binary output is observed. This situation often arises in practical cases, such that data measured during normal system operation can be used. However, a consistent identification can then only be performed if data from multiple experiments is combined.

The identification relies on making predictions $\hat{x}(k)$ for the different experiments. These are determined using the known input signals and an estimated Finite Impulse Response (FIR) model $\hat{G}(q)$. The best model is then found by minimzing a cost function that is composed by comparing the values of $\hat{x}(k)$ with the measured binary values $y(k)$, taking into account the known behaviour of the binary measurement. Two different methods are developed to do so:

- The first method directly uses the binary information and applies penalties for predicted values of $\hat{x}(k)$ that are not in the range corresponding to the binary value. This achieves a high prediction accuracy but yields constrained optimization problems.
- The second method is developed as an alternative to reduce the required computational load of the first. By assuming the output equals the threshold near the detected transition, a small error is introduced but the estimation reduces to an unconstrained linear least squares optimization problem. Solutions can therefore be found much faster, and it also becomes possible to find recursive solutions.

3 Experimental validation

For the experimental validation the test setup shown in Fig. 2 is available. It contains a sliding mass which is driven by an electromotor. The mass's position is measured with a linear encoder, while an optical sensor also provides binary measurements. The models estimated using the binary data can thus be evaluated by comparing their predictions to the true measurements, or by comparing the models to those estimated with the data from the linear encoder.

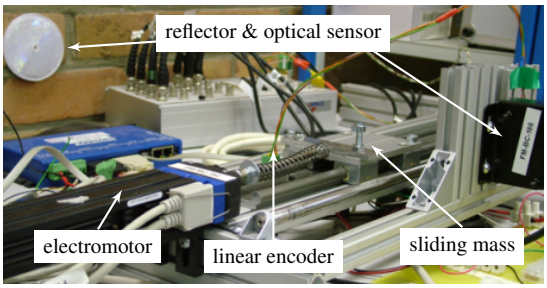

Figure 2: Test setup with binary output sensor.

Acknowledgement: This work has been carried out within the framework of projects IWT-SBO 80032 (LeCoPro) of the Institute for the Promotion of Innovation through Science and Technology in Flanders (IWT-Vlaanderen) and G.0422.08 of the Research Foundation -Flanders (FWO - Vlaanderen). This work also benefits from KU Leuven-BOF PFV/10/002 Center-of-Excellence Optimization in Engineering (OPTEC) and from the Belgian Programme on Interuniversity Attraction Poles, initiated by the Belgian Federal Science Policy Office.

Prediction Error Methods and Polynomial Root-Finding

Kim Batselier Philippe Dreesen Bart De Moor
Department of Electrical Engineering (ESAT), SCD
KU Leuven, 3001 Leuven
Belgium
Email: {kim.batselier,bart.demoor}@esat.kuleuven.be

1 Introduction

Prediction-error methods (PEMs) [1] have been the dominant method in system identification for the past 30 years. Despite their success these methods also have some drawbacks. For instance, an explicit parametrization of the model is always required and the search for the parameters can involve search surfaces that may have many local minima. Good initial parameter values are then of crucial importance. These are typically obtained by using subspace methods [2]. In this article we will present a numerical method for finding the global optimum which does not require any initial parameter value. It will be shown that PEMs are non-linear polynomial optimization problems and that these are equivalent to solving a non-linear multivariate polynomial system. An algorithm will be provided that effectively counts the number of affine solutions of the non-linear polynomial system and determines these solutions by solving a generalized eigenvalue problem. The whole theory is described in a numerical linear algebra framework.

2 Prediction Error Methods are Polynomial Optimization Problems

The model parameters of a LTI model

$$A(q)y(t) = \frac{B(q)}{F(q)}u(t) + \frac{C(q)}{D(q)}e(t) \tag{1}$$

are found from minimizing the prediction errors

$$e(t,\theta) = \frac{A(q)D(q)}{C(q)}y(t) - \frac{B(q)D(q)}{C(q)F(q)}u(t). \tag{2}$$

This can be written as the following optimization problem

$$\hat{\theta} = \underset{\theta}{\operatorname{argmin}} \sum_{t=n+1}^{N} l(e(t,\theta)) \tag{3}$$

subject to (2) where l refers to a suitable norm. We will assume the quadratic norm $l(e) = \frac{e^2}{2}$. By using Lagrange multipliers $\lambda_1, \ldots, \lambda_{N-n}$ these constraints can be added to the cost function

$$\sum_{t=1}^{N} \frac{e(t,\theta)^2}{2N} + \sum_{t=n+1}^{N} \lambda_{t-1}\left[e(t,\theta) = \frac{A(q)D(q)}{C(q)}y(t) - \frac{B(q)D(q)}{C(q)F(q)}u(t)\right] \tag{4}$$

which shows that for the quadratic norm PEMs correspond to a non-linear polynomial optimization problem. Taking the partial derivatives of (4) with respect to every unknown and equating these to zero results in a multivariate polynomial system. PEMs are therefore mathematically equivalent to solving a multivariate polynomial system.

3 Prediction Error Methods are Eigenvalue Problems

Since PEMs are equivalent with solving a multivariate polynomial system it can also be shown that they are in essence a generalized eigenvalue problem. In [3] the link between multivariate polynomial system solving and eigenvalue problems by means of the Macaulay matrix is discussed. This matrix contains all coefficients of the polynomial system and its nullity reveals the total number of solutions.

4 Counting and Finding Affine Roots

In practice, multivariate polynomial systems will have roots at infinity which are also counted by the nullity of the Macaulay matrix. These solutions are not desired and need to be removed when formulating the generalized eigenvalue problem. The concept of a reduced monomial system will be introduced and it will be shown how this monomial system guarantees to count and find only the affine roots. An algorithm will be provided and the main computational tool in the implementation is a sparse rank-revealing QR decomposition.

5 Acknowledgements

Kim Batselier is a research assistant at the Katholieke Universiteit Leuven, Belgium. Philippe Dreesen is supported by the Institute for the Promotion of Innovation through Science and Technology in Flanders (IWT-Vlaanderen). Bart De Moor is a full professor at the Katholieke Universiteit Leuven, Belgium. Research supported by Research Council KUL: GOA/11/05 Ambiorics, GOA/10/09 MaNet, CoE EF/05/006 Optimization in Engineering (OPTEC) en PFV/10/002 (OPTEC), IOF-SCORES4CHEM, several PhD/postdoc & fellow grants; Flemish Government: FWO: PhD/postdoc grants, projects: G0226.06 (cooperative systems and optimization), G0321.06 (Tensors), G.0302.07 (SVM/Kernel), G.0320.08 (convex MPC), G.0558.08 (Robust MHE), G.0557.08 (Glycemia2), G.0588.09 (Brain-machine) research communities (WOG: ICCoS, ANMMM, MLDM); G.0377.09 (Mechatronics MPC) IWT: PhD Grants, Eureka-Flite+, SBO LeCoPro, SBO Climaqs, SBO POM, O&O-Dsquare Belgian Federal Science Policy Office: IUAP P6/04 (DYSCO, Dynamical systems, control and optimization, 2007-2011); IBBT EU: ERNSI; FP7-HD-MPC (INFSO-ICT-223854), COST intelliCIS, FP7-EMBOCON (ICT-248940), FP7-SADCO (MC ITN-264735), ERC HIGHWIND (259 166) Contract Research: AMINAL Other: Helmholtz: viCERP ACCM.

References

[1] L. Ljung, "System Identification: Theory for the User (2nd Edition)," Prentice Hall, 1999.

[2] P. Van Overschee, B. De Moor, "Subspace Identification for Linear Systems: Theory, Implementation, Applications," Kluwer Academic Publishers, 1996.

[3] P. Dreesen, K. Batselier, B. De Moor, "Back to the Roots: Polynomial System Solving, Linear Algebra, Systems Theory," Internal Report ESAT-SISTA, KU Leuven, 2011.

Robust or Fast Local Polynomial Method: How to choose?

Griet Monteyne, Diana Ugryumova, Gerd Vandersteen and Rik Pintelon
Vrije Universiteit Brussel, Department of ELEC, Pleinlaan 2, 1050 Brussel, Belgium
Email: griet.monteyne@vub.ac.be

1 Introduction

The Robust (RLPM) and Fast (FLPM) Local Polynomial Methods were developed to find a non-parametric Frequency Response Function (FRF) estimate [1]. In this contribution the methods are compared and applied on experimental data coming from a heat diffusion experiment. Both methods assume that the excitation signal is a periodic signal and that the transient can be approximated locally in the frequency domain by a low-degree polynomial. FLPM also approximates the FRF by a local polynomial with a low degree. This approximation results in a bias error in case a low-degree polynomial cannot approximate the FRF well. RLPM does not approximate the FRF by a local polynomial. Thus, using RLPM avoids this bias error due to undermodeling. Unfortunately RLPM cannot estimate the level of the nonlinear distortions unless data coming from at least two experiments with uncorrelated inputs is available.

2 Theoretical analysis

The methods consider that the single-input, single-output system is disturbed by filtered white additive noise on the input and the output (Fig. 1).

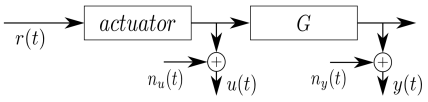

Figure 1: Scheme of measurement setup. G represents the considered system; r, the reference signal; u, y the noisy input, output signals; and n_u, n_y the input, output noise.

First, the reference $r(t)$, input $u(t)$ and output $y(t)$ signals are collected during P consecutive periods (N samples per period). The DFT spectra of the signals are calculated as

$$X(k) = \frac{1}{\sqrt{NP}} \sum_{i=0}^{NP-1} x(t) e^{-j\frac{2\pi kt}{NP}} \qquad (1)$$

where $X = R$, U or Y. Transforming the P consecutive periods to the frequency domain implies that only transient and noise are present on the $P-1$ lines in-between every two consecutive excited frequency lines.

Next, the non-excited frequency lines are used to estimate the transient on the input and output signal at the excited frequency lines. This is possible since the transient is locally approximated by a polynomial.

Finally, the estimated transient ($\hat{T}_Z = [\hat{T}_Y \ \hat{T}_U]^T$) is subtracted from the DFT spectra at the excited frequency lines.

$$Z_{new}(k) = Z(k) - \hat{T}_Z(k) \text{ with } Z = [Y \ U]^T \qquad (2)$$

FLPM then estimates the FRFs between the reference and input/output signal ($\hat{G}_{RY}$ and $\hat{G}_{RU}$) by approximating them locally by a polynomial. RLPM avoids the bias that is potentially introduced by FLPM by calculating the FRF estimates as $\hat{G}_{RY}(k) = Y_{new}(k)/R(k)$ and $\hat{G}_{RU}(k) = U_{new}(k)/R(k)$.

The FRF between input and output signal is for both methods found as $\hat{G}_{UY}(k) = \hat{G}_{RY}(k)/\hat{G}_{RU}(k)$.

3 Results and conclusion

Both methods were used to find FRF estimates for a simple heat diffusion problem. Fig. 2 shows that at low frequencies FLPM outperforms RLPM. This is due to the avoided bias and thus confirms the theoretical analysis.

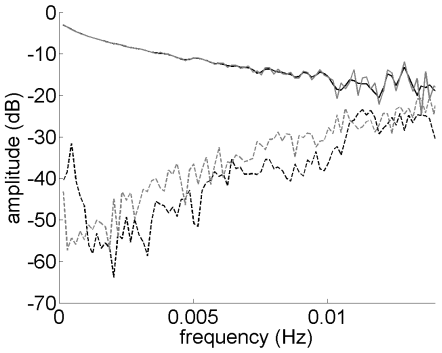

Figure 2: FRF estimates (solid lines) and root-mean-square errors (dotted lines) using FLPM (black) and RLPM (gray).

At higher frequencies FLPM seems to outperform RLPM. This is due to the smoothing over the neighboring frequencies caused by the local polynomial approximation of the FRFs. However, the information content of both FRF estimates is the same.

References

[1] R. Pintelon, G. Vandersteen, J. Schoukens, and Y. Rolain, "Improved (non-)parametric identification of dynamic systems excited by periodic signals–the multivariate case," Mechanical Systems and Signal Processing, vol. 25, no. 8, pp. 2892–2922, 2011.

Multi-level control for intelligent intermodal transport networks

Le Li*, Rudy Negenborn$^{\Delta}$, Bart De Schutter*
*Delft Center for Systems and Control
$^{\Delta}$Department of Marine and Transport Technology
Delft University of Technology, Mekelweg 2, 2628 CD Delft, The Netherlands
E-mail: {L.Li-1, r.r.negenborn, b.deschutter}@tudelft.nl

1 Introduction

Intermodal transportation may be defined as the transportation of a person or a load from its origin to its destination by a sequence of at least two transportation modes, the transfer from one mode to the next being performed at an intermodal terminal [1]. The reliable and efficient operation of large-scale intermodal transport networks, (such as road and railway networks, flight networks, ocean-shipping and coastal-shipping networks, etc.) is of huge importance for meeting the continuously increasing transport demand of goods in the national and international trade and promoting sustained development of the economy and the environment.

With the development of modern technology, various sensors, communication devices, embedded control units and actuators have been equipped in nearly every local node of large-scale transport networks, which takes up the task to monitor and manage the operating performance of its own relatively small part of the entire network. These equipments endow the local nodes with the intelligence, with which anyone of the local nodes can gain the ability to communicate with other nodes. The key issue that arises here is how these intelligent nodes will coordinate their actions, so as to guarantee the operating performance of the network as a whole. Our research aims at developing multi-level, coordinated, intelligent on-line control methods for large-scale intelligent intermodal transport networks.

2 Research Framework

In order to make optimal use of the intelligence in transport networks, model predictive control (MPC) will be applied for control of the nodes. When applying MPC to the intelligent transport network, the nodes are modeled as control agents that determine the optimal actions for the next control cycle by optimizing the objective function using different predictive models, the measurements of the initial state of the network at the beginning of the current control cycle and the predictions of the evolution of the possible disturbances over a certain prediction horizon.

Due to the large-scale nature of transport networks, single-agent control structures encounter challenges due to the computational complexity of control tasks and the limitations on communication bandwidth. Decentralized and distributed multi-agent control structures can reduce the amount of computation for each control agent in the system, although, typically lead to a lower system performance compared to that of an ideal single-agent control structure.

The multi-level multi-agent control structure (see Figure 1) provides the possibility to obtain a trade-off between system performance and computational complexity [2]. There are several control levels in a control structure. The control agents in lower levels take care of the fast dynamics of a small part of the network, while the control agents in higher levels take care of the slower dynamics of a larger part and coordinate the actions of the control agents in lower levels.

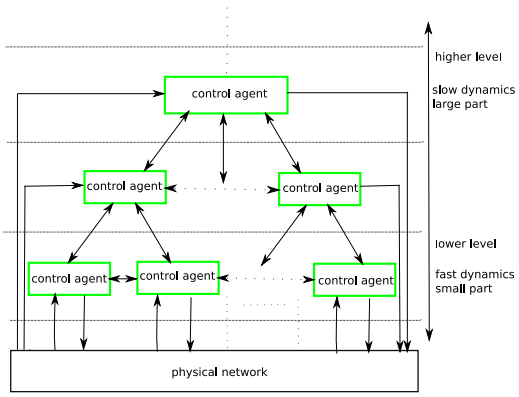

Figure 1: Multi-level multi-agent control structure

In order to ensure the stability and the control performance of the multi-level multi-agent control structure, special coordination mechanisms should be developed. Hence, we have the following three research objectives: 1) improve the computational efficiency of the existing coordination control methods or develop a new one; 2) analyze its theoretical properties; 3) investigate its control performance by case study in intelligent intermodal transport networks.

Acknowledgments This research is supported by China Scholarship Council under Grant 2011629027 and the VENI project "Intelligent multi-agent control for flexible coordination of transport hubs" (project 11210) of the Dutch Technology Foundation STW, a subdivision of the Netherlands Organization for Scientific Research (NWO).

References

[1] C. Barnhart, G. Laporte, *Transportation*, Elsevier, 2007.

[2] R. Scattolini. Architectures for distributed and hierarchical Model Predictive Control – A review, *J. of Proc. Ctrl.* 19(5): 723-731, 2009.

Optimal control of electricity generation from μ-CHPs in a network.

G. K. H. Larsen
University of Groningen
g.k.h.larsen@rug.nl

N. D. van Foreest
University of Groningen
n.d.van.foreest@rug.nl

J. M. A. Scherpen
University of Groningen
j.m.a.scherpen@rug.nl

1 Introduction

We have designed a model that describes the balance of electricity production and consumption in a multi-producer multi-consumer Smart Grid. A perfect balance between production and consumption is taken to be the control goal. One strategy to achieve balance in the network is to match production and consumption only inside each house. However, if neighbors cooperate and share some information with each other, the balancing could be done more efficiently.

Due to the many constraints on the μ-CHP, which produce at the same time heat and electricity, we will use Model Predictive Control (MPC) to solve the optimal control problem. We solve a central optimal control problem in a completely distributed way using a distributed MPC approach based on dual decomposition as described in [1]. Each house has a unique demand pattern based on realistic patterns generated by ECN pattern generator.

2 Dynamically coupled households

In the house one can make decisions for when to turn on (off) its μ-CHP, i.e. determining the change in electricity production $u_i(k)$. The real electricity imbalance $\tilde{x}_i(k)$ on node i is then

$$\tilde{x}_i(k+1) = \tilde{x}_i(k) + u_i(k) + w_i(k), \tag{1}$$

the imbalance at the previous time-step plus the change in production $u_i(k)$ and change in demand $w_i(k)$.

We realize communication in the network through dynamic coupling between the houses' notion of imbalance, $x_i(k)$. Each house i has a state equation also involving imbalance information from neighboring houses. The model for imbalance information in house i is given by

$$x_i(k+1) = A_{ii}x_i(k) + \sum_{j\neq i} A_{ij}x_j(k) + B_{ii}u_i(k) + w_i(k), \tag{2}$$

where B_{ii} is the input weight, A_{ii} is weighing the electricity imbalance information of house i itself, and A_{ij} weights the information received from neighbors. Notice that the *physical* imbalance enters the system at each house i through change in production $u_i(k)$ and change in demand $w_i(k)$, where it is included in the *information* about imbalance $x_i(k+1)$.

The control goal is to steer the states $x(k) = [x_1(k), \ldots, x_n(k)]$ to zero as cheaply as possible in $u(k) = [u_1(k), \ldots, u_n(k)]$:

$$J_{\text{opt}} = \min_{u(k)} \sum_{i=1}^{n} Q_{ii}x_i^2 + R_{ii}u_i^2, \tag{3}$$

where n is the number of households, $Q_{ii}, R_{ii} > 0$ are weights and (3) is subject to the constraints (2) and operational constraints on the μ-CHP. These *operational constraints involves* a minimum (maximum) production $p_{\min,(\max)}$, and a minimum time on (off) after start-up (shut-down).

3 A dynamic price mechanism

Distributed optimal control via dual decomposition methods [2], achieves distributed dynamic price patterns. The extension of the distributed optimal control settings via dual decomposition methods to an MPC setting is treated in [1].

We apply this distributed MPC method to the (large scale) embedding of μ-CHP's in the electricity grid. A simulation example is shown in figure 1.

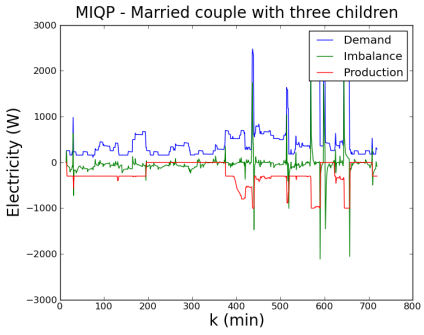

Figure 1: One house in a network where n=5.

References

[1] P. Giselsson and A. Rantzer. Distributed model predictive control with suboptimality and stability guarantees. In *Proceedings of the 49:th IEEE Conference on Decision and Control 2010*, pages 7272 – 7277, Atlanta, GA, USA, 2010.

[2] A. Rantzer. On prize mechanisms in linear quadratic team theory. In *Proc. 46th IEEE Conference on Decision and Control*, pages 1112 – 1116, New Orleans, LA, USA, 2007.

Moving horizon estimation for airborne wind energy systems

Kurt Geebelen[1,2], Jan Swevers[1], Moritz Diehl[2]
[1]Department of Mechanical Engineering, KU Leuven, Belgium
[2]Department of Electrical Engineering, KU Leuven, Belgium
Email: Kurt.Geebelen@mech.kuleuven.be

1 Introduction

In the search for sustainable energy sources as a replacement for fossil fuel based energy production, wind energy is one of the cheapest and most available resources for large-scale production. A new technology to harvest wind energy uses tethered airplanes at high altitudes and is referred to as '*Airborne Wind Energy*' (AWE). Several different AWE approaches are under development at several research groups and companies around the world. Our research focuses on AWE systems that consist of an airplane tethered to a ground-based generator that is performing periodic motions. During the first phase of its periodic motion, the airplane delivers a high traction force on the cable while it is being unrolled, causing the generator to produce electricity. When the cable is fully unrolled, the airplane is controlled such that the traction force is as low as possible, and the cable is retracted. Over the two phases combined, net electricity is produced.
A critical element in the development of AWE systems is automatic control of the airplanes, which depends a.o. on a reliable estimate of the pose of the airplane. This presentation discusses a Moving Horizon Estimator (MHE) for the pose of tethered airplanes.

2 Measurements and Estimation

A reliable airplane pose measurement system is developed that runs at a sufficiently high sampling frequency (500–1000 Hz). It is a combination of an absolute measurement system (e.g. a stereo vision system, a GPS, or an Ultra Wide Band (UWB) system) that runs at a low frequency (1–10 Hz) and an Inertial Measurement Unit (IMU) that runs at a high frequency (500–1000 Hz). The IMU is mounted on the aiprlane, and measures its acceleration and rotation speed in all three directions at a sampling frequency of up to 800 Hz. By integrating these measurements through a kinematic model, estimates of the pose are available at a high frequency. Without the absolute measurement system, the IMU would drift due to the integration of noisy measurements. Fusion of the IMU and the absolute pose measurements is therefore needed.

The Kalman filter is the most commonly used tool for state estimation and sensor fusion. The Kalman filter however only is optimal in case of a linear system and measurement model. In case of non-linear dynamics, an extended or unscented Kalman filter can be used, but they are suboptimal. A different approach comes in the form of MHE. A MHE estimates the system state by solving an optimal control problem online. In a typical MHE approach, the following optimisation problem is solved:

$$\begin{aligned} \min_{x,w,v} \; & \sum_{k=0}^{T-1} \| w_k \|^2_{Q_k^{-1}} + \sum_{k=0}^{T} \| v_k \|^2_{R_k^{-1}} \\ \text{subject to} \quad & x_{k+1} = f(x_k, w_k), \qquad \forall k = 0,..,T-1 \\ & y_k = h(x_k, u_k) + v_k, \qquad \forall k = 0,..,T \end{aligned} \tag{1}$$

where v and w are noise terms introduced to model the measurement noise and model uncertainty respectively, x is the system state, y represents the measurements and T is the considered time horizon. Because the IMU delivers measurements at a high sampling frequency, such an approach would quickly amount to very large optimisation problems to be solved. Therefore an approach in which the IMU measurements are approximated by polynomials is developed, with a basis equal to $\{1, t, ..., t^{m-1}\}$ and m the selected degree. The polynomial coefficients $c = \{c_1, c_2, ..., c_m\}$ are the decision variables for the optimisation problem. Each set of IMU measurements between two absolute pose measurements is represented by a polynomial. This yields the following optimisation problem to be solved:

$$\begin{aligned} \min_{x,c} \; & \sum_{k=0}^{T-1} \| \text{IMU}_k - h_{\text{IMU}}(c_k) \|^2_{Q_k^{-1}} + \sum_{k=0}^{T} \| y_k - h_a(x_k, u_k) \|^2_{R_k^{-1}} \\ \text{subject to} \quad & x_{k+1} = f(x_k, c_k), \qquad \forall k = 0,..,T-1 \end{aligned}$$

where h_a and h_{IMU} are the absolute pose and IMU measurement functions respectively. h_{IMU} returns the estimated IMU measurements according to the polynomial base and the respective weighting factors. By taking the degree of the polynomial base not too high, the number of decision variables can be dramatically reduced compared to problem (1), allowing for a faster solution of the problem. Simulation and experimental results will be shown during the presentation.

3 Acknowledgments

This research was supported by the European Uion via ERC HIGHWIND (259 166) and via FP7-EMBOCON (ICT-248940), by the K.U.Leuven-BOF via the Center of Excellence on Optimization in Engineering PFV/10/002 (OPTEC, http://www.kuleuven.be/optec/) and by the Belgian Programme on Interuniversity Attraction Poles, initiated by the Belgian Federal Science Policy Office (DYSCO).

Asymptotic Characteristics of Toeplitz Matrix in SISO Model Predictive Control

Quang N. Tran, Leyla Özkan, A.C.P.M. Backx
Department of Electrical Engineering
Eindhoven University of Technology
P.O. Box 513, 5600 MB Eindhoven
The Netherlands
Email: N.Q.Tran@tue.nl, L.Ozkan@tue.nl
A.C.P.M.Backx@tue.nl

Jobert H.A. Ludlage
Delft Center for Systems and Control
Delft University
Mekelweg 2, 2628 CD Delft
The Netherlands
Email: J.H.A.Ludlage@tudelft.nl

1 Introduction

The performance of Model Predictive Control (MPC) degrades over time if proper supervision is not performed, due to the model-plant mismatch. Since frequency-domain-based robust control approaches are better understood in dealing with uncertainty, we need to establish a connection between frequency-domain information and the finite horizon optimal control problem. For that reason, the singular value decomposition (SVD) of the Toeplitz matrix in the quadratic performance index of MPC is studied. It was shown in [2] that for sufficiently long prediction horizons, the eigenvalues of the Hessian matrix converge to the energy density spectrum of the associated system seen by the performance index. We extend that work and show that the left and right singular vectors of the Toeplitz matrix provide the phase information of the associated system for sufficiently long prediction and control horizons.

2 Results

The Toeplitz matrix in MPC reflects the connection between future inputs and future outputs of the system. Considering a stable SISO system, we can neglect the impulse response of the system from a time instant k_0: $H(k) = 0$ for $k > k_0$. Thus, the Toeplitz matrix $T \in \mathbb{R}^{N\times N}$ is given by:

$$T = \begin{pmatrix} H(0) & 0 & \dots & \dots & \dots & 0 \\ \vdots & \ddots & \ddots & & & \vdots \\ H(k_0) & \dots & H(0) & 0 & & \vdots \\ 0 & \ddots & & \ddots & \ddots & \vdots \\ \vdots & \ddots & \ddots & & \ddots & 0 \\ 0 & \dots & 0 & H(k_0) & \dots & H(0) \end{pmatrix} \quad (1)$$

where N is the control horizon and the prediction horizon of the MPC. We obtain the singular value decomposition of the Toeplitz matrix: $T = USV^\top$. The diagonal of S (i.e. singular values of T) contains the gain information of the system, and the singular vectors U and V are of sine wave shape and contain the phase information of the system. Fig. 1 shows the correspondence between the phase of the system and the information provided by the Toeplitz matrix.

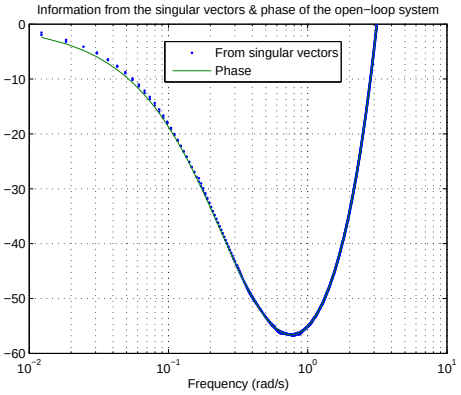

Figure 1: Arccos of the inner product of the Toeplitz matrix's singular vectors & phase

3 Conclusion

This information paves the way for the analysis of the finite horizon control problem and help us make use of frequency domain techniques in dealing with model uncertainties occurring at certain frequencies. Multi-variable systems with non-minimum phase zeros or delays will also be studied based on the results of [1].

References

[1] Jobert H.A. Ludlage. *Controllability Analysis of Industrial Processes: towards the industrial application*. PhD thesis, Eindhoven University of Technology, The Netherlands, 1997.

[2] Osvaldo J. Rojas, Graham C. Goodwin, María M. Serón, and Arie Feuer. An svd based strategy for receding horizon control of input constrained linear systems. *International Journal of Robust and Nonlinear Control*, 14:1207–1226, 2004.

Low-rank optimization on the set of low-rank non-symmetric matrices

Bamdev Mishra and Rodolphe Sepulchre
Department of Electrical Engineering and Computer Science
University of Liège
Emails: b.mishra@ulg.ac.be and r.sepulchre@ulg.ac.be

1 Introduction

We address unconstrained convex optimization problems with low-rank solutions. We propose an algorithm that alternates between fixed-rank optimization and rank-one updates. The fixed-rank optimization is characterized by different factorization models. The search space is nonlinear but is equipped with a particular Riemannian structure that leads to efficient computations. For each of the factorization we present a second-order trust-region algorithm with a guaranteed quadratic rate of convergence. Overall, the proposed optimization scheme converges super-linearly to the global solution while still maintaining complexity that is linear in the number of rows of the matrix. The performance of the proposed algorithm is illustrated on the low-rank matrix completion problem.

2 Problem formulation

We focus on the following convex unconstrained problem

$$\min_{\mathbf{X}\in\mathbb{R}^{n\times m}} \quad f(\mathbf{X}) \tag{1}$$

where f is a smooth convex function with the additional information that the solution $\mathbf{X}^*$ of the problem (1) is low-rank. Programs of this type have attracted much attention in the recent years as efficient convex relaxations of intractable rank minimization problems [Faz02, KO09, CCS10] with *trace* (nuclear) norm or *tikhonov* regularization. While most fixed-rank optimization algorithms assume a priori the search space and solve for a local minimum, we perform a systematic and efficient search for the global minimum of (1). The usefulness of this scheme has been presented in [MMBS11] in the context of trace norm.

Alternating between fixed-rank optimization and rank-one updates ensures that all intermediate iterates are low-rank while converging super-linearly to global minimum. Local minima are then escaped by incrementing the rank until the global minimum in reached. The rank-one update is always selected to ensure a decrease of the cost. This scheme of low-rank optimization differs from standard approaches which require singular value thresholding operations at each iteration [CCS10, MGC11].

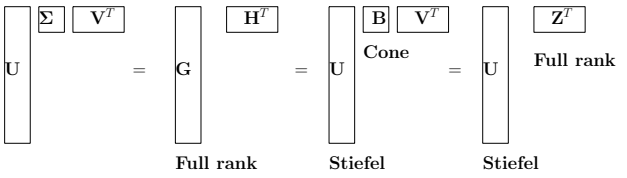

Figure 1: Different factorization models of a p-rank non-symmetric matrix.

3 Factorization models

We discuss the geometry associated with each of the factorization model and give the necessary insights to devise second-order schemes, shown in Figure 1. The search space of p-rank manifold is the quotient manifold defined by

$$\begin{aligned} &\mathbb{R}^{n\times p}\times\mathbb{R}^{m\times p}/\mathrm{GL}(r) && \leftarrow \quad \mathbf{GH}^T \\ &\mathrm{St}(p,n)\times S_{++}(p)\times\mathrm{St}(p,m)/O_p && \leftarrow \quad \mathbf{UBV}^T \\ &\mathrm{St}(p,n)\times\mathbb{R}^{m\times p}/O_p && \leftarrow \quad \mathbf{UZ}^T \end{aligned}$$

where $\mathrm{GL}(r)$ is the set of full rank $r\times r$ matrices and O_p is the set of $p\times p$ orthogonal matrices.

References

[CCS10] J.-F. Cai, E. J. Candès, and Z. Shen, *A singular value thresholding algorithm for matrix completion*, SIAM Journal On Optimization **20** (2010), no. 4, 1956–1982.

[Faz02] M. Fazel, *Matrix rank minimization with applications*, Ph.D. thesis, Stanford University, 2002.

[KO09] R. H. Keshavan and S. Oh, *A gradient descent algorithm on the Grassman manifold for matrix completion*, CoRR **abs/0910.5260** (2009).

[MGC11] S. Ma, D. Goldfarb, and L. Chen, *Fixed point and bregman iterative methods for matrix rank minimization*, Math. Program. **128** (2011), no. 1-2, 321–353.

[MMBS11] B. Mishra, G. Meyer, F. Bach, and R. Sepulchre, *Low-rank optimization with trace norm penalty*, Tech. report, arXiv 1112.2318, 2011.

Acknowledgments

This paper presents research results of the Belgian Network DYSCO (Dynamical Systems, Control, and Optimization), funded by the Interuniversity Attraction Poles Programme, initiated by the Belgian State, Science Policy Office. Bamdev Mishra is a research fellow of the Belgian National Fund for Scientific Research (FNRS). The scientific responsibility rests with its author(s).

Numerical modelling and calibration of an ultrasonic separator

Hans Cappon
HZ University of Applied Sciences
P.O. Box 364, 4380 AJ Vlissingen
hans.cappon@hz.nl

Karel J. Keesman
Systems & Control Group
Wageningen University
Bornse Weilanden 9, 6708 WG Wageningen
karel.keesman@wur.nl

1 Introduction

Design of ultrasonic equipment is more frequently facilitated with numerical models. These numerical models, however, need a calibration step, as usually not all characteristics of the materials used are known. Characterisation of material properties combined with numerical simulations and experimental data can be used to acquire valid estimates of the unknown material parameters. In our design application, a finite element (FE) model of an ultrasonic particle separator, driven by an ultrasonic transducer in thickness mode, is required. The particle separator consists of a glass cuvette with a piezoelectric transducer attached to the glass by means of epoxy adhesive. Separation occurs most efficiently when the system is operated at its main eigenfrequency.

2 Approach

A two-step approach was applied in order to obtain a calibrated model of the separator. Admittance measurements on the piezo transducer were used for all steps of model calibration and validation. In the first calibration step the unknown material parameters of the piezoelectric transducer were estimated with an optimisation routine [1], while preserving prior physical knowledge known from manufacturer data [2]. Starting point for the optimisation were parameter estimates obtained from a full factorial design of numerical experiments. In the second step the model was extended to the entire separator, also preserving known parameters and estimating the remaining unknowns or uncertain parameters, for instance the thickness of the adhesive layer between the piezoelectric transducer and the separator chamber's glass.

3 Results

The results show that the approach leads to a fully calibrated 2D model of the piezo transducer and the complete cuvette (see Figure 1). Nevertheless, both a sensitivity analysis on the piezo transducer and the results of the DOE show that very small changes to the input parameters, like the adhesive layer thickness or even the water temperature, will dramatically change the system response. This means that either such system should be made and operated within tight specifications to obtain the calculated performance or the operation of the system should be adaptable to cope with a slightly off-spec system, requiring a controller to find and maintain the eigenfrequency. Finally the separator model was 'filled' with water and validated with admittance measurements. The obtained pressure profiles show the typical nodal lines which cause the ultrasonic agglomeration of particles.

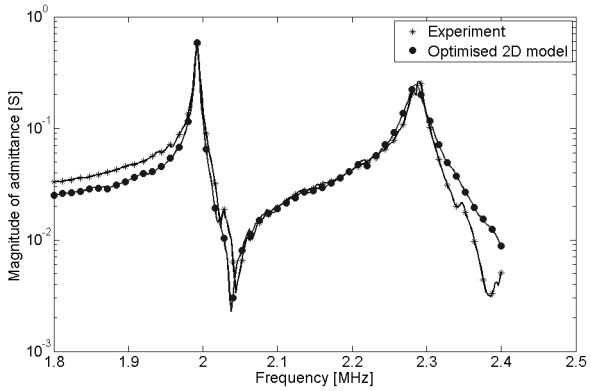

Figure 1: Measured and simulated admittance magnitude of the empty cuvette

4 Conclusion

Preserving known physical knowledge while optimising the response with unknown parameters was an efficient method for system calibration. The method does not only provide adequate input for future design, but also provides valuable insight into the influence of various parameters to the system response.

References

[1] K.J. Keesman, System Identification: an Introduction, Springer Verlag, London, 2011.

[2] H. Cappon, K. Keesman, Numerical modelling of piezoelectric transducers using physical parameters, IEEE trans. UFFC. Submitted 2011.

Community detection via kernel spectral clustering

Rocco Langone Carlos Alzate Johan A. K. Suykens
Department of Electrical Engineering (ESAT), SCD, KU Leuven, B-3001 Leuven Belgium
Email: {rocco.langone,carlos.alzate,johan.suykens}@esat.kuleuven.be

1 Introduction

We face the problem of community detection or clustering, which has been widely discussed in [2]. We use the kernel spectral clustering model (see [3]) to accomplish this task, by employing the primal-dual framework and making use of out-of-sample extension. The clustering model can be trained on a small subset of the whole graph (by solving an affordable eigenvalue problem) and then be applied to the rest of the network in a learning framework. The out-of-sample extension is a unique feature of our algorithm in the community detection field, and allows to analyze large networks. In this picture, two tasks become crucial:

- the choice of a good criterion to properly select the parameters to feed into the model, like the kernel parameters (if any) and the number of clusters.
- the extraction of a subgraph which is representative for the overall community structure characterizing the entire network.

In order to achieve the first goal we use a new method proposed in [4]. This criterion is based on Modularity, a quality function which, although with some drawbacks, has been shown to be a meaningful measure accounting for the presence of a significant community structure in networks. Regarding the selection of a small representative subgraph to use as training set, we propose an active selection method based on the greedy optimization of the expansion factor (see [5]). We demonstrate the effectiveness of our model on synthetic networks and benchmark data from real networks (power grid network and protein interaction network of yeast), ad we also make a comparison with the Nyström method.

2 Kernel spectral clustering model

Given N_{tr} training nodes $\mathscr{D} = \{x_i\}_{i=1}^{N_{\text{tr}}}, x_i \in \mathbb{R}^N$ and the number of communities k, the primal problem of spectral clustering via weighted kernel PCA is formulated as follows:

$$\min_{w^{(l)},e^{(l)},b_l} \frac{1}{2}\sum_{l=1}^{k-1} w^{(l)^T} w^{(l)} - \frac{1}{2N}\sum_{l=1}^{k-1} \gamma_l e^{(l)^T} D_\Omega^{-1} e^{(l)} \quad (1)$$

$$\text{such that } e^{(l)} = \Phi w^{(l)} + b_l 1_{N_{\text{tr}}} \quad (2)$$

where $\varphi : \mathbb{R}^N \to \mathbb{R}^{d_h}$ is the mapping to a high-dimensional feature space, Φ is the $N_{\text{tr}} \times d_h$ feature matrix $\Phi = [\varphi(x_1)^T; \ldots; \varphi(x_{N_{\text{tr}}})^T]$, $\gamma_l \in \mathbb{R}^+$ are regularization constants, b_l are bias terms, $l = 1, \ldots, k-1$. The dual problem related to this primal formulation is:

$$D_\Omega^{-1} M_D \Omega \alpha^{(l)} = \lambda_l \alpha^{(l)} \quad (3)$$

where Ω is the kernel matrix with ij-th entry $\Omega_{ij} = K(x_i, x_j) = \varphi(x_i)^T \varphi(x_j)$, D_Ω is the diagonal matrix with diagonal entries $d_i^\Omega = \sum_j \Omega_{ij}$, M_D is a centering matrix. The out-of-sample extension on the N_{test} new nodes becomes:

$$e_{\text{test}}^{(l)} = \Omega_{\text{test}} \alpha^{(l)} + b_l 1_{N_{\text{test}}} \quad (4)$$

where Ω_{test} is the $N_{\text{test}} \times N_{\text{tr}}$ kernel matrix.

3 Results

In the case of the synthetic networks in order to compare the memberships predicted by the kernel spectral clustering model with the true memberships the ARI index is used. On the other hand, in the case of the real datasets, to assess the quality of the clustering produced by the model, the Modularity of the predicted partition is calculated. The results obtained are good both in terms of the quality of the discovered partitions and the computation time needed to perform the analysis. Moreover, our model outperforms the Nyström method. The analysis of very large graphs and online clustering (by extending the trained model on every new test node arriving in a data stream) can be considered as future challenges.

Acknowledgements This work was supported by Research Council KUL: GOA/11/05 Ambiorics, GOA/10/09 MaNet, CoE EF/05/006 Optimization in Engineering(OPTEC), IOF-SCORES4CHEM, several PhD/postdoc & fellow grants;Flemish Government:FWO: PhD/postdoc grants, projects: G0226.06 (cooperative systems and optimization), G0321.06 (Tensors), G.0302.07 (SVM/Kernel), G.0320.08 (convex MPC), G.0558.08 (Robust MHE), G.0557.08 (Glycemia2), G.0588.09 (Brain-machine) research communities (WOG: ICCoS, ANMMM, MLDM); G.0377.09 (Mechatronics MPC) IWT: PhD Grants, Eureka-Flite+, SBO LeCoPro, SBO Climaqs, SBO POM, O&O-Dsquare; Belgian Federal Science Policy Office: IUAP P6/04 (DYSCO, Dynamical systems, control and optimization, 2007-2011); EU: ERNSI; FP7-HD-MPC (INFSO-ICT-223854), COST intelliCIS, FP7-EMBOCON (ICT-248940); Contract Research: AMINAL; Other:Helmholtz: viCERP, ACCM, Bauknecht, Hoerbiger. Rocco Langone is a phd student at the K.U. Leuven, Belgium. Carlos Alzate is a postdoctoral fellow of the Research Foundation - Flanders (FWO). Johan Suykens is a professor at the K.U.Leuven, Belgium. The scientific responsibility is assumed by its authors.

References

[1] R. Langone, C. Alzate, and J. A. K. Suykens, "Kernel spectral clustering for community detection in complex networks," (Submitted).

[2] S. Fortunato, "Community detection in graphs," *Physics Reports*, vol. 486, no. 3-5, pp. 75–174, 2010.

[3] C. Alzate and J. A. K. Suykens, "Multiway spectral clustering with out-of-sample extensions through weighted kernel PCA," *IEEE Transactions on Pattern Analysis and Machine Intelligence*, vol. 32, no. 2, pp. 335–347, February 2010.

[4] R. Langone, C. Alzate, and J. A. K. Suykens, "Modularity-based model selection for kernel spectral clustering," in *Proc. of the International Joint Conference on Neural Networks (IJCNN 2011)*, 2011, pp. 1849–1856.

[5] A. S. Maiya and T. Y. Berger-Wolf, "Sampling community structure," in *Proc. 19th ACM Intl. Conference on the World Wide Web (WWW '10)*, 2010.

Riemannian MADS for range-based ICA estimation

S. Easter Selvan, P. B. Borckmans and P.-A. Absil
Department of Mathematical Engineering
Université catholique de Louvain
Louvain-la-Neuve
Belgium
Email: {easter.suviseshamuthu,pierre.borckmans,pa.absil}@uclouvain.be

1 Introduction

This work briefly describes a geometrical approach—Riemannian Mesh Adaptive Direct Search (RMADS)—for optimizing a range-based contrast function in order to estimate independent components (ICs) respecting the unit-norm constraint. The empirical results using signal and image data show that the convergence quality of the RMADS algorithm employed in the IC estimation surpasses the state-of-the-art approaches.

2 RMADS optimizing range-based contrast

The RMADS is a Riemannian extension of the MADS algorithm [1] for minimizing a non-smooth function which ensures an asymptotically dense set of *polling* directions. Given an initial iterate, the MADS algorithm locates an optimizer of the objective function by evaluating the function at some trial points, and not requiring any of its derivative information. At each iteration, the trial points are selected such that they lie on a *mesh*, constructed using a finite set of directions scaled by a *mesh size parameter*. These directions must form a positive spanning set, and remain as the product of some fixed non-singular generating matrix and an integer vector. The objective function values are evaluated at the trial points, and the *improved mesh point* is selected as the one with a lower function value compared to the incumbent iterate without insisting on sufficient decrease. Following this *successful iteration*, the incumbent solution and the *mesh size parameter* are updated. If the iteration fails in producing an *improved mesh point*, the *mesh size parameter* is reduced, and the trial points closer to the incumbent solution are tried. Even though the convergence depends only on the aforementioned *poll step*, an optional *search step* may be included which enhances the exploratory capability of MADS.

Owing to the requirement to remove the scaling indeterminacy in the independent component analysis (ICA) problem, the ICs are constrained to have unit-norm. In other words, the optimization enforces the constraint that each IC lies on a unit-hypersphere. However, to avoid the accumulation of estimation errors in the deflation method, it is a common practice to resort to the simultaneous approach of IC estimation. Consequently, the underlying constraint on the IC estimate can be viewed as a cartesian product of unit-hyperspheres; this is equivalent to formulating the ICA problem on the *oblique manifold*.

Despite being non-smooth, the range-based contrast function enjoys the discriminacy property, which ensures that each local optimum of the function corresponds to a satisfactory IC estimate [2]. Interestingly, since the RMADS is endowed with the guarantee of convergence to a local optimum of a non-smooth objective function, it turns out to be a pertinent choice for optimizing the aforementioned contrast function. Nevertheless, the MADS designed for the Euclidean setting has to be carefully tailored to optimize on the *oblique manifold*, and in addition preserve the convergence guarantees. The RMADS algorithm utilizes the following ingredients of the *oblique manifold* optimization: (i) *exponential map* and (ii) *log map* to perform the vector addition and subtraction, respectively, such that the resultant quantity belongs to the manifold, and (iii) *parallel transport* to carry out a mathematical operation between the vectors on two different tangent spaces, by transporting one vector to the tangent space of the other. Since the range-based contrast function can easily be shown to have Lipschitz continuity, a convergence sketch can be provided to explain how the RMADS still guarantees a local optimum solution under mild assumptions.

3 Experimental validation

We performed a simulation by mixing the natural images/audio signals with a random non-orthogonal mixing matrix. The mixed images/signals are then *whitened* and separated using the ICA estimates obtained via the proposed and the state-of-the-art ICA approaches. The separation quality assessed using the performance index (PI) bears evidence to the benefits of our approach.

References

[1] C. Audet and J. E. Dennis, "Mesh adaptive direct search algorithms for constrained optimization," *SIAM Journal on Optimization*, vol. 17, no. 1, pp. 188–217, May 2006.

[2] F. Vrins, J. A. Lee, and M. Verleysen, "A minimum-range approach to blind extraction of bounded sources," *IEEE Transactions on Neural Networks*, vol. 18, no. 3, pp. 809–822, May 2007.

Controllability and Energy performance of the Drying Process

James C Atuonwu[1], Gerrit van Straten[1], Henk C van Deventer[2], Anton J B van Boxtel[1]
[1]Systems and Control Group, Wageningen University,
P. O. Box 17, 6700AA Wageningen, The Netherlands.
[2]TNO, P. O. Box 360, 3700AJ Zeist, The Netherlands.
Email[1]: {james.atuonwu, gerrit.vanstraten, ton.vanboxtel}@wur.nl
Email[2]: henk.vandeventer@tno.nl

1. Introduction

Drying is an important but energy intensive process applied in a wide variety of industries. Assuming a 100% energy efficient dryer, the amount of heat required to evaporate 1kg of free water from a product is in the order of 2.5MJ. The energy efficiencies of conventional dryers are however usually in the range 20 – 60%. With about 60000 products dried in application domains spanning virtually all industrial process systems, drying contributes about 15% of total industrial energy consumption. Dryer control is important for energy efficiency and product quality and many innovative dryer designs have been developed towards performance improvement. This work shows from energy balances and process resiliency analysis how dryer controllability and energy efficiency can be improved simultaneously. The viability of desiccant adsorption drying as a means of achieving this is shown.

2. Methodology

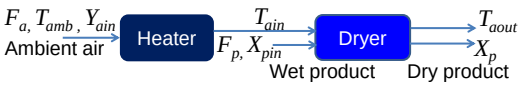

Fig. 1 Dryer schematic.

For the conventional drying system (Fig. 1), product moisture content X_p and outlet air temperature T_{aout} are outputs controlled by air flowrate F_a and inlet temperature T_{ain}. T_{amb} is the ambient temperature. The energy balance states that the drying air sensible heat loss across the dryer equals the latent heat gain plus heat loss Q_{loss}

$$F_a\left(C_{pa}+Y_{ain}C_{pv}\right)\left(T_{ain}-T_{aout}\right)=F_p\left(X_{pin}-X_p\right)\Delta H_v+Q_{loss} \quad (1)$$

The energy efficiency η, the ratio of the energy of the evaporated water to the dryer heat input is approximately

$$\eta=\left(T_{ain}-T_{aout}\right)/\left(T_{ain}-T_{amb}\right) \quad (2)$$

where F_p, X_{pin} are product flow and inlet moisture content respectively, Y_{ain} is inlet air humidity, C_{pa} and C_{pv} are specific heat capacities of air and water vapour while ΔH_v is the latent heat of vaporization of water. The process gain matrix which determines system controllability is given by

$$G=\begin{pmatrix}\partial X_p/\partial F_a & \partial X_p/\partial T_{ain}\\ \partial T_{aout}/\partial F_a & \partial T_{aout}/\partial T_{ain}\end{pmatrix} \quad (3)$$

Controllability can be analysed using tools like the relative gain array *RGA* (note: $\otimes$ is the Hadamard product) and the Morari Resiliency Index *MRI* given respectively by

$$RGA=G\otimes\left(G^{-1}\right)^T \quad (4)$$

$$MRI=\min\left(svd\left(G\right)\right) \quad (5)$$

Differentiating equation (1) with respect to F_a and T_{ain}, (assuming Q_{loss} does not vary with them), gives:

$$\left(F_a\,\partial T_{aout}/\partial F_a\right)-\left(1/K\right)\left(\partial X_p/\partial F_a\right)=T_{ain}-T_{aout} \quad (6)$$

$$\left(\partial T_{aout}/\partial T_{ain}\right)+\left(1/KF_a\right)\left(\partial X_p/\partial T_{ain}\right)=1 \quad (7)$$

where the constant $K=\left(C_{pa}+Y_{ain}C_{pv}\right)/\left(F_p\Delta H_v\right)$

The dryer process gain matrix which determines the system controllability properties is therefore seen to be related to the energy performance. When the drying air is dehumidified by passing through a desiccant adsorption system before the heater, the gain matrix elements change. Also, extra degrees of freedom and state variables are introduced, altering controllability and energy efficiency. Using modelling techniques, it can be shown how and under which conditions this modification can improve controllability and energy efficiency simultaneously.

3. Conclusion

Process design modifications affect both steady-state performance measures like energy efficiency and controllability. By including desiccant dehumidification as an add-on to the basic dryer, energy efficiency and controllability can be improved simultaneously .

Acknowledgements

This work is funded by the Energy Research Program EOS of the Dutch Ministry of Economics under Project EOSLT07043.

Benchmarking for CVT in CS-PTO Applications

Irmak Aladagli, Theo Hofman, Maarten Steinbuch
Control Systems Technology Group
Eindhoven University of Technology
The Netherlands
Email: i.aladagli@tue.nl

Bas Vroemen
Drivetrain Innovations
Croy 46, 5653 LD Eindhoven
The Netherlands
Email: vroemen@dtinnovations.nl

1 Introduction and Background

The coming years will see noise and emission regulations become ever more stringent, especially in the domain of heavy duty vehicles. The producers of these vehicles have already started looking for solutions. One of the promising solutions is powering the auxiliaries of these vehicles electrically, through a generator driven by the Internal Combustion Engine (ICE) of the vehicle, see [1].

Electrically powered auxiliaries require a constant voltage and frequency supply of electricity, like mains. Therefore, the generator, which is powered through the ICE, has to be driven at constant speed. This means a transmission that can convert the variable speed of the ICE to a constant speed input to the generator is required. The Continuously Variable Transmission (CVT) is such a device that has continuous ratio coverage through its range. This concept of drawing power from the ICE at constant speed is called the Constant-Speed Power Take-Off (CS-PTO).

In this research, the potential of the CVT in CS-PTO applications is investigated. One such application is completed on the test rig, and the resulting performance is discussed.

2 The CVT

This project concentrates on the pulley CVT among the many available types. The pulley CVT employs two sets of conical pulley sheaves with a belt in between that transfers the power from the input to the output side, see figure 2(a). On each side, one of the pulley sheaves can move axially, changing the radius at which the belt sits on the pulley, thus changing ratio. Certain clamping forces are required to keep or change the axial positions of the moveable pulley sheaves. These forces are supplied hydraulically, as depicted by the primary and secondary pressures p_1 and p_2 in figure 2(a).

The main mechanisms of operation of the CVT are friction and hydraulics. Therefore, its behaviour is highly nonlinear. This makes identification and control challenging, see [2]. Moreover, a cascaded control system is required as to track the desired ratio, one should also be able to control the hydraulic valves accurately, as can be seen in figure 1.

3 Control and Results

Manual tuning is employed in designing the controls of the system depicted in figure 1. In addition to linear feedback control, linear and nonlinear feedforward control and decoupling controls are employed. Moreover, various safety strategies have been included to safeguard the CVT.

Extensive performance tests prove that the maximum error

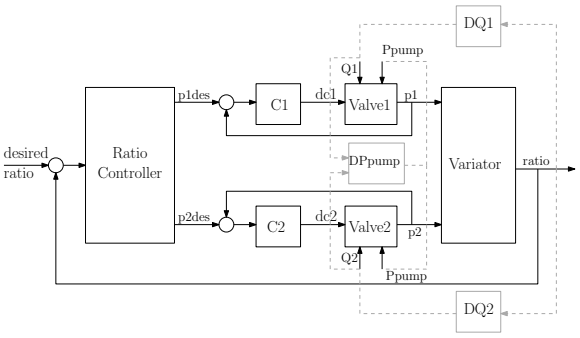

Figure 1: Control system overview.

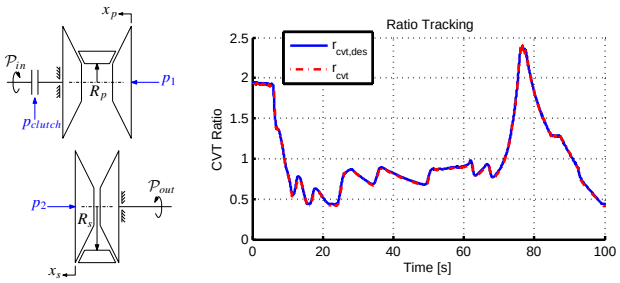

Figure 2: (a) The CVT. (b) Tracking performance of the designed controller.

in ratio tracking is 6%. The efficiency of the variator is estimated to be between 91 and 94%. These results comply with project requirements. However, it is clear that there is still room for improvement.

4 Conclusions and Looking Forward

Developing controls for the system and extensive performance tests established good benchmarking of the capabilities of this CVT setup and hydraulic valves as actuators. From this point on, the components of the system will be identified and modelled in computer environment where optimal controls can be developed according to the performance and robustness criteria.

References

[1] A. J. Klostermann, "New concepts for fuel efficient auxiliary systems for heavy duty vehicles," October 2011, in ATC Workshop Notes.

[2] T. Oomen, S. van der Meulen, O. Bosgra, M. Steinbuch, and J. Elfring, "A robust-control-relevant model validation approach for continuously variable transmission control," in *American Control Conference*, 2010.

Control for Low Emission, High Efficiency Diesel Engines

Chris Criens, Frank Willems, Maarten Steinbuch
Eindhoven University of Technology
Den Dolech 2, P.O. Box 513, Gem-Z -1.138
5600 MB Eindhoven, The Netherlands
c.h.a.criens@tue.nl

Introduction

In 2013 the new EURO VI emission standards will become active. As a result, the emissions of Nitrous Oxides (NO_x) and Particulate Matter (PM) will have to be lowered significantly. To realize this, tight control over the combustion conditions will have to be combined with exhaust gas aftertreatment.

Engine Air-Path

The amount and composition of the intake air of a diesel engine are managed by a Variable Geometry Turbine (VGT) and Exhaust Gas Recirculation (EGR) system.

By applying EGR, the combustion temperature and oxygen concentration are reduced, resulting in lowered emissions of NO_x. The combination of EGR valve and variable turbine enables independent control over both the amount and composition of the intake air.

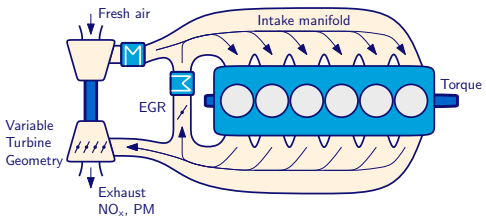

Figure 1: A schematic representation of the main components of a diesel engine air system

Control

Feedback control is used to adapt to disturbances, making the engine behavior more predictable and stay closer to its optimum. Optimal in this sense typically means the best possible efficiency within the constraints provided by the engine hardware and emission legislation.

A new control method has been developed that uses setpoint tracking of NO_x-emissions, PM-emissions and pumping losses (to represent efficiency). This results in a two-input (EGR, VGT), three-output (NO_x, PM, pumping losses) control problem. Using a singular value decomposition, the output-direction that is not influenced by the two actuators can be separated. Simultaneously the remaining steady-state input-output behavior is decoupled.

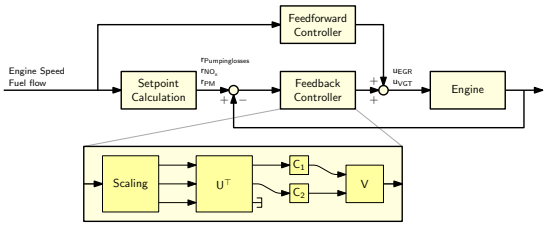

Figure 2: Overview of the engine control scheme

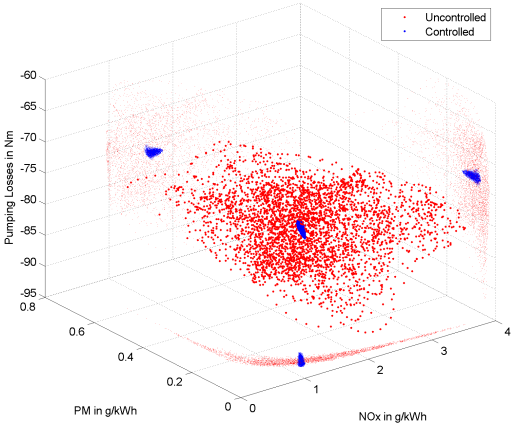

Figure 3: A feedback controlled engine vs. a traditional open loop controlled (Uncontrolled) engine with various disturbances present. The plot shows the results in 3-d with 2-d projections on the axes.

The new feedback controller decreases the effect of the disturbances by a factor 10. Additionally, the average emissions decrease by 10 to 20 percent and fuel consumption improves by 0.7 percent. Engines equipped with the new controller will have more dependable behavior and be more environmentally friendly.

References

Chris Criens, Frank Willems, Maarten Steinbuch, *Underactuated Control of a Heavy Duty Diesel Engine Airpath for Low Emissions and High Efficiency*, Submitted to ACC 2012

A New Robust Delay-Variable Repetitive Controller

With Application to Media Transport in a Printer

Ezequiel Bajonero Canonico
Eindhoven University of Technology
P.O. Box 513, Eindhoven, The Netherlands
Email: e.bajonero.canonico@student.tue.nl

Ewout van der Laan
Océ-Technologies B.V
P.O. Box 101, Venlo, The Netherlands
Email: ewout.vanderlaan@oce.com

Sjirk Koekebakker
Océ-Technologies B.V
Email: sjirk.koekebakker@oce.com

Maarten Steinbuch
Eindhoven University of Technology
Email: m.steinbuch@tue.nl

1 Introduction

In the industry is common to find systems that perform a task in a repetitive way, i.e., pick and place machines, printers, etc. It is desired for these systems to perform in the fastest way possible and with high accuracy, because this reflects productivity and quality. For example, bad performance in a printer system may end up in registration (dot position) errors which translate in a low print quality.
Because of the repetitive nature of these systems most of the errors will appear in each repetition they perform.When feedback is not capable to reject these repetitive disturbances, a repetitive controller (RC) can help us to reject the disturbances of a specific frequency.

2 Control structure

In cases where there is uncertainty in the frequency of the disturbance, High Order Repetitive Control (HORC) proposed in [2] can be used to compensate for it. HORC introduce a series of memory loops to widen the notch in a certain frequency at the expense of amplification in between harmonics so the HORC is robust to frequency mismatches. In [3] the notch is narrowed to achieve attenuation in between harmonics by choosing different weights in the loops so the RC becomes robust to noise.
In cases where the disturbances are spatial, delay-variable repetitive control (DVRC) [1] can be useful. DVRC is capable of calculating the RC delay in every iteration based on another spatial variable. One of the drawbacks of DVRC is that the robustness is limited for frequency uncertainties or noise.

Combining these two techniques HORC and DVRC, allows us to build a new Robust Delay-Variable Repetitive Controller (RDVRC). This new structure will be robust against frequency mismatch or noise in the disturbance by choosing the proper weights in accordance with our system properties (noise, dynamics, sensors, etc.). For stability of the RDVRC a new criterion is derived based on the stability proof presented in [1] and [2].

3 Experimental Results

Our experimental setup consists of a transporting belt and two rollers. It is clear that the position in any point of the belt depends on the rollers, and on the speed at which they operate. The belt is operated at 5 different speeds while measuring the error in the position of the belt.

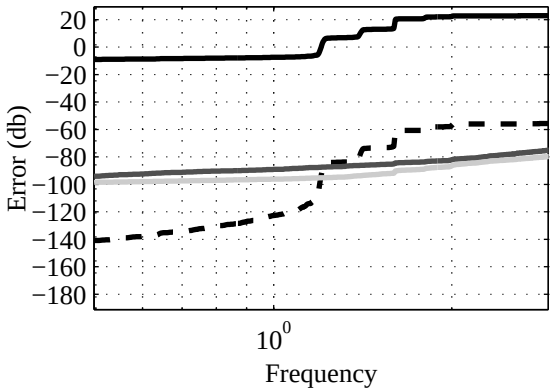

Figure 1: *Cumulative power spectrum density (CPSD) of the original disturbance (black), feedback error (black dashed), DVRC(dark grey) and obtained with new structure RDVRC (light grey)*

It can be observed in Figure 1 that the feedback is not capable to reject the repetitive disturbance. The DVRC is capable to do that but RDVRC is able to reduce noise in between harmonics, obtaining even more satisfactory results.

References

[1] R. Merry,"Performance-driven control of nanomotion systems", Eindhoven University of Tech., 2009

[2] M. Steinbuch,"Repetitive Control for Systems With Uncertain Period-Time", Automatica, 2002

[3] M. Steinbuch,S. Weiland,J. Van den Eerenbeemt,T. Singh, "On Noise- and Period-Time Sensitivity in High Order Repetitive Control", IEEE, 2004

Port-Hamiltonian approach to deployment on a line

Ewoud Vos[1,2], Jacquelien M.A. Scherpen[1], and Arjan J. van der Schaft[2]
University of Groningen
[1]Institute for Technology, Engineering & Management
[2]Johann Bernoulli Institute for Mathematics and Computer Science
Email: {e.vos,j.m.a.scherpen,a.j.van.der.schaft}@rug.nl

1 Introduction

In this talk we present a port-Hamiltonian approach to the deployment on a line of a robotic sensor network (see e.g. [3] for related work). Using the port-Hamiltonian modelling framework has some clear benefits. Including physical interpretation of the model, insight in the system's energy and structure, scalability, and use of the Hamiltonian for stability analysis. A concise overview of port-Hamiltonian systems theory can be found in [2].

Deployment on a line fits within the broader context of using robotic sensors networks for (autonomous) inspection of dikes. The aim of the autonomous dike inspection is to make a group (swarm) of robotic sensor move along the surface of the dike, while monitoring it with e.g. ground penetration radars (GPR).

The ideas in this talk are inspired by [1], who uses a passivity based-approach for coordination. It is well known that there is a strong link between port-Hamiltonian systems and passivity, which can be used in the stability analysis of the network.

In this talk we'll look at a network of N robots, which are modelled as fully actuated point masses. The interaction among the robots is represented by a graph G. The robots correspond to the vertices of the graph. The M edges of the graph correspond to virtual couplings [4], which are virtual springs and dampers. The dynamics of the interconnected system [4] are given by

$$\begin{aligned} \dot{q}^{vc} &= -B^T \frac{\partial H}{\partial p} \\ \dot{p} &= B \frac{\partial H}{\partial q^{vc}} - \left(D^r + BD^{vc}B^T\right) \frac{\partial H}{\partial p}, \end{aligned} \tag{1}$$

where q^{vc}, p, B, H, D^r, and D^{vc} denote respectively the relative distances, momenta, incidence matrix of graph G, Hamiltonian, robots dissipation matrix, and the virtual dampers dissipation matrix.

2 Deployment on a line

The deployment objective is to spatially distribute the robotic sensor network at equal relative distances on a line. We assume that all robots only interact with their nearest neighbors. The corresponding graph G is called a chain (or path) graph.

We extend the state with two static virtual walls, located at the boundaries of the line segment. Using a coordinate transformation we obtain the dynamics on the constrained state space [2]. At the equilibrium of this system the deployment objective is achieved. The equilibrium is globally (asymptotically) stable if the robots and/or virtual couplings are (strictly) passive. The corresponding (distributed) control law for the robots is given by

$$u = B \frac{\partial H}{\partial q^{vc}} - BD^{vc}B^T \frac{\partial H}{\partial p}. \tag{2}$$

Note that $\frac{\partial H}{\partial q^{vc}}$ and D^{vc} in (2) are design parameters, which can be used to shape the equilibrium and the transient response of the network.

3 Elementary simulation results

We have run elementary simulations for a network with eight robots, two virtual walls, and nine virtual springs. The robots are strictly passive ($D^r > 0$), while the virtual couplings are lossless ($D^{vc} = 0$). The figure below shows the time evolution of the robots.

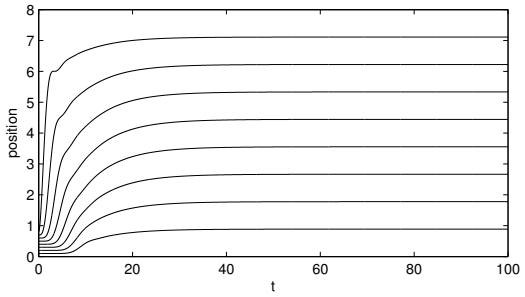

From their initial positions, the robots move towards a configuration where they are deployed at equal distances on the line segment.

References

[1] M. Arcak, "Passivity as a design tool for group coordination" IEEE Transactions on Automatic Control, 2007, 52, 1380-1390

[2] V. Duindam, A. Macchelli, and S. Stramigioli, "Modeling and Control of Complex Physical Systems: The Port-Hamiltonian Approach," Springer Verlag, 2009

[3] C. De Persis, H. Liu, and M. Cao, "Control of one-dimensional guided formations using coursely quantized information" Proc. 49th IEEE Conf. Dec. and Contr., pp. 2257-2262, Atlanta, GA, December 15-17, 2010.

[4] A.J. van der Schaft, and B. Maschke, "Discrete conservation laws and port-Hamiltonian systems on graphs and complexes," arXiv:1107.2006v1.

Probabilistic Multiple Hypothesis Reasoning in Robotics

Sjoerd van den Dries, Jos Elfring, René van de Molengraft, Maarten Steinbuch
Eindhoven University of Technology
P.O. Box 513, 5600 BM Eindhoven The Netherlands
Email: S.v.d.Dries@tue.nl

1 Introduction

In order to adequately perform tasks in a domestic setting, robots need to be aware of their environment and need to know the relations between objects in the world. A world model can be used to store and keep track of object positions and other attributes, such as velocity, color or weight. Typically, such world model is constructed based on observations received from sensors by fusing the received information into one global, consistent belief state. At the same time, a reasoning component can be used to translate the quantitative descriptions provided by the world model to qualitative, symbolic representations from which new symbolic properties can be derived. For example, the world model may track the positions of a cup and table in Cartesian coordinates, while the reasoning component translates this information to qualitative relations, such as 'the cup is on top of the table'.

However, the process described above is hindered by the fact that the world can only be partially observed due to occlusions, and is constructed from noisy data because of sensor limitations. To be able to adequately cope with these problems, uncertainty must be explicitly represented and dealt with, not only in the world model but also in the reasoning component.

2 Reasoning with Uncertainty

The problem of constructing a consistent world model from noisy observations is well-studied in literature. For example, the tracking community provides several well-established methods for fusing sensor information within a probabilistic framework [1]. At the same time, many methods exist for performing probabilistic inference in reasoning systems, such as [2]. However, the probabilistic output of the world model is typically first 'truncated' to strict facts, *e.g.*, the most probable state, before being fed to the reasoner. For example, the reasoning system described in [4] only uses the most probable location of the robot as input, while the localization module itself provides probabilistic information. This approach has the disadvantage that valuable information may be lost.

The implementation of the world model as used on our AMIGO robot is based on the multiple-hypothesis approach known from tracking literature [3]. This means that multiple possible states of the world are outputted, including the dependencies between those possible worlds. Our aim is to implement a reasoning module which makes explicit use of those multiple possibilities. For example, if a robot is asked to retreive a cup, and the world model outputs that the cup is either on coordinate C_1 or C_2 in room A or coordinate C_3 in room B, the reasoner may output that its best to go to room A, even if C_3 has the highest probability. The conversion of the quantitative information provided by the world model to the symbolic representation used in the reasoner will be performed by explicitly linking probability distributions over the attribute space of the objects to symbolic expressions. For example, a cup position probability distribution over a table surface can be linked to the expression 'the cup is on the table'.

A benefit of this approach is that qualitive information 'known' to the reasoner can also be used to update the world model. If John tells the robot that he will be in room A in one hour, the robot can represent this information as a probability distribution over the room for the attribute 'position'. Then, this type of information can be fed to the world model as if it was an observation. If the robot later receives observations of a person in room A, it will be able to associate these measurements to John. In a similar way, if the robot knows that it has succesfully picked up a cup with 90% certainty, the world model can be updated with this position information using a distribution centered around the robot's gripper. That way, it can keep track of the cup's position, even without observing it.

The research leading to these results has received funding from the European Union Seventh Framework Program FP7/2007-2013 under grant agreement n^{O}248942 RoboEarth.

References

[1] Y. Bar-Shalom. *Tracking and data association*. Academic Press Professional, Inc., San Diego, CA, USA, 1988.

[2] P. Domingos, S. Kok, H. Poon, M. Richardson, and P. Singla. Unifying logical and statistical ai. In *Proceedings of the Twenty-First National Conference on Artificial Intelligence*, pages 2–7. AAAI Press, 2006.

[3] D. B. Reid. An algorithm for tracking multiple targets. *IEEE Transactions on Automatic Control*, 24:843–854, 1979.

[4] M. Tenorth, D. Jain, and M. Beetz. Knowledge processing for cognitive robots. *KI - Künstliche Intelligenz*, 24:233–240, 2010. 10.1007/s13218-010-0044-0.

Global asymptotic tracking of one-DOF mechanical systems without velocity measurements

Yuxin Su, Jan Swevers, and Joris De Schutter
Department of Mechanical Engineering, Division PMA, Katholieke Universiteit Leuven
Celestijnenlaan 300B, B-3001 Leuven-Heverlee, Belgium
Email: {yuxin.su, Jan.swevers, Joris.deschutter}@mech.kuleuven.be)

Abstract

It is proven that simple PD position feedback plus feedforward dynamics compensation can achieve global asymptotic tracking for one-DOF mechanical systems under the assumption of exact model knowledge. In order to cope with model uncertainty, the control law is extended with a model parameter adaption algorithm.

1 Introduction

Loria [1] developed a position feedback controller for one-DOF mechanical systems yielding global asymptotic stability assuming exact model knowledge. The main disadvantage of this controller is that it involves hyperbolic tangent, sine, and cosine functions, which are not easy to implement and may induce very high value of the control effort. In addition, control parameter tuning is not at all straightforward.

In this work an alternative position feedback controller is presented. The proposed control is much simpler and more intuitive and hence easier to implement than the method presented in [1].

2 Problem statement

Starting from the dynamics of a one-DOF mechanical system [2, p.190], that is

$$J\ddot{q} + B\dot{q} + Mgl\sin(q) = \tau \tag{1}$$

the output tracking errors $e(t), \dot{e}(t) \in \Re^1$ are defined as:

$$e = q_d - q,\ \dot{e} = \dot{q}_d - \dot{q} \tag{2}$$

where $q_d(t) \in \Re^1$ is any C^3 reference trajectory. Our objective is to design a control input $\tau(t)$ that uses feedback of only position $q(t)$ such that $e(t), \dot{e}(t) \to 0$ as $t \to \infty$.

3 Control design

3.1 Output feedback PD plus (OPD+) control

The model-based control law is proposed as follows

$$\tau = k_p e + k_d \upsilon + J\ddot{q}_d + B\dot{q}_d + Mgl\sin(q) \tag{3}$$

$$\dot{q}_c = -a(q_c + be)\ ,\ \upsilon = q_c + be \tag{4}$$

where k_p, k_d, a, b are positive gains, respectively, and q_c is an auxiliary variable.

Theorem 1: The proposed (OPD+) control (3) and (4) ensures the globally asymptotic stability.

A Lyapunov based proof is given during the presentation.

3.2 Adaptive output feedback PD (AOPD) control

If the exact model is not known, the proposed control law equals

$$\tau = Y_d\hat{\theta} + k_p e + k_d \upsilon \tag{5}$$

$$\hat{\theta} = -kY_d e + k\int_0^t \left((\dot{Y}_d(\sigma) - \alpha Y_d(\sigma)\right)e(\sigma)d\sigma \tag{6}$$

where $Y_d\hat{\theta}$ represents the feedforward desired dynamics compensation with the estimated model parameters $\hat{\theta}$; k, α are positive adaptive gains, and υ is given by (4) and (5).

Theorem 2: The proposed AOPD control (4)-(6) ensures global asymptotic tracking, provided the control gains are chosen to satisfy some sufficient conditions (see the presentation).

A Lyapunov based proof is given during the presentation.

4 Illustrative example

Comparisons of the proposed OPD+ control with the method presented in [1] are performed. One of the examples is the tracking of a sinusoidal reference trajectory $q_d = 2(1-\sin(t))(\text{rad})$. Figure 1 shows the resulting position tracking errors and clearly illustrates the advantage of the proposed method.

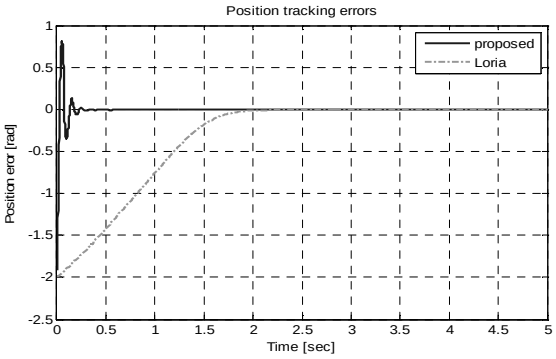

Fig. 1. Position tracking errors.

Reference

[1] A. Loria, "Global tracking control of one degree of freedom Euler-Lagrange systems without velocity measurements," *Eur. J. Control*, 1996, 2 (2): 144-151.

[2] M. W. Spong, S. Hutchinson, and M. Vidyasagar, *Robot Modeling and Control*. New York: Wiley, 2006.

ROP: Developing a Robotic Open Platform

Janno Lunenburg, René van de Molengraft and Maarten Steinbuch
Department of Mechanical Engineering, Eindhoven University of Technology
P.O. Box 513, 5600 MB Eindhoven, The Netherlands[1]
Email: j.j.m.lunenburg@tue.nl

1 Introduction

Before domestic robots will be part of our daily lives, further large-scale research on both hardware and software is required. In software, the Robot Operating System (ROS) [1] is nowadays acknowledged as a standard software platform that is used by numerous research institutions. This open source software is available to everyone and by sharing knowledge with the community there is no need to 'reinvent the wheel', hence drastically speeding up development. Similarly, this paper proposes the Robotic Open Platform (ROP): an open hardware platform available to all (www.roboticopenplatform.org). The more research groups will join and use ROP, the more ROP will become a valuable collection of configurable and affordable hardware components. Our target is that eventually a fully operational service robot can be built for around €15,000 (bill of material).

2 Modularity and Standards

Personal robots are expected to become a market with a similar influence as the personal computer market. Comparing the two markets, we are now in the era before the design of the IBM standard PC architecture. There are very few personal robotic systems on the market, they are expensive, and components are not interchangeable. Identical to how the IBM architecture revolutionized the PC market, the creation of design standards for personal robots will open up the great potential of the personal robotics market.

In the design of current research platforms, such as the PR2 [2] and the Care-O-bot 3 [3], the importance of modularity has been acknowledged. For example, the interfaces of the PR2 robot can be found on the manufacturers website. However, the mechanical, electrical and software interfaces of various manufacturers are still very different, making it impossible to, *e.g.*, straightforwardly equip one robot platform with the arm of another one. Having one platform where users are encouraged to share their designs with the community implicitly stimulates the development of common standard interfaces. Furthermore will the fast development of affordable actuators and sensors enable the construction of affordable modules for base, torso, arms and head, such that the bill of material is expected to drop rapidly in the coming years.

[1]The research leading to these results has received funding from the Dutch ministry of Economic affairs.

3 Current Status and Future Work

The first robot that was presented on ROP is the AMIGO service robot (see Figure 1). The ROP website contains all available documentation needed to create a full copy of AMIGO, and the corresponding software will be made publicly available on ROS. This robot was quickly followed by the Willow Garage TurtleBot and the Tech United Eindhoven TURTLE soccer robot will be added soon.

Figure 1: The AMIGO robot

Our hope is that research groups over the world will share their designs on ROP and will reuse available designs and knowledge, such that a strong community will grow and develop, similar to what happened with ROS over the recent years. We are currently focussing on the design of AMIGO 2.0, which will feature a unified interface between modules, and a completely open source robotic arm.

References

[1] Morgan Quigley, Ken Conley, Brian P. Gerkey, Josh Faust, Tully Foote, Jeremy Leibs, Rob Wheeler, and Andrew Y. Ng. ROS: an open-source robot operating system. In *ICRA Workshop on Open Source Software*, 2009.

[2] K.A. Wyrobek, E.H. Berger, H.F.M. Van Der Loos, and J.K. Salisbury. Towards a personal robotics development platform: Rationale and design of an intrinsically safe personal robot. In *Proceedings of ICRA 2008*

[3] Birgit Graf, Christopher Parlitz, and Martin Hägele. Robotic home assistant Care-O-bot®3 product vision and innovation platform. In *Proceedings of HCI International 2009*

A Novel Phase Portrait to Understand Neuronal Excitability

Guillaume Drion[1,2,#], Alessio Franci[3,#], Vincent Seutin[2] and Rodolphe Sepulchre[1]
[1]Department of Electrical Engineering and Computer Science and GIGA Research, University of Liège, Liège, Belgium
[2]Neurophysiology Unit and GIGA Neurosciences, University of Liège, Liège, Belgium
[3]L2S, Univ Paris Sud 11, Gif-sur-Yvette, France
# These authors contributed equally to this work. Email: gdrion@ulg.ac.be

Abstract

Rooted in the seminal work of Hodgkin and Huxley [1], conductance-based models have become a central paradigm to describe the electrical behavior of neurons. These models combine a number of advantages, including physiological interpretability (parameters have a precise experimental meaning) and modularity (additional ionic currents and/or spatial effects are easily incorporated using the interconnection laws of electrical circuits). Not surprisingly, the gain in quantitative description is achieved at the expense of mathematical complexity. The dimension of detailed quantitative models makes them mathematically intractable for analysis and numerically intractable for the simulation of large neuronal populations. For this reason, reduced modeling of conductance-based models has proven an indispensable complement to quantitative modeling [2]. In particular, the FitzHugh-Nagumo model [3], a two-dimensional reduction of Hodgkin-Huxley model, has played an essential role over the years to explain the mechanisms of neuronal excitability (see e.g. [4] for an excellent introduction and further references). More recently, Izhikevich has enriched the value of reduced-models by providing the Fitzugh-Nagumo model with a reset mechanism [5] that captures the fast (almost discontinuous) behavior of spiking neurons. Such models are used to reproduce the qualitative and quantitative behavior of a large family of neuron types [6]. Notably, their computational economy makes them good candidates for large-scale simulations of neuronal populations.

The Hodgkin-Huxley model and all reduced models derived from it [3, 6] focus on sodium and potassium currents, as the main players in the generation of action potentials: sodium is a fast depolarizing current, while potassium is slower and hyperpolarizing. Initally motivated by reduced modeling of dopaminergic neurons in which calcium currents are essential to the firing mechanisms [7], the present paper mimicks the classical reduction of the Hodgkin-Huxley model augmented with an additional calcium current. The calcium current is a distinct player because it is depolarizing, as the sodium current, but acts on the slower timescale of the potassium current.

To our surprise, the inclusion of calcium currents in the HH model before its planar reduction leads to a novel phase portrait that has been disregarded to date. Mimicking earlier classical work, we perform a normal form reduction of the global HH reduced planar model. The mathematical normal form reduction is fundamentally different in the classical and new phase portrait because it involves a different bifurcation. The classical fold bifurcation is replaced by a transcritical bifurcation.

The results of these mathematical analysis lead to a novel simple model that further enriches the modeling power of the popular hybrid model of Izhikevich. A single parameter in the new model controls the neuron calcium conductance. In low calcium conductance mode, the model captures the standard behavior of earlier models. But in high calcium conductance mode, the same model captures the electrophysiological signature of neurons with a high density of calcium channels, in agreement with many experimental observations. For this reason, the novel reduced model is particularly relevant to understand the firing mechanisms of neurons that switch from a low calcium-conductance mode to a high calcium-conductance mode. Because thalamocortical (TC) neurons provide a prominent example of such neurons, they are chosen as a proof of concept of the present paper, the benefits of which should extend to a much broader class of neurons.

References

[1] Hodgkin A and Huxley A (1952) A quantitative description of membrane current and its application to conduction and excitation in nerve. J. Physiol. 117: 500-44.

[2] Rinzel J (1985) Excitation dynamics: insights from simplified membrane models. Fed Proc. 44:2944-6.

[3] FitzHugh R (1961) Impulses and physiological states in theoretical models of nerve membrane. Biophys J. 1: 445-66.

[4] Ermentrout GB, Terman DH (2010) Mathematical Foundations of Neuroscience. Interdisciplinary Applied Mathematics. Springer.

[5] Izhikevich EM (2003) A simple model of spiking neurons. IEEE Trans Neural Netw. 14: 1569-72.

[6] Izhikevich, EM (2007) Dynamical Systems in Neuroscience: The Geometry of Excitability and Bursting. MIT Press.

[7] Drion G, Massotte L, Sepulchre R, Seutin V (2011) How modeling can reconcile apparently discrepant experimental results: The case of pacemaking in dopaminergic neurons. PLoS Comput. Biol. 7, e1002050.

Decision making in noisy bistable switches: a local analysis for non local predictions

Laura Trotta, Eric Bullinger and Rodolphe Sepulchre
Departement of Electrical Engineering and Computer Science,
University of Liège, B-4000 Liège, Belgium
l.trotta@ulg.ac.be, e.bullinger@ulg.ac.be, r.sepulchre@ulg.ac.be

1 Introduction

Bistable switches are frequently encountered in biology because binary decisions are at the core of many cellular processes. A bistable switch model is often described by a set of ordinary differential equations with two stable steady-states, each of them associated with a distinct decision. Depending on the external stimulus, the system can flip back and forth between these two stable states, choosing one of the two possible options. Examples of bistable switches are found in a broad variety of biological models including models of the cell cycle, the controlled cell death and development [1]. Most of these models are nonlinear and high dimensional which make them difficult to analyze. In addition, biological switches are often subject to different sources of noise which introduce some stochasticity in the system. Therefore, understanding which parameters and states govern the decision making process requires analyzing the transient behavior of a high-dimensional, nonlinear and possibly stochastic system. In this paper, we propose to use a local approach to study decision making in bistable switches subject to additive white noise. This local method is proposed as a valuable alternative to extensive numerical simulations generally required to understand the mechanism under investigation.

2 Method and Results

Let,

$$\frac{dx}{dt} = f(x) + \varepsilon\xi(t), \quad x \in \mathbb{R}^n \tag{1}$$

describe a system such that for $\varepsilon = 0$, the system is a bistable switch with two stable equilibrium points (x_1, x_2). $\xi(t)$ is a vector-valued random process of zero mean whose components are independent and each of which is an independent identically distributed random variable. This vector-valued random process is introduced to account for intrinsic fluctuations and is motivated by the Langevin theory. In this paper, we argue that it is possible to use a local approach to study decision making in (1). This work is based on the hypothesis that the deterministic bistable model $(\varepsilon = 0)$ has a saddle point (x_0) with some properties of time-scale separation between its attractive and repulsive directions. Our approach is motivated by the work of E. Stone and P. Holmes on random perturbations of heteroclinic attractors [2] and the work of Bogacz et al. on the physics of decision making [3]. In particular, we show that under appropriate assumptions, the decision process can be described locally by an Ornstein-Uhlenbeck process whose dynamics is governed by parameters directly related to the saddle point. For two examples of biological switches, we compare the results obtained with this local model with the results obtained for the global model.

3 Discussion

In this paper, we try to estimate some statistics about the decision making process in a bistable model submitted to noise by studying the local properties of the system around an hyperbolic saddle point. Despite the fact that the saddle is not an equilibrium point of the stochastic system, we show that a local approach is still instructive. Under appropriate assumptions, the system can be reduced to an Orstein-Uhlenbeck process whose dynamics depend on the properties of the saddle point. Yet, Orstein-Uhlenbeck processes have been used to study decision making under uncertainty in a broad variety of fields including statistics and cognitive neurosciences [3]. This local approach could also be a good starting point for the study of decision making in multi-stable models. Especially further work should discuss possible connections between our work and recent work on the transient behavior of stochastic gradient algorithms [4].

References

[1] J. Tyson, R. Albert, A. Goldbeter, P Ruoff and J Sible, “Biological switches and clocks”, J. R. Soc. Interface, 5(Suppl.1):S1-S8, 2008.

[2] E. Stone and P. Holmes, “Random Perturbations of Heteroclinic Attractors”, SIAM J. Appl. Math., 50: 726-743,1990

[3] R. Bogacz, E. Brown, J. Moehlis, P. Holmes and J.D. Cohen, “The physics of optimal decision making: A formal analysis of models of performance in two-alternative forced-choice tasks”, Psychological Review, 113(4):700-765, 2006.

[4] R. Brockett, “Modeling the transient behavior of stochastic gradient algorithms”, 50th IEEE Conference on Decision and Control and European Control Conference (CDC-ECC), USA, 2011

The modeling cycle in genetic network reconstruction: the XlnR regulon of *Aspergillus niger*

Jimmy Omony[1,3], Astrid R. Mach-Aigner[2], Leo H. de Graaff[3], Gerrit van Straten[1], Anton J.B. van Boxtel[1]
[1]Systems and Control group, Wageningen University, P.O. Box 17, 6700 AA Wageningen, The Netherlands.
[2]Gene Technology, Department of Gene Technology and Applied Biochemistry,
Institute of Chemical Engineering, TU Vienna, A-1060 Vienna, Austria.
[3]Laboratory of Systems and Synthetic Biology, Wageningen University,
Dreijenplein 10, 6703 HB, Wageningen, The Netherlands.
Email: {jimmy.omony,leo.degraaff,gerrit.vanstraten,ton.vanboxtel}@wur.nl
Email: aaigner@mail.zserv.tuwien.ac.at

1 Introduction

This work provides insight into the modeling cycle in biological network reconstruction. Understanding regulatory mechanisms in biological networks is a multi-stage process that involves acquisition and consolidation of prior knowledge, experimental design, data collection, hypothesis testing and model validation. Often, in parameter identification problems, models need to be fine-tuned and validated. This is a cyclic process that involves learning from both data and the model. This work involves reverse engineering biological networks using gene expression time course data sets. Following wet-lab experiments, transcription profiles for the genes that are involved in the D-xylose metabolism in the XlnR regulon of *Aspergillus niger* were categorized. The genes showed different transcription profiles as a result of the D-xylose perturbation on the XlnR regulon. The relationship between the model and data was analyzed.

2 Methods

The study of biological networks is often based upon experimentally measured data or *in silico* studies. We model the XlnR regulon of *Aspergillus niger* [1], and using the cyclic evaluation we adapt the models to improve our understanding of the dynamics exhibited in the gene expression data set. Nonlinear ordinary differential equations and Hill functions were used to model the gene regulation and their associated dynamics. By fixing the values of the less sensitive parameters, the estimates of the more sensitive parameters significantly improved. The gene expression profiles were analytically categorized for the data sets corresponding to the low (1 mM) and high (50 mM) D-xylose concentrations. The D-xylose concentration follows the expression:

$$u_1(t) = u_1(0)\frac{\theta}{\beta + e^{Kt}};\ \text{given}\ u_1(0) = u_{10} \qquad (1)$$

where θ, β and K are parameters and t is time. The transcription-translation model we used is given in (2). Here x_i is the mRNA abundance and z_i is the protein concentration; $k_{is}, k_{i1}^{'}, k_{i2}, k_{i3}, k_{id}, r_i$ and η_i are the system parameters.

$$\begin{cases} \dot{x}_i = k_{is}\dfrac{k_{i1}^{'}u_1}{1+k_{i1}^{'}u_1}\dfrac{1}{1+k_{i2}u_1}\varphi(z_i,:) - k_{id}x_i, \\ \dot{z}_i = r_i x_i - \eta_i z_i;\ \ x_i(t_0) = x_{i0},\ \text{and}\ z_i(0) = z_{i0} \end{cases} \qquad (2)$$

Here, $\varphi(z_i,:)$ is either an activator i.e. $\varphi(z_i,:) = k_{i3}z_i/(1+k_{i3}z_i)$ or repressor $\varphi(z_i,:) = 1/(1+k_{i3}z_i)$ Hill function.

3 Results and discussion

Under the experimental condition considered (low or high D-xylose concentration), the gene transcription levels implicitly relate to the amount of enzymes produced. The results show that for this group of genes, better model fits can be obtained if more is known on the precise role played by post-translation modification products and the associated D-xylose metabolism at high D-xylose concentrations. Most target gene transcription profiles show high order dynamics to the second and third order, indicating the existence of feedback loops in the network.

4 Conclusion

Different levels of perturbation with the 1 mM and 50 mM D-xylose on the regulon lead to different target gene expression dynamics. The bimodal responses exhibited by some target genes suggest a potential existence of other contributors to the regulation mechanism in the XlnR regulon. The dependence of the steady states on the parameter was highlighted by the system steady state analysis.

Acknowledgement: This work is supported by the graduate school VLAG and the IPOP program of Wageningen University.

References

[1] J. Omony, L.H. de Graaff, G. van Straten, A.J.B. van Boxtel. Modeling and analysis of the dynamic behavior of the XlnR regulon in *Aspergillus niger*. *BMC Syst. Biol*, **5(Suppl. 1)**:S14, 2011.

Invariance and contractiveness via comparison systems

Nikolaos Athanasopoulos
Electrical Engineering Department
Eindhoven University of Technology
P.O. Box 513, 5600 MB, Eindhoven
The Netherlands
Email: n.athanasopoulos@tue.nl

George Bitsoris
Electrical and Computer Engineering Department
University of Patras
26500, Patras
Greece
Email: bitsoris@ece.upatras.gr

1 Introduction

One particular extension of the standard Lyapunov stability theory concerns the use of Lyapunov-like vector functions instead of scalar ones. Vector valued functions combined with comparison theorems stemming from the theory of differential inequalities, have been initially used for the stability analysis of continuous-time nonlinear systems. Conceptually, the comparison systems approach lies in the following: if a stability analysis or control synthesis problem is too difficult to investigate, an attempt is made to establish a relationship between the system under consideration and another system via a vector function, such that both systems enjoy similar properties. Analogous methods have also been developed and applied to discrete-time systems using linear or nonlinear comparison systems. An overview of the existing methods can be found in [1], [2].

2 Positively invariant and contractive sets

Applying the comparison systems method, necessary and sufficient conditions verifying positive invariance and contractiveness of subsets defined by nonlinear vector inequalities of the form

$$S(v,d) = \{x \in \mathbb{R}^n : v(x) \leq d\} \tag{1}$$

with respect to continuous-time as well as discrete-time systems, have been established. The idea behind the approach is based on the following: If $v(x)$ is a vector valued function defined on the state-space of a system $x(t+1) = f(x(t))$ and $y(t+1) = h(y(t))$ is the associated comparison system constructed using function $v(x)$, then $v(x_0) \leq y_0$ implies $v(x(t)) \leq y(t)$ for $t \geq 0$. In other words, in the case of contractiveness, the rate of convergence of each border surface $v_i(x) = d_i$ of the set defined by the vector valued inequality $v(x) \leq d$ is upper bounded by the the rate of convergence of the corresponding component $y_i(t)$ of the state vector of the comparison system. Thus, positive invariance of the set defined by inequality $y \leq d$ with respect to the comparison system implies the positive invariance of the set $v(x) \leq d$ with respect to the original system.

3 Main results

In the case when $v(x) = Gx$, that is in the case when the set defined by the inequality $v(x) \leq d$ is a polyhedron, the rate of convergence of the components $y_i(t)$ of the vector $y(t)$ provides information about the rate of convergence of the facets $(Gx(t))_i = y_i(t)$ of the polyhedron. A polyhedron, however, can also be described in terms of its vertices. Motivated by this fact, this note is focused on two main issues, namely in developing new types of comparison systems providing information about the evolution of the vertices of a polyhedron and extending the approach to other complex types of sets.

Starting from recent results [3], [4], we first deal with the problem of establishing positive invariance and contractiveness for sets of a more general form than (1):

$$S(V,g,d) = \{x \in \mathbb{R}^n : (\exists y \in \mathbb{R}^p,\ y = Vx : g(y) \leq d)\}. \tag{2}$$

Then, we move on to the problem of establishing comparison systems associated with the original systems via sets described by their "generating vectors"

$$Q(W,g,r) = \{x \in \mathbb{R}^n : (\exists y \in \mathbb{R}^p, \quad g(y) \leq r : x = Wy)\}. \tag{3}$$

An application of these so called dual comparison systems, associated with sets (3), will be demonstrated for the case of discrete-time bilinear systems.

References

[1] W. Haddad, and V. Chellaboina, "Nonlinear dynamical systems and control: A Lyapunov-based approach,", Princeton University Press, 2006.

[2] V. Lakshmikantham, V.M. Matrosov, and S. Sivasundaram, "Vector Lyapunov functions and stability analysis of nonlinear systems", Kluwer Academic Publishers, 1991.

[3] G. Bitsoris, and N. Athanasopoulos, "A dual comparison principle for the analysis and design of discrete-time dynamical systems", in proceedings of the 18th IFAC World Congress, pp. 6437–6442, 2011.

[4] N. Athanasopoulos, and G. Bitsoris, "Stability analysis and control of bilinear systems: a dual approach", in proceedings of the 18th IFAC World Congress, pp. 6443–6448, 2011.

An Observer for a Piecewise-Affine Hybrid System on Polytopes

Luc C.G.J.M. Habets
Dept. of Mathematics and Computer Science
Eindhoven University of Technology
P.O. Box 513
5600 MB Eindhoven
The Netherlands
Email: l.c.g.j.m.habets@tue.nl

Jan H. van Schuppen
CWI
P.O. Box 94079
1090 GB Amsterdam
The Netherlands
Email: J.H.van.Schuppen@cwi.nl

1 Problem and Concepts

The motivation of the problem of observer construction is the need for observers for several engineering control problems. Examples of such problems are control of motorway traffic, control of electric circuits, etc.

Define a time-invariant continuous-time *piecewise-affine hybrid system on polytopes* (PAHSP) without inputs, see [2], as a dynamical system as understood in control and system theory, with the representation,

$$\begin{aligned} dx_q(t)/dt &= A(q)x_q(t)+a(q),\ x_g(t_0)=x_{q,0}, \\ y(t) &= C(q)x_q(t)+c(q), \\ q^+ &= f(q^-,e,x_{q^-}),\ q^-=q_0, \\ r(q^-,e,x_{q^-}) &= M(q^-,e)x_{q^-}+c_r(q^-), \\ & q\in Q,\ x_q(t)\in X(q),\ y(t)\in\mathbb{R}^p. \end{aligned}$$

The *observer problem* is to uniquely determine the state of a PAHSP at the end of a time-interval from the observations of the output of the PAHSP received during that time-interval. Earlier publications cover observability of linear hybrid systems but not the problem considered in this lecture. The problem of checking observability of piecewise-affine hybrid systems has been proven to be undecidable, see [1]. Therefore a more modest aim is considered: can a decidable sufficient condition for observability be proven?

Coobservability is defined as the system theoretic property that on any interval one can uniquely determine the state at the final time from the observations received on the interval.

2 Construction of an Observer

Assume that at any time-instant the discrete part of the state of a PAHSP can be determined uniquely from its output trajectory. Define the state estimate polytope (SEP) as the set of states within the continuous state set which are compatible with the current and past outputs. If the affine system at discrete state q is observable, or, equivalently, if $(A(q),C(q))$ is an observable pair, then the SEP shrinks shortly after the initial time to a vector in the state set and the state is then estimated. If at state q, the affine system is not observable then the SEP reduces to a polytope in the unobservable subspace. Once a discrete event occurs then the SEP is intersected with the current exit facet and is transformed by the reset map to a new SEP within the continuous state set of the new discrete state. This cycle repeats. If coobservability holds, then the SEP reduces to a single vector in the local state polytope, after a finite number of discrete transitions

3 Coobservability check

The second problem is the construction of a procedure to determine whether a piecewise-affine hybrid system is coobservable. Assume again that from the output the discrete state can be determined uniquely. At the initial time there is again an initial state estimate polytope (SEP). If at the local discrete state the affine system is not observable then reduce the SEP to a polytope in the unobservable subspace. Determine all exit facets of the state polytope at which the state trajectory can leave the polytope. It is in general a difficult and a practically almost-untractable problem to determine which exit facets can be reached from any particular initial state. Once the set of exit facets is determined or over approximated then one obtains from it a branching set of discrete state trajectories. If the state trajectory reaches an exit facet then it is first intersected with the exit facet, which may reduce its dimension. Subsequently the reduced SEP is transformed by the reset map to a new SEP in the state set of the new discrete state. Thus after one cycle of computations one obtains a new SEP at another discrete state which has a strictly smaller or equal dimension than the SEP at the previous discrete state. The cycle of computations then repeats. If for every branch of the finite set of branches of the discrete-state trajectories there exists a finite cycle of computations reducing the SEP to a single vector then the system is coobservable.

References

[1] Pieter Collins and Jan H. van Schuppen. Observability of hybrid systems and turing machines. In *Proceeedings of the 43th IEEE Conference on Decision and Control*, New York, 2004. IEEE Press.

[2] L.C.G.J.M. Habets, P.J. Collins, and J.H. van Schuppen. Reachability and control synthesis for piecewise-affine hybrid systems on simplices. *IEEE Trans. Automatic Control*, 51:938–948, 2006.

An evaluation list for model complexity assessment

George A.K. van Voorn
Biometris, Wageningen University and Research,
Radix, Building 107, Droevendaalsesteeg 1,
6708 PD, Wageningen, the Netherlands
george.vanvoorn@wur.nl

1 Abstract

The complexity of models and databases plays a pivotal part in model-based research. Simple models and databases contain only few processes and variables, and usually have only limited predictive value. More complex models and databases are aimed at more reliable and more accurate predictions. They contain more processes and variables, describing more details of the modelled system. However, in increasing the complexity there is also a larger need for data support, and factors may have been introduced into the model or database of which there is only limited knowledge. In practice, a significant increase in the complexity may actually increase rather than decrease the uncertainty with regard to the model or database output. Apart from that, several practical issues play a role in the complexity of simulation models and databases, for instance, the running time of more complex models easily outgrows computer capabilities, which reduces the possibilities for rigorous testing, verification, sensitivity analysis, bifurcation analysis, validation and calibration of the model, and thus decreases the confidence in the model [1].

We have developed the concept of 'equilibrium' in the complexity of a model or database [2], not to be confused with 'equilibrium' in the meaning of 'steady state'. A model or database is considered to be in equilibrium when it is sufficiently complex for making predictions within a certain accuracy demanded by the application, while the complexity is supported by adequate data of sufficient quality and minimised to fulfill practical conditions. The concept of 'equilibrium' is not unrelated to statistical model selection using, for instance, an automated selection criterion such as the Akaike Information Criterion (AIC [3]), but it is much broader and not fixed to one objective criterion – the above definition is specifically application-oriented, and the complexity is not limited to the number of parameters.

To analyse if models and databases are in 'equilibrium' we have developed an evaluation list. This 'Evaluation list Model Complexity' (EMC) consists of several questions on subjects with regard to model complexity. The list is to be filled out by people involved in the development and/or use of the model or database under evaluation and other stakeholders. Rather than a formal criterion with which a model or database is valued, like the AIC, the list consists of questions that are set up such that they generate 'conflicts'. This set-up proves useful for exposing weak spots. For example, if one question asks about the intended application of the model, then the next question will ask for what applications the model is actually being used currently. If the two answers do not match, a potential issue has been found.

Different versions of the list have been subjected to expert review, tested with cases from the scientific literature, and with cases provided by organisations that make ample use of simulation models and spatial databases for policy evaluations for the Dutch government [4]. In the presentation I will discuss the motivation and concepts behind the list, and some of the obtained results of the application of the list. Furthermore, I discuss some future work on the subject, including further testing of the new version of the evaluation list, the application of the list to a broad ranges of models and databases, the development of guidelines for model improvement based on the findings of applying the list, and the development of a EMC 'light' version that consists of only a couple of questions for quick scanning. For more information see the web page [5].

References

[1] Van Voorn, G.A.K., D.J.J. Walvoort, M. Knotters, P.W. Bogaart, H. Houweling, P.H.M. Janssen (2011). Een beoordelingslijst voor de complexiteit van modellen en bestanden (in Dutch). To appear as WOT paper, Wettelijke Onderzoekstaken Natuur & Milieu, Wageningen University & Research.

[2] Bogaart, P.W., G.A.K. van Voorn, L.M.W. Akkermans (2011). Evenwichtsanalyse modelcomplexiteit – Een verkennende studie (in Dutch). WOT working document 226, Wettelijke Onderzoekstaken Natuur & Milieu, Wageningen University & Research.

[3] Akaike, H. (1974). A new look at the statistical model identification. IEEE Transactions on Automatic Control, AC-19, 716–723.

[4] Van Voorn, G.A.K., D.J.J. Walvoort (2011). Evaluation of an evaluation list for model complexity. To appear as WOT working document, Wettelijke Onderzoekstaken Natuur & Milieu, Wageningen University & Research.

[5] www.biometris.wur.nl/UK/Research/Modeling-+Projects/Model+Complexity

How to obtain a broad band FRF with constant uncertainty?

Egon Geerardyn, Yves Rolain and Johan Schoukens
Department ELEC, Vrije Universiteit Brussel, Pleinlaan 2, 1050 Elsene, Belgium
Email: { egon.geerardyn, yves.rolain, johan.schoukens } @vub.ac.be

1 Introduction

Initial FRF measurements of an unknown system are often a cumbersome endeavor. How does one design a suitable excitation signal when very little is known about the system? Excitation signals with a logarithmic power spectral density (PSD) are often used, since these spread the available signal power evenly over the features of the system[1]. For multisine excitations, such a PSD is to be approximated in the sense that the PSD is discrete and confined to a linear frequency grid. This results in a quasi-logarithmic (quasi-log) multisine [2]. In this paper we present an elegant and simple way to design such a quasi-log multisine. This consists of a well-chosen amplitude spectrum such that it approximates the spectrum of the logarithmic signal closely and suitable choice of the spacing between frequency lines. Such a signal allows for a robust identification of unknown systems.

2 Approach

The studied method relies on periodic multisines as excitation signals. We determine a suited frequency ratio $\alpha_f = \frac{f_{k+1}}{f_k}$ of the (quasi) log frequency grid, which is related to the minimal damping that we expect in the class of systems under test. For a given linear grid spacing, the quasi-log grid will have a reduced frequency resolution at low frequencies compared to the desired signal. We compensate for this effect by concentrating the power carried by the neighboring lines of the logarithmic multisine on the available lines of the (compensated) quasi-log grid. In Figure 2 we show the spectrum of a linear and log grid multisine, together with a quasi-log multisine and the compensation described above.

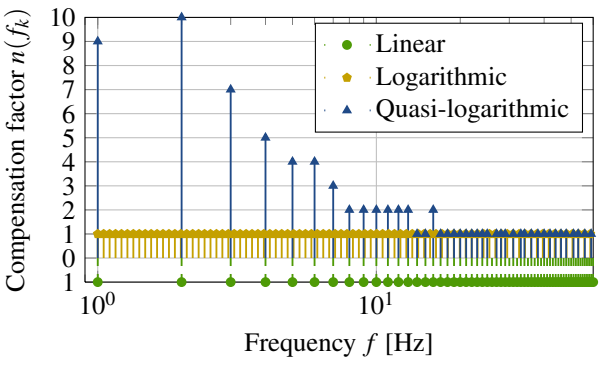

Figure 1: Different frequency grids and compensation factor.

3 Results

Simulations compare the performance of the different excitation signals. Within the band of interest, systems with identical damping but different resonance frequencies were identified for 1000 noisy realizations of the measurements. The variance on the FRFs is displayed in Figure 2.

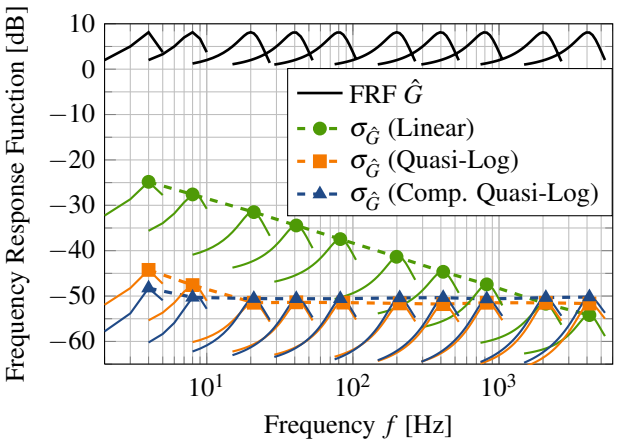

Figure 2: Variance $\sigma_{\hat{G}}$ of the FRF of systems with equal damping but different resonance frequencies, for different excitation signals with identical power.

We see that a linearly spaced multisine results in a high variability: the variances vary widely as a function of the resonance frequency. Both the quasi-log and the compensated quasi-log signal offer independence of the variance on the value of the resonance frequency.

4 Conclusion

The proposed quasi-log multisine allows to improve the FRF measurement and obtain a constant SNR over the frequency. When compared to the classical multisine, the variance at low frequencies is much lower at the cost of a modest increase of the variance at the high frequencies.

References

[1] C. C. Rojas, J. S. Welsh, G. C. Goodwin, and A. Feuer, "Robust optimal experiment design for system identification," *Automatica*, vol. 43, no. 6, pp. 993–1008, 2007.

[2] R. Pintelon and J. Schoukens, *System Identification: a Frequency Domain Approach*. Wiley-IEEE Press, 2001.

Full scale dynamics of biological sulfide oxidation at halo alkaline conditions

Johannes B.M. Klok
Systems and Control group
Wageningen University
P.O. Box 17, 6700 AA Wageningen
The Netherlands
Email: johannes.klok@wur.nl

Karel J. Keesman
Systems and Control group
Wageningen University
P.O. Box 17, 6700 AA Wageningen
The Netherlands
Email: karel.keesman@wur.nl

1 Abstract

Hydrogen sulfide is present in many hydrocarbon gas streams such as synthesis gas. Bulk removal proceeds by physicochemical processes, such as the amine-Clauss process[1]. These processes are associated with some distinct disadvantages as high temperatures and pressure. As microbiological sulfide oxidation proceeds around ambient temperatures and atmospheric pressure, the biological desulfurization process is considered as an alternative to the existing technology[2].

In the biotechnological process for hydrogen sulfide removal under halo alkaline conditions (see figure [3]), a variety of oxidation products can be formed. The process selectivity of the process depends on various substrate levels, as oxygen, sulfide and polysulphide. The formation of elemental sulfur is preferred as thiosulfate and sulfate formation will increase the process costs significantly. In order to scale-up the biological desulfurization process, more insight between the associated biological kinetics and hydraulic phenomena is needed. Hence, analytical models need to be developed to predict full scale gas-lift reactors.

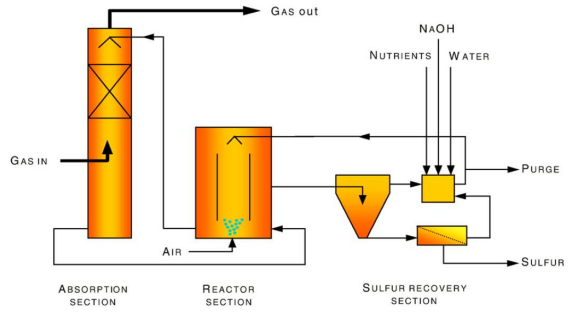

Figure 1: Flow scheme of the biotechnological process for biogas desulfurization.

References

[1] Janssen, A. J. H.; Van Leerdam, R. C.; Van den Bosch, P. L. F.; Van Zessen, E.; Van Heeringen, G.; Buisman, C. J. N. Development of a family of large-scale biotechnological processes to desulfurise industrial gases, 2nd International Congress on Biotechniques for air pollution control, A Corua, Spain, 2007

[2] Janssen, A.J.H.; Ruitenberg, R.; Buisman, C.J.N., Industrial applications of new sulfur biotechnology, Water Sci. Technol. 2001, 44 (8), 85-90

[3] Janssen, A.J.H.; Lens, P.N.L.; Stams, A.J.M.; Plugge, C.M.; Sorokin, D.Y.; Muyzer, G.; Dijkman, H.; Van Zessen, E.; Luimes, P.; Buisman, C.J.N., Application of bacteria involved in the biological sulfur cycle for paper mill effluent purification. Sci. Total Environ. 2009, 407 (4), 1333-1343.

Optimal input design for model discrimination

Karel J. Keesman
Systems and Control Group
Wageningen University
P.O. Box 17, 6700 AA Wageningen
The Netherlands
E-mail: karel.keesman@wur.nl

Eric Walter
Laboratoire des Signaux et Systèmes
CNRS, SUPELEC
Université Paris-Sud
91192 Gif-sur-Yvette, France

Abstract

Before attempting to estimate (identify) the parameters of a given model, one may have to choose the proper model structure among a set of candidates, which may correspond, for instance, to competing scientific hypotheses about the description of some phenomenon (see, e.g., some of the practical examples in [1]). Choosing between model structures is called *model discrimination*. For it to be possible on the basis of experimental data, these models must be *distinguishable*, a property that can be tested by techniques similar to those used to test models for identifiability (although identifiability of two structures is neither necessary nor sufficient for their distinguishability), see [2]. In practice, of course, the ability to discriminate distinguishable model structures depends of the informational content of the data collected. This is why optimal experiment design for model discrimination has received some attention in the statistical literature.

For optimal design to be possible, some performance index is needed. *T-optimal design* [3] aims at maximizing some measure of the lack of fit between the output of some model assumed to be true and that of an alternative structure. When experiment design boils down to input design for a dynamic state-space model, it can be seen as the search for an optimal control law for a specific cost function. Yet, surprisingly little seems to have been done to connect the fields of optimal control and experiment design for model discrimination. This presentation is a contribution to filling this gap.

Let two competitive model structures be defined by the following state and output equations

$$\begin{aligned} \dot{x_1}(t) &= f_1(x_1(t), \vartheta_1) + b_1 u(t) \\ y_1(t) &= g_1(x_1(t), \vartheta_1) \end{aligned} \quad (1)$$

and

$$\begin{aligned} \dot{x_2}(t) &= f_2(x_2(t), \vartheta_2) + b_2 u(t) \\ y_2(t) &= g_2(x_2(t), \vartheta_2) \end{aligned} \quad (2)$$

with $x_1(t)$ and $x_2(t)$ state vectors of appropriate dimensions, ϑ_1, ϑ_2 parameter vectors, $u(t)$ the joint control input vector, and $f_1(\cdot)$, $f_2(\cdot)$ non-linear vector functions. For the purpose of introducing the idea of optimal input design for model discrimination using analytical solutions and based on Pontryagin's maximum principle, we limit ourselves to the case of two non-linear scalar state equations that are affine in their joint input.

The methodology was applied to a fed-batch reactor case study with zero-, first-order and Monod kinetics. For details see [4]. Future work will focus on multi-state, parameterized and not fully observed models requiring numerical solutions to the problem.

References

[1] K.J. Keesman, "System Identification: an Introduction", Springer Verlag, London, 2011.

[2] E. Walter, Y. Lecourtier, and J. Happel, On the structural output distinguishability of parametric models, and its relation with structural identifiability, IEEE Transactions on Automatic Control, AC-29(1):5657, 1984.

[3] A.C. Atkinson and V.V. Fedorov, The design of experiments for discriminating between two rival models, Biometrika, 62:5770, 1975.

[4] K.J. Keesman and E. Walter, Optimal input design for model discrimination, SYSID'12, Brussels, Belgium, 2012.

Lyapunov based design of robust linear-feedback for time-optimal periodic quadcopter motion

J. Gillis[1,3], K. Geebelen[1], J. Sternberg[2], S. Gros[2], M. Diehl[2]
[1]Department of Mechanical Engineering, KU Leuven, Belgium
[2]Optimization in Engineering Center (OPTEC), KU Leuven, Belgium
[3]Doctoral Fellow of the Fund for Scientific Research – Flanders (F.W.O.) in Belgium.
Corresponding author: joris.gillis@mech.kuleuven.be
Celestijnenlaan 300a - bus 2421, 3001 Heverlee

1 Introduction

In recent years, Unmanned Aerial Vehicles (UAV), such as quadcopters, have received increasing attention. In the research world, they are an interesting platform for e.g. testing new control algorithms. An interesting challenge is the robust control of quadcopters. This presentation discusses how the period lyapunov differential equations can be used to obtain approximate robust control for a time-optimal periodic quadcopter flight task. The results are limited to computer simulation for now, but the KU Leuven quadcopter platform is available for demonstration in the future.

2 Quadcopter model

A quadcopter typically has 4 rotors, of which 2 rotate clockwise, and the other 2 rotate anti-clock-wise. The state vector of a quadcopter consists of the 3D postion, velocity, orientation and rotation speeds of the body, and of the spinning speeds of the 4 rotors. Orientation is parametrised by quaternions. This amounts to a total of 17 states. The control inputs to the system are torques applied on the 4 rotos. The aerdoynamic forces and torques are modelled according to [4].

3 Problem formulation

3.1 Flight scenario

In the investigated flight scenario, the quadcopter must meet two waypoints A and B in a periodic time-optimal fashion. The system is free to choose at what time these waypoint shall be met. A hard constraint is present in the form of an impermeable vertical cylinder that prohibits a line-of-sight connection between A and B.

3.2 Robust linear feedback control

To robustify the non-linear system in an approximate fashion, a Lyapunov based approach is taken [1]. In this formalism, the original system is augmented with extra states P that satisfy the following linear Lyapunov differential equations:

$$\dot{P}(t) = A(t).P(t) + P(t).A^T(t) + B(t).B^T(t) \quad P(0) = P(T) \tag{1}$$

where A and B are linearisations of the system dynamics with respect to states and disturbances respectively. P can be interpreted as an uncertainty ellipsoid on the states of the original system. Robustification is obtained by adding a P-weighted term to constraints.

To obtain a linear feedback control, original controls of the system are explicitized as $u = \bar{u} + \bar{K}\left[(x - \bar{x}) + w\right]$, where bar quantities become parameters of the optimal control problem and w models measurement noise.

An invariant appears in the system due to the use of quaternions, requiring modifications to the periodicity constraints [2].

4 Numerical approach

The resulting optimal control problem is treated numerically by a direct approach, using a collocation scheme on fully implicit model equations. A sparsity-exploiting interior point method is used to solve the resulting non-linear problem. The python interface of CasADi [3], is used as a development framework.

References

[1] B. Houska and M. Diehl, "Robust design of linear control laws for constrained nonlinear dynamic systems," Proc. of the 18th IFAC World Congress, 2011.

[2] J. Sternberg, S. Gros, B. Houska, M. Diehl "Approximate Robust Optimal Control of Periodic Systems with Invariants and High-Index Differential Algebraic Systems," submitted to ROCOND 2012 conference

[3] J. Andersson, J. Akesson, and M. Diehl "CasADi A symbolic package for automatic differentiation and optimal control," internal report, https://sourceforge.net/projects/casadi/

[4] P. Bristeau, P. Martin, E. Salaün and N. Petit, "The role of propeller aerodynamics in the model of a quadrotor UAV," Proc. of the European Control Conference, 2009.

Time-optimal robot path tracking with Cartesian acceleration constraint

Frederik Debrouwere[†], Wannes Van Loock[†], Moritz Diehl[‡], Joris De Schutter[†], Jan Swevers[†]
KU Leuven, BE-3001 Heverlee, Belgium
[†]Department of Mechanical Engineering, Division PMA
[‡]Department of Electrical Engineering, Devision SCD
Frederik.Debrouwere@mech.kuleuven.be

1 Introduction

Time-optimal path tracking problems often arise in industrial applications, such as welding, gluing and painting, as well as in applications such as programming by human demonstration, and target interception and capturing. Therefore time-optimal motion for robotic manipulators has significant importance from a productivity and economical point of view. But it is a highly complex task, due to the non-linear, coupled robot dynamics which make the optimization problem extremely non-convex. Therefore this work focuses on planning of robot motions along prescribed geometric paths, called path tracking. In this case the optimization problem can be reformulated as a convex problem [1] for which the global optimum can be found efficiently. This method exploits the fact that motion along a path can be expressed by a single path coordinate $s(t)$. By expressing the optimization problem in the variables $a(s) = \ddot{s}$ and $b(s) = \dot{s}^2$, it is transformed into a convex optimization problem [1].

In some applications it can be useful to also include a Cartesian acceleration constraint on the motion of the end effector of a robotic manipulator. This results in a constraint on the Cartesian end effector acceleration twist [2]. Some possible applications are moving loosely stacked objects on a plate, or moving an open barrel filled with a liquid. In these cases, the acceleration of the end effector, expressed in the end effector frame must be constrained to avoid the objects from falling off or to avoid the liquid from overflowing the barrel.

2 Cartesian acceleration constraint

The Cartesian acceleration twist $\dot{t}_{bs}^{ee}$ (see [2]) of the end effector $\{ee\}$, with respect to the base frame $\{bs\}$, can be represented in three ways (see [3]): *body-fixed*, *inertial* and *hybrid*, depending on the velocity reference point and coordinate reference frame. Hence three different Cartesian end effector acceleration constraints can be formulated.

In the presentation it will be shown that in all the cases the Cartesian acceleration constraint depends linearly on the two optimization variables $a(s)$ and $b(s)$:

$$\underline{\dot{t}}_{bs}^{ee} \leq j_1 a(s) + j_2 b(s) \leq \bar{\dot{t}}_{bs}^{ee}, \tag{1}$$

with $j_1 = J(q)q'$ and $j_2 = J(q)q'' + \dot{J}(q,q')q'$ where J is the geometrical Jacobian [2], q the joint angle vector and $\underline{\dot{t}}_{bs}^{ee}$ and $\bar{\dot{t}}_{bs}^{ee}$ the lower and upper bound on the Cartesian acceleration twist. Hence adding a Cartesian acceleration constraint preserves convexity of the problem.

In the presentation the application of this method is illustrated with numerical and experimental results for a KUKA LWR robot with seven degrees of freedom. For example, figure 1 shows the result of numerical simulation and gives the y component of the body-fixed acceleration twist for a linear path along the y axis of the robot base, in function of the path coordinate s for an unconstrained Cartesian acceleration twist (left) and a constrained Cartesian acceleration twist (right).

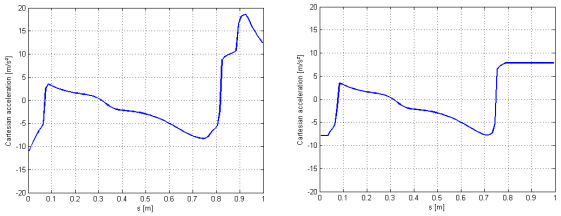

Figure 1: Cartesian acceleration (y component) along the path s

References

[1] D. Verscheure, B. Demeulenaere, J. Swevers, J. De Schutter, and M. Diehl, "Time-optimal path tracking for robots: A convex optimization approach," *Automatic Control, IEEE Transactions on*, vol. 54, pp. 2318 –2327, oct. 2009.

[2] M. W. Spong, *Robot Dynamics and Control*. New York, NY, USA: John Wiley & Sons, Inc., 1st ed., 1989.

[3] H. Bruyninckx and J. D. Schutter, "Symbolic differentiation of the velocity mapping for a serial kinematic chain," *Mechanism and Machine Theory*, vol. 31, no. 2, pp. 135 – 148, 1996.

Acknowledgement This work benefits from K.U.Leuven-BOF PFV/10/002 Center-of-Excellence Optimization in Engineering (OPTEC), the Belgian Programme on Interuniversity Attraction Poles, initiated by the Belgian Federal Science Policy Office (DYSCO), the European research project EMBOCON FP7-ICT-2009-4 248940, project G.0377.09 of the Research Foundation Flanders (FWO Vlaanderen), and K.U.Leuvens Concerted Research Action GOA/10/11.

Comparison of mechanical-hybrid vehicle concepts

Koos van Berkel[1], Sander Rullens[1], Theo Hofman[1], Bas Vroemen[2], Maarten Steinbuch[1]
[1]Department of Mechanical Engineering, Technische Universiteit Eindhoven,
P.O. Box 513, 5600 MB Eindhoven, The Netherlands
[2]Drive Train Innovations, Croy 46, 5653 LD Eindhoven, The Netherlands
E-mail: {k.v.berkel, t.hofman, m.steinbuch}@tue.nl, vroemen@dtinnovations.nl

1 Introduction

Since the early 1980s many mechanical-hybrid vehicle concepts have appeared in the literature with one mutual goal: to decrease fuel consumption. To be competitive in the automotive industry, however, other aspects such as costs and complexity should also be taken into account. Currently, it is not clear which mechanical-hybrid gives the best trade-off between these aspects. Comparison between these concepts is not trivial, because there are many variables, such as (1) topology, (2) components, (3) flywheel size, and (4) energy management strategy (EMS), amongst others. The following research question arises:

Which mechanical-hybrid vehicle gives the best trade-off between fuel saving and costs and complexity?

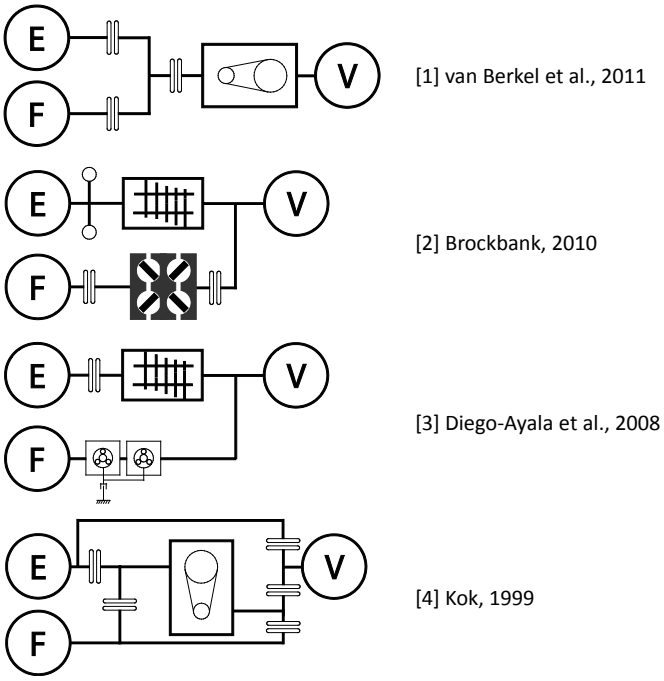

Figure 1: Selection of four mechanical-hybrid concepts that will be compared in fuel saving, costs, and complexity. Each concept consists of a combustion engine (E), flywheel (F), vehicle (V), and a dedicated transmission.

2 Approach

An extensive survey shows that (at least) 17 different mechanical-hybrid vehicle concepts have been studied in the literature. High-level comparison of the topologies shows that only few actually different topologies exist. Based on this observation, a selection of four competitive concepts is made for further investigation, as schematically depicted in Fig. 1. The fuel saving potential of each concept is computed for *one* reference vehicle, but for various flywheel sizes by using an optimal EMS that is obtained with dynamic programming (DP). To avoid excessive computation times, component models are simplified and the grid sizes of the DP algorithm are optimized based on the accuracy of the component models. The cost and complexity are estimated based on the expected mass and the number of mode switches, respectively. Finally, an overview is given that shows the trade-off between fuel saving, cost, and complexity.

3 Acknowledgements

This work is a part of the mecHybrid project which is a common project of Punch Powertrain, DTI, TU/e, CCM, SKF, and Bosch. The project is funded by the Dutch Ministry of Economic Affairs, Provincie Noord-Brabant and SRE.

References

[1] K. van Berkel et al., "Optimal Control of a Mechanical-Hybrid Powertrain", *IEEE Transactions on Vehicular Technology*, 2011.

[2] C. Brockbank., "Development of full-toroidal traction drive in flywheel based mechanical hybrids", In *Proc. of the 6th Int. Conf. on Continuously Variable and Hybrid Transmissions, Maastricht, Netherlands*, 2010.

[3] Diego-Ayala et al., "The mechanical hybrid vehicle: an investigation of a flywheel-based vehicular regenerative energy capture system", *Proc. IMechE, J. of Automobile Eng.*, 222 (11), 2087–2101, 2008.

[4] D. Kok., "Design optimization of a flywheel hybrid vehicle", PhD thesis, Technische Universiteit Eindhoven, Netherlands, 1999.

Towards Integrated Energy and Thermal Management for Parallel Hybrid Electric Vehicle

H.T. Pham, J.T.B.A. Kessels, P.P.J. van den Bosch
Department of Electrical Engineering, Control Systems Group
Eindhoven University of Technology
P.O. Box 513, 5600 MB Eindhoven
The Netherlands
Email: t.pham.hong@tue.nl, J.T.B.A.Kessels@tue.nl, P.P.J.v.d.Bosch@tue.nl

1 Abstract

Energy management (EM) in hybrid electric vehicles (HEVs) typically determines the optimal power split between the internal combustion engine (ICE) and the electric machine. To date, significant work has been done to solve this problem with various approaches. In general, this is divided into two main groups namely, heuristic based and optimal control techniques. The heuristic methods such as rule-based, fuzzy logic and genetic algorithm, are often applied in real-time implementation. However, the main disadvantage of these methods is that they are very sensitive to the tuning of rules and experience of the designers. The optimal control strategies, on the other hand, can offer an optimal solution to the stated EM problem. Besides many off-line optimization methods like dynamic programming (DP) and quadratic programming (QP), etc, a well known and promising on-line energy management is the equivalent consumption minimization strategy (ECMS) [1]. The ECMS strategy tries to minimize a local cost function, called Hamiltonian:

$$H = \dot{m}_{fuel}(\tau_{ice}, N_{ice}) + \lambda P_s$$

The Hamiltonian consists of the actual fuel consumption and a weighted electric consumption, where $\dot{m}_{fuel}[g/s]$ is the fuel mass flow depending on the engine torque $\tau_{ice}[Nm]$ and engine speed $N_{ice}[rpm]$. $P_s[W]$ is the net battery storage power and considered as a decision variable. Note that, the battery state of energy $E_s[J]$ is related to P_s by the equation $\dot{E}_s = P_s$. So far, the challenge was to find an optimal Lagrange costate λ minimizing the Hamiltonian function and satisfying additional constraints such as battery charge sustaining and power limitation of the ICE, the electric machine as well as the battery. The optimal solution can be achieved if some prior knowledge of the drive cycle is known. However, this assumption is not valid in real-time implementation of the energy management strategy.

Moreover, in order to achieve minimal fuel consumption in HEVs, an EM strategy is required to control not only the chemical and mechanical power flow but also the thermal power one (Fig. 1). The thermal buffers such as ICE and battery temperature have significant influence on fuel consumption in HEVs, since the performance of the ICE is very restricted during cold-start period and the battery is defective if its temperature is below/above a predefined level. The current solution with separated control loops for each thermal buffer does not achieve global energy efficiency in all situations. Hence, an integrated energy and thermal management (IETM) in HEVs is neccessary to obtained the complemented power management for HEVs. This integration brings more challenges in solving the optimal control problem due to the appearance of additional costates when other thermal states are taken into account. Few works have been reported about the aiming at integrated energy and thermal management in the more general framework of ECMS, see for example [2] and the references there in. However, online implementation is often not possible due to the difficulty in determining the initial conditions of the costates.
This work firstly presents a method to obtain the value of λ by using only the past information of the drive cycle. By utilizing the result of this method, the EM problem is then extended to the IETM with the integration of other thermal states.

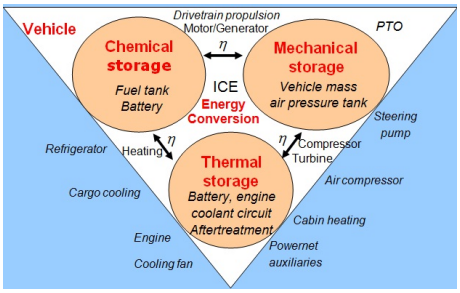

Figure 1: Schematic overview of the main subsystems and their interaction in HEVs

References

[1] L. Guzzella, and A. Sciarretta, "Vehicle Propulsion Systems-Introduction to Modeling and Optimization," Second edition, Berlin, Germany: Springer-Verlag, 2007.

[2] J. Lescot, A. Sciarretta, Y. Chamaillard, and A. Charlet, "On the integration of optimal enery management and thermal management of hybrid electric vehicles," in VPPC2010 IEEE , Sept. 2010.

Cooperative Planning of a class of Heterogeneous Multi-vehicle systems

Jean-François Determe, Emanuele Garone
Control and Systems Analysis Department
Université Libre de Bruxelles
50, av. F.D. Roosevelt, CP 165/55
1050 Brussels
Belgium
jdeterme@ulb.ac.be, egarone@ulb.ac.be,

Roberto Naldi
Department DEIS
Viale Risorgimento 2
University of Bologna
40136 Bologna
Italy
roberto.naldi@unibo.it

1 Introduction

This work addresses a mission planning problem for a scenario in which two autonomous vehicles with complementary characteristics have to cooperate in order to perform a desired task in an optimal way. In particular, inspired by real-world search-and rescue operations, we concentrate on a very simple system of heterogeneous vehicles, arising from the combination of (i) a slow autonomous surface carrier (typically a ship), with long range operational capabilities, and (ii) a faster vehicle (typically a helicopter, an UAV or an offshore vehicle) with a limited operative range. The carrier is able to transport the faster vehicle, as well as to deploy, recover, and service it.

In this work, we focus on a particular Travelling Salesman Problem (TSP) representing a generalization of the one proposed in [1] and that will be hereafter denoted as Generalized Carrier-Vehicle Travelling Salesman Problem (GCV-TSP). Informally we may state this problem as the one of determining the minimum-time trajectory allowing the faster vehicle to visit a given set of points and then to come back, along with the carrier one, to the initial position.

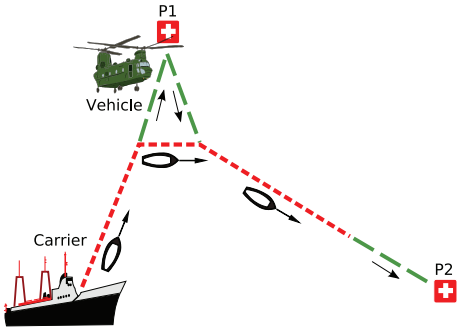

Figure 1: The *carrier-vehicle* system.

2 Methodology

To solve the GCV-TSP problem is quite a challenging task that involves several different decision variables belonging both to the continuous and integer worlds. More specifically it is necessary to determine

(a.) the **order of visit** of the points

(b.) the **number of take offs** and the **number of points** that have to be visited for each take-off

(c.) the continuous **trajectories** the two vehicles have to follow

that minimize the mission completion time. The resulting problem, having the classical Euclidean TSP as a particular case, is clearly at least an NP-Hard problem and thus, up to the actual knowledge, it cannot be solved in polynomial time. As a consequence, for practical applications, efficient polynomial-in-time heuristics have to be developed.

Here we propose a heuristic for the given problem based on a bottom-up approach. Namely, we will :

(1) **solve** the problem of **determining the continuous trajectories** for the two vehicles *(c.)* **assuming that** the values of the discrete variables associated with the **order** of the points *(a.)* and the **number** of points to visit for each take-off *(b.)* **are known**;

(2) **develop heuristics** to deal with the problem of **determining** the variables *(b.)* **assuming** that only the **order of visit** *(c.)* is given.

(3) Finally, **dropping the last assumption,** we will **develop a heuristic** for the determination of the order of visit of the n points.

To highlight the practical effectiveness of the proposed heuristic, the results of a significative numerical analysis will be shown and discussed.

References

[1] E. Garone, R. Naldi and E. Casavola, "A Traveling Salesman Problem for a Class of Carrier-Vehicle System", *AIAA Journal of Guidance, Control, and Dynamics*, Volume 34, No. 4, pp. 1272-1276, 2011.

Optimal Design of Reduced-Order LPV Controllers

Gijs Hilhorst, Goele Pipeleers, Jan Swevers
KU Leuven, Department of Mechanical Engineering, Division PMA
Celestijnenlaan 300b, 3001 Heverlee, Belgium
Email: gijs.hilhorst@mech.kuleuven.be

1 Introduction

The analysis and control of linear systems with varying parameters, so-called linear parameter-varying (LPV) systems, have become major research areas since the nineties. LPV systems arise naturally when modeling mechatronic systems such as wafer stages, pick-and-place robots, micro electromechanical systems and active vision systems. To meet the tightening performance and accuracy demands from industry, control design methodologies that account for the varying parameters as well as uncertainty of the system dynamics are becoming indispensable. Especially for high-order plants, design methods for reduced-order controllers are desired, due to their low implementation cost and high reliability.

Lyapunov based methods proved to be succesfull for setting up analysis and synthesis conditions for robust output-feedback control of linear time-invariant (LTI) systems [6, 2]. A given LTI system is stabilized while optimizing an $\mathscr{H}_2$ and/or $\mathscr{H}_\infty$ norm. However, this generally invokes bilinear matrix inequalities (BMIs) which, contrary to linear matrix inequalities (LMIs), are non-convex and hard to solve. Provided that the controller to be designed is of full order, a nonlinear change of variables exists that transforms the BMI problem into an LMI problem [5]. In case of reduced-order controller design a different characterization applies. One of the possibilities is to rewrite the BMI problem as a problem involving LMIs and a rank constraint. Unfortunately, the latter problem is NP-hard [4], due to non-convexity of the rank constraint.

2 Proposed Approach

Regarding full-order LPV control, several extensions exist. In [3], a full-order LPV controller design for discrete-time systems of the form

$$\begin{aligned} x(k+1) &= A(\alpha)x(k)+B_w(\alpha)w(k)+B_u(\alpha)u(k), \\ z(k) &= C_z(\alpha)x(k)+D_{zw}(\alpha)w(k)+D_{zu}(\alpha)u(k), \\ y(k) &= C_y(\alpha)x(k)+D_{yw}(\alpha)w(k) \end{aligned} \tag{1}$$

is proposed. Here k denotes discrete-time, and x, w, u, z, y denote the state, exogenous input, control input, exogenous output and measured output respectively. The system (1) is assumed to have a homogeneous polynomial parameter dependency on the scheduling parameter α that varies within a multi-simplex. Bounds on the rate of variation of α can be defined and taken into account. A polytopic uncertainty domain can then be constructed, of which the vertices are used to derive a finite set of sufficient LMI conditions for full-order LPV controller synthesis.

Extensions of the method from [3] to the case of reduced-order controllers are desired. However, a method to simplify the BMI conditions for reduced-order LPV controller synthesis is necessary. In recent work [1], a set of sufficient LMI conditions is derived for the existence of reduced-order robust controllers for continuous-time uncertain linear systems. This is done using a two-step procedure. First a parameter-dependent state-feedback is determined, which is then used to synthesize the robust output-feedback controller. The introduction of some conservatism seems unavoidable to obtain a convex optimization problem for such an intrinsically hard problem. Inspired by the method used in [1], we will investigate the possibilities of extending the results from [3]. Our choice for discrete-time systems stems from the fact that system identification and implementation is done in a digital way nowadays.

Acknowledgement This work benefits from K.U.Leuven-BOF PFV/10/002 Center-of-Excellence Optimization in Engineering (OPTEC), the Belgian Programme on Interuniversity Attraction Poles, initiated by the Belgian Federal Science Policy Office (DYSCO), project G.0712.11 of the Research Foundation - Flanders, and K.U.Leuven's Concerted Research Action GOA/10/11. Goele Pipeleers is Postdoctoral Fellow of the Research Foundation - Flanders.

References

[1] C.M. Agulhari, R.C.L.F. Oliveira, and P.L.D. Peres. LMI relaxations for reduced-order robust $\mathscr{H}_\infty$ control of continuous-time uncertain linear systems (preprint). 2011.

[2] S. Boyd, L. El Ghaoui, E. Feron, and V. Balakrishnan. *Linear Matrix Inequalities in System and Control Theory*. 1994.

[3] J. De Caigny, J.F. Camino, R.C.L.F. Oliveira, P.L.D. Peres, and J. Swevers. Gain-scheduled dynamic output feedback for discrete-time LPV systems. *International Journal of Robust and Nonlinear Control*, 2011.

[4] M. Fu and Z. Luo. Computational complexity of a problem arising in fixed order output feedback design. 1997.

[5] C.W. Scherer, P. Gahinet, and M. Chilali. Multiobjective output-feedback control via LMI optimization. 1997.

[6] C.W. Scherer and S. Weiland. *Linear Matrix Inequalities in Control*. 2005.

Transfer-Function-Data-based computation of closed-loop poles for lightly damped MIMO systems

Rob Hoogendijk*, René van de Molengraft and Maarten Steinbuch
Department of Mechanical Engineering, Eindhoven University of Technology
P.O. Box 513, 5600 MB Eindhoven, The Netherlands
Email: *r.hoogendijk@tue.nl

1 Introduction

The trend in the design of high precision motion systems is towards lightweight systems to enable high accelerations. At the same time, this causes the systems to become less stiff, causing flexible dynamics to shift to lower frequencies, which poses a challenge for the control design. The flexible dynamics of these systems tend to be lightly damped due to the materials that are used.

Since for these systems frequency response data (FRD) can be obtained with high accuracy and at low cost, controllers are conventionally designed in a data-based way using decoupling in combination with manual loopshaping. However, the analysis methods for these techniques are limited.

This research aims at the extension of data-based analysis methods using so-called *Transfer Function Data* (TFD) derived from FRD. Here, it is shown that TFD can be used to compute the closed-loop poles of the system in a data-based way.

2 Closed-loop poles from TFD

FRD contains the response of a system $H(s)$ at frequencies ω_n, i.e., $H(j\omega_n)$. Thus, FRD only gives information on the system for points s that lie on the imaginary axis. Therefore, the concept TFD is introduced here. TFD contains the response $H(s_i)$ of the system at a grid of complex frequencies $s_i = \sigma_i + j\omega_i$, which can lie anywhere in the complex plane. For stable, strictly proper systems, TFD in the right half plane can be computed from FRD by Cauchy integral [1]

$$H(s_i) = \frac{1}{2\pi}\int_{-\infty}^{\infty} \frac{H(j\omega)}{(j\omega - s_i)} d\omega, \quad s_i \in \mathbb{C}^+. \tag{1}$$

For lightly damped systems, TFD in the left half plane can be obtained from

$$H(s) = H(-s), \tag{2}$$

due to the symmetry of the poles with respect to the imaginary axis. It can be shown that for MIMO systems, this can be performed for each entry of the MIMO transfer function matrix separately. Using this method a sampled, data-based representation of the MIMO transfer function $H(s_i)$ can be obtained.

The closed-loop poles p_{cl} of a MIMO system $H(s)$ with feedback controller $C(s)$ can be computed using TFD from

$$\mathscr{D}(s_i) = det(I + H(s_i)C(s_i)) = 0, \tag{3}$$

A numerically reliable way to determine which points s_i satisfy (3), is to look for points s_i where the real and imaginary part of this determinant cross zero, see Fig. 1. The locations where these curves intersect are the pole-locations. As a bonus, the zero-crossing method also gives the open-loop poles of the system. The open-loop and closed-loop poles are distinguished easily since $\mathscr{D}(s_i) = \infty$ at the open-loop poles.

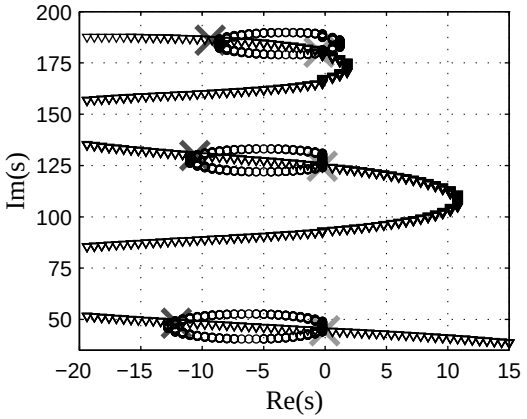

Figure 1: Data-based computation of the closed-loop poles using TFD. The points where the zero crossings of $\Re(\mathscr{D}(s_i))$ (▽) and $\Im(\mathscr{D}(s_i))$ (○) intersect are the pole locations. For comparison, the system poles (grey ×) and closed loop poles (black ×) obtained from a model are plotted as well.

References

[1] R. Hoogendijk, A.J. den Hamer, G.Z. Angelis, M.J.G. van de Molengraft and M. Steinbuch, Frequency response data based optimal control using the data based symmetric root locus, Proc. IEEE CCA 2010 p. 257-262.

Model-based control design for inferential and over-actuated control of lightweight motion systems

Frank Boeren, Robbert van Herpen, Tom Oomen, Okko Bosgra
Eindhoven University of Technology
f.a.j.boeren@student.tue.nl

Marc van de Wal
ASML Research

Introduction

Next-generation high-precision positioning systems are designed to be lightweight, in order to enable an increase of the speed of movement. As lightweight systems tend to have complex dynamical system behavior, model-based control design is essential to achieve high-performance. Model-based control typically requires weighting to specify the design objectives, e.g., disturbance attenuation and reference tracking. Hence, for successful control design, the design of weighting functions is of vital importance.

Weighting function design for lightweight systems

The main control challenge for lightweight systems is the presence of flexible dynamical behavior at frequencies relevant for control. In fact, to achieve high-performance, a controller should be designed that not only delivers accurate positioning at the sensor locations, but also prevents deformation of the structure. This is known as inferential control.

Conventional weighting function design for motion systems [1] poses magnitude bounds on the closed-loop transfer function matrices in order to specify design objectives, see weightings W_1 and W_2 in Fig.1. However, for lightweight motion systems with flexible phenomena close to the crossover region, i.e., $\sigma_i(L) \approx 1$, the lack of weighting in the mid-frequency range allows lightly damped closed-loop poles, hampering inferential performance. Therefore, weighting should be specified for the dominant gains of the system in all frequency ranges. Fig. 1 shows the proposed design W_{MF} in the mid-frequency range.

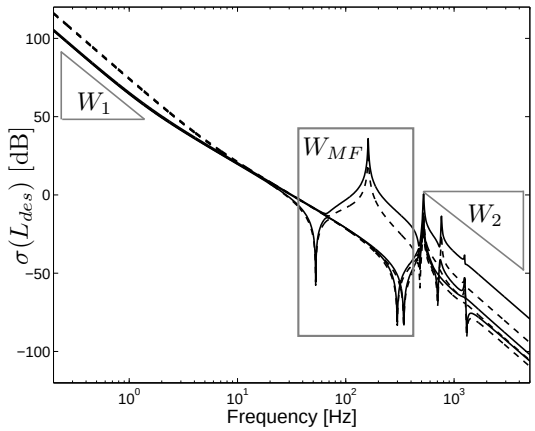

Figure 1: Singular values of the open loop L with (black) and without (black dashed) mid-frequency weighting

In this research, conventional design specifications expressed in the weightings W_1 and W_2 are extended by shaping the dominant gains of the system in the mid-frequency range. The dominant gains in a multivariable system can be shaped if the weighting functions explicitly address the input and output directionality of the system in control-relevant frequency ranges. This is critical, since the directionality associated with deformations of the system is different from the directionality of rigid-body dynamics. The resulting frequency-dependent decoupling enables explicit shaping of the dominant gains. After decoupling the system with respect to the dominant gains, a lead filter is used to create phase lead around the lightly damped flexible mode (Fig. 1).

Experimental results

The response of a multivariable lightweight motion system to a step excitation in a single motion degree-of-freedom as depicted in Fig 2 shows that the extended weighting function results in additional damping of the closed-loop poles.

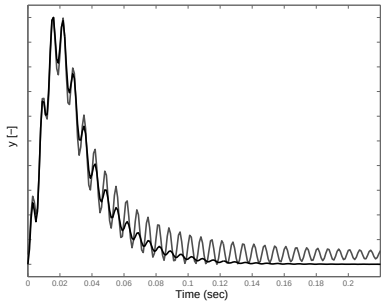

Figure 2: Response at the output y for a step in the input disturbance: conventional (gray) and extended (black)

This result shows that exploiting directionality of a multivariable plant is the key to high-performance inferential control for lightweight motion systems.

Outlook

Although the proposed weighting function design enhances high-performance model-based control, it can not effectively deal with transmission zeros. This typically results in degrading inferential performance. First promising results show that extending the number of actuators and sensors in conjunction with the proposed weighting function design enhances inferential performance.

References

[1] M. van de Wal, G. van Baars, F. Sperling, and O. H. Bosgra, Multivariable H_∞/μ feedback control design for high-precision wafer stage motion. *Contr. Eng. Pract.*, 10(7):735755, 2002.

Teleoperated endoscopic injection

Jérôme Janssens and Michel Kinnaert
Université Libre de Bruxelles (ULB)
50, Av. F.D. Roosevelt - CP 165/55. B-1050 Bruxelles. Belgium
Email : jerome.janssens@ulb.ac.be, michel.kinnaert@ulb.ac.be

1 Introduction

Endoluminal endoscopy consists of the insertion of an endoscope via a natural orifice of the human body. This technique allows the diagnostic as well as the treatment of several gastric diseases (e.g. gastroesophageal reflux disease, treatment of obesity, gastric tumors, ... [1]).

For some of these surgical interventions, such as gastric mucosa tumor ablation (figure 1), the gastroenterologist has first to inject saline water into the gastric wall. This injection

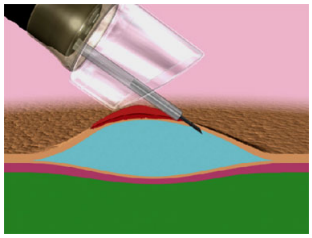

Figure 1: Saline injection beneath a gastric tumor

must be done precisely between the mucosa and the muscular layers, without completely piercing the gastric wall.
To do so, the equipment used is a needle carried by a catheter, itself introduced in the endoscope. The physician has to rely only on his feelings when manipulating the catheter to complete this task. Unfortunately, the flexibility of the catheter and the friction from the endoscope heavily deteriorate the force feeling of the operator.

The goal of this project is to develop a motorized endoscope which allows to perform a teleoperated needle insertion and injection, and consequently to be able to get rid of the aforementioned drawbacks.

2 The project

A first simplified master-slave tests bench (without neither catheter, neither endoscope) was built. Some classical teleoperation control scheme were then implemented allowing to compare their performance. An algorithm detecting the puncture of a layer when a needle is piercing a multi-layers soft tissue was developed. Both the force feedback and the algorithm were tested and validated during needle insertion in pig stomach.

A second tests bench, including both an endoscope and a catheter, is now under development. The master motor is directly driving a pulley itself driving a belt. This direct driving aims to keep the device compact while minimizing both inertia and friction effects. The use of a belt reminds the movement made when inserting the catheter in the endoscope.
A catheter driving system, set on the endoscope head, provides the position measurement. The interaction force between the needle and the tissue is measured by an in-situ sensor. A second position sensor will be used at the end of the catheter. Catheter position measurement on both proximal and distal sides of the endoscope will provide more information in order to characterize the flexibility and the backlash of the catheter and thereby to study their influence on the global system stability and performance.

3 Future developments

When the second tests bench will be finished, the influence of the catheter flexibility and backlash will be studied. The transition detection algorithm will then be adapted to take into account this flexibility and the backlash. Finally, a complete stability analysis of the global system will be performed.

Acknowledgement

This research project is funded by the Walloon Region.

References

[1] N. Tsesmeli, D. Coumaros, “The future of bariatrics: endoscopy, endoluminal surgery, and natural orifice transluminal endoscopic surgery”, Endoscopy 2010, 42, pp 155 - 162.

[2] L. Barbé, “Téléopération avec retour defforts pour les interventions percutanées”, PhD thesis, Université Louis Pasteur, 2007.

[3] T. Delwiche, “Contribution to the design of control laws for bilateral teleoperation with a view to applications in minimally invasive surgery”, PhD thesis, ULB, 2009.

World Modeling in Robotics

Jos Elfring, Sjoerd van den Dries, René van de Molengraft, Maarten Steinbuch
Eindhoven University of Technology
P.O. Box 513, 5600 MB, Eindhoven, The Netherlands
Email: J.Elfring@tue.nl

1 Introduction

Domestic robots are typically confronted with a complex, dynamically changing and unstructured environment. In such environments, robots must be able to perform a wide variety of tasks, *e.g.*, safe navigation, object manipulation, including many different objects. An important prerequisite for successfully accomplishing these tasks is the availability of an accurate description of the environment the robot is operating in. In this work, such a description of the environment will be referred to as world model. A world model usually contains 3D-positions of uniquely labeled objects. In dynamic scenarios, dynamic object attributes such as velocities are included as well [1] and depending on the tasks any other object attribute can be added. The robot perceives the world using a perceptual system possibly containing multiple sensors such as cameras and laser scanners. The perceptual system generates measurements, *i.e.*, time-stamped features, that can be anything from colored blobs in a camera image [2] to labeled object positions [1]. These measurements are the input for the algorithm that constructs the world model.

2 Requirements

The world modeling algorithm should link measurements from the perceptual system to semantically meaningful labeled objects in the world model. Creating and maintaining this link is called *anchoring* [3]. Updating the object attributes based on measurements is a non-trivial task due to the uncertainties the robot will be confronted with and measurement noise in the input data. Therefore, a proper *data association* algorithm is required. In addition, *model-based object tracking* can be used (i) for estimating attributes that can not be measured directly and (ii) to do predictions. Finally, the algorithm should allow *real-time execution* on a robot with limited computational resources.

3 Probabilistic Multiple Hypothesis Anchoring

A probabilistic multiple hypothesis anchoring (PMHA) algorithm was developed meeting these requirements. It is inspired on anchoring as described in [3] with an explicit data association algorithm based on multiple hypothesis tracking (MHT) [4]. The MHT algorithm solves the data association problem by considering all possible measurement to object associations. Each set of associations is called a hypothesis and gets a probability of being correct. Unlikely hypotheses are pruned in order to allow real-time execution. The main advantage of the MHT is the ability to correct previous decisions based on new measurements. By incorporating a multiple model tracker [5], any kind of prior knowledge can be exploited, *e.g.*, "John arrives at work at 8 am" or "humans approximately move according to a constant velocity motion model".

4 Results

The PMHA algorithm is implemented on our AMIGO robot and experiments have shown:

- Successful anchoring of measurements to objects.
- Probabilistic data association using MHT. As a result, new measurements can be used to correct previous decisions.
- Multiple model tracking exploiting any kind of prior knowledge that is available.
- Real-time execution at tens of Hertz in scenarios with many objects.

The research leading to these results has received funding from the European Union Seventh Framework Program FP7/2007-2013 under grant agreement n^{O}248942 RoboEarth.

References

[1] J. Silva, N. Lau, A.J. Neves, J. Rodrigues, J.L. Azevedo, "World modeling on an msl robotic soccer team," Mechatronics 21 (2), 411–422, 2011

[2] J. Elfring, M.J.G. van de Molengraft, R.J.M. Janssen, M. Steinbuch, "Two level world modeling for cooperating robots using a multiple hypotheses filter," 2011 IEEE Int. Conf. on Robotics and Automation, 815–820, 2011

[3] S. Coradeschi, A. Saffiotti, "An introduction to the anchoring problem," Robotics and Autonomous Systems 43 (2–3), 85–96, 2003

[4] D.B. Reid, "An algorithm for tracking multiple targets," IEEE Trans. on Automatic Control AC-24 (6), 843–854, 1979

[5] X.R. Li, V.P. Jilkov, "A survey of maneuvering target tracking. part v: Multiple-model methods," IEEE Trans. on Aerospace and Electronic Systems 41 (4), 1255–1274, 2005

Dynamic metabolic flux analysis using dynamic optimization techniques

Dominique Vercammen, Eva Van Derlinden, Jan Van Impe
BioTeC - Chemical and Biochemical Process Technology and Control
Katholieke Universiteit Leuven
Willem de Croylaan 46, 3001 Leuven, Belgium
Email: {dominique.vercammen,eva.vanderlinden,jan.vanimpe}@cit.kuleuven.be

1 Introduction

In the area of predictive microbiology, most models focus on simplicity and general applicability, and can be classified as black box models with the main emphasis on the description of the macroscopic (population level) microbial behavior as a response to the environment. Their validity to describe pure cultures in simple, liquid media under moderate environmental conditions is widely illustrated and accepted. However, experiments have shown that extrapolation to more complex (realistic) systems is not allowed as such. In general, the applicability and reliability of existing models under more realistic conditions can definitely be improved by unraveling the underlying mechanisms and incorporating intracellular (microscopic) information [1], effectively taking a look inside the black box. Following a systems biology approach, the link between the intracellular fluxes and the extracellular measurements can be established by techniques of metabolic flux analysis.

2 Methodology

A metabolic network is a graphical representation of (a subset of) all metabolic reactions occuring inside a cell. All information contained in this network is equally well described by the stoichiometric matrix. This matrix forms the basis for the mass balances of the concentrations of the intracellular metabolites. The number of metabolites and reactions is, even for a medium-scale network, quite extensive, so the intracellular mass balances turn into a rather large system of differential equations. By assuming a pseudo-steady state at the microscopic level (with respect to the macroscopic level), the mass balances reduce into an underdetermined homogeneous linear system. This system can be directly integrated into the macroscopic model structure, yielding a system of differential equations with time-varying controls, the so-called free fluxes. By parameterizing the free fluxes and collecting measurement data for the states (the macroscopic variables), a dynamic parameter estimation arises. To get a dynamic view of the fluxes, it is sufficient to parameterize the free fluxes as a function of time. By parameterizing the free fluxes as a function of the macroscopic concentrations and conditions (T,pH,...), it is possible to build a dynamic predictive model.

3 Methods

The dynamic parameter estimation problem is solved by discretizing the differential states via a multiple shooting scheme. The resulting nonlinear program is solved with IPOPT, an interior point method for NLP's. First- and second-order information is obtained by solving the first- and second-order sensitivity equations together with the original dynamic model.

4 Results

The methodology described above is exemplified for a small-scale metabolic network. The free fluxes are parameterized as a function of time by splines of varying order. These parameters are estimated based on simulated data with different levels of measurement noise. Confidence intervals for the estimated parameters, and thus for the free fluxes, are calculated.

5 Conclusion

The dynamic metabolic flux analysis methodology based on dynamic optimization is successful in estimating dynamic metabolic fluxes. In future work, this methodology will be applied to estimate fluxes during a lag-phase which is induced by a sudden temperature shift. By parameterizing the free fluxes as a function of macroscopic concentrations and temperature, a dynamic model for this specific transient behaviour will be developed.

Acknowledgements

Work supported in part by Projects OT/09/025/TBA, OPTEC (Center-of-Excellence Optimization in Engineering) PFV/10/002 and SCORES4CHEM KP/09/005 of the Katholieke Universiteit Leuven, and by the Belgian Program on Interuniversity Poles of Attraction, initiated by the Belgian Federal Science Policy Office. E. Van Derlinden is supported by grant PDKM/10/122 of the KULeuven research fund. J.F. Van Impe holds the chair Safety Engineering sponsored by the Belgian chemistry and life sciences federation essenscia. D. Vercammen is supported by a doctoral grant of the Agency for Innovation through Science and Technology (IWT).

References

[1] **S. Brul et al.**: Microbial systems biology: new frontiers open to predictive microbiology. Int J Food Microbiol., **128(1)**, 16-21 (2008)

Robustness analysis of apoptosis signalling

Monica Schliemann
Montefiore Institute
Université de Liège
4000 Liège
Belgium
Email: Monica.Schliemann@ulg.ac.be

Eric Bullinger
Montefiore Institute
Université de Liège
4000 Liège
Belgium
Email: E.Bullinger@ulg.ac.be

1 Introduction

Models of intracellular biochemical reaction networks are difficult to parameterise due to the low number of quantitative time series experimental values. Therefore, model validation or invalidation plays an important role, as it allows to check qualitatively whether a model structure is suited or not to reproduce qualitatively the experimental findings.

Apoptosis is an important form of programmed cell death for removing damaged or unwanted cells in organisms. Thus, the regulation of apoptosis is very important as its misregulation can induce severe pathologies: on the one hand, apoptosis is less present e.g. in cancer or viral infections, while on the other, cell death is enhanced in neurodegenerative diseases or AIDS.

2 Apoptosis model

In this presentation, we analyse the robustness of an experimentally validated polynomial differential equation model of TNF-induced pro-and anti-apoptotic signalling [1]. The model contains of 47 species, 89 complexes and 106 kinetic parameters (70 irreversible and 18 reversible reactions).

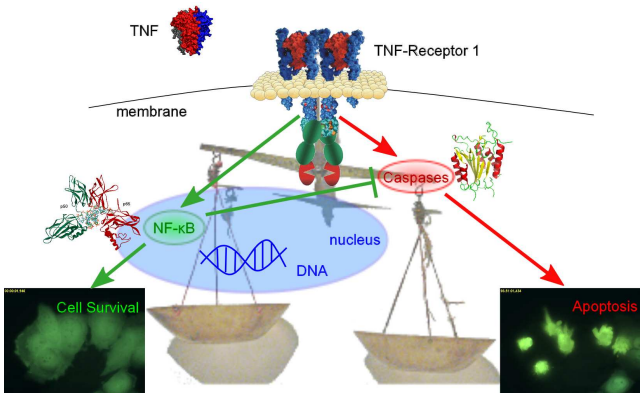

Figure 1: Sketch of TNF-induced Pro- and Anti-Apoptotic Signalling. The final decision of a cell to start the cell death program or not is taken by a carefully regulated network intertwined pro-apoptotic (via caspases) and anti-apoptotic (via NF-κB) pathways.

3 Robustness analysis

We show that the model's bistability is robust to large parameter variations. Only two parameters are shown to be fragile, in particular when changed simultaneously.

Many biological experiments quantify average concentrations or the percentage of viable cells, while other methods such as microscopy-based experiments observe single cells. The integration of single cell and cell population behaviour of TNF-induced pro- and anti-apoptotic signalling has been achieved via a cell ensemble model, whose robustness is also analysed here. We show that within the cell population there are cells with not only quantitative differences, but also qualitative ones. In particular, all cells are not bistable. The degree of robustness applicable for the nominal cell is expanded to combine mono- and bistable models. This measure, applied solely to the two-dimensional subspace of fragile parameters, is shown to correlate well with the time of death. While robustness of bistability can serve for model validation of the nominal cell model, it cannot for the model of the cell population.

4 Conclusion

The nominal apoptosis model [1] is robust with respect to bistability. Of the high-dimensional parameter space, two relatively fragile directions could be uncovered. Therefore, the model seems valid from a robustness point of view.

The robustness analysis of the model of apoptosis simultaneously describing single cells and cell population behaviour highlights the complexity of analysing robustness of cell population models, as within a cell population there might exist subpopulations with different qualitative properties (number of steady states, existence of limit cycles, etc.). By generalising the degree of robustness, we obtained a measure that correlates well with the time of death.

References

[1] M. Schliemann, E. Bullinger, S. Borchers, F. Allgöwer, R. Findeisen, and P. Scheurich. Heterogeneity reduces sensitivity of cell death for TNF-stimuli. *BMC Syst Biol*, 5(1):204, Dec 2011.

Estimating the prediction uncertainty of biological models

Simon van Mourik
Wageningen University and Research center
simon.vanmourik@wur.nl

Hans Stigter
Wageningen University and Research center
hans.stigter@wur.nl

Jaap Molenaar
Wageningen University and Research center
jaap.molenaar@wur.nl

1 Abstract

Models of biological systems are characterized by the unavailability of many physical parameters, despite the continuing development of experimental techniques [1]. Parameter estimation via time series data has proven to be a valuable alternative. However, measurement inaccuracies, data scarcity and parameter interdependencies create a high uncertainty in parameter values and thus also in model predictions [2, 3]. Estimation of the size of the region in which the true parameter values may be located (the confidence region), can help to determine the severity of the prediction uncertainty. Approximation of the confidence region can be done by random sampling, which is relatively accurate but computationally exhaustive [4]. The alternative is a local sensitivity analysis, which is fast and easily implementable [5]. However, this approximation is based on a linearization, which can cause considerable and unpredictable errors for nonlinear models.

We propose a method to sample the prediction region by adapting an existing global parameter search method. The sampled parameter values are each inserted into the model, and a prediction simulation is carried out. The result is an area covered with possible model predictions (the prediction region), indicating the size of the uncertainty.

Another trait of biological systems is extreme complexity, unavoidably resulting in model errors. We show how structural model errors can be modeled and approximated, based on discrepancies between model fit and data.

Altogether, our method follows a simple algorithm, has modest computational demands, and can be naturally integrated with optimal experiment design analysis. Some favorable properties of the algorithm could be demonstrated, suggesting a general reliability for a broad class of continuous-time models.

Figure 1 shows schematically the main idea. The theoretical parameter confidence region corresponding to the data set is sampled, whereafter the sampled parameter values are inserted into the model. The model simulations then cover an area of possible model predictions (the prediction region), indicating the size of the uncertainty.

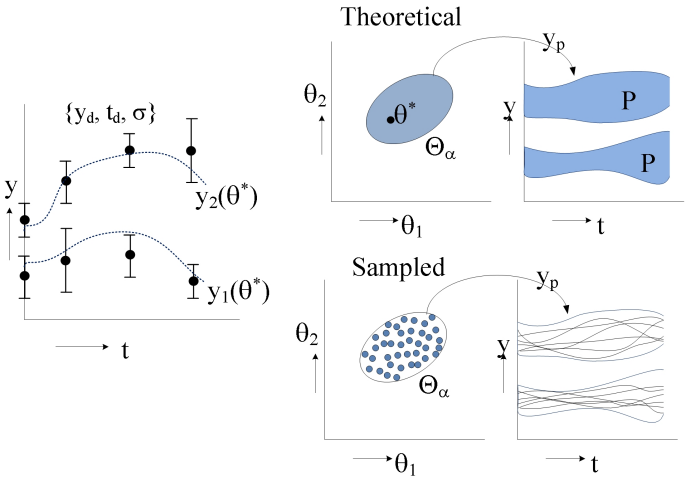

Figure 1: Schematic representation of parameter space and prediction region for two parameters and two outputs. Left: data set with measurement noise. Top right: theoretical confidence region and corresponding prediction region. Bottom right: approximation by sampling.

References

[1] S. J. Maerkl and S. R. Quake. A systems approach to measuring the binding energy landscapes of transcription factors. *Science*, 315:233–237, Jan 2007.

[2] D.E. Zak et al. Continuous-time identification of gene expression models. *OMICS*, 7(4):373–386, 2003.

[3] A. Raue, C. Kreutz, T. Maiwald, J. Bachmann, M. Schilling, U. Klingmuller, and J. Timmer. Structural and practical identifiability analysis of partially observed dynamical models by exploiting the profile likelihood. *Bioinformatics*, 25:1923–1929, Aug 2009.

[4] R. N. Gutenkunst, F. P. Casey, J. J. Waterfall, C. R. Myers, and J. P. Sethna. Extracting falsifiable predictions from sloppy models. *Ann. N. Y. Acad. Sci.*, 1115:203–211, Dec 2007.

[5] Janet R. Donaldson and Robert B. Schnabel. Computational experience with confidence regions and confidence intervals for nonlinear least squares. *Technometrics*, 29(1):pp. 67–82, 1987.

Game-Theoretical Approach to Multi-Agent Synchronization

Sofie Haesaert, and Robert Babuska
Delft Center for Systems and Control
Delft University
Mekelweg 2
2628 CD Delft
The Netherlands
Email: s.haesaert@student.tudelft.nl
r.babuska@tudelft.nl

Frank L. Lewis
Automation and Robotics Research Institute
The University of Texas at Arlington
7300 Jack Newell Blvd. S.
Ft. Worth, TX 76118
USA
Email: lewis@uta.edu

1 Introduction

In this paper symmetric Coupled difference Riccati Equations are considered associated with the Linear quadratic discrete-time graphical games. Linear quadratic graphical games represent several kinds of multi-agent problems that involve a communication graph. A synchronization problem, where a set of agents synchronize to the state of the leader, is one such example. Here the communication graph is used to define a tracking error. The setting of this control problem has a lot of similarities with multi-agent systems with global dynamics and individual quadratic performance indices ([1]). Each agent minimizes its own cost function, therefore the game-theoretical Nash equilibriums is a solution. Using the Bellman equations originating from the classical dynamic programming approach, a linear feedback law can be iterated.

This paper generalizes the knowledge from systems and control to solve and analyze the difference graphical games. Sufficient solvability conditions for the coupled Riccati equations are given.

2 The synchronization problem

Consider N agents with states z_i whose interaction is represented by the undirected graph $\mathcal{G}$, with edge weights e_{ij}, and the weighted in-degree d_i. Then the local tracking error is defined as x_i and the dynamics of this local tracking error can be given as the local neighborhood dynamics in Eq.(2.)

$$x_i(k) = \sum_{j\in\mathcal{N}_i} e_{ij}(z_i(k)-z_j(k)) + g_i(z_i(k)-z_0(k)) \quad (1)$$

$$x_i(k+1) = Ax_i(k) + (d_i+g_i)B_iu_i(k) - \sum_{j\in\mathcal{N}_i} e_{ij}B_ju_j(k)) \quad (2)$$

where $x_i(k)\in R^n$ is the state of the agent i, $u_i(k)\in R^{m_i}$ is the control input. g_i is a local gain. Rewriting (2), the global dynamics are

$$x(k+1) = \bar{A}x(k) + ((L+G)\otimes I_n)\bar{B}u(k) \quad (3)$$

with the global state $x^T(k) = \left[x_1^T(k),\ldots,x_N^T(k)\right]$ and global input vector $u^T(k) = \left[u_1^T(k),\ldots,u_N^T(k)\right]$. The Kronecker product, $\otimes$, is used to define $\bar{A} = (I_n\otimes A)$. And the diagonal matrix of local gains g_i is G. $\bar{B}$ is the block diagonal matrix $\bar{B} = \{B_1,\ldots,B_N\}$. L is the laplacian matrix of $\mathcal{G}$. Instead of looking at the error between each agent and the leader, one looks at a combination of tracking errors (1) to define the following distributed cost function for each agent

$$J_i = \sum_{k=0}^{\infty}\left(x_{i,k}^TQ_{ii}x_{i,k} + u_{i,k}^TR_{ii}u_{i,k} + \sum_{j\in\mathcal{N}_i} u_{j,k}^TR_{ij}u_{j,k}\right). \quad (4)$$

Though the performance indices are local and the action are applied locally, the individual actions have consequences for all agents in the graph. Hence the cost-to-go functions of the agents will consist of the states of all agents in the graph.

3 Coupled Riccati equations

The cost-to-go-function $V_i^*(x(k)) = x^T(k)S_ix(k)$ is quadratic due to the structure of the problem, and can be analyzed using symmetric coupled Riccati equations

$$\begin{aligned} S_i &= \bar{Q}_i + \Lambda^TS_i\Lambda \\ &+ \textstyle\sum_{j\in\{\mathcal{N}_i,i\}}\Lambda^TS_j\bar{B}_jR_{jj}^{-1}R_{ij}R_{jj}^{-1}\bar{B}_j^TS_j\Lambda \quad \forall i\in N \end{aligned} \quad (5)$$

Here block diagonal matrices $\bar{B}_j = \left\{0,...,B_j,\ldots,0\right\}$, and $\bar{Q}_i = \{0,\ldots,B_{ii},\ldots,0\}$ are used. If this solution exists then it can be shown that the global system is asymptotically stable, and the agents are in a global Nash equilibrium. The corresponding game values are $J_i^*(x_0) = x_0^TS_ix_0$. This solution can be iterated using the Coupled Difference Riccati Equations

$$\begin{aligned} S_i^{q+1} &= \bar{Q}_i + \Lambda^{q\,T}S_i^q\Lambda^q \\ &+ \textstyle\sum_{j\in\{\mathcal{N}_i,i\}}\Lambda^{q\,T}S_j^q\bar{B}_jR_{jj}^{-1}R_{ij}R_{jj}^{-1}\bar{B}_j^TS_j^q\Lambda^q \quad \forall i\in N \end{aligned} \quad (6)$$

If $\Lambda = \left[I+\sum_{j\in N}\bar{B}_iR_{ii}^{-1}\bar{B}_i^TS_i\right]^{-1}\bar{A}$ exists for all q then S_i^{q+1} can be iterated. The Coupled Riccati equations describe the expected behavior of multi-agent synchronizations, which have wide-spread application possibilities.

References

[1] Basar T., Olsder G.J., "Dynamic Noncooperative Game Theory ",1999.

Neuromorphic reinforcement learning

Julie Dethier, Damien Ernst, and Rodolphe Sepulchre
Systems and Modeling Research Unit, ULg
10 Grande Traverse, B-4000 Liege, Belgium
Emails: [jdethier, dernst, R.Sepulchre]@ulg.ac.be

1 Neuromorphic engineering

Living organisms are able to successfully perform challenging tasks such as perception, classification, association, and control. In hope for similar successes in artificial systems, *neuromorphic engineering* uses neurophysiological models of perception and information processing in biological systems to emulate their functions but also resemble their structure [1]. In this abstract, we focus on the basal ganglia (BG), brain region in control of primitive functions of the nervous system, and specifically on their involvement in action selection and reinforcement learning (RL). We hypothesize that neuromorphic-inspired systems will greatly benefit the RL community.

2 Computational architecture of the basal ganglia

The BG are a group of interconnected subcortical nuclei that participate in cortical- and sub-cortical loops. These loops are topographically organized in relatively discrete channels that loop back, via appropriate thalamic relays, to the same area of cortex (e.g. limbic, associative, sensorimotor) from which they originated [2]. Two essential functions of the BG are action selection and RL; we investigate how theses functions can be morphed and engineeringly exploited.

2.1 Action selection

Parallel processing functional systems that compete for behavioral expression loop through the BG, conveying phasic excitatory signals—"bids" for selection—to the input nuclei [2]. Through comparison of input magnitudes (competing bids), the tonic inhibitory output is withdrawn from "selected" channels—disinhibition via the direct pathway of thalamocortical targets—and maintained or increased on "non-selected" channels—inhibition via the indirect pathways to suppress unwanted actions [3]. This action selection model can be exploited in Cognitive Pattern Generators, by analogy to the motor system's Central Pattern Generators, rhythm generators that operate to organize cognition [4].

Integration of these rhythm generators in Reservoir Computing (RC) models could generate powerful neuromorphic processing systems. RC, emulating information processing in the cortex, relies on a fully connected one-hidden-layer recurrent neural network, the reservoir, with dynamics at the "edge of chaos" and with only trainable weights in the connections from hidden nodes to the multiple outputs [5]. This simplicity of training comes with challenges: creating a rich enough reservoir, particularly if many dynamics systems employ its different outputs with different sets of weights [5]. Cognitive Pattern Generators could select specific system dynamics for a set of desired outputs.

2.2 Reinforcement learning

The BG play also a critical role in reward and RL circuits. Phasic firing in dopamine (DA) neurons in the ventral tegmental area (VTA)—BG region providing important modulatory signals to other BG nuclei and external structures—complies with a *reward prediction error* signal of contemporary learning theories, e.g. in temporal difference (TD) learning [6]. One suggestion for biological RL is DA modulation of cortico-striatal synaptic plasticity [8]. Exploiting this reward-modulated plasticity could improve RC effectivity: the internal dynamics can autonomously tune themselves to the dynamic regime which is optimal for a given task [7]. This mechanism could also explain cognitive functions, e.g. conditioning and working memory, and dysfunctions, e.g. Parkinson's and schizophrenia [8].

3 Basal ganglia model

The first step in this learning-oriented neuromorphic engineering is the modeling of the BG and their parallel processing loops, a subject of ongoing research. Particular interest lies in phasic firing in DA neurons and its role in plasticity.

References

[1] C. A. Mead, *P IEEE*, **78(10)**, 1990: 1629–39.

[2] F. A. Middleton and P. L. Strick, *Brain Res Rev*, **31**, 2000: 236–50.

[3] T. J. Prescott, F. M. M. Gonzalez, K. Gurney, M. D. Humphries, and P. A. Redgrave, *Neural Networks*, **19**, 2006: 31–61.

[4] A. M. Graybiel, *Schizophr bull*, **23(3)**, 1997: 459–69.

[5] D. Prokhorov, *IEEE IJCNN*, Montreal, Canada, 2005.

[6] W. Schultz, *Annu Rev Psychol*, **57**, 2006: 87–115.

[7] B. Schrauwen, M. Wardermann, D. Verstraeten, J. J. Steil, and D. Stroobandt, *Neurocomputing*, **71(7-9)**, 2008: 1159–71.

[8] R. D. Samson, M. J. Frank, and J. M. Fellous, *Cogn Neurodyn*, **4(2)**, 2010: 91–105.

Randomized averaging algorithm: decoupling accuracy and convergence rate

Paolo Frasca
Dipertimento di Matematica
Politecnico di Torino
corso Duca degli Abruzzi 24
10126 Torino, Italy
Email: paolo.frasca@polito.it

Julien M. Hendrickx
ICTEAM
Université catholique de Louvain
4 Av G. Lemaitre
B-1348 Louvain la Neuve, Belgium
Email: julien.hendrickx@uclouvain.be

Abstract

We consider randomized discrete-time consensus systems that preserve the average on expectation, and provide an upper bound on the mean square deviation of the consensus value from the initial average. Our results are based on a new approach, unrelated to the convergence properties of the system.

1 Problem Statement

Given a set of nodes I of finite cardinality N, we consider a distributed state $x(t) \in \mathfrak{R}^I$ evolving according to a stochastic discrete-time system of the form

$$x_i(t+1) = \sum_{j \in I} a_{ij}(t) x_j(t) \qquad \forall i \in I, t \in \mathbb{Z}_{\geq 0} \qquad (1)$$

where for every $i, j \in I$, we assume $a_{ij}(t)$ to be a sequence of independent and identically distributed random variables such that $a_{ij}(t) \geq 0$ and $\sum_{l \in I} a_{il}(t) = 1$ for all $t \geq 0$. System (1) is run with the goal for the state of each node to provide a good estimate of the initial average $\frac{1}{N}\sum_{i \in I} x_i(0)$. Note that $x(0)$ is unknown but given, and our results are valid for any $x(0) \in \mathfrak{R}^I$. System (1) can be rewritten as

$$x(t+1) = x(t) - L(t)x(t) \qquad t \geq 0, \qquad (2)$$

where $L_{ij}(t) = -a_{ij}(t)$ if $i \neq j$ and $L_{ii}(t) = \sum_{j : j \neq i} a_{ij}(t)$.

Convergence of such systems has already been treated in the literature: If the graph induced by $\mathbb{E}[L(t)]$ is strongly connected and there exists $i \in I$ such that almost surely $L_{ii}(t) < 1$, then there exists a scalar random variable x_∞ such that $x(t)$ converges almost surely to $x_\infty \mathbf{1}$ [2]. Rather than in convergence, we are interested in the quality of the convergence value, in terms of its distance from the initial average $x_\infty - \bar{x}(0)$, where we use $\bar{x}(t) := \frac{1}{N}\sum_{i \in I} x_i(t)$. It can be easily verified that the expected limiting value of the system is the initial average $\mathbb{E}(x_\infty = \bar{x}(0))$ if and only if $\mathbf{1}^* \mathbb{E}(L(t)) = 0$. Such systems preserve the average *on expectation*.

2 Main result

Theorem 1 *Let x be an evolution of system (2) that converges to consensus, and denote $V(t) = \frac{1}{N}\sum_i \big(x_i(t) - \bar{x}(t)\big)^2$. If $\mathbf{1}^* \mathbb{E}[L(t)] = 0$ and there exists $\gamma > 0$ such that*

$$\mathbb{E}[L(s)^* \mathbf{1}\mathbf{1}^* L(s)] \leq \gamma \mathbb{E}[L(s) + L(s)^* - L(s)^* L(s)], \qquad (3)$$

then $\mathbb{E}\left[(x_\infty - \bar{x}(0))^2\right] \leq \frac{\gamma}{N} V(0)$.

The proof, available in [1], relies on showing that the expected increase of $(\bar{x}(t) - \bar{x}(0))^2$ can be bounded proportionally to the expected decrease of the disagreement $V(t)$. Our argument does not make use of the convergence properties of the system, and the bound we obtain does not a priori depend on "global" properties of the interaction graphs, such as its spectrum. The convergence rate, instead, does depend on the graph spectrum, and so did accuracy results previously available for particular cases of system (2) – see [1].

3 Application

The strength of the bound obtained in Theorem 1 depends on the value of γ. In general, the optimal γ can be large, as some systems do lead to large mean square deviations. As detailed in [1], there exist however important classes of systems for which the inequality (3) holds for values of γ that are small and independent of N, so that the mean square deviation is proportional to $1/N$. An example result is the following. If the node updates are mutually independent, i.e. $a_{ij}(t)$ and $a_{kl}(t)$ are independent random variables when $i \neq k$, and if there is a lower bound a^* on the self-confidence $a_{ii}(t)$ of the nodes, then one can prove that Theorem 1 holds with $\gamma = (a^*)^{-1} - 1$. This bound only depends on locally controllable quantities: unlike previous results, it therefore imposes no requirement on the network structure, which can be hard to implement in practice.

References

[1] P. Frasca, J.M. Hendrickx, "On the mean square error of randomized averaging algorithms arXiv:1111.4572", 2011.

[2] F. Fagnani and S. Zampieri, "Randomized consensus algorithms over large scale networks". IEEE Journal on Selected Areas in Communications, 26(4):634-649, 2008.

Port Hamiltonian modeling of Power Networks

F. Shaik [1] A.J. van der Schaft [1] J.M.A. Scherpen[1] D. Zonetti [2] R. Ortega [2]

1 Introduction

In this talk a full nonlinear model for the power network in port–Hamiltonian framework is derived to study its stability properties. For this we use the modularity approach i.e., we first derive the models of individual components in power network as port-Hamiltonian systems and then we combine all the component models using power-preserving interconnections to give a global port-Hamiltonian model of the power network. In this way we obtain a structure-preserving disaggregated model that basically preserves the original topology of the network, which will subsequently pave the way for energy based analysis.

2 Modeling of power network

A typical power network consists of 1. generators, 2. loads, 3. buses to which loads and generators are connected, and 4. transmission lines, connecting these buses, consisting of in-series inductive component and in-parallel capacitive components [1].

The port-Hamiltonian models of these components are derived by using their bond–graph representations [2]. The port-Hamiltonian models of generators and transmission line components are given by

$$\begin{aligned} \dot{x}_i &= [\mathcal{J}_i - \mathcal{R}_i]\nabla_{x_i} H_i(x_i) + g_i u_i \\ y_i &= g_i^t \nabla_{x_i} H_i(x_i) \end{aligned} \tag{1}$$

where x_i, u_i, y_i, $\mathcal{J}_i = -\mathcal{J}_i^T$, $\mathcal{R}_i = \mathcal{R}_i^T \geq 0$, $H_i(x_i)$ are the state vector, input vector, output vector, interconnection matrix, dissipation matrix and energy function, respectively of component i. For generator, the state vector consists of fluxes in inductances, angular displacement and momentum of the rotor. The inputs to generator are voltage across the field winding and mechanical torque applied to the rotor. The outputs are current in the field winding and speed of the rotor. For transmission line, the state vector consists of flux in inductance and charges across the capacitors. The inputs and outputs of transmission line are current flowing through and voltages across these components, respectively.

In this talk we assume that the loads are purely resistive i.e., it is given by static relation $y_i = R_L u_i$. To obtain the interconnection laws governing power network we define a graph on it. The graph is obtained by treating buses as nodes and all other elements as edges. If the the incidence matrix of this graph is given by M, then the interconnection laws are given by $MI_e = 0$ and $M^T V = V_e$ where I_e, V_e and V are vectors of edge currents, edge voltages and node voltages, respectively.

By combining all these individual models of the components and eliminating network constraints we get a global power network model as

$$\begin{aligned} \dot{x} &= [\mathcal{J} - \mathcal{R}]\nabla_x H(x) + gu \\ y &= g^t \nabla_x H(x) \end{aligned} \tag{2}$$

where state x consists of states of all individual components, and $H(x) = \Sigma H_i(x_i)$ is the total energy function. Input u is vector of all rotor field voltages and mechanical torques, and y is the vector of field currents and rotor speeds.

After having obtained the complete port–Hamiltonian model of the power network we study its stability, for which we assume a constant input in (2). In the talk we will show that for this forced Hamiltonian system the total energy function ceases to be a candidate Lyapunov function. For the remedy, we use the results obtained in [3] to construct a candidate Lyapunov function using the energy function. We will also discuss the influence of network interconnection structure on the stability of the overall system.

[1]Faculty of Mathematics and Natural Sciences, University of Groningen, P. O Box 800, 9700 AV Groningen, The Netherlands f.shaik@rug.nl, A.J.van.der.Schaft@math.rug.nl, j.m.a.scherpen@rug.nl

[2]Laboratoire des Signaux et Systèmes CNRS-SUPELEC, Plateau de Moulon, Supelec, 91192, Gif-sur-Yvette, France daniele.zonetti@gmail.com, romeo.ortega@lss.supelec.fr

References

[1] **Power System Stability and Control**, Kundur, P., McGraw-Hill, 1993, Engineering, 2009.

[2] **Modeling and Control of Complex Physical Systems: The Port Hamiltonian Approach**, Geoplex Consortium, Springer-Verlag, Berlin, Communications and Control Engineering, 2009.

[3] B. Maschke, R. Ortega and A. van der Schaft, Energy–based Lyapunov functions for forced Hamiltonian systems with dissipation, *IEEE Trans. on Automatic Control*, Vol. 45, No. 8, pp. 1498–1502, 2000.

Sensors for control of nuclear fusion plasmas

Gillis Hommen
Control Systems Technology Group
Eindhoven University of Technology P.O. Box 513
5600 MB Eindhoven The Netherlands
Email: g.hommen@tue.nl

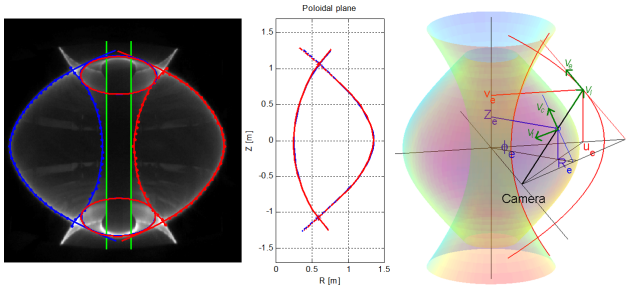

Figure 1: OFIT: edge detection in image, reconstructed boundary in poloidal plane and schematic of coordinate transform from image to tokamak coordinates.

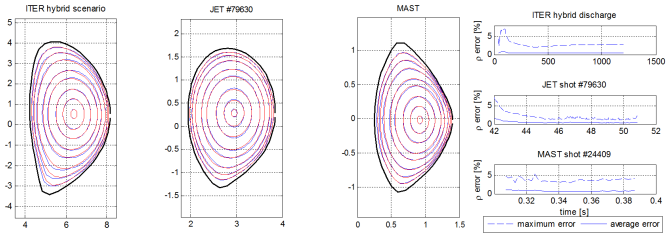

Figure 2: Example of estimates flux surfaces (OFIT+, blue) compared to results of magnetic reconstruction(red), for ITER, MAST, and JET equilibria. To focus on the flux surface shapes, identical plasma boundary and magnetic axis were used for both flux maps. Estimation errors are also shown, as a percentage offset of the minor radius.

1 Introduction

In the tokamak [1], a nuclear fusion reactor, a 100+ million degree plasma is confined by magnetic fields. The state of the plasma can be measured using a wide range of magnetic measurements. However, such magnetic interpretations of the plasma state suffer from drifts, signal to noise issues and rely on complex, iterative reconstructions to obtain a detailed measurement of the plasma. [2] Therefore, this work introduces a non-magnetic approach to the plasma-state reconstruction problem using visible light camera images, designed specifically with feedback control applications in mind.

2 Plasma boundary reconstruction

A new diagnostic, dubbed OFIT, to reconstruct the tokamak plasma boundary using visible wavelength images is developed for use in feedback control of tokamak plasma position and shape. [3] In the cold edge of the plasma, visible light is emitted. Exploiting this edge-localized and toroidally symmetric emission profile, a new coordinate transform is presented to reconstruct the plasma surface from a poloidal view image. A simple edge detection algorithm is applied to find the plasma edges in the image. These edges (lines) are then transformed from image coordinates to tokamak coordinates (surfaces) using the new toroidal surface reconstruction transform as illustrated in fig. 1.

3 Plasma internal reconstruction

The internal structure of the tokamak plasma is described by a set of concentric flux surfaces. Many important parameters of the plasma are so-called flux functions; their value is constant on each flux surface. The profiles of these parameters are controlled using actuators and sensors that are distributed two-dimensionally in the cross section of the plasma. As such, a distributed control system is described where the mapping of actuators and sensors to the coordinates of the control variables is given by the shape of the flux surfaces. The flux surface layout is a function of the spatial distribution of electrical current flowing through the plasma. Their shape can be obtained through magnetic reconstruction. Alternatively, their shape can be estimated by propagating the shape of the plasma boundary to the magnetic axis. An estimation algorithm is developed that provides fast flux surface estimates that are accurate to within 1% of the minor radius of the plasma. Fig. 2 shows examples of magnetically reconstructed and estimated flux surfaces in three tokamaks and also the estimation errors during the experiment. The efficiency of these techniques makes them ideally suited for real-time implementation and control applications.

References

[1] John Wesson, Tokamaks, Oxford University Press,ISBN 0-19-850922-7.

[2] R. Albanese, Plasma reconstruction in tokamaks with linearized approaches, Int. J. Appl. Electromagn. Mech. 26, 191 (2007).

[3] Hommen et. al., Rev. Sci. Instrum. 81, 113504 (2010)

Control strategy for print quality control

Carmen Cochior
Department of Electrical Engineering
Eindhoven University of Technology
P.O. Box 513, 5600 MB Eindhoven,
The Netherlands
Email: c.cochior@tue.nl

Paul van den Bosch
Department of Electrical Engineering
Eindhoven University of Technology
P.O. Box 513, 5600 MB Eindhoven,
The Netherlands
Email: p.p.j.v.d.bosch@tue.nl

René Waarsing
Océ-Technologies B.V.
5914 CA Venlo, The Netherlands
Email: rene.waarsing@oce.com

Jacques Verriet
Embedded System Institute
5600 MB Eindhoven, The Netherlands
Email: jacques.verriet@esi.nl [1]

1 Introduction

Industrial printers deliver high-quality prints and high throughput independently of the media type in the print queue (e.g. paper weight, paper size, thermal properties), the job type (simplex/duplex) and environment (e.g. temperature, humidity). They are composed of several subsystems and many states (speed, position, temperatures). The print quality depends on physical variables (e.g. temperatures, velocity) inside. If the print temperature is too low, the toner will not penetrate the paper sufficiently and it will remain on the top of the paper and will be erased. If the print temperature is too high, the toner will melt and stick to other surfaces.

The media properties (e.g. paper weight) are directly influencing the system dynamics. A specific characteristic of printers is that a few seconds in advance the properties of the sheet are known. This information can be used in feedfoward to obtain a better performance of the system. Main problems encountered in printing control are the nonlinear dynamics due to changes in controllable and measurable disturbances (e.g. change in the media type) and hard constraints which may vary in time. The process is limited by a variable maximum available power.

2 Problem Statement

The objective is to maximize the throughput and keep the printing quality within constraints under all operating conditions. An interesting problem for printers is also the cold start. To maximize the throughput of the machines, it is important to determine an optimal heating strategy, as temperature considerably influences the print quality. The machine needs to be warmed up to a certain temperature to make sure that the printing quality is not lost not even for one page. Also when switching between media types, once the printing process started, the quality has to be guaranteed.

The research challenge is to design a runtime adaptive control system that maintains a high level of performance under nonlinear dynamical behavior and changing partly known operational conditions. To deliver high performance, the system should adapt in runtime, based on the operating conditions and constraints. In our case, the adaptation is mainly related to changes in the media type (print queue). Since there is a direct influence of the system dynamics, dependent on the paper properties, different models should be used in control for cold start and warm process. A parameter dependent model of the system could catch all the dynamics for cold and warm process. A control approach is proposed to maximize the throughput while guaranteeing the quality of the system. It is based on a nonlinear dynamic parameter-dependent predictive controller. MPC is a good choice to control the behavior of printers, because it can deal in an optimal way with hard constraints and available information of the print queue [1, 2]. The controller has to track a time-varying target, given hard constraints of the plant and measured and unmeasured disturbances. A trade off is being made between maximizing the throughput and printing quality in the cost function. Since the proposed method gave good results in simulations, this encourage a full analysis of the properties in closed-loop as a next step, to prove the effectiveness of the method.

[1] This work has been carried out as part of the OCTOPUS project with Océ-Technologies B.V. under the responsibility of the Embedded Systems Institute. This project is partially supported by the Netherlands Ministry of Economic Affairs under the Bsik program.

References

[1] L.B. Rawlings and R. Amrit, "Optimizing Process Economic Perfomance Using Model Predictive Control", *Nonlinear Model Predictive Control*,LNCIS 384, pp. 119-138,2009

[2] A.Ferramosca, D Limon, I. Alvarado, T. Almo and E.F. Camacho, "MPC for tracking of constrained nonlinear systems", *48th IEEE Conference on Decision and Control and 28th Chinese Control Conference*, 2009, pp. 7978-7983.

Integrated design of far and large offshore wind turbines

Edwin van Solingen[1], Jan-Willem van Wingerden[1], Michel Verhaegen[1], Roeland de Breuker[2]
[1]Delft Center for Systems and Control, Delft University of Technology, The Netherlands
[2]Aerospace Structures & Computational Mechanics, Delft University of Technology, The Netherlands
Email: E.vanSolingen@tudelft.nl

1 Introduction

With a desired 20% integration level of sustainable energy in 2020 by the European Union, a desired capacity of 6000 MW offshore in The Netherlands by 2020 and the predicted lack of availability of fossil fuels, wind energy has a bright future. However, the largest bottleneck is still the cost of energy which is roughly twice the cost of their fossil alternative. For that reason, the Far and Large Offshore Wind (FLOW) innovation program was initiated. One of the targets of this program is to reduce the production costs with 20%, which would significantly strengthen the position of wind turbines. To achieve this goal, active control is becoming more and more important. For example, in a turbine the rotor torque, blade pitch angle, position of the rotor with respect to the wind, drive-train torsion and tower bending are actively controlled.

2 Integrated design approach

Typically, when designing turbines, first the structural dynamics and aerodynamical behavior of the wind turbine are optimized, followed by the independent design of the different controllers. Furthermore, the dynamics of the controlled turbine are a result of the interaction of the controller, the structural dynamics and aerodynamics. A consequence of independently designing the controllers is that each control loop is conservatively optimized, i.e., taking into account safety margins and cross-couplings between the different control loops, resulting in suboptimal designs. Also, the combined dynamics of turbine and controllers often do not yield optimal designs. For those reasons, the design of wind turbines is approached in an integrated design fashion. This means that both the structural dynamics and the controller design are simultaneously optimized, with the ultimate goal to minimize the production costs.

3 Research scope

The scope of the research is not to integrate all components of a wind turbine (as is done in [1]) in a single design, but to only focus on the simultaneous optimization of the structural design of the blades (aeroelastics) and the different controllers. To be more specific, the objective parameters in the blade design are the mass and stiffness, whereas the shape is assumed to be fixed. We will consider the torque and blade pitch regulators in our optimization framework.

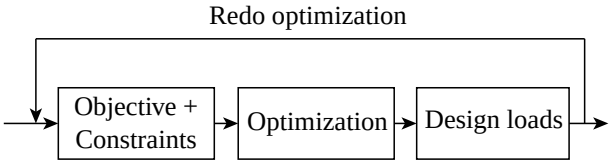

Figure 1: Optimization procedure for the integrated design of structural blade dynamics and controllers.

In literature, very few examples of such integrated structure and controller design are found. However, one example is the isolation of buildings against earthquakes [2].

In the optimization process, the objective is to optimize the structural dynamics of the blades and controllers, so that the blades have minimum weight on the one hand, but are able to withstand the different loads which they are subjected to in real-world on the other hand. Furthermore, the design is constrained by for example the placement of blade modes in order to avoid excitation by other modes present in a turbine. The integrated design is accomplished by iteratively optimizing the design and subjecting it to the design loads to check whether the design is satisfactory. If the design specifications are not met, the optimization procedure is repeated (see also Figure. 1).

The research is started with a demonstration of a simultaneous design of both structure and controller on an experimental 2D-airfoil with actuator flap. In this simplified approach, the framework for the integrated design of wind turbines is developed.

4 Acknowledgement

The research is funded by the FLOW innovation program.

References

[1] C.L. Bottasso and A. Croce. Computational procedures for the multi-disciplinary constrained optimization of wind turbines. Technical Report DIA-SR 10-02, Politecnico di Milano, January 2010.

[2] Juan F. Camino, M. C. de Oliveira, and R. E. Skelton. ”Convexifying” linear matrix inequality methods for integrating structure and control design. *Journal of Structural Engineering*, 129(7):978–988, 2003.

Towards online data-driven batch optimization using Partial Least Squares

G. Gins, J. Vanlaer, P. Van den Kerkhof, and J.F.M. Van Impe
BioTeC, Department of Chemical Engineering, KU Leuven – Catholic University of Leuven
W. de Croylaan 46 PB 2423, B-3001 Heverlee (Leuven), Belgium
{geert.gins, jef.vanlaer, pieter.vandenkerkhof, jan.vanimpe}@cit.kuleuven.be

1 Introduction

Batch processes are widely used in chemical and life sciences industries for the production of products with a high added value (e.g., medicines, enzymes, high-performance polymers). Accurately controlling the final quality of a batch process presents a major challenge. First of all, a batch process is dynamic in nature. In addition, physical measurements of the quality parameter that can be used to predict the final quality are often simply not available online.

Data-driven models provide an answer to this problem, and have been applied successfully both to simulation and industrial data. These techniques use simple, online available measurements (temperatures, pressures, flow rates, ...) to *monitor* the batch process or *predict* the final quality. Examples include Nomikos and MacGregor [1], Ündey *et al.* [2], Choi *et al.* [3] and Gins *et al.* [4]. In these works, abnormal quality is detected through (*i*) deviations from the nominal batch behavior or (*ii*) estimation of the batch-end quality (i.e., the quality after completion of the batch).

2 Online batch-end quality optimization

Most research effort for batch processes has been directed towards *process monitoring*; the number of applications where the data-driven models are used to actually *control* or *optimize* a batch is very limited. Recently, McCready optimized the production of a batch process with an MPLS model by adapting the manipulated variables (MVs) at three distinct decision moments [5]. Expansion to full batch production optimization requires, ideally, changes in MVs every few time points. As a result, more test runs are required to identify the MPLS model. The time required to perform these tests is a major drawback: successful industrial adaptation hinges on fast implementation. Hereto, as few test runs as possible should be conducted.

This paper investigates whether all possible decision moments must be considered during model identification. From training sets with a limited number of MV changes, predictive MPLS models are constructed. If these models are capable of predicting the final quality when MV changes occur at times not included in the training set, the number of tests required for model identification can be significantly reduced.

3 Results

Two case studies were performed: one where only a single change in the manipulated variable was allowed, and one where multiple changes could be performed. In both studies it was concluded that the inclusion of a few switch times in the training data sufficed: the final quality of batches with other switch times was accurately estimated on- and offline, provided the switches occur in the range of training switch times. This is a valuable result for practical (industrial) implementation and acceptance because the amount of test batches needed is reduced and the information content of each experiment is increased.

Acknowledgements. Work supported in part by Project PVF/10/002 (OPTEC Optimization in Engineering Center) of the Research Council of the KU Leuven, Project KP/09/005 (SCORES4CHEM) of the Industrial Research Council of the KU Leuven, and the Belgian Program on Interuniversity Poles of Attraction initiated by the Belgian Federal Science Policy Office. J. Vanlaer and P. Van den Kerkhof are funded by a Ph.D grant of the Agency for Innovation by Science and Technology (IWT). J. Van Impe holds the chair Safety Engineering sponsored by the Belgian chemistry and life sciences federation essenscia. The scientific responsibility is assumed by the authors.

References

[1] P. Nomikos and J.F MacGregor. Monitoring batch processes using multiway principal component analysis. *AIChE J.*, 40(8): 1361–1375, 1994.

[2] C. Ündey, S. Ertunç, and A. Çinar. Online batch/fed-batch process performance monitoring, quality prediction, and variable-contribution analysis for diagnosis. *Ind. Eng. Chem. Res.*, 42:4645–4658, 2003.

[3] S.W. Choi, A.J. Morris, and I.-B. Lee. Dynamic model-based batch process monitoring. *Chem. Eng. Sci.*, 63(3):622–636, 2008.

[4] G. Gins, J. Vanlaer, and J.F. Van Impe. Online batch-end quality estimation: does laziness pay off? In: J. Quevedo, T. Escobet and V. Puig (Eds.) *Proceedings 7th IFAC International Symposium on Fault Detection, Supervision and Safety of Technical Processes (SafeProcess2009)*, Barcelona (Spain), 1246–1251, 2009.

[5] C. McCready. Model Predictive Multivariate Control (MPMC). In: *2nd European Conference on Process Analytics and Control Technology (EuroPACT2011)*, Glasgow (United Kingdom), 82, 2011.

Hybrid Robust Output Regulation for the METIS Chopper[1]

Robert Huisman
SRON Netherlands Institute for Space Research
P.O. Box 800, 9700 AV Groningen
The Netherlands
Email: R.Huisman@sron.nl

Bayu Jayawardhana
Faculty of Mathematics and Natural Sciences
University of Groningen
The Netherlands
Email: B.Jayawardhana@rug.nl

1 Introduction

We present the design and analysis of a Hyrbid controller for the METIS Cold Chopper (MCC). The MCC is a 2D rotatable mirror in the optical path of the Mid-Infrared E-ELT Imager and Spectrograph (METIS) instrument [1]. It provides telescope beam chopping by rotating this internal mirror. The system has three degrees of freedom, two rotational and one parasitic translational movement in the direction of the mirror vertex. It has to satisfy stringent performance requirements while dealing with different noise sources, disturbances and constraints on the input signals.

2 Hybrid controller design

The developed controller combines time-optimal control design (for handling the constraints and transient performance) and a H_∞ controller (for achieving stability and robustness against uncertainties and disturbances). We note that our control strategy is motivated by recent results on periodic output regulation using a hybrid control framework [2]. The hybrid configuration is given in [2, Eq. (7)].

The matrices A_C, B_C and C_C of the controller's flow dynamics have the following structure

$$A_C = \begin{bmatrix} \star & 0 & 0 \\ 0 & 0 & 0 \\ 0 & 0 & 0 \end{bmatrix} \; B_C = \begin{bmatrix} \star & \star \\ -1 & 0 \\ 0 & 0 \end{bmatrix} \; C_C = \begin{bmatrix} \star & k_i & 0 \\ \star & 0 & 0 \end{bmatrix},$$

where the elements in $\star$ are obtained from the H_∞ design. An integrator with gain k_i is added to the controller for achieving zero angular steady state error. The matrices Φ and Ψ of the controller's jump dynamics have the following structure

$$\Phi = \begin{bmatrix} \mathrm{Id} & 0 & 0 \\ 0 & 0 & 1 \\ 0 & 1 & 0 \end{bmatrix} \; \Psi = \begin{bmatrix} 0 & 0 \\ k_1 & 0 \\ k_2 & 0 \end{bmatrix},$$

where k_1 and k_2 are the correction gains that can be added to the integrators. During the jump, the state for the H_∞ controller is kept constant whereas the integrators are exchanging values.

[1] METIS is a collaboration between NOVA, ATC, CEA Saclay, ETH, KU Leuven and MPIA. The MCCD is a collaboration between NOVA, ASTRON, JPE BV, the RUG, SRON, and TNO.

It can be shown that output regulation is guaranteed if the hybrid system satisfies:

$$\sigma_{\max}\left(\mathscr{J}_{cl}\exp\left(\mathscr{H}_{cl}(T/2-\tau_s)\right)\right) < 1, \qquad (1)$$

where $\mathscr{H}_{cl} := \begin{bmatrix} A_G & B_G C_C \\ B_C C_G & A_C \end{bmatrix}$, $\mathscr{J}_{cl} := \begin{bmatrix} M & 0 \\ \Psi C_G & \Phi \end{bmatrix}$, the tuple (A_G, B_G, C_G) is the system's matrices of the mechanism, $M := \exp(A_G\tau_s)$, T is the chop period and τ_s is the duration of the feedforward control input.

3 Analysis results

Matlab/Simulink was used to analyze the performance of the controller. In figure 1 the simulation results of two consecutive chops between 0 mrad and 8.5 mrad is shown. The settling time is approximately 5 msec, the positional stability is smaller than the required 1.7 μrad and the positional accuracy is $< 1\mu$rad.

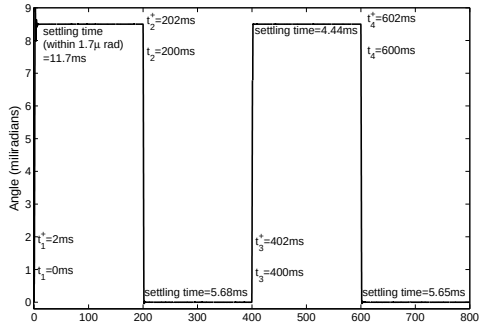

Figure 1: The closed-loop system behaviour with the hybrid controller with the desired positions of 0rad and 8.5mrad.

References

[1] B. Brandl *et.al.*, "METIS - the mid-infrared E-ELT imager and spectrograph," *in McLean IS, Casali MM, editors. Ground-based and airborne instrumentation for astronomy II*, SPIE 7014, 70141N, 2008.

[2] L. Marconi and A.R. Teel, "A note about hybrid linear regulation," Proc. 49th IEEE Conf. Dec. Contr., Atlanta, Georgia, 2010.

Implications of measurement noise for Partial Least Squares model order selection

J. Vanlaer, P. Van den Kerkhof, G. Gins, and J.F.M. Van Impe
BioTeC, Department of Chemical Engineering, KU Leuven – Catholic University of Leuven
W. de Croylaan 46 PB 2423, B-3001 Heverlee (Leuven), Belgium.
{jef.vanlaer, pieter.vandenkerkhof, geert.gins, jan.vanimpe}@cit.kuleuven.be

1 Introduction

The development of automated monitoring systems is an important challenge for the chemical and life sciences industries [4]. Especially for batch processes, which are commonly used for the production of goods with high added value, close process monitoring is of utmost importance. However, despite the frequent use of low-level controllers, detection of and response to abnormal events often remains a manual operation, severely complicated by the large size and complexity of modern process plants.
Multiway Partial Least Squares (MPLS [3]) models exploit the information arising from numerous online sensors in today's (bio)chemical processes for monitoring purposes. These models enable online prediction of the batch-end quality, which is generally only measured offline after batch completion. However, noise present on both online sensor measurements and offline quality measurements influences the predictive performance of the MPLS models, which has important consequences for the selection of the optimal model order. Up until today, no analytical relation has been identified to describe the influence of measurement noise on PLS batch-end quality predictions, which partly explains the reluctance of companies to accept this technique. The non-linear properties of the PLS predictor and the lack of knowledge about its statistical distribution make the derivation of such a relation extremely difficult [2].
Therefore, this work aims at investigating the influence of noise on PLS predictions of final batch quality and the implications for model order selection. Since most online sensors produce accurate measurements, the research focusses on noise on the (offline) quality measurements.

2 Methodology

To investigate the statistical properties of MPLS model predictions with respect to noise on the output measurements, a Monte Carlo simulation with 1000 repetitions is performed for 10 different levels of the output noise, using data of a penicillin production process from an extended version of the `Pensim` simulator [1]. For every repetition, the noise is resampled from a Gaussian distribution with zero mean and a standard deviation ranging from 1 to 10 percent of the mean penicillin concentration in the training batches. Bias and variance of the model predictions are studied and the results are used to assess the performance of several techniques for model order selection.

3 Results

Prediction bias and variance show inverse behaviour with respect to the model order. While prediction bias initially decreases to reach a minimum value at a model order that is independent of the noise level, prediction variance increases with increasing model order since more noise is included in the higher order components. This inverse behaviour holds important consequences for selection of the optimal model order, which corresponds to a trade-off between bias and variance. An adjusted Wold's *R* criterion that only includes extra components if they significantly improve the prediction according to a chosen significance level selects lower model orders than the minimum MSE and Wold's *R* criteria, trading variance for (small) bias. In general, the adjusted Wold's *R* criteria are shown to be slightly preferable to select the optimal model order.

Acknowledgements. Work supported in part by Project PVF/10/002 (OPTEC Optimization in Engineering Center) of the Research Council of the KU Leuven, Project KP/09/005 (SCORES4CHEM) of the Industrial Research Council of the KU Leuven, and the Belgian Program on Interuniversity Poles of Attraction initiated by the Belgian Federal Science Policy Office. J. Vanlaer and P. Van den Kerkhof are funded by a Ph.D grant of the Agency for Innovation by Science and Technology (IWT). J. Van Impe holds the chair Safety Engineering sponsored by the Belgian chemistry and life sciences federation essenscia. The scientific responsibility is assumed by the authors.

References

[1] G. Birol, C. Ündey, and A. Çinar. A modular simulation package for fed-batch fermentation: penicillin production. *Comput Chem Eng*, 26:1553–1565, 2002.

[2] M.C. Denham. Prediction intervals in partial least squares. *J Chemometr*, 11:39–52, 1997.

[3] P. Nomikos and J.F. MacGregor. Multiway partial least squares in monitoring batch processes. *Chemometr Intell Lab*, 30:97–108, 1995.

[4] V. Venkatasubramanian, R. Rengaswamy, K. Yin and S.N. Kavuri. A review of process fault detection and diagnosis. Part I: Quantitative model-based methods. *Comput Chem Eng*, 27:293–311, 2003.

Practical Design of an Extended Kalman Filter for an Animal Cell Culture

Ines Saraiva, Mihaela Sbarciog, Alain Vande Wouwer
Service d'Automatique, Université de Mons,
B-7000 Mons, Belgium
Email : Ines.Saraiva@umons.ac.be; MihaelaIuliana.Sbarciog@umons.ac.be

1. Introduction

Some very complex biochemical substances in the pharmaceutical field cannot be synthesized by traditional chemistry. However, animal cells can be programmed to synthesize them. One such method is to cultivate these cells extracted from animal tissue (eg. CHO, hybridoma) in a suspended continuous mode. A perfusion filter placed in the outstream allows the biomass to be kept in batch while other compounds are continuously extracted. Thus, small volumes can be operated for long periods, reaching high cell concentrations, low product residence time and high productivity. A small bleed outstream allows the operation to reach steady state.

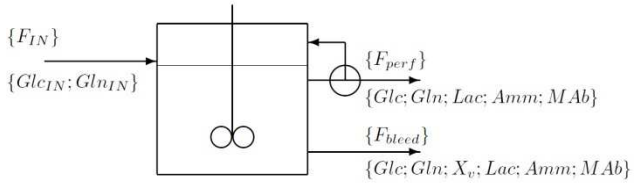

Fig. 1. Continuous Perfused Bioreactor

In this study, a nonlinear macroscopic model described in [1] of fairly general applicability to animal cell cultures is used. It considers reasonable assumptions such as that cell grow is limited by glucose and glutamine availability, cell death is promoted by accumulation of lactate and ammonia and glutamine exhaustion, a part of glucose is spent for cell maintenance, and the production of the product of interest, monoclonal antibodies, is partially growth-related and partially not.

$$Glc + Gln \xrightarrow{\varphi} X_v + Lac + Amm + MAb$$

The objective of this study is to evaluate several sensor configurations in terms of observability and practical performance of an extended Kalman filter. The selection of sensor configurations is also discussed in terms of equipment costs and measurement implementation.

The extended Kalman filter is intended for a control strategy based on a nonlinear model predictive controller as described in [2].

As an example, some estimation results are shown in Figure 2 for the estimation of biomass and metabolite concentrations based on the measurements of the two major substrates, glucose and glutamine.

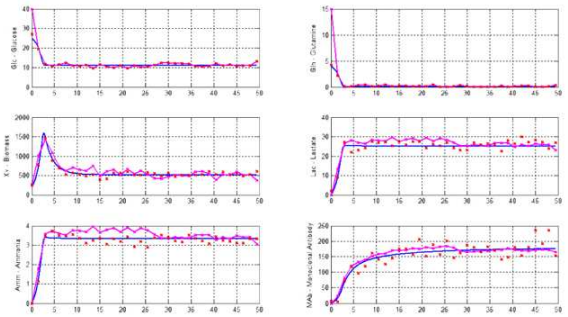

Fig. 2. EKF Estimation of Biomass and Metabolites

Acknowledgments

This work presents research results of the Belgian Network DYSCO (Dynamical Systems, Control, and Optimization), funded by the Interuniversity Attraction Poles Program, initiated by the Belgian State, Science Policy Office. The scientific responsibility rests with its authors. This work is carried out in the framework of the research project OCPAM (Hainaut-Biomed) funded by FEDER.

References

[1] M. de Tremblay, M. Perrier, C. Chavarie, J. Archambault, "Optimization of fed-batch culture of hybridoma cells using dynamic programming: single and multi feed cases" Bioprocess Engineering 7, 229-234, 1992.

[2] M. Sbarciog, I. Saraiva, A. Vande Wouwer, "Accelerating animal cell growth in perfusion mode by multivariable control" Chemical Engineering Research and Design, (submitted).

Application of Least Squares Support Vector Machines to online fault diagnosis of batch processes

P. Van den Kerkhof, J. Vanlaer, G. Gins, and J.F.M. Van Impe
BioTeC, Department of Chemical Engineering, KU Leuven – Catholic University of Leuven
W. de Croylaan 46 PB 2423, B-3001 Heverlee (Leuven), Belgium
{pieter.vandenkerkhof, jef.vanlaer, geert.gins, jan.vanimpe}@cit.kuleuven.be

1 Introduction

Fault detection and fault diagnosis of (bio)chemical batch processes is a difficult problem due to their dynamic nature. Principal Component Analysis (PCA)-based techniques, originating from the work of Nomikos and MacGregor [1], have become popular for data-driven fault detection. On the other hand, fault diagnosis of the detected disturbance remains a difficult issue. In this work, a new data-driven diagnosis technique is developed, using a statistical classifier based on Least Squares Support Vector Machines (LS-SVMs [2]). LS-SVMs exhibit a large generalization performance, especially when the number of training samples is small. This is an important advantage as the availability of faulty data is a common bottleneck in developing data-driven diagnosis techniques.

2 Fault diagnosis method

The identification of the LS-SVM classifier consists of three steps. In a first stage, past faulty batches are scanned with fault detection statistics based on the PCA model of normal operating conditions data. Based on process knowledge and operator experience, fault classes are defined and each of the detected faults is assigned to one fault class. The number of classes is a trade-off between classifier performance and practical use of the diagnosis results.

In the second step, the faulty data of each batch is scaled and an appropriate data window starting from the detection of the fault is selected. The goal of this step is to obtain a uniform characteristic data pattern for each fault class. Contrary to Fischer Discriminant Analysis (FDA)-based methods [3], the classifier is not trained on the data of each entire faulty batch because samples obtained at later time points might be influenced by different corrective actions (depending on the operator). Moreover, multiple faults can occur in a single faulty batch. An appropriate scaling increases similarity within each fault class and avoids overloading the classifier with irrelevant features. For example, normalizing around the mean trajectory reduces the difference between faults of the same class occurring at different time points.

Finally, the LS-SVM classifier is trained. An (LS-)SVM classifier is basically a binary classifier. Different techniques exist to decompose the multi-class diagnosis problem into a series of binary classification problems (e.g., *One-versus-One* and *One-versus-All*).

During the application phase, the current batch is monitored using an existing fault detection system. Upon detection, a window of pretreated data is passed to the classifier which assigns a fault class to the current disturbance. Based on this information, operators take corrective actions or abort the process if the batch can not be salvaged. Monitoring the fault detection statistics and successive fault classifications reveal if the operator actions bring the process back within normal operating conditions.

3 Results

The proposed approach is validated on data generated with an expanded version of the PENSIM simulator [4]. The simulated data contains faults from six different classes. The obtained results provide a proof of concept of the proposed technique and demonstrate the importance of appropriate data pretreatment.

Acknowledgements. Work supported in part by Project PVF/10/002 (OPTEC Optimization in Engineering Center) of the Research Council of the KU Leuven, Project KP/09/005 (SCORES4CHEM) of the Industrial Research Council of the KU Leuven, and the Belgian Program on Interuniversity Poles of Attraction initiated by the Belgian Federal Science Policy Office. P. Van den Kerkhof and J. Vanlaer are funded by a Ph.D grant of the agency for Innovation by Science and Technology (IWT). J. Van Impe holds the chair Safety Engineering sponsored by the Belgian chemistry and life sciences federation essenscia. The scientific responsibility is assumed by the authors.

References

[1] P. Nomikos and J.F MacGregor. Monitoring batch processes using multiway principal component analysis. *AIChE Journal*, 40(8):1361–1375, 1994.

[2] J.A.K. Suykens, T. Van Gestel, J. De Brabanter, B. De Moor and J. Vandewalle. Least Squares Support Vector Machines. World Scientific, Singapore, 2002.

[3] H.-W. Cho and K.-J. Kim. Fault diagnosis of batch processes using discriminant model. *International Journal of Production Research*, 42(3):597–612, 2004.

[4] G. Birol, C. Ündey, and A. Çinar. A modular simulation package for fed-batch fermentation: penicillin production. *Computers & Chemical Engineering*, 26:1553–1565, 2002.

Control of transportation networks modeled as port-Hamiltonian systems on graphs

Jieqiang Wei
JBI, University of Groningen, PO Box 407,9700AK Groningen, the Netherlands
j.wei@rug.nl

A.J.van der Schaft
JBI, University of Groningen, PO Box 407,9700AK Groningen, the Netherlands
A.J.van.der.Schaft@rug.nl

1 Abstract

Recently the connection of port-Hamiltonian systems theory with graph theory has been emphasized [2, 3]. In the current talk we are primarily interested in using the framework of port-Hamiltonian systems on graphs for studying the throughput and robustness of network models with sources and sinks under flow and capacity constraints [6].

As an initial problem we consider the following system as

$$\dot{x} = Bu + d$$
$$y = B^T x$$

where B is the incidence matrix of a graph, x is the vector of state variables associated to the vertices of the graph, u is the flow input associated to the edges, while d is an external input corresponding to flows at the sources and sinks of the graph. Furthermore, we assume there are flow constraints.

For controlling this system we use a classical PI controller. This can be represented as a port-Hamiltonian system with external input. By constructing an explicit Lyapunov function inspired by the construction in [5], we prove that the controlled system is asymptotically stable while the elements converge to a common value and the controller state converges to a value $\bar{u}$, such that $B\bar{u} + d = 0$.

References

[1] B. Bollobas, Modern Graph Theory, Graduate Texts in Mathematics 184, Springer, New York, 1998.

[2] A.J. van der Schaft, B.M. Maschke, Port-Hamiltonian systems on graphs and complexes, 2011 arXiv.

[3] A.J van der Schaft, B.M. Maschke, Port-Hamiltonian dynamics on graphs: Consensus and coordination control algorithms. In Proc. 2ned IFAC Workshop on Distributed Estimation and Control in Networked Systems,France 2010.

[4] Amirreza Rahmani, Meng Ji, Mehran Mesbahi, and Magnus Egerstedt, Controllability of multi-agent systems from a graph-theoretic perspective, SIAM J. Control Optim. Vol. 48, No. 1, pp.162-186,2009.

[5] Wei Ren, On Consensus Algorithms for Double-Integrator Dynamics, IEEE Transactions on Automatic Control, Vol. 53, No. 6, JULY 2008.

[6] Franco Blanchini, Stefano Miani, and Walter Ukovich, Control of Production-Distribution Systems with Unknown Inputs and System Failures, IEEE Transactions on Automatic Control, Vol.45, No. 6, 2000.

Notch filters for port-Hamiltonian systems

D.A. Dirksz[1], J.M.A. Scherpen[2], A.J. van der Schaft[2], and M. Steinbuch[1]

[1]Department of Mechanical Engineering, Eindhoven University of Technology, P.O. Box 513, 5600 MB Eindhoven, The Netherlands,
Emails: d.a.dirksz@tue.nl, m.steinbuch@tue.nl

[2]Faculty of Mathematics and Natural Sciences, University of Groningen, Nijenborgh 4, 9747 AG Groningen, The Netherlands,
Emails: j.m.a.scherpen@rug.nl, a.j.van.der.schaft@rug.nl

Introduction

Network modeling of lumped-parameter physical systems naturally leads to a geometrically defined class of systems, i.e., port-Hamiltonian (PH) systems [4, 6]. The PH modeling framework describes a large class of (nonlinear) systems including passive mechanical systems, electrical systems, electromechanical systems, mechanical systems with nonholonomic constraints, thermal systems and distributed parameter systems with boundary control. The popularity of PH systems can be largely accredited to its application for analysis and control design of multi-input multi-output (MIMO) physical systems

Nonlinear modeling and control methods, including the PH framework, have the great disadvantage of not including any frequency information in the modeling and control design. In practice the frequency-based control methods are preferred because of the importance of the system behavior in the frequency domain. In the frequency domain transfer functions, Bode plots, PID controllers, lag-lead compensators and filters are some examples of powerful tools for analysis and control [1]. However, such methods are only theoretically justified for linear systems. Many physical systems are actually nonlinear, for which linearization is then first required. However, the results only hold locally, (very) close to the linearization point. On the other hand, nonlinear control often offers methods to steer a nonlinear system to a desired state for any initial condition. When global convergence cannot be proven, techniques exist to define a region of attraction [3]. Some results on including frequency methods into nonlinear control can be found in [2, 5, 8].

Contribution

Here, we describe the standard notch filter in the PH form. In control applications a notch filter is often used for control of systems with lightly damped flexible modes (resonance frequencies). A notch filter is a filter that passes signals of all frequencies except those in a stop band centered around a center frequency. Furthermore, by a specific choice for the notch parameters it is possible to realize an *inverse* notch filter. An inverse notch filter does the opposite, it only passes signals which are centered around a center frequency. Inverse notch filters are usually used for disturbance attenuation since high feedback gain is applied at the disturbance frequency [7]. The main contribution here is to include frequency filtering into nonlinear control design by describing a standard notch filter in the PH framework. In a similar way we also present a PH description of the inverse notch filter. By having the notch filter in PH form we can simply interconnect it, in a passive way, with another (nonlinear) PH system, which then preserves the passivity property for the closed-loop system. We are able to combine the nonlinear control methodology of passivity based-control (PBC) [6] with a notch filter, which is tuned to reduce (or increase in the case of an inverse notch) the feedback gains at a specific frequency.

References

[1] G.F. Franklin, J.D. Powell, A. Emami-Naeini, 2006, *Feedback control of dynamic systems*, Upper Saddle River, Pearson Prentice Hall

[2] C.A. Jacobson, A.M. Stankovic, G. Tadmor, M.A. Stevens, 1996, Towards a dissipativity framework for power system stabilizer design, *IEEE Transactions on Power Systems*, Vol. 11, No. 4, 1963-1968

[3] H. Khalil, 1996, *Nonlinear Systems*, Prentice Hall, Upper Saddle River

[4] B.M. Maschke, A.J. van der Schaft, 1992, Port-controlled Hamiltonian systems: modeling origins and system-theoretic properties, *IFAC symposium on Nonlinear Control Systems*, Borbeaux, France, 282-288

[5] D. Rijlaarsdam, P. Nuij, J. Schoukens, M. Steinbuch, 2011, Frequency domain based nonlinear feedforward control design for friction compensation, *Mechanical Systems and Signal Processing*, doi:10.1016/j.ymssp.2011.08.008

[6] A.J. van der Schaft, 2000, *L_2-gain and passivity techniques in nonlinear control*, London, Springer

[7] M. Steinbuch, M.L. Norg, 1998, Advanced motion control, *European Journal of Control*, Vol. 4, No. 4 278-293

[8] N. van de Wouw, H. Pastink, M. Heertjes, A. Pavlov, H. Nijmeijer, 2008, Performance of convergence-based variable-gain control of optical storage drives, *Automatica*, Vol. 44, No. 1, 15-27.

On antiwindup control for port Hamiltonian systems

Fulvio Forni and Rodolphe Sepulchre

Department of Electrical Engineering and Computer Science,
University of Liège, B-4000 Liège, Belgium
fforni@ulg.ac.be, r.sepulchre@ulg.ac.be

1 Introduction

Every control methodology designed to achieve a desired performance is inevitably limited by actuators constraints, at implementation level. The mismatch between the controller output and the effective constrained actuation leads to performance degradation which may extend up to loss of stability. This problem can be encountered already in simple control design, like PI control, where the controller output is not driving the plant when saturation occurs, which causes a wrong update of its state, namely an excess of error accumulation in the integral part of the controller, with subsequent loss of performance (windup). These issues are well known and the literature contains several contributions, the so-called antiwindup correction, which characterize a well-established core of solutions with several tools ready for applications [1, 6].

Most of these techniques have been developed for linear plants while, despite the industrial relevance of the problem, few antiwindup approaches have been studied for nonlinear systems. Motivated by ongoing research on port Hamiltonian systems [3], and taking inspiration from the antiwindup approach for Lagrangian systems [2] and from the antiwindup solution for induction motors recently proposed in [5], we outline an antiwindup setup for port Hamiltonian systems which can be rendered incrementally passive by output injection [4]. This feature allows for an augmentation of the plant dynamics by an internal model, which is driven by the error between the ideal reference and the actual trajectory and is used to modify the controller input for performance recovery, as in [2].

2 The methodology

Consider the regulation problem of imposing a prescribed steady-state response x^* to a plant (saturation is denoted by σ). Using a linear settings for simplicity, consider

$$\dot{x} = Ax + B\sigma(u) \qquad y = Cx \tag{1}$$

and suppose that the feedback $u = K(x, x^*)$ guarantees regulation. To solve the problem by output feedback we introduce an observer

$$\dot{\hat{x}} = A\hat{x} + B\sigma(u) + v \qquad \hat{y} = C\hat{x}$$

which is rendered contractive w.r.t. x, independently on the input u, by the output injection $v = L(\hat{x} - x)$ (in a nonlinear setting, contraction by a suitable definition of v is entailed by incrementally passivity of (1)). Then, neglecting saturations, regulation is achieved by $u = K(\hat{x}, x^*)$.

A typical goal in presence of saturation is to preserve the unconstrained behavior given by $K(\hat{x}, x^*)$ for small signals, namely when $K(\hat{x}, x^*)$ does not saturate, and to recover from saturation-induced phenomena when $K(\hat{x}, x^*)$ saturate. With this aim, the constrained reference signal is decomposed as the sum $\hat{x} = x_U + x_{aw}$ with dynamics

$$\begin{aligned} \dot{x}_U &= Ax_U + Bu + v - w & y_U &= Cx_U \\ \dot{x}_{aw} &= Ax_{aw} + B[\mathrm{sat}_M(u) - u] + w & y_{aw} &= Cx_{aw}. \end{aligned}$$

The *unconstrained* dynamics x_U can now be regulated independently from the actuator limits, thus by enforcing $u = K(x_U, x^*)$, while the mismatch between x_U and $\hat{x}$ caused by saturation is now stored within the state x_{aw} of the *antiwindup* dynamics. Then, performance recovery can be imposed by stabilizing x_{aw} at zero, through w. In fact, $(x_U, x_{aw}) = (x^*, 0)$ implies $\hat{x} = x$ and, by contraction, $x = x^*$. Clearly, the two dynamics are coupled through $[\mathrm{sat}_M(u) - u]$ (zero when $\sigma(K(x_U, x^*)) = K(x_U, x^*)$) and w, which suggest limits in the stabilization performances achievable on x_{aw}.

3 Conclusions

We believe that the antiwindup approach proposed above is an effective framework to solve simple regulation problems on a large class of Hamiltonian systems which show an incremental passivity property like, for instance, electromechanical systems. An example with ad-hoc modifications and suitable selection of u and w is presented in the induction motor control in [5].

References

[1] M. V. Kothare, P. J. Campo, M. Morari, and C. N. Nett. A unified framework for the study of anti-windup designs. *Automatica*, 30:1869–1883, 1994.

[2] Federico Morabito, Andrew R. Teel, and Luca Zaccarian. Nonlinear antiwindup applied to euler-lagrange systems. *IEEE Transactions on Robotics*, 20(3):526–537, 2004.

[3] R. Ortega, A. J. Van Der Schaft, I. Mareels, B. Maschke, and Lss G. Y. Supelec. Putting energy back in control. *Contr. Syst. Magazine, IEEE*, 21(2):18–33, 2001.

[4] Alexey Pavlov and Lorenzo Marconi. Incremental passivity and output regulation. *Systems and Control Letters*, 57(5):400 – 409, 2008.

[5] R. Sepulchre, T. Davos, F. Jadot, and F. Malrait. Antiwindup design for induction motor control in the field weakening domain. *IEEE Trans. on Control Systems Technology,*, PP(99):1–15.

[6] L. Zaccarian and A.R. Teel. *Modern anti-windup synthesis: control augmentation for actuator saturation*. Princeton University Press, Princeton (NJ), 2011.

Identification and distributed control of large scale systems

Yue Qiu[†] , Jan-Willem van Wingerden[†], Martin van Gijzen [‡] and Michel Verhaegen [†]

[†] Delft Center for System and Control, Delft University of Technology
Mekelweg 2, 2628 CD, Delft, the Netherlands
[‡]Delft Institute of Applied Mathematics, Delft University of Technology
Mekelweg 4, 2628 CD, Delft, the Netherlands

Email: {Y.Qiu, J.W.vanWingerden, M.B.vanGijzen}@tudelft.nl

1 Introduction

The control of spatially distributed interconnected systems is of great interest in practical applications such as flexible structures, wind farms, biochemical reactions, etc.. The biggest challenge in distributed control of spatially interconnected systems is the complexity of the control algorithms. The system matrix that describes the input-state-output behavior of N interconnected subsystems, with subsystems of order n, will be of size $nN \times nN$ matrix. Therefore conventional solution algorithms will require $O(n^3N^3)$ floating point operations (flops), which makes traditional controller synthesis expensive for fine discretization or large number of distributed subsystems. To surmount this obstacle, a lot of research has been done during the past decade. Sequentially Semi-Separable(SSS) matrix provide an effective approach and this structured space matrix allows for decoupling of distributed controllers, thus distributed controllers can be designed separately. In [1], some efficient algorithms have been developed to do controller synthesis of 1-D system in $O(n^3N)$ flops, which is a linear computational complexity. To extend this to multi-dimensional systems, our research focuses on designing a fast solver for multi-level SSS matrices of linear computational complexity for 2-D systems, which is a big challenge for controller synthesis that requires advanced concepts form numerical linear algebra. This fast solver for multi-level SSS matrices can be applied for identification and distributed control of wind farm.

2 Distributed Control of Large-Scale Systems

In [1], some efficient algorithms for SSS matrix operation of linear computational complexity are designed for distributed control of 1-D systems as shown in Figure 1. To extend his research, we consider the 2-D spatially distributed interconnected subsystems, which are shown in Figure 2. By utilizing methods described in [1], we can first assemble the 1-D string system $\overline{\Sigma_s}$ to a state-space model. The matrices of $\overline{\Sigma_s}$ all have an SSS matrix structure. Then the 2-D distributed system is equivalent to another 1-D distributed system, with subsystems $\overline{\Sigma_s}$. Therefore, the matrices of the state-space model all have a multi-level SSS matrix structure, that is, generators of this type of matrix have an SSS matrix structure. These matrices are of size $nMN \times nMN$, where M and N are the number of subsystems along the vertical and horizon direction, respectively. The structured matrix approach of distributed control has the property that the distributed controller is decoupled and can therefore be designed separately, which leads to a flexible controller configuration.

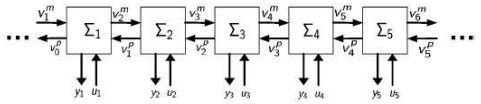

Figure 1: 1-D spatially distributed interconnected system structure

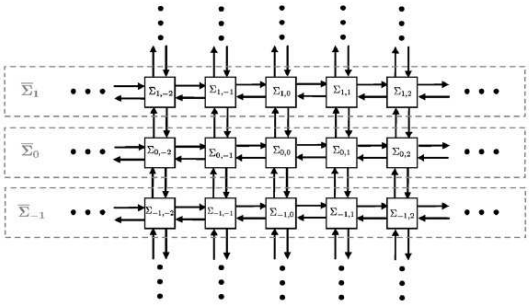

Figure 2: 2-D spatially distributed interconnected system structure

3 Expectation

Ordinary matrix operations have computational complexity of $O\big((nMN)^3\big)$, which is prohibitive for controller synthesis. The goal of this research is to develop a fast solver for multi-level SSS matrices that has linear computational complexity, and to apply this fast solver to the distributed control of wind farms with the same structure as the 2-D system shown in Figure 2.

References

[1] J. K. Rice. *Efficient Algorithms for Distributed Control: A Structured Matrix Approach*. PhD thesis, Delft University of Technology, 2010.

Modelling and identification of a double closed-loop industrial wet grinding circuit

Mose Mukepe Kahilu and Michel Kinnaert
Department of Automatic Control and Systems Analysis
Université Libre de Bruxelles (ULB)
CP165/55, 50 Av F.D.Roosevelt, 1050 Brussels
Belgium
Email: mmukepek@ulb.ac.be, michel.kinnaert@ulb.ac.be

The Kolwezi Concentrator (KZC) from Gécamines Company in the Democratic Republic of Congo is an industrial wet grinding process consisting of a double closed-loop circuit composed mainly of one rod mill, two ball mills, two hydrocyclones classifiers, one pump sump, one pump, one slurry distributor and several pipes and channels for material transport. For regulation purposes, product particle size, product flow rate and product density are regarded as controlled variables while fresh ore feed rate (u_1), rod mill feed water and dilution water flow rate (u_2 and u_3) are the three manipulated variables. The KZC circuit can be considered as a multi-input multi-output dynamical system with couplings, time delays, strong external disturbances such as ore hardness and feed particle size variations, and internal disturbances caused by model mismatch (see [1]).

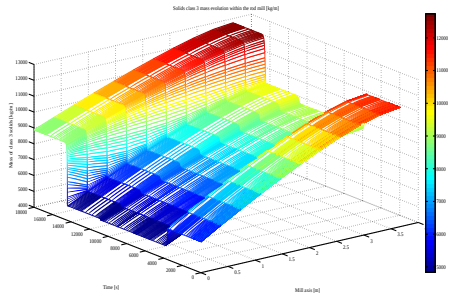

Figure 1: Time-axial position evolution of the mass of solid class 3 within the rod mill

In this work, a phenomenological approach combining population mass balance and pulp dynamics transport is used for rod mill and ball mill modelling. This leads to non-linear partial differential equations (PDE) (see [2]) containing six parameters for each mill. A steady-state model is sufficient to describe the hydrocyclones classifiers. The other components of the KZC flowsheet are simply considered as time delay elements. All model parameters are determined from experimental data by using the non-linear least squares algorithm. Both a steady-state simulator and dynamical simulator based on three classes of particle sizes have been developed within the MATLAB/SIMULINK software. The steady-state simulator is based on an analytical solution of the steady-state equations. For the dynamical simulator, the method of lines is used to transform the PDE of each mill into a set of ordinary differential equations which is solved by means of the ODE15s solver from MATLAB.

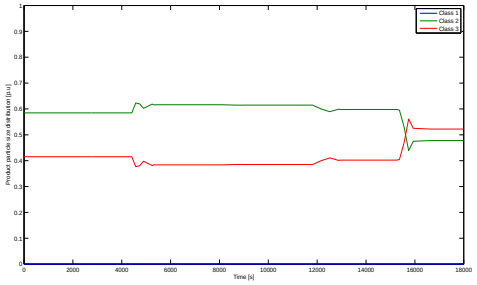

Figure 2: Time evolution of product particle size distribution, class 1 (in blue), class 2 (in green) and class 3 or fineness (in red)

The simulation results are close to the data observed in practice, which allows us to validate our mathematical models. Figure 1 shows the 3-D space evolution of class 3 (fineness) mass within the rod mill and figure 2 shows the time evolution of the particle sizes at the circuit output after step variations of u_1 (t/h) at $t = 3600$ s, u_2 (m^3/h) at t=7200 s, u_3 (m^3/h) at $t = 9000$ s, ore hardness at $t = 10800$ s and feed particle size at $t = 14400$ s.

References

[1] J. Yang, S. Li, X. Chen and Q. Li. Disturbance rejection of ball mill grinding circuits using DOB and MPC. itPowder Technology, 198:219-228, 2010.

[2] R. Lepore. Nonlinear optimization-based control techniques applied to cement grinding and polymerization processes. PhD Thesis, Faculté Polytechnique de Mons, 2006.

Computing $\mathscr{H}_2$ norms and their derivatives for time-delay systems, using Krylov based model order reduction

Jelle Peeters, Wim Michiels
Department of Computer Science, Katholieke Universiteit Leuven,
Celestijnenlaan 200A, B-3001 Heverlee, Belgium
Email: {jelle.peeters, wim.michiels}@cs.kuleuven.be

1 Introduction

The $\mathscr{H}_2$ norm plays an important role in the field of systems and control as a robustness measure with respect to noise or external disturbances and has numerous applications in many fields, such as robust optimization and $\mathscr{H}_2$ optimal control. For time-delay systems with transfer function

$$\gamma(s) := C(sI - \Sigma_{i=0}^{m} A_i e^{-s\tau_i})^{-1} B,$$

it was shown in [1], that the $\mathscr{H}_2$ norm $||\gamma(s)||_2$ can be calculated by rewriting the time-delay system in a linear infinite-dimensional form and applying a spectral discretization to become a system without delay. The $\mathscr{H}_2$ norm of this (larger) standard LTI system, $||\gamma_N(s)||_2$, can be easily calculated, resulting in an approximation for $||\gamma(s)||_2$. Downside of this method is the fact that the discretized model is of order nN, with n the size of the original time-delay system and N the number of discretization points. In [2], a Krylov based model order reduction technique for time-delay systems is suggested which allows to reduce the order of the discretized model further down to a chosen value $k << N$, matching several moments of $\gamma(s)$ and $\gamma_N(s)$ around zero and infinity. Our approach builds on this technique and extends it into a two-sided Krylov method. This not only allows to choose smaller values of k as we match double the amount of moments, but more importantly also to efficiently calculate derivatives of the $\mathscr{H}_2$ norm w.r.t. matrices of the original time-delay system.

2 Contributions

The idea behind the approach consists of discretizing a delay system of order n into a standard linear system of the form

$$G_N \dot{z}(t) = z(t) + H_N u(t), \quad y(t) = F_N z(t), \quad z(t) \in \mathbb{R}^{nN \times nN},$$

in such a way that several moments at zero and infinity are preserved. Subsequently, the system matrices F_N, G_N, H_N are projected on the Krylov spaces $\mathscr{K}_k(G_N, H_N)$ and $\mathscr{K}_k(G_N^T, (G_N^T)^{-1} F_N)$ as

$$\hat{F} = F_N V, \qquad \hat{G} = W^T G_N V, \qquad \hat{H} = W^T H_N,$$

where V, W contain the vectors respectively spanning the right and left Krylov spaces and $\hat{F}, \hat{G}, \hat{H}$ the system matrices of the reduced model of dimension k, such that these moments are again preserved, as shown in Fig 1. Moreover, our construction is such that the matrices of the reduced system are *independent of* N as long as $N > 2k$, hence the implementation does not involve a choice of N. As the reduced order system closely approximates the original time-delay system, we can approximate $||\gamma(s)||_2$ in function of the small matrices $\hat{F}, \hat{G}, \hat{H}$ of the reduced model.

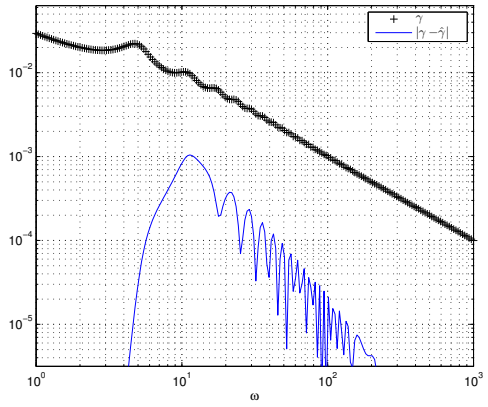

Figure 1: Frequency response and error after reducing a time-delay system or order $n = 100$ to a reduced model of order $k = 10$. Notice a smaller error around zero and towards infinity.

By constructing both a right and left Krylov space of G_N, we are able to not only evaluate the $\mathscr{H}_2$ norm, but also its *derivatives* w.r.t. the system matrices A_i, B, C in function of $\hat{F}, \hat{G}, \hat{H}$, thus again independently of N. For low-order feedback control, control parameters typically appear in the system matrices A_i, B, C, therefore being able to express and efficiently evaluate elements of $\frac{\partial(\gamma^2)}{\partial A_i}, \frac{\partial(\gamma^2)}{\partial B}, \frac{\partial(\gamma^2)}{\partial C}$ is most interesting from optimization and control point of view.

References

[1] J. Vanbiervliet, W. Michiels and E. Jarlebring, *Using spectral discretization for the optimal $\mathscr{H}_2$ design of time-delay systems*, Int. J. Control, 84(2):228-241, 2011.

[2] W. Michiels, E. Jarlebring and K. Meerbergen, *Krylov based model order reduction of time-delay systems*, SIAM J. Matrix Anal. Appl. 32(4):1399-1421, 2011.

Interacting multi-agent systems

Rahayu Prihatin
Department of Applied Mathematics
University of Twente
P.O. Box 217, 7500 AE Enschede
The Netherlands
Email: r.prihatin@ewi.utwente.nl

Anton Stoorvogel
Department of Applied Mathematics
University of Twente
P.O. Box 217, 7500 AE Enschede
The Netherlands
Email: a.a.stoorvogel@utwente.nl

1 Introduction

Decentralized control systems are characterized by systems that are made up of smaller systems, or agents, which have only indirect information about the other systems. That is, agents do not share the same measurements nor does one agent know the inputs to all the other agents. Examples of decentralized systems are abundant and include power systems, economic systems, and systems of multiple autonomous agents, to name a few. Control of such systems has been the subject of much research since Wang and Davison's seminal paper [2] in 1973, in which they prove necessary and sufficient conditions for stabilization of linear, time-invariant (LTI) decentralized systems by LTI controllers.

In some cases the agents have no interaction and the interaction only comes from a common objective. This is a very active research area anf early results were reported in [1]. In this presentation, however, we investigate agents which do have interaction between the different agents. In other words, we have agents whose dynamics interact and the interaction is not solely coming from a common objective.

2 Problem formulation

We consider systems of the form:

$$\dot{x}_i = A_i x_i + B_i u_i + \sum_{j=1}^{N} E_{ij} y_j$$

$$y_i = C_i x_i$$

We first consider the relatively simple case where we need to design a protocol for agent i with only local measurements y_i and local input u_i. It can be shown that the minimum-phase property of (A_i, B_i, C_i) guarantees that we can obtain stabilization of systems. Next, we consider the more general case where agent i has measurement:

$$z_i = \sum_{j=1}^{N} g_{ij} y_j$$

and we need a protocol to design u_i. In that case, we investigate different objectives. The first case is consensus where we require $y_i - y_j$ converges to zero for all i and j. The second objective is regulation where we have a reference signal r and we want to obtain that $y_i - r$ converges to zero for all i. In the latter case, we obviously need that at least some agents have access to the reference signal. Clearly results in the latter case also requires knowledge about the reference signal. In this presentation we concentrate on sinusoidal reference signals.

3 Results

This first case with only local measurements has been completely resolved. We will also present preliminary results for the second class of problems.

References

[1] J.A. FAX AND R.M. MURRAY, "Information flow and cooperative control of vehicle formations", IEEE Trans. Aut. Contr., 49 (2004), pp. 1465–1476.

[2] S.H. WANG AND E.J. DAVISON, "On the stabilization of decentralized control systems", IEEE Trans. Aut. Contr., 18 (1973), pp. 473–478.

Controllability of Diffusively Coupled Multi-Agent Systems with Switching Topologies

S. Zhang, M. K. Camlibel and M. Cao

Faculty of Mathematics and Natural Sciences, University of Groningen, Nijenborgh 4, 9747AG Groningen, the Netherlands

Email: {shuo.zhang, m.k.camlibel, m.cao}@rug.nl

1 Diffusively coupled multi-agent systems with switching topologies

Let $G_i = (V, E_i)$ with $i \in \{1, 2, \ldots, p\}$ be simple, undirected graphs where $V = \{1, 2, \ldots, n\}$ is the vertex set and $E_i \subseteq V \times V$ is the edge set. For each G_i, we group vertices into two categories as follows: let $V_{\mathrm{L}}^i = \{\ell_1^i, \ldots, \ell_{m_i}^i\} \subseteq V$ and $V_{\mathrm{F}}^i = V \setminus V_{\mathrm{L}}^i$. Then the diffusively coupled multi-agent system associated with G_i can be given by

$$\dot{x}_j = -\sum_{(j,k)\in E_i} (x_j - x_k), \text{ if } j \in V_{\mathrm{F}}^i$$
$$\dot{x}_j = -\sum_{(j,k)\in E_i} (x_j - x_k) + u_j, \text{ if } j \in V_{\mathrm{L}}^i$$

where $x_j \in \mathbb{R}$ is the state of agent j and $u_j \in \mathbb{R}$ is the external input to agent j.

By defining $x = \begin{bmatrix} x_1 & \ldots & x_n \end{bmatrix}^T$ and $u = \begin{bmatrix} u_1 & \ldots & u_n \end{bmatrix}^T$, this system can be written into a compact form

$$\dot{x} = -L_i x + M_i u_i$$

where L_i is the Laplacian matrix of G_i and $M_i \in \mathbb{R}^{n\times n}$ is defined by

$$[M_i]_{jk} = \begin{cases} 1 & \text{if } j = \ell_k^i \\ 0 & \text{otherwise.} \end{cases}$$

In this note, we consider the switched multi-agent system given by

$$\dot{x}(t) = -L_{\sigma(t)} x(t) + M_{\sigma(t)} u(t), \tag{1}$$

where $\sigma(t) : \mathbb{R}_+ \to \{1, 2, \ldots, p\}$ is a right-continuous piecewise constant *switching signal*.

2 Graph partitions

We quickly review graph partitions that will be used in the sequel. More details can be found in [1]. Any nonempty subset of the vertex set V is called a *cell*. A collection of mutually disjoint cells $\pi = \{C_1, \ldots, C_r\}$ is said to be a *partition* of V if $\bigcup_{j=1}^r C_j = V$. Let Π denote the set of all the partitions of V. A partition π_1 is said to be *finer* than a partition π_2, denoted by $\pi_1 \leqslant \pi_2$, if each cell of π_1 is a subset of some cell of π_2.

Let $\Pi_{\mathrm{AEP}}(G)$ denote the set of all almost equitable partitions of a given graph $G = (V, E)$ [1]. For the collection of graphs $\{G_1, \ldots, G_p\}$, define

$$\Pi_{\mathrm{AEP}}(\pi_1, \ldots, \pi_p) = \{\pi \mid \pi \in \Pi_{\mathrm{AEP}}(G_i) \text{ and } \pi \leqslant \pi_i \text{ for all } i\} \tag{2}$$

where π_i is a given partition of G_i. It can be shown that there exists a unique partition, say $\pi^* = \pi^*(\pi_1, \ldots, \pi_p)$, such that

$$\pi^* \in \Pi_{\mathrm{AEP}}(\pi_1, \ldots, \pi_p)$$
$$\pi \leqslant \pi^* \text{ for all } \pi \in \Pi_{\mathrm{AEP}}(\pi_1, \ldots, \pi_p)$$
$$\pi \leqslant \pi' \text{ for all } \pi \in \Pi_{\mathrm{AEP}}(\pi_1, \ldots, \pi_p) \implies \pi^* \leqslant \pi'.$$

We denote the distance partition relative to a vertex v of a graph G by $\pi_{\mathrm{D}}(v; G)$ (see [1] for more details).

3 Main results

Let $\mathscr{K}$ denote the controllable subspace of the system (1). Then, we prove that

$$\mathscr{K} \subseteq \operatorname{im} P(\pi^*(\pi_1^{\mathrm{L}}, \ldots, \pi_p^{\mathrm{L}})) \tag{3}$$

where π_i^{L} is the partition $\{\{\ell_1^i\}, \ldots, \{\ell_{m_i}^i\}, V_{\mathrm{F}}^i\}$ and $P(\pi)$ denotes the characteristic matrix of the partition π. After this upper bound in terms of the almost equitable partitions, we prove the following lower bound on the dimension of the controllable subspace $\mathscr{K}$:

$$\dim(\mathscr{K}) \geqslant \max_{\substack{i \in \{1,2,\ldots,p\} \\ k \in \{1,2,\ldots,m_i\}}} \operatorname{card}(\pi_{\mathrm{D}}(\ell_k^i; G_i)). \tag{4}$$

Moreover, these two bounds are tight in the sense that there are examples for which one of them is attained whereas the other holds strictly. Such examples will also be provided in the presentation.

References

[1] S. Zhang, M. K. Camlibel and M. Cao. "Controllability of diffusively-coupled multi-agent systems with general and distance regular coupling topologies". *Proc. of the 50th IEEE Conference on Decision and Control and 2011 European Control Conference,* 759-764, 2011

Performance of a synchronized community detection algorithm

A.Browet
ICTEAM, UCLouvain
4 Av. G. Lemaître
1348 Louvain-la-Neuve
Belgium
arnaud.browet@uclouvain.be

P.-A. Absil
ICTEAM, UCLouvain
4 Av. G. Lemaître
1348 Louvain-la-Neuve
Belgium

P. Van Dooren
ICTEAM, UCLouvain
4 Av. G. Lemaître
1348 Louvain-la-Neuve
Belgium

Networks are everywhere. In many applications, they are used to represent interactions between the different elements of interest. But at the same time as theoretical knowledge and practical tools of graph theory were developed, network sizes grew tremendously. Social networks, which were studied for a few dozens of individuals, are now composed of millions of people sharing online friendships; mobile phone networks have a penetration rate that grew from around 20% in the late nineties to almost 100% nowadays in developed countries; biological networks such as protein-to-protein interactions, may have billions of nodes; etc.

Many network properties (degree distribution, average distance or flow propagation for example) have been studied extensively. A key feature of real networks lies in the non-homogeneous local distribution of edges. Each node tends to be more densely connected with a specific subset of the vertices of the graph than with the rest of the network. These structural organizations of nodes are called communities.

Extracting communities from large networks have been a challenging problem for years, and a popular class of methods consists of optimizing the so-called modularity. This quality function introduced by Newman and Girvan [1] defines good communities as group of nodes with an internal edge density larger than the associated density expected from the degree distribution of the graph. Optimizing the modularity has been shown to be a NP-hard problem and while many heuristics have been developed for specific contexts, a lot of them are not suitable for more general framework due to their computational requirements or the structure of the network. The Louvain method [2] provides a good tradeoff between the complexity of the algorithm and the quality of the clustering. However the method still struggles to extract community structures for very large networks and is not suitable for parallel implementation.

We propose a synchronized version of the Louvain method where the synchronization also allows an efficient parallelization of the algorithm. Even if our implementation is built upon modularity maximization, we point out that our algorithm is also suitable for different quality functions like the Potts model of Reichardt and Bornholdt for example. First, each node chooses an assignment to one of its neighbors, independently of the choice of the other nodes, based on the local gain of the quality function to merge the two nodes. Communities are then defined as the connected components in this directed assignment graph. Then, knowing the local decision of each node, we build a recursive synchronized correction step designed to guarantee some global convergence of the method. Three levels of correction are proposed: first we impose that the sum of the global gains for each community must be positive; we also impose that the gain of assigning each node to its community must be positive; the last correction level imposes that the gain to assign a node to its community is larger than the gain to assign it to any other community. Those correction levels may produce switches of nodes between communities but also merge and split of communities. Finally, when a steady state has been found, communities are aggregated to form a new graph where each node represents a community and each vertex is the sum of the edges between two communities.

We compare the results of our algorithm on the popular benchmark of Lancichinetti and Fortunato [3] with the classical Louvain method, the fast modularity algorithm by Clauset and the Infomap algorithm by Rosvall (not based on modularity optimization). Results show that our algorithm is able to produce good community structure of comparable quality with the other methods. On the other hand, we demonstrate that the computational cost required by our method is considerably lower than for the other methods, indicating that our solution might be very appropriate to initialize a finer tuning of the communities when required.

References

[1] M. E. J. Newman, and M. Girvan, “Finding and evaluating community structure in networks,” Physical Review E - Statistical, Nonlinear and Soft Matter Physics, 2003.

[2] V. D. Blondel, J.-L. Guillaume, R. Lambiotte, and E. Lefebvre, “Fast unfolding of communities in large networks,” Journal of Statistical Mechanics: Theory and Experiment, 2008.

[3] A. Lancichinetti, and S. Fortunato, “Benchmarks for testing community detection algorithms on directed and weighted graphs with overlapping communities,” Physical Review E, 2009.

Stability and synchronization analysis of multi-agent systems with switching topologies

N. Monshizadeh H.L. Trentelman M.K. Camlibel

J. B. Inst. for Mathematics and Computer Science, University of Groningen, The Netherlands

{n.monshizadeh@rug.nl, h.l.trentelman@math.rug.nl, m.k.camlibel@rug.nl}

1 Introduction

The distributed control of multi-agent systems has gained lots of attention during the last decade. In particular, consensus problem has been widely investigated for networks of agents. The pioneering works in this regard have been carried out for the case where the agents' dynamics are single or double integrators. An excellent review can be found in [2]. The consensus results for the case where the agents have a general, yet identical, linear dynamics with time-independent communication topology are reported in [1].

Despite the extensive amount of research available in the context of consensus/synchronization of multi-agent systems, there are few works which have considered network of agents with general linear dynamics together with time-dependent communication topology (see e.g. [3]).

In this talk, we consider the network of agents with general, but identical, linear dynamics, and the communication topology may switch within a set of admissible topologies. We allow switching to be arbitrary meaning that the switching may occur at arbitrary time instances. It will be observed that synchronization is essentially an *output stability* problem. Given the agents' dynamics, coupling rule, and set of admissible topologies, we derive conditions under which synchronization is achieved.

2 Preliminaries

Let $G_i = (V, E_i)$ with $i = 1, 2, \ldots, N$ be an undirected (unweighted) graph where $V = \{1, 2, \ldots, p\}$ is the vertex set and $E_i \subseteq V \times V$ is the edge set. A diffusively coupled multi-agent system with switching topology consists of a collection of identical linear input/state/output systems given by

$$\dot{x}_j(t) = Ax_j(t) + Bu_j(t) \tag{1a}$$
$$y_j(t) = Cx_j(t) \tag{1b}$$

together with the diffusive coupling rule

$$u_j(t) = \sum_{(i,j)\in E_{\sigma(t)}} (y_i(t) - y_j(t)), \tag{1c}$$

where $j \in V$, $x_j \in \mathbb{R}^n$ is the state of agent j, σ is a right-continuous piecewise constant function of time taking its value from the index set $\{1, 2, \ldots, N\}$, and $u_j \in \mathbb{R}^m$ is the diffusive coupling term. For each $i = 1, 2, \ldots, N$, let L_i denote the Laplacian matrix corresponding to the graph $G_i = (V, E_i)$. Then, the multi-agent system (1) can be written in the compact form of

$$\dot{x}(t) = \mathscr{A}_{\sigma(t)} x(t), \tag{2}$$

where $x = \mathrm{col}(x_1, \ldots, x_p)$, and $\mathscr{A}_{\sigma(t)} := I_p \otimes A - L_{\sigma(t)} \otimes BC$, where "$\otimes$" denotes the Kronecker product.

We say the multi-agent system (1) is *synchronized* if every solution of (2) satisfies $\lim_{t\to\infty}(x_j(t) - x_k(t)) = 0$ for all $j, k = 1, 2, \ldots, p$.

3 Main Contribution

As mentioned earlier, several conditions to guarantee the synchronization of network (2) are provided in this talk. The proposed conditions are mostly derived form the following crucial result.

Theorem 3.1 *Consider the network* (2)*. Let the eigenvalues of L_i be denoted as $0 = \lambda_1^i \leqslant \lambda_2^i \leqslant \lambda_3^i \leqslant \ldots \leqslant \lambda_p^i$, for each $i = 1, 2, \ldots, N$. Let $\underline{\lambda}$ and $\overline{\lambda}$ denote the minimum and maximum values of λ_j^i, for $i \in \{1, 2, \ldots, N\}$ and $j \in \{2, 3, \ldots, p\}$, respectively. Then, the network* (2) *is synchronized if there exists a common quadratic Lyapunov function for the pair of matrices $A - \underline{\lambda}BC$ and $A - \overline{\lambda}BC$.*

References

[1] Z.-K. Li, Z.-S. Duan, G.-R. Chen, and L. Huang. Consensus of multiagent systems and synchronization of complex networks: a unified viewpoint. *IEEE Transactions on Circuits and Systems*, 57(1):213–224, 2010.

[2] R. Olfati-Saber, J. A. Fax, and R.M. Murray. Consensus and cooperation in networked multi-agent systems. *Proceedings of the IEEE*, 95(1):215–233, 2007.

[3] L. Scardovia and R. Sepulchreb. Synchronization in networks of identical linear systems. *Automatica*, 14(11):2557–2562, 2009.

Consensus on nonlinear spaces and graph coloring

A.Sarlette
Ghent University
alain.sarlette@ugent.be

1 Context and idea

Dynamical systems where agents interact with each other according to a graph structure have recently drawn a lot of attention. For instance, "consensus" studies a problem where agents attract each other to finally all have the same state. Interactions among agents is thereby defined by an externally imposed graph. For agents in $\mathbb{R}^k$, the issue is to find minimal requirements on the interconnection graph – that can be directed and time-varying way – guaranteeing convergence of all agents to a common state; see e.g. [1, 2]. For agents on nonlinear spaces, like a sphere, the problem can be difficult also for fixed undirected graphs: although the interconnected system converges towards an equilibrium set, determining all stable equilibria as a function of graph properties is an open problem [3]; the dual problem of repulsive agents is similar.

The broad research field of *analog computation* relaxes discrete computational questions to a continuous state space, and lets a dynamical system evolving on this state space converge to a "solution" of the algorithmic problem. The link is obvious through optimization problems, but this requires introducing a problem-specific geometry; see e.g. [4, 5] in the control community.

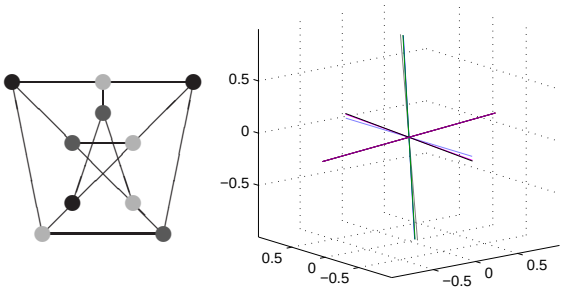

It is then tempting to link one of the many graph-based computational problems, to simple dynamical systems with agents interacting according to the same graph. We make this link between

- *graph k-coloring* (see figure, left): k colors are available to 'color' the nodes of a graph; two nodes that are connected by a graph edge must always have different colors.
- repulsive agents on projective space (see figure, right): a geometry is taken where each agent state can be visualized as representing a line of $\mathbb{R}^k$. A distance measure is defined between any two such lines, and agents move in order to maximize the distance to their graph-defined neighbors.

2 Results

Let S_o denote that the agent states belong to a set of mutually orthogonal lines of $\mathbb{R}^k$. Consider the question, taking a graph as argument: Does the system of repulsive agents have a stable equilibrium in S_o?

We show that answering this question is as difficult as deciding k-colorability of the graph. Thus, for $k > 2$, characterizing the stable equilibria of repulsive agents on projective space is NP-hard in the number of agents. The Bell-Kochen-Specker Theorem developed in the context of quantum systems, implies that unfortunately the converse reasoning does not help: Letting a swarm of repulsive agents reach a globally stable equilibrium, does not necessarily solve graph coloring. See [6] for more details.

Acknowledgments

This talk presents research results of the Belgian Network DYSCO (Dynamical Systems, Control, and Optimization), funded by the Interuniversity Attraction Poles Program, initiated by the Belgian State, Science Policy Office. The author did most of this work as an FNRS postdoctoral researcher at University of Liège.

References

[1] J.N. Tsitsiklis, *Problems in decentralized decision making and computation*, PhD Thesis, MIT (1984).

[2] V.D. Blondel et al., *Convergence in multiagent coordination, consensus and flocking*, Proc. 44th IEEE Conf. Decision and Control, 2996-3000 (2005).

[3] A. Sarlette and R. Sepulchre, *Consensus optimization on manifolds*, SIAM J. Control and Optimization 48,1 : 56–76 (2009).

[4] R.W. Brockett, *Dynamical systems that sort lists, diagonalize matrices, and solve linear programming problems*, Lin. Alg. Appl. 146: 79–91 (1991).

[5] P-A. Absil and R. Sepulchre, *Continuous dynamical systems that realize discrete optimization on the hypercube*, Systems & Control Letters 52 : 297–304 (2004).

[6] A. Sarlette, *Consensus on nonlinear spaces and graph coloring*, Proc. 50th IEEE Conf. Decision and Control, 4885-4890 (2011).

Real-time Control of Electrical Power Systems

Ana Virag, Andrej Jokić, Paul van den Bosch
Department of Electrical Engineering, Eindhoven University of Technology
P.O. Box 513, 5600 MB Eindhoven, The Netherlands, Email: a.virag@tue.nl

1 Introduction

As a market commodity, electricity is characterized by several unique and important features: *i)* the inability of efficiently storing large quantities of energy, which, as a consequence, leads to *ii)* the necessity for supply to meet the demand in real-time (power balancing), and *iii)* the transportation of power through a transmission system of limited capacity. Currently, *i)* and *ii)* are handled by real-time power balancing, primary and secondary control. They are the essentially the same service, with different time frame. Load frequency control (LFC) takes into account limitations of the transmission system, i.e. *iii)*, by controlling the total sum of flows of all tie-lines connected to a control area. The current implementation is shown in Fig. 1.

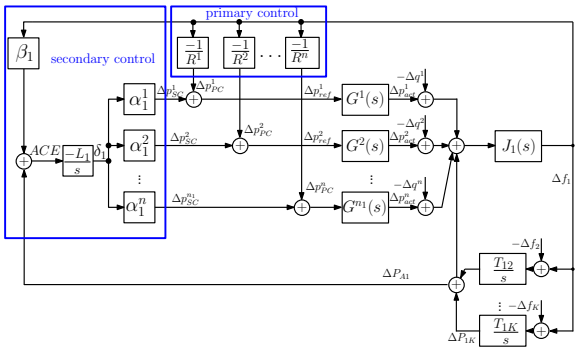

Figure 1: Representation of a power system control area, based on [1] and [2].

2 Inefficiencies in the system

In this work, we focus on the inefficiencies of current real-time balancing of power systems and propose an alternative solution. Table 1 summarizes the inefficiencies. Each inefficiency is accompanied by a proposal for improving the system.

3 Proposed solutions

Our approach is based on the introduction of double-sided markets for provision of LFC, conceptually introduced in [3], and their real-time implementation, see Table 1. We propose ancillary service (AS) markets which deliver the needed ancillary services, i.e. LFC, such that in real-time an optimal solution exists for any considered power disturbance, without violating network constraints. Focus is on the real-time control structure which enables consistent implementation of AS contracts made in forward time AS markets. We explain how these changes influence current LFC implementation and which new commodities are to be created to increase the efficiency and the reliability of the system. We argue that by changing the participation factors in secondary control provision in real-time, transmission constraints can explicitly be taken into account. The presented real-time control structure is compared with the currently existing solutions.

INEFFICIENCY	**ALTERNATIVE**
transmission constraints not explicitly taken into account during procurement of reserve capacity	creating markets for secondary control ancillary services, which take into account position in the grid
single-buyer market for secondary control	creating two-sided market for secondary control
provision of primary control not (adequately) rewarded	creating markets for primary control with droop gain as commodity
available transmission capacity calculated in a conservative way	taking transmission constraints in an explicit manner, per transmission line; better cooperation of control areas

Table 1: List of inefficiencies in the current system and proposed improvements.

Acknowledgment

This work was supported by the European Commission Research Project FP7-ICT-249096 *Price-based Control of Electrical Power Systems (E-Price)*, www.e-price-project.eu.

References

[1] P. Kundur, "Power System Stability and Control," 1994, McGraw-Hill Professional, ISBN 007035958X

[2] ENTSO-E, "UCTE Operation Handbook", 2004, available at https://www.entsoe.eu

[3] P.P.J. van den Bosch et al., "Reduced risks and improved economic operation of ancillary services", 2010, the 7th International Conference on the European Energy Market

Boiling-based thermal conditioning in battery electric vehicles

R.W. van Gils*,[1], M.F.M. Speetjens[2] and H. Nijmeijer[1]
Eindhoven University of Technology, PO Box 513, 5600 MB Eindhoven
Department of Mechanical Engineering,[1]Dynamics and Control, [2]Energy Technology
Email: *r.w.v.gils@tue.nl

1 Introduction

Nonuniform and elevated temperature distributions within a battery pack of a battery electric vehicle (BEV) can be harmful to the battery, see [1]. Boiling heat transfer has great potential to overcome these thermal issues as it allows for (i) large cooling capacities, (ii) a high degree of temperature uniformity and (iii) efficient waste heat recovery. However, applying boiling to its fullest efficiency, requires stabilisation of unstable modes. In this study, a model-based controller to stabilise these unstable modes is designed.

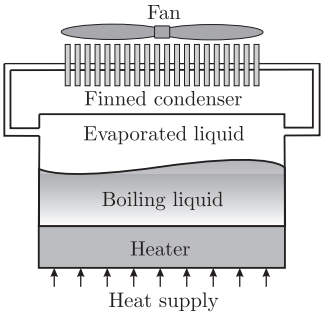

Figure 1: Schematic representation of a pool-boiling system.

2 Model description

A pool-boiling system, see Figure 1, may serve as physical model for thermal-conditioning applications based on boiling heat transfer. The two-dimensional (2D) pool-boiling model to represent the thermal management scheme describes the heat transfer within the heater, i.e. the battery cell wall, see Figure 2, by

$$\frac{\partial T}{\partial t}(x,y,t) = \alpha \nabla^2 T(x,y,t), \tag{1}$$

with the boundary conditions

$$\left.\frac{\partial T}{\partial x}\right|_{x=0,L} = 0, \quad \left.\frac{\partial T}{\partial y}\right|_{y=0} = -\frac{1}{\lambda}(Q_H + u(t)), \tag{2}$$

$$\left.\frac{\partial T}{\partial y}\right|_{y=H} = -\frac{1}{\lambda} q_F(T_F), \tag{3}$$

with λ and α the thermal conductivity and diffusivity of the heater, respectively, L and H its length and height, $T_F := T(x,H,t)$ the fluid-heater interface temperature, $q_F(T_F)$ a nonlinear relation that describes the heat flux from heater to boiling liquid, $u(t)$ the (uniform) system input and Q_H the nominal heat generation of the battery cell, also see [1].

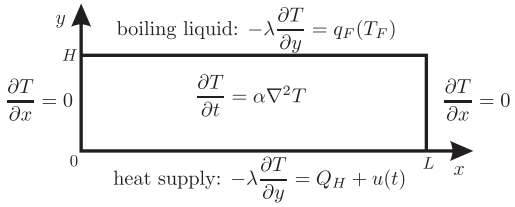

Figure 2: Pool-boiling model.

3 Control strategy

Stabilisation of the unstable modes is to be accomplished by variation $u(t)$ of the pressure in the boiling chamber. The intended control strategy is a feedback law, based on the error $v(x,y,t) = T(x,y,t) - T_\infty(x,y)$ between the heater temperature $T(x,y,t)$ and its desired distribution $T_\infty(x,y)$, given by

$$u(t) = \int_0^H \int_0^L v(x,y,t) g(x,y) \mathrm{d}x\mathrm{d}y. \tag{4}$$

Here, $g(x,y)$ is the feedback weight function with which the properties of the feedback law, and thus the closed-loop system, will be prescribed. In order to be able to apply this kind of feedback law to the system, an observer that estimates the system state is implemented. This observer is an exact copy of the system (1) – (3) with output error injection in (3).
It turns out that the unstable modes can only be stabilised for specific combinations of the heater properties λ, α (heater material) and L, H (heater dimensions), when Q_H (nominal heat generation) is given. This means that in the design of a thermal management system for BEVs, it is important to determine the typical value for the heat generation Q_H and choose heater dimensions and material accordingly.

4 Future work

First exploratory experiments will be carried out in the (near) future, to see whether boiling heat transfer can indeed thermally condition battery packs in BEVs.

Acknowledgements

This research is funded by the HTAS-REI (Range Extender Innovations) project.

References

[1] R. van Gils, M. Speetjens, and H. Nijmeijer, *Boiling heat transfer in battery electric vehicles*, in EEVC 2011, Brussels, Belgium, October 26 – 18, 2011.

Idealized voltage control of variable reluctance actuators

A. Katalenic and C.M.M. van Lierop
Department of Electrical Engineering, Eindhoven University of Technology
P.O. Box 513, 5600MB Eindhoven, The Netherlands
Email: a.katalenic@tue.nl

1 Introduction

Current-mode control of variable reluctance actuators was shown to be very sensitive to disturbances, e.g. unknown air gap variations and hysteresis [1]. Those disturbances make the feed-forward models inaccurate, which raises performance limitations for the feed-back control. In this presentation, we propose a voltage based control strategy consisting of a high bandwidth analog sensing coil voltage control loop. With such a controller, the reluctance actuator behaves as an ideal transformer between the primary coil voltage and the sensing coil voltage. The actuator behavior between the input voltage and the air-gap magnetic flux is then modelable with a single integrator, i.e. parasitic effects such as hysteresis and air gap dependency are eliminated. Good correlation between the air gap magnetic flux and the actuator force [2] further motivates this approach. The control of the remaining drift and the set-point generation can be implemented in a digital computer.

2 Actuator model and control design

The first principle behavior of the primary coil circuit can be written as:

$$\frac{d\Phi}{dt} = \frac{1}{N}(u - R\cdot i). \tag{1}$$

It is clear from (1), that if the primary coil current can be measured and the resistance estimated, a new input signal $u = u^* + R_{est}\cdot i$ will yield the following primary coil circuit behavior:

$$\frac{d\Phi}{dt} = \frac{1}{N}\cdot u^* + \frac{\Delta R}{N} i, \tag{2}$$

where $\Delta R = R_{est} - R$, Φ is the magnetic flux encircled by the primary coil and N is the number of primary coil turns.

On the other hand, the voltage on the sensing coil, i.e. the secondary coil, can be written as:

$$u_{sc} = \frac{N_{sc}}{N} u^* - \Delta(s), \tag{3}$$

where N_{sc} is the number of secondary coil turns, and $\Delta(s) = \frac{N_{sc}}{N}(R - R_{est})i + N_{sc}\frac{d\Phi_{leak}}{dt} + ME(s)$ is an error component containing the resistance estimate error, the unknown leakage flux error, and the error due to the approximative nature of the used first-principle models. The sensing-coil voltage is measurable, and a high-bandwidth analog PI controller can be added to reduce the unknown model error

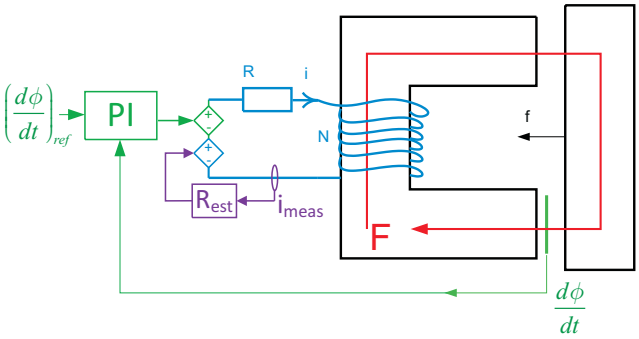

Figure 1: A sketch of the analog sensing coil voltage controller

$\Delta(s)$. Then, since the current in the sensing coil is negligible, $u_{sc} = N_{sc}\frac{d\Phi_{sc}}{dt}$, and the following holds:

$$\Phi_{sc} = \frac{1}{N}\int_0^t u^* dt. \tag{4}$$

The quadratic relationship between the magnetic flux picked up by the sensing coil and the attractive force produced by the actuator $F \approx k\cdot\Phi_{sc}^2$ yields the final model of the plant containing the analog control circuitry, the power amplifier and the reluctance actuator:

$$F = k\left(\frac{1}{N}\int_0^t u^* dt\right)^2. \tag{5}$$

The advantages and disadvantages of the obtained plant behavior, which contain issues with feed-forward and feed-back force control of (5), will be discussed in the presentation.

References

[1] A. Katalenic, C.M.M. van Lierop, P.P.J. van den Bosch,"On hysteresis and air gap disturbance in current and voltage mode feed-forward control of variable reluctance actuators," Proceedings Joint 50th IEEE conference on Decision and Control and European Control Conference, December 12-15, 2011, Orlando.

[2] F.J. Keith, "Implicit Flux Feedback Control for Magnetic Bearings,", PhD thesis, University of Virginia, 1993, Source: Dissertation Abstracts International, Volume: 54-08, Section: B, page: 4316.

Design and Active Structural Acoustic Control of an axisymmetric rotational inertia shaker

G. Zhao[1], G.Pinte[2], W. Symens[2], P. Sas[1]
Department of Mechanical Engineering, Division PMA, Katholieke Universiteit Leuven
Flanders' Mechatronic Technology Centre,
e-mail: guoying.zhao@mech.kuleuven.be

1 Introduction

Excessive noise radiation from a structure housing a rotating device is a common problem in many industrial applications such as gearboxes, compressors, etc.. In these applications the noise is often caused by a disturbance force acting on the rotating element. For the control of the noise radiation, several active solutions have already been tested. On the one hand, the vibro-acoustic response of the noise radiating surfaces of the housing can be controlled e.g. by smart panels with piezo-electric patches. A drawback of this solution is that an active element has to be installed on each radiating surface. On the other hand the disturbance forces can be blocked by the introduction of active elements in the force transmission paths towards these noise radiating surfaces e.g. by active bearings [1]. A drawback of this solution is that the installation of the active element in the force transmission path will affect the system's stiffness.

The goal of this research is therefore to develop an active component which generates secondary forces directly on the shaft. To this end, an axisymmetric rotational inertia shaker has been developed, which can be installed directly on the shaft as an add-on device parallel to the functional bearings. This shaker, which tackles the disturbance at its source, does not affect the machine stiffness.

2 Design

(a) **(b)**

Figure 1: (a) The axisymmetric rotational inertia shaker and (b) the experimental test bed

Figure 1(a) shows a photo of the developed rotational axisymmetric inertia shaker. This inertia shaker consists of a ring-shaped mass and a piezostack. Radial forces can be generated on a rotating shaft by accelerating the ring-shaped mass. The axisymmetric inertia shaker is tested on an experimental test bed comprising a rotating shaft, which is mounted in a frame (Figure 1(b)). Noise is radiated by a plate that is attached to the frame. The disturbance force is introduced by an electrodynamic shaker.

3 Adaptive shunt control

To evaluate the behaviour of the developed inertia shaker, an adaptive shunt circuit is developed for the control of the piezostack. This shunt circuit, consisting of operational amplifiers, passive electrical components such as (voltage-controlled) resistors, inductors and capacitors, emulates the impedance of a variable inductance [2]. Connecting such an inductance to the piezostack will create a strong noise reduction in a narrow frequency band. By adapting the inductance value of the shunt circuit, the suppressed frequency band can be adjusted depending on the vibration disturbance frequency.

The performance of the inertia shaker was first evaluated during non-rotating tests, where the orientation of the shaft was chosen such that the piezostack was oriented in the same direction as the disturbing force. When the virtual inductance was tuned optimally, a noise reduction of more than 15 dB was obtained. Afterwards, the performance has been also checked during a rotational test. As expected, a strong reduction, which is more or less the same as the value in the non-rotational test, can be obtained when the piezostack is in the same direction as the disturbance force, while there is nearly no reduction in the perpendicular direction to the disturbance.

4 Conclusions

An axisymmetric rotational inertia shaker has been developed and successfully applied to reduce the structure-borne noise radiation of a experimental test bed with a rotating element. Since the developed prototype consists of one piezo element and can only generate forces in one direction, future work consists of the design and control of a 2-dimensional axisymmetric rotational inertia shaker, which can generate shaft vibrations in all radial directions.

References

[1] G. Pinte, S. Devos, B. Stallaert, W. Symens, J. Swevers, P. Sas, *A piezo-based bearing for the active structural acoustic control of rotating machinery*, Journal of Sound and Vibration, Vol. 329, Iss. 9, P. 1235-1253 (2010)
[2] D. Niederberger, *Smart Damping Materials using Shunt Control*, PhD. thesis, Swiss Federal Institute of Technology (ETH), Zurich (2005)

Cooperative Adaptive Cruise Control: Tradeoffs Between Control and Network Specifications

Sinan Öncü, Nathan van de Wouw, Henk Nijmeijer
Department of Mechanical Engineering, Eindhoven University of Technology
Email: s.oncu@tue.nl

1 Introduction

In this study, we consider a Cooperative Adaptive Cruise Control (CACC) system which regulates inter-vehicle distances in a vehicle string. Improved performance can be achieved by utilizing information exchange between vehicles through wireless communication besides local sensor measurements. However, wireless communication introduces network-induced effects that may compromise the performance of the CACC system. Therefore, we approach the design of a CACC system from a Networked Control System (NCS) perspective and obtain tradeoff curves between CACC performance and network specifications.

2 Problem Statement

We use an existing CACC controller design which has been successfully implemented in the scope of the Connect and Drive project and demonstrated with CACC equipped vehicles [1]. Each vehicle in the string shown in Fig. 2 has a control structure as shown in Fig. 1 where the CACC controller ($C_{i,CACC}(s)$) produces control input in addition to the ACC controller ($C_{i,ACC}(s)$) in a feedforward fashion to maintain a desired spacing

$$d_{r,i} = r_i + h_{d,i} v_i, \tag{1}$$

with its predecessor where i is the vehicle index, r_i is the distance at stand-still, $h_{d,i}$ is the so-called headway-time and v_i is the velocity. This spacing policy is implemented through $H_i(s)$ in Fig. 1.

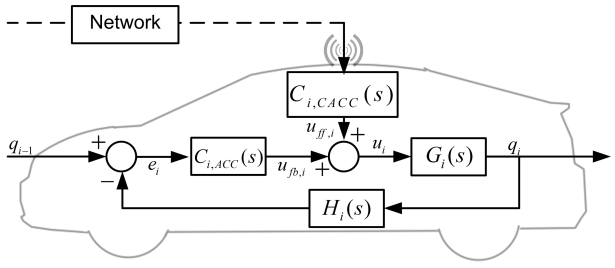

Fig. 1: Schematic representation of a single vehicle in the string.

In this work, we present a NCS framework that incorporates sampling-and-hold effects and constant network delays that occur due to wireless communication and inspect the string stability of the string in which vehicles are interconnected by a vehicle following control law and a constant time headway spacing policy. Schematic representation of the interconnected vehicle string is as shown in Fig. 2.

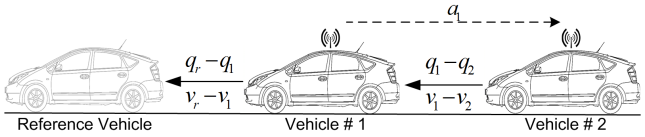

Fig. 2: Schematic representation of the CACC vehicle string with two cars.

A NCS model of the system was obtained as in [2] by using exact discretization. Roughly speaking, string stability can be considered as the attenuation of specific signals throughout the vehicle string and can be inspected by using a discrete-time frequency response analysis of the following transfer function which is constructed using the discrete-time NCS model:

$$SS_{i,i-1} = \left| \frac{V_i(z)}{V_{i-1}(z)} \right| \leq 1, \qquad i \in \{1,2,....,n\} \tag{2}$$

where $V_i(z)$ denotes the velocity of the i-th vehicle. In Fig. 3, maximum allowable ratio $\left(\frac{\tau_k}{T_s}\right)$ of the time delay (τ_k) to sampling interval (T_s) where (2) is satisfied is depicted with a color code for each sampling interval/headway distance pair.

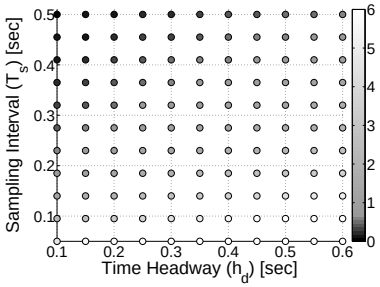

Fig. 3: Maximum allowable ratio of time delays (τ_k) to sampling interval (T_s) for different headway times (h_d).

Results can be used as guidelines for making tradeoffs in the design of CACC. Future studies will focus on extending the framework to incorporate time-varying delays.

References

[1] J. Ploeg, B.T.M. Scheepers, E. Nunen, N.van de Wouw, and H. Nijmeijer, "Design and Experimental Evaluation of Cooperative Adaptive Cruise Control," *in Proceedings of the 14th International IEEE Conference on Intelligent Transportation Systems*, pp. 260-265, 2011.

[2] Öncü S., van de Wouw N., Nijmeijer, H., Cooperative Adaptive Cruise Control: Tradeoffs Between Control and Network Specifications, *in Proceedings of the 14th International IEEE Conference on Intelligent Transportation Systems*, pp. 2051-2056, 2011.

Joint order and dependency reduction for LPV state-space models

Muhammad Mohsin Siraj
Department of Electrical Engineering- Control Systems
Eindhoven University of Technology
P.O Box 513, 5600 MB Eindhoven
The Netherlands
Email: m.s.siraj@student.tue.nl

Roland Tóth
Delft Center for Systems and Control
Delft University
Mekelweg 2, 2628 CD Delft
The Netherlands
Email: R.Toth@tudelft.nl

1 Introduction

The principle question that always arises in modeling of most physical and chemical systems is how to decrease the complexity of the resulting model without sacrificing its accuracy. In case of *Linear Parameter-Varying* (LPV) systems, a system class that allows describing non-linear phenomena by a linear structure where the parameters are dependent on a so called scheduling signal expressing varying operating conditions and the cause of nonlinear effects, decreasing the complexity includes not only the reduction of the complexity w.r.t the order of the system model (state reduction), but also w.r.t dependency on the scheduling variable. Various methods available for state reduction of LTI system models can be extended to LPV system models [1]. However, reduction of the scheduling dependency is still an open problem. In this work, we focus on the question of model reduction of LPV system models from the view point of both state order and scheduling dependency reduction.

2 The LPV Ho-Kalman algorithm

The LPV Ho-Kalman algorithm is studied in [1]. It is an extension of the famous LTI Ho-Kalman algorithm. A unique property of the LPV Ho-Kalman approach is that it does not require quadratic stabilizability or detectability of the model and can be employed in both stable and unstable cases without imposing any modifications. However, this algorithm focuses only on the state-order reduction, hence it does not offer reduction w.r.t the scheduling dependency.

3 ℓ_1 Recovery

In many identification and modeling problems a loss function $f(x)$ is minimized, where x represents the parameters of the system model. Under given conditions, this results in an accurate model of a system. However, it is not known that whether all the elements of x are needed for a good representation of the system or a few elements can represent the systems in an adequate way. This demands the minimization of the support of x as follows:

$$\min \quad \|x\|_{\ell_0}$$

where $\|.\|_{\ell_0}$ is the ℓ_0 pseudo-norm that returns the number of non zero components in its arguments. It is obvious that both objectives can not be achieved together. Therefore, they are often combined in one optimization problem as follows:

$$\begin{aligned} &\text{minimize} && \|x\|_{\ell_0} && \text{(1a)}\\ &\text{subject to} && \|b-\Phi x\|_{\ell_2} < \varepsilon && \text{(1b)} \end{aligned}$$

As minimization of $\|.\|_{\ell_0}$ is an NP hard problem, a fruitful alternative is a convex relaxation based on the ℓ_1 norm. Such a relaxation is known to have a close approximation of the ℓ_0 norm.

4 The Improved LPV Ho-Kalman algorithm

The concept of reducing the support can be utilized with the LPV Ho-Kalman algorithm to offer a reduction of complexity in terms of the scheduling dependence as well. For the sake of simplicity in discussing this idea, only the *Single-Input Single-Output* (SISO) case is considered. It is assumed that the Markov parameters $g_0, g_1, ..., g_N$ of the LPV model w.r.t different trajectories of the scheduling variable $p(k)$ are given, while the system matrices, associated with the underlaying minimal representation and the scheduling dependency are unknown.

The problem of scheduling dependency reduction is formulated as a linear problem i.e., $\Phi x = b$, where the block diagonal matrix Φ is filled with the different combinations of the sequence $\{P_k\}_{k=1}^{N}$ defined as $P_k = p(k)$, b is a column vector of the Markov parameters of the data generating system i.e., $b = \begin{bmatrix} g_0 & g_1 & \dots & g_N \end{bmatrix}^\top$ and x is the unknown column vector of the Markov parameters associated with the minimal scheduling dependency of a state-space model in terms of predefined bases functions, like polynomials, on p. ℓ_1 optimization is used to recover the support of x and then, the LS fit is used to recover the true vector x. From this vector x, a mapping is defined to the so called Hankel matrix. Finally the LPV Ho-Kalman algorithm [1] is used with some improvements to recover a reduced model with both state order and scheduling dependency reduction.

References

[1] Roland Tóth, Hossam Seddik Abbas and Herbert Wener, "On the State-Space Realization of LPV Input-Output Models: Practical Approaches," IEEE Transactions on Control Systems Technology, 2012.

Modal Decoupling of a Lightweight Motion Stage Using Algebraic Constraints on the Decoupling Matrices

E. Silvaş[1], R. Hoogendijk[1],W. Aangenent[2], M.M.J. van de Wal[2] M. Steinbuch[1]

[1]Department of Mechanical Engineering, Technische Universiteit Eindhoven, P.O. Box 513, 5600 MB Eindhoven, The Netherlands

[2]R&D ASML Netherlands B.V., P.O. Box 324, 5500 AH Veldhoven, The Netherlands

Email: e.silvas@tue.nl

1 Introduction

Current trends towards lightweight positioning systems from the lithography industry demand the usage of advanced servo control design methods that can actively control the unavoidable flexibilities. One solution is to use overactuation, [1], and over-sensing and to control the rigid and flexible modes of the system in a decentralized manner.

Compared with the traditional decentralized control approach, in this work a more effective and a less conservative way towards a decentralized modal control is investigated for a 6 degrees of freedom motion stage. This paper describes a method to compute decoupling matrices Φ_u and Φ_y (Figure 1) that decouple the system in its rigid body(RB) modes and a number of non-rigid body(NRB) modes. Alignment and scaling of the rigid body modes are ensured. The decoupling enables the design of multi-loop SISO controllers, K, for the decoupled MIMO system, G_d.

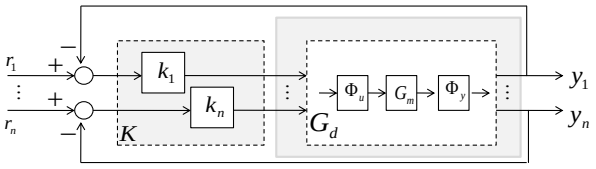

Figure 1. Multi-loop SISO modal control.

2 A new decoupling method for flexible motion systems

As described in [2] the transfer function of a dynamical system in modal coordinates $G_m(s)$ can be written as a sum of transfer functions for each mode i,

$$G_m(s) \quad = \sum_{i=1}^{n} C_{mi}(sI - A_{mi})^{-1} B_{mi}, \tag{1}$$

where A_m, B_m and C_m refer to the state space matrices in modal coordinates with compatible dimensions and n is the number of degrees of freedom of the system. When only positioning sensors are used the term $(sI - A_{mi})^{-1}$ from (1) will be diagonal.

In theory $\Phi_u = B_m^{-1}$ and $\Phi_y = C_m^{-1}$, but this is not possible since in practice the number of modes is larger then the number of inputs and outputs. Typically the RB modes are decoupled and controlled for high-feedback gains and the NRB modes critical for performance are damped using active vibration control methods.

The key idea is to decouple the modal system using geometric knowledge and by imposing a set of constrains. Therefore, to decouple for each mode i in terms of the modal input, the following equations should hold for the input matrix Φ_u

$$B_{mi} \cdot \Phi_{uj} = 1 \quad for \;\; i = j, \tag{2a}$$

$$B_{mi} \cdot \Phi_{uj} = 0 \quad for \;\; i \neq j, \tag{2b}$$

where $i = 1...n_d$ represents the $i-th$ row of B_m and $j = 1...n_d$ represents the $j-th$ column on Φ_u. Equation (2a) ensures that the mode i is controllable. By following the same approach the output decoupling matrix Φ_y can be found.

3 Results and conclusions

The proposed approach is applied to an experimental setup that has 14 inputs and 14 outputs. The traditional approach, 6 RB decoupled modes (case 1) is compared with the approach described in this paper, where beside the 6 RB also 7 NRB modes have been considered for decoupling (case 2). The results in Figure 2 clearly show a better decoupling (especially in low frequencies). This can enable the achievability of better servo-performance with control.

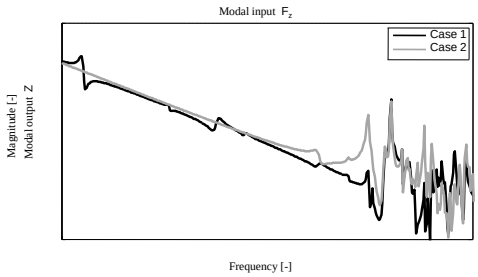

Figure 2. Z-direction mode for two decoupling cases: (case 1) when only the 6 RB modes are decoupled and (case 2) when 7 more NRB are decoupled together with the 6 RB modes .

If the system is oversensed/overactuated, then by a proper choice of modes to be made explicitly controllable, observable or uncontrollable/unobservable the maximum values of achievable bandwidths can be increased.

References

[1] M.G.E. Schneiders, M.J.G. van Molengraft, and M. Steinbuch. Benefits of Over-actuation in Motion Systems. *Proceeding of the 2004 American Control Conference, Boston, Massachusetts*, June 30 July2, 2004.

[2] Wodek K. Gawronski. *Advanced Structural Dynamics and Active Control of Structures*. Springer, 2004.

Dynamic Simulation and Control of a Recirculating Aquaculture System

P. Almeida, A. Donoso Bravo and A. Vande Wouwer
Automatic Control Laboratory
University of Mons
7000 Mons
Belgium
Email: pedro.almeida;andres.donosobravo;alain.vandewouwer@umons.ac.be

1 Introduction

Due to the growth of world population and change in food consumption habits, the aquaculture industry has become one of the world's fastest growing sector of food production [3]. Recirculating aquaculture systems (Figure 1) result from the need of more intensive practices, growing environmental constraints on water consumption and effluent quality, as well as the possibility to supply fish in places where it would be otherwise difficult [1, 3]. In these systems, nitrification and denitrification units are used to remove ammonia and nitrate from the system, which would otherwise accumulate and become toxic for fish [2, 3]. In order to keep key

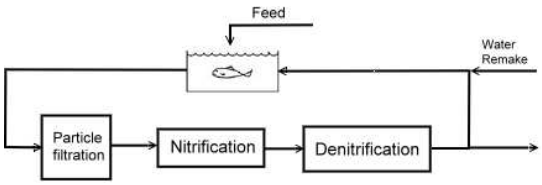

Figure 1: Diagram of an aquaculture recirculation unit.

variables of the system (such as ammonia, nitrate, oxygen) under control, either due to security or economical reasons, control strategies should be applied. Being a multivariable system, either a decentralized or centralized approach could be applied. In this study, attention is focused on decentralized control and an analysis of the plant is achieved in order to select the best input-output pairing.

Results and discussion

A dynamic model representing a recirculation aquaculture plant composed of fish rearing tanks, a physical filtration system and nitrification and denitrification biofilters is derived. The model takes fish feeding, growth and excretion into account as well as the biological removal of the nitrogen compounds in a closed loop system. The resulting system of differential-algebraic equations is implemented in a dynamic simulator coded in MATLAB©.

The interaction between the different variables is studied using classical tools such as the relative gain array, and classical control strategies are applied to the regulation of the main variables of interest. As an example, the results for the control of the oxygen concentration using a PI controller in the Fish Tanks when setpoint changes are introduced, can be seen in Figure 2. The oxygen concentration is controlled by manipulating the k_{la} variable, i.e. by changing the air flowrate or the way the oxygen diffuses in the water.

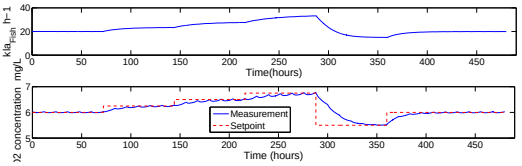

Figure 2: Oxygen concentration variation with the value of k_{la} in the fish tanks.

2 Acknowledgments

The authors gratefully acknowledge the support of the WAGRALIM project NUTRIVERT funded by the Walloon Region. This paper presents research results of the Belgian Network DYSCO (Dynamical Systems, Control, and Optimization), funded by the Interuniversity Attraction Poles Programme, initiated by the Belgian State, Science Policy Office. The scientific responsibility rests with its author(s).

References

[1] M. T. Gutierrez-Wing and R. F. Malone, *Biological filters in aquaculture: Trends and research directions for freshwater and marine applications*, Aquacultural Engineering., 34(3):163-171, 2006.

[2] J. van Rijn and Y. Tal and H. J. Schreier, *Denitrification in recirculating systems: Theory and applications*, Aquacultural Engineering., 34(3):364-376, 2006.

[3] T.E.I. Wik and B.T. Linden and P. I. Wramner, *Integrated dynamic aquaculture and wastewater treatment modelling for recirculating aquaculture systems*, Aquaculture., 287(3-4):361-370, 2009.

Pre-crash passenger safety in cars: a model based control approach

Mark Mutsaers Siep Weiland
Department of Electrical Engineering
Eindhoven University of Technology
P.O. Box 513, 5600 MB Eindhoven
The Netherlands
Email: {M.E.C.Mutsaers,S.Weiland}@tue.nl

Lex van Rooij Olaf op den Camp
TNO Science and Industry
Automotive, Integrated Vehicle Safety
P.O. Box 756, 5700 AT Helmond
The Netherlands
Email: {lex.vanrooij,olaf.opdencamp}@tno.nl

Motivation

Dynamical systems are often represented in much detail using mathematical models that consist of a large number of ordinary differential equations. Model order reduction can then be applied to approximate the complex models by simpler ones, however keeping in tact the most important physical phenomena of the original model. These models are often used to design (low-order) controllers or observers, which are connected to the original system. In "classical" strategies, one needs to apply two disjoint steps, namely the reduction of the model and the optimization to design a controller or observer, or vice versa. Since one can not guarantee the desired behavior of interconnecting the original system and the controller or observer, we propose to take one of the following routes:

1. combine the two disjoint steps into one to model the desired closed-loop behavior as low-order system, and afterwards construct the controller or observer;
2. develop model reduction techniques that keep the desired control objective invariant, implying that no control relevant information is lost when approximating.

In the presentation, we will use theoretical results from the first proposed strategy in practice, by applying it to an application in the automotive industry.

Safety in future cars

Safety in cars is an important research topic in automotive industry. Modern cars are already becoming safer due to advanced safety systems, as airbags and autonomous braking systems, that decrease injuries and fatalities in a crash. To make future cars even safer, current research focuses on what happens *before* a crash occurs, which is named the pre-crash phase. In this phase, future safety systems can possibly prevent crashes. More specifically, we focus on the pre-crash behavior of the human in the vehicle, which already can be simulated in much detail using commercial software as e.g. Madymo (see Figure 1).

From Active Human Model...

Instead of using the commercial software to simulate the (kinematic) pre-crash behavior of the human, a fast model that could do this in *real time* is desired. This model describes the *active* behavior of the human in the vehicle, where active means that we want to include the human's muscular behavior in the model. To obtain this, two steps need to be performed:

1. describe the passive human behavior using a detailed model;
2. introduce a controller to make the model active.

The modeling can be done using the equations of motion, resulting in a complex non-linear, or after linearization, a high-order linearized model. The active behavior can be included using an LQ controller. In the presentation we will combine the reduction and the controller design to obtain a fast model for the active human behavior, and make a comparison with the "classical" strategy where two disjoint steps are performed.

to Active Human State Estimator!

The reason why a fast model that describes the active kinematic behavior of a human needs to be designed is that it is part of the so called active human state estimator (AHSE). With a limited number of measurements available, the goal is to design an estimator, that runs in real time, to estimate the kinematic behavior of the human in the vehicle. This information can be used for a variety of applications in new safety systems in cars, to increase robustness and improve occupant safety further.

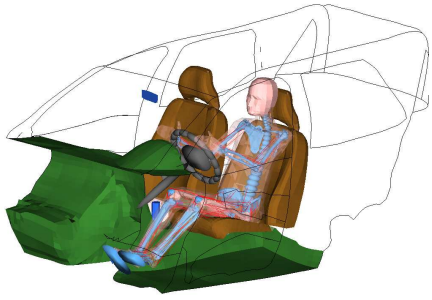

Figure 1: Simulation of a driver using Madymo software.

Modeling of a waste heat recovery system for control purposes

E. Feru, F. Willems, M. Steinbuch
Department of Mechanical Engineering, Eindhoven University of Technology, P.O. Box 513, 5600 MB Eindhoven, The Netherlands
{e.feru, f.p.t.willems, m.steinbuch}@tue.nl

1 Introduction

Engine exhaust gas heat utilisation has attracted a lot of interest due to the substantial amount of heat that can be recovered. Exhaust heat utilisation can reduce fuel consumption up to 7%, lower emissions and improve the overall engine efficiency. To recover the energy from the exhaust a waste heat recovery device (WHR) is used. The objective is to control the WHR system in order to maximize the heat recovery efficiency. To this end, a new model of an evaporator within a waste heat recovery system is proposed. Using experimental data the simulation results show that the proposed model provides a good approximation of the real system.

2 System description

A promising technology in waste heat recovery systems is based on Organic Rankine Cycles (ORC). Two of the main advantages of this technology are simplicity and availability of its components. In Fig. 1 a simplified scheme of the ORC system is illustrated.

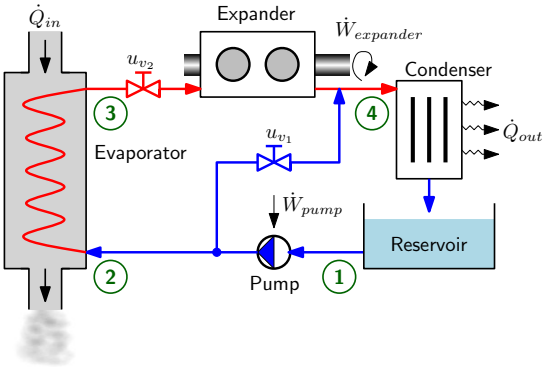

Fig. 1. Physical layout of the Rankine cycle.

In such a system, the organic fluid enters the evaporator in a liquid phase and exits as superheated vapour. Next, as the vapour is expanded mechanical power $\dot{W}_{expander}$ is generated. The condenser is characterized by entering a superheated vapour and leaving saturated liquid at its output.

In order to maximize the heat recovery efficiency and avoid that unwanted conditions occur in the WHR system, solve the following optimization problem:

$$\min_{u_{v_1}, u_{v_2}} -\|q_1 \dot{W}_{expander}\| + \|q_2 \dot{W}_{pump}\| + \|q_3 \dot{Q}_{out}\| \quad (1)$$

subject to *physical limitations* and *drivability constraints* which ensures ideal torque split between engine and WHR system. Parameters q_1, q_2 and q_3 are penalties on mechanical power produced by the expander, mechanical power consumed by the pump and heat flow rate out of the condenser, respectively. For a vector $x \in \mathbb{R}^n$, $\|x\|$ denotes the arbitrary p-norm. These types of optimization problem can be solved efficiently using an accurate model of the system. Therefore, the model of an evaporator within a waste heat recovery system is presented.

3 Nonlinear model of the evaporator

Modeling of the evaporator [1] is a challenging task because of its complex dynamics and nonlinearity. This work describes the modeling of the evaporator in a detailed way which covers the case of two-phase flow with subcooled liquid at the inlet and superheated vapour at the outlet (see Fig. 2).

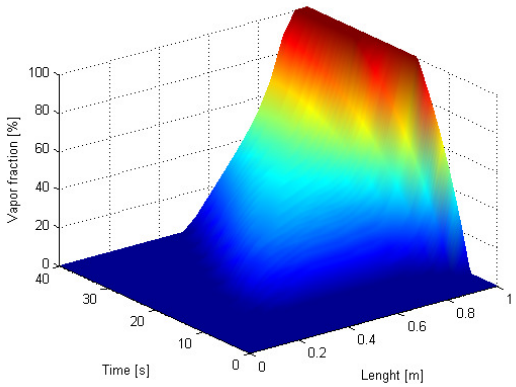

Fig. 2. Vapour fraction as a function of time and length.

In fact, a finite volume model is developed because of higher robustness during start-up and load-change in comparison with other types of evaporators. The evaporator is discretized into n cells in which the mass conservation principle and energy conservation principle are applied. One of the main constraint in these kind of systems is to make sure the evaporator delivers superheated vapour to the input of the expander. Therefore, the aim of the modeling phase is to obtain a mathematical representation of the system which can be used to solve the optimization problem (1).

A comparison of the simulation results with the experimental data shows that the essential dynamics of the evaporator within a waste heat recovery system are captured.

References

[1] J.M. Jensen, *Dynamic Modeling of Thermo-Fluid Systems*, Ph.D. Thesis, Technical University of Denmark, March, 2003.

Some Preliminary Results on Modeling and Control of MBR Process

Guilherme ARAUJO PIMENTEL [a], Alain VANDE WOUWER [a],
Alain RAPAPORT [b], Daniel COUTINHO [c]

[a]Service d'Automatique, Université de Mons, Bd. Dolez 31, 7000 Mons - Belgique

[b]UMR 'MISTEA' Mathmatique, Informatique et STatistique pour l'Environnement et l'Agronomie (INRA/SupAgro), 2, place P.Viala, 34060 Montpellier - France

[c] Departamento de Automação e Sistemas, Universidade Federal de Santa Catarina, Florianópolis - Brasil

guilherme.araujopimentel@umons.ac.be, alain.vandewouwer@umons.ac.be

1 Introduction

There are many water shortage problems in the world, and the reuse of treated water is very important. The Membrane bioreactor (MBR) technology produces a permeate effluent with an exceptional purity and the process has advantages as small footprint and reactor requirements, high effluent quality, good disinfection capability, higher volumetric loading and less sludge production [**?**][**?**]. The MBR process combines the biological degradation process by activated sludge, with a direct solid−liquid separation by membrane filtration. Using micro or ultrafiltration membrane technology (with pore sizes ranging from 0.05 to 0.4 μm), MBR systems allow the complete physical retention of bacterial flocks and virtually all suspended solids within the bioreactor.

2 Biological Population Model for a MBR

Modelling of wastewater treatment plants is still under development. The biological population models (or biomass kinetic models) are generally based on the Activated Sludge Model (ASM), that is used worldwide for modelling wastewater treatment plants. ASM1 was presented by the IAWQ Task Group on Mathematical Modelling for Design and Operation of Biological Wastewater Treatment Processes [**?**]. In the present study, a dynamic simulator has been developed for a pilot plant, based on a slightly modified version of ASM1, and a membrane model. The pilot process includes a denitrification tank, that contains anaerobic bacteria, and a nitrification tank, that contains aerobic bacteria and the membrane. At this stage, an ideal MBR is considered.

3 Control of dissolved Oxygen in the Nitrification Tank

The process is a nonlinear system subject with perturbations in flow and load, together with uncertainties concerning the composition of the incoming wastewater. In [**?**], two main control strategies are presented: control of the dissolved oxygen level in the nitrification reactor by manipulation of the oxygen transfer coefficient (K_La) and control of the nitrate level in the anoxic compartment by manipulation of the internal recycle flow rate. In the present study, the control of the nitrification process based on the dissolved oxygen concentration is investigated. As the microorganisms responsible for the degradation of ammonia uses oxygen for the conversion into nitrate, we propose the regulation of the ammonia concentration by acting on the quantity of oxygen (K_La) that is injected into the tank. An adaptive controller is developed, which can be applied with minimal prior process knowledge. A parallel is also drawn with another control strategy proposed by Antonelli and Astolfi et al.[**?**].

4 Acknowledgments

This paper presents research results of the Belgian Network DYSCO (Dynamical Systems, Control, and Optimization), funded by the Interuniversity Attraction Poles Programme, initiated by the Belgian State, Science Policy Office and INRA-INRIA 'MODEMIC' (Modeling and Optimisation of the Dynamics of Ecosystems with MICro-organisms), France.

References

[1] S.Judd and C.Judd, *"The MBR book, principles and applications of membrane bioreactors in water and wastwater treatment"*, Elsevier, 2011.

[2] T.Wintgens, J.Rosen, T.Melin, C.Brepols, K.Brensla and N.Engelhardt, *"Moddeling of membrane bioreactor system for municipal wastewater treatment"*, Journal of Membrane Science, 2003,Vol. 216,p. 55-65.

[3] M.Henze, C.P.Leslie Grandy Jr, W.Gujer, G.V.R. Marais and T. Matsuo, *"A general model for single-sludge wastewater treatment system"*, Water Research, 1987,Vol. 21,p. 505 - 515.

[4] J. Alex, L.Benedetti, J.Copp, K.V.Gernaey, U.Jeppsson, I.Nopens, M.N.Pons, C.Rosen, J.P.Steyer and P.Vanrolleghem, *"Benchmark Simulation Model no. 1 (BSM1)"*, IWA Taskgroup on Benchmarking of Control Stategies for WWTPs, 2008, April.

[5] R.Antonelli, J.Harmand, J.P.Steyer and A.Astolfi, *Set-point regulation of an anaerobic digestion process with bounded output feedback*, Transactions on control systems technology, 2003, Vol. 11(4),p. 495-504.

Comparative study of a few state estimation techniques for monitoring microalgae cultures

Micaela Benavides[a], Alain Vande Wouwer[a]
[a]Service d'Automatique, Université de Mons
31 Boulevard Dolez, 7000 Mons
Belgium
Micaela.BENAVIDES@umons.ac.be
Alain.VandeWouwer@umons.ac.be

Jan Van Impe
BioTeC & OPTEC, Dept. of Chemical Engineering
Katholieke Universiteit Leuven
W. de Croylaan 46, 3001 Leuven
Belgium
Email: jan.vanimpe@cit.kuleuven.be

1 Introduction

In this study, we analyze and compare three different state estimation techniques:

- An Extended Luenberger Observer (ELO), which is designed using Lyapunov arguments and LMI (Linear Matrix Inequalities)-based techniques, so as to ensure some robustness properties (against model uncertainties and measurement noise) [1].
- An Extended Kalman Filter (EKF), which is by far the most common approach to bioprocess estimation [4].
- An Ensemble Kalman Filter (EnKF), which a nonlinear stochastic state estimation technique [3].

The first two techniques make use of a linearization of the model around the estimated trajectory. Whereas ELO is a deterministic algorithm which can be made - to some extend - robust to model discrepancies and measurement noise, the EKF is a suboptimal minimum variance approach. The main advantage of EnKF is that it directly applies to the nonlinear model (without requiring any linearization) and provides a more rigorous probabilistic approach.

These techniques are applied to two case studies related to the cultures of micro-algae in continuous photobioreactors.

The first model is Droop model [2], which is a popular model to describe the capability of microalgae to uncouple substrate absorption and biomass growth. It is the simplest model for describing microalgae growth in the chemostat. Droop model considers as states the substrate (s) (inorganic nitrogen), the internal quota (q_n) of nutrients and the biomass (x) in terms of organic carbon.

$$\begin{aligned} \dot{s} &= -\rho(s)x - Ds + Ds_{in} \\ \dot{q_n} &= \rho(s) - \mu(q_n)q_n \\ \dot{x} &= \mu(q_n)x - Dx \end{aligned} \tag{1}$$

The second model is much more recent [5], and considers that the organic carbon is composed of a sugar reserve compartment (g), a neutral lipid reserve compartment (l) and a functional compartment (f), i.e., $x = f + g + l$. The principal advantage of this model is to describe the evolution of the lipid quota (q_l), which is of interest in applications related to the production of biofuels. The equations of this model are the combination of equations (1) and (2).

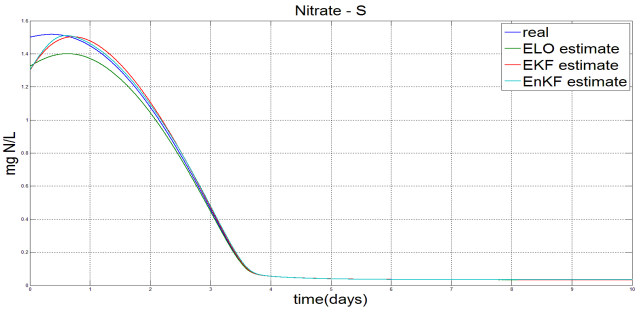

Figure 1: Real and estimated values for the substrate.

$$\begin{aligned} \dot{q_l} &= (\beta q_n - q_l)\mu(q_n) - \gamma\rho(s) \\ \dot{q_f} &= -q_f\mu(q_n) + (\alpha+\gamma)\rho(s) \end{aligned} \tag{2}$$

2 Results

Figure 1 shows the evolution of the real and estimated substrate in the following conditions: the dilution rate is $D = 0.8\mathrm{d}^{-1}$, the influent nitrate concentration is $s_{in} = 5mg\,\mathrm{L}^{-1}$, the state measured is the biomass with measurement noise $v = 0.1$ and the process noise in each state $w = 0.01$.

3 Acknowledgments

This work presents research results of the Belgian Network DYSCO, funded by the Interuniversity Attraction Poles Program, initiated by the Belgian State, Science Policy Office.

References

[1] S. Boyd, L. El Ghaoui, E. Feron, and V. Balakrishnan. *Linear matrix inequalities in system and control theory*, volume 15. Society for Industrial Mathematics, 1994.

[2] M. Droop. 25 years of algal growth kinetics a personal view. *Botanica marina*, 26(3):99–112, 1983.

[3] G. Evensen. *Data assimilation: the ensemble Kalman filter*. Springer Verlag, 2009.

[4] A. Gelb. *Applied optimal estimation*. MIT press, 1999.

[5] F. Mairet, O. Bernard, P. Masci, T. Lacour, and A. Sciandra. Modelling lipid production in microalgae. *9th International Symposium on Dynamics and Control of Process Systems (DYCOPS)*, 2010.

Identification and Modeling of Distillation Columns From Transient Response Data

Diana Ugryumova, Gerd Vandersteen
Vrije Universiteit Brussel, dept. ELEC
Pleinlaan 2, 1050 Brussels, Belgium
Email: dugryumo@vub.ac.be

Bart Huyck, Filip Logist
Katholieke Universiteit Leuven, dept. CIT
W. de Croylaan 46, 3001 Heverlee, Belgium

1 Introduction

In this research, we model a binary distillation column using a frequency domain identification approach. The goal is to find an accurate but simple black-box model of a distillation column to be used in e.g. model predictive control. A distillation column is in essence a multiple-input-multiple-output (MIMO) non-linear system whose system dynamics vary due to changes in the ambient temperature. Here, we consider the modeling of a system which is not in steady-state, and hence introduces leakage errors in the frequency domain, and whose dynamics depend on external factor, i.e. the ambient temperature.

In the next sections, firstly, the modeling approach is introduced. Secondly, the results of a binary distillation column modeling using simulation data are presented.

2 Identification and modeling approach

A recently developed robust local polynomial method (RLPM) together with random-phase multisine inputs are used to eliminate the leakage error and to obtain better estimates of the non-parametric frequency response matrix (FRM) and its variance [1]. This non-parametric FRM is then used to fit a low-order rational form parametric model which also includes a time-delay term.

The extracted parametric models are then extended to capture its dependency on changes in the ambient temperature. In the proposed solution, the parameters (time-delays τ_i, zeros z_i and poles p_i) of the distillation column model depend on the difference between the reboiler power and the heat loss over the column, ΔQ:

$$\hat{G}(s,\Delta Q) = \exp\left(-\tau(\Delta Q)s\right)\frac{\prod_{i=1}^{n_z} s - z_i(\Delta Q)}{\prod_{i=1}^{n_p} s - p_i(\Delta Q)},$$

where $\hat{G}(s,\Delta Q)$ denotes an estimate of the FRM in continuous Laplace domain s and where n_z and n_p denote the amount of zeros and poles, respectively. Using this parameterization, the operation of the column with respect to the changes in ambient temperature becomes approximately constant and hence easier to model.

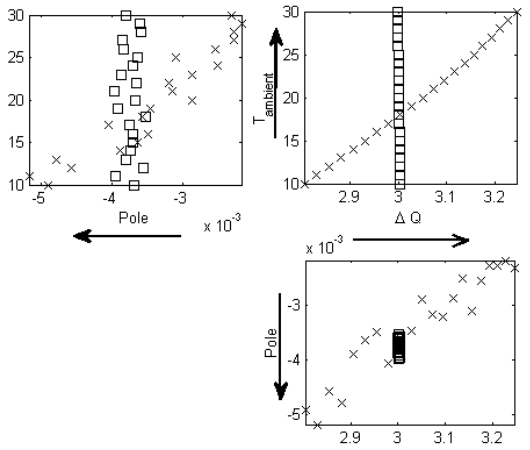

Figure 1: Plot of one of the poles of the parametric model from the reboiler power to the temperature at the bottom. The operating point varies with ambient temperature (cross), ΔQ, and hence, the operating point is more or less constant when using our approach (square).

3 Simulation results

Figure 1 displays one of the poles of the 3rd order rational model from the reboiler power (one of the input variables) to the temperature at the bottom (an output). This transfer function model has zero delay. For a constant level of reboiler power, the total heat loss varies with the ambient temperature and consequently, the pole location varies with the ambient temperature. If the reboiler power is adjusted such that the difference between the reboiler power and the heat loss, ΔQ, is independent of the ambient temperature, then the pole location becomes almost independent of the ambient temperature. This makes it possible to extract more accurate system models.

References

[1] R. Pintelon, G. Vandersteen, J. Schoukens, and Y. Rolain, "Improved (non-)parametric identification of dynamic systems excited by periodic signals - the multivariate case," Mechanical Systems and Signal Processing, vol. 25, no. 8, pp. 2892–2922, 2011.

Macroscopic modelling of overflow metabolism in fed-batch cultures of hybridoma cells

Zakaria Amribt, Hongxing Niu and Philippe Bogaerts
3BIO-BioControl, Brussels School of Engineering
Université Libre de Bruxelles,
Av. F.-D. Roosevelt 50 C.P. 165/61, 1050 Brussels, Belgium
Email: Zakaria.Amribt@ulb.ac.be, Hongniu@ulb.ac.be, Philippe.Bogaerts@ulb.ac.be

1 Introduction

Mammalian cell cultures are now well established as an industrial production platform for recombinant proteins, and with the recent PAT (Process Analytical Technology) initiative from the FDA, it now seems valuable to obtain a thorough metabolic characterization of cell lines and of the relationships between the cell environment and cellular behaviour.

This study aims at constructing a simple and identifiable macroscopic model of hybridoma cells that takes into account phenomena of overflow metabolism within glycolysis and glutaminolysis. These phenomena have been widely recognized in microbial biotechnology, e.g. in the case of ethanol production by *Saccharomyces cerevisie* and acetate by *Escherichia coli* [1]. In animal cell cultures cells convert a significant amount of glucose and glutamine to lactate and ammonia under high glucose and glutamine concentrations [2]. Therefore, mathematically describing this phenomenon is important in order to control cells at the most desirable metabolism state without unnecessary overflow metabolism.

The macroscopic model proposed in this work aims at simulating fed-batch cultures of hybridoma HB-58 cells. The model of central carbon metabolism is reduced to a set of macroscopic reactions describing three metabolism states: respiratory metabolism, overflow metabolism and critical metabolism (Fig.1). It is validated with experimental data of fed-batch hybridoma cultures and successfully predicts the dynamics of cell growth and death, substrate consumption (glutamine and glucose) and metabolites production (lactate and ammonia). Model parameters and confidence intervals are obtained via a non linear least squares identification. This model, on the one hand, allows quantitatively describing overflow metabolism in mammalian cell cultures and, one the other hand, will be valuable for monitoring and control of fed-batch cultures in order to optimize the process.

2 Model development and results

The mathematical model of the complex kinetics is inspired from a simplified metabolic network and from studies of overflow metabolism in yeast cultures [1], using Monod-type kinetics. We obtain 7 dynamic equations (mass balances) with 17 parameters to be identified.

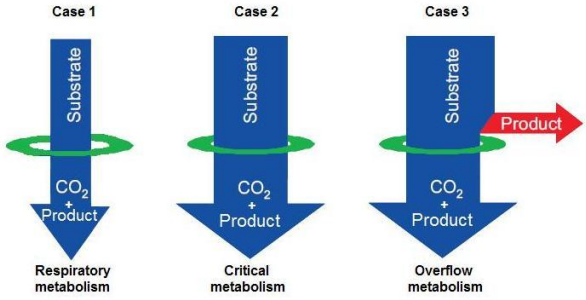

Fig. 1. Illustration of the overflow metabolism in hybridoma cells. Case 1: Respiratory metabolism with glucose and glutamine completely consumed for cell growth; Case 2: Critical metabolism (maximum respiratory capacity) with cells maximum specific growth rate; Case 3: Overflow metabolism with glucose and/or glutamine excess, and production of the associated metabolites (lactate and/or ammonium).

The proposed model gives satisfactory predictions during all periods of cultures (Fig.2). Nevertheless, a few identified parameters have large confidence intervals, which indicates that the model could be further reduced.

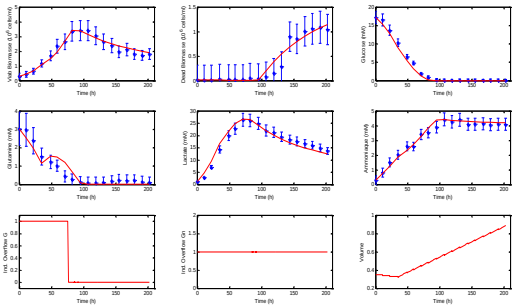

Fig. 2. Comparison between model simulation and experimental data of hybridoma HB-58 cells after parameter identification (direct validation).

References

[1] Xu, B., Jahic, M., and Enfors, S.O. (1999). *Modeling of overflow metabolism in batch and fed batch cultures of Escherichia coli*. Biotechnology Progress, 15, 81-90.

[2] Friesewinkel, P., Niu, H., Drugmand, J.-Ch. and Bogaerts, Ph.: *Simple Metabolic Modelling of Vero Cell Growth on Glucose in Fixed-bed Bioreactors*. Proceedings of the 11th IFAC Symposium on Computer Applications in Biotechnology (CAB2010), Leuven (Belgium), 7-9/7/2010.

Modelling a hyper-proliferative *E. coli*

Cristina Retamal[1], Laurent Dewasme, Anne-Lise Hantson and Alain Vande Wouwer
Automatic Control Laboratory, University of Mons
31, Boulevard Dolez,B-7000, Mons (Belgium)
Email[1]: cristina.retamal@umons.ac.be

1 Introduction

Escherichia coli is one of the most popular host microorganisms for the production of several compounds relevant for the industry. However, an excessive presence of a rich carbon source in the culture can lead, under aerobic conditions, to acetate production which inhibits cells growth. This phenomenon is known as "Overflow metabolism". Oxygen limiting conditions and a saturation of the central metabolic pathways (CPMs) for energy generation purposes have been suggested as the causes of the aerobic acetate production. On the other hand, the conditions considered as the trigger of the acetate production are a high specific growth rate, a high specific glucose uptake rate and a high glucose concentration [1].

The research team of the LGPB (Université Libre de Bruxelles) has developed a mutant *Escherichia coli* capable to produce less acetate, to resist high acetate concentrations and to grow at higher cell density than its wild type strain. This strain is called a hyper-proliferative *E. coli* [2]. The main purposes of this work are the monitoring and supervision of an hyper-proliferative *E. coli*. Moreover, one of the important question is: will the mutant strain be capable to produce higher biomass concentration than its wild type under a controller? To achieve the objective and answer this question, a first important step is the development of mathematical models which would allow to describe the dynamics of the culture of both bacteria and to reach an optimal design and operation of the process.

2 Parameter identification: first results

Batch et fed-batch experiments with the wild type strain MG1655 and the mutant strain were performed in order to estimate the parameters of macroscopic models. First, a partial decoupling method is employed which allows estimating part of the pseudo-stoichiometry independently of the kinetics [3]. The second step is devoted to the estimation of the kinetics using a nonlinear least-squares estimator, as well as the estimation of confidence intervals for the parameters and the predicted states based on the Fisher information matrix. When identifying partially the pseudo-stoichiometric coefficients, one can observe that the mutant strain produces more biomass in the oxidative phase and produces less acetate per gram of substrate consumed than the wild type strain. On the other hand, there is no significant difference in the kinetic terms. It may imply that the mutant strain does not grow necessarily faster and one might conclude that the hyper-proliferation is mainly related to the stoichiometry. However, these results were obtained with limited accuracy. A series of more informative experiments are being carried out in order to increase the level of confidence in the models. The included figure shows, for the wild type strain, the comparison of the real data and simulation results obtained after parameter identification.

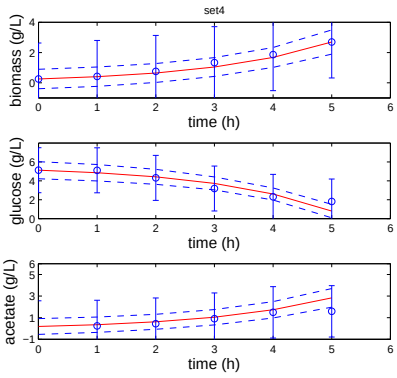

Figure 1: A direct validation of the model. Wild type strain MG1655. Circles: experimental data. Solid lines: predicted values with a 95% of confidence on the simulation errors (discontinuous lines)

3 Acknowledgments

The authors gratefully acknowledge the support of the Waleo 3 project HYPRO2COM funded by the Wallonia Region and the Belgian Network DYSCO funded by the Interuniversity Attraction Poles Program, initiated by the Belgian State, Science Policy Office.

References

[1] M.J. Alba, and E. Calvo, "Characterization of bioreaction processes: Aerobic Escherichia coli cultures" Journal of Biotechnology 84, 107-118, 2000.

[2] J. Timmermans, "Global regulation in E. Coli mediated by the post-transcriptional regulator CsrA and by two proteins of unknown functions, TldD ad TldE" Ph.D. Thesis, Université Libre de Bruxelles, 2009.

[3] L. Chen, and G. Bastin, "Structural Identifiability of the yield coefficients in bioprocess models when the reaction rates are unknown" Mathematical biosciences 132, 35-67, 1996.

Distributed Control of Large-Scale Hybrid Systems

Shuai Liu, Bart De Schutter

Delft Center for Systems and Control, Delft University of Technology
Mekelweg 2, 2628 CD Delft, The Netherlands
Email: {S.Liu-1, B.Deschutter}@tudelft.nl

1 Introduction

Hybrid systems, which are described by a combination of continuous dynamics and discrete-event dynamics, have attracted widespread interest. Hybrid systems can be used in many areas, such as traffic networks, power networks, water distribution networks, industrial processes, bio-processes, robotics, aerospace, etc. Hence, It is of great significance to develop control methods for hybrid systems.

Currently, many research efforts in the field of control of hybrid systems focus on tractability and efficiency. There are already some tractable control methods for small-sized hybrid systems. However, no efficient control methods for large-scale hybrid systems have been developed yet. Therefore, we focus on tractable efficient control methods for large-scale hybrid systems.

2 Research Approach

Due to the computational complexity, scalability issues, and communication bandwidth limitations, on-line, real-time centralized control for large-scale hybrid systems is infeasible. Therefore, distributed control methods are required for such systems.

To develop systematic distributed on-line real-time control methods for large-scale systems, the following issues must be considered:

- How to get coordination and cooperation between the distributed local controllers?
- How to address the computational complexity of the distributed hybrid control problem?
- How to subdivide the overall system and assign local controllers to subsystems?

We propose to use a model-based control approach with intelligent control agents. Through prediction using a model of the system and numerical optimization, model predictive control (MPC) determines a sequence of control actions that optimize a given performance criterion in a rolling horizon fashion. The use of intelligent agents in distributed MPC allows obtaining coordination through negotiation. The application of models allows predicting the influence of control operations on the future development of system. Many types of models can be used for prediction in MPC. In order to reduce the computational complexity, special tractable classes of hybrid systems are considered. In particular, we choose piecewise-affine (PWA) model as a starting point. For a PWA model [1], the input-state space is divided into several regions and in each region the system is characterized by linear or affine dynamics.

For small-scale PWA systems, there are some available MPC methods, which do not perform well when applied in large-scale PWA systems. In order to extend the MPC methods for small-scale PWA systems towards use for large-scale PWA systems, we will combine them with conventional and newly developed distributed control methods [2]. To this aim, we will integrate methods from integer optimization, operations research, intelligent agents, and systems and control.

3 Expected Results

The research will result in systematic distributed on-line real-time control methods for special classes of hybrid systems. These methods will be efficient and robust, providing levels of reliability and dependability for large-scale hybrid systems that cannot be obtained through current control methods.

References

[1] A. Bemporad and M. Morari. Control of systems integrating logic, dynamics, and constraints. *Automatica*, 35(3):407–427, 1999.

[2] R. Scattolini. Architectures for distributed and hierarchical model predictive control-a review. *Journal of Process Control*, 19(5):723–731, 2009.

Networked Control System Toolbox: A Numerical Tool for Stability Analysis[1]

N.W. Bauer, S.J.L.M. van Loon, M.C.F. Donkers, N. van de Wouw, W.P.M.H Heemels
Dept. of Mechanical Engr., Eindhoven University of Technology, P.O. Box 513, 5600 MB Eindhoven, The Netherlands
{N.W.Bauer, S.J.L.M.v.Loon, M.C.F.Donkers, N.v.d.Wouw, W.P.M.H.Heemels}@tue.nl

1 Introduction

There have been many theoretical developments in the area of stability analysis for networked control systems but a lack of computational tools which implement the theory. The purpose of this paper is to present a MATLAB toolbox which has implemented the theoretical developments in [1, 2, 3, 4]. In these papers, a discrete-time framework is used to assess stability of a continuous-time linear time-invariant (LTI) plant and a LTI controller interconnected via a communication network which introduces varying delays, varying transmission intervals, dropouts, quantization and the need for scheduling protocols. This toolbox automates creating a polytopic overapproximation and solving the corresponding linear matrix inequalities [1, 3, 4] to determine if stability can be guaranteed.

2 Functionality

Below, we elaborate on this toolbox, which is equipped with a graphical user interface (GUI), see Fig. 1, that allows the user to easily construct the NCS model under study. The input data that the user needs to specify are:

- The state-space data, A^p, B^p and C^p of the LTI continuous-time plant;
- The state-space data, A^c, B^c, C^c and D^c of the discrete-time LTI output-feedback controller. Note that, the NCS Toolbox also supports continuous-time LTI output-feedback controllers and state-feedback controllers;
- The bounds on the transmission intervals and delays;
- A bound on the maximum allowable number of successive packet dropouts;
- If the communication medium is shared, the user can construct the topology of the network in terms of the sensor and actuator nodes using the GUI. Moreover, the user can select two well-known protocols, namely, the TOD and the RR protocol;
- The type of quantizer that is used, i.e., a uniform or logarithmic quantizer;

[1]This work is supported by the Innovational Research Incentives Scheme under the VICI grant "Wireless control systems: A new frontier in automation" (No. 11382) awarded by NWO (The Netherlands Organization for Scientific Research) and STW (Dutch Science Foundation), and the European 7th Framework Network of Excellence "Highly-complex and networked control systems" (HYCON2).

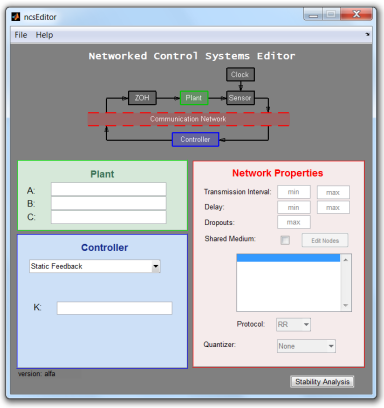

Figure 1: NCS Toolbox Graphical User Interface.

Based on these input data provided by the user, the NCS Toolbox provides the following functionality:

- Three overapproximation techniques are implemented in this NCS Toolbox, i.e., overapproximation techniques based on gridding and norm bounding (GNB), [4], the Jordan normal form approach (JNF), [1], and an approach based on the Cayley-Hamilton theorem (CH), [2];
- Stability and performance analysis using one of the three available overapproximation techniques combined with LMI-based conditions.

By using this toolbox, the user is able to make design tradeoffs between control properties such as stability and performance, and network-related properties such as delays, scheduling, bandwidth limitations etc., in a user-friendly manner.

References

[1] M.B.G. Cloosterman, N. van de Wouw, W.P.M.H. Heemels, and H. Nijmeijer. Stability of networked control systems with uncertain time-varying delays. *IEEE Trans. Autom. Control*, 54(7):1575–1580, Jul. 2009.

[2] R. Gielen, S. Olaru, M. Lazar, W.P.M.H. Heemels, N. van de Wouw, and S. Niculescu. On polytopic inclusions as a modeling framework for systems with time-varying delays. *Automatica*, 46(3):615–619, 2010.

[3] W.P.M.H. Heemels, N. van de Wouw, R.H. Gielen, M.C.F. Donkers, L. Hetel, and et. al. Comparison of overapproximation methods for stability analysis of networked control systems. In *HSCC 2010: Proc. 13th ACM Int. Conf. on Hybrid systems*, pages 181–190.

[4] S.J.L.M. van Loon, M.C.F. Donkers, N.W. Bauer, N. van de Wouw, and W.P.M.H Heemels. Stability analysis of networked and quantized control systems: A switched linear systems approach. *Submitted*.

Robust sawtooth period control based on adaptive online optimization

J.J. Bolder[1], G. Witvoet[1,2,3], M.R. de Baar[1,2], N. van de Wouw[1], M.A.M. Haring[1], E. Westerhof[2], N.J. Doelman[3] and M. Steinbuch[1]

[1] Eindhoven University of Technology, Dept. of Mechanical Engineering, The Netherlands

[2] FOM Institute DIFFER, Association EURATOM-FOM, Nieuwegein, The Netherlands

[3] TNO Technical Sciences, Opto-mechatronics, Delft, The Netherlands

1 Introduction

The sawtooth instability is a repetitive phenomenon occurring in plasmas of tokamak nuclear fusion reactors. Experimental studies of these instabilities and the effect they have on the plasma (notably the drive of secondary instabilities and consequent performance reduction) for a wide variety of plasma conditions is an important line of study in nuclear fusion research. Variations in the plasma conditions have a significant influence on the dynamical behavior of the sawtooth instability. We present the design of a sawtooth period controller which is robust against such variations [1].

2 The sawtooth control problem

The variable to be controlled is the interval between two sawtooth crashes, the sawtooth period. The actuator is a mirror (launcher), which is used to deposit energy in the plasma using microwaves. The dynamical behavior of the sawtooth period is nonlinear, the control direction may change as the plasma conditions vary. A control strategy which is able to handle such changes is Extremum Seeking Control [2].

3 Extremum seeking control

Extremum seeking control (ESC) is an adaptive control strategy that incorporates on-line optimization techniques to slowly drive a process to a desired operating point. The ESC is model-free and therefore inherently robust against model uncertainties. In this technique a cost function in terms of the desired sawtooth period is optimized on-line by changing the deposition location. Figure 1 shows the topology of the extremum seeking controller which is adapted to the sawtooth control problem.

4 Simulation results

The robustness of the controller is tested for two different sets of plasma parameters. The simulation results are shown in figure 2. There is a large difference between the steady state input-to-output (I/O) maps. Nevertheless, the reference is successfully tracked for the cases 1 and 2. The sawtooth period τ_s is shown in (a), the launcher angle ϑ and estimated minimizer $\hat{\vartheta}$ in (b) and the sawtooth period trajectory in (c).

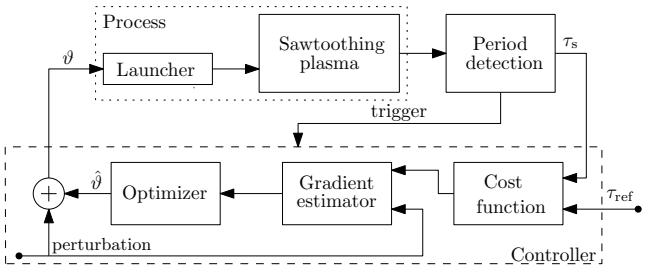

Figure 1: Extremum seeking controller topology

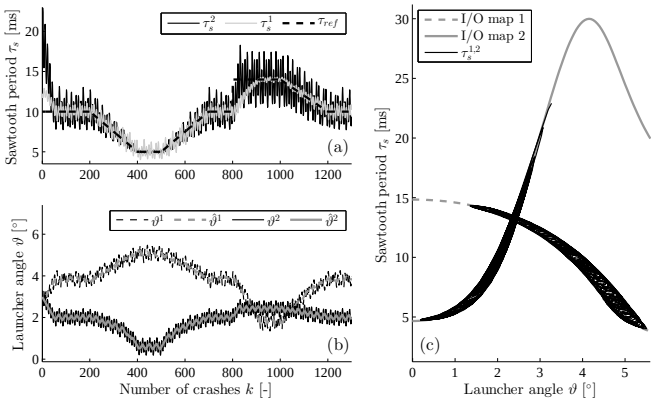

Figure 2: Simulation results with different plasma parameters.

5 Conclusions and recommendations

The successful tracking of a sawtooth period reference for two completely different operating conditions has been demonstrated. The implementation of the controller on a tokamak is future research.

References

[1] J. Bolder, G. Witvoet *et al.*, "Robust sawtooth period control based on adaptive online optimization," *Submitted to Nuclear Fusion*, 2012.

[2] D. Nešić, Y. Tan *et al.*, "A unifying approach to extremum seeking: adaptive schemes based on estimation of derivatives," *49th IEEE Conference on Decision and Control, Atlanta, Georgia, USA*, pp. 4625–4630, 2010.

Variable gain control for transient performance improvement

Bram Hunnekens, Nathan van de Wouw, Henk Nijmeijer
Mechanical Engineering, Section Dynamics and Control, Eindhoven University of Technology
P.O. Box 513, NL 5600 MB Eindhoven, The Netherlands
Email: B.G.B.Hunnekens@tue.nl

1 Introduction

It is well-known that steady-state errors due to constant disturbances can be removed by including integral action in the controller. However, inclusion of the integrator increases the amount of overshoot in a transient response. Here, a nonlinear variable gain integral controller (VGIC) is proposed to balance this tradeoff in a more desirable manner.

2 Variable Gain Integral Control

Consider the SISO closed-loop variable gain control scheme in Figure 1, consisting of a plant $P(s)$, $s \in \mathbb{C}$, nominal linear controller $C_{nom}(s)$, which does not include integral action, reference r, disturbance d and measured output y. The variable gain part of the controller consists of the variable gain element $\varphi(e)$, i.e. $w = -\varphi(e)$, depending on the error e, and a weak integrator described by

$$C_I(s) = \frac{s+\omega_i}{s}, \tag{1}$$

with $\omega_i > 0$ the zero of the weak integrator.

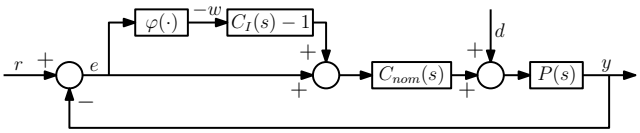

Figure 1: Variable gain control structure.

By a suitable choice of the nonlinear element $\varphi(e)$ we aim to limit the amount of integral action when the error e is large, thereby reducing the amount of overshoot of the transient response. Consider the saturation nonlinearity depicted in Figure 2. For errors $|e| \leq \delta$, $\varphi(e) = e$, and hence a linear controller $C(s) = C_{nom}(s)C_I(s)$ is active. For $|e| > \delta$, the amount of integral action is limited due to the saturation characteristic in $\varphi(e)$.

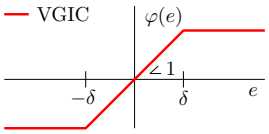

Figure 2: Variable gain element $\varphi(e)$.

Using circle-criterion arguments it can be shown that, under mild assumptions, if the transfer function $G_{ew}(s) = \frac{\omega_i}{s}\frac{P(s)C_{nom}(s)}{1+P(s)C_{nom}(s)}$ satisfies the frequency domain condition

$$\mathrm{Re}(G_{ew}(j\omega)) \geq -1 \quad \forall \omega \in \mathbb{R}, \tag{2}$$

the equilibrium point satisfying $e = 0$ is globally asymptotically stable. In other words, the VGIC still removes steady-state errors in the presence of constant disturbances.

3 Experimental results

To illustrate the effectiveness of the approach in terms of improving the transient performance (decreased overshoot), consider experimental results from a setup consisting of two rotating inertias interconnected by a flexible shaft in Figure 3. A unit step-reference r acts at $t = 1$ s and a constant force disturbance d acts at $t = 5$ s. Clearly, the VGIC, with $\delta = 0.1$ rad, limits the amount of overshoot but is still capable of removing the effect of the constant force-disturbance.

A nonlinear VGIC has been proposed that improves transient performance in terms of overshoot and steady-state errors. The design uses linear loop-shaped controllers as building blocks, which makes the design intuitive and performance driven.

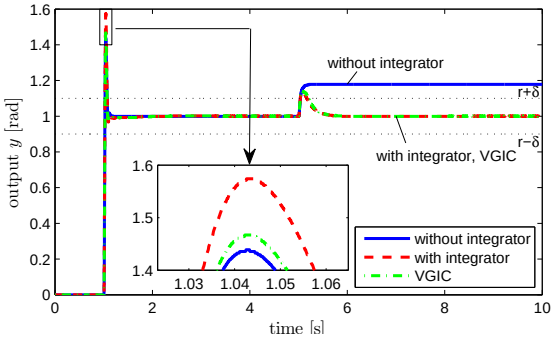

Figure 3: Illustrative example of VGIC.

References

[1] M.F. Heertjes, S. Schuurbiers, H. Nijmeijer, Performance-improved design of NPID controlled motion systems with applications to wafer stages, *IEEE Trans. Indust. Electron*. 2009; 56(5):134755.

This research is financially supported by STW

Tracking control of mechanical systems with impacts

Benjamin Biemond, Nathan van de Wouw, Maurice Heemels, and Henk Nijmeijer
Eindhoven University of Technology
P.O. Box 513, 5600 MB Eindhoven, The Netherlands
Email: {j.j.b.biemond, n.v.d.wouw, m.heemels, h.nijmeijer}@tue.nl

Introduction

A tracking control problem is considered for mechanical systems with impacts. For these systems, conventional control approaches are unfeasible when jumps of the plant do not coincide with jumps of the reference. To illustrate this problem, consider a ball bouncing on a table, (see figure on the right) described by

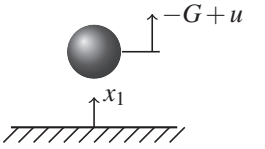

$$\dot{x} = \begin{pmatrix} x_2 \\ -G+u+\lambda(x_1,x_2) \end{pmatrix}, \text{ for } x_1 \geq 0, \qquad (1a)$$

during flight, where x_1 and x_2 are the distance and velocity of the ball with respect to the table, respectively, G is the gravitational acceleration, u is an applied force, and the contact force λ avoids penetration of the table. Impacts between the ball and the table are modelled with:

$$x^+ = \begin{pmatrix} x_1 \\ -x_2 \end{pmatrix}, \text{ for } x_1 = 0 \text{ and } x_2 < 0. \qquad (1b)$$

For a desired bouncing ball trajectory r as given in the figure below, an appropriate controller might induce the depicted trajectory x of the plant.

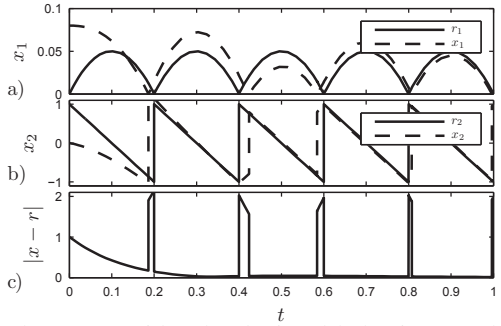

Intuitively, we consider the depicted behaviour as desired, since the controller ensures that the trajectories converge to each other during flight, and the impact time mismatch converges to zero. However, the depicted Euclidean tracking error $|x-r|$ shows unstable "peaking" behaviour.

Control problem formulation

For the bouncing ball system (1), a tracking control problem that requires asymptotic behaviour of $|x-r|$ will be unfeasible due to the depicted "peaking" behaviour. Hence, we reformulate the tracking problem using the following error measure, that does not show the depicted "peaking" behaviour and, when evaluated along closed-loop trajectories, is a continuous function of time:

$$d(r,x) = \min(|x-r|, |x+r|). \qquad (2)$$

In the figure on the right, the neighbourhoods $\{x \in C \cup D : d(r^i,x) < \delta\}$ of two different points r^i, $i = 1,2$, are shown. Essentially, the tracking error measure d allows to compare a reference trajectory with a plant trajectory, "as if" both of them already jumped. For this reason, the measure d does not show the "peaking" behaviour, and can be used to formulate a feasible tracking problem as follows, cf. [1]:

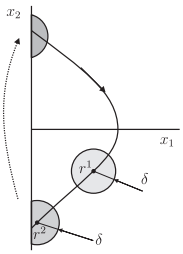

Definition 1 (Tracking problem) *Given the impacting system* (1) *with reference trajectory r, design a control law* $u(r,x)$ *such that the trajectory r is asymptotically stable with respect to the error measure d in* (2)*.*

Controller design

The tracking problem given in Definition 1 is feasible, and a switching controller that solves this problem is designed as follows:

$$u(r,x) = \begin{cases} -[k_p\, k_d](x-r), & \text{for } V_d \leq V_m \\ -2G-[k_p\, k_d](x+r), & \text{for } V_d > V_m, \end{cases}$$

where $k_p, k_d > 0$, and the switches of the controller are designed by using the following functions:

$$V_d(r,x) = \tfrac{1}{2}(x-r)^T P(x-r); \quad V_m(r,x) = \tfrac{1}{2}(x+r)^T P(x+r),$$

for appropriate $P = P^T \succ 0$. The Lyapunov function $V(r,x) = \min(V_d(r,x), V_m(r,x))$ is used to prove that the tracking problem is solved and $d(r(t),x(t))$ converges asymptotically to zero for $t \to \infty$, as depicted below.

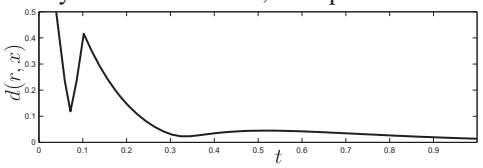

Discussion

We formulated a feasible tracking problem for a mechanical system with impacts using a non-Euclidean tracking error measure d. This measure embeds an intuitive notion of tracking, and does not show the peaking behaviour. This approach is applicable to a large class of hybrid systems with state-triggered jumps, and does not require the jump times to coincide, [2].

[1] J. J. B. Biemond, N. van de Wouw, W.P.M.H. Heemels, H. Nijmeijer, "Tracking control of mechanical systems with impacts," *submitted to American Control Conference*, 2012.

[2] J. J. B. Biemond, N. van de Wouw, W.P.M.H. Heemels, H. Nijmeijer, "Tracking Control for Hybrid Systems with State-Triggered Jumps," *submitted to IEEE Transactions on Automatic Control*, 2012.

This research is supported by the Netherlands Organisation for Scientific Research (NWO) and the European Union HYCON2 Network of Excellence.

Period control in nuclear fusion plasmas

Menno Lauret
Den Dolech 2, 5612 AZ Eindhoven, The Netherlands
m.lauret@tue.nl

Lauret, Felici, Witvoet, Goodman, Vandersteen, de Baar, Sauter, TCV team

1 Abstract

Tokamaks are machines in which very hot plasmas are confined with intend to create circumstances suited for nuclear fusion and thereby energy production without waste. The sawtooth instability, typically present in Tokamak plasmas, is a periodic instability that causes periodic drops in the core temperature. For ITER, the time between two consecutive sawtooth crashes (i.e. the natural sawtooth period) will be much too large. In past experiments the sawtooth period has been feedback controlled with a variable electron cyclotron current drive (ECCD) deposition location. Here, recent experiments [1] on TCV are presented where the ECCD power is periodically modulated. Simulations [2] predict that for a range of modulation periods and duty cycles (percentage of power on during modulation) the sawtooth period becomes the same as the power modulation period (i.e. sawtooth locking). Experiments on TCV, see the figures, show convincing evidence of sawtooth locking thereby confirming the simulations. It appears that for this system open loop control, based on the nonlinear phenomenon of period locking, can be at least as efficient as classical feedback control of the sawtooth period.

Experimental evidence of sawtooth locking on the TCV tokamak

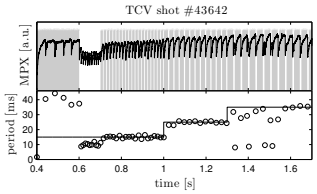

Figure 1: Sawtooth cycle measured with central soft X-ray channel (black) and power modulation in grey (top-box). The measured sawtooth period (circles) and power modulation period (line) shown in the bottom box show sawtooth locking for modulation periods of 15 ms and 25 ms.

Conclusions

The shown experiments confirm that the sawtooth period can be precisely controlled by modulating the ECCD power, without using real-time measurements. For certain combinations of the modulation periods, power levels and duty cycles the sawtooth period becomes the modulation period. In ongoing work this phenomenon is used to design a robust (feedback) controller for the sawtooth period, that is based on power modulation. The locking phenomenon probably also occurs for other dynamical processes in the plasma like ELMs for which similar control methods might also work.

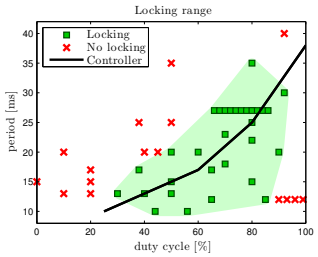

Figure 2: Locking occurs only for certain combinations of modulation period and duty cycle. The green area is the locking-range.

References

[1] Lauret, Felici, Witvoet, Goodman, Vandersteen, Sauter, de Baar and the TCV team. *Demonstration of sawtooth period locking with power modulation in TCV plasmas.* Submitted to Nucl. Fusion.

[2] Witvoet, Lauret, de Baar, Westerhof, Steinbuch. *Numerical demonstration of injection locking of the sawtooth period by means of modulated EC current drive.* Nucl. Fusion 51 (2011).

Port-Hamiltonian Systems on Simplicial Complexes

Marko Šešlija
Discrete Technology and Production Automation
University of Groningen
Nijenborgh 4, Groningen 9747 AG
The Netherlands
Email: m.seslija@rug.nl

Jacquelien M.A. Scherpen
Discrete Technology and Production Automation
University of Groningen
Nijenborgh 4, Groningen 9747 AG
The Netherlands
Email: j.m.a.scherpen@rug.nl

Arjan van der Schaft
Johann Bernoulli Institute for Mathematics and Computer Science
University of Groningen
Nijenborgh 9, Groningen 9747 AG
The Netherlands
Email: a.j.van.der.schaft@math.rug.nl

1 Introduction

Geometric structures behind a variety of physical systems stemming from mechanics, electromagnetism and chemistry exhibit a remarkable unity enunciated by Dirac structures. The open dynamical systems defined with respect to these structures belong to the class of so-called port-Hamiltonian systems. These systems arise naturally from the energy-based modeling. Apart from offering a geometric content of Hamiltonian systems, Dirac structures supply a framework for modeling port-Hamiltonian systems as interconnected and constrained systems. From a network-modeling perspective, this means that port-Hamiltonian systems can be reticulated into a set of energy-storing elements, a set of energy-dissipating elements, and a set of energy port by which the interconnection of these blocks and environment is modeled. It is well-known that such a modeling strategy also utilizes control synthesis for these systems.

The port-Hamiltonian formalism transcends the lumped-parameter scenario and has been successfully applied to study of a number of distributed-parameter systems [1]. The centrepiece of the efforts concerning infinite-dimensional case is the Stokes-Dirac structure. The canonical Stokes-Dirac structure is an infinite-dimensional Dirac structure defined in terms of differential forms on a smooth manifold with boundary. The Hamiltonian equations associated to this Dirac structure allow for non-zero energy exchange through the boundary.

2 Problem and recent antecedents

Having finite-dimensional approximations of distributed-parameter systems is of a great importance for numerical simulation and control design. Standard tools from numerical analysis, however, in principle fail to preserve the underlying geometric structure frequently leading to physically bogus results. Most of the research efforts have been directed toward structure-preserving discretization of port-Hamiltonian systems described by partial differential equations on one-dimensional spatial domains (see e.g. [2]). Recently in [4, 5] we have proposed a discrete geometry approach [3] to structure-preserving discretization of open Hamiltonian systems defined on arbitrary n-dimensional manifolds with boundaries.

3 Results

In this contribution we shall present a geometric framework for defining port-Hamiltonian systems on simplicial complexes. Dirac structures capturing the topological laws of the system are constant finite-dimensional Poisson structures. We shall address the issue of representation of these so-called simplicial Dirac structures, as discrete analogues of the Stokes-Dirac structure, and show how they predetermine dynamics of lumped-parameter systems. The formalism will be illustrated on a few examples originating from classical mechanics, electromagnetism and chemistry.

References

[1] A.J. van der Schaft, B.M. Maschke, "Hamiltonian formulation of distributed-parameter systems with boundary energy flow", *Journal of Geometry and Physics*, vol. 42, pp. 166–194, 2002.

[2] G. Golo, V. Talasila, A.J. van der Schaft, B. Maschke, "Hamiltonian discretization of boundary control systems," Automatica, vol. 40, no. 5, pp. 757–771, May 2004.

[3] A. N. Hirani, *Discrete exterior calculus*, Ph.D. thesis, California Institute of Technology, 2003.

[4] M. Seslija, J.M.A. Scherpen, A.J. van der Schaft, "A discrete exterior approach to structure-preserving discretization of distributed-parameter port-Hamiltonian systems," *Proc. 50th IEEE Conf. on Decision and Control*, Orlando, Florida, December 12-15, 2011.

[5] M. Seslija, A.J. van der Schaft, J.M.A. Scherpen, "Discrete Exterior Geometry Approach to Structure-Preserving Discretization of Distributed-Parameter Port-Hamiltonian Systems," http://arxiv.org/abs/1111.6403

Assimilation of PM 10 measurements in the air quality model AURORA by using Kalman filtering techniques

Oscar Mauricio Agudelo and Bart De Moor
Department of Electrical Engineering (ESAT),SCD-SISTA, KU Leuven
Kasteelpark Arenberg 10, B-3001 Heverlee, Belgium.
Email: {mauricio.agudelo, bart.demoor}@esat.kuleuven.be

1 Introduction

Data assimilation is the common name given to several numerical techniques that combine the outputs of a numerical model with observational data in order to improve the quality of the model predictions. This work presents the results of using data assimilation techniques such as the Ensemble Kalman Filter (EnKF)[1] and the Deterministic Ensemble Kalman Filter (DEnKF) [2], for improving the PM 10 (particles with diameters ranging from 0 to 10 micrometers) estimations of the air quality model AURORA. The EnKF and the DEnKF are built around a stochastic formulation of the model, where some of its parameters are assumed to be uncertain. The uncertainty in these parameters turns out to be the main reason behind the differences between the model predictions and the real measurements. The filters estimate these parameters as well as the PM 10 concentrations by using ground-based measurements provided by IRCEL, the Belgian Interregional Environment Agency. The assimilation experiments are carried out over a region that consists of Belgium, Luxembourg, and some small parts of Germany, France and the Netherlands. The horizontal domain is divided into 59 x 49 grid-cells with a resolution of 5 km. Regarding the vertical domain, 22 layers are used to span an altitude of 2000 m. The model was set up for simulating a period of 12 days starting on January 20th, 2010 at midnight. This period is of special interest since within it a PM 10 episode took place, that is, elevated PM 10 concentrations were registered. In this study, we used the measurements provided by 21 air quality stations. These stations were split into two groups: (i) assimilation stations and (ii) validation stations. The first group was used in the assimilation process to obtain the optimal estimate of the state. The second group was not used in the assimilation, but only to verify the results.

2 Results and Future research

Figure 1 shows the average of the PM 10 concentration over the validation stations. Notice that AURORA is not able to properly follow the data. In spite of the big gap between AURORA and the measurements, both data assimilation techniques manage to notably reduce this gap. For the case of the EnKF, the error is decreased by 65.39% in the assimilation stations and by 53.44% in the validation stations. For the DEnKF the error in the assimilation and validation stations is reduced by 68.27% and 55.88% respectively. Future work will be focused on performing assimilation experiments for longer periods, e.g., 6 months or 1 year, while keeping the current spatial domain and the resolution of 5 km.

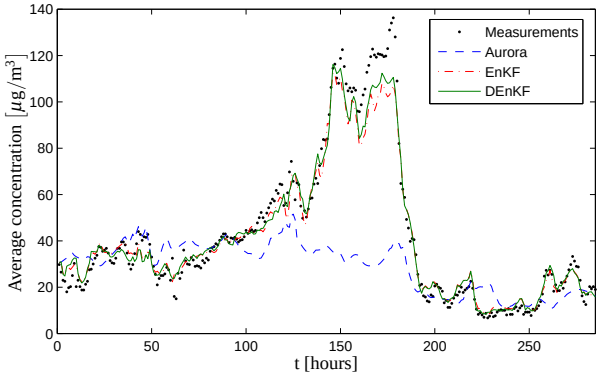

Figure 1: Average of the PM 10 concentration over the validation stations. Starting date: January 10th, 2010.

Acknowledgments. This research has been supported by: • Research Council KUL: GOA/11/05 Ambiorics, GOA/10/09 MaNet, CoE EF/05/006 Optimization in Engineering (OPTEC) and PFV/10/002 (OPTEC), IOF-SCORES4CHEM, several PhD/postdoc & fellow grants; • Flemish Government: ○ FWO: PhD/postdoc grants, projects: G0226.06 (cooperative systems and optimization), G0321.06 (Tensors), G.0302.07 (SVM/Kernel), G.0320.08 (convex MPC), G.0558.08 (Robust MHE), G.0557.08 (Glycemia2), G.0588.09 (Brain-machine) research communities (WOG: ICCoS, ANMMM, MLDM); G.0377.09 (Mechatronics MPC); ○ IWT: PhD Grants, Eureka-Flite+, SBO LeCoPro, SBO Climaqs, SBO POM, O&O-Dsquare; • Belgian Federal Science Policy Office: IUAP P6/04 (DYSCO, Dynamical systems, control and optimization, 2007-2011); • IBBT • EU: ERNSI; FP7-HD-MPC (INFSO-ICT-223854), COST intelliCIS, FP7-EMBOCON (ICT-248940), FP7-SADCO (MC ITN-264735), ERC HIGHWIND (259 166) • Contract Research: AMINAL • Other: ○ Helmholtz: viCERP ○ ACCM. Dr. Bart De Moor is a full professor at the Katholieke Universiteit Leuven, Belgium. The scientific responsibility is assumed by its authors.

References

[1] G. Burgers, P. Jan van Leeuwen, and G. Evensen, "Analysis scheme in the Ensemble Kalman Filter," *Monthly Weather Review*, vol. 126, no. 6, pp. 1719–1724, 1998.

[2] P. Sakov and P. R. Oke, "A deterministic formulation of the ensemble Kalman filter: an alternative to ensemble square root filters," *Tellus*, vol. 60A, pp. 361–371, 2008.

Observer design for a class of switching servers

Dirk van Zwieten, Erjen Lefeber, Ivo Adan and Koos Rooda
Manufacturing Networks, Department of Mechanical Engineering, Eindhoven University of Technology
P.O. Box 513, 5600 MB Eindhoven, The Netherlands
Email: d.a.j.v.zwieten@tue.nl

1 Introduction

Networks of switched servers are all around, e.g. manufacturing systems, supply chains, urban traffic networks, etc. When the layout and policy of the network is known, under certain conditions it is possible for a server to reconstruct the global state of the system. Therefore, we propose to use the idea of observers for deriving distributed policies for switching networks. However, first a criterium for observability of these networks and design of observers for arbitrary observable networks must be considered. We present the design of observers for a specific class of switching servers.

2 System

We consider switching servers as fluid models with constant input and using a clearing policy with a fixed switching order. The server can serve only one flow at a time and switching between serving different flows might require a switching/setup time. When a flow is served by a server more than once we speak of a re-entrant flow. Figure 1 depicts two examples of switching servers with and without re-entrant flows.

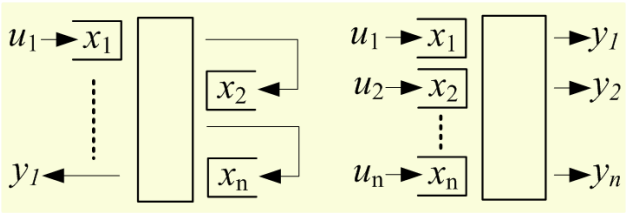

Figure 1: Switching servers with (left) and without (right) re-entrant flows.

The server dynamics can be described by the following linear hybrid model:

$$\dot{x} = B_m u + E_m, \tag{1}$$
$$y = C_m \tag{2}$$

where x and y are the continuous state vector and output vector. The discrete state or mode is denoted by m. Matrices B_m, C_m and E_m are mode dependent. Note that the output vector is piecewise constant and unrelated to the continuous state of the system.

3 Observer design

The observer problem concerns the estimation of unmeasured states of a system using the information of inputs and outputs. For the class of systems under consideration we present a step-by-step approach to derive an observer. First, events are defined. An event is a time-instant where the observable output, i.e. output known by the observer, switches between values. This indicates the beginning or end of a specific mode. Second, the system dynamics are copied by the observer. Third, the switching rules are adapted. A switch to and from modes with observable output is only allowed at the accompanying events. This step entails two extra modes per observable output, which occur during the time that the observer expects a certain event and the actual occurrence of that event. Fourth, the dynamics of these modes are derived. Last, updates of the state vector at events are derived. For example, when an event indicates the end of a mode, the buffer that is served during this mode is known to be zero.

Using this approach an observer is derived which can completely estimate the states of the system if and only if information of all inputs and at least a single output is known.
Furthermore, the time it takes for the observer to completely estimate the states of the system is in finite time and has an upper bound depending on the number of inputs between two consecutive observable outputs.

4 Conclusions

An approach has been developed to derive observers for a class of multi-class switching servers. Also, an observability criterium and the maximal time it takes for the observer to completely estimate the states of the system has been derived.
Interesting future work is expanding this approach to; discrete event systems, systems with stochastically distributed arrival and process times and systems with different policies.

Acknowledgement

This work is supported by the Netherlands Organization for Scientific Research (NWO-VIDI grant 639.072.072).

Part 3

Plenary Lectures

Dynamic Value Functions

Towards Constructive Nonlinear Control Systems Analysis and Design

M. Sassano and A. Astolfi

EEE Dept, Imperial College London, UK

and

DISP, Università di Roma “Tor Vergata”, Italy

Outline

- Introduction
- Preliminaries and Motivations
- Dynamic Lyapunov Functions ($DLf's$)
- A Simple Example
- Dynamic Value Functions ($DVf's$)
  - Optimal Control
  - $\mathcal{L}_2$-disturbance Attenuation
- Examples
- Conclusions

Introduction

The solutions of several analysis and design problems for linear control systems are given in terms of the solutions of matrix equations or inequalities (Lyapunov, Riccati, Sylvester, ...).

Usually, the extension to the nonlinear case is

- conceptually straightforward (leading to partial differential equations or inequalities);
- computationally impracticable.

Goal of this talk is to

- introduce the notion of Dynamic Lyapunov and Value functions;
- demonstrate the applicability of the novel concept in the analysis (Lyapunov’s stability) and design (optimal control, $\mathcal{L}_2$-disturbance attenuation) of nonlinear control systems;
- compare the new methodology with standard approaches.

Preliminaries and Motivations

Consider the problem of studying the stability properties of equilibrium points

$$\dot{x}(t) = f(x(t)) \qquad x(t) \in \mathbb{R}^n, \quad f(0) = 0$$

$x = 0$ asymptotically stable

$$\Updownarrow$$

$$\exists V : \mathbb{R}^n \to \mathbb{R}_+,\ V \in \mathcal{C}^1, \text{ such that } \frac{\partial V}{\partial x} f(x) < 0,\ x \in \mathbb{R}^n \setminus \{0\}$$

Preliminaries and Motivations (cont'd)

Asymptotic stability

$\Rightarrow$ First-order linear partial differential inequality with positivity constraint

$\Rightarrow$ Explicit solution available only in simple cases

A possible solution: Fix the structure of the function, $e.g.$ quadratic, polynomial, and "optimize" the parameters, $e.g.$

$$V(x) = \frac{1}{2} x^\top P x \quad \Rightarrow \quad x^\top P f(x) < 0$$

A simple (negative) example

$$\begin{aligned} \dot{x}_1 &= -x_1 \\ \dot{x}_2 &= x_1^2 - x_2 \end{aligned}$$

The origin is globally asymptotically stable and locally exponentially stable.

$$V = x^\top P x \quad P = P^\top > 0 \qquad \Rightarrow \qquad \mathcal{N} \triangleq \{x \in \mathbb{R}^2 : \dot{V} \leq 0\} \subset \mathbb{R}^2$$

Algebraic Solution

Idea: "Relax" the integrability and (partly) the positivity constraints

$V > 0 : \frac{\partial V}{\partial x} f(x) < 0$ first-order partial differential inequality with positivity constraint

Algebraic Solution

Idea: "Relax" the integrability and (partly) the positivity constraints

$P(x)f(x) \leq 0$ ~~first-order partial differential~~ inequality ~~with positivity constraint~~

with the tangency condition

$$\frac{\partial P}{\partial x}(x)\Big|_{x=0} = \bar{P}$$

where $\bar{P} = \bar{P}^\top > 0$ is such that

$$\bar{P}A + A^\top \bar{P} < 0\,, \qquad A \triangleq \frac{\partial f}{\partial x}(x)\Big|_{x=0}$$

Algebraic Solution

Idea: "Relax" the integrability and (partly) the positivity constraints

$P(x)f(x) \leq 0$ ~~first-order partial differential~~ inequality ~~with positivity constraint~~

$P : \mathbb{R}^n \to \mathbb{R}^n$ does not have to be the gradient of any scalar function

How do we *integrate* the mapping P to obtain a Lyapunov function?

A naive approach (SDLE): $V(x) \triangleq P(x)x$

$$\frac{dV}{dt} = \frac{\partial V}{\partial x} f(x) = P(x)f(x) + x^\top \frac{\partial P^\top}{\partial x} f(x) \leq x^\top \frac{\partial P^\top}{\partial x} f(x)$$

$\Downarrow$

A partial differential inequality (again) with no additional degree of freedom

$\Downarrow$

Not a good idea!

A more sophisticated (??) idea

Consider the extended system $(\xi(t) \in \mathbb{R}^n)$

$$\dot{x} = f(x) \qquad \dot{\xi} = \alpha(x, \xi)$$

(i) Define $V : \mathbb{R}^n \times \mathbb{R}^n \to \mathbb{R}$ such that:

- $V > 0$, for all $(x,\, \xi) \in \Omega \subseteq \mathbb{R}^n \times \mathbb{R}^n$
- $\dfrac{\partial V}{\partial x} = P(x) + \delta(x,\, \xi)$
- $\delta(x,\, x) = 0$
- no specific structure for $\dfrac{\partial V}{\partial \xi}$

(ii) Select $\alpha : \mathbb{R}^n \times \mathbb{R}^n \to \mathbb{R}^n$, $\alpha(0, 0) = 0$ such that

$$\frac{dV}{dt} = \frac{\partial V}{\partial x} f(x) + \frac{\partial V}{\partial \xi} \alpha(x,\, \xi) < \delta(x,\, \xi) f(x) + \frac{\partial V}{\partial \xi} \alpha(x,\, \xi) < 0$$

A more sophisticated (??) idea

Consider the extended system $(\xi(t) \in \mathbb{R}^n)$

$$\dot{x} = f(x) \qquad \dot{\xi} = \alpha(x, \xi)$$

(i) Define $V : \mathbb{R}^n \times \mathbb{R}^n \to \mathbb{R}$ such that:

- $V > 0$, for all $(x,\, \xi) \in \Omega \subseteq \mathbb{R}^n \times \mathbb{R}^n$
- $\dfrac{\partial V}{\partial x} = P(x) + \delta(x,\, \xi)$
- $\delta(x,\, x) = 0$
- no specific structure for $\dfrac{\partial V}{\partial \xi}$

(ii) Select $\alpha : \mathbb{R}^n \times \mathbb{R}^n \to \mathbb{R}^n$, $\alpha(0, 0) = 0$ such that

$$\frac{dV}{dt} = \frac{\partial V}{\partial x} f(x) + \frac{\partial V}{\partial \xi} \alpha(x,\, \xi) < \delta(x,\, \xi) f(x) + \underbrace{\frac{\partial V}{\partial \xi} \alpha(x,\, \xi)}_{} < 0$$

The ξ-dynamics are an additional "design" parameter

A class of pairs (α, V)

$$R = R^\top > 0 \qquad V(x,\, \xi) = P(\xi)x + \frac{1}{2}\|x - \xi\|_R^2 \qquad \|v\|_R^2 \triangleq v^\top R v$$

$$\Downarrow$$

(i) $\exists\, \bar{R} = \bar{R}^\top > 0$, $\Omega \subset \mathbb{R}^n \times \mathbb{R}^n$ such that (by the tangency condition) V is positive definite for all $R > \bar{R}$ and $(x,\, \xi) \in \Omega$

(ii) partial derivatives of V:

$$V_x = P(x) + (x - \xi)^\top (R - \Phi(x, \xi))^\top \qquad P(x) - P(\xi) = (x - \xi)^\top \Phi(x,\, \xi)^\top$$

$$V_\xi = x^\top P_\xi(\xi) - (x - \xi)^\top R$$

A class of pairs (α, V)

$$R = R^\top > 0 \qquad V(x,\, \xi) = P(\xi)x + \frac{1}{2}\|x - \xi\|_R^2 \qquad \|v\|_R^2 \triangleq v^\top R v$$

$$\Downarrow$$

(i) $\exists\, \bar{R} = \bar{R}^\top > 0$, $\Omega \subset \mathbb{R}^n \times \mathbb{R}^n$ such that (by the tangency condition) V is positive definite for all $R > \bar{R}$ and $(x,\, \xi) \in \Omega$

(ii) partial derivatives of V:

$$V_x = P(x) + \overbrace{(x - \xi)^\top (R - \Phi(x, \xi))^\top}^{\delta(x,\, \xi)} \qquad P(x) - P(\xi) = (x - \xi)^\top \Phi(x,\, \xi)^\top$$

$$V_\xi = x^\top P_\xi(\xi) - (x - \xi)^\top R$$

A class of pairs (α, V)

$$R = R^\top > 0 \qquad V(x,\xi) = P(\xi)x + \frac{1}{2}\|x-\xi\|_R^2 \qquad \|v\|_R^2 \triangleq v^\top R v$$

$$\alpha = -k\frac{\partial V}{\partial \xi}^\top = -k\left(x^\top P_\xi(\xi) - (x-\xi)^\top R\right)$$

$$\Downarrow$$

$\exists \bar{k} \geq 0$, $\Omega \subset \mathbb{R}^n \times \mathbb{R}^n$ such that (not trivial since $\{(x,\xi) \in \Omega : \frac{\partial V}{\partial \xi} = 0\} \neq \emptyset$)

$$\delta(x,\xi)f(x) - k\frac{\partial V}{\partial \xi}\frac{\partial V}{\partial \xi}^\top < 0$$

for all $k \geq \bar{k}$ and $(x,\xi) \in \Omega$

Dynamic Lyapunov function (DLf)

A Dynamic Lyapunov function $\mathcal{V}$ is a pair (D_α, V), where

- D_α is the ordinary differential equation $\dot{\xi} = \alpha(x,\xi)$, with $\xi(t) \in \mathbb{R}^n$ and $\alpha(0,0) = 0$
- $V : \Omega \subseteq \mathbb{R}^n \times \mathbb{R}^n \to \mathbb{R}$ is positive definite around $(x,\xi) = (0,0)$ and it is such that

$$\frac{dV}{dt} = \frac{\partial V}{\partial x}f(x) + \frac{\partial V}{\partial \xi}\alpha(x,\xi) < 0,$$

for all $(x,\xi) \in \Omega \setminus \{0\}$

$DLf's$ vs Lyapunov functions

There exists a Dynamic Lyapunov function for $\dot{x} = f(x)$

$$\Downarrow$$

$x = 0$ is an asymptotically stable equilibrium point of $\dot{x} = f(x)$

The origin is a locally exponentially stable equilibrium of $\dot{x} = f(x)$

$$\Downarrow$$

There exists a Dynamic Lyapunov function for $\dot{x} = f(x)$

$$\Downarrow$$

$DLf's$ provide a tool to study stability properties of equilibrium points as Lyapunov functions

- There are "canonical" $DLf's$

$$\mathcal{V} = \left(\dot{\xi} = -k\left(\frac{\partial P}{\partial \xi}x - R(x-\xi)\right),\ P(\xi)x + \frac{1}{2}\|x-\xi\|_R^2\right),$$

provided P is an algebraic solution

- The construction does not rely on the solution of any partial differential equation

From DLf's to Lyapunov functions

Suppose that $\mathcal{V} = (D_\alpha, V)$ is a DLf and that there exists $h : \mathbb{R}^n \to \mathbb{R}^n$ such that

$$\frac{\partial h}{\partial x}f(x) = -k\frac{\partial V}{\partial \xi}(x,\xi)\Big|_{\xi = h(x)}$$

$$\Downarrow$$

$$V_{\mathcal{M}} \triangleq P(h(x))x + \frac{1}{2}\|x - h(x)\|_R^2$$

is a paramterized family of Lyapunov functions

Proof/Comments

- $\mathcal{M} = \{(x,\xi) \in \Omega : \xi = h(x)\}$ is an invariant manifold, parameterized by x
- $V_{\mathcal{M}}$ describes the restriction of the function $V(x,\xi)$ to the manifold $\mathcal{M}$
- h is the solution of a partial differential equation without constraint on the sign of the solution or of the right-hand side

A Simple Example (cont'd)

$$\begin{aligned}\dot{x}_1 &= -x_1\\ \dot{x}_2 &= x_1^2 - x_2\end{aligned}$$

- Construction of DLf: The mapping $P(x) = x^\top$ is an algebraic solution. Then

$$\mathcal{V} = (\dot{\xi} = -k\xi,\ \frac{1}{2}(x^\top x + \xi^\top \xi))$$

is a Dynamic Lyapunov function

- Invariance pde: The system of partial differential equations reduces to two identical (decoupled) pde's

$$-\frac{\partial h_i}{\partial x_1}(x_1, x_2)x_1 + \frac{\partial h_i}{\partial x_2}(x_1, x_2)(x_1^2 - x_2) + kh_i(x_1, x_2) = 0$$

A Simple Example (cont'd)

$$\begin{aligned}\dot{x}_1 &= -x_1\\ \dot{x}_2 &= x_1^2 - x_2\end{aligned}$$

- Construction of DLf: The mapping $P(x) = x^\top$ is an algebraic solution. Then

$$\mathcal{V} = (\dot{\xi} = -k\xi,\ \frac{1}{2}(x^\top x + \xi^\top \xi))$$

is a Dynamic Lyapunov function

- Invariance pde: The system of partial differential equations reduces to two identical (decoupled) pde's

$$-\frac{\partial h_i}{\partial x_1}(x_1, x_2)x_1 + \frac{\partial h_i}{\partial x_2}(x_1, x_2)(x_1^2 - x_2) + kh_i(x_1, x_2) = 0$$

Similar to Lyapunov partial differential equation for exponential stability, *i.e.* $\frac{\partial V}{\partial x} f(x) = -kV$, but without the sign constraint

A Simple Example (cont'd)

$$\begin{aligned}\dot{x}_1 &= -x_1\\ \dot{x}_2 &= x_1^2 - x_2\end{aligned}$$

- Solution and Invariant Manifold:

$$h_1(x) = h_2(x) = L\left(\frac{x_2 + x_1^2}{x_1}\right)x_1^k \qquad \text{not positive definite}$$

$k \geq 1$, where $L : \mathbb{R} \to \mathbb{R}$ is any differentiable function

- Family of Lyapunov functions: let $L(a) = a$, then

$$V_{\mathcal{M}}(x) = \frac{1}{2}(x_1^2 + x_2^2) + (x_2 + x_1^2)^2\left(x_1^{k-1}\right)^2$$

$$k = 1 \qquad \Rightarrow \qquad V_{\mathcal{M}}^1 = \frac{1}{2}(x_1^2 + x_2^2) + (x_2 + x_1^2)^2$$

For all $k \geq 1$, $V_{\mathcal{M}}(x)$ is such that $\mathcal{N} = \mathbb{R}^2$

A Simple Example (cont'd)

$$\begin{aligned}\dot{x}_1 &= -x_1\\ \dot{x}_2 &= x_1^2 - x_2\end{aligned}$$

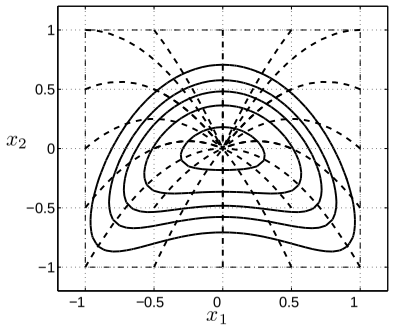

Phase portraits of the trajectories of the system together with the level lines of the Lyapunov function $V_{\mathcal{M}}^1$

Optimal Control

$$\dot{x} = f(x) + g(x)u \qquad J(x(0), u) = \tfrac{1}{2}\int_0^\infty (q(x) + u^\top u)dt$$

$$x(t) \in \mathbb{R}^n, u(t) \in \mathbb{R}^m \qquad q(\cdot) : \mathbb{R}^n \to \mathbb{R}_+, q(0) = 0$$

Assumptions

- $f(0) = 0, \;\Rightarrow\; \exists F : \mathbb{R}^n \to \mathbb{R}^{n\times n}$ such that $f(x) = F(x)x$
- $(f(x),\, q(x))$ zero-state detectable

Goal: determine a control law u_o such that

- the zero equilibrium of the system is asymptotically stable
- the cost is minimized, *i.e.*

$$J(x, u_o) < J(x, u) \qquad u \neq u_o$$

Optimal Control

$$\dot{x} = f(x) + g(x)u \qquad J(x(0), u) = \tfrac{1}{2}\int_0^\infty (q(x) + u^\top u)dt$$

$$x(t) \in \mathbb{R}^n, u(t) \in \mathbb{R}^m \qquad q(\cdot) : \mathbb{R}^n \to \mathbb{R}_+, q(0) = 0$$

Assumptions

- $f(0) = 0, \;\Rightarrow\; \exists F : \mathbb{R}^n \to \mathbb{R}^{n\times n}$ such that $f(x) = F(x)x$
- $(f(x),\, q(x))$ zero-state detectable

Classical solution

$$\frac{\partial V}{\partial x} f(x) - \frac{1}{2}\frac{\partial V}{\partial x} g(x) g(x)^\top \frac{\partial V}{\partial x}^\top + \frac{1}{2} q(x) = 0$$

$$\Downarrow$$

$$u_o = -g(x)^\top \frac{\partial V}{\partial x}^\top$$

Dynamic Value Function (DVf)

A Dynamic Value function $\mathcal{V}$ is a pair (D_α, V), where

- D_α is the dynamical system

$$\begin{aligned} \dot{\xi} &= \alpha(x,\, \xi)\,, \\ u &= -g(x)^\top V_x(x,\, \xi)^\top\,, \end{aligned}$$

  with $\xi(t) \in \mathbb{R}^n$, $\alpha : \mathbb{R}^n \times \mathbb{R}^n \to \mathbb{R}^n$, $\alpha(0, 0) = 0$;
- $V : \Omega \subseteq \mathbb{R}^n \times \mathbb{R}^n \to \mathbb{R}$ is positive definite around $(x,\, \xi) = (0, 0)$ and it is such that

$$\frac{\partial V}{\partial x} f(x) + \frac{\partial V}{\partial \xi}\alpha(x, \xi) - \frac{1}{2}\frac{\partial V}{\partial x} g(x) g(x)^\top \frac{\partial V}{\partial x}^\top + \frac{1}{2} q(x) \leq 0\,,$$

  for all $(x, \xi) \in \Omega$.

$DVf's$ and optimal control

(i) Extended state-space $\Rightarrow$ dynamic feedback

(ii) V solves a partial differential inequality in place of an equation

$DV\,f's$ and optimal control

(i) Extended state-space $\Rightarrow$ dynamic feedback

(ii) V solves a partial differential inequality in place of an equation

$$\dot{x} = f(x) + g(x)u \qquad J(x(0), u) = \tfrac{1}{2}\int_0^\infty (q(x) + u^\top u)dt$$

$$x(t) \in \mathbb{R}^n, u(t) \in \mathbb{R}^m \qquad q(\cdot) : \mathbb{R}^n \to \mathbb{R}_+, q(0) = 0$$

$DV\,f's$ and optimal control

(i) extended state-space

(ii) V solves a partial differential inequality in place of an equation

$$\dot{x} = f(x) + g(x)u \qquad J(x(0), u) = \tfrac{1}{2}\int_0^\infty (q(x) + u^\top u)dt$$

$$\dot{\xi} = \alpha(x, \xi)$$

$$x(t) \in \mathbb{R}^n, \xi(t) \in \mathbb{R}^n, u(t) \in \mathbb{R}^m \qquad q(\cdot) : \mathbb{R}^n \to \mathbb{R}_+, q(0) = 0$$

$DV\,f's$ and optimal control

(i) extended state-space

(ii) V solves a partial differential inequality in place of an equation

$$\dot{x} = f(x) + g(x)u \qquad J(x(0), u) = \tfrac{1}{2}\int_0^\infty (q(x) + u^\top u + c(x, \xi))dt$$

$$\dot{\xi} = \alpha(x, \xi)$$

$$x(t) \in \mathbb{R}^n, \xi(t) \in \mathbb{R}^n, u(t) \in \mathbb{R}^m \qquad q(\cdot) : \mathbb{R}^n \to \mathbb{R}_+, q(0) = 0$$

$$c : \mathbb{R}^n \times \mathbb{R}^n \to \mathbb{R}_+, c(0, 0) = 0$$

$DV\,f's$ and optimal control (cont'd)

(i) extended state-space

(ii) V solves a partial differential inequality in place of equation

Interpretation

$DVf's$ and optimal control (cont'd)

(i) extended state-space

(ii) V solves a partial differential inequality in place of equation

Interpretation

- D_α is a dynamic control law that approximates the optimal control law

$DVf's$ and optimal control (cont'd)

(i) extended state-space

(ii) V solves a partial differential inequality in place of equation

Interpretation

- D_α is a dynamic control law that approximates the optimal control law
- c is an additional cost (the cost of solving an algebraic equation)

$DVf's$ and optimal control (cont'd)

(i) extended state-space

(ii) V solves a partial differential inequality in place of equation

Interpretation

- D_α is a dynamic control law that approximates the optimal control law
- c is an additional cost (the cost of solving an algebraic equation)

Comments

The additional cost can be reduced

- initializing the dynamic extension: $\xi^*(x) = \arg\min_\xi V(x,\xi)$
- using $k = k(x,\xi)$ to *shape* the running cost c

Algebraic Solution and Construction of $DVf's$

Let $\sigma(x) \triangleq x^\top \Sigma(x) x \geq 0$. A $\mathcal{C}^1$ mapping $P : \mathbb{R}^n \to \mathbb{R}^{1\times n}$, $P(0) = 0$, is said to be an algebraic $\bar{P}$ solution of the HJB pde if

(i) for all $x \in \mathbb{R}^n$

$$P(x)f(x) + \frac{1}{2}q(x) - \frac{1}{2}P(x)g(x)g(x)^\top P(x)^\top + x^\top \Sigma(x) x = 0$$

(ii) P is tangent in $x = 0$ to the symmetric positive definite solution of

$$\bar{P}A + A^\top \bar{P} - \bar{P}BB^\top \bar{P} + Q = 0$$

Algebraic Solution and Construction of $DVf's$

Let $\sigma(x) \triangleq x^\top \Sigma(x) x \geq 0$. A $\mathcal{C}^1$ mapping $P : \mathbb{R}^n \to \mathbb{R}^{1\times n}$, $P(0) = 0$, is said to be an algebraic $\bar{P}$ solution of the HJB pde if

(i) for all $x \in \mathbb{R}^n$

$$P(x)f(x) + \frac{1}{2}q(x) - \frac{1}{2}P(x)g(x)g(x)^\top P(x)^\top + x^\top \Sigma(x)x = 0$$

(ii) P is such that

$$\Psi(x) \triangleq \frac{\partial P(x)^\top}{\partial x}\Big|_{x=0} = \bar{P}$$

Algebraic Solution and Construction of $DVf's$

Let $\sigma(x) \triangleq x^\top \Sigma(x) x \geq 0$. A $\mathcal{C}^1$ mapping $P : \mathbb{R}^n \to \mathbb{R}^{1\times n}$, $P(0) = 0$, is said to be an algebraic $\bar{P}$ solution of the HJB pde if

(i) for all $x \in \mathbb{R}^n$

$$P(x)f(x) + \frac{1}{2}q(x) - \frac{1}{2}P(x)g(x)g(x)^\top P(x)^\top + x^\top \Sigma(x)x = 0$$

(ii) P is such that

$$\Psi(x) \triangleq \frac{\partial P(x)^\top}{\partial x}\Big|_{x=0} = \bar{P}$$

Note:

- The mapping P does not need to be a gradient vector
- Only local positivity is imposed

Construction of $DVf's$

"Integrate" the algebraic $\bar{P}$ solution in the sense defined for $DLf's$:

$$V(x,\, \xi) = P(\xi)x + \frac{1}{2}\|x - \xi\|_R^2$$

Then $\mathcal{V} = (D_\alpha,\, V)$ with V as above and D_α as

$$\begin{aligned} \dot{\xi} &= -k\left(\frac{\partial P}{\partial \xi}x - R(x-\xi)\right) \\ u &= -g(x)^\top \left(P(x)^\top + (R - \Phi(x,\, \xi))(x-\xi)\right) \end{aligned}$$

is a Dynamic Value function if

$$\frac{1}{2}A_{cl}(x)^\top \Delta(x,\xi) + \frac{1}{2}\Delta(x,\xi)^\top A_{cl}(x) < \Sigma(x) + \frac{1}{2}\Delta(x,\xi)^\top g(x)g(x)^\top \Delta(x,\xi)$$

$$\Delta(x,\xi) = (R - \Phi(x,\xi))R^{-1}\Psi(\xi)^\top \qquad A_{cl}(x) = F(x) - g(x)g(x)^\top N(x)$$

$$P(x) - P(\xi) = (x-\xi)^\top \Phi(x,\, \xi)^\top$$

$N : \mathbb{R}^n \to \mathbb{R}^{n\times n}$ such that $P(x) = x^\top N(x)^\top$

Comments on DVf's

- Suppose that $\Sigma(0) = \bar{\Sigma} > 0$ in the definition of algebraic $\bar{P}$ solution. Then, by continuity, there exists a neighborhood $\Omega \subset \mathbb{R}^n \times \mathbb{R}^n$ of the origin such that the condition (C) is satisfied for all $(x, \xi) \in \Omega$, hence $\mathcal{V}$ is a Dynamic Value function in Ω
- The vector field $A_{cl}(x)x$ describes the closed-loop nonlinear system obtained when only the *algebraic* input $u = -g(x)^\top P(x)^\top$ is applied
- We are able to construct a (dynamic) value function for a nonlinear (approximate) optimal control problem by simply solving an algebraic scalar inequality
- The explicit expression of Φ is not needed:

$$u = -g(x)^\top \left(P(\xi)^\top + R(x-\xi)\right)$$

Sketch of the Proof

HJB equation for the extended system

$$\Downarrow$$

$$\mathcal{HJB}(x,\,\xi) \triangleq \frac{\partial V}{\partial x} f(x) - k\frac{\partial V}{\partial \xi}\frac{\partial V}{\partial \xi}^{\top} - \frac{1}{2}\frac{\partial V}{\partial x} g(x) g(x)^{\top} \frac{\partial V}{\partial x}^{\top} + \frac{1}{2} q(x) \leq 0$$

$$\Downarrow$$

$$\mathcal{HJB}(x,\,\xi) = -[x^{\top}\;(x-\xi)^{\top}][M(x,\xi) + kC(\xi)^{\top}C(\xi)] \begin{bmatrix} x \\ (x-\xi) \end{bmatrix} \leq 0$$

$$M(x,\xi) = \begin{bmatrix} \Sigma(x) & \Gamma_1(x,\xi) \\ \Gamma_1(x,\xi)^{\top} & \Gamma_2(x,\xi) \end{bmatrix}$$

$$C(\xi) = [\Psi(\xi)^{\top} \; -R] \qquad \Gamma_1 = -\frac{1}{2} A_{cl}^{\top}(x)(R - \Phi(x,\xi))$$

$$\Gamma_2 = \frac{1}{2}(R - \Phi(x,\xi))^{\top} g(x) g(x)^{\top} (R - \Phi(x,\xi))$$

Sketch of the Proof

HJB equation for the extended system

$$\Downarrow$$

$$\mathcal{HJB}(x,\,\xi) \triangleq \frac{\partial V}{\partial x} f(x) - k\frac{\partial V}{\partial \xi}\frac{\partial V}{\partial \xi}^{\top} - \frac{1}{2}\frac{\partial V}{\partial x} g(x) g(x)^{\top} \frac{\partial V}{\partial x}^{\top} + \frac{1}{2} q(x) \leq 0$$

$$\Downarrow$$

$$\mathcal{HJB}(x,\,\xi) = -[x^{\top}\;(x-\xi)^{\top}][M(x,\xi) + kC(\xi)^{\top}C(\xi)] \begin{bmatrix} x \\ (x-\xi) \end{bmatrix} \leq 0$$

There exists $\bar{k} \geq 0$ such that $\mathcal{HJB} \leq 0$ for all $k \geq \bar{k}$

$$\Updownarrow$$

$$(C(\xi)^{\perp})^{\top} M(x\,\xi) C(\xi)^{\perp} > 0$$

$$\Uparrow$$

$\mathcal{V}$ is a DVf

Shaping the Additional Running Cost

The additional running cost is

$$h(x,\xi) = [x^{\top}\;(x-\xi)^{\top}][M(x,\xi) + kC(\xi)^{\top}C(\xi)] \begin{bmatrix} x \\ (x-\xi) \end{bmatrix} \geq 0$$

$$k(x,\xi) = (CC^{\top})^{-1} CMZ \left((C^{\perp})^{\top} MC^{\perp}\right)^{-1} (C^{\perp})^{\top} MC^{\top} - CMC^{\top}(CC^{\top})^{-1}$$

$$\Downarrow$$

$$h(x,\xi)\big|_{\Omega \setminus Ker(C(\xi))} = 0$$

Additionally if there exists $\varepsilon \in \mathbb{R}_+$ such that

$$0 < \Sigma(x) + \frac{1}{2}\Delta^{\top} g(x) g(x)^{\top} \Delta - \frac{1}{2} A_{cl}(x)^{\top}\Delta - \frac{1}{2}\Delta^{\top} A_{cl}(x) < \varepsilon I$$

then $h(x,\xi) \leq \varepsilon T(x,\xi)$, for all $(x,\xi) \in Ker(C(\xi))$, with T some known continuous function

Time-varying DVfs

Let

$$V(t,x,\xi) = P(\xi)x + \frac{1}{2}(x-\xi)^{\top} R(t)(x-\xi)$$

with $R(t) = \Phi(x(t), \xi(t))$, for all $t \geq 0$. Suppose

- V is positive definite uniformly in t
- $\Phi = \Phi^{\top} > 0$
- $\Psi(\xi) R^{-1} \dot{\Phi}(x,\xi) R^{-1} \Psi(\xi)^{\top} < \Sigma(x)$

Then V solves the HJB partial differential inequality

$$\frac{\partial V}{\partial t} + \mathcal{HJB}(x,\xi) \leq 0$$

Time-varying DVfs

Let

$$V(t,x,\xi) = P(\xi)x + \frac{1}{2}(x-\xi)^\top R(t)(x-\xi)$$

with $R(t) = \Phi(x(t),\xi(t))$, for all $t \geq 0$. Suppose

- V is positive definite uniformly in t
- $\Phi = \Phi^\top > 0$
- $\Psi(\xi)R^{-1}\dot{\Phi}(x,\xi)R^{-1}\Psi(\xi)^\top < \Sigma(x)$

$\mathcal{V} = (D_\alpha, V)$, with D_α defined as

$$\begin{aligned}\dot{\xi} &= -k(\Psi(\xi)^\top x - R(t)(x-\xi))\\ u &= -g(x)^\top\left(P(x)^\top + (R(t)-\Phi(x,\xi))(x-\xi)\right) = -g(x)^\top P(x)^\top\end{aligned}$$

is a time-varying DVf

The control law u does not depend on ξ!

$\mathcal{L}_2$-disturbance Attenuation

Consider a perturbed system

$$\begin{aligned}\dot{x} &= f(x) + g(x)u + p(x)d\\ z &= \begin{bmatrix} h(x) \\ u \end{bmatrix}\end{aligned}$$

Goal: ensure that the "effect" of d on z, in the $\mathcal{L}_2$-gain sense, is smaller than a given γ.

Modify the definition of algebraic solution to include the disturbance attenuation objective

$$P(x)f(x) + \frac{1}{2}P(x)\left[\frac{1}{\gamma^2}p(x)p(x)^\top - g(x)g(x)^\top\right]P(x)^\top + \frac{1}{2}h(x)^\top h(x) + \sigma(x) \leq 0.$$

Construct a Dynamic Storage function in the same spirit of a DVf

Example – The Van der Pol Oscillator

$$\begin{aligned}\dot{x}_1 &= x_2\\ \dot{x}_2 &= -x_1 - \frac{1}{2}(1-x_1^2)x_2 + x_1 u\end{aligned}$$

$$J(x(0),u) = \frac{1}{2}\int_0^\infty (x_2^2 + u^2)dt$$

The oscillator has a stable equilibrium at the origin surrounded by an unstable limit cycle.

The linearized system around the origin is uncontrollable ($B = 0$).

The value function is

$$V_o(x_1,x_2) = \frac{1}{2}(x_1^2 + x_2^2)$$

allowing the comparison between the optimal control, the optimal control for the linearized problem, and the approximate dynamic optimal control

Example – The Van der Pol Oscillator

Algebraic Solution: Let $\Sigma(x) = \lambda/2\, diag\{x_2^2,\, x_1^2\}$, $\lambda > 0$.

$P(x) = [x_1(1-\lambda x_1 x_2)\,, x_2]$ is an algebraic $\bar{P}$ solution (P is not a gradient)

Dynamic Value function: Let $R = diag(\kappa,\kappa)$ with $\kappa > 1$.

$$V(x,\xi) = x_1\xi_1(1-\xi_1\xi_2) + x_2\xi_2 + \frac{\kappa}{2}(x_1-\xi_1)^2 + \frac{\kappa}{2}(x_2-\xi_2)^2$$

$$\begin{aligned}\dot{\xi}_1 &= -k(x_1 - 2\lambda x_1\xi_1\xi_2 - \lambda\xi_1^2 x_2 - \kappa(x_1-\xi_1))\\ \dot{\xi}_2 &= -k(x_2 - \kappa(x_1-\xi_1))\\ u &= -\kappa x_1 x_2 + (\kappa-1)x_1\xi_2\end{aligned}$$

The Dynamic Value function is such that for any $\epsilon > 0$ there exists $\kappa > 1$ such that

$$V_o(x(0)) \leq V(x(0),\, \xi^*(x(0))) \leq V_o(x(0)) + \epsilon$$

... but (in principle) we need to solve a pde to compute V_o, while only a scalar algebraic equation must be solved to compute the DVf.

Example – The Van der Pol Oscillator

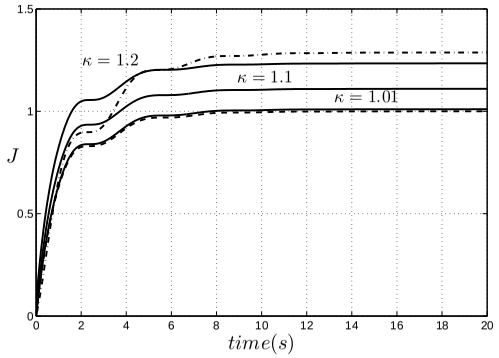

Integral of the running cost
u_o (dashed line), $u = 0$, *i.e.* the optimal solution of the linearized problem (dash-dotted line), dynamic control law (solid lines)

Example – Fully Actuated Mechanical Systems – Optimal Control

Consider mechanical systems described by equations of the form

$$\begin{aligned}\dot{x}_1 &= x_2\,,\\ \dot{x}_2 &= M(x_1)^{-1}\left[\boxed{\mathsf{u}} - C(x_1,x_2)x_2 - G(x_1) + G(0)\right]\,.\end{aligned}$$

$x_1(t) \in \mathbb{R}^n$, $x_2(t) \in \mathbb{R}^n$, $M(x_1) = M(x_1)^\top > 0$, $G(x_1) - G(0) = \bar{G}(x_1)x_1$.

Let

$$q(x) = \mu_1^2 x_1^\top x_1 + \mu_2^2 x_2^\top x_2$$

$$f(x) \triangleq \begin{bmatrix} x_2 \\ -M(x_1)^{-1}\left(C(x_1,x_2)x_2 + G(x_1) - G(0)\right)\end{bmatrix}$$

$$g(x) \triangleq \epsilon \begin{bmatrix} 0 \\ M(x_1)^{-1}\end{bmatrix}\,, \qquad \boxed{\epsilon = 1}$$

Example – Fully Actuated Mechanical Systems – Dist. Attenuation

Consider mechanical systems described by equations of the form

$$\begin{aligned}\dot{x}_1 &= x_2\,,\\ \dot{x}_2 &= M(x_1)^{-1}\left[\boxed{\mathsf{u + d}} - C(x_1,x_2)x_2 - G(x_1) + G(0)\right]\,.\end{aligned}$$

$x_1(t) \in \mathbb{R}^n$, $x_2(t) \in \mathbb{R}^n$, $M(x_1) = M(x_1)^\top > 0$, $G(x_1) - G(0) = \bar{G}(x_1)x_1$.

Let

$$q(x) = \mu_1^2 x_1^\top x_1 + \mu_2^2 x_2^\top x_2$$

$$f(x) \triangleq \begin{bmatrix} x_2 \\ -M(x_1)^{-1}\left(C(x_1,x_2)x_2 + G(x_1) - G(0)\right)\end{bmatrix}$$

$$g(x) \triangleq \epsilon \begin{bmatrix} 0 \\ M(x_1)^{-1}\end{bmatrix}\,, \qquad \boxed{\epsilon \in [0,1)}$$

Example – Fully Actuated Mechanical Systems – Algebraic Solution

$$x_i^\top \Upsilon_i^\top(x)\Upsilon_i(x)x_i = x_i^\top(\mu_i^2 I_n + \Sigma_i(x))x_i \;>\; 0 \qquad i = 1,2$$

Let $W_1(x_1,x_2)$ be such that

$$\Upsilon_1^\top \Upsilon_1 = W_1 M^{-1}\bar{G} + \bar{G}^\top M^{-1} W_1 + \epsilon^2 W_1 M^{-2} W_1$$

and let

$$V_1 = W_1 M^{-1}\left[C + \epsilon^2 M^{-1} W_2\right] + \bar{G}^\top M^{-1} W_2$$

$$V_2 = W_2 M^{-1}\left[C + \frac{1}{2}\epsilon^2 M^{-1} W_2\right] - \frac{1}{2}\Upsilon_2^\top \Upsilon_2$$

with $W_2(x_1,x_2)$ such that $W_2(0,0) = \bar{P}_3$.

$P(x) = [x_1^\top V_1 + x_2^\top V_2, x_1^\top W_1 + x_2^\top W_2]$ is an algebraic solution of the HJB equation

Example – Fully Actuated Mechanical Systems – Algebraic Solution

$$x_i^\top \Upsilon_i^\top(x)\Upsilon_i(x)x_i = x_i^\top(\mu_i^2 I_n + \Sigma_i(x))x_i \;>\; 0 \qquad i = 1,2$$

Let $W_1(x_1, x_2)$ be such that

$$\underbrace{\Upsilon_1^\top \Upsilon_1 = W_1 M^{-1}\bar{G} + \bar{G}^\top M^{-1} W_1 + \epsilon^2 W_1 M^{-2} W_1}_{\text{Algebraic matrix equation in the unknown } W_1}$$

For planar mechanical systems, *i.e.* $G(x_1) = 0$, the algebraic solution has a closed-form

$$\Downarrow$$

$$W_1(x_1,\, x_2) = \frac{1}{\epsilon}\Upsilon_1^\top M(x_1)$$

Example – Fully Actuated Mechanical Systems – DVf

$$P(x) = [x_1^\top V_1 + x_2^\top V_2, x_1^\top W_1 + x_2^\top W_2]$$

$$\Downarrow$$

$$V = (\xi_1^\top V_1(\xi) + \xi_2^\top V_2(\xi))x_1 + (\xi_1^\top W_1(\xi) + \xi_2^\top W_2(\xi))x_2 + \frac{1}{2}\|x-\xi\|_R^2$$

$$D_\alpha : \begin{cases} \dot{\xi} & = -k\left(\dfrac{\partial P}{\partial \xi}^\top x - R(x-\xi)\right) \\ u & = -g(x)^\top\left[P(\xi)^\top + R(x-\xi)\right] \end{cases}$$

Example – Fully Actuated Mechanical Systems – 2R planar robot

$$\begin{aligned} \dot{x}_1 &= x_2 \\ \dot{x}_2 &= M(x_1)^{-1}\left[\tau - C(x_1,x_2)x_2\right] \end{aligned}$$

$\tau = u$ (optimal control) $\qquad$ $\tau = u + d$ (disturbance attenuation)

$$M = \begin{bmatrix} a_1 + 2a_2\cos(\chi_2) & a_2\cos(\chi_2) + a_3 \\ a_2\cos(\chi_2) + a_3 & a_3 \end{bmatrix} \quad C = \begin{bmatrix} 0 & -a_2\sin(\chi_2)(\chi_4 + 2\chi_3) \\ a_2\sin(\chi_2)\chi_3 & 0 \end{bmatrix}$$

- Compute the Algebraic Solution (closed-form)
- Design the dynamic control law with $R = \kappa\Phi(0,0)$
- Compare with the optimal solution of the linearized problem (no closed-form solution of the HJB pde)

Example – Fully Actuated Mechanical Systems – Optimal Control

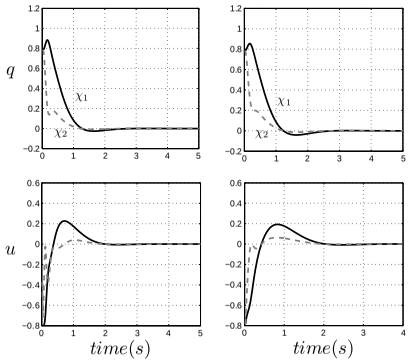

Dynamic control law (left) and linearized control law (right graph)

$$V_d(x(0), \xi^*(x(0))) = 0.2081 < V_l(x(0)) = 0.2606$$

Example – Fully Actuated Mechanical Systems – Dist. Attenuation

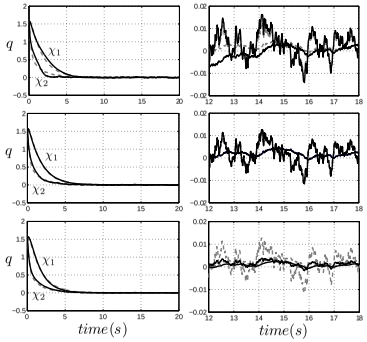

Dynamic control law (left) and linearized control law (right graph)

$\kappa = 0.8$ (top) $\kappa = 1$ (middle) $\kappa = 5$ (bottom)

Example – Optimal Control of Air Path in a Diesel Engine

Regulated outputs: fresh mass airflow (MAF)/absolute pressure in intake manifold (MAP)

Inputs: variable geometry turbo-charger (VGT) and exhaust gas recirculation valve (EGR)

Model: from input/output measurements, approximated by a polynomial Nonlinear Auto Regressive model with eXogenous inputs (NARX)

$$y(k) = \theta_0 + \sum_{m=1}^{l} \sum_{\substack{i_1 \dots i_m = 1 \\ i_1 \le i_2 \le \dots \le i_m}}^{n} \theta_{i_1 \dots i_m} \prod_{p=1}^{m} x_{i_p}(k) + \varepsilon(k)$$

(i) Obtain a state-space discrete time representation $x(k+1) = F(x(k), v)$ (x_1 and x_3 describe the regulated outputs MAP and MAF, respectively)

(ii) Obtain a continuous-time representation (inverse Euler transformation)

$$\dot{x}(t) = \frac{1}{T}(-x(t) + F(x(t), v(t))) \qquad \text{T sampling time}$$

Example – Optimal Control of Air Path in a Diesel Engine

Let $x_1^* \in \mathbb{R}$ and $x_3^* \in \mathbb{R}$. Determine a control law of the form

$$\dot{\xi} = \alpha(x, \xi, x_1^*, x_3^*) \qquad u = \beta(x, \xi, x_1^*, x_3^*)$$

such that

(i) $x(t) \in \mathcal{L}_\infty$

(ii) $\lim_{t\to\infty} \|x_1(t) - x_1^*\| = 0, \lim_{t\to\infty} \|x_3(t) - x_3^*\| = 0$

(iii) the cost

$$J(x(0), u) = \int_0^\infty (q(x(t) - x^*) + u(t)^\top u(t))dt$$

is minimized

Example – Optimal Control of Air Path in a Diesel Engine

Add stable filters for the input v to obtain an input-affine nonlinear model

$$\dot{x}(t) = \frac{1}{T}(-x(t) + F(x(t), v(t)))$$

$$\Downarrow$$

$$\begin{aligned} \dot{x}(t) &= \frac{1}{T}(-x(t) + F(x(t), p_1, p_2, z(t))) \\ \dot{z}(t) &= Az(t) + Hv(t) \end{aligned}$$

$$\sigma(A) \subset \mathbb{C}^-$$

p_1 and p_2 uncontrolled inputs (engine speed, injected fuel amount)

Example – Optimal Control of Air Path in a Diesel Engine

Let x_2^*, x_4^*, z_1^* and z_2^* be the solution of

$$0 = \frac{1}{T}\left(-x^* + F(x^*, p_1, p_2, z^*)\right)$$

Then the control law

$$\dot{\xi} = -k\left(\Psi(\xi)^\top e - R(e-\xi)\right),$$
$$v = v^* - B^\top P(\xi) - B^\top R(e-\xi),$$

with $e = [x - x^*, z - z^*]$ and $v^* = -H^{-1}Az^*$, approximately solve the optimal control problem

System of 4 quadratic equations in 4 unknown

There exists a solution if the references are feasible

Example – Optimal Control of Air Path in a Diesel Engine

The dynamic control law has been tested on a Combustion Engine Test Bench at the Institute for Design and Control of Mechatronical Systems of the J. Kepler University, Linz, Austria.

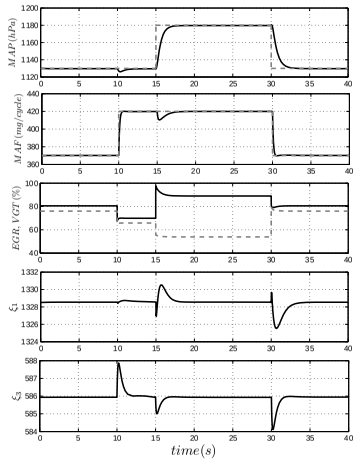

Conclusions

- Dynamic Value function
  - DVf can be constructed by solving an algebraic equation
  - DVf provides a dynamic (in place of static) control law that approximates optimal control laws
  - the additional cost can be reduced by initializing the dynamic extension and by shaping the running cost
- For autonomous systems $DVf's$ reduce to $DLf's$
  - $DLf's$ *generalize* Lyapunov functions
  - The existence result is constructive
- The applicability of the novel concept has been illustrated by non-trivial examples

Model reduction by moment matching

A. Astolfi

a.astolfi@ic.ac.uk

EEE Dept, Imperial College London, UK

and

DISP, Università di Roma "Tor Vergata", Italy

Outline

- Introduction
  - The model reduction problem
  - Goal of this work and its foundations
- Model reduction by moment matching for linear systems – Revisited
- Reduction by projection
- Nonlinear systems
- Frequency response of nonlinear systems
- Petrov-Galerkin projection
- The Markov parameters of nonlinear systems
- A brief discussion

Introduction

The model reduction problem for linear and nonlinear systems has been widely studied over the past decades.

Applications: reduced order models are often used in analysis and design

- Mechanical systems: study based on a rigid body perspective
- Large scale systems (IC, weather forecast): study based on simplified models

Theory: the model reduction problem generates important theoretical questions and requires advanced tools from linear algebra, functional analysis and numerical analysis

Introduction – The model reduction problem

Given an I/O system $\Rightarrow$ Compute a *simpler* system which *approximates* its I/O behavior

To render precise this problem formulation it is necessary to define:

the meaning of the approximation — the concept of simplicity

Introduction – The model reduction problem (cont'd)

The meaning of the approximation

- Approximation error in terms of
  - the frequency response of a suitably defined *error system*
  - the response of the system for classes of input signals
    (the moment matching method, which zeroes the transfer function of the error system at specific points)

  (Linear systems: Antoulas, Jaimoukha, Sorensen, van Dooren, ...)
- Approximation error in terms of H_2 or H_∞ norm of the error system
  (Linear systems: Kavranoglu and Bettayeb, Huang and co-workers, ...)
  (Nonlinear systems: Scherpen, van der Schaft)
- Approximation error based on the Hankel operator
  (Linear systems: Glover)
  (Nonlinear systems: Scherpen, van der Schaft, Fujimoto, Krener)

Introduction – The model reduction problem (cont'd)

The concept of simplicity

Linear systems: simplicity = dimension of the system

Nonlinear systems: dimensional argument inappropriate, need to take into consideration also the complexity of the functions

Introduction – The model reduction problem (cont'd)

The concept of simplicity

Linear systems: simplicity = dimension of the system

Nonlinear systems: dimensional argument inappropriate, need to take into consideration also the complexity of the functions

Other issues

- Properties of the reduced order model
  (e.g. stability, passivity, ... , of the system retained by the reduced model).
- Computational cost associated with the construction of the reduced model.
- Systems theoretic interpretation of the reduction process.

Introduction – Goals of this work and its foundations

- Goals
  - To take a first step towards the development of a theory for model reduction, based on the notion of moment, for nonlinear systems.
  - To revisit the linear theory, providing new perspectives and results.

Introduction – Goals of this work and its foundations

- Goals
  - To take a first step towards the development of a theory for model reduction, based on the notion of moment, for nonlinear systems.
  - To revisit the linear theory, providing new perspectives and results.
- Foundations
  - The steady-state response of nonlinear systems (Isidori-Byrnes).
  - Center manifold theory (Carr).
  - The theory of output regulation for nonlinear systems (Byrnes-Isidori, Huang).
  - The *frequency response* of nonlinear systems (Byrnes-Isidori, Isidori-Astolfi, Hu-Teel-Lin, Huang, Chua-Ng).

Linear systems – The notion of moment

Consider a linear SISO system ($x(t) \in \mathbb{R}^n$, $u(t) \in \mathbb{R}$, $y(t) \in \mathbb{R}$)

$$\begin{array}{rcl} \dot{x} & = & Ax + Bu \\ y & = & Cx \end{array} \qquad W(s) = C(sI - A)^{-1}B$$

Frequency-domain description of moments

- 0-moment at $s^\star \in \mathbb{C}$:
$$\eta_0(s^\star) = C(s^\star I - A)^{-1}B$$
- k-moment at $s^\star \in \mathbb{C}$:
$$\eta_k(s^\star) = \frac{(-1)^k}{k!}\left[\frac{d^k}{ds^k}\left(C(sI - A)^{-1}B\right)\right]_{s=s^\star} = C(s^\star I - A)^{-(k+1)}B$$

Linear systems – The notion of moment

Consider a linear SISO system ($x(t) \in \mathbb{R}^n$, $u(t) \in \mathbb{R}$, $y(t) \in \mathbb{R}$)

$$\begin{array}{rcl} \dot{x} & = & Ax + Bu \\ y & = & Cx \end{array} \qquad W(s) = C(sI - A)^{-1}B$$

Time-domain description of moments (for all $s^\star \notin \sigma(A)$)

- $\eta_0(s^\star) = C\Pi$, Π is the (unique) solution of the Sylvester equation $A\Pi + B = \Pi s^\star$.

Linear systems – The notion of moment

Consider a linear SISO system ($x(t) \in \mathbb{R}^n$, $u(t) \in \mathbb{R}$, $y(t) \in \mathbb{R}$)

$$\begin{array}{rcl} \dot{x} & = & Ax + Bu \\ y & = & Cx \end{array} \qquad W(s) = C(sI - A)^{-1}B$$

Time-domain description of moments (for all $s^\star \notin \sigma(A)$)

- $\begin{bmatrix} \eta_0(s^\star) & \cdots & \eta_k(s^\star) \end{bmatrix} = C\Pi\Psi_k$,

  Π is the (unique) solution of the Sylvester equation $A\Pi + BL_k = \Pi\Sigma_k$

$$\Psi_k = \mathrm{diag}(1, -1, \cdots, (-1)^k) \qquad L_k = \begin{bmatrix} 1 & 0 & \cdots & 0 \end{bmatrix}$$

$$\Sigma_k = \begin{bmatrix} s^\star & 1 & 0 & \cdots & 0 \\ 0 & s^\star & 1 & \cdots & 0 \\ \vdots & \vdots & \ddots & \ddots & \vdots \\ 0 & \cdots & 0 & s^\star & 1 \\ 0 & \cdots & \cdots & 0 & s^\star \end{bmatrix}$$

Linear systems – The notion of moment (cont'd)

- The pair (L_k, Σ_k) is observable for any $s^\star$.
- Σ_k and L_k are complex valued and have a special structure.
- Moments are coordinates invariant and, by a property of real rational functions,

$$\eta_k(\bar{s}^\star) = \overline{\eta_k(s^\star)}.$$

Linear systems – The notion of moment (cont'd)

Consider a linear system and

$$s^\star \in \mathbb{R} \qquad (s^\star = \alpha^\star + i\omega^\star \in \mathbb{C} \setminus \mathbb{R})$$

Suppose $s^\star \notin \sigma(A)$.

$\eta_0(s^\star), \ldots, \eta_k(s^\star)$ are in one-to-one relation with the matrix $C\Pi$, where Π is the (unique) solution of the Sylvester equation

$$A\Pi + BL = \Pi S,$$

with S any non-derogatory real matrix such that

$$\det(sI - S) = (s - s^\star)^{k+1} \qquad (= \left(s^2 - 2\alpha^\star s + (\alpha^\star)^2 + (\omega^\star)^2\right)^{k+1}) \qquad (1)$$

and L such that the pair (L, S) is observable.

Linear systems – The notion of moment (cont'd)

Consider a linear system, $s^\star \in \mathbb{C}$, $k \geq 0$ and assume $\sigma(A) \subset \mathbb{C}^-$ and $s^\star \in \mathbb{C}^0$.

Let

$$\dot{\omega} = S\omega, \qquad \begin{matrix}\omega(t) \in \mathbb{R}^\kappa \\ \omega(0) \neq 0\end{matrix} \qquad \kappa = \begin{cases} k+1 & \text{if } s^\star \in \mathbb{R}, \\ 2(k+1) & \text{if } s^\star \in \mathbb{C} \setminus \mathbb{R}, \end{cases}$$

and S any non-derogatory real matrix with characteristic polynomial as in (1).

Linear systems – The notion of moment (cont'd)

Consider a linear system, $s^\star \in \mathbb{C}$, $k \geq 0$ and assume $\sigma(A) \subset \mathbb{C}^-$ and $s^\star \in \mathbb{C}^0$.

Let

$$\dot{\omega} = S\omega, \qquad \begin{matrix}\omega(t) \in \mathbb{R}^\kappa \\ \omega(0) \neq 0\end{matrix} \qquad \kappa = \begin{cases} k+1 & \text{if } s^\star \in \mathbb{R}, \\ 2(k+1) & \text{if } s^\star \in \mathbb{C} \setminus \mathbb{R}, \end{cases}$$

and S any non-derogatory real matrix with characteristic polynomial as in (1).

Consider the interconnection ((L, S) observable)

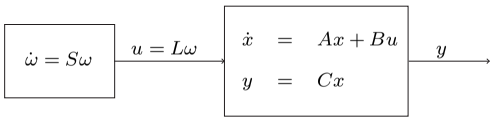

Linear systems – The notion of moment (cont'd)

Consider a linear system, $s^\star \in \mathbb{C}$, $k \geq 0$ and assume $\sigma(A) \subset \mathbb{C}^-$ and $s^\star \in \mathbb{C}^0$.

Let

$$\dot{\omega} = S\omega, \qquad \begin{matrix}\omega(t) \in \mathbb{R}^\kappa \\ \omega(0) \neq 0\end{matrix} \qquad \kappa = \begin{cases} k+1 & \text{if } s^\star \in \mathbb{R}, \\ 2(k+1) & \text{if } s^\star \in \mathbb{C} \setminus \mathbb{R}, \end{cases}$$

and S any non-derogatory real matrix with characteristic polynomial as in (1).

Consider the interconnection ((L, S) observable)

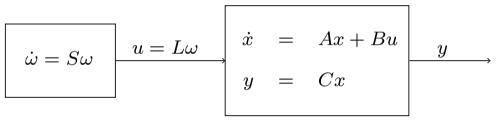

Steady state response
⇕
Moments
⇕
Π

The moments $\eta_0(s^\star), \ldots, \eta_k(s^\star)$ are in one-to-one relation with the (well-defined) steady-state response of the output of the interconnected system

Linear systems – The notion of moment (cont'd)

Consider a linear system, $s^\star \in \mathbb{C}$, $k \geq 0$ and assume $\sigma(A) \subset \mathbb{C}^-$ and $s^\star \in \mathbb{C}^0$.

Let

$$\dot{\omega} = S\omega, \qquad \begin{matrix}\omega(t) \in \mathbb{R}^\kappa \\ \omega(0) \neq 0\end{matrix} \qquad \kappa = \begin{cases} k+1 & \text{if } s^\star \in \mathbb{R}, \\ 2(k+1) & \text{if } s^\star \in \mathbb{C} \setminus \mathbb{R}, \end{cases}$$

and S any non-derogatory real matrix with characteristic polynomial as in (1).

Consider the interconnection ((L, S) observable)

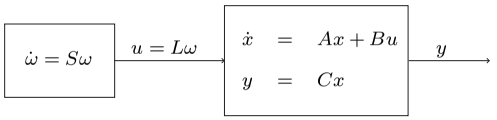

Steady state response
⇕
Moments
⇕
Π

The moments $\eta_0(s^\star), \ldots, \eta_k(s^\star)$ are in one-to-one relation with the (well-defined) steady-state response of the output of the interconnected system

This property is instrumental to derive a nonlinear enhancement of the notion of moment

31^{st} Benelux Meeting on Systems and Control – p. 11/39

A first *Intermezzo* – Reduction by projection

Consider a linear SISO system ($x(t) \in \mathbb{R}^n$, $u(t) \in \mathbb{R}$, $y(t) \in \mathbb{R}$)

$$\Sigma : \begin{cases} \dot{x} &= Ax + Bu \\ y &= Cx \end{cases} \qquad W(s) = C(sI - A)^{-1}B$$

Families of reduced order models, achieving moment matching at $\sigma(S) = \{s_1, \cdots, s_\nu\}$, can be obtained by *projection*

$$R_W : \begin{cases} \dot{\xi} &= W^\star AV\xi + W^\star Bu \\ \psi &= CV\xi \end{cases} \qquad V = \begin{bmatrix}(s_1 I - A)^{-1}B & \cdots & (s_\nu I - A)^{-1}B\end{bmatrix} \quad W^\star V = I$$

$$R_V : \begin{cases} \dot{\xi} &= W^\star AV\xi + W^\star Bu \\ \psi &= CV\xi \end{cases} \qquad W^\star = \begin{bmatrix} C(s_1 I - A)^{-1} \\ \vdots \\ C(s_\nu I - A)^{-1} \end{bmatrix} \quad W^\star V = I$$

A first *Intermezzo* – On Krylov projectors

The matrices V and W are called Krylov projectors.

We develop a systems theoretic interpretation of the Krylov *projectors* based on the interconnection of the system to be reduced ($x(t) \in \mathbb{R}^\nu$)

$$\Sigma : \begin{cases} \dot{x} &= Ax + Bu \\ y &= Cx \end{cases} \qquad W(s) = C(sI - A)^{-1}B$$

with the signal generator ($\omega(t) \in \mathbb{R}^\nu$)

$$E : \ \dot{\omega} = S\omega$$

Recall that the eigenvalues of the matrix S are the interpolation points

31^{st} Benelux Meeting on Systems and Control – p. 13/39

A first *Intermezzo* – On Krylov projectors – The projector V

Consider the systems Σ and E and the interconnection equation

$$u = L\omega$$

i.e. the system

$$E \xrightarrow{L} \Sigma : \left\{ \begin{array}{rcl} \dot{\omega} & = & S\omega \\ \dot{x} & = & Ax + BL\omega \end{array} \right. \qquad (L, S) \text{ observable}$$

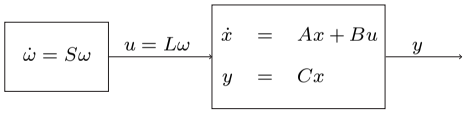

The system $E \xrightarrow{L} \Sigma$ has an invariant subspace $x = \Pi\omega$,

with Π the unique solution of the Sylvester equation $A\Pi + BL = \Pi S$

There exists a square, non-singular, matrix T such that $\Pi = VT$

A first *Intermezzo* – On Krylov projectors – The projector W

Consider the system Σ, the system E *augmented* with the addition of an input signal, *i.e.*

$$\dot{\omega} = S\omega + \kappa$$

and the interconnection equation

$$\kappa = My$$

i.e. the system

$$\Sigma \xrightarrow{M} E : \left\{ \begin{array}{rcl} \dot{x} & = & Ax + Bu \\ \dot{\omega} & = & S\omega + MCx \end{array} \right. \qquad (S, M) \text{ controllable}$$

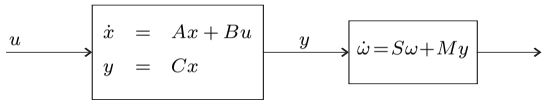

A first *Intermezzo* – On Krylov projectors – The projector W

$$\Sigma \xrightarrow{M} E : \left\{ \begin{array}{rcl} \dot{x} & = & Ax + Bu \\ \dot{\omega} & = & S\omega + MCx \end{array} \right. \qquad (S, M) \text{ controllable}$$

Let $d(t) \in I\!R^{\nu}$ be such that, along the trajectories of $S \xrightarrow{M} E$ and for some Υ

$$\dot{d} = Sd + \Upsilon u$$

Then (uniquely)

$$S\Upsilon = \Upsilon A + MC \qquad \text{rank}\Upsilon = \nu$$

There exists a square, non-singular, matrix R such that $\Upsilon = RW$

A first *Intermezzo* – On Krylov projectors – The projector W

$$\Sigma \xrightarrow{M} E : \left\{ \begin{array}{rcl} \dot{x} & = & Ax + Bu \\ \dot{\omega} & = & S\omega + MCx \end{array} \right. \qquad (S, M) \text{ controllable}$$

The system $\Sigma \xrightarrow{M} E$, in the x and d coordinates and with output $\chi = d$, is described by

$$\begin{array}{rcl} \dot{x} & = & Ax + Bu \\ \dot{d} & = & Sd + \Upsilon Bu \\ \chi & = & d \end{array}$$

which is an unobservable system with unobservable modes $\sigma(A)$.

Linear systems – A *new* notion of moment

Consider the interconnected system $\Sigma \overset{M}{\to} E$ with output d.

Assume $\sigma(A) \subset \mathbb{C}^-$, $\sigma(S) \in C^0$, $x(0) = 0, \omega(0) = 0$, and $u(t) = \delta_0(t)$.

The moments of Σ at $\sigma(S)$ are in one-to-one relation

with the steady-state response of the output $d(t)$

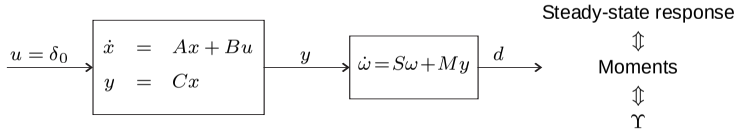

Linear systems – A family of reduced order models – R_G

The system

$$\begin{array}{rcll} \dot{\xi} & = & F\xi + Gu & \xi(t) \in \mathbb{R}^\nu \qquad \psi(t) \in \mathbb{R} \\ \psi & = & H\xi & \end{array}$$

is a model of the given linear system at $S \in \mathbb{R}^{\nu \times \nu}$, with S such that $\sigma(S) \cap \sigma(A) = \emptyset$, if

$$\sigma(S) \cap \sigma(F) = \emptyset \qquad C\Pi = HP$$

$$(L, S) \text{ observable} \qquad A\Pi + BL = \Pi S \qquad FP + GL = PS$$

The model is a reduced order model if $\nu < n$.

Linear systems – A family of reduced order models – R_G

- The matrices F and S have the same dimensions.
- S and A do not have common eigenvalues.
- S and F do not have common eigenvalues.

A family of reduced order models for the given linear system at S is

$$R_G : \left\{ \begin{array}{rcll} \dot{\xi} & = & (S - GL)\xi + Gu & \\ \psi & = & C\Pi\xi & \end{array} \right. \qquad \sigma(S) \cap \sigma(S - GL) = \emptyset$$

where G is a free matrix.

Linear systems – A family of reduced order models – R_H

Consider a system described by ($\xi(t) \in \mathbb{R}^\nu$, $u(t) \in \mathbb{R}$, $\eta(t) \in \mathbb{R}$)

$$R : \left\{ \begin{array}{rcl} \dot{\xi} & = & F\xi + Gu \\ \eta & = & H\xi \end{array} \right.$$

interconnected to the *augmented* signal generator by the interconnection equation

$$\kappa = M\eta$$

i.e. the system

$$R \overset{M}{\to} E : \left\{ \begin{array}{rcl} \dot{\xi} & = & F\xi + Gu \\ \dot{\omega} & = & S\omega + MH\xi \end{array} \right. \qquad (S, M) \text{ controllable}$$

Linear systems – A family of reduced order models – R_H

$$R \xrightarrow{M} E : \left\{ \begin{array}{rcl} \dot{\xi} & = & F\xi + Gu \\ \dot{\omega} & = & S\omega + MH\xi \end{array} \right. \qquad (S, M) \text{ controllable}$$

Let F, G and H be such that there exists $\delta(t) \in I\!R^\nu$ with the property that, along the trajectories of $R \xrightarrow{M} E$,

$$\dot{\delta} = S\delta + \Upsilon Bu$$

Select

$$\delta = \omega + \xi \qquad \text{(equivalently } \delta = \omega + \mathcal{R}\xi \quad \det\mathcal{R} \neq 0)$$

$$\Updownarrow$$

$$F = S - MH \qquad G = \Upsilon B$$

$$\Downarrow \ ?$$

$$R_H : \left\{ \begin{array}{rcl} \dot{\xi} & = & (S - MH)\xi + \Upsilon Bu \\ \eta & = & H\xi \end{array} \right.$$

Linear systems – A family of reduced order models – R_H

$$R_H : \left\{ \begin{array}{rcl} \dot{\xi} & = & (S - MH)\xi + \Upsilon Bu \\ \eta & = & H\xi \end{array} \right.$$

Consider system Σ, the signal generator E and the family of reduced order models R_H.

Assume (S, M) is controllable, $\sigma(A) \cap \sigma(S) = \emptyset$, $\sigma(S - MH) \cap \sigma(S) = \emptyset$.

Let Υ be the (unique) solution of $S\Upsilon = \Upsilon A + MC$.

Any model in the family R_H is a reduced order model

of system Σ achieving moment matching at $\sigma(S)$.

Linear systems – A family of reduced order models – R_H vs. R_G

$$R_H : \left\{ \begin{array}{rcl} \dot{\xi} & = & (S - MH)\xi + \Upsilon Bu \\ \eta & = & H\xi \end{array} \right. \qquad \sigma(S) \cap \sigma(S - MH) = \emptyset$$

$$R_G : \left\{ \begin{array}{rcl} \dot{\xi} & = & (S - GL)\xi + Gu \\ \psi & = & C\Pi\xi \end{array} \right. \qquad \sigma(S) \cap \sigma(S - GL) = \emptyset$$

The family R_H is *dual* to the family R_G:

- H enters as a state feedback matrix and the input matrix depends on the moments
- G enters as an output injection matrix and the output matrix depends on the moments

Linear systems – Families of reduced order models

$$R_G : \left\{ \begin{array}{rcl} \dot{\xi} & = & (S - GL)\xi + Gu \\ \psi & = & C\Pi\xi \end{array} \right. \qquad \sigma(S) \cap \sigma(S - GL) = \emptyset$$

$$R_W : \left\{ \begin{array}{rcl} \dot{\xi} & = & W^\star AV\xi + W^\star Bu \\ \psi & = & CV\xi \end{array} \right. \qquad V = \left[(s_1 I - A)^{-1}B \ \cdots \ (s_\nu I - A)^{-1}B \right] \qquad W^\star V = I$$

$$R_V : \left\{ \begin{array}{rcl} \dot{\xi} & = & W^\star AV\xi + W^\star Bu \\ \psi & = & CV\xi \end{array} \right. \qquad W^\star = \left[\begin{array}{c} C(s_1 I - A)^{-1} \\ \vdots \\ C(s_\nu I - A)^{-1} \end{array} \right] \qquad W^\star V = I$$

$$R_H : \left\{ \begin{array}{rcl} \dot{\xi} & = & (S - MH)\xi + \Upsilon Bu \\ \eta & = & H\xi \end{array} \right. \qquad \sigma(S) \cap \sigma(S - MH) = \emptyset$$

Linear systems – Families of reduced order models

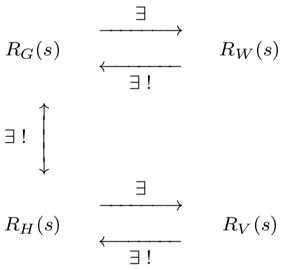

Nonlinear systems – The notion of moment

Consider a nonlinear SISO system

$$\begin{aligned} \dot{x} &= f(x,u) & x(t) \in \mathbb{R}^n \quad u(t) \in \mathbb{R} \quad y(t) \in \mathbb{R} \\ y &= h(x) & f(0,0) = 0 \quad h(0) = 0 \end{aligned}$$

a signal generator

$$\begin{aligned} \dot{\omega} &= s(\omega) & \omega(t) \in \mathbb{R}^\nu \quad \omega(0) \neq 0 \quad \theta(t) \in \mathbb{R} \\ \theta &= l(\omega) & s(0) = 0 \quad l(0) = 0 \end{aligned}$$

and the interconnected system

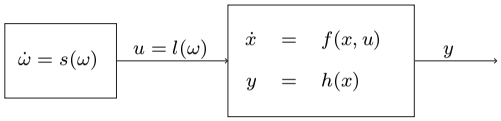

Nonlinear systems – The notion of moment (cont'd)

The signal generator captures the requirement that one is interested in studying the behavior of the system only in *specific circumstances*.

For this to make sense and to provide a generalization of the notion of moment, we need some assumptions and definitions.

Nonlinear systems – The notion of moment (cont'd)

For this to make sense and to provide a generalization of the notion of moment, we need some assumptions and definitions.

- There is a unique mapping $\pi(\omega)$, locally defined in a neighborhood of $\omega = 0$, which solves the PDE

$$f(\pi(\omega), l(\omega)) = \frac{\partial \pi}{\partial \omega} s(\omega).$$

$$\Downarrow$$

The interconnected system possesses an invariant manifold, described by $x = \pi(\omega)$ and the dynamics restricted to the invariant manifold are $\dot{\omega} = s(\omega)$, *i.e.* are a copy of the dynamics of the signal generator.

Nonlinear systems – The notion of moment (cont'd)

For this to make sense and to provide a generalization of the notion of moment, we need some assumptions and definitions.

- The signal generator is observable, *i.e.* for any pair of initial conditions $\omega_a(0)$ and $\omega_b(0)$, such that $\omega_a(0) \neq \omega_b(0)$, the corresponding output trajectories $l(\omega_a(t))$ and $l(\omega_b(t))$ are such that

$$l(\omega_a(t)) - l(\omega_b(t)) \not\equiv 0.$$

$\Downarrow$

$h(\pi(\omega))$ is (by definition) *the moment of the nonlinear system at* $s(\omega)$ *(at* $(s(\omega), l(\omega))$*)*

Nonlinear systems – The notion of moment (cont'd)

For this to make sense and to provide a generalization of the notion of moment, we need some assumptions and definitions.

- The signal generator is observable, *i.e.* for any pair of initial conditions $\omega_a(0)$ and $\omega_b(0)$, such that $\omega_a(0) \neq \omega_b(0)$, the corresponding output trajectories $l(\omega_a(t))$ and $l(\omega_b(t))$ are such that

$$l(\omega_a(t)) - l(\omega_b(t)) \not\equiv 0.$$

$\Downarrow$

$h(\pi(\omega))$ is (by definition) *the moment of the nonlinear system at* $s(\omega)$ *(at* $(s(\omega), l(\omega))$*)*

$\Downarrow$

This coincides with the linear notion

Nonlinear systems – The notion of moment (cont'd)

Consider the nonlinear system, the signal generator and the observability assumption.

Assume the zero equilibrium of $\dot{x} = f(x, 0)$ is locally exponentially stable and the signal generator is Poisson stable.

Then

- the PDE

$$f(\pi(\omega), l(\omega)) = \frac{\partial \pi}{\partial \omega} s(\omega)$$

  has a (local) solution;

- the moment of the nonlinear system at $s(\omega)$ coincides with the (locally well-defined) steady-state response of the output of the interconnected system.

For linear systems it is possible to define k-moments for every $s^\star \in \mathcal{C}$ and for any $k \geq 0$.

For nonlinear systems it may be difficult to deal with unbounded $l(\omega(t))$.

Nonlinear systems – The notion of moment: an example

Consider a linear, asymptotically stable, system with $x(t) \in \mathbb{R}^n$, $n > 3$, $u(t) \in \mathbb{R}$, $y(t) \in \mathbb{R}$ and the signal generator

$$\dot{\omega} = \begin{bmatrix} \dot{\omega}_1 \\ \dot{\omega}_2 \\ \dot{\omega}_3 \end{bmatrix} = s(\omega) = \begin{bmatrix} \frac{I_2 - I_3}{I_1} \omega_2 \omega_3 \\ \frac{I_3 - I_1}{I_2} \omega_3 \omega_1 \\ \frac{I_1 - I_2}{I_3} \omega_1 \omega_2 \end{bmatrix} \qquad I_1 > 0 \quad I_2 > 0 \quad I_3 > 0$$

$$I_i \neq I_j \text{ for } i \neq j$$

$$\theta = l(\omega) = L\omega = \begin{bmatrix} L_1 & L_2 & L_3 \end{bmatrix} \omega \qquad L_1 L_2 L_3 \neq 0$$

Nonlinear systems – The notion of moment: an example (cont'd)

The moment of the linear system at $s(\omega)$ can be computed as follows.

Let

$$\pi(\omega) = \sum_i \pi_i(\omega) \qquad \pi_i(\omega) = \begin{bmatrix} \pi_i^1(\omega) \\ \vdots \\ \pi_i^n(\omega) \end{bmatrix} \qquad \begin{array}{l} \pi_i^j(\omega) \text{ homogeneous} \\ \text{polynomial of degree } i \end{array}$$

Then

$$\pi_1(\omega) = -A^{-1}BL\omega \quad \pi_2(\omega) = -A^{-2}BL\dot{\omega} \quad \cdots \quad \pi_i(\omega) = -A^{-i}BL\frac{d^{i-1}\omega}{dt^{i-1}} \quad \cdots$$

The moment of the linear system at $s(\omega)$ is (formally)

$$C\pi(\omega) = -CA^{-1}\left[BL\omega + A^{-1}BL\dot{\omega} + \cdots + A^{-i+1}BL\frac{d^{i-1}\omega}{dt^{i-1}} + \cdots\right].$$

A second *Intermezzo* – Frequency response of nonlinear systems

Consider the interconnected system

$$\dot{\omega} = \begin{bmatrix} 0 & \omega^\star \\ -\omega^\star & 0 \end{bmatrix}\omega \qquad \begin{array}{rcll} \dot{x} & = & f(x,[L_1\ L_2]\omega)) & \omega^\star > 0,\ \ \omega(0) \neq 0 \\ y & = & h(x) & L_1^2 + L_2^2 \neq 0 \end{array}$$

Under suitable hypotheses, the output converges towards a periodic steady state response.

A second *Intermezzo* – Frequency response of nonlinear systems

Consider the interconnected system

$$\dot{\omega} = \begin{bmatrix} 0 & \omega^\star \\ -\omega^\star & 0 \end{bmatrix}\omega \qquad \begin{array}{rcll} \dot{x} & = & f(x,[L_1\ L_2]\omega)) & \omega^\star > 0,\ \ \omega(0) \neq 0 \\ y & = & h(x) & L_1^2 + L_2^2 \neq 0 \end{array}$$

Suppose such a steady state response has the same period of $\omega(t)$

$\Downarrow$

Steady state response

$$h(\pi(\omega(t))) = \sum_{k=-\infty}^{\infty} c_k e^{k\omega^\star t} \quad \Rightarrow \quad \text{Fourier truncation operator} \quad \mathcal{P}_+\Big(\sum_{k=-\infty}^{\infty} \alpha_k e^{k\omega^\star t}\Big) = \sum_{k=0}^{\infty} \alpha_k e^{k\omega^\star t}$$

$\Downarrow$

The frequency response

$$F(\omega(0),\omega^\star) = \frac{\mathcal{P}_+(h(\pi(\omega(t))))}{\mathcal{P}_+(l(\omega(t))} \quad \Leftarrow \quad \text{The frequency response depends upon } \omega^\star \text{ and } \omega(0)$$

A second *Intermezzo* – Frequency response of nonlinear systems

Consider the interconnected system

$$\dot{\omega} = \begin{bmatrix} 0 & \omega^\star \\ -\omega^\star & 0 \end{bmatrix}\omega \qquad \begin{array}{rcll} \dot{x} & = & f(x,[L_1\ L_2]\omega)) & \omega^\star > 0,\ \ \omega(0) \neq 0 \\ y & = & h(x) & L_1^2 + L_2^2 \neq 0 \end{array}$$

Suppose such a steady state response has the same period of $\omega(t)$

$\Downarrow$

Steady state response

$$h(\pi(\omega(t))) = \sum_{k=-\infty}^{\infty} c_k e^{k\omega^\star t} \quad \Rightarrow \quad \text{Fourier truncation operator} \quad \mathcal{P}_+\Big(\sum_{k=-\infty}^{\infty} \alpha_k e^{k\omega^\star t}\Big) = \sum_{k=0}^{\infty} \alpha_k e^{k\omega^\star t}$$

$\Downarrow$

The frequency response

$$F(\omega(0),\omega^\star) = \frac{\mathcal{P}_+(h(\pi(\omega(t))))}{\mathcal{P}_+(l(\omega(t))} \quad \Leftarrow \quad \text{The frequency response depends upon } \omega^\star \text{ and } \omega(0)$$

For linear systems: $F(\omega(0),\omega^\star) = |W(i\omega^\star)|e^{\angle W(i\omega^\star)}$, where $W(s) = C(sI-A)^{-1}B$.

Nonlinear systems – Reduced order model

The system

$$\begin{aligned}\dot{\xi} &= \phi(\xi, u) \\ \psi &= \kappa(\xi)\end{aligned} \qquad \xi(t) \in I\!R^{\nu} \qquad \psi(t) \in I\!R$$

is a *model* at $s(\omega)$ of the nonlinear system if it has the same moment at $s(\omega)$.

The system is said to *match* the moment of the nonlinear system at $s(\omega)$.

Furthermore, the system is a reduced order model of the nonlinear system if $\nu < n$.

Nonlinear systems – Reduced order model

The system	The model	The signal generator
$\dot{x} = f(x,u)$	$\dot{\xi} = \phi(\xi,u)$	$\dot{\omega} = s(\omega)$
$y = h(x)$	$\psi = \kappa(\xi)$	$\theta = l(\omega)$

Under suitable assumptions, the model *matches* the moments of the system at $s(\omega)$ if

$$\phi(p(\omega), l(\omega)) = \frac{\partial p}{\partial \omega} s(\omega)$$

has a unique solution $p(\omega)$ such that

$$h(\pi(\omega)) = \kappa(p(\omega)),$$

where $\pi(\omega)$ is the solution of

$$f(\pi(\omega), l(\omega)) = \frac{\partial \pi}{\partial \omega} s(\omega).$$

Nonlinear systems – A family of reduced order models

A family of reduced order models, all achieving moment matching, is

$$\begin{aligned}\dot{\xi} &= s(\xi) - \delta(\xi) l(\xi) + \delta(\xi) u \\ \psi &= h(\pi(\xi))\end{aligned} \qquad \delta(\cdot) \text{ is a free mapping}$$

The free mapping can be used to achieve specific properties of the reduced order model.

For example, a reduced order model, for which the zero equilibrium is locally asymptotically stable, achieving matching at $s(0) = 0$ is

$$\dot{\xi} = -\delta(\xi)(\xi - u) \qquad \psi = h(\pi(\xi))$$

where $\delta(\xi)$ is such that $\delta(0) > 0$ and $\pi(\omega)$ is such that $f(\pi(\omega), \omega) = 0$.

Nonlinear systems – The Ćuk converter

The averaged model of the DC–to–DC Ćuk converter is

$$\begin{aligned} L_1 \frac{d}{dt} i_1 &= -(1-u)\, v_2 + E \\ C_2 \frac{d}{dt} v_2 &= (1-u)\, i_1 + u\, i_3 \\ L_3 \frac{d}{dt} i_3 &= -u\, v_2 - v_4 \\ C_4 \frac{d}{dt} v_4 &= i_3 - G\, v_4 \\ y &= v_4 \end{aligned}$$

$i_1(t) \in I\!R^{+} \quad i_3(t) \in I\!R^{-}$

$v_2(t) \in I\!R^{+} \quad v_4(t) \in I\!R^{-}$

$L_1 > 0 \quad C_2 > 0 \quad L_3 > 0$

$C_4 > 0 \quad E > 0 \quad G > 0$

$u(t) \in (0, 1)$

0-moment of the system at $s^{\star} = 0$

$$h(\pi(\omega)) = \frac{\omega}{\omega - 1} E$$

Nonlinear systems – The Ćuk converter

The averaged model of the DC–to–DC Ćuk converter is

$$\begin{aligned} L_1 \frac{d}{dt} i_1 &= -(1-u)\, v_2 + E \\ C_2 \frac{d}{dt} v_2 &= (1-u)\, i_1 + u\, i_3 \\ L_3 \frac{d}{dt} i_3 &= -u\, v_2 - v_4 \\ C_4 \frac{d}{dt} v_4 &= i_3 - G\, v_4 \\ y &= v_4 \end{aligned} \qquad \begin{aligned} & i_1(t) \in I\!R^+ \quad i_3(t) \in I\!R^- \\ & v_2(t) \in I\!R^+ \quad v_4(t) \in I\!R^- \\ & L_1 > 0 \quad C_2 > 0 \quad L_3 > 0 \\ & C_4 > 0 \quad E > 0 \quad G > 0 \\ & u(t) \in (0,1) \end{aligned}$$

0-moment of the system at $s^\star = 0$

$$h(\pi(\omega)) = \frac{\omega}{\omega - 1} E$$

A stable reduced order model achieving moment matching

$$\dot{\xi} = -\delta(\xi)(\xi - u) \qquad \psi = E \frac{\xi}{\xi - 1} \qquad \delta(0) > 0$$

both well-defined for $\omega \neq 1$

A third *Intermezzo* – Petrov-Galerkin projection

Consider a nonlinear SISO system (all functions and mappings are sufficiently smooth)

$$\Sigma : \left\{ \begin{aligned} \dot{x} &= f(x,u) \\ y &= h(x) \end{aligned} \right. \qquad \begin{aligned} & x(t) \in I\!R^n \quad u(t) \in I\!R \quad y(t) \in I\!R \\ & f(0,0) = 0 \quad h(0) = 0 \end{aligned}$$

and a pair of matrices

$$V \in I\!R^{n \times \nu} \quad W \in I\!R^{n \times \nu} \qquad \nu < n \qquad W'V = I$$

A reduced order model, of dimension ν, is given by

$$\Sigma_{PG} : \left\{ \begin{aligned} \dot{\xi} &= W' f(V\xi, u) \\ \psi &= h(V\xi) \end{aligned} \right.$$

The matrix VW' is called the Petrov-Galerkin projection

Nonlinear systems – A new family of reduced order models

Consider a nonlinear SISO system

$$\Sigma : \left\{ \begin{aligned} \dot{x} &= f(x,u) \\ y &= h(x) \end{aligned} \right. \qquad \begin{aligned} & x(t) \in I\!R^n \quad u(t) \in I\!R \quad y(t) \in I\!R \\ & f(0,0) = 0 \quad h(0) = 0 \end{aligned}$$

the signal generator

$$\mathcal{G} : \left\{ \begin{aligned} \dot{\omega} &= s(\omega) \\ \theta &= l(\omega) \end{aligned} \right. \qquad \begin{aligned} & \omega(t) \in I\!R^\nu \quad \theta(t) \in I\!R \\ & s(0) = 0 \quad l(0) = 0 \end{aligned}$$

and the (new) family of models

$$\Sigma_\rho : \left\{ \begin{aligned} \dot{\xi} &= \left[\frac{\partial \rho}{\partial x} f(x,u) \right]_{x = \pi(\xi)} \\ \psi &= h(\pi(\xi)) \end{aligned} \right. \qquad \begin{aligned} & f(\pi(\omega), l(\omega)) = \frac{\partial \pi}{\partial \omega} s(\omega) \\ & \rho \circ \pi(\cdot) = \mathrm{Id} \end{aligned}$$

Nonlinear systems – A new family of reduced order models

Consider a nonlinear SISO system

$$\Sigma : \left\{ \begin{aligned} \dot{x} &= f(x,u) \\ y &= h(x) \end{aligned} \right. \qquad \begin{aligned} & x(t) \in I\!R^n \quad u(t) \in I\!R \quad y(t) \in I\!R \\ & f(0,0) = 0 \quad h(0) = 0 \end{aligned}$$

the signal generator

$$\mathcal{G} : \left\{ \begin{aligned} \dot{\omega} &= s(\omega) \\ \theta &= l(\omega) \end{aligned} \right. \qquad \begin{aligned} & \omega(t) \in I\!R^\nu \quad \theta(t) \in I\!R \\ & s(0) = 0 \quad l(0) = 0 \end{aligned}$$

and the (new) family of models

$$\Sigma_\rho : \left\{ \begin{aligned} \dot{\xi} &= \left[\frac{\partial \rho}{\partial x} f(x,u) \right]_{x = \pi(\xi)} \\ \psi &= h(\pi(\xi)) \end{aligned} \right. \qquad \begin{aligned} & f(\pi(\omega), l(\omega)) = \frac{\partial \pi}{\partial \omega} s(\omega) \\ & \rho \circ \pi(\cdot) = \mathrm{Id} \end{aligned}$$

Suppose that the zero equilibrium of Σ, with $u = 0$, is LES and $\mathcal{G}$ is Poisson stable.

Then Σ_ρ yields a family of reduced order models achieving moment matching at $s(\omega)$.

Nonlinear systems – A new family of reduced order models

LES of Σ, with $u = 0$, can be replaced by hyperbolicity of $x = 0$.

The family

$$\Sigma_\rho : \left\{ \begin{array}{rcl} \dot{\xi} & = & \left[\frac{\partial \rho}{\partial x} f(x,u)\right]_{x=\pi(\xi)} \\ \psi & = & h(\pi(\xi)) \end{array} \right. \qquad \begin{array}{l} f(\pi(\omega), l(\omega)) = \frac{\partial \pi}{\partial \omega} s(\omega) \\ \rho \circ \pi(\cdot) = \mathrm{Id} \end{array}$$

yields a nonlinear version of the Petrov-Galerkin method with *projector*

$$\pi \circ \rho : I\!R^n \to I\!R^n$$

The families Σ_δ and Σ_ρ are *strongly* related.

Nonlinear systems – A new family of reduced order models

$$\Sigma_\delta : \left\{ \begin{array}{rcl} \dot{\xi} & = & s(\xi) - \delta(\xi) l(\xi) + \delta(\xi) u \\ \psi & = & h(\pi(\xi)) \end{array} \right. \qquad \begin{array}{l} \delta(\cdot) \text{ free} \\ s(p(\omega)) - \delta(p(\omega))\big(l(p(\omega)) - l(\omega)\big) = \frac{\partial p}{\partial \omega} s(\omega) \end{array}$$

$$\Updownarrow$$

$$p(\omega) = \omega$$

$$\Sigma_\rho : \left\{ \begin{array}{rcl} \dot{\xi} & = & \left[\frac{\partial \rho}{\partial x} f(x,u)\right]_{x=\pi(\xi)} \\ \psi & = & h(\pi(\xi)) \end{array} \right. \qquad \begin{array}{l} f(\pi(\omega), l(\omega)) = \frac{\partial \pi}{\partial \omega} s(\omega) \\ \rho \circ \pi(\cdot) = \mathrm{Id} \end{array}$$

Assume $f(x,u) = f(x) + g(x)u$ (with some abuse of notation)

Nonlinear systems – A new family of reduced order models

$$\Sigma_\delta : \left\{ \begin{array}{rcl} \dot{\xi} & = & s(\xi) - \delta(\xi) l(\xi) + \delta(\xi) u \\ \psi & = & h(\pi(\xi)) \end{array} \right. \qquad \begin{array}{l} \delta(\cdot) \text{ free} \\ s(p(\omega)) - \delta(p(\omega))\big(l(p(\omega)) - l(\omega)\big) = \frac{\partial p}{\partial \omega} s(\omega) \end{array}$$

$$\Updownarrow$$

$$p(\omega) = \omega$$

$$\Sigma_\rho : \left\{ \begin{array}{rcl} \dot{\xi} & = & \left[\frac{\partial \rho}{\partial x} f(x,u)\right]_{x=\pi(\xi)} \\ \psi & = & h(\pi(\xi)) \end{array} \right. \qquad \begin{array}{l} f(\pi(\omega), l(\omega)) = \frac{\partial \pi}{\partial \omega} s(\omega) \\ \rho \circ \pi(\cdot) = \mathrm{Id} \end{array}$$

Assume $f(x,u) = f(x) + g(x)u$ (with some abuse of notation)

(a)' For any $\rho(\cdot)$ there exists a (unique) $\delta(\cdot)$ such that Σ_δ and Σ_ρ *coincide*.

(b)' Suppose $\mathrm{rank} \left[\begin{array}{cc} \frac{\partial \pi}{\partial \xi} & g(\pi(\xi)) \end{array} \right] = \nu + 1$.

For any $\delta(\cdot)$ there exists a $\rho(\cdot)$ such that hat Σ_δ and Σ_ρ *coincide*.

Linear systems – Matching at $s(\omega)$

Consider the linear system Σ_l, with state $x(t) \in I\!R^n$ and the matrix A such that $\sigma(A) \subset \mathbb{C}^-$.

Consider the signal generator $\mathcal{G}$, with state $\omega(t) \in I\!R^\nu$, $n > \nu$ and $l(\omega) = L\omega$.

Assume that the signal generator is Poisson stable and that, locally around $\omega = 0$,

$$s(\omega) = \sum_{i \geq 1} s^{[i]}(\omega) \qquad s^{[1]}(\omega) = 0 \qquad s^{[i]}(\cdot) \text{ is homogeneous of degree } i$$

Then a family of reduced order models achieving moment matching at $s(\omega)$ is

$$\begin{array}{rcl} \dot{\xi} & = & s(\xi) - \delta(\xi) L\xi + \delta(\xi) u, \\ \psi & = & C\pi(\xi), \end{array} \qquad \delta(\cdot) \text{ is a free mapping}$$

$$\pi(\xi) = \sum_{i \geq 1} \pi^{[i]}(\xi) \qquad \pi^{[1]}(\xi) = -A^{-1} B L \xi \qquad \pi^{[k]}(\xi) = A^{-1} \sum_{i=1}^{k-1} \frac{\partial \pi^{[i]}(\xi)}{\partial \xi} s^{[k-i+1]}(\xi), \quad k \geq 2$$

Linear systems – Matching at $s(\omega)$ – Example

A reduced order model for a linear asymptotically stable system Σ_l at

$$s(\omega) = \begin{bmatrix} \frac{I_2 - I_3}{I_1}\omega_2\omega_3 \\ \frac{I_3 - I_1}{I_2}\omega_3\omega_1 \\ \frac{I_1 - I_2}{I_3}\omega_1\omega_2 \end{bmatrix} \qquad l(\omega) = L\omega = \begin{bmatrix} L_1 & L_2 & L_3 \end{bmatrix}\omega$$

with $I_i \neq I_j$, for $i \neq j$, $I_i > 0$ and $L_1L_2L_3 \neq 0$, is given by

$$\begin{aligned} \dot{\xi} &= s(\xi) - \delta(\xi)L\omega + \delta(\xi)u \\ \psi &= -CA^{-1}\left(BL\omega + A^{-1}BL\dot{\omega}\cdots + A^{-i+1}BL\tfrac{d^{i-1}\omega}{dt^{i-1}}\cdots\right). \end{aligned}$$

Linear systems – Matching at $s(\omega)$ – Example

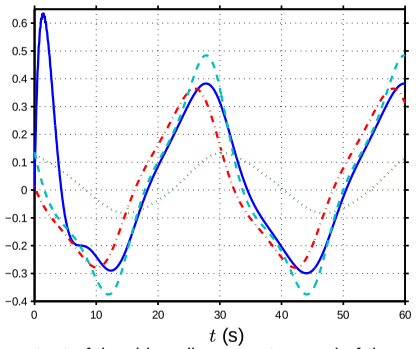

Time histories of the output of the driven linear system and of the *approximating* outputs of the driven reduced order model: $y(t)$ (–), $\psi^{I(t)}$ (··), $\psi^{II(t)}$ (-.) and $\psi^{III}(t)$ (--).

$$\max(|y(t)-\psi^{I}(t)|) = 0.2765 > \max(|y(t)-\psi^{II}(t)|) = 0.1644 > \max(|y(t)-\psi^{III}(t)|) = 0.0764$$

Nonlinear systems – Matching at $S\omega$

Consider the model reduction problem for Σ at $s(\omega) = S\omega$, *i.e.* $\mathcal{G}$ is a linear system.

This problem is of particular interest since reduced order models have a very simple description, *i.e.* the family $\mathcal{F}$ is given

$$\begin{aligned} \dot{\xi} &= (S - \delta(\xi)L)\xi + \delta(\xi)u \\ \psi &= h(\pi(\omega)) \end{aligned} \qquad \delta(\cdot)\text{is a free mapping}$$

Selecting $\delta(\xi) = \Delta$, for some constant Δ, the family $\mathcal{F}$ is described by a linear differential equation with a nonlinear output map.

This structure has two advantages:

- the matrix Δ can be selected to achieve additional goals;
- the computation of (an approximation of) the reduced order model boils down to the computation of (an approximation of) the output map $h(\pi(\omega))$.

Nonlinear systems – Matching at $S\omega$ – The Ćuk converter (cont'd)

$$\Sigma: \begin{cases} L_1\dfrac{d}{dt}i_1 = -(1-u)\,v_2 + E & C_2\dfrac{d}{dt}v_2 = (1-u)\,i_1 + u\,i_3 \\ L_3\dfrac{d}{dt}i_3 = -u\,v_2 - v_4 & C_4\dfrac{d}{dt}v_4 = i_3 - G\,v_4 \\ y = v_4 \end{cases}$$

$$i_1(t) \in \mathbb{R}^+, i_3(t) \in \mathbb{R}^-, v_2(t) \in \mathbb{R}^+, v_4(t) \in \mathbb{R}^-, u(t) \in (0,1)$$

The moment of the system at $\{s(\omega), l(\omega)\} = \{0, \omega\}$ is

$$h(\pi(\omega)) = \frac{\omega}{\omega - 1}E \qquad \pi(\omega) = \begin{bmatrix} GE\dfrac{\omega^2}{(1-\omega)^2} \\ E\dfrac{1}{1-\omega} \\ GE\dfrac{\omega}{\omega-1} \\ E\dfrac{\omega}{\omega-1} \end{bmatrix}$$

Nonlinear systems – Matching at $S\omega$ – The Ćuk converter (cont'd)

$$\Sigma : \begin{cases} L_1 \dfrac{d}{dt} i_1 = -(1-u)\, v_2 + E & C_2 \dfrac{d}{dt} v_2 = (1-u)\, i_1 + u\, i_3 \\ L_3 \dfrac{d}{dt} i_3 = -u\, v_2 - v_4 & C_4 \dfrac{d}{dt} v_4 = i_3 - G\, v_4 \\ y = v_4 \end{cases}$$

$$\Sigma_\delta : \begin{cases} \dot{\xi} = -\delta(\xi)(\xi - u) \\ \psi = E \dfrac{\xi}{\xi - 1} \end{cases} \qquad \delta(0) \neq 0$$

Nonlinear systems – Matching at $S\omega$ – The Ćuk converter (cont'd)

$$\Sigma : \begin{cases} L_1 \dfrac{d}{dt} i_1 = -(1-u)\, v_2 + E & C_2 \dfrac{d}{dt} v_2 = (1-u)\, i_1 + u\, i_3 \\ L_3 \dfrac{d}{dt} i_3 = -u\, v_2 - v_4 & C_4 \dfrac{d}{dt} v_4 = i_3 - G\, v_4 \\ y = v_4 \end{cases}$$

$$\Sigma_\delta : \begin{cases} \dot{\xi} = -\delta(\xi)(\xi - u) \\ \psi = E \dfrac{\xi}{\xi - 1} \end{cases} \qquad \delta(0) \neq 0$$

$$\Sigma_\rho : \begin{cases} \dot{\xi} = -\tilde{\delta}(\xi)(\xi - u) \\ \psi = E \dfrac{\xi}{\xi - 1} \end{cases} \qquad \tilde{\delta}(\xi) = \left[\frac{\alpha(x_3, x_4)(\xi - 1)}{L_3 G} + \frac{G\xi(\alpha(x_3, x_4) - 1)}{C_2} \right]_{x = \pi(\xi)}$$

$$\rho \circ \pi = \mathrm{Id} \Rightarrow \rho(x) = \frac{\dfrac{\alpha x_3}{G} + (1-\alpha) x_4}{\dfrac{\alpha x_3}{G} + (1-\alpha) x_4 - E} \qquad \alpha = \alpha(x)$$

Nonlinear systems – Matching at $S\omega$ – The Ćuk converter (cont'd)

$$\Sigma_\delta : \begin{cases} \dot{\xi} = -\delta(\xi)(\xi - u) \\ \psi = E \dfrac{\xi}{\xi - 1} \end{cases} \qquad \delta(0) \neq 0$$

$$\Sigma_\rho : \begin{cases} \dot{\xi} = -\tilde{\delta}(\xi)(\xi - u) \\ \psi = E \dfrac{\xi}{\xi - 1} \end{cases} \qquad \tilde{\delta}(\xi) = \left[\frac{\alpha(x_3, x_4)(\xi - 1)}{L_3 G} + \frac{G\xi(\alpha(x_3, x_4) - 1)}{C_2} \right]_{x = \pi(\xi)}$$

$$\Sigma_\delta \quad \underset{\alpha(x)_{x=\pi(\xi)} = L_3 G \frac{G\xi - \delta(\xi) C_2}{C_2(\xi - 1) + G^2 L_3 \xi}}{\Longleftrightarrow} \quad \Sigma_\rho$$

Nonlinear systems – The Ćuk converter (cont'd)

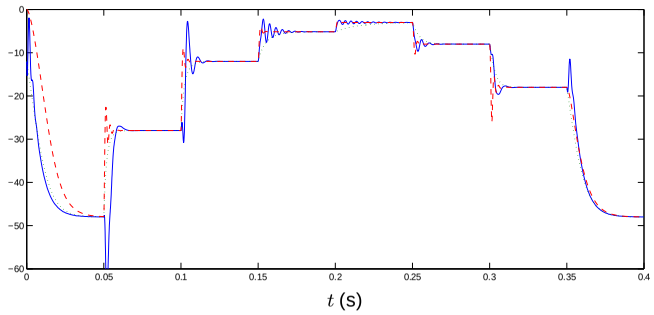

Time histories of the output of the averaged model of the Ćuk converter and of the *approximating* outputs of the reduced order models: $y(t)$ (–), $\psi(t)$ (··), $\psi^{2d}(t)$ (- -).

A fourth *Intermezzo* – The Markov parameters of a nonlinear system

We provide a nonlinear counterpart of the notion of moment at $s = \infty$ of a linear system.

For linear systems this notion is associated with the impulse response: it is not possible to use the results discussed above.

For a linear system

$$\Sigma_l : \left\{ \begin{array}{rcl} \dot{x} & = & Ax + Bu \\ y & = & Cx \end{array} \right.$$

the k-moments at $s = \infty$ are defined as $\eta_k(\infty) = CA^kB$.

To obtain a nonlinear counterpart of this notion recall that

$$CA^kB = \frac{d^k}{dt^k}(Ce^{At}B)\Big|_{t=0} = y_I^{(k)}(0) = y_{F,B}^{(k)}(0)$$

- $y_I(\cdot)$ denotes the impulse response of the system;
- $y_{F,B}(\cdot)$ denotes the free output response from $x(0) = B$.

A fourth *Intermezzo* – The Markov parameters of a nonlinear system

Consider a nonlinear affine system

$$\Sigma_a : \left\{ \begin{array}{rcll} \dot{x} & = & f(x) + g(x)u & x(t) \in I\!R^n \quad u(t) \in I\!R \quad y(t) \in I\!R \\ y & = & h(x) & f(0) = 0 \quad h(0) = 0 \end{array} \right.$$

Integrating the differential equation[a] with $x(0) = 0$ and $u(t) = \delta_0(t)$, evaluating for $t = 0$, and substituting in the output equation yields

$$y_I(0) = y_I^0(0) = h(g(0)) \qquad y_I^{(k)}(0) = L_f^k h \circ g(0), \quad k > 0.$$

The k-moment at $s = \infty$, for $k \geq 0$, of Σ_a are defined as

$$\eta_k(\infty) = y_I^{(k)}(0) = y_{F,g(0)}^{(k)}(0),$$

where $y_{F,g(0)}(\cdot)$ denotes the free output response of the system from $x(0) = g(0)$.

[a] See, e.g., Bressan-Piccoli, "Introduction to the Mathematical Theory of Control", AIMS Series on Applied Mathematics, 2007.

A fourth *Intermezzo* – The Markov parameters of a nonlinear system

A reduced order model, matching the $0, \cdots, k-1$ moments at $s = \infty$, for Σ_a is a linear system Σ_l, with state $x(t) \in I\!R^k$, and matrices A, B and C such that

$$CA^iB = y_I^{(i)}(0) \qquad i = 0, \cdots, k-1.$$

The matrices A, B and C can be computed using standard realization algorithms.

These matrices are not uniquely defined, hence it is possible, for example, to assign the eigenvalues of the reduced order model.

The computation of the reduced order model does not require the solution of any PDE.

A brief discussion

- Parameterized models can be exploited to achieve stability, relative degree, minimum phaseness, passivity, dissipativity, optimality, ...dimensional reduction.
- Model reduction of structured systems: from passive systems to passive models, from Hamiltonian systems to Hamiltonian models, from *physical systems* to *physical models*.
- Connections with balancing, interpolation theory, realization theory.
- Numerical recipes.

Event-Based Control: Theory and Application

Jan Lunze
Ruhr-University Bochum, 44780 Bochum, Germany
Lunze@atp.rub.de

Abstract

Event-based control is a means to reduce the communication between the sensors, the controller and the actuators in a control loop by invoking a communication among these components only after an event has indicated that the control error exceeds a tolerable bound. This working principle differs fundamentally from that of the usual feedback loop, in which data are communicated continuously or at periodic sampling instances. Hence, in the control schemes currently used a communication takes place also in case of small control errors when no information feedback is necessary to satisfy the performance requirements.

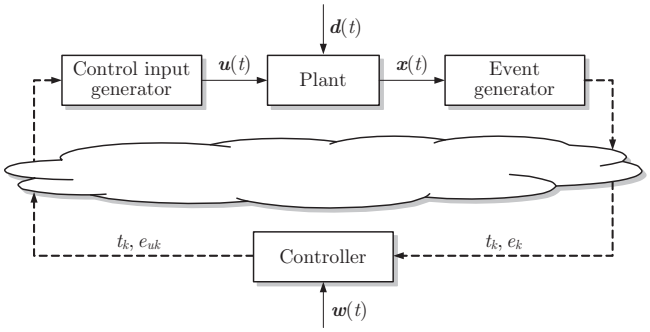

Fig. 1: Event-based control loop

This paper considers the event-based control loop shown in Fig. 1. The event generator determines the time instants t_k, $(k = 0,1,...)$ at which the next communication from the event generator via the controller towards the control input generator is invoked. The control input generator determines the inpuz $u(t)$ for the time interval $t \in [t_k, t_{k+1})$ in dependence upon the information $x(t_k)$ obtained at time t_k. The dashed arrows in the figure indicate information links that are only used after an event has been generated, whereas the solid arrows are used continuously.

The aim of this paper is to propose a new scheme of event-based control, where the communication link is only used if the disturbance $d(t)$ has caused an intolerable effect on the loop performance. As the main result, algorithms for the event generation and the control input generation are described for which the event-based control loop mimics the continuous state-feedback loop with adjustable accuracy.

In comparison with the numerous recent publications on event-based control, the approach described in this talk has three novelties. First, the control input generator is no longer a zero-order hold, but uses a model of the continuous closed-loop system to adapt the input continuously to the plant state. Second, the event generator evaluates the current plant state in comparison with the state that a continuous state-feedback system has. Hence, an event does not indicate a large control error but a large deviation of the event-based control loop from the continuous loop. Third, both the event generator and the control input generator include a disturbance estimator.

The talk also reports on the experimental evaluation of event-based control for a thermofluid process. The experiments show that event-based control leads to a considerable reduction of the communication within the control loop in comparison with sampled-data control (Fig. 2). Furthermore, the experiments demonstrate a considerable robustness of the closed-loop system with respect to model uncertainties.

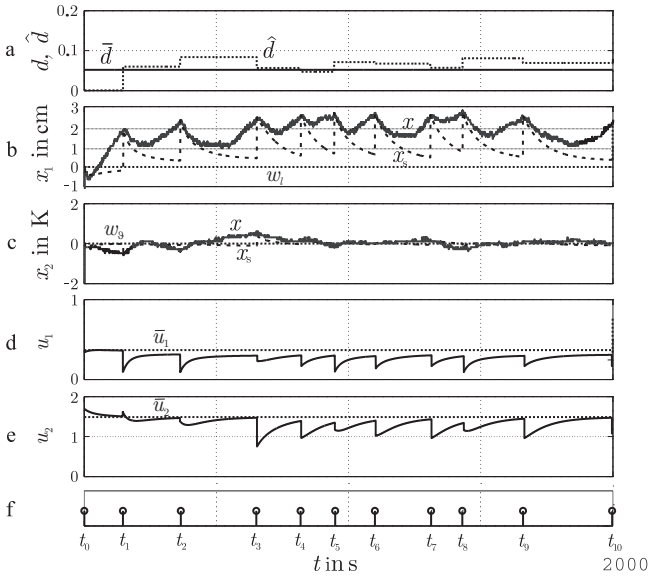

Fig. 2: Experimental results

The paper is based on the references [1] and [2].

References

[1] D. Lehmann, J. Lunze, Extension and experimental evaluation of an event-based state-feedback approach, *Control Engineering Practice* **19** (2011), 101-112.

[2] J. Lunze, D. Lehmann, A state-feedback approach to event-based control, *Automatica* **46** (2010), pp. 211-215.

Synchronization of Autonomous Agents with Individual Dynamics

Jan Lunze
Ruhr-University Bochum, 44780 Bochum, Germany
Lunze@atp.rub.de

Abstract

Synchronization is an important phenomenon occurring in multi-agent systems. The overall system consists of a (large) number of subsystems the interconnections of which give the whole system a coherent behaviour, in which the subsystems follow the same dynamical pattern. In this paper, synchronization is investigated as the process of moving the subsystem outputs $\mathbf{y}_i(t)$, $(i = 1,2,...,N)$ onto a common trajectory $\mathbf{y}_s(t)$.

In control theory, synchronization has become an important topic in connection with networked control systems. The research aim is to find methods for choosing the interactions among autonomous agents, which are implemented by a digital communication network, for which the overall system becomes synchronised satisfying the following two requirements:

1. **Synchronous behaviour:** For specific initial states of the agents, all outputs $\mathbf{y}_i(t)$ should follow a common trajectory $\mathbf{y}_s(t)$, which is called the synchronous trajectory:

$$\mathbf{y}_1(t) = \mathbf{y}_2(t) = ... = \mathbf{y}_N(t) = \mathbf{y}_s(t), \quad t \geq 0. \qquad (1)$$

2. **Asymptotic synchronization:** For all other initial states, the networked controller should asymptotically synchronise the agents:

$$\lim_{t\to\infty} \|\mathbf{y}_i(t) - \mathbf{y}_s(t)\| = 0, \quad i = 1,2,...,N. \qquad (2)$$

As an important issue of synchronization, the agents should be able to follow the synchronous trajectory $\mathbf{y}_s(t)$ due to their internal dynamics. On the synchronous trajectory (1) the interactions are not active and the agents have to generate the synchronous outputs as their free motion. The paper shows that the synchronization of agents with individual dynamics requires the controlled agents to include the dynamics of the synchronous trajectory in sense that is explained in the talk.

In contrast to the majority of publications on consensus and synchronization of identical agents, this paper deals with multi-agent systems in which the agents P_i have individual dynamical properties and, thus, are said to be heterogeneous. Such agents cannot be synchronized by some static networked controller K, but the synchronization problem has to be posed in the more general setting shown in Fig. 1. The agents P_i are extended by dynamical local units C_i (also called local controllers), which are interconnected over a digital communication network K. The local units together with the network represent the networked controller.

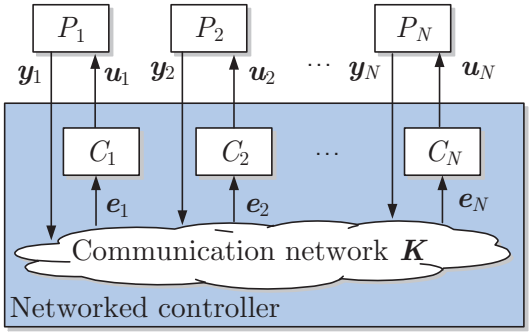

Fig. 1: Synchronization of autonomous agents

The paper solves two important problems:

- **Internal-reference principle for synchronization.** It answers the question under what conditions heterogeneous agents can be synchronized on some trajectory $\mathbf{y}_s(t)$. The result is the internal-reference principle for synchronization, which claims that all agents P_i together with their local unit C_i have to include the model Σ_s of the reference trajectory $\mathbf{y}_s(t)$.
- **Synchronization test.** It provides a necessary and sufficient condition under which the overall system is synchronized. For the particular case of a cycle-free communication topology this condition breaks down to separate conditions on the controlled agents.

The paper is based on the references [1] and [2].

References

[1] Lunze, J.: Synchronisable nodes in networked systems, *J. Phys. A: Math. Theor.* **44** (2011) 045103.

[2] Lunze, J.: An internal-model principle for the synchronization of autonomous agents with individual dynamics, *IEEE Conf. on Decision and Control*, Orlando 2011, pp. 2106-2111.

Part 4

List of Participants

Alessandro Abate
Dept. of Delft Center for Systems and Control
Technische Universiteit Delft
32
2628 CD Delft
The Netherlands
a.abate@tudelft.nl

Dieky Adzkiya
Dept. of Delft Center for Systems and Control
Technische Universiteit Delft
32
2628 CD Delft
The Netherlands
D.adzkiya@tudelft.nl

Irmak Aladagli
Control Systems Technology Group
Technische Universiteit Eindhoven
PO Box 513
5600 MB Eindhoven
The Netherlands
i.aladagli@gmail.com

Desti Alkano
Industrial Engineering and Management
University of Groningen
Nijenborgh 4
9747 AG Groningen
The Netherlands
d.alkano@rug.nl

Pedro ALMEIDA
Automatic Control Laboratory, Polytech
University of Mons
31 Boulevard Dolez
7000 Mons
Belgium
Pedro.Almeida@umons.ac.be

Zakaria Amribt
3BIO-BioControl, Brussels School of Engineering
Universit Libre de Bruxelles
Av. F.-D. Roosevelt 50 C.P. 165/61
1050 Ixelles Brussels
Belgium
zakaria.amribt@ulb.ac.be

Prof. A. Astolfi
Dept. of Electrical and Electronic Engineering
Imperical College
South Kensington Campus
SW7 2AZ London
United Kingdom
a.astolfi@imperial.ac.uk

Dr N. Athanasopoulos
Dept. of Electrical Engineering
Technische Universiteit Eindhoven
PO Box 513
5600 MB Eindhoven
The Netherlands
n.athanasopoulos@tue.nl

J C Atuonwu
Systems and Control Group
Wageningen University
P O Box 17
6700AA Wageningen
The Netherlands
james.atuonwu@wur.nl

Prof.dr.ir. A.C.P.M. Backx
Dept. of Electrical Engineering
Technische Universiteit Eindhoven
P.O. Box 513
5600 MB Eindhoven
The Netherlands
a.c.p.m.backx@tue.nl

Ezequiel Bajonero Canonico
Dept. of Mech. Eng, Control Systems Technology Group
Technische Universiteit Eindhoven
PO Box 513
5600 MB Eindhoven
The Netherlands
e.bajonero.canonico@student.tue.nl

kim batselier
Department of Electrical Engineering
Katholieke Universiteit Leuven
Kasteelpark Arenberg 10 - bus 2446
3010 Leuven
Belgium
kim.batselier@esat.kuleuven.be

N.W. Bauer
Dept. of Mechanical Engineering
Technische Universiteit Eindhoven
PO Box 513
5600 MB Eindhoven
The Netherlands
n.w.bauer@tue.nl

Micaela Benavides
Service d'Automatique
UMONS
31 Boulevard Dolez
7000 Mons
Belgium
MicaelaLucia.BENAVIDESCASTRO@umons.ac.be

Ir. J.J.B. Biemond
Dept. of Mechanical Engineering
Eindhoven University of Technology
PO Box 513
5600 MB Eindhoven
the Netherlands
j.j.b.biemond@tue.nl

Ir. C. Bikcora
Dept. of Electrical Engineering
Technische Universiteit Eindhoven
PO Box 513
5600 MB Eindhoven
The Netherlands
c.bikcora@tue.nl

F.A.J. Boeren
Dept. of Mechanical Engineering
Eindhoven University of Technology
PO Box 513
5600 MB Eindhoven
The Netherlands
F.A.J.Boeren@student.tue.nl

ir. J.J. Bolder
Dept. of Mechanical Engineering
Technische Universiteit Eindhoven
PO Box 513
5600 MB Eindhoven
The Netherlands
j.j.bolder@tue.nl

Ton Boom, van den
Dept. of Delft Center for Systems and Control
Technische Universiteit Delft
32
2628 CD Delft
The Netherlands
a.j.j.vandenboom@tudelft.nl

Maarten Breckpot
Dept. of Eletrical Engineering, ESAT-SCD
KU Leuven
Kasteelpark Arenberg 10, bus 2446
3001 Leuven
Belgium
maarten.breckpot@esat.kuleuven.be

Arnaud BROWET
INMA
Universit catholique de Louvain
Avenue Georges Lemaitre 4
1348 Louvain la Neuve
Belgium
arnaud.browet@uclouvain.be

Dr Eric Bullinger
Institut Montefiore
Universit de Lige
B28
4000 Lige Sart Tilman
Belgium
E.Bullinger@ulg.ac.be

ANGELO BUTTAFUOCO
S A A S
UNIVERSITE LIBRE DE BRUXELLES
AVENUE F.D. ROOSEVELT 50 CP 165/55
1050 BRUXELLES
BELGIUM
angelo.buttafuoco@ulb.ac.be

Kanat Camlibel
Dept. of Mathematics
University of Groningen
Sint Jansstraat 17C
9712 JM Groningen
Netherlands
kanat.camlibel@gmail.com

Ir. H.J. Cappon
Delta Academy
HZ University of Applied Sciences
PO Box 364
4380 AJ Vlissingen
The Netherlands
hans.cappon@hz.nl

Dr R. Carloni
Dept. of Electrical Engineering
University of Twente
PO Box 217
7500 AE Enschede
The Netherlands
R.Carloni@ewi.utwente.nl

C. Cochior
Department of Electrical Engineering
Eindhoven University of Technology
P.O. Box 513
5600 MB Eindhoven
The Netherlands
c.cochior@tue.nl

Anne Collard
Montefiore Institute
University of Lige
Grande Traverse 10
4000 Lige
Belgium
anne.collard@ulg.ac.be

Ir C.H.A. Criens
Mechanical Engineering
Technische Universiteit Eindhoven
PO Box 513
5600MB Eindhoven
Netherlands
c.h.a.criens@tue.nl

Pter Zoltn Csurcsia
DEPT ELEC
Vrije Universiteit Brussel
Pleinlaan 2
1050 Brussels
Belgium
peter.zoltan.csurcsia@vub.ac.be

Arne Dankers
Dept. of Delft Center for Systems and Control
Technische Universiteit Delft
32
2628 CD Delft
The Netherlands
a.g.dankers@tudelft.nl

Bram de Jager
Dept. of Mechanical Engineering
TU/e
PO Box 513
5600 MB Eindhoven
The Netherlands
A.G.de.Jager@tue.nl

Prof. C. de Persis
Smart Manufacturing Systems
University of Groningen
Nijenborgh 4
9747 AG Groningen
The Netherlands
c.de.persis@rug.nl

Ir. Frederik Debrouwere
Mechanical Engineering/PMA
KU Leuven
Celestijnenlaan 300B
3001 Heverlee
Belgium
Frederik.Debrouwere@mech.kuleuven.be

Adeline DECUYPER
INMA
Universit catholique de Louvain (UCL)
Avenue Georges Lemaitre 4
1348 Louvain la Neuve
Belgium
adeline.decuyper@uclouvain.be

Jonathan Dehaye
Dept. of Mathematics
University of Namur (FUNDP)
rue de Bruxelles, 61
B-5000 Namur
Belgium
jonathan.dehaye@fundp.ac.be

Jrmy Dehaye
Dept. of Mathematics
University of Namur (FUNDP)
8 Rempart de la Vierge
B-5000 Namur
Belgium
jeremy.dehaye@fundp.ac.be

Bruno Depraetere
Mechanical Engineering/PMA
KU Leuven
Celestijnenlaan 300B
3001 Heverlee
Belgium
bruno.depraetere@mech.kuleuven.be

JEAN-FRANCOIS DETERME
S A A S
UNIVERSITE LIBRE DE BRUXELLES
AVENUE F.D. ROOSEVELT 50 CP 165/55
1050 BRUXELLES
BELGIUM
pascale.lathouwers@ulb.ac.be

Julie Dethier
Dept. of Electrical Engineering and Computer Science
University of Liege
Grande Traverse, 10
4000 Liege
Belgium
jdethier@ulg.ac.be

Pierre DEVILLE
INMA
Universit catholique de Louvain (UCL)
Avenue Georges Lemaitre 4
1348 Louvain la Neuve
Belgium
pierre.deville@uclouvain.be

Dr. Ir. D.A. Dirksz
Dept. of Mechanical Engineering
Eindhoven University of Technology
PO Box 513
5600 MB Eindhoven
The Netherlands
d.a.dirksz@tue.nl

Guillaume Drion
Dept. of Electrical Engineering and Computer Science
University of Lige
Grande Traverse n10
B-4000 Lige
Belgium
gdrion@ulg.ac.be

Tong Duy Son
Mechanical Engineering/PMA
KU Leuven
Celestijnenlaan 300B
3001 Heverlee
Belgium
duyson.hut@gmail.com

Ir J. Elfring
Dept. of Mechanical Engineering
Technische Universiteit Eindhoven
PO Box 513
5600 MB Eindhoven
The Netherlands
j.elfring@tue.nl

J.C. Engwerda
Dept. of Econometrics and O.R.
Tilburg University
PO Box 90153
5000 LE Tilburg
The Netherlands
engwerda@uvt.nl

Sadegh Esmaeilzadeh
Dept. of Delft Center for Systems and Control
Technische Universiteit Delft
32
2628 CD Delft
The Netherlands
S.EsmaeilZadehSoudjani@tudelft.nl

E. Feru
Dept. of Mechanical Engineering
Technische Universiteit Eindhoven
PO Box 513
5600 MB Eindhoven
The Netherlands
e.feru@tue.nl

Marco Forgione
Dept. of Delft Center for Systems and Control
Technische Universiteit Delft
32
2628 CD Delft
The Netherlands
m.forgione@tudelft.nl

Fulvio Forni
Dept. of Electrical Engineering and Computer Science
University of Lige
Grande Traverse, 10, Building B28
B-4000 Liege Sart-Tilman
Belgium
fforni@ulg.ac.be

Ir D.F. Fu
Dept. of Electrical Energy, System and Automation
Universiteit Gent
Technologiepark 913
9052 Gent
Belgium
dongfei.fu@ugent.be

Matteo Fumagalli
EWI
University of Twente
PO Box 217
7500 AE Enschede
The Netherlands
m.fumagalli@utwente.nl

H.J. Garcia de Marina Peinado
DTPA
Groningen University
Nijenborgh 4
9747 GA Groningen
The Netherlands
h.j.garcia.de.marina.peinado@rug.nl

EMANUELE GARONE
S A A S
UNIVERSITE LIBRE DE BRUXELLES
AVENUE F.D. ROOSEVELT 50 CP 165/55
1050 BRUXELLES
BELGIUM
pascale.lathouwers@ulb.ac.be

Kurt Geebelen
ESAT-SCD:sista
KU Leuven
Kasteelpark Arenberg 10
3001 Heverlee
Belgium
kurt.geebelen@mech.kuleuven.be

ir. E. Geerardyn
Dept. of Fundamental Electricity and Instrumentation (ELEC)
Vrije Universiteit Brussel
Pleinlaan 2
1050 Elsene
Belgium
egon.geerardyn@vub.ac.be

Ir. R.H. Gielen
Electrical Engineering
Eindhoven University of Technology
PO Box 513
5600MB Eindhoven
The Netherlands
r.h.gielen@tue.nl

Geert Gins
Dept. of Chemical Engineering - BioTeC
KU Leuven
W. de Croylaan 46 PB 2423
3001 Heverlee
Belgium
geert.gins@cit.kuleuven.be

ir. T.M.P. Gommans
Dept. of Mechanical Engineering
Eindhoven University of Technology
P.O. Box 513
5600 MB Eindhoven
The Netherlands
t.m.p.gommans@tue.nl

Ir G.F. Goormaghtigh
3BIO-BIOCONTROL
Universit Libre de Bruxelles
165/61
1050 Bruxelles
Belgium
fred.goormaghtigh@gmail.com

Ir. Jan Goos
ELEC
Vrije Universiteit Brussel
Pleinlaan 2
1050 Elsene
Belgium
jan.goos@vub.ac.be

Ir T.G. Gosset
Biosystems, Biomodelling and Bioprocesses Dept.
Universit Libre de Bruxelles
165/61
1050 Bruxelles
Belgium
tgosset@ulb.ac.be

Mr. Sasanka Gottimukkala
Systems Control and Applied Analysis, Johann Bernoulli Institute for Mathematics and Computer Science
UIniversity of Groningen
P. O Box 800
9700 AV Groningen
The Netherlands
s.v.gottimukkala@rug.nl

Sofie Haesaert
Dept. of Delft Center for Systems and Control
Technische Universiteit Delft
2628
CD Delft
The Netherlands
s.haesaert@student.tudelft.nl

Mohammad Hajiahmadi
Dept. of Delft Center for Systems and Control
Technische Universiteit Delft
32
2628 CD Delft
The Netherlands
m.hajiahmadi@tudelft.nl

Ir. D.J.F. Heck
Dept. of Mechanical Engineering
Technische Universiteit Eindhoven
PO Box 513
5600 MB Eindhoven
The Netherlands
d.j.f.heck@tue.nl

Prof. Julien M. Hendrickx
ICTEAM
Universit catholique de Louvain
av G Lemaitre 4
B-1348 Louvain la Neuve
Belgium
julien.hendrickx@uclouvain.be

Ir. R. M. Hermans
Dept. of Electrical Engineering
Eindhoven University of Technology
P.O. Box 513
5600 MB Eindhoven
The Netherlands
r.m.hermans@tue.nl

Peter Heuberger
Dept. of Delft Center for Systems and Control
Technische Universiteit Delft
32
2628 CD Delft
The Netherlands
p.s.c.heuberger@tudelft.nl

Gijs Hilhorst
Mechanical Engineering/PMA
KU Leuven
Celestijnenlaan 300B
3001 Heverlee
Belgium
gijs.hilhorst@mech.kuleuven.be

Ir. P.G.M. Hoeijmakers
Mechanical Engineering
Eindhoven University of Technology
P.O. Box 513
5600 MB Eindhoven
The Netherlands
p.g.m.hoeijmakers@tue.nl

Ir. G. Hommen
Control Systems Technology
Eindhoven University of Technology & Dutch Institute for Fusion Energy Research
PO Box 513
5600 MB Eindhoven
The Netherlands
g.hommen@tue.nl

ir. R, Hoogendijk
Dept. of Mechanical Engineering
Technische Universiteit Eindhoven
PO Box 513
5600 MB Eindhoven
The Netherlands
r.hoogendijk@tue.nl

Erik Hostens
Engineering
FMTC
Celestijnenlaan 300D - 4027
3001 Leuven
Belgium
erik.hostens@fmtc.be

Yu Hu
Dept. of Delft Center for Systems and Control
Technische Universiteit Delft
32
2628 CD Delft
The Netherlands
yu.hu@tudelft.nl

R. Huisman
DTPA
Universiteit Groningen
Nijenborgh 4
9747 AG Groningen
The Netherlands
r.huisman@sron.nl

Bram Hunnekens
Mechanical Engineering
Eindhoven University of Technology
PO Box 513
5600 MB Eindhoven
The Netherlands
B.G.B.Hunnekens@tue.nl

Bart Huyck
Department of Electrical Engineering (ESAT-SCD)
KU Leuven
Kasteelpark Arenberg 10, bus 2446
3001 Heverlee
BELGIUM
bart.huyck@esat.kuleuven.be

M. Jafarian
Smart Manufacturing Systems
University of Groningen
Nijenborgh 4
9747 AG Groningen
The Netherlands
m.jafarian@rug.nl

ir. R.J.M. Janssen
Dept. of Mechanical Engineering
Eindhoven University of Technology
PO BOX 513
5600 MB Eindhoven
The Netherlands
r.j.m.janssen@tue.nl

Pieter Janssens
Mechanical Engineering/PMA
KU Leuven
Celestijnenlaan 300B
3001 Heverlee
Belgium
Pieter.Janssens@mech.kuleuven.be

JEROME JANSSENS
S A A S
UNIVERSITE LIBRE DE BRUXELLES
AVENUE F.D. ROOSEVELT 50 CP 165/55
1050 BRUXELLES
BELGIUM
jerome.janssens@ulb.ac.be

Dr. Bayu Jayawardhana
Discrete Technology and Production Automation
University of Groningen
Nijenborgh 4
9747 AG Groningen
The Netherlands
b.jayawardhana@rug.nl

M.D. Kaba
JBI for Mathematics and Computer Science
University of Groningen
PO Box 407
9700 AK Groningen
The Netherlands
m.d.kaba@rug.nl

dipl.-Ing. A. Katalenic
Dept. of Electrical Engineering
Technische Universiteit Eindhoven
PO Box 513
5600MB Eindhoven
Nederland
a.katalenic@tue.nl

Dr Keesman
Systems & Control Group
Wageningen University
Bornse Weilanden 9
6708 WG Wageningen
Netherlands
karel.keesman@wur.nl

Bart Kersbergen
Dept. of Delft Center for Systems and Control
Technische Universiteit Delft
32
2628 CD Delft
The Netherlands
b.kersbergen@tudelft.nl

Dr Islam S. M. Khalil
Dept. of Control Engineering
University of Twente
Calslaan 38 009, Enschede
7522 ME Enschede
The Netherlands
i.s.m.khalil@utwente.nl

MICHEL KINNAERT
S A A S
UNIVERSITE LIBRE DE BRUXELLES
AVENUE F.D. ROOSEVELT 50 CP 165/55
1050 BRUXELLES
BELGIUM
pascale.lathouwers@ulb.ac.be

Ir. J.B.M. Klok
Systems and Control group
Wageningen Universiteit
PO Box 17
6700 AA Wageningen
The Netherlands
johannes.klok@wur.nl

dr ir S.H. Koekebakker
Dept. Mech. Eng, Control Systems Technology Group
Technische Universiteit Eindhoven / Oc
PO Box 513
5600MB Eindhoven
The Netherlands
S.H.Koekebakker@tue.nl

Anil Kunnappillil Madhusudhanan
Dept. of Delft Center for Systems and Control
Technische Universiteit Delft
32
2628 CD Delft
The Netherlands
a.k.madhu@tudelft.nl

Rocco Langone
, Department of Electrical Engineering-ESAT, SCD-SISTA
KU Leuven
Kasteelpark Arenberg 10
B-3001 Leuven
Belgium
rocco.langone@esat.kuleuven.be

msc Larsen
Faculty of Mathematics and Natural Sciences
University of Groningen
DTPA
9747AG Groningen
The Netherlands
g.k.h.larsen@rug.nl

John Lataire
Dept. ELEC
Vrije Universiteit Brussel
Pleinlaan 2
1050 Elsene
Belgium
jlataire@vub.ac.be

ir. M. Lauret
Dept. of Mechanical Engineering
Technische Universiteit Einhoven / FOM DIFFER
PO Box 513
5600 MB Eindhoven
The Netherlands
m.lauret@tue.nl

Quang Thuan Le
Department of Mathematics
University of Groningen
P.O. Box 800
9700 AV Groningen
The Netherlands
t.q.le@rug.nl

Le Li
Dept. of Delft Center for Systems and Control
Technische Universiteit Delft
32
2628 CD Delft
The Netherlands
l.li-1@tudelft.nl

Raphal Liegeois
Montefiore Institute (EECS)
University of Lige
Grande Traverse 10
4000 Lige
Belgium
r.liegeois@ulg.ac.be

Shuai Liu
Dept. of Delft Center for Systems and Control
Technische Universiteit Delft
32
2628 CD Delft
The Netherlands
s.liu-1@tudelft.nl

Ir Louarroudi
ELEC
Vrije Universiteit Brussel
Pleinlaan 2
1050 Brussels
Belgium
elouarro@vub.ac.be

Ir. Janno Lunenburg
Department of Mechanical Engineering
Eindhoven University of Technology
PO Box 513
5600 MB Eindhoven
The Netherlands
j.j.m.lunenburg@tue.nl

Prof. Dr. J. Lunze
Institute of Automation and Computer Control
Ruhr-Universitt Bochum
Universittsstrae 150
44780 Bochum
Germany
Lunze@atp.rub.de

R. Maas, van der
Dept. of Mechanical Engineering
Eindhoven University
PO Box 513
5600 MB Eindhoven
The Netherlands
r.j.r.v.d.Maas@tue.nl

Anna Marconato
Dept. ELEC
Vrije Universiteit Brussel
Pleinlaan 2
1050 Brussel
Belgium
anna.marconato@vub.ac.be

S Marinkov
Dept. of Mechanical Engineering
Eindhoven University of Technology
PO Box 513
5600 MB Eindhoven
The Netherlands
s.marinkov@tue.nl

Siamak Mehrkanoon
Department of Electrical Engineering, ESAT-SCD
K U Leuven
Kasteelpark Arenberg 10,
B-3001 Leuven,
Belgium
Siamak.Mehrkanoon@esat.kuleuven.be

Samuel MELCHIOR
INMA
Universit catholique de Louvain (UCL)
Avenue Georges Lemaitre 4
1348 Louvain la Neuve
Belgium
samuel.melchior@uclouvain.be

Bamdev Mishra
Dept. of Electrical Engineering and Computer Science
University of Liege
10, Grand Traverse, B28, Sart-Tilman
4000 Liege
Belgium
b.mishra@ulg.ac.be

Dr S. Misra
Electrical Engineering
Twente University
PO Box 217
7500 AE Enschede
The Netherlands
s.misra@utwente.nl

Nima Monshizadeh Naini
Control systems and applied analysis
University of Groningen
Noorderstationsstraat 10A
9717KN Groningen
Netherlands
n.monshizadeh@gmail.com

Ir G. Monteyne
Dept. of ELEC
Vrije Universiteit Brussel
Pleinlaan 2
1050 Elsene
Belgium
gmonteyn@vub.ac.be

Ir. Sikandar Moten
Mechanical Engineering/PMA
KU Leuven
Celestijnenlaan 300B
3001 Heverlee
Belgium
sikandar.moten@student.kuleuven.be

MOISE MUKEPE KAHILU
S A A S
UNIVERSITE LIBRE DE BRUXELLES
AVENUE F.D. ROOSEVELT 50 CP 165/55
1050 BRUXELLES
BELGIUM
pascale.lathouwers@ulb.ac.be

Eng. Muoz Arias
Faculty of Mathematics and Natural Sciences
University of Groningen
9716HW
9716HW Groningen
The Netherlands
m.munoz.arias@rug.nl

Mark Mutsaers
Dept. of Electrical Engineering
Eindhoven University of Technology
PO Box 513
5600 MB Eindhoven
The Netherlands
m.e.c.mutsaers@tue.nl

Oscar Olarte
Department of Fundamental Electricity and Instrumentation
Vrije Universiteit Brussels
Buiding K - Room K440 Pleinlaan 2
1050 Brussels
Belgium
oolarter@vub.ac.be

D. Oliva Uribe
ELEC
Vrije Universiteit Brussel
Pleinlaan 2
1050 Brussels
Belgium
dolivaur@irexchange.vub.ac.be

Drs. J. Omony
Systems and Control group
Wageningen University
P.O. Box 17
6700 AA Wageningen
The Netherlands
jimmy.omony@wur.nl

Sinan Oncu
Mechanical Engineering
Eindhoven University of Technology
PO Box 513
5600 MB Eindhoven
Netherlands
s.oncu@tue.nl

Dr. ir. T.A.E. Oomen
Department of Mechanical Engineering
Technische Universiteit Eindhoven
PO Box 513
5600 MB Eindhoven
The Netherlands
t.a.e.oomen@tue.nl

Ir r.y. Ouyang
Discrete technology and production automation
University of Groningen
Nijenborgh 4
9747 AG Groningen
The Netherlands
r.y.ou.yang@gmail.com

Dr. L. Ozkan
Dept of Electrical Engineering
Technische Universiteit Eindhoven
PO Box 513
5600 Eindhoven
The Netherlands
l.ozkan@tue.nl

Jelle Peeters
Department of Computer Science
Katholieke Universiteit Leuven
Celestijnenlaan 200A
B-3001 Heverlee
Belgium
jelle.peeters@cs.kuleuven.be

MSc. H.T. Pham
Electrical Engineering/Control System
Technische Universiteit Eindhoven
P.O. Box 513
5600 MB Eindhoven
The Netherlands
t.pham.hong@tue.nl

BORCKMANS Pierre
INMA
Universit catholique de Louvain (UCL)
Avenue Georges Lemaitre 4
1348 Louvain la Neuve
Belgium
pierre.borckmans@uclouvain.be

Guilherme PIMENTEL
Automatic Control Laboratory, Polytech
University of Mons
31 Boulevard Dolez
7000 Mons
Belgium
Guilherme.AraujoPimentel@umons.ac.be

Rik Pintelon
ELEC
Vrije Universiteit Brussel
Pleinlaan 2
B-1050 Brussel
Belgium
Rik.Pintelon@vub.ac.be

Goele Pipeleers
Dept. of Mechanical Engineering
KU Leuven
Celestijnenlaan 300B
B-3001 Heverlee
Belgie
goele.pipeleers@mech.kuleuven.be

Dr J.W. Polderman
Applied Mathematics
University of Twente
PO Box 217
7500 AE Enschede
The Netherlands
j.w.polderman@math.utwente.nl

Max Potters
Dept. of Delft Center for Systems and Control
Technische Universiteit Delft
32
2628 CD Delft
The Netherlands
m.g.potters@tudelft.nl

Wisnu Adi Pradana
Dept. of Applied Mathematics
Universiteit Twente
PO Box 217
7500 AE Enschede
The Netherlands
w.a.pradana@utwente.nl

R. Prihatin
Applied Mathematics
University of Twente
PO Box 217
7500 AE Enschede
Netherlands
r.prihatin@ewi.utwente.nl

Yue Qiu
Dept. of Delft Center for Systems and Control
Technische Universiteit Delft
32
2628 CD Delft
The Netherlands
Y.qiu@tudelft.nl

Dr S.S. Rao
DTPA
Groningen University
Nijenborgh 4
9747 AG Groningen
The Netherlands
s.s.rao@rug.nl

Ir. Retamal
Service d'Automatique
Universit de Mons
Boulevard Dolez 31
7000 Mons
Belgique
cristina.retamal@umons.ac.be

Ir. A. Richelle
3BIO-BIOCONTROL
Universit Libre de Bruxelles
Avenue Franklin Roosevelt, 50 - CP 165/61
1050 Brussels
Belgium
arichell@ulb.ac.be

Pierre Sacr
Montefiore Institute (EECS)
University of Lige
Grande Traverse 10
4000 Lige
Belgium
pierre.sacre@ulg.ac.be

Ines SARAIVA
Automatic Control Laboratory, Polytechnic Faculty
University of Mons
31 Boulevard Dolez
7000 Mons
Belgium
Ines.Saraiva@umons.ac.be

Alain Sarlette
SYSTeMS
Universiteit Gent
Technologiepark Zwijnaarde 914
9052 Gent
Belgium
alain.sarlette@ugent.be

Prof. dr. ir. J.M.A. Scherpen
Fac. Mathematics and Natural Sciences
University of Groningen
Nijenborgh 4
9747 AG Groningen
The Netherlands
j.m.a.scherpen@rug.nl

Johan Schoukens
ELEC
Vrije Universiteit Brussel
Pleinlaan 2
B1050 Brussels
Belgium
johan.schoukens@vub.ac.be

Rodolphe Sepulchre
Dept. of Electrical Engineering and Computer Science
University of Liege
Insitut Montefiore, B28
4000 Liege Sart-Tilman
Belgium
r.sepulchre@ulg.ac.be

Marko Seslija
Faculty of Mathematics and Natural Sciences
University of Groningen
Nijenborgh 4
9712GW Groningen
Netherlands
m.seslija@rug.nl

Dr. F. Shaik
Faculty of mathematics and natural sciences
University of Groningen
P.O. Box 407
9700 AK Groningen
The Netherlands
F.Shaik@rug.nl

Hanumant Singh Shekhawat
Dept. of Applied mathematics
University of Twente
P.O. Box 217
7500 AE Enschede
The Netherlands
h.s.shekhawat@utwente.nl

MSc E. Silvas
Dept. of Mechanical Engineering
Technische Universiteit Eindhoven
PO Box 513
5600 MB Eindhoven
The Netherlands
E.Silvas@tue.nl

Muhammad Mohsin Siraj
Dept. of Electrical Engineering
Technische Universiteit Eindhoven
PO Box 513
5600 MB Eindhoven
The Netherlands
m.s.siraj@student.tue.nl

Edwin Solingen
Dept. of Delft Center for Systems and Control
Technische Universiteit Delft
32
2628 CD Delft
The Netherlands
e.vansolingen@tudelft.nl

Prof.dr.ir. M. Steinbuch
Dept. of Mechanical Engineering - Control Systems Technology
University of Technology Eindhoven
PO Box 513, GEM-Z 0.141
5600 MB Eindhoven
The Netherlands
m.steinbuch@tue.nl

dr. ir. E. Steur
Dept. of Mechanical Engineering
Eindhoven University of Technology
P.O.Box 513
5600 MB Eindhoven
The Netherlands
e.steur@tue.nl

Dr J.D. Stigter
Biometris
Wageningen UR
PO Box 100
6700 AC Wageningen
The Netherlands
jdstigter@gmail.com

Dr J. Stoev
FMTC
KU Leuven
Celestijnenlaan 300B
BE-3001 Leuven
Belgium
Julian.Stoev@fmtc.be

Prof.dr. A.A. Stoorvogel
Dept. of Electrical Engineering, Mathematics and Computer Science
Universiteit Twente
P.O. Box 217
7500 AE Enschede
The Netherlands
A.A.Stoorvogel@utwente.nl

Prof.Dr. S. Stramigioli
Electrical Engineering
Twente University
PO Box 217
7500 AE Enschede
The Netherlands
S.Stramigioli@utwente.nl

Yuxin Su
Mechanical Engineering/PMA
KU Leuven
Celestijnenlaan 300B
3001 Heverlee
Belgium
yuxin.su@mech.kuleuven.be

Paul SUVAROV
Automatic Control Laboratory, Polytech
University of Mons
31 Boulevard Dolez
7000 Mons
Belgium
Paul.Suvarov@umons.ac.be

Easter Selvan SUVISESHAMUTHU
INMA
Universit catholique de Louvain (UCL)
Avenue Georges Lemaitre 4
1348 Louvain la Neuve
Belgium
easter.suviseshamuthu@uclouvain.be

Jan Swevers
Mechanical Engineering/PMA
KU Leuven
Celestijnenlaan 300B
3001 Heverlee
Belgium
jan.swevers@mech.kuleuven.be

Koen Tiels
Dept. ELEC
Vrije Universiteit Brussel
Pleinlaan 2
1050 Brussel
Belgium
Koen.Tiels@vub.ac.be

Ilya Tkachev
Dept. of Delft Center for Systems and Control
Technische Universiteit Delft
32
2628 CD Delft
The Netherlands
I.tkachev@tudelft.nl

Patricio Torres
Dept. of Delft Center for Systems and Control
Technische Universiteit Delft
32
2628 CD Delft
The Netherlands
p.i.torrestapia@tudelft.nl

Quang N. Tran
Dept. of Electrical Engineering
Technische Universiteit Eindhoven
PO Box 513
5600 MB Eindhoven
The Netherlands
n.q.tran@tue.nl

Maguy TREFOIS
INMA
Universit catholique de Louvain (UCL)
Avenue Georges Lemaitre 4
1348 Louvain la Neuve
Belgium
maguy.trefois@uclouvain.be

Laura Trotta
Dept. of Electrical Engineering and Computer Science
University of Lige
Grande Traverse, 10
4000 Lige
Belgium
l.trotta@ulg.ac.be

Diana Ugryumova
Dept. of ELEC
Vrije Universiteit Brussel
Pleinlaan 2
1050 Brussels
Belgium
diana.ugryumova@vub.ac.be

Ir K. van Berkel
Deptartment of Mechanical Engineering
Technische Universiteit Eindhoven
PO Box 513
5600 MB Eindhoven
The Netherlands
k.v.berkel@tue.nl

MSc. P.J.M. van Beveren
Farm Technology Group
Wageningen University
Postbus 317
6700 AH Wageningen
The Netherlands
peter.vanbeveren@wur.nl

Sjoerd van den Dries
Dept. of Mechanical Engineering
Technische Universiteit Eindhoven
PO Box 513
5600 MB Eindhoven
The Netherlands
S.v.d.Dries@tue.nl

Prof.dr.ir. P.M.J. Van den Hof
Dept. EE Control Systems
Technische Universiteit Eindhoven
P.O. Box 513
5600 MB Eindhoven
The Netherlands
p.m.j.vandenhof@tue.nl

Pieter Van den Kerkhof
Dept. of Chemical Engineering - BioTeC
KU Leuven
W. de Croymaan 46 PB 2423
3001 Heverlee
Belgium
pieter.vandenkerkhof@cit.kuleuven.be

Ir. P van der Hulst
Electrical engineering
Technische Universiteit Eindhoven
PO Box 513
5600 MB Eindhoven
The Netherlands
p.v.d.hulst@tue.nl

Ir. T.P.J. Van der Sande
Dynamics and Control
Eindhoven University of Technology
PO Box 513
5600MB Eindhoven
The Netherlands
t.p.j.v.d.sande@tue.nl

Prof.dr. van der Schaft
Bernoulli Institute for Mathematics and Computer Science
Rijksuniversiteit Groningen
PO Box 407
9700 AK Groningen
The Netherlands
a.j.van.der.schaft@rug.nl

ir. R.W. van Gils
Dept. of Mechanical Engineering, Dynamics and Control group
Eindhoven University of Technology
PO Box 513, GEM-Z -1.144
5600 MB Eindhoven
The Netherlands
r.w.v.gils@tue.nl

Dr Ir T.A.C. van Keulen
Engine Development
DAF Trucks N.V.
PO Box 90065
5600 PT Eindhoven
The Netherlands
thijs.van.keulen@daftrucks.com

Wannes Van Loock
Mechanical Engineering/PMA
KU Leuven
Celestijnenlaan 300B
3001 Heverlee
Belgium
wannes.vanloock@mech.kuleuven.be

ir. S.J.L.M. van Loon
Dept. of Mechanical Engineering
Technische Universiteit Eindhoven
PO Box 513
5600 MB Eindhoven
The Netherlands
s.j.l.m.v.loon@tue.nl

Dr ir van Mourik
Plant Sciences Group
Wageningen University
P.O. Box 100
6700 AC Wageningen
Netherlands
simon.vanmourik@wur.nl

Vital van Reeven
Dept. of Mechanical Engineering
Technische Universiteit Eindhoven
PO Box 513
5600 MB Eindhoven
The Netherlands
v.v.reeven@tue.nl

Prof. J.H. van Schuppen
Cluster MAC
CWI
PO Box 94079
1090 GB Amsterdam
Netherlands
J.H.van.Schuppen@cwi.nl

dr G.A.K. Van Voorn
Biometris
Wageningen University & Research
P.O. Box 100
6700 AC Wageningen
The Netherlands
george.vanvoorn@wur.nl

Ir. P.W.M. van Zutven
Dept. of Mechanical Engineering
Eindhoven University of Technology
PO Box 513
5600 MB Eindhoven
the Netherlands
p.w.m.v.zutven@tue.nl

ir. D.A.J. van Zwieten
Dept. of Mechanical Engineering
Technische Universiteit Eindhoven
PO Box 513
5600 MB Eindhoven
The Netherlands
d.a.j.v.zwieten@tue.nl

Dr Vanbeylen
Dept. of Fundamental Electricity (ELEC)
Vrije Universiteit Brussel
Pleinlaan 2
1050 Brussel Brussel
Belgium
lvbeylen@vub.ac.be

Jef Vanlaer
Dept. of Chemical Engineering - BioTeC
KU Leuven
W. de Croylaan 46 PB 2423
3001 Heverlee
Belgium
jef.vanlaer@cit.kuleuven.be

Dominique Vercammen
Dept. of Chemical Engineering - BioTeC
Katholieke Universiteit Leuven
W. de Croylaan 46 PB 2423
3001 Heverlee
Belgium
dominique.vercammen@cit.kuleuven.be

Prof. Dr. M. Verhaegen
DCSC
TU Delft
Mekelweg 2
2618 CD Delft
The Netherlands
m.verhaegen@tudelft.nl

Ana Virag
Dept. of Electrical Engineering
Technische Universiteit Eindhoven
PO Box 513
5600 MB Eindhoven
The Netherlands
a.virag@tue.nl

ir. M. Volckaert
Dept. of Mechanical Engineering
KU Leuven
Celestijnenlaan 300B
3001 Leuven
Belgium
marnix.volckaert@mech.kuleuven.be

Ir. E Vos
Discrete technology and product automation
University of Groningen
Nijenborgh 4
9747AG Groningen
The Netherlands
e.vos@rug.nl

Thijs Vromen
Mechanical Engineering
Eindhoven University of Technology
PO Box 513
5600 MB Eindhoven
The Netherlands
t.g.m.vromen@tue.nl

Yihui Wang
Dept. of Delft Center for Systems and Control
Technische Universiteit Delft
32
2628 CD Delft
The Netherlands
yihui.wang@tudelft.nl

ir.X Wang
Mechanical Engineering/PMA
KU Leuven
Celestijnenlaan 300B
3001 Heverlee
Belgium
xin.wang@mech.kuleuven.be

Chen Wang
Faculty of Mathematics and Natural Sciences
University of Groningen
Nijenborgh 4, Room 5117.0116
9747 AG Groningen
The Netherlands
wangchen@pku.edu.cn

J Wei
Johann Bernoulli Institute of mathematics and computer sciences
University of Groningen
P.O.BOX 407
9700AK Groningen
The Netherlands
j.wei@rug.nl

Prof. Dr. S. Weiland
Dept. of Electrical Engineering
TU Eindhoven
PO Box 513
5600 MB Eindhoven
The Netherlands
S.Weiland@tue.nl

Dr. Ir. W. D. Widanage
Dept. of Fundamental Electricity and Instrumentation
Vrije Universiteit Brussel
Pleinlaan 2
1050 Brussels
Belgium
wwidanag@vub.ac.be

Jan-Willem Wingerden
Dept. of Delft Center for Systems and Control
Technische Universiteit Delft
32
2628 CD Delft
The Netherlands
j.w.vanwingerden@tudelft.nl

Professor J. J. Winkin
Mathematics
University of Namur (FUNDP)
Rempart de la vierge 8
5000 Namur
Belgium
joseph.winkin@fundp.ac.be

Dr M. Witters
FMTC
KU Leuven
Celestijnenlaan 300D - bus 4027
BE-3001 Leuven
Belgium
Maarten.Witters@fmtc.be

H.K. Wong
School of Engineering / ELEC
Uni. of Warwick / Vrije Uni. Brussels
School of Engineering, University of Warwick
CV4 7AL Coventry
United Kingdom
hin.wong@warwick.ac.uk

Dr. J. Woude, van der
Applied Mathematics
TU Delft
Mekelweg 4
2628 CD Delft
The Netherlands
J.W.vanderWoude@tudelft.nl

Weiguo Xia
Faculty of Mathematics and Natural Sciences
University of Groningen
Nijenborgh 4
9747 AG Groningen
The Netherlands
w.xia@rug.nl

J. Xin
Department of Marine and Transport Technology
Delft University of Technology
Mekelweg 2
2628 CD Delft
The Netherlands
j.xin@tudelft.nl

Yashar Zeinaly
Dept. of Delft Center for Systems and Control
Technische Universiteit Delft
32
2628 CD Delft
The Netherlands
Y.zeinaly@tudelft.nl

Shuo Zhang
Faculty of Mathematics and Natural Sciences
University of Groningen
Nijenborgh 4
9747AG Groningen
The Netherlands
shuo.zhang@rug.nl

F. Zhang
DTPA
Groningen University
Nijenborgh 4
9747 AG Groningen
The Netherlands
fan.zhang@rug.nl

Guoying Zhao
Mechanical Engineering/PMA
KU Leuven
Celestijnenlaan 300B
3001 Heverlee
Belgium
paul.sas@mech.kuleuven.be

Part 5

Organizational Comments

Welcome

The Organizing Committee has the pleasure of welcoming you to the *31st Benelux Meeting on Systems and Control*, at Centerparcs "Heijderbos" in Heijen, The Netherlands.

Aim

The aim of the Benelux Meeting is to promote research activities and to enhance cooperation between researchers in Systems and Control. This is the thirty-first in a series of annual conferences that are held alternately in Belgium and The Netherlands.

Overview of the Scientific Program

1. Plenary lectures by invited speaker *Alessandro Astolfi* (Imperial College, London, United Kingdom) on
   - **Dynamic Value Functions – Towards Constructive Nonlinear Control Systems Analysis and Design**
   - **Model reduction by moment matching**
2. Plenary lectures by invited speaker *Jan Lunze* (Ruhr-Universität, Germany) on
   - **Event-Based Control: Theory and Application**
   - **Synchronization of Autonomous Agents with Individual Dynamics**
3. Mini course by *Stefano Stramigioli* (Twente University, The Netherlands) on
   - **Port Based Thinking: What is it and why is this useful?**
   - **Port Based Modeling for Robotics**
   - **Port Based Control for Robotics**
4. Contributed short lectures. See the list of sessions for the titles and authors of these lectures.

Directions for speakers

For a contributed lecture the available time is 25 minutes. Please leave a few minutes of this period for discussion and room changes and adhere to the indicated schedule. In each room overhead projectors and beamers will be available. Be careful with this equipment, because the beamers are supplied by some of the participating groups. *When using a beamer/projector, you have to provide a notebook yourself and you have to start your lecture with the notebook up and running and the external video port switched on.*

Registration

The Benelux Meeting registration desk, located in the foyer, will be open on Tuesday, March 27, from 10:00 to 14:00. Late registrations can be made at the Benelux Meeting registration desk, when space is still available. The on-site fee schedule is:

Arrangement	Price
single room	€ 540.–
twin-bedded room	€ 435.–
meals only (no dinner)	€ 300.–
one day (no dinner)	€ 155.–

The registration fee includes:

- Admission to all sessions.
- A copy of the Book of Abstracts.
- Coffee and tea during the breaks.
- In the case of an accommodation arrangement: lunch and dinner on Tuesday, breakfast, lunch, and dinner on Wednesday, and breakfast and lunch on Thursday.
- In the case of a "meals only" arrangement: lunch on Tuesday, Wednesday, and Thursday.
- In the case of a "one day" arrangement: lunch on Tuesday, or Wednesday, or Thursday.
- Free use of a wireless Internet connection (WiFi) in each cottage.

The registration fee does *not* include:

- Cost of phone calls
- Special ordered drinks during lunch, dinner, in the evening, etc.

Organization

The Organizing Committee of the 31^{st} Benelux Meeting consists of

D. Aeyels
Gent University
Systems Group

Email: Dirk.Aeyels@UGent.be

V. Blondel
Universit catholique de Louvain
Department of Mathematical Engineering
E-mail: vincent.blondel@uclouvain.be

R. Boel
Gent University
Systems Group
Email: Rene.Boel@UGent.be

B. De Moor
Catholic University of Leuven
Dept. ESAT-SCD
Email: bart.demoor@esat.kuleuven.ac.be

B. De Schutter
Delft University of Technology
Delft Center for Systems and Control
Email: B.DeSchutter@tudelft.nl

G. Meinsma
Twente University
Department of Applied Mathematics
Email: g.meinsma@math.utwente.nl

H. Nijmeijer
Eindhoven Univesity
Faculteit Werktuigbouwkunde
Email: H.Nijmeijer@tue.nl

J. Scherpen
Rijksuniversiteit Groningen
Faculty of Mathematics and Natural Sciences
Email: j.m.a.scherpen@wur.nl

J. Schoukens
Vrije Universiteit Brussel
Departement ELEC
Email: Johan.schoukens@vub.ac.be

M. Steinbuch
Eindhoven University
Dept. of Mechanical Engineering
Email: M.Steinbuch@tue.nl

J.D. Stigter
Wageningen University
Biometris (Mathematical and Statistical Methods)
Email: Hans.Stigter@wur.nl

A.A. Stoorvogel
Twente University
Dept. of Applied Mathematics
Email: a.a.stoorvogel@utwente.nl

S. Stramigioli
Twente University
Dept. of Electrical Engineering
Email: s.stramigioli@ieee.org

T.J.J. van den Boom
Delft University of Technology
Delft Center for Systems and Control
Email: a.j.j.vandenboom@tudelft.nl

A.J. van der Schaft
Rijksuniversiteit Groningen
Faculteit Wiskunde
Email: a.j.van.der.schaft@math.rug.nl

P. Van Dooren
Catholic University of Louvain
Mathematical Engineering
Email: paul.vandooren at uclouvain.be

J.F.M. van Impe
Catholic University of Leuven
Dept. of Chemical Engineering
Email: jan.vanimpe@cit.keuleuven.be

G. van Straten
Wageningen Universiteit
Dept. of Agrotechnology and Food Sciences
Email: Gerrit.vanStraten@wur.nl

M. Verhaegen
Delft University of Technology
Delft Center for Systems and Control
Email: m.verhaegen@tudelft.nl

S. Weiland
Technische Universiteit Eindhoven
Faculteit Elektrotechniek
Email: s.weiland@ele.tue.nl

J. Willems
Catholic University of Leuven
Department of Electrical Engineering,
Email: Jan.Willems@esat.kuleuven.be

The meeting is sponsored or supported by the following organizations:

- Dutch Institute for Systems and Control (DISC),
- Nederlandse Organisatie voor Wetenschappelijk Onderzoek (NWO).

The meeting has been organized by Hans Stigter (Wageningen University) and Ton van den Boom (Delft University).

Conference location

The lecture rooms of "Centerparcs Heijderbos" are situated on the ground floor. Consult the map at the end of this booklet to locate rooms. During the breaks, coffee and tea will be served in the foyer. Announcements and personal messages will be posted near the main conference room. Accommodation is provided in the conference center and in your cottage. Breakfast will be served between 7:30 and 8:30. Room/Cottage keys can be picked up at lunch time on the first day and need to be returned before 10:00 on the day of departure. Parking is free of charge. The address of "Centerparcs Heijderbos" is

Hommersumseweg 43
6598 MC Heijen
The Netherlands

Facilities

The facilities at the center include a restaurant, bar, and recreation and sports facilities. We refer to the reception desk of the center for detailed information about the use of these facilities.

Best junior presentation award

Continuing a tradition that started in 1996, the Benelux meeting will close with the announcement of the winner of the Best Junior Presentation Award. This award is given for the best presentation at the meeting given by a junior researcher (*i.e.*, someone working towards a PhD degree). The award is specifically given for quality of presentation rather than quality of research, which is judged in a different way. At the meeting, the chairs of sessions will ask three volunteers in the audience to fill out an evaluation form. After the session, the evaluation forms will be collected by the Prize Commissioners who will then compute a ranking. The winner will be announced on Thursday, March 29, in room **Jasmijn**, immediately after the final lectures of the meeting and he or she will be presented with the award, which consists of a trophy that may be kept for one year and a certificate. The evaluation forms of each presentation will be returned to the junior researcher who gave the presentation. The Prize Commissioners are Prof. Johan Schoukens (Vrije Universiteit Brussel), and Dr Simon van Mourik (Wageningen University).

The organizing committee counts on the cooperation of the participants to make this contest a success.

Website

An *electronic version* of the Book of Abstracts can be downloaded from the Benelux Meeting web site.

Meetings

The following meetings are scheduled:

- Board DISC on Tuesday, March 27, room Narcis, 18:00–19:30.
- Management Team DISC on Wednesday, March 28, room Narcis, 17:30–19:00.
- UNIT DISC on Thursday, March 29, room Narcis, 12:30–13:30.

Tuesday March 27

11:25 – 11:30	P0 Jasmijn *Opening*					
11:30 – 12:30	P1 Jasmijn *"Dynamic Value Functions – Towards Constructive Nonlinear Control Systems Analysis"* Astolfi					
12:30 – 13:45	Lunch					
13:45 – 14:45	P2 Jasmijn *"Model Reduction by Moment Matching"* Astolfi					
Room TuP	Gerbera TuP01 *System Theory A*	Jasmijn TuP02 *System Identification A*	Hyacinth TuP03 *Optimal Control A*	Iris TuP04 *Optimization A*	Klaproos TuP05 *Non-Linear Control A*	Lelie TuP06 *Robotics A*
15:10 – 15:35	Bauer	Forgione	Hajiahmadi	Trefois	Pradana	Khalil
15:35 – 16:00	Hermans	Dankers	van Reeven	Mutsaers	Ouyang	van Zutphen
16:00 – 16:25	Tkachev	Decuyper	Zeinaly	Fu	Breckpot	Marinkov
16:25 – 16:50	Gommans	Hoeijmakers	Wang	Van Loock	Volckaert	Heck
16:50 – 17:20	Coffee Break					
TuE	TuE01 *System Theory B*	TuE02 *System Identification B*	TuE03 *Optimal Control B*	TuE04 *Optimization B*	TuE05 *Non-Linear Control B*	TuE06 *Robotics B*
17:20 – 17:45	Kaba	Wong	Alkano	Liégeois	Thuan	Fumagalli
17:45 – 18:10	Adzkiya	Vanbeylen	Suvarov	Mehrkanoon	Madhusudhanan	Munos-Arias
18:10 – 18:35	Shekhawat	Lataire	Witters	Borckmans	Jafarian	Janssen
18:35 – 19:00	Soudjani	Marcanoto	Huyck	Bikcora	Sepulchre	Wang
18:00 – 19:30	Board DISC (room Narcis)					
19:30 – 21:00	Dinner					

Wednesday March 28

Room WeA	Gerbera WeA01 *Systems Theory C*	Jasmijn WeA02 *System Identification C*	Hyacinth WeA03 *Optimal Control C*	Iris WeA04 *Optimization C*	Mimosa WeA05 *Mechanical Engineering A*	Lelie WeA06 *Medical Applications*	
08:30 – 08:55	van der Hulst	Louarroudi	van Keulen	Deville	van Loon	Olarte	
08:55 – 09:20	Gielen	Torres	Son	Kersbergen	van der Sande	Collard	
09:20 – 09:45	Melchior	Csurcsia	Hostens	Hu	Vroomen	Buttafuoco	
09:45 – 10:10	Polenkova	Goos	Xin	Wang	Janssens	Uribe	
10:10 – 10:35	Coffee Break						
Room WeP	Gerbera WeP01 *Systems Theory D*	Jasmijn WeP02 *System Identification D*	Hyacinth WeP03 *Optimal Control D*	Iris WeP04 *Optimization D*	Mimosa WeP05 *Mechanical Engineering B*	Lelie WeP06 *Robotics C*	Klaproos WeP07 *Systems Biology A*
10:35 – 11:00	Jeltsema	Tiels	Li	Mishra	Atuonwu	Vos	Drion
11:00 – 11:25	Sacré	Depraetere	Larsen	Cappon	Aladagli	van den Dries	Trotta
11:25 – 11:50	Gottimukkala	Batselier	Larsen	Langone	Criens	Su	Omony
11:50 – 12:15	Xia	Monteyne	Tran	Easter Selvan	Canonico	Lunenburg	-
12:30 – 13:45	Lunch						
Room WeE	Gerbera WeE01 *Systems Theory E*	Jasmijn WeE02 *System Identification E*	Hyacinth WeE03 *Optimal Control E*	Iris WeE04 *Optimization E*	Mimosa WeE05 *Mechanical Engineering C*	Lelie WeE06 *Robotics D*	Klaproos WeE07 *Systems Biology B*
13:45 – 14:10	Athanasopoulos	Geerardyn	Gillis	van Berkel	Hilhorst	Janssens	Vercammen
14:10 – 14:35	Habets	Klok	Debrouwere	Pham	Hoogendijk	Elfring	Schliemann
14:35 – 15:00	van Voorn	Keesman	-	Determe	Boeren	-	van Mourik
15:00 – 15:20	Coffee Break						
15:20 – 15:30	P3: DISC Certificate Awards						
15:30 – 16:30	P4 Jasmijn *"Port Based Thinking: What is it and why is it useful?"* Stramigioli						
16:30 – 17:30	P5: *"Port Based Modeling for Robotics"* Stramigioli						
17:30 – 19:00	Meeting Management Team DISC (room Narcis)						
18:00 – 19:00	P6: *"Port Based Control for Robotics"* Stramigioli						
19:30 – 21:00	Dinner						

Thursday March 29

8:30 – 9:30	P7 Jasmijn *"Event-Based Control: Theory and Application"* Jan Lunze					
9:30 – 9:45	Break					
9:45 – 10:45	P8 Jasmijn *"Synchronization of Autonomous Agents with Individual Dynamics"* Jan Lunze					
10:45 – 11:15	Break					
Room ThM	Lelie ThM01 *Games and Agent-Based Models A*	Hyacinth ThM02 *Electro-Mechanical Engineering A*	Klaproos ThM03 *Modeling for Control A*	Gerbera ThM04 *Biochemical Engineering A*	Iris ThM05 *Non-Linear Control C*	Mimosa ThM06 *Distributed Parameter Systems A*
11:15 – 11:40	Haesaert	Shaik	van Solingen	Vanlaer	Wei	Qiu
11:40 – 12:05	Dethier	Hommen	Gins	Saraiva	Dirksz	Kahilu
12:05 – 12:30	Frasca	Cochior	Huisman	van den Kerkhof	Forni	Peeters
12:30 – 13:45	Lunch					
Room	Lelie	Hyacinth	Klaproos	Gerbera	Iris	Mimosa
ThP	ThP01 *Games and Agent-Based Models B*	ThP02 *Electro-Mechanical Engineering B*	ThP03 *Modeling for Control B*	ThP04 *Biochemical Engineering B*	ThP05 *Non-Linear Control D*	ThP06 *Distributed Parameter Systems B*
13:45 – 14:10	Prihatin	Virag	Siraj	Pimentel	Liu	Lauret
14:10 – 14:35	Zhang	van Gils	Silvas	Benavides	Bauer	Seslija
14:35 – 15:00	Browet	Katalenic	Almeida	Ugryumova	Bolder	Agudelo
15:00 – 15:25	Monshizadeh	Zhao	Mutsaers	Amribt	Hunnekens	van Zwieten
15:25 – 15:50	Sarlette	Oncu	Feru	Retamal	Biemond	-
16:00 – 16:15	Best Junior Presentation Award Ceremony					
16:15	Closure of 31st Benelux Meeting					

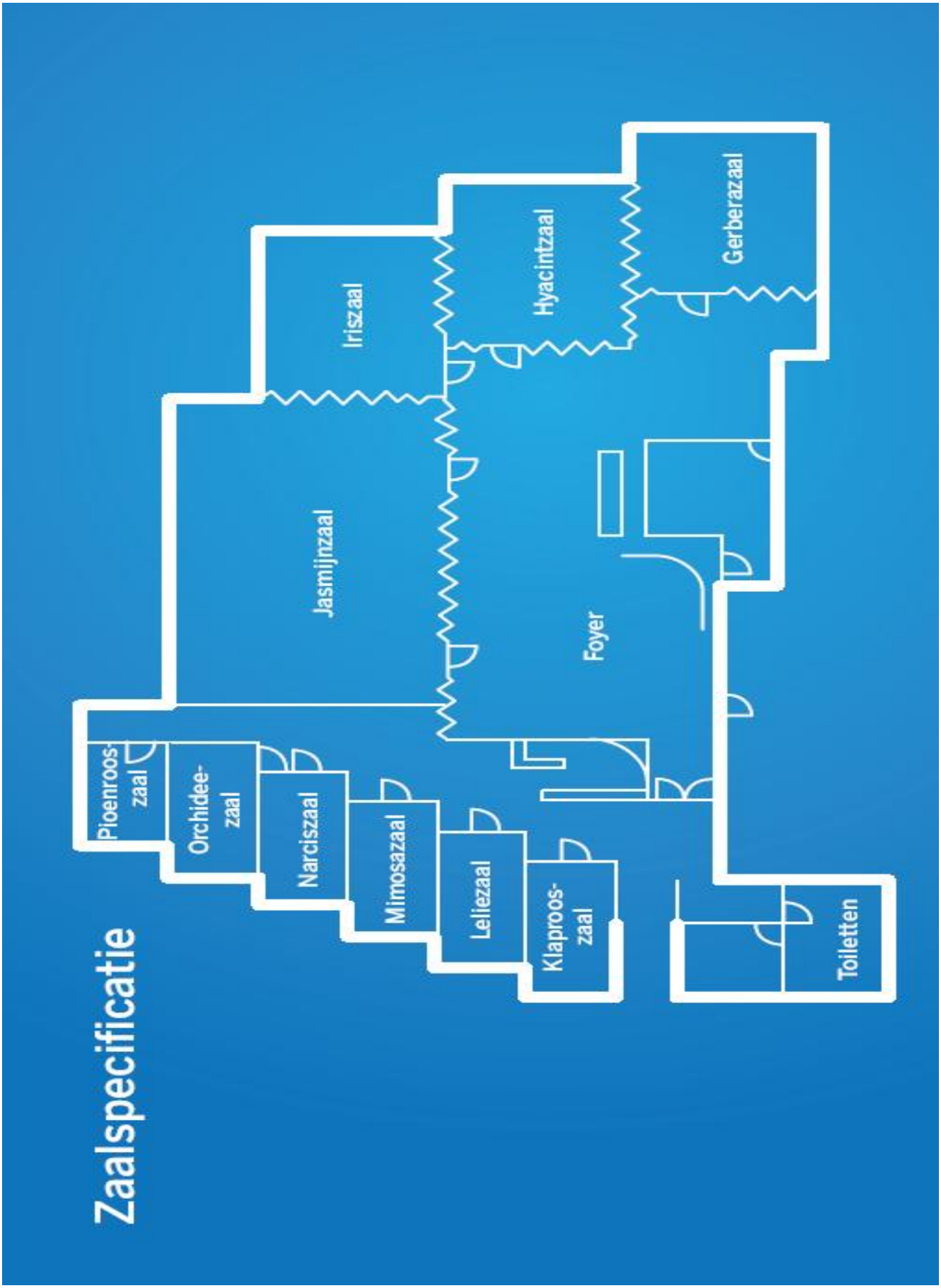
Zaalspecificatie
Ploenroos-zaal
Orchidee-zaal
Narciszaal
Mimosazaal
Leliezaal
Klaproos-zaal
Jasmijnzaal
Iriszaal
Hyacintzaal
Gerberazaal
Foyer
Toiletten